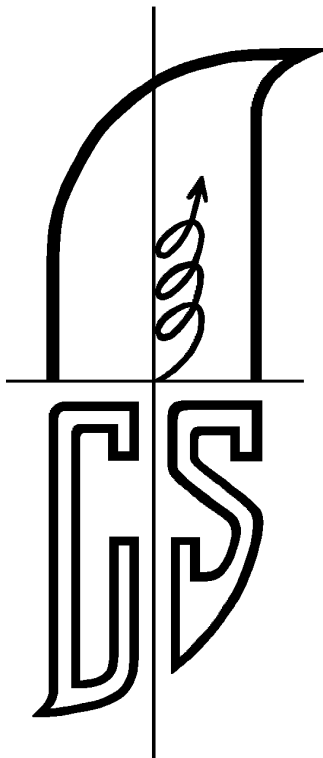
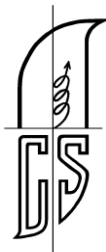


16th Czech and Slovak Conference on Magnetism



Book of Abstracts

**June 13 – 17, 2016
Košice, Slovakia**



16th Czech and Slovak Conference on Magnetism

Organized by



Faculty of Science
Pavol Jozef Šafárik University in Košice



Institute of Experimental Physics
Slovak Academy of Sciences, Košice

in cooperation with



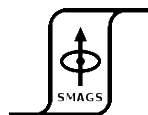
Technical University of Košice



Slovak Physical Society



Czech Physical Society



Slovak Magnetic Society

16th Czech and Slovak Conference on Magnetism

June 13 – 17, 2016

Košice, Slovakia

Book of Abstracts

Editors: Pavol Sovák, Ivan Škorvánek, Martin Orendáč,
Jozef Marcin, Marián Reiffers

Copyright ©2016 Slovak Physical Society
All rights reserved.

The abstracts are reproduced as received from authors.

ISBN 978-80-971450-9-5

INTERNATIONAL ADVISORY COMMITTEE

Andrej Bobák	Košice
Horia Chiriac	Iași
Alexander Feher	Košice
Karol Flachbart	Košice
Giselher Herzer	Hanau
Bogdan Idzikowski	Poznań
Pavel Javorský	Prague
Jiří Kamarád	Prague
Tadeusz Kulik	Warsaw
Mark W. Meisel	Gainesville
Marcel Miglierini	Bratislava
Marek Pękała	Warsaw
Jaromír Pištora	Ostrava
Oldřich Schneeweiss	Brno
Józef Spalek	Kraków
Peter Švec	Bratislava
Ilja Turek	Brno
Lajos K. Varga	Budapest

ORGANIZING COMMITTEE

Conference Chairs:	Pavol Sovák	FS UPJŠ Košice
	Ivan Škorvánek	IEP SAS Košice
Programme:	Martin Orendáč	FS UPJŠ Košice
	Jozef Marcin	IEP SAS Košice
Publication:	Jozef Kováč	IEP SAS Košice
	Peter Kollár	FS UPJŠ Košice
	Rastislav Varga	FS UPJŠ Košice
	Natália Tomašovičová	IEP SAS Košice
	Hana Čenčariková	IEP SAS Košice
Treasurer:	Marián Reiffers	IEP SAS Košice
Local Committee:	Ján Füzer	FS UPJŠ Košice
Members:	Adriana Zelenáková	FS UPJŠ Košice
	Milan Timko	IEP SAS Košice
	Martina Koneracká	IEP SAS Košice

Scope of the Conference

The objective of the conference is to offer the opportunity for the Slovak and Czech scientists and guests from other countries working in the field of basic and applied magnetism to present their recent results and to exchange ideas and technical information.

Technical Content

The programme of the conference covers the following areas:

1. Theoretical problems of magnetically ordered materials, magnetization processes,
2. Amorphous, nanocrystalline and other soft magnetic materials,
3. Magnetic materials for energy applications (permanent magnets, magnetocaloric materials, motors, transformers, ...),
4. Magnetic thin films and surfaces, spintronics, particles and nanostructures,
5. Low-dimensional magnetic materials, molecular magnets and ferrofluids,
6. Rare-earth and 5f-systems,
7. Strongly correlated electron systems, superconducting materials,
8. Multifunctional magnetic materials (multiferroic, magnetoelastic, shape memory, ...),
9. Applications and other magnetic materials not included in 1-8.

The scientific programme consists of plenary, invited and contributed talks and poster sessions.

Conference Language

The working language of the conference is English.

Proceedings

The Proceedings of the Conference will be published in [Acta Physica Polonica](#), the Journal recognised by the Current Contents database.

Conference Date and Location

The conference will be held at [Technical University](#) in [Košice](#), during June 13-17, 2016. Conference sessions will take place in the [Lecture hall Aula Maxima](#), Technical University, Letná 9, Košice. Poster sessions will take place in the [Library foyer](#), Technical University, Boženy Němcovej 7, Košice.

CSMAG'16 Conference Secretariat

Institute of Physics, P. J. Šafárik University

Park Angelinum 9

041 54 Košice,

Slovakia

www: <http://csmag.saske.sk>

e-mail: info.csmag@saske.sk

Exhibitors and Supporters



CHROMSPEC-SLOVAKIA, spol. s r. o.
Slovakia
www.chromspec.sk



CRYOGENIC Limited
United Kingdom
www.cryogenic.co.uk



CRYOSOFT spol. s r. o.
Slovakia
www.cryosoft.euweb.cz



KEPCO
Czech Republic
www.kepcopower.com | www.teste.cz



LOT – QuantumDesign GmbH
Germany
lot-qd.com



SOS electronic s.r.o.
Slovakia
www.sos.sk



TESTOVACÍ TECHNIKA s.r.o.
Czech Republic
www.teste.cz

P R O G R A M M E

Programme at a Glance

Monday June 13	Tuesday June 14	Wednesday June 15	Thursday June 16	Friday June 17
10:00 Registration	08:45-10:30 Session 6	08:45-10:30 Session 3	08:45-10:30 Session 4	09:00-10:30 Session 7
	10:30-10:50 Coffee Break	10:30-10:50 Coffee Break	10:30-10:50 Coffee Break	10:30-10:50 Coffee Break
	10:50-12:20 Session 2	10:50-12:20 Session 4	10:50-12:20 Session 8	10:50-12:20 Session 9 & Closing
12:20-14:00 Lunch	12:20-14:15 Lunch	12:20-14:15 Lunch	12:20-14:15 Lunch	12:20-14:00 Lunch
14:00-16:15 Opening Session	14:15-16:15 Session 5	14:15-16:15 Session 1	14:15-16:15 Session 7	14:00 Trip to Tokaj
16:15-16:45 Coffee Break	16:15-16:30 Coffee Break	16:15-16:30 Coffee Break	16:15-16:30 Coffee Break	
16:45-18:15 Session 2	16:30-18:00 Poster Sessions P1, P3, P9	16:30-18:00 Poster Sessions P2, P4, P8	16:30-18:00 Poster Sessions P5, P6, P7	
18:30 Welcome Reception	19:00 Concert		19:00 Barbecue	

Conference Sessions

- 1. Theoretical problems of magnetically ordered materials, magnetization processes**
- 2. Amorphous, nanocrystalline and other soft magnetic materials**
- 3. Magnetic materials for energy applications (permanent magnets, magnetocaloric materials, motors, transformers, ...)**
- 4. Magnetic thin films and surfaces, spintronics, particles and nanostructures**
- 5. Low-dimensional magnetic materials, molecular magnets and ferrofluids**
- 6. Rare-earth and 5f-systems**
- 7. Strongly correlated electron systems, superconducting materials**
- 8. Multifunctional magnetic materials (multiferroic, magnetoelastic, shape memory, ...)**
- 9. Applications and other magnetic materials not included in 1-8**

MONDAY, JUNE 13

10:00 Registration

12:20 Lunch

14:00

OPENING SESSION

Pavol Sovák, Co-Chair
Ivan Škorvánek, Co-Chair

14:15 PL-01 (plenary)

MAGNETO-OPTICAL DOMAIN IMAGING

R. Schäfer

14:55 PL-02 (plenary)

**SPIN CONFIGURATION AND MAGNETIZATION REVERSAL OF
INDIVIDUAL COFE BASED CYLINDRICAL NANOWIRES**

*M. Vazquez, C. Bran, A. Asenjo, R. Perez, O. Chubykalo-Fesenko,
E. Palmero, E. Berganza and J. A. Fernandez Roldan*

15:35 PL-03 (plenary)

**INVESTIGATION OF Ce AND Yb INTERMETALLICS:
THE IMPORTANCE OF PHASE DIAGRAMS AND CRYSTAL
CHEMISTRY**

M. Giovannini

16:15 Coffee Break

MONDAY, JUNE 13

**AMORPHOUS, NANOCRYSTALLINE AND
OTHER SOFT MAGNETIC MATERIALS**

Giselher Herzer, Chair

16:45 I2-01 (invited)

**STRUCTURAL ORIGIN OF CREEP INDUCED MAGNETIC
ANISOTROPY OF AMORPHOUS ALLOYS**

M. Ohnuma, P. Kozikowski, G. Herzer and C. Polak

17:15 O2-01

**INFLUENCE OF ANNEALING CONDITIONS ON THE MAGNETIC
PROPERTIES OF $\text{Fe}_{73.5}\text{Cu}_1\text{Nb}_3\text{Si}_{13.5}\text{B}_9$ GLASS-COATED
NANOWIRES**

S. Corodeanu, T. A. Óvári, G. Stoian, L. C. Whitmore, H. Chiriac and
N. Lupu

17:30 O2-03

**Co_2FeX (X = Al, Si) HEUSLER COMPOUNDS PREPARED BY
PLANAR FLOW CASTING AND ARC MELTING METHODS:
MICROSTRUCTURE AND MAGNETISM**

A. Titov, O. Zivotsky, Y. Jiraskova, J. Bursik, A. Hendrych and
D. Janickovic

17:45 O2-04

**EFFECTS OF SWIFT HEAVY-IONS ON Fe-BASED METALLIC
GLASSES STUDIED BY SYNCHROTRON DIFFRACTION**

S. Michalik, M. Pavlovic, J. Gamcova, P. Sovak and M. Miglierini

18:00 O9-01

**MAGNETIC PROPERTIES OF THE IONIC LIQUIDS $\text{Edimim}(\text{FeX}_4)$
(X = Cl and Br) IN ITS SOLID STATE**

I. de Pedro, A. García-Sáiz, J. L. Espeso, L. F. Barquín and
J. Rodríguez-Fernández

18:30 Welcome Reception

TUESDAY, JUNE 14

RARE-EARTH AND 5f-SYSTEMS

Julian Sereni, Chair

08:45 I6-01 (invited)

FERROMAGNETIC CRITICALITY OF URANIUM COMPOUNDS

J. Prokleška, P. Opletal, M. Vališka, M. Míšek and V. Sechovský

09:15 O6-01

MAGNETISM AND CRYSTAL FIELD IN PrCuAl_3 AND NdCuAl_3

P. Novák and M. Diviš

09:30 O6-02

MAGNETIC PROPERTIES OF SOLID SOLUTIONS $\text{HoCo}_{1-x}\text{Ni}_x\text{C}_2$

H. Michor, V. Levytsky, V. Babizhetskyy, M. Hembara, A. Schumer, S. Özcan and B. Ya. Kotur

09:45 O6-03

**WEAKLY ANISOTROPIC MAGNETISM IN URANIUM
INTERMETALLIC $\text{U}_4\text{Ru}_7\text{Ge}_6$**

M. Vališka, J. Valenta, P. Doležal, V. Tkáč, J. Prokleška, M. Diviš and V. Sechovský

10:00 O6-04

**MAGNETIC PROPERTIES AND MAGNETOCALORIC EFFECT IN
STRUCTURALLY DISORDERED RECo_2 (RE = Y, Gd, Tb)
COMPOUNDS**

Z. Śniadecki, N. Pierunek and B. Idzikowski

10:15 O6-05

**MAGNETIC PHASE DIAGRAMS AND STRUCTURES IN R_2TIn_8
(T = Rh, Ir, Co) AND RELATED TETRAGONAL COMPOUNDS**

P. Javorský, P. Čermák, M. Kratochvílová, J. Zubáč, K. Pajskr, K. Prokeš and B. Ouladdiaf

10:30 Coffee Break

TUESDAY, JUNE 14

**AMORPHOUS, NANOCRYSTALLINE AND
OTHER SOFT MAGNETIC MATERIALS**

Rastislav Varga, Chair

10:50 I2-02 (invited)

**DEVELOPMENT OF SELECTED AMORPHOUS AND
NANOCRYSTALLINE SOFT MAGNETIC SYSTEMS WITH
ENHANCED FUNCTIONAL PROPERTIES**

P. Svec, I. Janotova, J. Zigo, I. Matko, D. Janickovic, J. Marcin, I Skorvanek
and *P. Svec Sr.*

11:20 O2-05

**OPTIMISATION OF FRAME-SHAPED FLUXGATE SENSOR'S
CORE MADE OF AMORPHOUS ALLOY USING GENERALIZED
MAGNETOSTATIC METHOD OF MOMENTS**

R. Szewczyk and *P. Frydrych*

11:35 O2-06

**SIZE DEPENDENT HEATING EFFICIENCY OF MULTICORE
IRON OXIDE PARTICLES IN LOW-POWER ALTERNATING
MAGNETIC FIELDS**

I. S. Smolkova, *N. E. Kazantseva*, *L. Vitkova*, *V. Babayan*, *J. Vilcakova* and
P. Smolka

11:50 O2-07

LOSS PREDICTION IN 6.5% ELECTRICAL STEELS

J. Szczygłowski

12:05 O2-08

**EFFECT OF DISK VELOCITY IN MELT SPINNING METHOD ON
MAGNETIC PROPERTIES OF AMORPHOUS RIBBONS**

N. Amini, *M. Miglierini* and *M. Hasiak*

12:20 Lunch

TUESDAY, JUNE 14

**LOW-DIMENSIONAL MAGNETIC MATERIALS,
MOLECULAR MAGNETS AND FERROFLUIDS**

Alexander Feher, Chair

14:15 I5-01 (invited)

**THE ROUTE TO MAGNETIC ORDER IN THE KAGOME
ANTIFERROMAGNET**

J. Richter

14:45 I5-02 (invited)

**LONG-RANGE MAGNETIC ORDER IN A PURELY ORGANIC 2D
LAYER ADSORBED ON EPITAXIAL GRAPHENE**

A. L. Vázquez de Parga

15:15 O5-01

**UNUSUAL MAGNETIC-PRESSURE RESPONSE OF AN
S = 1 QUASI-ONE-DIMENSIONAL ANTIFERROMAGNET NEAR
D/J ~ 1**

M. K. Peprah, P. A. Quintero, A. Garcia, J. M. Pérez, J. S. Xia,
J. M. Manson, S.E. Brown and *M. W. Meisel*

15:30 O5-02

**DOUBLE MAGNETIC RELAXATION AND MAGNETOCALORIC
EFFECT IN TWO CLUSTER-BASED MATERIALS $\text{Mn}_9[\text{W}(\text{CN})_6]\text{-L}$**

P. Konieczny, R. Pelka, W. Nogaś, S. Choraży, M. Kubicki, R. Podgajny,
B. Sieklucka and T. Wasiutyński

15:45 O5-03

**AC MAGNETIC SUSCEPTIBILITY OF FERROFLUIDS EXPOSED
TO AN EXTERNAL ELECTRIC FIELD**

M. Rajňák, B. Dolník, J. Kováč, J. Kurimský, R. Cimbala, K. Paulovičová,
P. Kopčanský and M. Timko

16:00 O5-04

**UNIVERSAL SEQUENCE OF GROUND STATES IN
ANTIFERROMAGNETIC FRUSTRATED RINGS WITH A SINGLE
BOND DEFECT**

M. Antkowiak, G. Kamieniarz and W. Florek

16:15 Coffee Break

16:30 Poster Sessions – P1, P3, P9

19:00 Concert

WEDNESDAY, JUNE 15

**MAGNETIC MATERIALS FOR ENERGY APPLICATIONS
(PERMANENT MAGNETS, MAGNETOCALORIC MATERIALS,
MOTORS, TRANSFORMERS, ...)**

Nicoleta Lupu, Chair

08:45 I3-01 (invited)

**ENERGY-EFFICIENT REFRIGERATION NEAR ROOM
TEMPERATURE WITH TRANSITION METAL BASED
MAGNETIC REFRIGERANTS**

*E. Brück, H. Yibole, Van Thang Nguyen, Xuefei Miao, M. Boeije, L. Caron,
Lian Zhang, F. Guillou and N. Van Dijk*

09:15 I3-02 (invited)

**SOFT MAGNETIC, NANOCRYSTALLINE MATERIALS FOR
INDUCTORS AND SHIELDING APPLICATIONS - OPTIMIZED
FOR HIGHER FREQUENCY**

C. Polak

09:45 O3-01

**MAGNETOCALORIC EFFECT OVER A WIDE TEMPERATURE
RANGE DUE TO MULTIPLE MAGNETIC TRANSITIONS IN
GdNi_{0.8}Al_{1.2} ALLOY**

*T. P. Rashid, S. Nallamuthu, K. Arun, I. Curlik, S. Ilkovic, A. Dzubinska,
M. Reiffers and R. Nagalakshmi*

10:00 O3-02

THE SCHOTTKY EFFECT IN YbCoGaO₄ SINGLE CRYSTALS

*I. Radelytskyi, T. Zajarniuk, A. Szewczyk, M. Gutowska, H. A. Dabkowska,
P. Dłużewski and H. Szymczak*

10:15 O3-03

**ANALYSIS OF THE CRYSTALLIZATION PROCESSES AS A
BASIS FOR OPTIMIZATION OF MAGNETIC PROPERTIES OF
Hf₂Co₁₁B ALLOYS**

A. Mustał, Z. Śniadecki, J. Kováč, I. Škorvánek and B. Idzikowski

10:30 Coffee Break

WEDNESDAY, JUNE 15

**MAGNETIC THIN FILMS AND SURFACES, SPINTRONICS,
PARTICLES AND NANOSTRUCTURES**

Oleg Heczko, Chair

10:50 I4-01 (invited)

**LOW TC GLASSY MAGNETIC ALLOYS FOR MEDICAL
APPLICATIONS**

H. Chiriac

11:20 O4-01

**FOCUSED ION BEAM PATTERNING OF METASTABLE FCC
IRON THIN FILMS – A NOVEL TEMPLATE FOR MAGNETIC
METAMATERIALS**

*M. Urbánek, V. Křížáková, J. Gloss, M. Horký, L. Flajšman, M. Schmid,
T. Šikola and P. Varga*

11:35 O4-02

**IN-PLANE EDGE MAGNETISM IN GRAPHENE-LIKE
NANOSTRUCTURES**

S. Krompiewski

11:50 O4-03

**HIGH-RESOLUTION FULLY VECTORIAL SCANNING KERR
MAGNETOMETRY**

L. Flajšman, M. Urbánek, V. Křížáková, M. Vaňatka and T. Šikola

12:05 O4-04

**TOWARDS MEASURING MAGNETISM WITH ATOMIC
RESOLUTION IN A TRANSMISSION ELECTRON MICROSCOPE**

J. Rusz, J. C. Idrobo, S. Muto, J. Spiegelberg and K. Tatsumi

12:20 Lunch

WEDNESDAY, JUNE 15

**THEORETICAL PROBLEMS OF MAGNETICALLY ORDERED
MATERIALS, MAGNETIZATION PROCESSES**

Jan Rusz, Chair

14:15 I1-01 (invited)

**EFFECT OF ELECTRON CONFINEMENT ON MAGNETISM OF
NANOSTRUCTURES**

M. Przybylski

14:45 O1-01

**MICROSCOPIC ORIGIN OF HEISENBERG AND NON-
HEISENBERG EXCHANGE INTERACTIONS IN
FERROMAGNETIC BCC Fe**

Y. O. Kvashnin, R. Cardias, *A. Szilva*, I. Di Marco, M. I. Katsnelson,
A. I. Lichtenstein, L. Nordström, A.B. Klautau and O. Eriksson

15:00 O1-02

**MAGNETISM AND TRANSPORT PROPERTIES OF
Mn-DOPED TOPOLOGICAL INSULATOR Bi₂Te₃ AND Bi₂Se₃: AB
INITIO CALCULATIONS**

K. Carva, P. Baláž, V. Tkáč, R. Tarasenko, V. Sechovský, J. Kudrnovský,
F. Máca and J. Honolka

15:15 O1-03

**NON- PLATEAU BEHAVIOR OF THE ZERO-TEMPERATURE
MAGNETIZATION IN SPIN-CLUSTERS AND CHAINS**

V. Ohanyan, O. Rojas, J. Strecka and S. Bellucci

15:30 O1-04

**AB INITIO THEORY OF GILBERT DAMPING IN RANDOM
ALLOYS**

I. Turek, J. Kudrnovsky and V. Drchal

15:45 O1-05

**PHOTO-MECHANICAL COUPLING IN MAGNETIC SHUTTLE
DEVICE**

A. Parafilo, S. Kulinich, L. Gorelik, M. Kiselev, R. Shekhter and M. Jonson

16:00 O1-06

BROKEN SYMMETRY IN THE MAGNETISATION DYNAMICS

J. Tóbiš and V. Cambel

16:15 Coffee Break

16:30 Poster Sessions – P2, P4, P8

THURSDAY, JUNE 16

**MAGNETIC THIN FILMS AND SURFACES, SPINTRONICS,
PARTICLES AND NANOSTRUCTURES**

Alžbeta Orendáčová, Chair

08:45 I4-02 (invited)

**TEMPLATE ASSISTED DEPOSITION OF FERROMAGNETIC
NANOSTRUCTURES: FROM ANTIDOT THIN FILMS TO
MULTISEGMENTED NANOWIRES AND METALLIC NANOTUBES**

*V. M. Prida, V. Vega, S. González, M. Salaheldeen, J M. Mesquita,
A. Fernández and B. Hernando*

09:15 O4-05

**MAGNETIC VORTEX NUCLEATION MODES STUDIED BY
ANISOTROPIC MAGNETORESISTANCE AND MAGNETIC
TRANSMISSION X-RAY MICROSCOPY**

*M. Vaňatka, M. Urbánek, R. Jíra, L. Flajšman, M. Dhankhar, V. Uhlíř,
M.-Y. Im and T. Šikola*

09:30 O4-06

**MAGNETIC PROPERTIES OF HEXAGONAL GRAPHENE
NANOMESHES**

M. Zwierzycki

09:45 O4-07

**MAGNETOTRANSPORT IN Mn-DOPED Bi₂Se₃ TOPOLOGICAL
INSULATORS**

*V. Tkáč, V. Komanický, R. Tarasenko, M. Vališka, V. Holý, G. Springholz,
V. Sechovský and J. Honolka*

10:00 O4-08

**STUDY OF MAGNETIC MICRO-ELLIPSES BY CANTILEVER
SENSOR**

K. Sečianska, J. Šoltýs and V. Cambel

10:15 O4-09

**MAGNETIC PHASE TRANSITION ASYMMETRY IN MESOSCALE
FeRh STRIPES**

V. Uhlíř, J. A. Arregi and E. E. Fullerton

10:30 Coffee Break

THURSDAY, JUNE 16

**MULTIFUNCTIONAL MAGNETIC MATERIALS
(MULTIFERROIC, MAGNETOELASTIC, SHAPE MEMORY, ...)**

Mark Meisel, Chair

10:50 I8-01 (invited)

RECENT RESEARCH IN MAGNETIC SHAPE MEMORY ALLOYS

J. M. Barandiaran and V. A. Chernenko

11:20 O8-01

**MAGNETIC DOMAIN STRUCTURE TRANSFORMATION DURING
FERROELASTIC TWIN BOUNDARY PASSAGE IN Ni-Mn-Ga
SINGLE CRYSTAL**

V. Kopecký, O. Perevertov, L. Fekete and O. Heczko

11:35 O8-02

**INVESTIGATION OF MAGNETOELASTIC PROPERTIES OF
Ni_{0.36}Zn_{0.64}Fe₂O₄ FERRITE MATERIAL IN LOW MAGNETIZING
FIELDS CORRESPONDING TO RAYLEIGH REGION**

M. Kachniarz, A. Bieńkowski and R. Szewczyk

11:50 O8-03

**MAGNETIC PHASE DIAGRAM OF TbMn_{1-x}Fe_xO₃
(0 ≤ x ≤ 1) SUBSTITUTIONAL SYSTEM**

*M. Mihalik jr., M. Mihalik, Z. Jagličić, R. Vilarinho, J. Agostinho Moreira,
A. Almeida and M. Zentková*

12:05 O8-04

**MAGNETIC PROPERTIES OF THE Bi_{0.65}La_{0.35}Fe_{0.5}Sc_{0.5}O₃
PEROVSKITE**

*A. V. Fedorchenko, E. L. Fertman, V. A. Desnenko, O. V. Kotlyar,
E. Čížmár, V. V. Shvartsman, D. C. Lupascu, S. Salamon, H. Wende,
A. N. Salak, D. D. Khalyavin, N. M. Olekhovich, A. V. Pushkarev,
Yu. V. Radyush and A. Feher*

12:20 Lunch

THURSDAY, JUNE 16

**STRONGLY CORRELATED ELECTRON SYSTEMS,
SUPERCONDUCTING MATERIALS**

Herwig Michor, Chair

14:15 I7-01 (invited)

**SAMARIUM HEXABORIDE: THE FIRST STRONGLY
CORRELATED TOPOLOGICAL INSULATOR?**

*O. Rader, P. Hlawenka, K. Siemensmeyer, E. Weschke, A. Varykhalov,
J. Sánchez-Barriga, N. Y. Shitsevalova, A. V. Dukhnenko, V. B. Filipov,
S. Gabáni, K. Flachbart and E. D. L. Rienks*

14:45 O7-01

**TRANSITION FROM MOTT INSULATOR TO
SUPERCONDUCTOR IN GaNb₄S₈ AT HIGH PRESSURE**

*X. Wang, K. Syassen, F. J. Litterst, J. Prchal, V. Sechovsky, D. Johrendt
and M. M. Abd-Elmeguid*

15:00 O7-02

**TESTING THE THIRD LAW OF THERMODYNAMICS
AT $T \rightarrow 0$ IN MAGNETIC SYSTEMS**

J. G. Sereni

15:15 O7-03

**PROTON DISORDER IN D₂O - ICE, A NEUTRON DIFFRACTION
STUDY**

*K. Siemensmeyer, J.-U. Hofmann, S. V. Isakov, B. Klemke, R. Moessner,
J. P. Morris and D. A. Tennant*

15:30 O7-04

**STRUCTURAL AND PHYSICAL PROPERTIES OF NEW
COMPOUNDS IN THE Yb-Pd-Sn TERNARY SYSTEM**

*F. Gastaldo, M. Giovannini, A. Strydom, I. Čurlík, M. Reiffers, P. Solokha
and A. Saccone*

15:45 O7-05

**SYNTHESIS AND PHYSICAL PROPERTIES CePdIn₅, A NEW
COMPOUND OF Ce_nPd_mIn_{3n+2m} HOMOLOGOUS SERIES**

*K. Uhlířová, J. Prokleška, B. Vondráčková, M. Kratochvilová, M. Dušek,
J. Custers and V. Sechovský*

16:00 O7-06

SUPERCONDUCTOR – INSULATOR TRANSITION

*P. Szabó, T. Samuely, V. Hašková, J. Kačmarčík, M. Žemlička,
M. Grajcar, R. Hlubina, R. Martoňák and P. Samuely*

16:15 Coffee Break

THURSDAY, JUNE 16

16:30 Poster Sessions – P5, P6, P7

19:00 Barbecue

FRIDAY, JUNE 17

**STRONGLY CORRELATED ELECTRON SYSTEMS,
SUPERCONDUCTING MATERIALS**

Konrad Siemensmeyer, Chair

09:00 I7-02 (invited)

**SCANNING TUNNELING MICROSCOPY STUDY OF
SUPERCONDUCTING VORTEX MOTION**

T. Samuely, M. Timmermans, D. Lotnyk, B. Raes, J. Van de Vondel and
V. V. Moshchalkov

09:30 O7-07

SUPERCONDUCTING STATE IN $\text{LaPd}_2\text{Al}_{(2-x)}\text{Ga}_x$

P. Doležal, M. Klicpera, J. Pásztorová, J. Prchal and P. Javorský

09:45 O7-08

**THE EFFECT OF Sm ADDITION ON SUPERCONDUCTING
PROPERTIES OF YBCO BULK SUPERCONDUCTORS**

D. Volochová, P. Diko, S. Piovarči, V. Antal and J. Kováč

10:00 O7-09

**HALL EFFECT AND HIDDEN QUANTUM CRITICALITY IN
 $\text{Mn}_{1-x}\text{Fe}_x\text{Si}$**

V. V. Glushkov, I. I. Lobanova, V. Yu. Ivanov, V. V. Voronov,
V. A. Dyadkin, N. M. Chubova, S. V. Grigoriev and S. V. Demishev

10:15 O7-10

**ELECTRIC CURRENTS AND VORTEX PINNING IN REBaCuO
SUPERCONDUCTING TAPES**

M. Jirsa, M. Rameš, I. Ďuran, T. Melišek and P. Kováč

10:30 Coffee Break

FRIDAY, JUNE 17

**APPLICATIONS AND OTHER MAGNETIC MATERIALS
NOT INCLUDED IN 1-8**

Roman Szewczyk, Chair

10:50 I9-01 (invited)

**STRESS MONITORING & ANNIHILATION IN STEELS BASED ON
MAGNETIC TECHNIQUES**

E. Hristoforou, P. Vourna, A. Ktena and P. Svec

11:20 O9-02

MAGNETIC ANISOTROPY OF HARD MILLED SURFACE

A. Mičietová, J. Uriček, M. Čilliková, M. Neslušan and P. Kejzlar

11:35 O9-03

**CHARACTERIZATION OF ODS STEELS AFTER GAMMA
IRRADIATION FOR APPLICATION IN ALLEGRO REACTOR**

V. Slugeň, I. Bartošová and J. Dekan

11:50 O9-04

**MRI GRADIENT ECHO PULSE SEQUENCE AS A PHYSICAL
TOOL IN DIFFERENTIATION OF NATIVE AND
RECONSTRUCTED FERRITIN**

*L. Balejcikova, O. Strbak, L. Baciak, J. Kovac, M. Masarova, A. Krafcik,
M. Peteri, P. Kopcansky and I. Frollo*

12:05

CLOSING

Pavel Javorský, Chair

12:20 Lunch

14:00 Trip to Tokaj (optional)

POSTER SESSIONS

TUESDAY, JUNE 14

16:30 – 18:00

- P1 THEORETICAL PROBLEMS OF MAGNETICALLY ORDERED MATERIALS, MAGNETIZATION PROCESSES**
- P3 MAGNETIC MATERIALS FOR ENERGY APPLICATIONS (PERMANENT MAGNETS, MAGNETOCALORIC MATERIALS, MOTORS, TRANSFORMERS, ...)**
- P9 APPLICATIONS AND OTHER MAGNETIC MATERIALS NOT INCLUDED IN 1-8**

WEDNESDAY, JUNE 15

16:30 – 18:00

- P2 AMORPHOUS, NANOCRYSTALLINE AND OTHER SOFT MAGNETIC MATERIALS**
- P4 MAGNETIC THIN FILMS AND SURFACES, SPINTRONICS, PARTICLES AND NANOSTRUCTURES**
- P8 MULTIFUNCTIONAL MAGNETIC MATERIALS (MULTIFERROIC, MAGNETOELASTIC, SHAPE MEMORY, ...)**

THURSDAY, JUNE 16

16:30 – 18:00

- P5 LOW-DIMENSIONAL MAGNETIC MATERIALS, MOLECULAR MAGNETS AND FERROFLUIDS**
- P6 RARE-EARTH AND 5f-SYSTEMS**
- P7 STRONGLY CORRELATED ELECTRON SYSTEMS, SUPERCONDUCTING MATERIALS**

POSTERS - TUESDAY, JUNE 14

P1

THEORETICAL PROBLEMS OF MAGNETICALLY ORDERED MATERIALS, MAGNETIZATION PROCESSES

P1-01 EXACT STUDIES OF THE HUBBARD PAIR-CLUSTER IN EXTERNAL FIELDS

T. Balcerzak and K. Szałowski

P1-02 THERMODYNAMICS OF FRUSTRATED MAGNETS: HIGH-TEMPERATURE EXPANSION REVISITED

J. Richter, A. Lohmann and H.-J. Schmidt

P1-03 SPONTANEOUS MAGNETIZATION AND PHASE DIAGRAMS OF THE MIXED SPIN-1/2 AND SPIN-S ISING MODEL ON THE BETHE LATTICE

C. Ekiz and J. Strečka

P1-04 MAGNETIC HYSTERESIS AS A CHAOTIC SEQUENCE

P. Frydrych, M. Nowicki and R. Szewczyk

P1-05 APPLICATION OF ANISOTROPIC VECTOR PREISACH MODEL FOR BULK MATERIALS

P. Frydrych, R. Szewczyk and M. Nowicki

P1-06 LOCALIZED-MAGNON CHAINS AND INTERCHAIN COUPLINGS

O. Krupnitska, O. Derzhko and J. Richter

P1-07 SPIN-CHAIN OF ALTERNATING ISING SPINS-CANTED AND HEISENBERG SPINS WITH TWO DIFFERENT LOCAL ANISOTROPY AXES: ZERO TEMPERATURA PHASE DIAGRAM AND MAGNETIZATION, AND THERMODYNAMICS MAGNETIZATION AND SUSCEPTIBILITY

J. Torrico, M. L. Lyra, O. Rojas, S. M. de Souza, M. Rojas, M. Hagiwara, Y. Han and J. Strečka

P1-08 BREAKDOWN OF A MAGNETIZATION PLATEAU IN FERRIMAGNETIC MIXED-SPIN HEISENBERG CHAINS DUE TO A QUANTUM PHASE TRANSITION TOWARDS A SPIN-LIQUID PHASE

J. Strečka

P1-09 INVERSE MAGNETOCALORIC EFFECT IN THE SPIN-1/2 FISHER'S SUPER-EXCHANGE ANTIFERROMAGNET

L. Gálisová and J. Strečka

- P1-10 ISOTHERMAL ENTROPY CHANGE AND ADIABATIC CHANGE OF TEMPERATURE DURING THE MAGNETIZATION PROCESS OF THE ISING OCTAHEDRON AND DODECAHEDRON**
K. Karľová, J. Strečka and T. Madaras
- P1-11 SELF-CONSISTENT MODEL OF A SOLID FOR THE LATTICE AND MAGNETIC PROPERTIES DESCRIPTION**
T. Balcerzak, K. Szałowski and M. Jaščur
- P1-12 FRACTIONAL SCALING OF MAGNETIC COERCIVITY IN ELECTRICAL STEELS**
M. Najgebauer
- P1-13 THEORETICAL STUDY OF THE FRUSTRATED ISING ANTIFERROMAGNET ON THE HONEYCOMB LATTICE**
A. Bobák, T. Lučivjanský, M. Žukovič, M. Borovský and T. Balcerzak
- P1-14 DEPENDENCE OF "LIFETIME" OF THE SPIRAL MAGNETIC DOMAIN ON THE MATERIAL PARAMETERS**
V. N. Mal'tsev and A. A. Nesterenko
- P1-15 ULTRAFast SPIN TRANSFER TORQUE GENERATED BY A FEMTOSECOND LASER PULSE**
P. Baláž, K. Carva, P. Maldonado and P. Oppeneer
- P1-16 THERMAL ENTANGLEMENT AND QUANTUM NON-LOCALITY ALONG THE MAGNETIZATION CURVE OF THE SPIN-1/2 ISING-HEISENBERG TRIMERIZED CHAIN**
J. Pavličko and J. Strečka
- P1-17 STRONG-COUPLING APPROACH TO THE SPIN-1/2 ORTHOGONAL-DIMER CHAIN**
T. Verkholyak and J. Strečka
- P1-18 STUDY OF AXIAL DIMENSION OF STATIC HEAD-TO-HEAD DOMAIN BOUNDARY IN AMORPHOUS GLASS-COATED MICROWIRE**
M. Kladivová, J. Ziman, J. Kecer and P. Duranka
- P1-19 THEORETICAL INVESTIGATIONS ON THE STRUCTURAL, MAGNETIC AND ELECTRONIC PROPERTIES OF $\text{Fe}_{2-x}\text{MnGe:Cu}_x$ ALLOY**
K. Gruszka and M. Nabiałek
- P1-20 MAGNETIZATION CURVES OF GEOMETRICALLY FRUSTRATED EXCHANGE-BIASED FM-AFM BILAYERS**
M. Pankratova and M. Žukovič

- P1-21 ENHANCED MAGNETOCALORIC EFFECT DUE TO SELECTIVE DILUTION IN A TRIANGULAR ISING ANTIFERROMAGNET**
M. Borovský and M. Žukovič
- P1-22 MOKE STUDY OF THE DOMAIN WALL DYNAMICS IN MAGNETIC MICROWIRES**
O. Váhovský and R. Varga
- P1-23 MIXED SPIN-1/2 AND SPIN 3/2 ISING MODEL WITH THREE-SITE FOUR-SPIN INTERACTIONS ON A DECORATED TRIANGULAR LATTICE**
V. Štubňa and M. Jaščur
- P1-24 CRITICAL DYNAMICS OF PLANAR MAGNETS: RENORMALIZATION GROUP ANALYSIS**
M. Dančo, M. Hnatič and T. Lučivjanský

P3 MAGNETIC MATERIALS FOR ENERGY APPLICATIONS (PERMANENT MAGNETS, MAGNETOCALORIC MATERIALS, MOTORS, TRANSFORMERS, ...)

- P3-01 INVESTIGATIONS OF THE MAGNETIZATION REVERSAL PROCESSES IN NANOCRYSTALLINE Nd-Fe-B ALLOYS DOPED BY Nb**
M. Kaźmierczak, P. Gębara, P. Pawlik, K. Pawlik, A. Przybył, I. Wnuk and J. J. Wysłocki
- P3-02 MAGNETOCALORIC PROPERTIES OF $(\text{Fe}_{46.9}\text{Co}_{20.1}\text{B}_{22.7}\text{Si}_{5.3}\text{Nb}_5)_{90}\text{M}_{10}$ (M=Tb, Pr, Nd) ALLOYS PREPARED BY MECHANICAL ALLOYING**
K. Sarlar, A. Adam, E. Civan and I. Kucuk
- P3-03 DC MAGNETIC PROPERTIES OF Ni-Fe BASED COMPOSITES**
F. Onderko, M. Jakubčín, S. Dobák, D. Olekšáková, P. Kollár, J. Füzér, M. Fáberová, R. Bureš and P. Kurek
- P3-04 SCALLING ANALYSIS OF THE MAGNETOCALORIC EFFECT IN Co@Au NANOPARTICLES**
P. Hrubovčák, A. Zelenáková, V. Zelenák and V. Franco
- P3-05 INVESTIGATION OF THE MAGNETIC PHASE TRANSITION IN THE $\text{LaFe}_{11.14}\text{Co}_{0.66}\text{Si}_{1.1}\text{M}_{0.1}$ (WHERE M=Al OR Ga) ALLOYS**
P. Gębara

- P3-06 MAGNETIC PROPERTIES AND MAGNETOCALORIC EFFECT IN SPUTTER DEPOSITED THIN FILMS OF Mn-RICH HEUSLER ALLOYS FROM Ni-Mn-X (X = Ga, Sn) SYSTEMS**
M. Chojnacki, K. Fronc, I. Radelytskyi, T. Wojciechowski, R. Minikayev and H. Szymczak
- P3-07 MEASUREMENT OF MAGNETOCALORIC EFFECT WITH MICROCALORIMETRY**
A. Chudikova, D. Gonzalez, T. Ryba, Z. Vargova, V. Komanicky, J. Kacmarcik, R. Gyepes and R. Varga
- P3-08 THE EFFECT OF Mn AND Ni ADMIXTURE ON MAGNETIZATION REVERSAL PROCESSES IN (Pr, Dy)-(Fe, Co)-B RIBBONS**
A. Przybył
- P3-09 APPLICATION OF MODIFIED TAKACS MODEL FOR ANALYSIS OF MAGNETOCALORIC EFFECT IN $\text{Fe}_{60}\text{Co}_{10}\text{Mo}_5\text{Cr}_4\text{Nb}_6\text{B}_{15}$**
J. Rzaccki and M. Dospial
- P3-10 SCALING OF ANHYSTERETIC CURVES FOR LAFECOSI ALLOY NEAR THE TRANSITION POINT**
R. Gozdur, K. Chwastek, M. Najgebauer, M. Lebioda, Ł. Bernacki and A. Wodzyński
- P3-11 INFLUENCE OF SPARK PLASMA SINTERING ON MICROSTRUCTURE AND PROPERTIES OF La-Ca-Sr-Mn-O MAGNETOCALORIC CERAMIC MATERIALS**
K. Zmorayová, V. Antal, J. Kováč, J. Noudem and P. Diko
- P3-12 MAGNETIC PROPERTIES AND STRUCTURE OF FeCo ALLOYS**
D. Olekšáková, P. Kollár, F. Onderko, J. Füzer, S. Dobák and J. Viňáš
- P3-13 INVESTIGATION OF MAGNETIC ANISOTROPY INFLUENCE ON TOTAL LOSS COMPONENTS OF GRAIN-ORIENTED ELECTRICAL STEELS**
W. A. Pluta
- P3-14 MAGNETOCALORIC EFFECT IN NOVEL $\text{Gd}_2\text{O}_3@\text{SiO}_2$ NANOCOMPOSITES**
A. Berkutova, A. Zelenáková, P. Hrubovčák, O. Kapusta and V. Zeleňák
- P3-15 THE INFLUENCE OF $\text{NiZnFe}_2\text{O}_4$ CONTENT ON MAGNETIC PROPERTIES OF SUPERMALLOY TYPE MATERIAL**
L. Ďáková, J. Füzer, S. Dobák, P. Kollár, M. Fáberová, M. Strečková, R. Bureš and H. Hadraba

P3-16 THE INFLUENCE OF PREPARATION METHODS ON MAGNETIC PROPERTIES OF Fe/SiO₂ SOFT MAGNETIC COMPOSITES

J. Füzervová, J. Füzér, P. Kollár, M. Kabátová and E. Dudrová

P3-17 MAGNETIC PROPERTIES AND STRUCTURE OF NON-ORIENTED ELECTRICAL STEEL SHEETS AFTER DIFFERENT SHAPE PROCESSINGS

T. Bulín, E. Švábenská, M. Hapla, Č. Ondrůšek and O. Schneeweiss

P9 APPLICATIONS AND OTHER MAGNETIC MATERIALS NOT INCLUDED IN 1-8

P9-01 MAGNETIC AND MÖSSBAUER STUDY OF A CERIUM-BASED REACTIVE SORBENT

Y. Jiraskova, J. Bursik, O. Zivotsky, J. Lunacek and P. Janos

P9-02 ANALYSIS OF STRUCTURE TRANSFORMATIONS IN RAIL SURFACE INDUCED BY PLASTIC DEFORMATION VIA BARKHAUSEN NOISE EMISSION

M. Neslušan, K. Zgutová, K. Kolařík and J. Šramka

P9-03 MÖSSBAUER STUDY OF CHANGES IN OLIVINE AFTER TREATMENTS IN AIR

M. Kądziołka-Gaweł and Z. Adamczyk

P9-04 HIGH SENSITIVITY CURRENT TRANSDUCER BASED ON FLUXGATE SENSOR WITH ULTRALOW COERCIVITY CORE

P. Frydrych, M. Nowicki and R. Szewczyk

P9-05 BSA EFFECT ON CONTRAST PROPERTIES OF MAGNETITE NANOPARTICLES DURING MRI

O. Strbak, M. Kubovcikova, L. Baciak, I. Khmara, D. Gogola, M. Koneracka, V. Zavisova, I. Antal, M. Masarova, P. Kopcansky and I. Frollo

P9-06 THE EFFECT OF CRYO-ROLLING AND ANNEALING ON MAGNETIC PROPERTIES IN NON-ORIENTED ELECTRICAL STEEL

T. Kvačkaj, P. Bella, R. Bidulský, R. Kočiško, P. Petroušek, A. Fedoriková, J. Bidulská, P. Jandačka, M. Lupták1 and M. Černík

P9-07 COMPARISON OF IRON OXIDES-RELATED MRI ARTIFACTS IN HEALTHY AND NEUROPATHOLOGICAL HUMAN BRAIN TISSUE

M. Masarova, A. Krafcik, M. Teplan, O. Strbak, D. Gogola, P. Boruta and I. Frollo

- P9-08 THALES - THREE-AXIS LOW ENERGY NEUTRON SPECTROSCOPY AT THE INSTITUT LAUE-LANGEVIN**
M. Klicpera, M. Boehm, S. Roux, J. Kulda, V. Sechovský, P. Svoboda, J. Saroun and P. Steffens
- P9-09 THERMAL EXPANSION MEASUREMENT METHODS**
P. Proschek, P. Opletal, A. Bartha, J. Valenta, J. Prokleška and V. Sechovský
- P9-10 EFFECT OF STOCHASTIC DYNAMICS ON THE NUCLEAR MAGNETIC RESONANCE IN A FIELD GRADIENT**
J. Tóthová and V. Lisý
- P9-11 THE INFLUENCE OF ANNEALING TEMPERATURE ON THE MAGNETIC PROPERTIES OF CRYO-ROLLED NON-ORIENTED ELECTRICAL STEEL**
T. Kvačkaj, P. Bella, R. Bidulský, R. Kočiško, A. Fedoriková, P. Petroušek, J. Bidulská, P. Jandačka, M. Lupták, L. Gembalová and M. Černík
- P9-12 THE EFFECT OF RESIDUAL STRESSES ON THE COERCIVE FIELD STRENGTH OF DRAWN WIRES**
M. Suliga, R. Kruzel, K. Chwastek, A. Jakubas and P. Pawlik
- P9-13 MAGNETIC AURA MEASUREMENT IN DIAGNOSTICS AND CONTROL OF A SMALL TURBOJET ENGINE**
R. Andoga and L. Főző
- P9-14 MECHANOCHEMICAL PREPARATION AND MAGNETIC PROPERTIES OF $\text{Fe}_3\text{O}_4/\text{ZnS}$ NANOCOMPOSITE**
Z. Bujňáková, A. Zorkovská and J. Kováč
- P9-15 ESTIMATION OF MULTICHANNEL MAGNETOMETER NOISE FLOOR IN ORDINARY LABORATORY CONDITIONS**
D. Praslička, P. Lipovský, J. Hudák and M. Šmelko
- P9-16 NON-STATIONARY NOISE ANALYSIS OF MAGNETIC SENSORS USING ALLAN VARIANCE**
K. Draganová, V. Moucha, T. Volčko and K. Semrád
- P9-17 CALIBRATION OF MAGNETOMETER FOR SMALL SATELLITES USING NEURAL NETWORK**
T. Kliment, D. Praslička, P. Lipovský, K. Draganová and O. Závodský
- P9-18 BARKHAUSEN NOISE INVESTIGATIONS OF 5.5 MM WIRE RODS WITH VARIOUS CARBON CONTENT**
M. Suliga and T. Garstka
- P9-19 SUPERCONDUCTIVITY AND QUANTUM CRITICALITY IN $\text{Cr}_{100-z}\text{Os}_z$**
P. R. Fernando, C. J. Sheppard and A. R. E. Prinsloo

- P9-20 MAGNETIC PROPERTIES OF $\text{Sc}_{1-x}\text{Ti}_x\text{Fe}_2$ UNDER HIGH PRESSURE**
Z. Arnold, M. Mišek, O. Isnard, J. Kaštil and J. Kamarád
- P9-21 INFLUENCE OF MAGNETIC SHIELD ON THE HIGH FREQUENCY ELECTROMAGNETIC FIELD PENETRATION THROUGH THE BUILDING MATERIAL**
I. Kolcunová, M. Pavlík, J. Zbojovský, S. Ilenin, Z. Čonka, M. Kanálik, D. Medved', A. Mészáros, Ľ. Beňa and M. Kolcun
- P9-22 ADDITIONAL MODIFICATION OF THERMOMAGNETIC PROPERTIES OF OBJECTS OF LOW RELATIVE PERMEABILITY IN ELECTROMAGNETIC FIELD**
D. Medved', M. Pavlík, J. Zbojovský, S. Ilenin, Z. Čonka, M. Kanálik, I. Kolcunová, A. Mészáros, Ľ. Beňa and M. Kolcun
- P9-23 ELECTRO-RHEOLOGICAL PROPERTIES OF TRANSFORMER OIL-BASED MAGNETIC FLUIDS**
K. Paulovičová, J. Tóthová, M. Rajňák, M. Timko, P. Kopčanský and V. Lisý
- P9-24 SOLID STATE ^{13}C NUCLEAR MAGNETIC RESONANCE STUDY OF MORPHOLOGY AND MOLECULAR MOBILITY OF POLYHYDROXYBUTYRATE**
A. Baran, P. Vrábel and D. Olčák
- P9-25 OPTIMIZED FREQUENCY SELECTIVE SURFACE FOR THE DESIGN OF MAGNETIC TYPE THIN BROADBAND RADIO ABSORBERS**
V. Babayan, N. E. Kazantseva, Yu. N. Kazantsev, J. Vilčáková and R. Moučka
- P9-26 APPLICATIONS OF BISTABLE MAGNETIC MICROWIRES**
R. Sabol, P. Klein, T. Ryba, R. Varga, M. Rovnak, I. Sulla, D. Mudronova, J. Gálik, I. Poláček and R. Hudak
- P9-27 KINETICS OF SOLID STATE SYNTHESIS OF QUATERNARY $\text{Cu}_2\text{FeSnS}_4$ (STANNITE) NANOCRYSTALS FOR SOLAR ENERGY APPLICATIONS**
P. Baláž, A. Zorkovská, I. Škorvánek, M. Baláž, E. Dutková, Z. Bujňáková, J. Trajić and J. Briančin
- P9-28 MECHANOCHEMICAL SYNTHESIS AND CHARACTERIZATION OF TERNARY CuFeS_2 and CuFeSe_2 NANOPARTICLES**
E. Dutková, I. Škorvánek, M. J. Sayagués, A. Zorkovská, J. Kováč and J. Kováč Jr.

- P9-29 ELIMINATION OF MAGNETIC NANOPARTICLES WITH VARIOUS SURFACE MODIFICATIONS FROM THE BLOODSTREAM IN VIVO**
I. Khmara, V. Zavisova, M. Koneracka, N. Tomasovicova, M. Kubovcikova, J. Kovac, M. Muckova and P. Kopcansky
- P9-30 DYNAMICS OF ^1H - ^{13}C CROSS POLARIZATION IN NUCLEAR MAGNETIC RESONANCE OF POLYHYDROXYBUTYRATE**
M. Kovaľaková, O. Fričová, M. Hutníková, V. Hronský and D. Olčák
- P9-31 MECHANOCHEMICAL REDUCTION OF CHALCOPYRITE CuFeS_2 : CHANGES IN COMPOSITION AND MAGNETIC PROPERTIES**
P. Baláž, A. Zorkovská, J. Kováč, M. Tešínský, M. Baláž, T. Osserov, G. Guseynova and T. Ketegenov
- P9-32 UTILIZATION OF EDDY CURRENT TOMOGRAPHY IN AUTOMOTIVE INDUSTRY**
P. Nowak, M. Nowicki, A. Juś and R. Szewczyk
- P9-33 MÖSSBAUER SPECTROSCOPY STUDY OF LABORATORY PRODUCED ODS STEELS**
J. Degmová, J. Dekan, J. Simeg Veterníková and V. Slugeň
- P9-34 DUAL-CONTROLLED PHOTSENSITIVE MESOPOROUS SILICA-COATED MAGNETITE NANOPARTICLES**
E. Beňová, O. Kapusta, A. Zeleňáková and V. Zeleňák
- P9-35 ISOLATED DC AND AC CURRENT AMPLIFIER WITH MAGNETIC FIELD SENSOR IN LOOP AND AMORPHOUS RING CORE**
O. Petruk, M. Kachniarz and R. Szewczyk
- P9-36 NOVEL METHOD OF OFFSET VOLTAGE MINIMIZATION IN HALL-EFFECT SENSOR**
O. Petruk, M. Kachniarz and R. Szewczyk
- P9-37 AIR-GAP TOROIDAL MAGNETIC MICRO-FORCE SENSOR**
M. Nowicki, M. Kachniarz, A. Juś, T. Charubin and R. Szewczyk
- P9-38 NANOCRYSTALLINE MAGNETIC GLASS-COATED MICROWIRES USABLE AS TEMPERATURE SENSORS IN BIOMEDICAL APPLICATIONS**
R. Hudak, I. Polacek, P. Klein, R. Varga, R. Sabol and J. Zivcak
- P9-39 INFLUENCE OF TEMPERATURE ON MAGNETOSTRICTIVE DELAY LINE PROPERTIES**
J. Salach and D. Jackiewicz
- P9-40 IMPLEMENTATION OF CONDUCTANCE TOMOGRAPHY IN DETECTION OF THE HALL SENSORS INHOMOGENEITY**
O. Petruk, P. Nowak and R. Szewczyk

- P9-41 MODELLING THE INFLUENCE OF STRESSES ON MAGNETIC CHARACTERISTICS OF THE ELEMENTS OF THE TRUSS USING EXTENDED JILES-ATHERTON MODEL**
D. Jackiewicz and R. Szewczyk

POSTERS - WEDNESDAY, JUNE 15

P2 AMORPHOUS, NANOCRYSTALLINE AND OTHER SOFT MAGNETIC MATERIALS

- P2-01 BOSON PEAK AND RELAXATION PHENOMENA IN $\text{Zn}(\text{PO}_3)_2\text{Er}(\text{PO}_3)_3$ PHOSPHATE GLASS**
M. Orendáč, K. Tibenská, E. Čížmár, V. Tkáč, A. Orendáčová, E. Černošková, J. Holubová and Z. Černošek
- P2-02 THE COMPARISON HARDNESS AND COERCIVITY EVOLUTION IN VARIOUS $\text{Fe}(\text{TM})$ BASED GLASSES (INCLUDING FINEMET PRECURSOR) DURING RELAXATION AND CRYSTALLIZATION**
Z. Weltsch, K. Kittl and A. Lovas
- P2-03 THE CHANGES IN MAGNETIC AND MECHANICAL PROPERTIES OF FINEMET - TYPE ALLOYS DURING ISOTHERMAL, AND PULSE HEAT TREATMENTS**
L. Hubač, L. Novák and A. Lovas
- P2-04 DC MAGNETIC PROPERTIES OF AMORPHOUS VITROVAC RIBBON**
P. Kollár, Z. Birčáková, J. Füzer and M. Kuźmiński
- P2-05 ANALYSIS OF THE THERMAL AND MAGNETIC PROPERTIES OF AMORPHOUS $\text{Fe}_{61}\text{Co}_{10}\text{B}_{20}\text{Y}_8\text{Me}_1$ (WHERE $\text{Me} = \text{W}, \text{Zr}, \text{Nb}, \text{Mo}$) RIBBONS**
P. Pietrusiewicz and M. Nabiałek
- P2-06 EFFECT OF CURRENT ANNEALING ON DOMAIN STRUCTURE IN AMORPHOUS AND NANOCRYSTALLINE FeCoMoB MICROWIRES**
P. Klein, R. Varga, G. A. Badini-Confalonieri and M. Vazquez
- P2-07 INVESTIGATION OF MAGNETIZATION PROCESSES FROM THE ENERGY LOSSES IN SOFT MAGNETIC COMPOSITE MATERIALS**
Z. Birčáková, P. Kollár, B. Weidenfeller, J. Füzer, R. Bureš and M. Fáberová

- P2-08 HIGH-FREQUENCY ABSORBING PERFORMANCES OF CARBONYL IRON/MnZn FERRITE/PVC POLYMER COMPOSITES**
R. Dosoudil and M. Ušáková
- P2-09 MICROSTRUCTURAL AND MAGNETIC CHARACTERISTICS OF DIVALENT Zn, Cu AND Co DOPED Ni FERRITES**
M. Šoka, R. Dosoudil and M. Ušáková
- P2-10 NICKEL/ZINC RATIO AND LANTHANUM SUBSTITUTION EFFECT ON STRUCTURAL AND MAGNETIC PROPERTIES OF NICKEL ZINC FERRITES**
V. Jančárik, M. Šoka, M. Ušáková and R. Hartánský
- P2-11 THE ROLE OF TEMPERATURE ON THE MAGNETIZATION PROCESS IN CoFeZrB/FeCuNbMoSiB HYBRID FERROMAGNETS**
S. Dobák, J. Füzer and P. Kollár
- P2-12 MAGNETIC PROPERTIES OF AMORPHOUS GEHLENITE GLASS MICROSPHERES**
M. Majerová, A. Dvurečenskij, A. Cigáň, M. Škrátek, A. Prnová, J. Kraxner, D. Galusek and J. Maňka
- P2-13 THERMOPOWER CHARACTERIZATION OF STRUCTURAL RELAXATION AND CRYSTALLIZATION IN FINEMET TYPE AMORPHOUS PRECURSOR ALLOY**
K. Bán, A. Szabó, R. Ipach and B. Szabó
- P2-14 COMPLEX MAGNETOIMPEDANCE IN JOULE HEATED $\text{Co}_{71.1}\text{Fe}_{3.9}\text{Si}_{10}\text{B}_{15}$ MICROWIRES**
E. Komova, P. Klein, R. Varga and J. Kozár
- P2-15 MAGNETIC PROPERTIES OF NANOCRYSTALLINE ALLOYS AFTER ELECTRONS IRRADIATION**
J. Sitek, D. Holková, J. Dekan and P. Novák
- P2-16 ACCENTS IN MODERN HIGH SATURATION NANOCRYSTALLINE Fe-RICH ALLOYS**
B. Butvinová, P. Butvin, I. Mat'ko, D. Janičkovič, M. Kuzminski, A. Slawska-Waniewska, P. Švec Sr. and M. Chromčíková
- P2-17 IMAGING OF MAGNETIC DOMAIN STRUCTURE IN $\text{FeSi/Mn}_{0.8}\text{Zn}_{0.2}\text{Fe}_2\text{O}_4$ COMPOSITE USING MAGNETIC FORCE MICROSCOPY**
M. Streckova, I. Batko, M. Batkova, R. Bures, M. Faberova, H. Hadraba and I. Kubena
- P2-18 EFFECTS OF COBALT ADDITION ON MAGNETIC PROPERTIES IN Fe-Co-Si-B-P-Cu ALLOYS**
M. Kuhnt, M. Marsilius, T. Strache, K. Durst, C. Polak and G. Herzer

- P2-19 MAGNETIC PROPERTIES OF $\text{Ni}_{0.3}\text{Zn}_{0.7}\text{Fe}_2\text{O}_4$ FERRITES WITH Fe IONS PARTLY SUBSTITUTED BY Eu**
E. Ušák, M. Ušáková, M. Šoka and D. Vašut
- P2-20 STRUCTURAL RELAXATIONS IN THE AMORPHOUS FeMeMoCrNbB (Me = Ni OR CO) ALLOYS**
J. Rzącki and K. Błoch
- P2-21 THE STRUCTURE AND POROSITY OF $\text{Fe}_{62-x}\text{Co}_{10}\text{W}_y\text{Me}_x\text{Y}_8\text{B}_{20-y}$ (WHERE Me = Mo, Nb; $x = 0, 1, 2$; $y = 0, 1, 2$) ALLOYS IN THE AMORPHOUS AND CRYSTALLINE STATE**
J. Gondro, S. Garus, M. Nabiałek, J. Garus and P. Pietrusiewicz
- P2-22 STRUCTURAL RELAXATIONS IN THE MASSIVE ALLOYS $\text{Fe}_{60}\text{Co}_{10}\text{W}_x\text{Mo}_2\text{Y}_8\text{B}_{20-x}$ (X = 0, 1, 2)**
K. Błoch, S. Garus, M. Nabiałek and J. Garus
- P2-23 THE STUDY OF MAGNETIZATION IN STRONG MAGNETIC FIELDS FOR $\text{Fe}_{62-x}\text{Co}_{10}\text{Nb}_x\text{Y}_8\text{B}_{20}$ (X = 0, 1, 2) ALLOYS**
M. Szota, S. Garus, J. Garus, K. Gruszka and K. Błoch
- P2-24 COMPARISON OF MAGNETIC PROPERTIES OF AMORPHOUS AND CRYSTALLINE $\text{Fe}_{60}\text{Co}_{10}\text{W}_2\text{Nb}_2\text{Y}_8\text{B}_{18}$ ALLOY**
S. Garus, M. Nabiałek, J. Garus and J. Gondro
- P2-25 MEASUREMENTS OF MAGNETIC PROPERTIES OF POLYMER-METALLIC COMPOSITES**
A. Jakubas, P. Gębara, A. Gnatowski and K. Chwastek
- P2-26 THE INFLUENCE OF TEMPERATURE ON UNIDIRECTIONAL EFFECT IN DOMAIN WALL PROPAGATION**
J. Onufer, J. Ziman, M. Rezníček and S. Kardoš
- P2-27 STRUCTURE AND MAGNETIC PROPERTIES OF Fe-B-Si-Zr METALLIC GLASSES**
R. Babilas, A. Radoń and P. Gębara
- P2-28 STRUCTURE AND COERCIVITY OF AMORPHOUS RAPIDLY QUENCHED FeCrB ALLOY**
J. Kecer and L. Novák
- P2-29 MAGNETIC PROPERTIES OF $\text{Ni}_{0.2}\text{Zn}_{0.8}\text{Fe}_2\text{O}_4$ FERRITE FIBERS PREPARED BY NEEDLE-LESS ELECTROSPINNING TECHNIQUES**
M. Streckova, E. Mudra, M. Sebek, T. Sopcak, J. Kovac and J. Duzsa
- P2-30 STUDY OF THE MAGNETIZATION PROCESSES IN AMORPHOUS AND NANOCRYSTALLINE FINEMET BY THE NUMERICAL DECOMPOSITION OF THE HYSTERESIS LOOPS**
J. Kováč and L. Novák

- P2-31 MESOPOROUS SILICA SBA-15 FUNCTIONALIZED BY NICKEL-PHOSPHONIC UNITS STUDIED BY RAMAN AND SQUID MAGNETOMETRY**
M. Laskowska and L. Laskowski
- P2-32 MAGNETIC AND STRUCTURAL CHARACTERIZATION OF NICKEL AND IRON BASED HEUSLER RIBBON Ni_2FeZ ($\text{Z} = \text{In}, \text{Sn}, \text{Sb}$)**
L. Bujnakova, T. Ryba, Z. Vargova, V. Komanicky, J. Kovac, R. Gyepes and R. Varga
- P2-33 XAFS SIGNALS MEASURED ON POLYCRYSTALLINE Fe AND $\text{Zr}_{60}\text{Cu}_{20}\text{Fe}_{20}$ ALLOY IN TRANSMISSION AND TOTAL ELECTRON YIELD MODE**
K. Saksl, S. Michalik, O. Milkovič, J. Gamcová, V. Girman and D. Balga
- P2-34 STRUCTURAL AND THERMOMAGNETIC PROPERTIES OF $\text{Fe}_{86-x}\text{Zr}_7\text{M}_x\text{Nb}_2\text{Cu}_1\text{B}_4$ { $\text{M}=\text{Co}, \text{Ni}, (\text{CoCr})$; $x=0$ OR 6} ALLOYS**
A. Łukiewska
- P2-35 THE CORRELATION OF MAGNETIC AND STRUCTURAL PROPERTIES OF Ni-Ti-Zr BULK METALLIC GLASS AT ELEVATED TEMPERATURES**
M. Lisnichuk, J. Katuna, K. Saksl, V. Girman, J. Gamcová, D. Balga, M. Ďurišin, J. Kováč and P. Sovák
- P2-36 TEMPERATURE EVOLUTION OF HYPERFINE MAGNETIC FIELDS ON 57-Fe IN A Fe-Co-Si-B-Mo-P METALLIC GLASS**
M. Cesnek, M. Miglierini, T. Kmječ, J. Kohout, N. Amini and D. Janičkovič
- P2-37 STRUCTURE AND MAGNETIC PROPERTIES OF IRON/IRON-OXIDE NANOPARTICLES PREPARED BY PRECIPITATION FROM SOLID STATE SOLUTION**
O. Milkovič, M. Sopko, J. Gamcová and I. Škorvánek
- P2-38 THE STRUCTURAL CHARACTERIZATION OF Ni-Ti-Zr BULK METALLIC GLASS USING TRANSMISSION AND SCANNING ELECTRON MICROSCOPY**
J. Katuna, M. Lisnichuk, K. Saksl, V. Girman, J. Gamcová, D. Balga, M. Ďurišin, J. Kováč and P. Sovák
- P2-39 THE INFLUENCE OF PULSE HEATING ON THE RAYLEIGH REGION IN AMORPHOUS FINEMET ALLOY**
L. Novák, J. Kováč and L. Hubač
- P2-40 EFFECT OF THICKNESS OF ELECTROPLATED NiFe CORES ON THE NOISE OF FLUXGATES**
M. Butta

- P2-41 INFLUENCE OF Co DOPING ON INDUCED ANISOTROPY AND DOMAIN STRUCTURE IN MAGNETIC FIELD ANNEALED $(\text{Fe}_{1-x}\text{Co}_x)_{79}\text{Mo}_8\text{Cu}_1\text{B}_{12}$ ALLOY**
B. Kunca, J. Marcin, P. Švec, J. Kováč, P. Švec Sr. and I. Škorvánek
- P2-42 FORMATION AND MOTION OF DOMAIN WALLS IN RAPIDLY SOLIDIFIED AMORPHOUS MAGNETIC NANOWIRES**
M. Tibu, M. Lostun, D. A. Allwood, H. Chiriac, N. Lupu and T.-A. Óvári
- P2-43 HOPKINSON EFFECT IN SOFT AND HARD MAGNETIC FERRITES**
J. Sláma, M. Ušáková, M. Šoka, R. Dosoudil and V. Jančárik
- P2-44 INFLUENCE OF VITROVAC CONTENT ON MAGNETIC PROPERTIES IN COMPOSITE MATERIALS BASED ON THE MIXTURE OF TWO FERROMAGNETS**
L. Hegedűs, P. Kollár, J. Füzer, R. Bureš, M. Fáberová and P. Kurek
- P2-45 MAGNETIC PROPERTIES OF Fe-BASED SOFT METALLIC ALLOY AFTER ION IRRADIATION**
M. Hasiak and M. Miglierini
- P2-46 FeSiBAlNiMo HIGH ENTROPY ALLOY PREPARED BY MECHANICAL ALLOYING**
R. Bureš, H. Hadraba, M. Fáberová, P. Kollár, J. Füzer, P. Roupcová and M. Strečková
- P2-47 EFFECT OF SAMPLE THICKNESS ON GMI BEHAVIOR OF AMORPHOUS $(\text{Fe}_{1-x}\text{Ni}_x)_{73}\text{Nb}_7\text{B}_{20}$ RIBBONS**
F. Andrejka, J. Marcin, D. Janičkovič, P. Švec and I. Škorvánek
- P2-48 EVIDENCE OF GRIFFITHS LIKE PHASE IN NANOCRYSTALLINE MANGANITE $\text{La}_{0.85}\text{Ca}_{0.15}\text{MnO}_3$**
M. Pękała, J. Szydłowska, K. Pękała and V. Drozd
- P2-49 EFFECT OF LASER SCRIBING ON THE MAGNETIC PROPERTIES OF CONVENTIONAL GO SILICON STEEL**
I. Petryshynets, V. Puchý, F. Kováč and M. Šebek
- P2-50 MICROWAVE SINTERED Fe/MgO SOFT MAGNETIC COMPOSITE**
M. Fáberová, R. Bureš, P. Kollár, J. Füzer, S. Dobák, F. Onderko, M. Strečková and P. Kurek
- P2-51 IMPROVEMENT OF MAGNETIC PROPERTIES AND CRYSTALLOGRAPHIC TEXTURE OF Fe-Si STEELS BY THERMAL PROCESSING IN HIGH MAGNETIC FIELD**
F. Kováč, I. Petryshynets, J. Marcin and I. Škorvánek

P4

MAGNETIC THIN FILMS AND SURFACES, SPINTRONICS, PARTICLES AND NANOSTRUCTURES

- P4-01 MAGNETISM AND STRUCTURE EVOLUTION IN Ni-Zn FERRITES THIN FILMS – CEMS STUDY**
T. Szumiata, M. Gzik-Szumiata, K. Brzózka, B. Górka, M. Gawroński, A. Javed, K. Farman and T. Fatima
- P4-02 EXACT DIAGONALIZATION-BASED CALCULATIONS OF INDIRECT MAGNETIC COUPLING IN GRAPHENE NANOSTRUCTURES**
K. Szałowski
- P4-03 GROWTH OF Pt-Ni NANOPARTICLES OF DIFFERENT COMPOSITION USING ELECTRODEPOSITION AND CHARACTERIZATION OF THEIR MAGNETIC PROPERTIES**
M. Kozejová, D. Hložná, Y. Hua Liu, K. Ráczová, E. Čižmár, M. Orendáč and V. Komanický
- P4-04 LSMO/YBCO HETEROSTRUCTURES AND INVESTIGATION OF “NEGATIVE” RESISTANCE EFFECT IN THE INTERFACE**
M. Sojková, T. Nurgaliev, V. Štrbík, Š. Chromik, B. Blagoev and M. Španková
- P4-05 GENERALIZATION OF MAGNETOSTATIC METHOD OF MOMENTS FOR THIN LAYERS WITH REGULAR RECTANGULAR GRIDS**
R. Szewczyk
- P4-06 SPECTROSCOPIC PROPERTIES OF SBA-15 MESOPOROUS SILICA FREE-STANDING THIN FILMS ACTIVATED BY COPPER IONS**
L. Laskowski and M. Laskowska
- P4-07 TRANSPORT AND MAGNETIC PROPERTIES OF SUPERCONDUCTOR-FERROMAGNET-SUPERCONDUCTOR NANOJUNCTIONS**
N. Gál, V. Štrbík, Š. Beňačka, Š. Gaži, M. Španková, Š. Chromik, M. Sojková and M. Pisarčík
- P4-08 HIGH RESOLUTION X-RAY CHARACTERIZATION OF MANGANITE FILMS GROWN ON VARIOUS SUBSTRATES**
M. Španková, V. Štrbík, E. Dobročka, Š. Chromik, N. Gál and M. Sojková
- P4-09 LOW-TEMPERATURE PROPERTIES OF ONE-DIMENSIONAL MAGNETO-PHOTONIC CRYSTALS IN MAGNETIC FIELD**
Yu. Kharchenko, I. Lukienko, O. Miloslavskaya, M. F. Kharchenko, A. V. Karavainikov, A. R. Prokopov and A. N. Shaposhnikov

- P4-10 MAGNETIC PROPERTIES OF NICKEL HEXACYANOFERRATE/CHROMATE THIN FILMS**
M. Fitta, T. Korzeniak, P. Czaja and M. Bałanda
- P4-11 Ni_2FeSi HEUSLER MICROWIRES FOR SPINTRONIC APPLICATIONS**
L. Galdun, T. Ryba, V. M. Prida, B. Hernando, V. Zhukova, A. Zhukov, Z. Vargová and R. Varga
- P4-12 SPIN WAVE CHARACTERISTICS OF INHOMOGENEOUS FERROMAGNETIC LAYERED COMPOSITES**
A. Urbaniak-Kucharczyk
- P4-13 MAGNETIC AND STRUCTURAL CHARACTERIZATION OF NiMnSb HEUSLER RIBBON**
T. Ryba, Z. Vargová, S. Ilkovic, M. Reiffers, V. Haskova, P. Szabo, J. Kravcak, R. Gyepes and R. Varga
- P4-14 MAGNETIC PROPERTIES FE AND GD OXIDES EMBEDDED IN MESOPOROUS SILICA**
O. Kapusta, A. Zeleňáková, V. Girman, P. Hrubovčák and V. Zeleňák
- P4-15 SYSTEMATIC ANALYSIS OF ANISOTROPIC MAGNETORESISTANCE IN $(\text{Ga},\text{Mn})\text{As}$**
K. Vyborny
- P4-16 PHASE ANALYSIS OF MAGNETIC INCLUSIONS IN NANOMATERIALS BASED ON MULTIWALL CARBON NANOTUBES**
K. Brzózka, M. Krajewski, A. Małolepszy, L. Stobiński, T. Szumiata, B. Górka, M. Gawroński and D. Wasik
- P4-17 INFLUENCE OF Mn DOPING ON MAGNETIC AND STRUCTURAL PROPERTIES OF Co_2FeSi HEUSLER ALLOY**
L. Galdun, T. Ryba, V. M. Prida, B. Hernando, Z. Vargová and R. Varga
- P4-18 EXCHANGE BIAS EFFECT IN NdFeO_3 SYSTEM OF NANO PARTICLES**
M. Vavra, M. Zentková, M. Mihalik, M. Mihalik jr., J. Lazúrová, V. Girman, M. Perovic, V. Kusigerski, P. Roupčova and Z. Jaglicic
- P4-19 SUPERSPIN GLASS STATE IN MAGNETIC NANOPARTICLES**
A. Zeleňáková, P. Hrubovčák and V. Zeleňák
- P4-20 THE INVESTIGATION OF SPIN-SEEBECK EFFECT IN Ni_xFe_y ALLOYS**
Ł. Bernacki, R. Gozdur and W. Pawlak

P4-21 EFFECT OF THE JAHN TELLER DISTORTION ON DOUBLE EXCHANGE INTERACTION IN $\text{La}_{1-x}\text{K}_x\text{MnO}_3$ NANO PARTICLES

M. Mihalik, M. Zentková, M. Vavra, M. Mihalik Jr., J. Lazúrová, V. Girman, M. Fitta and S. Il'kovič

P4-22 THE MAGNETIC EQUATION OF STATE AND TRANSPORT PROPERTIES IN REDUCED DIMENSIONS

K. Warda and L. Wojtczak

P4-23 THE ELECTRICAL RESISTIVITY OF METALLIC ALLOYS

K. Warda and L. Wojtczak

P4-24 STRUCTURE OF MELT-SPUN Co_2MnAl HEUSLER ALLOY

S. Piovarči, P. Diko, V. Kavečanský, T. Ryba, Z. Vargová and R. Varga

P8 MULTIFUNCTIONAL MAGNETIC MATERIALS (MULTIFERROIC, MAGNETOELASTIC, SHAPE MEMORY, ...)

P8-01 SPIN DISORDER RESISTIVITY OF THE HEUSLER Ni_2MnGa -BASED ALLOYS

J. Kamarád, J. Kaštil, F. Albertini, S. Fabbrici and Z. Arnold

P8-02 MAGNETIC CHARACTERIZATION OF MELT-SPUN CoNiGa FERROMAGNETIC SUPERELASTIC ALLOY

J. Mino, M. Ipatov, J. Gamcova, V. Zhukova, Z. Vargova, A. Zhukov and R. Varga

P8-03 MAGNETO-CRYSTALLINE ANISOTROPY OF $\text{NdFe}_{x-1}\text{Mn}_x\text{O}_3$ SINGLE CRYSTALS

M. Mihalik, M. Mihalik jr., M. Zentková, J. Lazúrová, K. Uhlířová and M. Kratochvílová

P8-04 TUNING OF MAGNETISM IN $\text{DyFe}_{x-1}\text{Mn}_x\text{O}_3$ SINGLE CRYSTALS BY IRON SUBSTITUTION

M. Zentková, M. Mihalik, M. Mihalik Jr., J. Lazúrová, K. Uhlířová, M. Kratochvílová, M. K. Peprah and M. W. Meisel

P8-05 IDENTIFICATION OF MAGNETIC PHASES IN HIGHLY CORROSION-RESISTANT STEEL BY MÖSSBAUER SPECTROMETRY

L. Pašteka, M. Miglierini and M. Bujdoš

P8-06 SUPERPARAMAGNETIC BEHAVIOUR OF IRON IN BIOLOGICAL TISSUES STUDIED BY MÖSSBAUER SPECTROMETRY

I. Bonková, M. Miglierini, M. Bujdoš and M. Kopáni

P8-07 ASSESMENT OF THE MAGNETOSTRICTIVE PROPERTIES OF THE SELECTED CONSTRUCTION STEELS

A. Juš, P. Nowak and R. Szewczyk

P8-08 MAGNETIC SUSCEPTIBILITY OF MULTIFERROIC PEROVSKITES

M. Maryško, V. V. Laguta, P. Novák and I. P. Raevski

POSTERS - THURSDAY, JUNE 16

P5

LOW-DIMENSIONAL MAGNETIC MATERIALS, MOLECULAR MAGNETS AND FERROFLUIDS

P5-01 MAGNETIC-FIELD INDUCED SLOW RELAXATION IN THE ISING-LIKE QUASI-ONE-DIMENSIONAL FERROMAGNET $\text{Ker}(\text{MoO}_4)_2$

V. Tkáč, A. Orendáčová, Ľ. Dlháň, M. Orendáč, R. Boča and A. Feher

P5-02 INFLUENCE OF PRESSURE ON THE MAGNETIC RESPONSE OF THE LOW-DIMENSIONAL QUANTUM MAGNET $\text{Cu}(\text{H}_2\text{O})_2(\text{C}_2\text{H}_8\text{N}_2)\text{SO}_4$

M. K. Peprah, D. VanGennep, B. D. Blasiola, P. A. Quintero, R. Tarasenko, J. J. Hamlin, M. W. Meisel and A. Orendáčová

P5-03 EXPERIMENTAL STUDY OF THE MAGNETOCALORIC EFFECT IN $\text{Ni}(\text{en})(\text{H}_2\text{O})_4\text{SO}_4 \cdot 2\text{H}_2\text{O}$ - an $S = 1$ MOLECULAR MAGNET WITH EASY-PLANE ANISOTROPY

R. Tarasenko, A. Orendáčová, E. Čižmár, M. Orendáč, I. Potočník and A. Feher

P5-04 GENERATION OF Fe_3O_4 NANOPARTICLE AGGREGATES IN A FERROFLUID DRIVEN BY EXTERNAL ELECTRIC FIELD

J. Kurimský, M. Rajňák, R. Cimbala, K. Paulovičová, M. Timko, P. Kopčanský, M. Kostelec, L. Kruželák and M. Kolcun

P5-05 ULTRASOUND FREQUENCY ANALYSIS OF A MAGNETIC FLUID IN LOW-INTENSITY EXTERNAL MAGNETIC FIELD

J. Kurimský, M. Rajňák, R. Cimbala, B. Dolník, J. Tóthová, K. Paulovičová, M. Timko, P. Kopčanský, J. Petráš, I. Kolcunová, J. Džmura and J. Balogh

P5-06 STRUCTURAL CHANGES IN LIQUID CRYSTALS WITH ROD-LIKE MAGNETIC PARTICLES STUDIED BY SURFACE ACOUSTIC WAVES

P. Bury, J. Kúdelčík, M. Veverčík, P. Kopčanský, M. Timko and V. Závistová

- P5-07 THE SPIN-1 J1-J3 HEISENBERG MODEL ON A TRIANGULAR LATTICE: EXACT DIAGONALIZATION STUDY**
P. Rubin and A. Sherman
- P5-08 GROUND STATE SPIN OF HUBBARD LADDER MODELS WITH INFINITE ELECTRON REPULSION**
V. O. Cheranovskii, E. V. Ezerskaya, D. J. Klein and V. V. Tokarev
- P5-09 STUDY OF STRUCTURAL CHANGES OF WATER-BASED MAGNETIC-FLUID BY ACOUSTIC SPECTROSCOPY**
J. Kúdelčík, Š. Hardoň, P. Bury, M. Timko and P. Kopčanský
- P5-10 ENHANCED MAGNETOCALORIC EFFECT IN $\text{NiCl}_2(\text{bipy})$ AT LOW TEMPERATURES**
K. Ráczová, E. Čižmár and A. Feher
- P5-11 MAGNETIC HEAT CAPACITY OF ANION-RADICAL SALT $\text{Ni}(\text{bipy})_3(\text{TCNQ})_4 \cdot (\text{CH}_3)_2\text{CO}$ AT VERY LOW TEMPERATURES**
D. Šoltésová, E. Čižmár, G. Vasylets, V. Starodub and A. Feher
- P5-12 THE ENERGY SPECTRUM AND THERMODYNAMICS OF THE SPIN-1/2 XX CHAIN WITH ISING IMPURITIES**
E. V. Ezerskaya
- P5-13 MEASUREMENT OF COMPLEX PERMITTIVITY OF OIL-BASED FERROFLUID**
J. Kúdelčík, Š. Hardoň and L. Varačka
- P5-14 LOW MAGNETIC FIELD RESPONSE IN FERRONEMATICS**
V. Gdovinova, N. Tomasovicova, V. Zavisova, N. Eber, T. Toth-Katona, F. Royer, D. Jamon, J. Jadzyn and P. Kopcansky
- P5-15 ANALYSIS OF THERMAL FIELD IN MINERAL TRANSFORMER OIL BASED MAGNETIC FLUIDS**
M. Kosterec, J. Kurimský, R. Cimbala, L. Kruželák, M. Rajňák, M. Timko and P. Kopčanský
- P5-16 FRUSTRATED ZIG-ZAG SPIN CHAINS FORMED BY HYDROGEN BONDS IN COMPOUND $[\text{Cu}(\text{H}_2\text{O})(\text{OH})(\text{tmen})]_2[\text{Pd}(\text{CN})_4] \cdot 2\text{H}_2\text{O}$**
E. Čižmár, A. Orendáčová, M. Orendáč, J. Kuchár, A. Feher, J.-H. Park and M. W. Meisel
- P5-17 TEMPERATURE DEPENDENCE OF A DIELECTRIC RELAXATION IN WEAKLY POLAR FERROFLUIDS**
M. Rajňák, J. Kurimský, B. Dolník, R. Cimbala, K. Paulovičová, P. Kopčanský and M. Timko
- P5-18 THE RESPONSE OF A MAGNETIC FLUID TO RADIO FREQUENCY ELECTROMAGNETIC FIELD**
B. Dolník, M. Rajňák, R. Cimbala, I. Kolcunová, J. Kurimský, J. Balogh, J. Džmura, J. Petráš, P. Kopčanský, M. Timko, J. Briančin and M. Fabián

P5-19 KINETICS OF NEMATIC TO ISOTROPIC PHASE TRANSITION IN LIQUID CRYSTAL DOPED WITH MAGNETIC NANOPARTICLES

K. Csach, A. Juríková, J. Miškuf, N. Tomašovičová, V. Gdovinová, V. Závišová, P. Kopčanský, N. Éber, K. Fodor-Csorba and A. Vajda

P5-20 CHARACTERIZATION OF CARBON NANOTUBES

M. Jeníková, K. Zakuťanská, J. Kováč, V. Girman, P. Kopčanský and N. Tomašovičová

P5-21 THE INFLUENCE OF MAGNETIC PARTICLES AND MAGNETIC FIELD ON THE SHAPE OF DROPLETS OF LIQUID CRYSTAL

J. Majorošová, V. Gdovinová, N. Tomašovičová, A. Juríková, V. Závišová, J. Jadzyn and P. Kopčanský

P5-22 THERMAL CONDUCTIVITY OF LOW-DIMENSIONAL MAGNETIC SYSTEMS

D. Legut, D. U. Wdowik and A. Orendáčová

P5-23 AFM STUDIES OF INTERACTION OF MAGNETIC NANOPARTICLES WITH LYOTROPIC LIQUID CRYSTAL

N. Tomašovičová, L. Balejíčková, V. Gdovinová, M. Kubovčíková, C.-W. Yang, I.-S. Hwang, S. Hayryan, C.-K. Hu and P. Kopčanský

P5-24 THE LOW AND HIGH SPIN GROUND STATES IN NEW TETRANUCLEAR MANGANESE MOLECULES WITH $[\text{Mn}^{\text{II}}_3\text{Mn}^{\text{III}}]$ AND $[\text{Mn}^{\text{II}}_2\text{Mn}^{\text{III}}_2]$ METALLIC CORES

M. Antkowiak, M. Sobocińska, M. Wojciechowski, G. Kamieniarz, J. Utko and T. Lis

P5-25 THE STUDY OF MAGNETIC MOLECULES CONTAINING CHROMIUM-BASED RINGS WITHIN DENSITY FUNCTIONAL THEORY

B. Brzostowski, M. Wojciechowski and G. Kamieniarz

P5-26 CORRELATION BETWEEN THE STRUCTURE AND MAGNETIC SUSCEPTIBILITY OF BiOX ($\text{X}=\text{Cl}, \text{Br}, \text{I}$) SINGLE CRYSTALS

V. Bunda, S. Bunda, J. Kovac, D. Lotnyk and A. Feher

P5-27 MAGNETIC PROPERTIES OF $\text{BiOCl}:\text{Ti}$ AND $\text{BiOCl}:\text{Sm}$ SINGLE CRYSTALS

S. Bunda, V. Bunda, J. Kovac, D. Lotnyk and A. Feher

P6 RARE-EARTH AND 5f-SYSTEMS

- P6-01 THE MACROSCOPIC AND MICROSCOPIC PROPERTIES STUDY ON CeTIn COMPOUNDS, WHERE $T = \text{Ni, Pd, Pt}$**
M. Klicpera, M. Boehm and P. Javorský
- P6-02 CRYSTAL FIELD IN NdPd_5Al_2 AND ITS INFLUENCE ON MAGNETIC PROPERTIES**
J. Zubáč, M. Diviš, B. Fák and P. Javorský
- P6-03 ANOMALOUS HALL EFFECT IN $\text{Ho}_{0.5}\text{Lu}_{0.5}\text{B}_{12}$ ANTIFERROMAGNET WITH CAGE-GLASS CRYSTAL STRUCTURE**
N. E. Sluchanko, V. N. Krasnorussky, A. V. Bogach, V. V. Glushkov, S. V. Demishev, A. L. Khoroshilov, A. V. Dukhnenko, N. Yu. Shitsevalova, V. B. Filipov, S. Gabani, K. Flachbart and G. E. Grechnev
- P6-04 MAGNETIC ANISOTROPY IN ANTIFERROMAGNET GdB_6**
M. Anisimov, V. Glushkov, S. Demishev, N. Samarin, A. Bogach, A. Samarin, N. Shitsevalova, A. Levchenko, V. Filipov, S. Gabani, K. Flachbart and N. Sluchanko
- P6-05 TRANSPORT PROPERTIES OF DILUTED MAGNETIC HEXABORIDES $\text{R}_{0.01}\text{La}_{0.99}\text{B}_6$ ($R = \text{Ce, Pr, Nd, Gd, Eu, Ho}$)**
M. Anisimov, V. Glushkov, S. Demishev, N. Samarin, N. Shitsevalova, A. Levchenko, V. Filipov, A. Bogach, V. Voronov, S. Gabani, K. Flachbart and N. Sluchanko
- P6-06 ELECTRON SPIN RESONANCE IN PARAMAGNETIC AND ANTI-FERROMAGNETIC STATES OF $\text{Ho}_{0.5}\text{Lu}_{0.5}\text{B}_{12}$**
M. I. Gilmanov, A. V. Semeno, S. V. Demishev, V. V. Glushkov, A. L. Khoroshilov, V. N. Krasnorussky, N. Y. Shitsevalova, V. B. Filipov, K. Flachbart and N. E. Sluchanko
- P6-07 MAGNETORESISTANCE ANISOTROPY IN HoB_{12}**
A. Khoroshilov, V. Krasnorussky, A. Bogach, V. Glushkov, S. Demishev, A. Levchenko, N. Shitsevalova, V. Filipov, S. Gabani, K. Flachbart, K. Siemensmeyer and N. Sluchanko
- P6-08 GLASS FORMING ABILITIES AND CRYSTALLIZATION PROCESS IN AMORPHOUS Pr-Fe-Co-Zr-Nb-B ALLOYS OF VARIOUS B CONTENTS**
K. Pawlik, P. Pawlik and J. J. Wysocki
- P6-09 INFLUENCE OF PRESSURE ON THE ELECTRIC TRANSPORT PROPERTIES OF CARBON-DOPED EuB_6**
G. Pristáš, S. Gabáni, I. Baťko, M. Baťková, V. Filipov and E. Konovalova

- P6-10 PREPARATION AND BASIC PHYSICAL PROPERTIES OF YbT_2X_2 (T – Pd, Au; X – Si, Ge) COMPOUNDS**
J. Kaštil, K. Vlášková, J. Prchal, M. Míšek, J. Kamarád and Z. Arnold
- P6-11 CHARGE TRANSPORT AND MAGNETISM IN $\text{Tm}_{0.03}\text{Yb}_{0.97}\text{B}_{12}$**
V. Glushkov, A. Azarevich, M. Anisimov, A. Bogach, S. Demishev, A. Dukhnenko, V. Filipov, K. Flachbart, S. Gabáni, S. Gavrilkin, N. Shitsevalova and N. Sluchanko
- P6-12 X-RAY DIFFRACTION STUDY OF $\text{CeT}_2\text{Al}_{10}$ (T= Ru, Os) AT LOW TEMPERATURE AND UNDER PRESSURE**
Y. Kawamura, J. Hayashi, K. Takeda, C. Sekine, T. Tanida, M. Sera, S. Nakano, T. Tomita, H. Takahashi and T. Nishioka
- P6-13 SPECIFIC HEAT STUDY ON $\text{CeCu}_x\text{Al}_{4-x}$ AND $\text{Ce}_x\text{La}_{1-x}\text{CuAl}_3$ COMPOUNDS**
K. Vlášková, P. Javorský and M. Klicpera
- P6-14 VARIATIONS OF ANTIFERROMAGNETISM IN UIrGe IN MAGNETIC FIELDS AND EXTERNAL PRESSURES**
M. Vališka, J. Prchal and V. Sechovský
- P6-15 EFFECT OF SOLVENTS ON MAGNETIC PROPERTIES OF METAL-ORGANIC FRAMEWORK MOF-76(Gd)**
M. Almáši, V. Zeleňák and A. Zeleňáková
- P6-16 CHARACTERIZATION OF NEW UNiX_2 SPLATS AND STUDY OF THEIR PHYSICAL PROPERTIES**
Z. Molcanova, M. Mihalik, M. Mihalik jr., M. Paukov and L. Havela
- P6-17 MAGNETIC PROPERTIES OF A DyCo_2 CRYSTAL**
J. Prchal, V. Latoňová, M. Kratochvílová and V. Sechovský
- P6-18 EXPERIMENTAL STUDY OF PHYSICAL PROPERTIES OF NEW $\text{Gd}_{1-x}\text{Ce}_x\text{Ni}_5$ SYSTEM**
A. Džubinská, M. Reiffers, J. I. Espeso and J. Rodríguez Fernández
- P6-19 MAGNETORESISTANCE OF THE $\text{CeCo}_{1-x}\text{Fe}_x\text{Ge}_3$ ALLOYS**
P. Skokowski, K. Synoradzki and T. Toliński
- P6-20 CRYSTAL STRUCTURE AND PHYSICAL PROPERTIES OF THE NOVEL Eu COMPOUNDS**
I. Čurlík, F. Gastaldo, M. Giovannini, A. M. Strydom and M. Reiffers
- P6-21 CROSSOVER BETWEEN FERMI-LIQUID AND NON-FERMI-LIQUID IN $\text{Th}_{1-x}\text{U}_x\text{Be}_{13}$ ($0 \leq x \leq 1$)**
N. Miura, K. Uhlířová, J. Prchal, C. Tabata, V. Sechovský, H. Hidaka, T. Yanagisawa and H. Amitsuka

P6-22 HALL COEFFICIENT IN TOROIDAL MAGNETIC ORDERED STATE OF UNi_4B

H. Saito, N. Miura, C. Tabata, H. Hidaka, T. Yanagisawa and H. Amitsuka

P7 STRONGLY CORRELATED ELECTRON SYSTEMS, SUPERCONDUCTING MATERIALS

P7-01 THERMODYNAMIC PROPERTIES OF A CUBIC HUBBARD CLUSTER AT QUARTER FILLING

K. Szałowski, T. Balcerzak, M. Jaščur, A. Bobák and M. Žukovič

P7-02 PARAMAGNETISM OF TASAKI-HUBBARD MODEL

V. Baliha, O. Derzhko and J. Richter

P7-03 MAGNETIC, THERMODYNAMIC AND TRANSPORT PROPERTIES OF POLYCRYSTALLINE NdAgAl_3 COMPOUND

S. Nallamuthu, A. Džubinská, M. Reiffers and R. Nagalakshmi

P7-04 MAGNETIC PHASE DIAGRAM OF $\text{UCo}_{1-x}\text{Ru}_x\text{Al}$ WITH LOW Ru CONCENTRATION

P. Opletal, J. Prokleška, J. Valenta and V. Sechovský

P7-05 MAGNETORESISTANCE STUDY OF C-AXIS ORIENTED YBCO THIN FILM

M. Chrobak, W. M. Woch, M. Kowalik, R. Zalecki, M. Giebułtowski, J. Przewoźnik, Cz. Kapusta and G. Szwachta

P7-06 PHASE DIAGRAMS AND REENRANT TRANSITIONS OF A SPIN-ELECTRON MODEL ON A DOUBLY DECORATED HONEYCOMB LATTICE

H. Čenčariková and J. Strečka

P7-07 SPIN-GLASS BEHAVIOR IN LaCu_4Mn COMPOUND

K. Synoradzki

P7-08 CLEAN BULK YBaCuO SUPERCONDUCTORS DOPED BY PARAMAGNETIC IONS OF Sm AND Yb

M. Jirsa, D. Volochová, J. Kováč and P. Diko

P7-09 STM STUDIES OF THE SUPERCONDUCTOR-INSULATOR TRANSITION IN MoC ULTRATHIN FILMS

P. Szabó, V. Hašková, T. Samuely, J. Kačmarčík, M. Žemlička, M. Grajcar and P. Samuely

P7-10 SUPERCONDUCTIVITY OF NIOBIUM THIN FILM IN THE BiOCl/Nb HETEROSTRUCTURE

D. Lotnyk, V. Komanicky, V. Bunda and A. Feher

- P7-11 NON BCS SUPERCONDUCTING DENSITY OF STATES IN B-DOPED DIAMOND**
O. Onufriienko, T. Samuely, G. Zhang, P. Szabó, V. V. Moshchalkov and P. Samuely
- P7-12 INFLUENCE OF THERMO – CHEMICAL TREATMENTS ON SUPERCONDUCTING PROPERTIES OF LITHIUM DOPED $\text{YBa}_2\text{Cu}_3\text{O}_{7-\delta}$ BULK SUPERCONDUCTORS**
V. Antal, D. Volochová, V. Kavečanský, J. Kováč and P. Diko
- P7-13 SUPERCONDUCTIVITY IN $\text{Lu}_x\text{Zr}_{1-x}\text{B}_{12}$ DODECABORIDES WITH CAGE-GLASS CRYSTAL STRUCTURE**
N. E. Sluchanko, A. N. Azarevich, A. V. Bogach, S. Yu. Gavrillin, M. I. Gilmanov, V. V. Glushkov, S. V. Demishev, K. V. Mitsen, A. V. Levchenko, N. Yu. Shitsevalova, V. B. Filipov, S. Gabani and K. Flachbart
- P7-14 INFLUENCE OF PRESSURE ON THE ELECTRON-PHONON INTERACTION IN SUPERCONDUCTORS**
Mat. Orendáč, S. Gabáni, G. Pristáš, E. Gažo, K. Flachbart and N. Shitsevalova
- P7-15 SIMPLIFIED PARQUET EQUATION SOLVER FOR THE ANDERSON IMPURITY MODEL**
V. Pokorný, V. Janiš and A. Kauch
- P7-16 ANOMALOUS HALL EFFECT IN MnSi**
V. V. Glushkov, I. I. Lobanova, V. Yu. Ivanov and S. V. Demishev
- P7-17 ELECTROMAGNON CONTRIBUTION TO THE COOPER PAIR FORMATION AND SUPERCONDUCTIVITY**
Z. Bak
- P7-18 SUPERCONDUCTING AND MAGNETIC PROPERTIES OF Sn-DOPED $\text{EuBa}_2\text{Cu}_3\text{O}_{7-\delta}$ COMPOUND**
A. Dvurečenskij, A. Cigáň, I. Van Driessche, M. Škrátek, M. Majerová, J. Maňka and E. Bruneel
- P7-19 TRAPPED FIELD OF YBCO BULK SUPERCONDUCTORS PREPARED BY INFILTRATION GROWTH PROCESS**
L. Vojtkova, P. Diko and S. Piovarči
- P7-20 ON THE MAGNETIC PENETRATION DEPTH IN SUPERCONDUCTING ULTRATHIN LEAD FILMS**
A. P. Durajski and R. Szczesniak
- P7-21 DC NANOSQUID FROM Nb THIN FILMS**
V. Štrbík, M. Pisarčík, Š. Gaži and M. Španková

- P7-22 MAGNETIC AND STRUCTURAL CHARACTERIZATION OF SUPERCONDUCTIVE Ni_2NbSn HEUSLER ALLOY**
P. Kanuch, T. Ryba, J. Gamcová, M. Kanuchova, M. Durisin, K. Saksli, Z. Vargova and R. Varga
- P7-23 EVOLUTION OF LOCK-IN EFFECT IN Cu_xTiSe_2 SINGLE CRYSTALS**
Z. Medvecká, T. Klein, V. Cambel, J. Šoltýs, G. Karapetrov, F. Levy-Bertrand, B. Michon, C. Marcenat, Z. Pribulová and P. Samuely
- P7-24 VORTEX LATTICE IN HEAVY-FERMION CeCoIn_5 PROBED BY AC-CALORIMETRY**
J. Kačmarčík, P. Pedrizzini, C. Marcenat, Y. Fasano, V. Correa, Z. Pribulová and P. Samuely
- P7-25 SUPPRESSION OF SUPERCONDUCTIVITY IN HOMOGENEOUSLY DISORDERED ULTRATHIN MoC FILMS INTRODUCED BY INTERFACE BETWEEN THE SAMPLE AND THE SUBSTRATE**
V. Hašková, M. Kopčík, P. Szabó, T. Samuely, J. Kačmarčík, M. Žemlička, M. Grajcar and P. Samuely
- P7-26 HALL PROBE MAGNETOMETRY OF SUPERCONDUCTING YB_6**
M. Marcin, Z. Pribulová, J. Kačmarčík, S. Gabáni, T. Mori, V. Cambel, J. Šoltýs and P. Samuely
- P7-27 ANGULAR DEPENDENCIES OF ESR PARAMETERS IN ANTIFERROQUADRUPOLEAR PHASE OF CeB_6**
A. V. Semeno, M. I. Gilmanov, N. E. Sluchanko, V. N. Krasnorussky, N. Y. Shitzevalova, V. B. Filipov, K. Flachbart and S. V. Demishev
- P7-28 THERMODYNAMIC CRITICAL FIELD IN HEXAGONAL BaSn_5 SUPERCONDUCTOR**
M. W. Jarosik and A. D. Woźniak
- P7-29 UNIFORMLY DISORDERED ULTRATHIN SUPERCONDUCTING MoC FILMS CLOSE TO INSULATING STATE. TRANSPORT STUDIES.**
J. Kačmarčík, P. Szabó, M. Rajňák, M. Žemlička, M. Grajcar, P. Markoš and P. Samuely
- P7-30 DETECTING OF LIGHT BY MEANS OF “HTSC / PHOTOSEMICONDUCTOR “ HYBRID CONTACT STRUCTURES**
V. Bunda, S. Bunda, D. Lotnyk, V. Komanicky and A. Feher

- P7-31 EFFECT OF PRESSURE ON CRITICAL PARAMETERS AND MICROSTRUCTURE OF DOPED MgB_2 MATERIAL**
G. Gajda, A. Morawski, A. Presz, R. Diduszko, T. Cetner, K. Gruszka, S. Hossain and D. Gajda
- P7-32 LOCAL MAGNETOMETRY USING SCANNING HALL PROBE MICROSCOPE**
Z. Pribulová, Z. Medvecká, J. Kačmarčík, E. Gažo and P. Samuely
- P7-33 PHOTON-ASSISTED CHARGE TRANSPORT IN A HYBRID JUNCTION WITH TWO NON-COLLINEAR FERROMAGNETS AND A SUPERCONDUCTOR**
K. Bocian and W. Rudziński
- P7-34 MAGNETIC-FIELD INDUCED TRANSITION IN A SPIN-GLASS STATE OF CATION DEFICIENT LaMnO_3**
V. Eremenko, V. Sirenko, E. Čížmár, A. Baran and A. Feher

A B S T R A C T S

PL-01**MAGNETO-OPTICAL DOMAIN IMAGING**Rudolf Schäfer¹*¹Leibniz Institute for Solid State and Materials Research (IFW) Dresden, Helmholtzstrasse 20, D-01069 Dresden, Germany and Institut für Material Science, Technical University Dresden, Germany*

The characterization of magnetic materials in research and development usually relies on the measurement of hysteresis curves. For the interpretation of such curves it is often helpful to study the magnetic domains and magnetization processes that are responsible for hysteresis effects. Magneto-optical microscopy, in particular Kerr microscopy, is just one among many techniques to image domains and processes, and it may be considered a „classical“ method (compared to „modern“ magnetic microscopy based, for instance, on circular X-ray dichroism or spin-polarized tunneling). Nevertheless, it is the most flexible and versatile technique and due to substantial technical progress in recent time magneto-optical domain imaging becomes very powerful again.

In this presentation, a review will be given on the possibilities and recent developments of magnetic domain imaging by wide-field magneto-optical microscopy. Besides some basics, this includes depth-sensitive and time-resolved domain imaging, a mathematical deconvolution method to enhance the lateral resolution, and on the other hand an overview imaging tool to maximize the field of view. Novel light-emitting diode (LED) lamps allow for contrast separation and -enhancement, vector magnetometry and in-situ quantitative Kerr microscopy of complete magnetization processes, as will be demonstrated on magnetic film and bulk materials.

By using magneto-optic indicator films (MOIF) with perpendicular or in-plane anisotropy, it is possible to image magnetic poles by Faraday microscopy. With the MOIF technique domain information can be obtained in cases where the sample surface is coated like on electrical steel. By using perpendicular MOIF films the domain contrast is even strong enough to allow for single-shot time-resolved imaging of coated transformer steel up to power frequencies. MOIF films also provide the potential to investigate the role of grain boundaries for flux propagation in such material.

PL-02**SPIN CONFIGURATION AND MAGNETIZATION REVERSAL OF INDIVIDUAL CoFe BASED CYLINDRICAL NANOWIRES**

M. Vazquez¹, C. Bran¹, A. Asenjo¹, R. Perez¹, O. Chubykalo-Fesenko¹, E. Palmero¹, E. Berganza¹ and J.A. Fernandez Roldan¹

¹*Instituto de Ciencia de Materiales de Madrid, CSIC. 28049 Madrid. Spain*

Magnetic nanowires, NWs, and their arrays are widely investigated for their applications in magnetic sensors, RE-free novel magnets, biomedical functionalization or magnetic storage. The tailoring of the spin reversal process of such NWs nanowires becomes essential for the design and control of those applications [1].

The magnetic domain structure and the magnetization reversal process of CoFe-based individual cylindrical nanowires (20 to 200 nm diameter and 100 nm up to tens of microns long) have been investigated. NWs were electrochemically grown into self-assembled porous templates and then chemically released from the membranes. The study has been extended to NWs with controlled alloy composition and geometry: single and modulated in diameter and composition (multisegmented) NWs. Their magnetocrystalline anisotropy (determined by the *hcp*, *fcc* or *bcc* crystal symmetry of NWs, as checked by XRD and HRTEM) is controlled by the alloy composition and various synthesis parameters [2].

Hysteresis loops of individual NWs have been obtained by magneto-optical Kerr effect magnetometry while their spin configuration at remanence has been imaged at remanence by Magnetic Force Microscopy and Photoemission Electron microscopy (PEEM) combined with X-ray Magnetic Circular Dichroism (XMCD) in transmission [3]. Micromagnetic simulations identify two main spin reversal modes involving the nucleation of a vortex-like structure at the ends followed by its propagation along the NW, and an additional rotational mode in wires with strong perpendicular anisotropy.

In this presentation, we will pay particular attention to the influence in the magnetic configuration of the presence of transition (compositional and diameter) regions in periodically modulated NWs.

[1] H.J. Gao *et al.*, Nanotechnology 21 (2010)105107; X.M. Kou *et al.*, Adv. Mater. 23 (2011) 1393.

[2] Y.P. Ivanov *et al.*, Nanotechnology 25 (2014) 475702; C. Bran *et al.*, J. Phys. D: Appl. Phys. 48 (2015) 145304; J. Phys. D: Appl. Phys. 46 (2013) 485001.

[3] C. Bran *et al.*, J. Mater. Chem. C 4 (2016) 978; E. Palmero *et al.*, Nanotechnology 26 (2015) 461001; O. Iglesias-Freire *et al.*, Nanotechnology 26 (2015) 395702.

PL-03**INVESTIGATION OF Ce AND Yb INTERMETALLICS:
THE IMPORTANCE OF PHASE DIAGRAMS AND CRYSTAL
CHEMISTRY**M. Giovannini^{1,2}¹*Department of Chemistry, University of Genova, Via Dodecaneso 31,
I-16146 Genova, Italy*²*CNR-SPIN, Corso Ferdinando Maria Perrone 24, 15152, Genova, Italy*

In recent years a growing interest has been devoted to investigation of strongly correlated electron systems, where hybridization of f-electrons and conduction electrons can cause a number of outstanding low temperature features. Among the rare earths, a large number of these phenomena is found in Ce- and Yb- based compounds and alloys. Chemical composition, as well as pressure and magnetic field, can play an important role in ground state properties of these compounds. Regarding the influence of chemical composition on physical properties of intermetallic compounds, in many cases compounds previously thought to be stoichiometric are later on recognized to be point of crystallographic order of solid solutions. Therefore an investigation of the homogeneity range is a fundamental task to be carried out before investigating the ground state properties. Another aspect which will be discussed is the doping of one element with another in order to study the evolution of the ground state in a compound.

In this talk a few examples of compounds, which have been recently investigated by us are discussed, with the aim to stress the importance of crystal chemistry and compositional phase diagrams for the challenging activity of synthesis and characterization of novel promising strongly correlated electron intermetallic compounds.

I1-01**EFFECT OF ELECTRON CONFINEMENT ON MAGNETISM OF NANOSTRUCTURES**M. Przybylski¹*¹Academic Centre for Materials and Nanotechnology and Faculty of Physics and Applied Computer Science, AGH University of Science and Technology, al. Mickiewicza 30, 30-059 Kraków, Poland*

In thin films (and any other nanoobjects), electron motion can be confined by the potential barriers at the surfaces/interfaces (or at the edges of nanoobjects), leading to the formation of quantum well states (*QWS*). *QWS* in thin films modify electronic structure oscillatory with increasing film thickness. It causes, e.g., oscillatory tunnelling between the electrodes of varying thickness.

Any manipulation of the *d*-electron bands, in particular if resulting in the change of occupied and/or unoccupied states close to the Fermi level (E_F) can change magnetic properties of transition metals significantly. Thus, the confinement of *d*-electrons in transition metal films is particularly interesting, since the *d*-electrons themselves determine magnetic anisotropy. If significant contribution to magnetic anisotropy is due to spin-polarized *QWS* formed in the *d*-electron bands, an effect of enhanced anisotropy can occur at specific thicknesses. Since the oscillation period is determined by k_{z0} , i.e., k_z of the bulk *d*-band corresponding to *QWS* that cross E_F , it helps to identify the symmetry of the quantized states.

However, the mechanism of oscillatory anisotropy can be more complex and is suggested to be explored by combining magneto-optical Kerr effect, photoemission spectroscopy and x-ray magnetic circular dichroism for better understanding. For example, only then the magnetic anisotropy oscillations in Fe films have been concluded as a direct consequence of the quantization of *d* states with Δ_5 spatial symmetry (and majority-spin character) coupled with majority-spin states with Δ_2 symmetry.

The mechanisms discussed here can be extended to other magnetic materials, opening the possibility of tailoring magnetic anisotropy by appropriate electronic-structure engineering.

O1-01**MICROSCOPIC ORIGIN OF HEISENBERG AND NON-HEISENBERG EXCHANGE INTERACTIONS IN FERROMAGNETIC BCC Fe**

Y. O. Kvashnin¹, R. Cardias², A. Szilva¹, I. Di Marco¹, M. I. Katsnelson^{3,4},
A. I. Lichtenstein^{4,5}, L. Nordström¹, A. B. Klautau² and O. Eriksson¹

¹*Department of Physics and Astronomy, Division of Material Theory, Uppsala University, Box 516, SE-75120, Uppsala, Sweden*

²*Faculdade de Física, Universidade Federal do Para, Belem, PA, Brazil*

³*Radboud University of Nijmegen, Institute for Molecules and Materials, Heijendaalseweg 135, 6525 AJ Nijmegen, The Netherlands*

⁴*Theoretical Physics and Applied Mathematics Department, Ural Federal University, Mira Str.19, 62002, Ekaterinburg, Russia and*

⁵*Institute of Theoretical Physics, University of Hamburg, Jungiusstrasse 9, 20355 Hamburg, Germany*

By means of first principles calculations we investigate the nature of exchange coupling in ferromagnetic bcc Fe on a microscopic level. Analyzing the basic electronic structure reveals a drastic difference between the 3d orbitals of E_g and T_{2g} symmetries. The latter ones define the shape of the Fermi surface, while the former ones form weakly-interacting impurity levels. We demonstrate that, as a result of this, in Fe the T_{2g} orbitals participate in exchange interactions, which are only weakly depend on the configuration of the spin moments and thus can be classified as a Heisenberg-like. These couplings are shown to be driven by Fermi surface nesting. In contrast, for E_g states the Heisenberg picture breaks down, since the corresponding contribution to the exchange interactions is shown to strongly depend on the reference state they are extracted from. Our analysis of the nearest-neighbour coupling indicates that the interactions among E_g states are mainly proportional to the corresponding hopping integral and thus can be attributed to be of double-exchange origin. By comparing to other magnetic transition metals, we put the results of bcc Fe into context and argue the iron has a unique behaviour when it comes to magnetic exchange interaction.

Ref: <http://arxiv.org/pdf/1510.01872v1.pdf>

O1-02**MAGNETISM AND TRANSPORT PROPERTIES OF MN-DOPED TOPOLOGICAL INSULATOR Bi_2Te_3 AND Bi_2Se_3 : AB INITIO CALCULATIONS**

K. Carva¹, P. Baláž¹, V. Tkáč¹, R. Tarasenko³, V. Sechovský¹, J. Kudrnovský², F. Máca² and J. Honolka²

¹*Department of Condensed Matter Physics, Faculty of Mathematics and Physics, Charles University, Ke Karlovu 5, CZ-12116 Prague 2, Czech Republic*

²*Institute of Physics, ASCR, Na Slovance 2, CZ-18221 Prague 8, Czech Republic*

³*P.J. Šafárik University, Institute of Physics, Park Angelinum 9, 041 54 Košice, Slovakia*

Magnetic doping is a way to add novel functionality to topological insulators [1], as well as a test of stability of topological properties. We calculate on ab initio level electronic structure of Bi_2Te_3 and Bi_2Se_3 doped by Mn at different possible positions in the lattice and also in the presence of native antisites. This provides for the first time a comprehensive map of possible behavior affecting strongly the bulk resistivity, carrier concentration and magnetism. Density of states calculations reveal in which case the Fermi level lies at low conducting impurity Mn peak and which effects shift it. This allows us to tune the bulk resistivity, and also help to uncover the location of Mn atoms. Concentration dependence of resistivity exhibits significant difference between substitutional or interstitial Mn position, the resistivity for pure substitutional doping is significantly higher. Calculations indicate that at least two of the considered defects have to be present simultaneously in order to explain the observations, and the role of interstitials may be more important than expected.

Exchange interactions between the Mn magnetic moments in bulk Mn-doped Bi_2Se_3 and Bi_2Te_3 have been calculated using ab initio methods. From these ferromagnetic Curie temperature and other magnetic properties are systematically studied by means of atomistic Monte Carlo simulations. Curie temperatures are shown to be significantly dependent on the concentration of Mn atoms in substitutional and interstitial positions. Theoretical results were compared to recent experimental studies [2].

[1] Y. S. Hor et al., Phys. Rev. B 81, 195203 (2010).

[2] R. Tarasenko et al., Physica B: Condensed Matter 481, 262 (2016).

O1-03**NON- PLATEAU BEHAVIOR OF THE ZERO-TEMPERATURE
MAGNETIZATION IN SPIN-CLUSTERS AND CHAINS**V. Ohanyan¹, O. Rojas², J. Strečka³ and S. Bellucci⁴¹*Laboratory of Theoretical Physics, Yerevan State University, 1 Alex Manoogian, 0025 Yerevan, Armenia*²*Departamento de Fisica, Universidade Federal de Lavras, CP 3037, 37200000, Lavras, MG, Brazil*³*Department of Theoretical Physics and Astrophysics, Faculty of Science, P. J. Šafárik University, Park Angelinum 9, 040 01, Košice, Slovak Republic*⁴*INFN-Laboratori Nazionali di Frascati, Via E. Fermi 40, 000 44 Frascati, Italy*

We examine the general features of the non-commutativity of the magnetization operator and Hamiltonian for small quantum spin clusters. The source of this non-commutativity can be a difference in the Landé g-factors for different spins in the cluster, XY-anisotropy in the exchange interaction and the presence of the Dzyaloshinskii-Moriya term in the direction different from the direction of the magnetic field. As a result, zero-temperature magnetization curves for small spin clusters mimic those for the macroscopic systems with the band(s) of magnetic excitations, i.e. for the given eigenstate of the spin cluster the corresponding magnetic moment can be an explicit function of the external magnetic field yielding the non-constant (non-plateau) form of the magnetization curve within the given eigenstate. In addition, the XY-anisotropy makes the saturated magnetization (the eigenstate when all spins in cluster are aligned along the magnetic field) inaccessible for finite magnetic field magnitude (asymptotical saturation). We demonstrate all these features on three examples: spin-1/2 dimer, mixed spin-(1/2,1) dimer, spin-1/2 ring trimer. We consider also the simplest Ising-Heisenberg chain, the Ising-XYZ diamond chain with four different g-factors. In the chain model the magnetization curve has a more complicated and non-trivial structure which that for clusters.

O1-04**AB INITIO THEORY OF GILBERT DAMPING IN RANDOM ALLOYS**I. Turek^{1,2}, J. Kudrnovský³ and V. Drchal³¹*Institute of Physics of Materials, Academy of Sciences of the Czech Republic, Žitkova 22, 616 62 Brno, Czech Republic*²*Faculty of Mathematics and Physics, Department of Condensed Matter Physics, Charles University, Ke Karlovu 5, 121 16 Praha 2, Czech Republic*³*Institute of Physics, Academy of Sciences of the Czech Republic, Na Slovance 2, 182 21 Praha 8, Czech Republic*

We present a recently developed *ab initio* theory of the Gilbert damping in substitutionally disordered ferromagnetic alloys [1]. The theory rests on introduced nonlocal torques which replace traditional local torque operators in the well-known torque-correlation formula and which can be formulated within the atomic-sphere approximation. The formalism is sketched in a simple tight-binding model and worked out in detail in the relativistic tight-binding linear muffin-tin orbital (TB-LMTO) method and the coherent potential approximation (CPA). The resulting nonlocal torques are represented by nonrandom, non-site-diagonal and spin-independent matrices, which simplifies the configuration averaging. The CPA-vertex corrections play a crucial role for the internal consistency of the theory and for its exact equivalence to other first-principles approaches based on the random local torques.

The developed theory has been applied to a broad class of itinerant ferromagnets including (i) binary (fcc NiFe, bcc FeCo) and ternary (permalloy doped by transition-metal impurities) random alloys, (ii) pure iron with a model atomic-level disorder, and (iii) stoichiometric FePt alloys with a varying degree of L1₀ atomic long-range order. Besides a comparison of the obtained results to those of other authors and to experiment, following aspects will be discussed: concentration trends of the Gilbert damping and their relation to the density of states at the Fermi energy, to the alloy magnetization and to the strength of the alloy disorder and of the spin-orbit interaction. Moreover, the non-monotonic temperature dependence of the Gilbert damping, which is conductivity-like at low temperatures and resistivity-like at elevated temperatures, has been reproduced for pure iron in semi-quantitative agreement with experiment.

[1] I. Turek, J. Kudrnovský, V. Drchal: Phys. Rev. B 92 (2015) 214407.

O1-05**PHOTO-MECHANICAL COUPLING IN MAGNETIC SHUTTLE DEVICE**A. Parafilo¹, S. Kulinich², L. Gorelik³, M. Kiselev¹, R. Shekhter⁴ and M. Jonson^{4,5}¹*The Abdus Salam International Centre for Theoretical Physics, Strada Costiera 11, I-34151 Trieste, Italy*²*B. Verkin Institute for Low Temperature Physics and Engineering, Prospekt Nauky 47, Kharkov 61103, Ukraine*³*Department of Physics, Chalmers University of Technology, SE-412 96 Göteborg, Sweden*⁴*Department of Physics, University of Gothenburg, SE-412 96 Göteborg, Sweden*⁵*SUPA, Institute of Photonics and Quantum Sciences, Heriot-Watt University, Edinburgh, EH14 4AS, Scotland, UK*

Recent years many attentions were devoted for investigation of an electronic spin degree of freedom in a nano-electromechanical (NEM) device. In such device magnetic (exchange) interaction provides additional mechanism for electronic transport control due to high sensitivity to an external magnetic field or magnetically polarized electrodes.

In our work we theoretically show that electronic spin can mediate a strong coupling between high frequency electromagnetic field and low-frequency mechanical vibrations in magnetic NEM system. The prototype shuttle device is based on a suspended carbon nanotube (CNT) deposited between two ferromagnetic electrodes with opposite magnetizations. A magnetic tip is placed at some distance from the top of CNT and produces non-homogeneous magnetic field, which induces magnetic force that acts on the suspended part of CNT. The NEM system is subjected into external microwave field, where orientation of magnetic component is perpendicular to the electron spin projections in the leads. The specific orientation of magnetic component of the microwave field and additional condition for coincidence of its frequency and Zeeman energy splitting induce spin-flip processes. To analyze effective coupling we investigate the time evolution of the CNT flexural oscillations with respect to electron degree of freedom.

We predicted, that in the case when microwave frequency exceed the threshold value, which is associated with Zeeman splitting, effective photo-mechanical coupling produces instability in vibrational “ground state” of the system (shuttle instability). It develops into pronounced self-sustained oscillations of CNT resonator with the charge and spin transfer between source and drain electrodes.

O1-06**BROKEN SYMMETRY IN THE MAGNETISATION DYNAMICS**J. Tóvik¹ and V. Cambel¹¹*Institute of Electrical Engineering, Slovak Academy of Sciences*

Magnetic structure in sub-micron structures is subject of intense research, motivated by applications. We have studied permalloy nano-dots with vortex magnetic structure in the absence of the external field [1, 2]. Solving numerically magnetic structure of cylindrical dot with defect we have observed asymmetry in vortex nucleation process. It can be shown by symmetry arguments that the magnetic vortex state is degenerated, however simulations showed preference for one of them. The symmetry breaking mechanism is hidden in magnetisation dynamics. We analyse the symmetry breaking mechanism on the phenomenological level of the theory described by Landau-Lifshitz-Gilbert equation. One mechanism responsible for symmetry breaking is time dependence of the external field. Second one is related to particular topology of the total energy surface in the configuration space [3]. While the symmetry breaking induced by time dependent external field is more volatile to external noise induced by temperature, the intrinsic symmetry breaking induced by topology can be robust even for elevated temperatures. Both mechanisms are shown on toy-model.

[1] V. Cambel and G. Karapetrov, Phys. Rev. B 84, 014424 (2011).

[2] J. Tóvik, V. Cambel, and G. Karapetrov, Phys. Rev. B 86, 134433 (2012).

[3] J. Tóvik, V. Cambel, and G. Karapetrov, Sci. Rep. 5, 12301 (2015).

P1-01**EXACT STUDIES OF THE HUBBARD PAIR-CLUSTER
IN EXTERNAL FIELDS**T. Balcerzak¹ and K. Szałowski¹*¹Department of Solid State Physics, University of Łódź, ul. Pomorska 149/153,
PL 90-236 Łódź, Poland*

The cluster, consisting of a pair of atoms embedded in the external magnetic and electric fields, is studied within the Hubbard model. The Hamiltonian, represented by 16x16 matrix, is diagonalized exactly by analytical methods. Thermodynamic properties are determined in the framework of the grand canonical ensemble, assuming the average number of electrons in the system between 0 to 4 (depending on the chemical potential).

The numerical studies are based on the grand thermodynamic potential and involve a variety of statistical-thermodynamic properties. In particular, the chemical potential, mean kinetic energy of the electrons, on-site magnetization, mean occupation numbers with given polarization, spin-spin and occupation number correlations are calculated.

The phase diagram, showing the critical magnetic field which switches between ferromagnetically saturated and partially ordered (or disordered) phase, is obtained as a function of electron concentration. The critical magnetic field dependence on the electric field, Hubbard U parameter and temperature is investigated. In the ground state, discontinuous changes of the mean occupation numbers of electrons vs. chemical potential illustrate the quantum behavior of the system. At zero temperature also all related quantities, for instance, magnetization and correlation functions, show the stepwise changes. It is found that the most distinct effect of switching between paramagnetic and ferromagnetic phase can be obtained in the ground state and at half-filling, i.e., with 2 electrons present in the cluster.

Below the critical magnetic field, an anomalous behavior of the magnetization vs. temperature is found. Namely, the magnetization demonstrates a smooth maximum as a function of temperature, which is strictly connected with the stepwise behavior of the magnetization vs. magnetic field observed in the ground state.

P1-02**THERMODYNAMICS OF FRUSTRATED MAGNETS:
HIGH-TEMPERATURE EXPANSION REVISITED**J. Richter¹, A. Lohmann¹ and H.-J. Schmidt²¹*Institute for Theoretical Physics, University Magdeburg, D-39016 Magdeburg, Germany*²*Universität Osnabrück, Fachbereich Physik,, D - 49069 Osnabrück, Germany*

We present the high-temperature expansion (HTE) up to 10th order of the specific heat C and the uniform susceptibility χ for Heisenberg models with arbitrary exchange patterns and arbitrary spin quantum number s . We encode the algorithm in a C++ program provided at [1] which allows to get explicitly the HTE series for concrete Heisenberg models [2,3]. We use our HTE scheme to study the specific heat and the susceptibility of frustrated quantum magnets. In particular, we consider magnetic systems with highly degenerate classical ground states, such as the kagome, the J_1 - J_2 , as well as the pyrochlore magnets. We investigate to what extent strong frustration is evident at moderate and high temperatures. Moreover, we discuss the influence of the spin quantum number s on the thermodynamic properties and compare this way quantum and classical systems.

[1] <http://www.uni-magdeburg.de/jschulejschulen/HTE10/>.

[2] H.-J. Schmidt, A. Lohmann, and J. Richter, Phys. Rev. B 84, 104443 (2011).

[3] A. Lohmann, H.-J. Schmidt, and J. Richter, Phys. Rev. B 89, 014415 (2014).

P1-03**SPONTANEOUS MAGNETIZATION AND PHASE DIAGRAMS OF THE MIXED SPIN-1/2 AND SPIN-S ISING MODEL ON THE BETHE LATTICE**
C. Ekiz¹ and J. Strečka²

¹*Department of Physics, Faculty of Art and Science, Adnan Menderes University, 09010 Aydın, Turkey*

²*Department of Theoretical Physics and Astrophysics, Faculty of Science, P. J. Šafárik University, Park Angelinum 9, 040 01 Košice, Slovak Republic*

Effect of the single-ion anisotropy on magnetic properties of the mixed spin-1/2 and spin-S ($S \geq 1$) Ising model on the Bethe lattice with the coordination number $q=3$ is investigated by combining star-triangle and triangle-star mapping transformations with exact recursion relations. First, the star-triangle mapping transformation is used to connect the mixed spin-1/2 and spin-S Ising model on the Bethe lattice with $q=3$ to an equivalent spin-1/2 Ising model on the triangular Husimi lattice. This spin-1/2 Ising model on the Husimi lattice is then converted to a simple spin-1/2 Ising model on the Bethe lattice by means of the triangle-star transformation. The latter spin-1/2 Ising model on the Bethe lattice was exactly solved using the method of recursion relations.

Exact results are obtained for the phase diagrams, total and sublattice magnetizations. The particular attention is focused on the effect of single-ion anisotropy on the temperature dependences of spontaneous magnetizations and finite-temperature phase diagrams, which are established for several values of quantum spin number S . The single-ion anisotropy basically changes the magnetic behavior of the spin-S atoms that constitute the sublattice B of the mixed spin-1/2 and spin-S Ising model on the three-coordinated Bethe lattice. Depending on the quantum spin number S and the single-ion anisotropy strength, thermal variations of sublattice and total magnetizations have been found to be either of Q-, R-, P-, L- or S-type. The N- and W-type magnetization dependences with one or two compensation temperatures, respectively, do not appear in the system under consideration because of the single-ion anisotropy effect. The present results on the Bethe lattice are in a good qualitative accordance with those obtained for the same mixed-spin Ising model on the honeycomb and bathroom-tile (4-8) lattices.

This work was financially supported by ERDF EU (European Union European regional development fond) grant provided under the contract No. ITMS26220120005 (activity 3.2).

P1-04**MAGNETIC HYSTERESIS AS A CHAOTIC SEQUENCE**P. Frydrych¹, M. Nowicki² and R. Szewczyk¹¹*Institute of Metrology and Biomedical Engineering, Warsaw University of Technology, Warsaw, Poland,*²*Research Institute for Automation and Measurements, Warsaw, Poland.*

In this paper hypothesis of magnetic hysteresis being a kind of chaotic sequence was tested. It was assumed that external magnetic field changes parameter of magnetization sequence: $M_i = f(H)M_{i-1}$. System entropy and Lyapunov exponent for different values of external magnetic field was computed. Results leads to similar conclusions as Gibbs considerations about entropy and free energy in magnetic materials. Developed hypothesis is useful for static and dynamic hysteresis simulations and can be complemented by stress and temperature dependence analysis. Outcome of chaotic assumption is system relaxation ability for constant magnetic field, which enables to return to anhysteretic curve. That curve is kind of fixed point of sequence for given magnetic field. Unfortunately this hypothesis is hardly verifiable due to long relaxation time. Presented considerations are purely theoretical and hypothetical. They are in need of further development and discussion.

P1-05

APPLICATION OF ANISOTROPIC VECTOR PREISACH MODEL FOR BULK MATERIALS

P. Frydrych¹, R. Szewczyk¹ and M. Nowicki²

¹Institute of Metrology and Biomedical Engineering, Warsaw University of Technology, Warsaw, Poland, p.frydrych@mchtr.pw.edu.pl

²Research Institute for Automation and Measurements, Warsaw, Poland

Recently developed models of domain wall motion and domain rotation simulates magnetic hysteresis for anisotropic amorphous alloy ribbons. In this paper possibility of two dimensional vector Preisach model application for bulk materials is investigated.

Physical magnetization mechanisms in bulk cores and thin ribbons were analyzed. Model was generalized for Neel and Bloch domain walls. Model is based on collection of Preisach planes which describe material state in different angles on rotation plane. Presented model exhibits good conformity with experimental data for bulk as well for ribbon shaped cores. Model includes anisotropy and describes not only mean magnetization vector, but also distribution of magnetic moments for different angles.

P1-06**LOCALIZED-MAGNON CHAINS AND INTERCHAIN COUPLINGS**O. Krupnitska¹, O. Derzhko¹ and J. Richter²¹*Institute for Condensed Matter Physics, National Academy of Sciences of Ukraine, Svientsitskii Street 1, 79011 L'viv, Ukraine*²*Institut für theoretische Physik, Otto-von-Guericke-Universität Magdeburg, P.O. Box 4120, 39016 Magdeburg, Germany*

Quantum Heisenberg antiferromagnet on the lattices which support a completely dispersionless (flat) lowest-energy magnon band exhibits many spectacular properties at low temperatures around the saturation magnetic field. For example, the ground-state magnetization curve has a jump at the saturation field, the specific heat has an extra low-temperature maximum etc. These properties can be explained using the concept of localized-magnon states [1,2]. Among many highly-frustrated lattices in different dimensions which support localized-magnon states, a frustrated diamond chain is of special interest. The reason for that is that there is a solid-state realization of the spin-1/2 (distorted) frustrated diamond-chain antiferromagnetic Heisenberg system. The natural mineral azurite $\text{Cu}_3(\text{CO}_3)_2(\text{OH})_2$ is probably the most promising candidate to show localized-magnon physics [2,3]. Among the observable low-temperature properties of azurite there are such as the plateau at 1/3 of the saturation magnetization and further steep increase to saturation reached at about 32.5 T, see Ref. 4. These features are expected within the localized-magnon picture. However, the successful description of all available experimental data for azurite requires an accurate treatment of interchain couplings (azurite orders below 2 K).

In our study we consider a spin-1/2 frustrated diamond-chain Heisenberg antiferromagnet and examine the effect of interchain couplings on some basic localized-magnon features. To this end, we perform exact diagonalizations and elaborate an effective low-energy description using perturbation theory.

- [1] J. Schulenburg, A. Honecker, J. Schnack, J. Richter, and H.-J. Schmidt, Phys. Rev. Lett. 88, 167207 (2002).
- [2] O. Derzhko, J. Richter, and M. Maksymenko, Int. J. Mod. Phys. B 29, 1530007 (2015).
- [3] H. Jeschke, I. Opahle, H. Kandpal, R. Valenti, H. Das, T. Saha-Dasgupta, O. Janson, H. Rosner, A. Brühl, B. Wolf, M. Lang, J. Richter, S. Hu, X. Wang, R. Peters, T. Pruschke, and A. Honecker, Phys. Rev. Lett. 106, 217201 (2011).
- [4] H. Kikuchi, Y. Fujii, M. Chiba, S. Mitsudo, T. Idehara, T. Tonegawa, K. Okamoto, T. Sakai, T. Kuwai, and H. Ohta, Phys. Rev. Lett. 94, 227201 (2005).

P1-07**SPIN-CHAIN OF ALTERNATING ISING SPINS-CANTED AND HEISENBERG SPINS WITH TWO DIFFERENT LOCAL ANISOTROPY AXES: ZERO TEMPERATURA PHASE DIAGRAM AND MAGNETIZATION, AND THERMODYNAMICS MAGNETIZATION AND SUSCEPTIBILITY**

J. Torrico¹, M. L. Lyrá¹, Onofre Rojas², S. M. de Souza², M. Rojas², M. Hagiwara³, Y. Han³ and J. Strečka⁴

¹*Instituto de Física, Universidade Federal de Alagoas, 57072-970, Maceió, AL, Brazil*

²*Departamento de Física, Universidade Federal de Lavras, 37200-000, Lavras-MG*

³*KYOKUGEN (Center for Quantum Science and Technology under Extreme Conditions), Osaka University, 1-3 Machikaneyama, Toyonaka, Osaka 560-8531, Japan*

⁴*Department of Theoretical Physics and Astrophysics, Faculty of Science, P. J. Šafárik University, Park Angelinum 9, 040 01 Kosice, Slovak Republic*

Motivated by some real material, such as the polymer $\text{Dy}(\text{NO})_3(\text{DMSO})_2\text{Cu}(\text{opba})(\text{DMSO})_2$ this material could be well represented by spin-1/2 chain with alternating Ising spins-canted and Heisenberg spins. We consider two different local anisotropy axes and in an arbitrarily oriented magnetic field. The zero temperature properties of the model are quite interesting, besides the canted phase diagram; the model exhibits some peculiar properties, such as frustrated phase under the influence of magnetic field. Another interesting property is the non-null net magnetization in the absence of magnetic field, this property arise due to the Ising spin are canted. We analyzed for different temperature zero the magnetization curves of the spins, the total magnetization and powder magnetization, in addition to susceptibility in the x-axis and z-axis, the total susceptibility and powder susceptibility. We exhibits the fit of the experimental data for the magnetization powder and powder susceptibility, and we shows that our model is a very good approximation with the experimental data.

P1-08**BREAKDOWN OF A MAGNETIZATION PLATEAU IN FERRI-MAGNETIC MIXED-SPIN HEISENBERG CHAINS DUE TO A QUANTUM PHASE TRANSITION TOWARDS A SPIN-LIQUID PHASE**J. Strečka¹¹*Department of Theoretical Physics and Astrophysics, Faculty of Science,
P. J. Šafárik University, Park Angelinum 9, 040 01 Košice, Slovak Republic*

Magnetization curves of the ferrimagnetic mixed spin- (S_A, S_B) Heisenberg chains are calculated with the help of density-matrix renormalization group (DMRG) method for several combinations of quantum spin numbers S_A and S_B . In general, the zero-temperature magnetization curves of the ferrimagnetic mixed-spin Heisenberg chains involve a quantized plateau due to the Lieb-Mattis ferrimagnetic ground state, which breaks down at a quantum phase transition towards the Luttinger spin liquid caused by closing of an energy gap by the external magnetic field. Subsequently, the total magnetization continuously rises with increasing the magnetic field within the Luttinger spin-liquid phase until it reaches the full moment at the saturation field $h_s = 2J(S_A + S_B)$ connected with another field-induced quantum phase transition.

The observed fractional magnetization plateaux of the ferrimagnetic mixed-spin Heisenberg chains are in agreement with the Oshikawa-Yamanaka-Affleck rule $S_u - m_u = \text{integer}$ [1], which provides necessary (but not sufficient) quantization condition for the total magnetization per unit cell m_u within the intermediate magnetization plateaux ($S_u = S_A + S_B$ is the total spin per unit cell). It will be demonstrated that both field-induced quantum phase transitions related to an existence of the Luttinger spin-liquid phase manifest themselves through a divergence of the magnetic susceptibility.

This work was financially supported by ERDF EU (European Union European regional development fond) grant provided under the contract No. ITMS26220120005 (activity 3.2).

[1] M. Oshikawa, M. Yamanaka, I. Affleck, Phys. Rev. Lett. 78 (1997) 1984.

P1-09**INVERSE MAGNETOCALORIC EFFECT IN THE SPIN-1/2 FISHER'S SUPER-EXCHANGE ANTIFERROMAGNET**L. Gálisová¹ and J. Strečka²¹*Department of Applied Mathematics and Informatics, Faculty of Mechanical Engineering, Technical University, Letná 9, 042 00 Košice, Slovakia*²*Institute of Physics, Faculty of Science, P. J. Šafárik University, Park Angelinum 9, 040 01 Košice, Slovakia*

The present work deals with magnetocaloric properties of the exactly solved spin-1/2 Fisher's super-exchange antiferromagnet [1], i.e. the spin-1/2 Ising model on a decorated square lattice, in which the antiferromagnetic (ferromagnetic) coupling J on horizontal (vertical) bonds and the external magnetic field H acting on the decorating spins are supposed. The investigated model provides a valuable paradigmatic example of exactly soluble two-dimensional spin system, which allows us to examine the magnetocaloric effect in a vicinity of the continuous (second-order) phase transition at non-zero magnetic fields.

The magnetocaloric quantities, such as the isothermal entropy change ΔS_T and the adiabatic temperature change ΔT_{ad} , are rigorously calculated by using the Fisher's exact solution for the magnetic entropy [1]. It is shown that the inverse magnetocaloric effect, i.e., negative values of $-\Delta S_T$ and ΔT_{ad} , occurs around the temperature interval $T_c(H \neq 0) < T < T_c(H = 0)$ for any magnetic-field change ΔH : $0 \rightarrow H$. If $\Delta H \in (0, J)$, the observed inverse magnetocaloric effect increases and shifts to lower temperatures upon the increase of the magnetic-field variation ΔH . By contrast, the inverse magnetocaloric effect is reduced with increasing the field change ΔH for any $\Delta H > J$. The most pronounced inverse magnetocaloric effect is found for the magnetic-field change $\Delta H = J$, which exactly coincides with the critical field $H_c = J$ of a zero-temperature phase transition to the paramagnetic ground state. These observations are confirmed by temperature variations of the corresponding adiabatic temperature change ΔT_{ad} . The largest negative adiabatic temperature change ΔT_{ad} can also be detected for $\Delta H = J$.

[1] M. E. Fisher, Proc. Roy. Soc. A 254 (1960) 66, 256 (1960) 502.

P1-10**ISOTHERMAL ENTROPY CHANGE AND ADIABATIC CHANGE OF TEMPERATURE DURING THE MAGNETIZATION PROCESS OF THE ISING OCTAHEDRON AND DODECAHEDRON**K. Karl'ová¹, J. Strečka¹ and T. Madaras²¹*Department of Theoretical Physics and Astrophysics, Faculty of Science, P. J. Šafárik University, Park Angelinum 9, 040 01 Košice, Slovak Republic*²*Department of Discrete Mathematics, Faculty of Science, P. J. Šafárik University, Park Angelinum 9, 040 01 Košice, Slovak Republic*

A recent systematic study of the regular Ising polyhedra has evidenced a giant magnetocaloric effect during the magnetization process of the Ising octahedron and dodecahedron, which occurs in a vicinity of zero magnetic field due to an absence of zero magnetization plateau and an abrupt magnetization jump [1]. In the present work we will rigorously examine temperature dependences for the isothermal entropy change and the adiabatic change of temperature of the Ising octahedron and dodecahedron, which can be viewed as their two basic magnetocaloric response functions.

The Ising octahedron and dodecahedron generally exhibit a large negative isothermal entropy change upon increasing of the magnetic field, which serves in evidence of their cooling performance during the adiabatic demagnetization. The working temperature interval with the large magnetocaloric effect monotonically increases with increasing of the magnetic-field change until the midpoint of the first magnetization plateau is reached. The largest isothermal entropy change can be found whenever the field change is greater than the saturation field of the relevant Ising spin cluster.

The adiabatic change of temperature confirms an outstanding cooling capability of the Ising octahedron and dodecahedron, which may reach during the adiabatic demagnetization absolute zero temperature. The Ising octahedron and dodecahedron can be therefore regarded as promising frustrated spin structures for magnetic refrigerators, whereas the maximum of the adiabatic change of temperature shifts to higher initial temperatures with increasing the magnetic-field change.

This work was financially supported by ERDF EU (European Union European regional development fond) grant provided under the contract No. ITMS26220120005 (activity 3.2).

[1] J. Strečka, K. Karl'ová, T. Madaras, Physica B 466 (2015) 76-85.

P1-11**SELF-CONSISTENT MODEL OF A SOLID FOR THE LATTICE AND MAGNETIC PROPERTIES DESCRIPTION**T. Balcerzak¹, K. Szałowski¹ and M. Jaščur²¹*Department of Solid State Physics, Faculty of Physics and Applied Informatics, University of Łódź, ulica Pomorska 149/153, PL 90-236 Łódź, Poland*²*Department of Theoretical Physics and Astrophysics, Faculty of Science, P. J. Šafárik University, Park Angelinum 9, 041 54 Košice, Slovak Republic*

In the paper, a self-consistent theoretical description of the lattice and magnetic properties of a model system is presented. The framework is based on summation of the Gibbs free energies for lattice subsystem [1,2], complemented with the energy of magnetic subsystem. The lattice energy is composed of elastic contribution stemming from the Morse interatomic potential and of vibrational contribution taken within Debye approximation. The anharmonicity is included by means of deformation-dependent Grüneisen parameter [2]. The magnetic energy is derived using the Mean Field Approximation for the system with localized spins. The power law dependence of exchange integral on the distance between interacting spins is assumed, which couples the magnetic subsystem and the lattice one. On the basis of minimization principle for the Gibbs energy, a set of coupled equations of state (EOS) for the entire system is derived. These EOS combine the parameters describing the elastic properties (volume deformation) and magnetic properties (magnetization) with such independent parameters as temperature, external magnetic field and external pressure.

The formalism is extensively illustrated with the numerical calculations performed for a model system of ferromagnetically coupled spins $S=1/2$, localized at the sites of simple cubic lattice. In particular, significant influence of the magnetic subsystem on the elastic properties is demonstrated. It manifests itself in modification of such quantities as the volume deformation, thermal expansion coefficient or isothermal compressibility. The effect is most noticeable in the vicinity of magnetic phase transition. On the other hand, the influence of lattice subsystem on the magnetic one is also evident. It is illustrated, for example, by the dependence of critical (Curie) temperature, magnetization and the magnetic response functions on the external pressure, as well as on the parameters of elastic interatomic interactions.

[1] T. Balcerzak, K. Szałowski, M. Jaščur, J. Phys. Condens. Matter 116 (2014) 043508.

[2] T. Balcerzak, K. Szałowski, M. Jaščur, J. Appl. Phys. 22 (2010) 425401.

P1-12**FRACTIONAL SCALING OF MAGNETIC COERCIVITY IN ELECTRICAL STEELS**M. Najgebauer¹*¹Faculty of Electrical Engineering, Czestochowa University of Technology,
al. Armii Krajowej 17, 42-200 Czestochowa, Poland*

A scaling hypothesis was first postulated by B. Widom on the basis of phenomenological grounds. It provides data collapse and a relation between critical exponents, what allows reducing the number of independent parameters characterizing the critical behavior.

Scaling and data collapse are usually used to analyze critical phenomena and phase transitions. However, these can also be applied to analyze phenomena far from the critical point, e.g. magnetization processes.

The Widom scaling has been successfully applied in analysis of power losses for various types of soft magnetic materials. Some attempts to apply scaling and data collapse to analyze magnetic coercivity have also been undertaken. However, the obtained results of coercivity scaling were not satisfactory.

In the paper, a new approach to scaling of magnetic coercivity based on the fractional procedure is presented. In the case of fractional scaling, exponents of all scaled variables are fractional numbers in spite of previously used scaling, where exponents of some scaled variables are integer numbers. Therefore, the fractional scaling provides more flexible expressions describing analyzed phenomena. The fractional scaling of magnetic coercivity is examined for electrical steels with different internal structure as non-oriented, grain-oriented and microcrystalline ones. Experimental data, subjected to the fractional scaling, include frequency dependencies of magnetic coercivity measured at various levels of maximum magnetic induction. For each sample, a family of measured coercivity dependencies is collapsed onto a single, universal curve. These results might be considered as a confirmation of scaling behavior of magnetic coercivity in electrical steels.

The obtained results of the fractional scaling of coercivity are promising. These results also indicate the possibility of using the fractional scaling for coercivity modeling. However, this assumption requires further research.

P1-13**THEORETICAL STUDY OF THE FRUSTRATED ISING ANTIFERROMAGNET ON THE HONEYCOMB LATTICE**A. Bobák¹, T. Lučivjanský^{1,2}, M. Žukovič¹, M. Borovský¹ and T. Balcerzak³¹*Institute of Physics, P.J. Šafárik University, Park Angelinum 9, 041 54 Košice, Slovak Republic*²*Fakultät für Physik, Universität Duisburg-Essen, Lotharstraße 1, D-47048 Duisburg, Germany*³*Department of Solid State Physics, University of Łódź, Pomorska 149/153, PL 93-414 Łódź, Poland*

Since a honeycomb lattice antiferromagnet with only nearest-neighbour (nn) interactions ($J_1 < 0$) is considered as a bipartite lattice, the ground state exhibits long-range ordering. However, the system is rather fragile against the onset of frustrating interactions. In recent years, therefore, it has become of great interest to investigate the corresponding model where the nn bonds are augmented by frustrating next-nearest-neighbour bonds with the strength $J_2 < 0$, possibly also in conjunction with next-next-nearest-neighbour bonds of the strength $J_3 < 0$. The resulting spin-1/2 J_1 - J_2 - J_3 Ising antiferromagnet on the honeycomb lattice in a special case when $J_3 = 0$ has been investigated in a previous study by present authors [1].

In this paper we study effects of the J_3 interaction on critical properties (or phase diagram) of the frustrated spin-1/2 J_1 - J_2 - J_3 Ising model on the honeycomb lattice by using the same effective-field theory with correlations as in Ref. [1]. We present results for the ground-state energy, the finite temperature phase diagram and the temperature dependence of the order parameter, in an attempt to provide even more information about the model. In particular, we find that when $J_3 \neq 0$ there is a region in which the frustrated honeycomb lattice antiferromagnet exhibits a tricritical point, at which the phase transition changes from the second order to the first one on the line between antiferromagnetic and paramagnetic phases. On the other hand, a similar tricritical behaviour does not exist in the spin-1/2 J_1 - J_2 model (i.e., when $J_3 = 0$) by using the same effective-field approach.

This work was supported by the Scientific Grant Agency of Ministry of Education of Slovak Republic (Grant VEGA No.1/0331/15). The authors acknowledge the financial support by the ERDF EU (European Union European regional development fund) grant provided under the Contract No. ITMS26220120005 (activity 3.2).

[1] A. Bobák, T. Lučivjanský, M. Žukovič, M. Borovský, T. Balcerzak, Phys. Lett. A (in press).

P1-14**DEPENDENCE OF "LIFETIME" OF THE SPIRAL MAGNETIC DOMAIN ON THE MATERIAL PARAMETERS**V. N. Mal'tsev¹ and A. A. Nesterenko¹¹*Institute of Natural Sciences, Ural Federal University, Mira Street 19, 620002 Yekaterinburg, Russia*

Spiral magnetic domains (SD) are a fairly common type of domain structure. It can be formed as a result of the quasi-static process, and as a result of the dynamic magnetization reversal. For example, stable spiral dynamic domains were formed under certain conditions in iron garnet films with perpendicular anisotropy, if they had been placed in the alternating magnetic field (frequency~ 0.1-30 kHz), i.e. a complete magnetization reversal of films does not occur [1]. Feature of SD is that it combines the properties of the bubble magnetic domain and stripe magnetic domain. However, until now there is not any theoretical description of dynamic SD, and there is not any explanation why in some films SD garnets occur, but not in others. We have developed a model of SD, in which it is possible to calculate the changing in the domain width - d , the spiral period - p , the outer spiral size - f and the size of the inner core - a during "lifetime» of SD. SD stability we associate with the SD "lifetime»: the bigger it is, the more stable SD. Two cases were considered: in static one when SD relaxes to its equilibrium state in the absence of an external field, and the dynamic one, in which the effect of an external field on the SD "lifetime» was investigated. The calculations were performed for the material parameters used in the experiments [1]. Calculations have shown that in the absence of field the equilibrium SD exists for a fairly wide range of values of p , but this interval is very narrow for films in which dynamic SDs were not observed. It has been found that in the general case, there is only one equilibrium value f for SD, but in films in which the dynamic SDs are formed, two values of the equilibrium f exist. Furthermore, it was found that if the size of the inner spiral core can be changing, SD becomes less stable, as reported in [1]. Research of dependencies of "lifetime" on the parameters of the material showed that all films with a stable dynamic SD have small values of magnetization and large values of the characteristic length of the film (in relation to film thickness).

[1] Kandaurova G. S. (2002), *Phys. Usp.* 45 1051–1072.

P1-15**ULTRAFAST SPIN TRANSFER TORQUE GENERATED BY A FEMTOSECOND LASER PULSE**P. Baláž¹, K. Carva¹, P. Maldonado² and P. Oppeneer²¹*Department of Condensed Matter Physics, Faculty of Mathematics and Physics, Charles University, Ke Karlovu 5, CZ-12116 Prague 2, Czech Republic*²*Department of Physics and Astronomy, Uppsala University, Box 516, SE-75120 Uppsala, Sweden*

Ultrafast demagnetization induced by a laser pulse is a distinctive physical phenomenon interesting from applicational as well as theoretical point of view. It is already well established knowledge that a laser impulse can substantially reduce magnetization on a femtosecond time-scale. Theoretically, this feature has possibly been explained as a consequence of spin relaxation via phonon and magnon scattering [1]. Another remarkable mechanism of ultrafast demagnetization becomes available in magnetic multilayers consisting of transition metals and/or their alloys featuring spin polarized 3d valence band and conduction 4s band. In this case an ultrashort laser pulse excites electrons occupied the d band into the s band, which is characterized by higher electron mobility. As a result of nonequilibrium situation due to laser heating, the hot charge carriers move away from the heated spot and remarkably reduce the local magnetic moment. This process is described by a superdiffusive spin transport model [2]. An important feature for the research in the field of spintronics is that this mechanism results in ultrafast generation spin currents which emerge in an adjacent nonmagnetic layer. Consequently, the spin current of hot electrons can exert spin transfer torque on another magnetic layer in a multilayer structure, as recently observed in experiments [3].

In this work, we study the the spin transfer torque and magnetization dynamics induced by a spin current of hot electrons excited by femtosecond laser pulse. The superdiffusive transport model has been generalized to noncollinear magnetic configurations to be applied to spin valve structures with laser heated fixed magnetic layer.

[1] B. Koopmans et al., *Nature Mat.* 9, 259 (2010).

[2] M. Battiato, K. Carva, P. Oppeneer *Phys. Rev. Lett.* 105, 027203 (2010); *Phys. Rev. B* 86, 024404 (2012).

[3] A.J. Schellekens, K.C. Kuiper, R.R.J.C. de Wit, B. Koopmans, *Nature Comm.* 5, 4333 (2014); G.-M. Choi, B.-Ch. Min, K.-J. Lee, D.G. Cahill, *Nature Comm.* 5, 4334 (2014).

P1-16**THERMAL ENTANGLEMENT AND QUANTUM NON-LOCALITY
ALONG THE MAGNETIZATION CURVE OF THE SPIN-1/2 ISING-
HEISENBERG TRIMERIZED CHAIN**J. Pavličko¹ and J. Strečka¹*¹Department of Theoretical Physics and Astrophysics, Faculty of Science,
P. J. Šafárik University, Park Angelinum 9, 040 01 Košice, Slovak Republic*

The spin-1/2 Ising-Heisenberg trimerized chain in a presence of external magnetic field is exactly solved using the decoration-iteration transformation and transfer-matrix method [1]. The magnetization curve exhibits two intermediate magnetization plateaus at zero and one-third of the saturation magnetization, which correspond to two unusual quantum ground states with antiferromagnetic and ferrimagnetic character [1]. To bring an insight into quantum features of the investigated spin-chain model, we have exactly calculated the concurrence and Bell function that quantify a degree of the quantum entanglement and quantum nonlocality at zero as well as nonzero temperatures.

It is demonstrated that the zero-temperature magnetization jumps between the intermediate magnetization plateaus are also reflected in the respective field-induced changes of the concurrence and Bell function. More strikingly, the concurrence and Bell function are both increasing when the magnetic field drives the investigated spin chain towards the intermediate one-third magnetization plateau what is in contrast with general expectations. Although the sudden changes of the concurrence and Bell function are mostly smoothened upon increasing temperature, the rising temperature may alternatively lead to an increase of the thermal entanglement and quantum non-locality close to the magnetization jump towards the intermediate one-third magnetization plateau. The threshold temperature for a disappearance of the thermal entanglement and quantum non-locality is examined in detail as a function of the magnetic field and the relative ratio between two different coupling constants.

This work was financially supported by ERDF EU (European Union European regional development fond) grant provided under the contract No. ITMS26220120005 (activity 3.2).

[1] J. Strečka, M. Jaščur, J. Phys.: Condens. Matter. 15 (2003) 4519.

P1-17**STRONG-COUPLING APPROACH TO THE SPIN-1/2
ORTHOGONAL-DIMER CHAIN**T. Verkholyak¹ and J. Strečka²*¹Institute for Condensed Matter Physics, NASU, 1 Svientsitskii Street, 79011 L'viv, Ukraine**²Institute of Physics, Faculty of Science, P. J. Šafárik University, Park Angelinum 9, 04001 Košice, Slovakia*

Magnetic properties of the spin-1/2 Heisenberg orthogonal-dimer chain are calculated within the perturbative approach, which is elaborated when starting from the exactly solved spin-1/2 Ising-Heisenberg orthogonal-dimer chain with the Heisenberg intradimer and Ising interdimer interactions. Although the latter model lacks the quantum XY part of the interdimer coupling in comparison with the fully Heisenberg model, both models exhibit some common features as intermediate plateaux at one-quarter and one-half of the saturation magnetization. More subtle behaviour like an infinite series of plateaux between one-quarter and one-half, as well as the spin-liquid phase above one-half plateau is not reproduced by the simplified Ising-Heisenberg model.

We treat the quantum XY part of the interdimer interaction within the many-body perturbation theory for degenerate states to restore some features of the magnetization curve of the pure Heisenberg model when starting from the exactly solved Ising-Heisenberg model. It is shown how quantum perturbation may create a series of fractional plateaux in the Heisenberg orthogonal-dimer chain. Moreover, the perturbation theory leads to the effective quantum model at the boundary between the one-half plateau and saturated phase, where a continuous change of the magnetization emerges due to an existence of the quantum spin-liquid phase for the effectively coupled horizontal dimers.

P1-18**STUDY OF AXIAL DIMENSION OF STATIC HEAD-TO-HEAD DOMAIN BOUNDARY IN AMORPHOUS GLASS-COATED MICROWIRE**M. Kladivová¹, J. Ziman¹, J. Kecer¹ and P. Duranka¹¹*Department of Physics, Technical University of Košice, Park Komenského 2, 042 00 Košice, Slovakia*

The dynamics of a single domain wall in so-called bistable microwires has been the subject of many studies. However, many questions about the structure and dimension of this type of domain wall still remain open. Most authors dealing with this subject deduce the shape and dimension of this wall from the analysis of voltage peaks induced in Sixtus-Tonks experiments [1]. The information obtained from this analysis is about a moving wall. The properties of the pick-up coil and stray field around this type of domain boundary have to be taken into account for correct interpretation of the results obtained in this way.

In our contribution a new experiment allowing the study of static domain boundary dimensions in bistable microwire is described. In this experiment a static domain boundary is created by an inhomogeneous axial magnetic field. The changes of axial magnetic flux due to the presence of this boundary were measured along the microwire using two pick-up coils. Experimental results were compared with a simple theoretical model. For $\text{Fe}_{77.5}\text{Si}_{15}\text{B}_{7.5}$ microwire with total diameter of 30 μm and metal nucleus diameter of 15 μm , good agreement between theoretical and experimental data was obtained for axial dimension of the domain boundary of about $200 \times$ diameter of the wire metallic core.

- [1] Gudoshnikov, S. A., Grebenshchikov, Yu. B., Ljubimov, B. Ya., Palvanov, P. S., Usov, N. A., Ipatov, M., Zhukov, A. and Gonzalez, J. (2009), Ground state magnetization distribution and characteristic width of head to head domain wall in Fe-rich amorphous microwire. *Phys. Status Solidi A*, 206: 613–617. doi: 10.1002/pssa.200881254.

P1-19**THEORETICAL INVESTIGATIONS ON THE STRUCTURAL, MAGNETIC AND ELECTRONIC PROPERTIES OF $\text{Fe}_{2-x}\text{MnGe}:\text{Cu}_x$ ALLOY**K. Gruszka¹ and M. Nabiałek¹*¹Institute of Physics, Częstochowa University of Technology,
Armii Krajowej av. 19, 42-200 Częstochowa, Poland*

The paper presents results of theoretical investigations on the structural, magnetic and electronic properties of $\text{Fe}_{2-x}\text{MnGe}:\text{Cu}_x$ Heusler alloy focusing on the role of iron-copper substitution effects on selected parameters. The calculations were performed on the basis of the density functional theory approach using the plane-wave basis set. The substitution of $[\text{Ar}]4s^1 3d^{10}$ copper in place of $[\text{Ar}]4s^2 3d^6$ iron site was investigated.

Among the many interesting properties exhibited by those alloys such as shape memory effect, half-metallicity, magnetoresistance etc. they also demonstrate significant sensitivity to various doping affecting their magnetic characteristics such as magnetic ordering or total magnetic moment, often demonstrating the Slater-Pauling behavior.

P1-20**MAGNETIZATION CURVES OF GEOMETRICALLY FRUSTRATED EXCHANGE-BIASED FM-AFM BILAYERS**M. Pankratova¹ and M. Žukovič¹¹*Institute of Physics, P. J. Šafárik University in Košice, Park Angelinum 9, 040 01 Košice, Slovakia*

We study the exchange bias phenomenon (EB) and magnetization curves of the geometrically frustrated ferromagnetic-antiferromagnetic (FM-AFM) bilayers. The EB manifests itself in the shift of the magnetization dependence along the field axis. This effect has been widely studied in the FM-AFM bilayers but still has no comprehensive explanation. The impact of the geometrical frustration on the EB in such bilayer systems has been little studied so far.

The problem is considered in the planar Heisenberg model with periodic boundary conditions. In particular, we consider a FM-AFM bilayer made of two monolayers on a triangular lattice. The exchange interaction through the FM-AFM interface is assumed to be ferromagnetic. In addition to the strong easy-plane anisotropy of the model we also consider the presence of single-ion anisotropies in both the AFM and FM layers.

Magnetization curves as the external magnetic field functions have been obtained for the above described bilayer. In addition, we have considered a so-called frozen AFM when the AFM layer in the FM-AFM bilayer is magnetically hard: the magnetic structure in the magnetic fields that are less than the spin-flop transition is fixed during the entire magnetization process. Hysteresis loops have been obtained for different values of the exchange interaction and the single-ion anisotropy. Horizontal plateaus and a splitting of the hysteresis loop are observed in both cases. We have shown that the horizontal plateaus correspond to the antiparallel states in the FM-AFM bilayer. Phase diagrams have been calculated for both the frozen and non-frozen AFM cases.

The EB is observed in the case of the frozen AFM layer. The cause of the shift of the hysteresis loop in this case is the uncompensated AFM interface and pinned AFM magnetic moments. However, for some values of the single-ion anisotropy, in the non-frozen case, we obtain the split of the hysteresis loop when one part of the curve has a positive bias while the second part is shifted in the negative direction.

Acknowledgments: This work was supported by the Scientific Grant Agency of Ministry of Education of Slovak Republic (Grant No. 1/0331/15). The author acknowledge the financial support by the ERDF EU (European Union European Regional Development Fund) grant provided under the contract No. ITMS26220120005 (activity 3.2).

P1-21**ENHANCED MAGNETOCALORIC EFFECT DUE TO SELECTIVE DILUTION IN A TRIANGULAR ISING ANTIFERROMAGNET**M. Borovský¹ and M. Žukovič¹¹*Institute of Physics, P. J. Šafárik University in Košice, Park Angelinum 9, 040 01 Košice, Slovak Republic*

An Ising antiferromagnet on a triangular lattice is a classical and the simplest example of a geometrically frustrated spin system. Due to the inability of the system to simultaneously minimize local energy contributions of all couplings it exhibits infinite-fold degeneracy in the ground state and non-zero residual entropy [1].

In our previous work [2], we showed that perturbations in the form of an external magnetic field and a selective dilution with non-magnetic impurities, applied to only one of the three sublattices, can relieve the degeneracy and may lead to long-range ordering in the system. However, relieving the massive degeneracy is also related to considerable entropic changes, which are relevant in a magnetocaloric effect.

In the present study, we employ an effective-field theory with correlations [3] to investigate the effect of the selective dilution on magnetocaloric properties of the system at moderate external fields. When the field is increased from zero to finite values in a non-diluted case, one can observe at low temperatures a negative isothermal entropy change $\Delta S \approx -S_0$, where S_0 is the Wannier's zero-field residual entropy value. For some range of temperatures, an increasing temperature is found to increase the magnitude of ΔS and to shift its maximum to higher fields. We show, that by applying a relatively small selective dilution the magnitude of ΔS can be further increased and thus the magnetocaloric effect enhanced. The fact that the maximum isothermal entropy changes are achieved at still moderate fields and relatively high temperatures gives such a system potential for practical application as a near room temperature magnetic refrigerator.

Acknowledgments: This work was supported by the Scientific Grant Agency of Ministry of Education of Slovak Republic (Grant No. 1/0331/15). The author acknowledge the financial support by the ERDF EU (European Union European Regional Development Fund) grant provided under the contract No. ITMS26220120005 (activity 3.2).

[1] G.H. Wannier, Phys. Rev. 79 (1950) 357.

[2] M. Borovský, M. Žukovič and A. Bobák, Physica A 392 (2013) 157.

[3] T. Kaneyoshi, Acta Phys. Polon. A 83 (1993) 703.

P1-22**MOKE STUDY OF THE DOMAIN WALL DYNAMICS IN MAGNETIC MICROWIRES**O. Váhovský¹ and R. Varga¹¹*Institute of Physics, Faculty of Sciences, P. J. Safarik University, Park Angelinum 9, 041 54 Kosice, Slovakia,*

Controlled manipulation of a single domain wall and its dynamic properties has become of great interest in the light of possible applications. Prototypes of logic devices based on encoding information in a position of the domain wall in ferromagnetic wires (composed of sputter-deposited thin films on a Si substrate) has been shown [1]. Apart from magnetic logic, other promising applications are magnetic domain – wall memories. Such is racetrack memory comprised of magnetic nanowires, where motion of domain walls is controlled by current pulses [2]. In any case, the speed of such devices depends on the domain wall velocity that propagates along the wire.

Classically, the domain wall velocity is measured by induction method. However, many problems appears when fast domain wall velocity should be measured. The problems appear due to the relatively large relaxation time of pick-up coils. Hence, application of Kerr-effect-based measuring methods is desirable, since they have much shorter relaxation times and the results are comparable [3, 4]. In the given contribution, we present the Kerr-effect-based system for study of the domain wall dynamics in glass-coated microwires that are characterized by fast domain wall propagation. Apart from simple domain wall propagation, we present the different effect that influence the domain wall velocity as a result of complex stress and defect distribution in glass-coated microwires

Acknowledgment

This research was supported by the projects APVV-0027-11, Slovak VEGA grant. No. 1/0164/16 and ITMS 26220120019.

- [1] Currivan-Incorvia, J. A. et al.: Logic circuit prototypes for three-terminal magnetic tunnel junctions with mobile domain walls. Nat. Commun. 7:10275 doi: 10.1038/ncomms10275 (2016).
- [2] Parkin, S. S. P. – Hayashi, M. – Thomas, L.: Magnetic Domain-Wall Racetrack Memory, Science 320, (2008).
- [3] Tibu, M. – Lostun, M. – Ovari, T. A. – Chiriac, H.: Simultaneous Magneto-optical Kerr Effect and Sixtus-Tonks Method for Analyzing the Shape of Propagating Domain Walls in Ultrathin Magnetic Wires, Rev. Sci. Instr. 83, 064708 (2012).
- [4] Chizhik, A. – Varga, R. – Zhukov, A. – Gonzalez, J. – Blanco, J. M.: Kerr-effect Based Sixtus-Tonks Experiment for Measuring the Single Domain Wall Dynamics, J. Appl. Phys. 103, 07E707 (2008).

P1-23**MIXED SPIN-1/2 AND SPIN 3/2 ISING MODEL WITH THREE-SITE FOUR-SPIN INTERACTIONS ON A DECORATED TRIANGULAR LATTICE**V. Štubňa¹ and M. Jaščur¹*¹Department of Theoretical Physics and Astrophysics, Institute of Physics, Faculty of Science, P. J. Šafárik University in Košice, Park Angelinum 9, 040 01 Košice, Slovakia*

Exactly solvable models of magnetic systems have considerable value for their deep insight into physical properties from the fundamental point of view. The exact analytical approach allows one to accurately identify key microscopic properties affecting the behaviour of systems at the macroscopic level. Unlike of other physical systems, the localized spin models are particularly suitable for the investigation of many-body interactions. For this reason, we will study in this work the mixed spin-1/2 and spin-3/2 Ising model on a decorated triangular lattice, where except of the conventional pair interaction, the multi-spin term involving three nearest-neighbour spins is taken into account. Influence of a single ion anisotropy is also included. Using a generalized decoration-iteration transformation, we obtain exact analytical results for all relevant physical quantities of the system. Numerical results for the ground state, phase diagrams, magnetization, heat capacity and entropy will be analysed and discussed in detail.

P1-24**CRITICAL DYNAMICS OF PLANAR MAGNETS: RENORMALIZATION GROUP ANALYSIS**M. Dančo^{1,2}, M. Hnatič^{1,2,3} and T. Lučivjanský^{3,4}¹*Institute of Experimental Physics, SAS, Košice, Slovakia*²*Joint Insitute for Nuclear Research, Dubna, Russia*³*Faculty of Sciences, P.J. Šafarik University, Košice, Slovakia*⁴*Fakultät für Physik, Universität Duisburg-Essen, D-47048 Duisburg, Germany*

The renormalization group method is applied to two-field symmetric (asymmetric) planar spin model E (model F) of critical dynamics, whose behavior near the phase transition point belong to the same universality class as that of superfluid helium. The true effective model, which results from the first microscopic principles, is the F model based on the Langevin equation with specific hydrodynamic modes and the model E is its simplified counterpart in fixed point of the renormalization group (RG). The proof of this correspondence is based on the approach within the framework of which the small-scale chaotic motion is considered as a random force, i.e., as white noise, while the equations of motion are written for large-scale motion in the basin of this noise. The RG functions, critical exponents and critical dynamical exponent z , which determines the growth of the relaxation time near the critical point, have been calculated in the two-loop approximation in the framework of ε -expansion.

I2-01**STRUCTURAL ORIGIN OF CREEP INDUCED MAGNETIC ANISOTROPY OF AMORPHOUS ALLOYS**M. Ohnuma¹, P. Kozikowski², G. Herzer² and C. Polak²¹*Faculty of Engineering, Hokkaido University, 060 8628 Sapporo, Japan*²*Vacuumschmelze GmbH & Co. KG, D-63450 Hanau, Germany*

Creep-induced magnetic anisotropy of amorphous alloys has been known since 1970's and commercially used for magnetic sensors etc.. The structural origin of the magnetic anisotropy, however, was not clear till recently. Using X-ray diffraction technique with transmission mode, we found the structural anisotropy as the difference of peak positions along and perpendicular to the applied stress directions in several amorphous alloys with different compositions of Fe-based, Ni-based and Co-based systems. The results indicate that elastic strain was introduced and remained after releasing the stress. In addition, it is succeeded to observe strain releasing by second annealing after the first creep annealing. This strain relaxation process has been observed by both XRD and dilatometry measurements. Interestingly, the maximum rate of strain releasing is observed at about the temperature of the first creep annealing. The residual strain and „temperature memory" effects strongly suggest that the structural heterogeneity with different relaxation temperatures exist in amorphous structure and they do not change even after the first annealing process.

I2-02**DEVELOPMENT OF SELECTED AMORPHOUS AND NANOCRYSTALLINE SOFT MAGNETIC SYSTEMS WITH ENHANCED FUNCTIONAL PROPERTIES**

P. Svec¹, I. Janotova¹, J. Zigo¹, I. Matko¹, D. Janickovic¹, J. Marcin², I. Skorvanek² and P. Svec Sr.¹

¹*Institute of Physics, Slovak Academy of Sciences, Bratislava, Slovakia*

²*Institute of Experimental Physics, Slovak Academy of Sciences, Kosice, Slovakia*

Selected results will be presented on formation, structure and properties of two new alloy systems based on Fe-B with additions of Co, Cu, C, P, Sn and other elements. Successful compositional and processing design has lead to a new class of so-called NANOMET alloys based on Fe-Co-Si-B-P-Cu/C which fulfill requirements on modern soft magnetic materials, especially demands for high saturation magnetization while preserving low coercivity. The second promising alloy system developed recently is based on Fe-Sn-B. Here the nanostructure-forming and stabilizing effect due to the presence of Nb or Zr in NANOPERM and HITPERM alloys and addition of small amounts of Cu in FINEMET alloys, namely nanograin size control, is obtained by addition of Sn. Enhanced functionality will be presented in systems of rapidly quenched alloys with increased thickness achieved by layering during preparation or by combination of layers with different compositions. Added value of such materials will be presented on specific cases of applications.

O2-01**INFLUENCE OF ANNEALING CONDITIONS ON THE MAGNETIC PROPERTIES OF $\text{Fe}_{73.5}\text{Cu}_1\text{Nb}_3\text{Si}_{13.5}\text{B}_9$ GLASS-COATED NANOWIRES**

S. Corodeanu¹, T. A. Óvári¹, G. Stoian¹, L. C. Whitmore¹, H. Chiriac¹ and N. Lupu¹

¹National Institute of R&D for Technical Physics, 700050 Iași, Romania

Amorphous and nanocrystalline glass-coated magnetic nanowires have been recently prepared by means of rapid solidification [1]. Here we report on the evolution of the magnetic properties (B-H loop, coercivity, axial permeability) and domain wall velocity with the annealing conditions (time - t_a and temperature - T_a) in $\text{Fe}_{73.5}\text{Cu}_1\text{Nb}_3\text{Si}_{13.5}\text{B}_9$ glass-coated nanowires and submicron wires with metallic nucleus diameters between 100 and 500 nm and the glass coating thickness of 5 μm . The aim was to study the dependence of their magnetic behavior on the structural changes induced by annealing at T_a from 250 to 650°C and various annealing times (5 min $\leq t_a \leq$ 60 min).

The microstructure evolves into a nanocrystalline one (α -Fe embedded into the residual amorphous matrix), as evidenced by HRTEM images, once the annealing temperature and time are increasing to 550÷600°C and 60 min., respectively. The nanograins distribution is more uniform in thinner samples, independent of the annealing conditions. All samples are magnetically bistable, irrespective of dimensions and annealing conditions. The maximum relative permeability of the 450 nm sample begins to saturate at 600°C, while for the thinner ones, a larger T_a is required to reach their maxima. Thinner samples also require longer annealing times to get their permeability saturated, since much larger stresses induced by the thick glass coating in the ultrathin metallic nucleus need to be relieved. A similar evolution has been observed for the coercivity, with larger values obtained for thinner nanowires, due to the larger anisotropy induced by the thicker glass coating. Maximum wall velocities, $v > 2000$ m/s, are measured in the annealed nanowires as a result of the nanocrystalline phase formation, this evolution being strongly dependent on the diameter of the samples, as well as on T_a and t_a , since domain walls move faster in the nanocrystalline state due to the smaller effective magnetic anisotropy.

Work supported by the NUCLEU Programme (PN 16 37 02 02). L.C. Whitmore acknowledges the financial support by the European Commission (FP7-REGPOT-2012-2013-1, Grant Agreement no. 316194, NANOSENS).

[1] H. Chiriac, S. Corodeanu, T.A. Óvári, and N. Lupu, J. Appl. Phys. 113 (2013) 17A329.

O2-03**Co₂FeX (X = Al, Si) HEUSLER COMPOUNDS PREPARED BY PLANAR FLOW CASTING AND ARC MELTING METHODS: MICROSTRUCTURE AND MAGNETISM**

A. Titov^{1,2}, O. Zivotsky¹, Y. Jiraskova², J. Bursik², A. Hendrych¹ and D. Janickovic³

¹*Department of Physics, VSB-Technical University of Ostrava, 17.listopadu 15, 708 33 Ostrava-Poruba, Czech Republic*

²*Institute of Physics of Materials, AS CR, Žitkova 22, 616 62 Brno, Czech Republic*

³*Institute of Physics, Slovak Academy of Sciences, Dubravská cesta 9, 845 11 Bratislava, Slovakia.*

Ferromagnetic Co₂FeX (X = Al, Si) Heusler compounds are often prepared in a form of thin films and applied mainly in spintronics. This paper is devoted to these alloys produced by non-traditional technologies: planar flow casting and arc melting in a protective argon atmosphere. This resulted in thin ribbons and small button-type ingots which were subsequently cut into thin discs and polished. The assessment of an influence of technologies on the structural/compositional and magnetic properties is the main goal of present study.

The chemical stoichiometry of both alloys was checked by energy dispersive X-ray spectroscopy and the structure morphology by scanning electron microscopy. Slight differences are visible between studied compositions as concerns both chemical homogeneity and crystal size. The X-ray patterns analysis has yielded lattice constants (0.557±0.001) nm and (0.573±0.001) nm for the Co₂FeSi and Co₂FeAl, respectively. The topography and surface mapping were analyzed by atomic force microscopy.

The surface and bulk magnetic properties were investigated by magneto-optical Kerr effect and vibrating sample magnetometer. Results obtained from the bulk hysteresis curves show nearly the same values of coercivity for both ribbons and discs; namely 120 A/m for Co₂FeAl and 1 kA/m for Co₂FeSi, unlike the saturation magnetization being by about 10 Am²/kg higher for ribbons, 151 Am²/kg for Co₂FeAl and 160 Am²/kg for Co₂FeSi, as compared to discs. The surface magnetic behavior of the discs indicates a marked increase of coercivity determined by the surface magnetic anisotropy inside the grains and on the grain boundaries for both compositions. Contrary to the rough surfaces of the ribbons, the smooth polished surfaces of the discs allowed us supplemental magnetic domain observations using the magneto-optical Kerr microscopy and magnetic force microscopy.

O2-04**EFFECTS OF SWIFT HEAVY-IONS ON Fe-BASED METALLIC GLASSES STUDIED BY SYNCHROTRON DIFFRACTION**S. Michalik¹, M. Pavlovic², J. Gamcova³, P. Sovak³ and M. Miglierini^{2,4}¹*Diamond Light Source Ltd., Harwell Science and Innovation Campus, Didcot, Oxfordshire OX11 0DE, UK*²*Faculty of Electrical Engineering and Information Technology, Slovak University of Technology, Ilkovicova 3, 812 19 Bratislava, Slovak Republic*³*Institute of Physics, Faculty of Science, P.J. Safarik University, Park Angelinum 9, 041 54 Kosice, Slovak Republic*⁴*Department of Nuclear Reactors, Czech Technical University in Prague, Prague 180 00, Czech Republic*

Fe-based metallic glasses (MGs) are considered to be radiation hard due to their homogeneous disordered structure. This makes them appropriate materials for applications at which they are exposed to radiation, like in magnetic cores of accelerator radio-frequency cavities. However, some observations indicated that high-energy heavy-ion irradiation did induce changes of their macroscopic magnetic properties. Therefore, it is important to study ion-induced modifications of MGs to understand the physical nature of underlying structural damage on microstructural scale and its impact upon the resulting magnetic properties.

In this work, the influence of U ions (5.9 MeV/u) on the as-prepared Fe-Cu-Nb-Si-B MG was investigated by *in situ* temperature X-ray diffraction of synchrotron radiation. Characteristics of the first diffuse peak (FDP) were used as parameters to describe the structural changes caused by ion irradiation. The FDP broadened as the irradiation fluence increased suggesting a higher degree of disorder. At the same time, its position was faintly shifted to lower values. Ion irradiation has also strongly affected the temperature evolution of the FDP characteristics. We conclude that ion irradiation induces structural rearrangement that, in turn, increases the degree of disorder of the amorphous structure. During heating treatment, structural relaxation and annealing out of this ion-induced degradation takes place. Consequently, the structure is recovered as demonstrated by the behaviour of the FDP broadening.

This work was supported by the grants GACR 14-12499S, VEGA 1/0182/16 and VEGA 1/0036/16.

O2-05**OPTIMISATION OF FRAME-SHAPED FLUXGATE SENSOR'S CORE MADE OF AMORPHOUS ALLOY USING GENERALIZED MAGNETOSTATIC METHOD OF MOMENTS**R. Szewczyk¹ and P. Frydrych²¹*Industrial Research Institute for Automation and Measurements PIAP, Al. Jerozolimskie 202; 02-486 Warsaw, Poland*²*Institute of Metrology and Biomedical Engineering, Warsaw University of Technology ; sw. A. Boboli 8; 02-525 Warsaw, Poland*

Fluxgate sensors utilizing cores made of amorphous alloys ribbons are very promising area of development of miniaturized magnetic field sensors [1]. Such sensors can be easily miniaturized. Moreover, technology of production of cores made of amorphous alloys is cost-effective due to the possibility of use of photolithographic processes. Finally, sensors can be produced using multilayer PCB, what is very useful for industrial applications.

In opposite to race track-shaped cores, fluxgates with the frame-shaped cores [2] enable measurements of 2D magnetic field. However, the shape of frame-shaped core has to be optimised from the point of view of sensor's sensitivity considering the geometry and technology of the sensor.

Unfortunately, commonly used 3D finite elements method is not effective for magnetostatic simulations of thin layers. In the case of this method, reduction of the thickness of the layer causes the radical increase of the number of tetrahedral elements in the layer, leading to lack of technical possibility to carrying out the simulation.

Proposed, thin layer oriented, generalization of the method of moments overcomes this problem. As a result, on the base of the simulations, the optimal geometry of frame-shaped core of fluxgate sensor was determined. Moreover, the thin layers thickness was considered during the optimisation. Finally, the paper presents the practical guidelines for development of frame-shaped, thin layer fluxgate sensors cores made of amorphous alloys.

[1] P. Ripka et al., IEEE Sensors 5 (2005) 433.

[2] P. Frydrych et al., IEEE Trans. Magn. 48 (2012) 1485.

O2-06**SIZE DEPENDENT HEATING EFFICIENCY OF MULTICORE IRON OXIDE PARTICLES IN LOW-POWER ALTERNATING MAGNETIC FIELDS**

I. S. Smolkova¹, N. E. Kazantseva¹, L. Vitkova¹, V. Babayan¹, J. Vilcakova¹ and P. Smolka¹

*¹Centre of Polymer Systems, Tomas Bata University in Zlin,
Trida Tomase Bati 5678, 760 01 Zlin, Czech Republic*

Superparamagnetic (SPM) iron oxide nanoparticles are nowadays finding broad applications in magnetic resonance imaging, drug delivery, cells separation and magnetic hyperthermia cancer treatment. Each of these methods requires nanoparticles with defined magneto-structural properties. Recently a big interest arose in dense aggregates of SPM iron oxide nanoparticles, so called multicore particles as they display ferromagnetic-like behavior due to magnetic interactions between SPM cores. Despite the fact, that their coercivity and remanence are significantly lower than for a particle of comparable size, multicore particles generate large amount of heat under exposure to alternating magnetic field (AMF). This makes them attractive for application in magnetic hyperthermia. However, the mechanisms of magnetization in multicore particles exposed to AMF are not clear. It is established that the main parameters influencing the heating efficiency are multicore particle size, shape and size distribution of SPM cores. Detailed experimental investigations are required with a view to determine the optimal size of multicore particle and the AMF parameters (frequency and amplitude within the allowed medical limits) to obtain maximal heat.

In this study, we demonstrated how hydrodynamic size of multicore particles influences the heating efficiency in AMF at 1048 kHz and 5.8 kA/m. The magnetic cores, i.e. iron oxide nanoparticles of 13 nm size and polydispersity 0.3 were obtained by coprecipitation method. Further peptization procedure allowed to gain aqueous dispersions of multicore particles with different hydrodynamic size from 90 to 180 nm, due to electrostatic stabilization. Multicore particles in aqueous dispersion have saturation magnetization of 40 emu/g_{Fe₃O₄} and coercivity of about 1 Oe regardless of their size. Dispersion of multicore particles with average hydrodynamic size of 180 nm has low stability, and does not heat in AMF. Whereas, the dispersion of 90 nm multicore particles is stable and provides specific loss power of about 30 W/g_{Fe}.

O2-07**LOSS PREDICTION IN 6.5% ELECTRICAL STEELS**J. Szczygłowski¹¹*Faculty of Electrical Engineering, Czestochowa University of Technology,
al. Armii Krajowej 17, 42-200 Czestochowa, Poland*

The high silicon steel is one of the most prospective materials for magnetic circuits in electrical machines operating at increased excitation frequencies, in particular for applications that require low core loss. A statistical model of energy loss in ferromagnets has been advanced by G. Bertotti; its basic assumption was that energy dissipation was the result of eddy currents generated in different time- and spatial scales. It was assumed that the so-called excess loss was controlled in the intermediate scale, i.e. the scale particular to magnetic domains. The domain structure, which undergoes changes during the magnetization process due to domain wall movements, causes variations in the distribution of eddy currents in the materials, what in turn results in excess loss. Domain structure in this model is considered as an ensemble of n so-called magnetic objects (MOs). In the case of grain-oriented steel, the MO is equivalent to a single domain wall, whereas in the case of microcrystalline materials – the whole domain structure within a single grain. Assuming that $n(t)$ is the number of MOs being active during the magnetization process, whereas $H_{exc}(t)$ denotes a fraction of externally applied magnetic field necessary for compensation of the counter-field from eddy currents generated by these MOs, the average value of the excess loss may be represented as $P_{exc} = 1/T \int_0^T H_{exc}(t) \frac{dB(t)}{dt} dt$. Assuming that the excess field is proportional to rate variation of magnetic flux induced by moving MOs, the relationship may be written $H_{exc}(t) = \sigma G S \frac{1}{n(t)} \frac{dB(t)}{dt}$. The dependence $n(t) = g[H_{exc}(t)]$ is necessary to calculate excess loss. The following series $n(H_{exc}(t)) = n_0 + \frac{H_{exc}(t)}{V_0} + \frac{1}{2} \left(\frac{H_{exc}(t)}{V_0} \right)^2 + \dots$ was proposed in some papers, where $n(t)$, V_0 are phenomenological model parameters. The good agreements between the measured and the modelled loss values for 3% Si-Fe GO and NO electrical sheets were obtained for the $n(H_{exc}(t))$ with just two terms of series expansion. This assumption in 6.5% Si-Fe leads to erroneous results.

The paper shows that taking into account the higher terms of the expansion $n(H_{exc}(t))$ allows improving the accuracy of loss prediction for 6.5% Si-Fe steel.

O2-08**EFFECT OF DISK VELOCITY IN MELT SPINNING METHOD ON MAGNETIC PROPERTIES OF AMORPHOUS RIBBONS**N. Amini^{1,2}, M. Miglierini^{1,3} and M. Hasiak⁴¹*Institute of Nuclear and Physical Engineering, Slovak University of Technology, Ilkovičova 3, 812 19 Bratislava, Slovakia*²*Department of Physics, Bu-Ali Sina University, 65174-4161, Hamedan, Iran*³*Department of Nuclear Reactors, Czech Technical University in Prague, V Holešovičkách 2, 180 00 Prague, Czech Republic*⁴*Department of Mechanics and Materials Science, Wrocław University of Science and Technology, Smoluchowskiego 25, 50-370 Wrocław, Poland*

Changes in magnetic parameters of $\text{Fe}_{78}\text{Si}_9\text{B}_{13}$ ribbons were investigated as a function of a quenching wheel velocity during their production by the melt casting method. It was shown that the ribbon thickness decreases monotonically with the velocity.

The main aim of the present paper is to study the effect of the disk's velocity upon selected magnetic properties of the produced ribbons. Amorphicity of the samples was checked by X-ray diffraction and Mössbauer spectrometry measurements. Hysteresis loops were measured at different temperatures from 50 K up to 400 K. Temperature dependence of magnetization $M(T)$ in zero field cooling (ZFC) mode was considered for all produced materials. Moreover, the influence of external magnetic field on $M(T)$ curves were analyzed.

The relation between magnetic properties and microstructure of the as-quenched ribbons was analyzed. From Mössbauer spectrometry results it is seen that no dependence of the mean value of the hyperfine field on the quenching velocity is observed. The Curie temperatures of the produced metallic glass are higher than 400 K so these ribbons are good candidates for industrial applications.

Along with as-quenched ribbons, we have also investigated the samples which were thermally annealed at temperatures that are well below the onset of crystallization.

This work was supported by the grants GACR 14-12499S and VEGA 1/0182/16.

P2-01**BOSON PEAK AND RELAXATION PHENOMENA IN $\text{Zn}(\text{PO}_3)_2\text{Er}(\text{PO}_3)_3$ PHOSPHATE GLASS**

M. Orendáč¹, K. Tibenská², E. Čížmár¹, V. Tkáč¹, A. Orendáčová¹, E. Černošková³, J. Holubová⁴ and Z. Černošek⁴

¹*Institute of Physics, P. J. Šafárik University, Park Angelinum 9, 041 54 Košice, Slovak Republic*

²*Faculty of Aeronautics, Technical University, Rampová 7, 041 21 Košice, Slovak Republic*

³*Joint Laboratory of Solid State Chemistry of IMC CAS, v.v.i., and University of Pardubice, Faculty of Chemical Technology, Studentská 84, 532 10 Pardubice, Czech Republic*

⁴*Dept Gen & Inorgan Chem, Faculty of Chemical Technology, Studentská 573, University of Pardubice, Pardubice 53210, Czech Republic*

Specific heat and alternating (ac) susceptibility of $\text{Zn}(\text{PO}_3)_2\text{Er}(\text{PO}_3)_3$ phosphate glass are reported. The specific heat measurements were performed in zero magnetic field from 2 K to nominally 50 K, whereas ac susceptibility studies were conducted from 2 K to 15 K in frequencies from 0.1 Hz to 1 kHz in dc magnetic field up to 2 T. The existence of the boson peak in specific heat is revealed below nominally 15 K. The energy scale of the involved phonon modes is estimated using soft-mode-dynamics model. Overcoming Ioffe – Regel crossover and subsequent strong scattering of the acoustic phonons on the local modes is suggested to occur above 7 K. The temperature of the crossover reasonably agrees with anomalous deceleration of spin dynamics with increasing temperature observed in magnetic relaxation studies. Excluding the formation of a spin glass state by analyzing Cole - Cole diagrams, the relaxation modes are investigated separately. The relaxation below 7 K is dominated by a direct relaxation process with pronounced influence of the phonon bottleneck. In addition, temperature independent relaxation mode with characteristic frequency nominally 70 Hz is tentatively attributed to cross – tunneling relaxation. Structural properties inevitable for the onset of the cross – tunneling are discussed.

The obtained results suggest that the phonon modes in glasses may be investigated by magnetic doping of glasses and subsequent calorimetric and magnetic relaxation studies.

The work was supported by the project ITMS 26220120005.

P2-02**THE COMPARISON HARDNESS AND COERCIVITY EVOLUTION IN VARIOUS Fe(TM) BASED GLASSES (INCLUDING FINEMET PRECURSOR) DURING RELAXATION AND CRYSTALLIZATION**Z. Weltsch¹, K. Kittl¹ and A. Lovas²*¹Department of Materials Technology, Faculty of Mechanical Engineering and Automation, Kecskemét College, H-6000 Kecskemét, Hungary, Izsáki út 10.**²Budapest University of Technology and Economics, Faculty of Transportation Engineering and Vehicle Engineering, Department of Automobiles and Vehicles Manufacturing, H 1111, Budapest Hungary, Stoczek utca 6.*

During various heat treatments, leading to the optimization of soft magnetic properties a wide spectra of other physical properties (including transport and mechanical) are also alter. The drastic change of brittleness and hardness are especially important, which have to be taken into any further step in the technology or application. It is especially trough during the amorphous nanocrystalline transformation. Among the mechanical properties the hardness and brittleness change do supply useful information about the degree of transformations.

In this presentation the hardness change will be analyzed in which the magnetic softening is also reflected indirectly –during run of heat treatments.

Comparing the behavior of several Fe-metalloid glasses, it was found (supposing nearly identical thickness) the hardness depends primarily on the type of metalloid and its concentration in the glass. The hardness in as quenched state especially sensitively depends on the B-content.

The degree of relaxation hardening (at a given temperature) is dominantly influenced by the T_h/T_{crys} (T_h is the heat treatment temperature, T_{crys} is the crystallization temperature)

In contrast to the gradual and slight hardness increase associated with the relaxation, the hardness increases rapidly increases during the crystallization process. The maximum value of HV after the completed crystallization predominantly influenced by the metalloid, and - especially - on the boron content. Hence, the total hardening associated with the amorphous nanocrystalline transformation in FINEMET precursors is lower, than that, in the crystallization of binary Fe-B glasses.

P2-03**THE CHANGES IN MAGNETIC AND MECHANICAL PROPERTIES OF FINEMET - TYPE ALLOYS DURING ISOTHERMAL, AND PULSE HEAT TREATMENTS**L. Hubáč¹, L. Novák¹ and A. Lovas²*¹Department of Physics, Faculty of Electrical Engineering and Informatics, Technical University of Košice, Park Komenského 2, 042 00 Košice, Slovakia**²Department of Automobiles and Vehicle Manufacturing, Budapest University of Technology and Economics, Stoczek u .2. 1111, Hungary*

The FINEMET-type nanocrystalline alloys are attractive for high frequency applications since they exhibit high effective permeability and high saturation magnetic flux density at high frequencies [1]. Additional advantage of these alloys is a wide range of possibilities for tailoring the shape of their magnetization curve by magnetic field or stress annealing [2]. However, during traditional, isothermal heat treatments (leading to amorphous-nanocrystalline transition) mechanical flexibility of precursor material significantly deteriorates, (it turns brittle), which prevents any mechanical applications. The aim of this study is to compare the influence of isothermal and pulse heat treatments on some soft magnetic and mechanical properties of these alloys. Isothermal heat treatments usually resulted in structural relaxation or, in various stages of the amorphous–nanocrystalline transformation. The method and equipment for the pulse heat treatment have been reported recently [3].

In the present paper, the first results on the kinetics of coercivity decrease as well as the evaluation of brittleness of the studied material, which was subject to pulse heat treatments are reported. It is found, that time courses of brittleness and coercivity decrease differ considerably, especially in the first period of pulse heat treatments.

- [1] Makino M, Inoue A and Masumoto T 1995 Nanocrystalline Soft Magnetic F-M-B (M= Zr, Hf, Nb) Alloys Produced by Crystallization of Amorphous Phase Materials Transactions JIM Vol. 36 No.7 pp. 924-938.
- [2] Herzer G 1997 Handbook of Magnetic Materials ed. Buschow K H J v.10 chap. 3 p. 415 Elsevier Science Amsterdam.
- [3] Kováč J, Novák L, Hubáč L, Impulse annealing as possibility of modification of magnetic properties of amorphous metallic alloys, In: Journal of Electrical Engineering, Vol. 66, 2015 No. 7/s pp. 142-145.

P2-04**DC MAGNETIC PROPERTIES OF AMORPHOUS VITROVAC RIBBON**P. Kollár¹, Z. Birčáková¹, J. Füzér¹ and M. Kuźmiński²¹*Institute of Physics, Faculty of Science, P. J. Šafárik University,
Park Angelinum 9, 040 01 Košice, Slovak Republic*²*Institute of Physics, Polish Academy of Sciences, Al. Lotników 32/46,
PL-02-668 Warsaw, Poland*

Soft magnetic amorphous Co-based materials prepared by rapid quenching method in the form of thin ribbon are well-known due to their excellent soft magnetic properties as high permeability, low coercivity and low magnetic loss in kHz-range. These properties determine these materials for many applications as signal transformers, chokes and power transformers for the kHz-range. The amorphous Co-Fe-B-Si material VITROVAC® 6155 U55 F produced by VACUUMSCHMELZE GmbH & Co. KG belongs to this class of materials and was investigated in as-delivered state. The sample was the 8.2 m long ribbon wound as a core of the toroidal transformer (with diameter of 5.8 cm) with primary magnetization coil and secondary pick-up coil. Third coil was used for generating of AC magnetic field with decreasing amplitude.

The aim of this work was to study DC magnetization process by various experimental methods. We have measured magnetization curve and anhysteretic curve by fluxmeter based hysteresisgraph and hysteresis loops by three different fluxmeter based hysteresisgraphs. First hysteresisgraph performs the hysteresis loops measurement by commutation method, second one measures the hysteresis loops by summing method and the last one is AC fluxmeter based hysteresisgraph working at very low magnetization frequencies down to 7 mHz (with triangle waveform). The measured hysteresis loops by three different methods exhibit significant differences. The explanation of this result is based on the structural after effect influencing the domain walls displacement. We assumed that the domain structure consists of very small number of domain walls responsible for magnetization process. This assumption was confirmed by visualization of the static domain structure by a computer-controlled set-up based on the Kerr effect.

*Acknowledgment**This work was realized within the project ITMS 26220120019.*

P2-05

ANALYSIS OF THE THERMAL AND MAGNETIC PROPERTIES OF AMORPHOUS $\text{Fe}_{61}\text{Co}_{10}\text{B}_{20}\text{Y}_8\text{Me}_1$ (WHERE Me = W, Zr, Nb, Mo) RIBBONS

P. Pietrusiewicz¹ and M. Nabiałek¹

¹Institute of Physics, Czestochowa University of Technology, 19 Armii Krajowej Av, 42-200 Czestochowa, Poland

The paper presents the results of thermal and magnetic studies of rapidly cooled alloy $\text{Fe}_{61}\text{Co}_{10}\text{B}_{20}\text{Y}_8\text{Me}_1$ (where Me = Nb, Zr, W, Mo). The resulting tapes have amorphous structure. It has been found that the effect of the addition of Me elements alters the thermal and magnetic properties. It is noted that with increasing amount of unpaired electrons on the valence shells, saturation magnetization decreases. Also the value of the coercivity and effective anisotropy were determined.

P2-06**EFFECT OF CURRENT ANNEALING ON DOMAIN STRUCTURE IN AMORPOUS AND NANOCRYSTALLINE FeCoMoB MICROWIRES**P. Klein¹, R. Varga^{1,2}, G. A. Badini-Confalonieri³ and M. Vazquez³¹*RVmagnetics s.r.o., Hodkovce 21, 04421 Košice, Slovakia*²*Faculty of Science, Institute of Physics, Univesity of Pavol Jozef Safarik, Park Angelinum 9, 041 54 Košice, Slovakia*³*Instituto de Ciencia de Materiales de Madrid, CSIC, Sor Juana Inés de la Cruz 3, 28049 Cantoblanco, Madrid, Spain*

Current annealing is more effective method of thermal treatment since it decreases the time necessary for annealing (it was shown in previous work that 10 minutes of current annealing corresponds to 1 hour of classical annealing in furnace). Moreover, current annealing leads to the more homogeneous final nanocrystalline microstructure in comparison to the classical annealing [1]. Electrical current flowing through microwire produces Oersted magnetic field and therefore circular magnetic anisotropy is induced during annealing. Induced circular anisotropy prefers vortex domain walls with faster velocities as was already showed in previous work [2].

In the given contribution, effect of current annealing on internal stress distribution has been studied in amorphous and nanocrystalline FeCoMoB microwires. As a result of current annealing, distribution of internal stresses was changed. Particularly, the values of the thickness of axial monodomain and switching field of single domain wall were changed as a consequence of variation of internal stresses inside metallic nucleus. Moreover, values of the switching field are in good accordance with that of thickness of axial monodomain. In addition, observed switching field variation can be satisfactorily explained by the effect of shape anisotropy.

This research was supported by the projects APVV-0027-11 and Slovak VEGA grant. No. 1/0164/16.

- [1] P. Klein, R. Varga, V. Komanicky, G. A. Badini-Confalonieri, and M. Vazquez, Effect of current annealing on domain wall dynamics in bistable FeCoMoB microwires, *Solid State Phenomena* 233-234 (2015) pp. 281-284.
- [2] P. Klein, R. Varga, M. Vazquez, Enhancing the velocity of the single domain wall by current annealing in nanocrystalline FeCoMoB microwires, *J. Phys. D: Appl. Phys.* 47 (2014) 255001 1-5.

P2-07**INVESTIGATION OF MAGNETIZATION PROCESSES FROM THE ENERGY LOSSES IN SOFT MAGNETIC COMPOSITE MATERIALS**Z. Birčáková¹, P. Kollár¹, B. Weidenfeller², J. Füzér¹, R. Bureš³ and M. Fáberová³¹*Institute of Physics, Faculty of Science, P. J. Šafárik University,
04154 Košice, Slovakia*²*Institute of Electrochemistry, Technical University of Clausthal,
38678 Clausthal-Zellerfeld, Germany*³*Institute of Materials Research, SAS, 04001 Košice, Slovakia*

Soft magnetic composites (SMCs) are composed of small ferromagnetic particles insulated from each other resulting in some unique properties as magnetic isotropy or low classical losses, which makes SMCs well suited for various AC and DC electromagnetic applications. The aim of this work was to study the reversible and irreversible magnetization processes on different SMCs from the view of inner demagnetizing fields, frequency dependence of excess losses and the separation of total losses in low and high induction components.

Samples of sieved granulometric classes of ASC 100.29 pure iron powder were prepared by wet homogenization of the powder with 15, 10 and 5 vol. % of phenolphormaldehyde resin and acetone, followed by a compaction at 800 MPa and curing at 165 °C for 60 min in electric furnace in air. Second type samples were prepared by mixing Somaloy powder with 5, 10 and 30 wt. % of Vitroperm powder, then compacted at 800 MPa and cured at 530 °C for 60 min in electric furnace in air atmosphere.

The increase of dynamic losses W_{dyn} with frequency was steeper in samples with higher resin content and also in samples with smaller magnetic particles. As the inter-particle classical losses W_c^{inter} were lower in samples with higher resin content due to higher specific resistivity, and the intra-particle classical losses W_c^{intra} were lower in samples with smaller particle sizes, both the effects can be thus explained by higher excess losses W_{exc} ($W_{dyn} = W_c^{inter} + W_c^{intra} + W_{exc}$) given by lower numbers of movable domain walls, meaning lower proportion of irreversible processes.

Inner demagnetizing fields were increasing with decreasing particle size and with increasing resin content, resulting in the weakening of magnetic interaction between particles, which reflects in lower numbers of movable domain walls.

Total losses were divided into low and high induction loss components (W_{AC}^{low} and W_{AC}^{high}) plotted vs. frequency. W_{AC}^{low} revealed the proportion of energy dissipation due to domain wall displacements and W_{AC}^{high} were related to rotation of magnetization vector and domain wall annihilation or recreation.

*Acknowledgment**This work was realized within the project ITMS 26220120019.*

P2-08**HIGH-FREQUENCY ABSORBING PERFORMANCES OF CARBONYL IRON/MnZn FERRITE/PVC POLYMER COMPOSITES**R. Dosoudil¹ and M. Ušáková¹¹*Institute of Electrical Engineering, Slovak University of Technology in Bratislava, Ilkovičova 3, 812 19 Bratislava, Slovakia*

With the rapid advances and broad implementation of radio communication and computer technology, and with the ongoing miniaturization of electronic equipments, there is an increased functionality of high-frequency absorbing materials that can provide effective shielding of electromagnetic interferences, especially in microwave frequency range (over 500 MHz). Although a lot of work on characteristics of polymer-based composites with single soft magnetic filler has been reported in recent years, there seem to be only a few reports on the high-frequency absorbing properties of composites with combined metal/ferrite filler. In this investigation, the high-frequency absorbing properties of metal/ferrite/polymer composites have been studied. The composite samples were prepared by mixing commercially available carbonyl iron and MnZn ferrite (with composition $\approx \text{Mn}_{0.52}\text{Zn}_{0.43}\text{Fe}_{2.05}\text{O}_4$) in different filler volume ratios of 1:0, 0.75:0.25, 0.5:0.5, 0.25:0.75 and 0:1 in polyvinylchloride (PVC). Then, hot pressing was carried out. Blend of metal/ferrite filler with PVC was plasticized and fired at 135°C and 5 MPa. Curing time was 30 min. The total volume concentration of combined metal/ferrite filler in composites was kept at 50 vol%. The pressed composites were prepared in the form of rings with an outer diameter of 7 mm, an inner diameter of 3.1 mm and a height of 2-3 mm. Variation of complex permeability $\mu = \mu' - j\mu''$ versus frequency f in the range of 1 MHz – 6.5 GHz was studied by means of a coaxial transmission line method using a vector network analyser. Electromagnetic wave absorption parameters such as return loss RL , matching frequency f_m , matching thickness d_m and bandwidth Δf for $RL \leq -20$ dB were obtained by numerical simulations. High-frequency absorbing properties of the composites are influenced by the strong correlation between return loss and complex permeability of the metal/ferrite/polymer composites. The investigated composite materials make possible to design thin, broadband and flexible microwave absorbers.

Acknowledgement

This work was supported by the Slovak Research and Development Agency under the contracts no. APVV-0062-11 and APVV-15-0257 and by the Scientific Grant Agency of the Ministry of Education, Science, Research and Sport of the Slovak Republic, and in part by the Slovak Academy of Sciences, under projects no. 1/0571/15 and 1/0405/16.

P2-09**MICROSTRUCTURAL AND MAGNETIC CHARACTERISTICS OF DIVALENT Zn, Cu AND Co DOPED Ni FERRITES**M. Šoka¹, R. Dosoudil¹ and M. Ušáková¹¹*Institute of Electrical Engineering, Slovak University of Technology in Bratislava, Ilkovičova 3, 812 19 Bratislava, Slovakia*

Divalent zinc, copper and cobalt doped nickel ferrites with the chemical formula $\text{Ni}_{1-x-y-z}\text{Zn}_x\text{Cu}_y\text{Co}_z\text{Fe}_2\text{O}_4$ where x values ranging from 0.4 to 0.6 in steps of 0.1, $y = 0.1$, $z = 0.01$ and 0.02 have been synthesized by conventional ceramic method. Calcination and sintering of the samples were carried out at 950°C and 1200°C respectively for 6 hours each in air atmosphere followed by natural cooling. The effect of Zn^{2+} , Cu^{2+} and Co^{2+} ions substitution on the selected microstructural properties (X-ray diffraction pattern, lattice parameter, average crystallite size, density and porosity) and magnetic characteristics (Curie temperature, magnetic moment and frequency dependence of complex initial permeability) have been investigated to examine the utility of prepared ferrite materials for high-frequency applications. X-ray diffraction measurements confirmed the single-phase spinel cubic structure in all the samples and modifications in lattice constant according to the ionic radii size of doped cations. The total magnetic moment per formula unit, given by the differences between the magnetic moments of A and B sublattice, increases with raising substitution of Ni^{2+} ions.

The measurements of frequency dependences of real (μ') and imaginary (μ'') parts of complex initial permeability ($\mu = \mu' - j\mu''$) have been made for all the synthesized ferrite samples from 100 kHz to 3 GHz by means of an impedance analysis method. The frequency at which the real part μ' of complex permeability μ starts to decrease coincides with the increase at which the imaginary part μ'' starts to raise. The obtained results are discussed in terms of the changes in chemical composition, microstructure and the associated processes of resonance and/or relaxation due to domain wall movements and damping of spin rotations contributing to the fall of permeability and rise of magnetic losses.

Acknowledgement

This work was supported by the Slovak Research and Development Agency under the contracts no. APVV-0062-11 and APVV-15-0257 and by the Scientific Grant Agency of the Ministry of Education, Science, Research and Sport of the Slovak Republic, and in part by the Slovak Academy of Sciences, under projects no. 1/0571/15 and 1/0405/16.

P2-10**NICKEL/ZINC RATIO AND LANTHANUM SUBSTITUTION EFFECT ON STRUCTURAL AND MAGNETIC PROPERTIES OF NICKEL ZINC FERRITES**V. Jančárik¹, M. Šoka¹, M. Ušáková¹ and R. Hart'anský¹*¹Institute of Electrical Engineering, Faculty of Electrical Engineering and Information Technology, Slovak University of Technology in Bratislava, Ilkovičova 3, 812 19 Bratislava, Slovakia*

Nowadays, attention is still focused on soft magnetic spinel ferrites. They are important and extensively used in several high-frequency applications. There are several approaches to improve their parameters by modification of preparation procedure as well as by definition of an optimum chemical composition. The aim of presented work is to prepare thermally stable nickel zinc ferrite with suitable structural and magnetic parameters by modification of $\text{Ni}^{2+}/\text{Zn}^{2+}$ ratio as well as to study the effect of partial substitution of Fe^{3+} ions by La^{3+} ions in these ferrites.

For that purpose, $\text{Ni}_x\text{Zn}_{1-x}\text{Fe}_2\text{O}_4$ ($x = 0.30, 0.36, 0.42, 0.50, 0.70, 1.0$) and $\text{Ni}_x\text{Zn}_{1-x}\text{La}_{0.02}\text{Fe}_{1.98}\text{O}_4$ ferrite powders were prepared by the self-propagated combustion method, then they were annealed at $850^\circ\text{C}/6\text{h}$. Such method of preparation allows to obtain oxide based materials with small particles.

Structure, phase composition and the magnetic properties of this set of non-substituted as well as lanthanum substituted samples were studied. X-ray spectroscopy was used for structural analysis. Diffraction patterns were collected with a diffractometer equipped with a conventional X-ray tube (Cu K α radiation, $\lambda = 1.5418\text{\AA}$).

Measurement of magnetic susceptibility temperature dependence was performed. Besides other analysis method, it represents quick and effective way of thermomagnetic analysis. Shape of the dependence brings a lot of information about the sample since the susceptibility is highly sensitive to chemical and phase composition, moreover also to ferrite particles size. Semi-automatic inductance bridge capable of analysis of very small amount of powder sample was used.

Acknowledgement

This work was supported by the Slovak Research and Development Agency under the contract No. APVV14-0076 and by the Scientific Grant Agency of the Ministry of Education, Science, Research and Sport of the Slovak Republic, No. VG 1/0571/15.

P2-11**THE ROLE OF TEMPERATURE ON THE MAGNETIZATION PROCESS IN CoFeZrB/FeCuNbMoSiB HYBRID FERROMAGNETS**S. Dobák¹, J. Füzer¹ and P. Kollár¹*¹Department of Condensed Matter Physics, Institute of Physics, Faculty of Science, P. J. Šafárik University, Park Angelinum 9, 041 54 Košice, Slovakia*

The study has been devoted to the investigation of the broadband complex permeability and energy loss in a dual-phase bulk hybrid ferromagnetic system from room temperature up to 110 °C. Two sets of samples have been prepared by mixing of short-time ball-milled amorphous Co₅₆Fe₁₆Zr₈B₂₀ (at.%) ribbon flakes either with (i) amorphous or (ii) nanocrystalline Fe_{72.5}Cu₁Nb₂Mo₂Si_{15.5}B₇ (at.%) powder in different mass ratios. So-prepared mixtures were consolidated at the pressure of 700 MPa at 590 °C for 2 min.

The materials were characterized by means of complex permeability spectra and energy loss determined by a digital hysteresisgraph-wattmeter in a broad range of frequencies from quasi-dc up to about 1 MHz at different defined peak inductions. The measurement has been carried out at the conditions where the material can be regarded as linear to fulfill the validity of used complex permeability approach.

The low-frequency permeability and losses are attributed to the domain wall motion up to the wall relaxation that is mainly controlled by eddy-current damping. The remaining parts of permeability spectra and energy loss are due to the magnetic moments rotation as has been clarified by the measurement at various peak inductions, which revealed that for each sample the permeability curves tend to coalesce into one line on attaining few tens kHz.

It has been observed that the operating temperature affects the studied magnetic properties in particular at low frequencies, i.e. those connected to domain walls displacement, and differently in regard of various amorphous/nanocrystalline FeCuNbMoSiB fraction in hybrid material. The findings have been elucidated from the view of temperature-influenced magnetization processes and phenomena associated to the increasing of temperature, e.g. reduction of anisotropies induced during the processing and weakening of intergranular exchange coupling in nanocrystalline materials.

Furthermore, the theoretical prediction of dc permeability in dual-phase ferromagnets has been made. We have used the phenomenological model based on the permeability and fraction of individual components in hybrid ferromagnet.

*Acknowledgment**This work was realized within the project ITMS 26220120019.*

P2-12**MAGNETIC PROPERTIES OF AMORPHOUS GEHLENITE GLASS MICROSPHERES**

M. Majerová¹, A. Dvurečenskij¹, A. Cigáň¹, M. Škrátek¹, A. Prnová², J. Kraxner², D. Galusek² and J. Maňka¹

¹*Department of Magnetometry, Institute of Measurement Science, Slovak Academy of Sciences, Dúbravská cesta 9, 841 04 Bratislava, Slovak Republic*

²*Vitrum Laugaricio – Joint Glass Center of the IIC SAS, TnU AD, FCHTP STU and Rona, a.s., Študentská 2, SK-911 50 Trenčín, Slovak Republic*

Gehlenite ($\text{Ca}_2\text{SiAl}_2\text{O}_7$) belongs to calcium aluminosilicates. From the mineralogical point of view, gehlenite regularly occurs in traditional ceramic materials, such as building ceramic materials and cookware. Gehlenite is also used in the preparation of biosoluble glass fibers and glass ceramics. Gehlenite has excellent physical, thermal and chemical stability. It is a suitable host for optically active dopants, with potential applications as phosphors for LEDs.

Regardless of the increasing importance of calcium aluminosilicate glasses, the question of the cation ordering-disordering in the ceramics is still open. Up to now, far less information is available in the area of knowledge of their magnetic properties, namely of gehlenite glass. We have only found a publication of R. Noller and H. Knoll referring to magnetic properties of iron doped gehlenite, showing magnetization curves at 298 K.

In the paper, gehlenite amorphous microspheres were prepared by the flame synthesis of a powder precursor. In the first step, the precursor was prepared from a stoichiometric mixture of CaCO_3 , Al_2O_3 , SiO_2 high-purity powders by a standard solid-state reaction method. Next, a fine powder mixture was sprayed into a $\text{CH}_4\text{-O}_2$ flame of the temperature around 2200°C and molten droplets of gehlenite were rapidly cooled by deionised water.

The amorphous character of microspheres was verified by the powder X-ray diffraction. Magnetic properties of the microspheres were measured by the QD SQUID magnetometer MPMS XL7.

Temperature dependences of the zero-field cooled (ZFC), the field cooled (FC) DC magnetic moment, at an increasing and decreasing temperature, at different values of applied magnetic field and the DC magnetization curves at different temperatures were measured. Based on the result of the magnetic measurements, the microspheres show complicated magnetic behaviour that is the function of the temperature and the magnetic field. Some characteristics of spin glass, magnetic AFM-Ferrimagnetic transition and contributions of itinerant electrons, were determined.

P2-13**THERMOPOWER CHARACTERIZATION OF STRUCTURAL RELAXATION AND CRYSTALLIZATION IN FINEMET TYPE AMORPHOUS PRECURSOR ALLOY**K. Bán¹, A. Szabó¹, R. Ipach¹ and B. Szabó¹*¹Department of Automobiles and Vehicle Manufacturing, Budapest University of Technology and Economics, Stoczek street 6., 1111 Budapest, Hungary*

In an earlier research the change of thermopower $U(T)$ was observed in various Fe-based glasses if a structural relaxation or even the amorphous-crystalline phase transition occurred. During the experiments the parallel shift of $U(T)$ curves was detected in the case of a structural relaxation, while a drastically change in the slope of $U(T)$ curves can be observed if crystalline phases are precipitated from the glassy phase.

In the present paper, a FENEMET precursor alloy was examined, where the composition is more complex, than that of the binary Fe-B glasses. The phenomenon of relaxation and the onset of crystallization were successfully distinguished, using the thermopower measurement. During the experiments an increase of the $U(T)$ slope is experienced at the beginning of the crystallization. In the present work the character of the $U(T)$ curves have been also compared in the samples subjected to traditional isotherm and pulse heat treatments.

P2-14**COMPLEX MAGNETOIMPEDANCE IN JOULE HEATED
Co_{71.1}Fe_{3.9}Si₁₀B₁₅ MICROWIRES**E. Komova¹, P. Klein², R. Varga² and J. Kozár¹¹ *Faculty of Aeronautics of Technical University, Rampova 7,**041 21 Kosice, Slovakia*² *Institute of Physics, Faculty of Science, UPJS, Park Angelinum 9,**041 54 Kosice, Slovakia*

Complex magnetoimpedance study is an alternating current technique that can be used to probe some properties of magnetic materials. In our paper, we report complex impedance measurements in low - negative magnetostrictive ferromagnetic CoFeSiB microwire. In these wires, the domain structure consist from two parts: an inner core, with domains oriented to the longitudinal direction of the wire, and an outer shell with circumferentially oriented domains. This magnetic structure is modified by AC current flowing through the microwire which produces an additional circumferential magnetic field H_ϕ and significantly affects magnetic structure inside the wires. The additional circular magnetization process in wires was studied by impedance measurements as a function of the amplitude and the frequency of the AC current after gradual Joule-heating. Changes in the behavior of magnetization processes are reflected in the real permeability values and loss factor values.

P2-15**MAGNETIC PROPERTIES OF NANOCRYSTALLINE ALLOYS AFTER ELECTRONS IRRADIATION**J. Sitek¹, D. Holková¹, J. Dekan¹ and P. Novák¹*¹Institute of Nuclear and Physical Engineering, Faculty of Electrical Engineering and Information Technology, Slovak University of Technology, Ilkovičova 3, 812 19 Bratislava, Slovakia*

Nanocrystalline $(\text{Fe}_1\text{Ni}_3)_{81}\text{Nb}_7\text{B}_{12}$ and $\text{Fe}_{77}\text{Co}_8\text{B}_{15}$ alloys were irradiated by electron beams of doses 2 MGy and 4 MGy, respectively. Irradiation had an influence on the magnetic microstructure of the studied alloys. It has manifested as a change in the direction of the net magnetic moment, intensity of the internal magnetic field and volumetric fraction of the constituent phases. All these parameters were determined from the measured Mössbauer spectra. The direction of the net magnetic moment was the most sensitive parameter. Structural changes were identified by X-ray diffraction. The results indicated that the changes of the microscopic magnetic parameters induced by irradiation depend also on the constituent elements and phase composition. Results of nanocrystalline samples were compared with their amorphous precursors.

P2-16**ACCENTS IN MODERN HIGH SATURATION NANOCRYSTALLINE Fe-RICH ALLOYS**

B. Butvinová¹, P. Butvin¹, I. Maľko¹, D. Janičkovič¹, M. Kuzminski²,
A. Slawska-Waniewska², P. Švec¹ and M. Chromčíková³

¹*Institute of Physics, SAS, Dubravská c. 9, 845 11 Bratislava, Slovakia*

²*Institute of Physics, PAS, Al. Lotnikow 32/46, 02-668 Warsaw, Poland*

³*Institute of Inorg. Chemistry, SAS, Centrum VILA, Študentská 2,
911 50 Trenčín, Slovakia*

Contemporary trend to raise saturation induction B_s simultaneously preserving the well-known advantages brought by optimal percentage of nanocrystalline, high B_s and high Curie temperature Fe phase rearranged the importance of properties known to be crucial for applicability of Fe-Nb-Cu-B-Si Finemets in power electronics. Perhaps the most important is the omitting of grain-growth blockers (Nb, Mo) in the composition of hiB materials – it severely limits the temperature and/or duration range of nanocrystallization annealing. Fe-rich and metalloid-poor compositions also increase the risk of lowering critical temperatures for Fe crystallization as well as for (magnetically harder) boride formation. Mainly to counter the latter, phosphorus and/or carbon is incorporated.

We checked/reviewed certain important properties in the alloy system Fe-Cu-B-Si-P. DSC revealed slight only differences due to composition in onset of the first crystallization just below 430°C and for T_C (amorphous) similarly small spread around 340°C. Variation neither of T_x , nor of T_C attributable to individual metalloid component (B, Si, P) percentage difference could be clearly resolved. Contrary to higher-temperature ($\geq 500^\circ\text{C}/1\text{hour}$) annealing, lower temperatures and/or shorter durations do not produce hard-ribbon-axis magnetic anisotropy i. e. slant hysteresis loops. This means that there is no significant in-plane compressive stress exerted by surfaces on positively magnetostrictive ribbon interior despite of possible boride formation or Fe(Si) grain growth. The latter effects are presumably considered to contribute to the observed larger coercivity, which is notably larger after Ar anneal than after equivalent vacuum anneal. Although 420° C is enough to produce surface oxides at technical purity Ar annealing, especially in P-containing ribbons, we find no obvious consequences of surface stress and it means that oxides without preferred surface Fe(Si) crystallization do not generate appreciable stress. This presents a welcome chance to attain highest possible induction without too much excitation (H).

P2-17**IMAGING OF MAGNETIC DOMAIN STRUCTURE IN
FeSi/Mn_{0.8}Zn_{0.2}Fe₂O₄ COMPOSITE USING MAGNETIC FORCE
MICROSCOPY**

M. Streckova¹, I. Batko², M. Batkova², R. Bures¹, M. Faberova¹, H. Hadraba³ and I. Kubena³

¹*Institute of Materials Research, Slovak Academy of Sciences, Watsonova 47, 040 01 Kosice, Slovak Republic*

²*Institute of Experimental Physics, Slovak Academy of Sciences, Watsonova 47, 040 01 Kosice, Slovak Republic*

³*Ceitec IPM, Institute of Physics of Materials, Academy of Sciences of Czech Republic, Ziskova 22, 616 62 Brno, Czech Republic*

Soft magnetic composites (SMCs), which are of technological relevance in electromagnetic applications, can be described as ferromagnetic powder particles surrounded by an electrically insulating film. A design of the novel microcomposite material composed of commercial spherical FeSi particles (produced by Högānas Corporation) and Mn_{0.8}Zn_{0.2}Fe₂O₄ ferrite is reported together with a basic characterization of mechanical, electrical and magnetic properties. The sol-gel auto-combustion method was used for a preparation of Mn_{0.8}Zn_{0.2}Fe₂O₄ ferrite, which has a spinel-type crystal structure as verified by XRD and TEM analysis. The atomization is a standard thermal treatment process for the FeSi powder production, which consequently leads to an internal recrystallization of the original grains. Each separate grain has a random orientation of the easy magnetization axis and is sufficiently large to split into several magnetic domains. The ferrite nanoparticles represent the mono-domain structures located between large spherical FeSi particles. The present work takes advantage of the magnetic force microscopy (MFM) for imaging the magnetic domains and domain walls in the micro-nano composite sample as well as to understand ability to conduct electron flow through ferrite thin layer between FeSi particles. The preparation of sample for a visualization of domain structure using MFM techniques is the hardest problem because polishing introduces internal stress. The focused ion beam (FIB) technology represents the most nondestructive way of polishing FeSi/Mn_{0.8}Zn_{0.2}Fe₂O₄ in comparison with mechanical, electrolytic or mechano-chemical way. The polishing of composite samples by means of FIB allows tracking of magnetic domain structure close to its natural state in comparison with the various kinds of domain structures examined after alternative mentioned polishing methods.

P2-18**EFFECTS OF COBALT ADDITION ON MAGNETIC PROPERTIES
IN Fe-Co-Si-B-P-Cu ALLOYS**M. Kuhnt¹, M. Marsilius², T. Strache², K. Durst¹, C. Polak² and G. Herzer²¹*Department of Materials Science, TU Darmstadt, D-64287 Darmstadt, Germany*²*Vacuumschmelze GmbH Co KG, D-63450 Hanau, Germany*

Nanocrystalline Fe-Co-Si-B-P-Cu alloys show high saturation polarization J_s above 1.8 T combined with good soft magnetic properties and good glass forming ability [1,2]. In this work, we investigated systematically the effects of partial substitution of Fe with Co in $\text{Fe}_{85.2}\text{Si}_{10.5}\text{B}_{9.5}\text{P}_4\text{Cu}_{0.8}$ on nanocrystallization, saturation polarization, coercivity and saturation magnetostriction.

Amorphous ribbons of $\text{Fe}_{85.2}\text{Co}_x\text{Si}_{10.5}\text{B}_{9.5}\text{P}_4\text{Cu}_{0.8}$ ($x=0,4,10,20,40$ and 57) have been produced by rapid solidification in 25 mm width and 22 μm thickness. The material was annealed for about 11 seconds (cf. [3]) between temperatures of about 350°C and 560°C. As a result of nanocrystallization, a bcc structure was achieved after annealing. Annealing at higher temperatures lead to the precipitation of borides accompanied by a degradation of the soft magnetic properties. With increasing Co, coercivity and saturation magnetostriction increases. Saturation polarization has a broad maximum of $J_s = 1.88$ T at about 20 at% Co.

[1] Zhang, Y. et al.: *IEEE Trans. Magn.* 50 (2014) 1-4.

[2] Takenaka, K. et al.: *Mat. Trans.* 56 (2015) 372-376.

[3] Herzer, G. et al.: *Phys. Stat. Sol. B* 248 (2011) 2382-2388.

P2-19**MAGNETIC PROPERTIES OF $\text{Ni}_{0.3}\text{Zn}_{0.7}\text{Fe}_2\text{O}_4$ FERRITES WITH Fe IONS PARTLY SUBSTITUTED BY Eu**E. Ušák¹, M. Ušáková¹, M. Šoka¹ and D. Vašut¹¹*Institute of Electrical Engineering, Faculty of Electrical Engineering and Information Technology, Slovak University of Technology, Ilkovičova 3, 812 19 Bratislava, Slovakia*

Recently, the influence of Eu^{3+} rare-earth (RE) ions on structural, electrical and magnetic properties of ferrites was investigated by many researchers [1-3]. In this work, the effect of Eu substitution of Fe on the magnetic properties of NiZn ferrites was studied. The samples of soft magnetic ferrite with the chemical composition $\text{Ni}_{0.3}\text{Zn}_{0.7}\text{Eu}_x\text{Fe}_{2-x}\text{O}_4$ where $x = 0.00, 0.02, 0.04, 0.06, 0.08$ and 0.10 were prepared by means of ceramic technology at the sintering temperature of 1200°C . Basic composition of the non-substituted ferrite $\text{Ni}_{0.3}\text{Zn}_{0.7}\text{Fe}_2\text{O}_4$ was chosen due to the fact that this ferrite exhibits the largest value of the initial permeability [4, 5] whilst the coercivity is the smallest.

Fundamental magnetic properties such as e.g. the Curie temperature T_C , coercive field H_c , remanent magnetic flux density B_r , hysteresis loop area A_l proportional to the total magnetization loss, amplitude and initial permeability at low frequencies were examined.

This work was supported by the Slovak Research and Development Agency under the contracts No. APVV-0062-11 and by the Scientific Grant Agency of the Ministry of Education, Science, Research and Sport of the Slovak Republic and the Slovak Academy of Sciences, under projects No. 1/0571/15 and 1/0405/16.

- [1] M. Asif Iqbal, Misbah-ul-Islamn, Irshad Ali, Hasan M. Khan, Ghulam Mustafa, Ihsan Ali: Study of electrical transport properties of Eu^{3+} substituted MnZn-ferrites synthesized by co-precipitation technique, *Ceramics International* 39 (2013) 1539–1545.
- [2] M. A. Hossain, M. N. I. Khan, S. S. Sikder: Effect of Resistivity, Permeability and Curie temperature of Rare Earth Metal Europium (Eu) Substitution on $\text{Ni}_{0.60}\text{Zn}_{0.40-x}\text{Eu}_x\text{Fe}_2\text{O}_4$ ($x = 0.05, 0.10, 0.15$) Ferrites, *ARPN Journal of Science and Technology*, vol. 5, No. 10, (2015), 520-524.
- [3] M. Šoka, M. Ušáková, E. Ušák, R. Dosoudil, J. Lokaj: Magnetic Properties Analysis of Rare-Earth Substituted Nickel Zinc Ferrites, *IEEE Transactions on Magnetism*, Vol. 50, No. 4, (2014), Art. No. 2800304, DOI: 10.1109/TMAG.2013.2284053.
- [4] J. Rekošová, R. Dosoudil, M. Ušáková, E. Ušák, I. Hudec: Magnetopolymer Composites With Soft Magnetic Ferrite Filler, *IEEE Transactions on Magnetism*, Vol. 49, No. 1, (2013), 38-41.
- [5] E. Ušák, M. Ušáková: Influence of Ni/Zn Ratio Variation on Structural and Magnetic Properties of NiZn Ferrites, *Journal of Electrical Engineering*, Vol 63, No. 7s, (2012), 141-143.

P2-20**STRUCTURAL RELAXATIONS IN THE AMORPHOUS FeMeMoCrNbB (Me = Ni OR Co) ALLOYS**J. Rzącki¹ and K. Błoch¹*¹Faculty of Production Engineering and Materials Technology, Czestochowa University of Technology, 19 Armii Krajowej Av., 42-200 Czestochowa, Poland*

In this paper the results of the structural and magnetic investigation for FeMeMoCrNbB (Me = Ni or Co) alloys was presented. For the structural investigation was performed by X-ray diffractometry. It was found that investigated samples were amorphous in the as-cast state. The magnetisation was measured within magnetic fields ranging from 0 to 1T using a vibrating sample magnetometer (VSM). The investigation of the 'magnetisation in the area close to ferromagnetic saturation' showed that the magnetisation process in strong magnetic fields is connected with the rotation of the magnetic moments in the vicinity of the defects, which are the sources of the short-range stresses. Analysis of the high-field magnetization curves has facilitated the calculation of the spin wave stiffness parameter.

P2-21**THE STRUCTURE AND POROSITY OF $\text{Fe}_{62-X}\text{Ce}_{10}\text{W}_Y\text{ME}_X\text{Y}_3\text{B}_{20-Y}$ (WHERE ME = Mo, Nb; X = 0, 1, 2; Y = 0, 1, 2) ALLOYS IN THE AMORPHOUS AND CRYSTALLINE STATE**J. Gondro¹, S. Garus¹, M. Nabiałek¹, J. Garus¹ and P. Pietrusiewicz¹¹*Institute of Physics, Częstochowa University of Technology,
Armii Krajowej av. 19, 42-200 Częstochowa, Poland*

Prepared samples were obtained by crystallization of a liquid alloy on a water cooled copper plate and in the amorphous state produced by injection casting method. The structure of the samples was determined by X-ray diffraction patterns. Diffraction patterns of samples produced by injection casting characterized by a single broad peak called "amorphous halo". In the samples cooled on a copper plate has been shown the existence of phases: YB_2 , Fe_2Y , $\alpha\text{-Fe}$, Co_5Y , B_6Co_{23} . The research performed using computer tomography revealed the existence of pores inside of the samples. A lower average pore diameter was in the crystal structure samples.

P2-22

STRUCTURAL RELAXATIONS IN THE MASSIVE ALLOYS

Fe₆₀Co₁₀W_xMo₂Y₈B_{20-x} (x = 0, 1, 2)

K. Błoch¹, S. Garus¹, M. Nabiałek¹ and J. Garus¹

*¹Institute of Physics, Częstochowa University of Technology,
Armii Krajowej av. 19, 42-200 Częstochowa, Poland*

The paper presents the results of structural and magnetic properties of bulk Fe₆₀Co₁₀W_xMo₂Y₈B_{20-x} (x = 0, 1, 2) alloys. Samples of this alloy were prepared by injection casting method in the form of 1 mm thickness plates. The structure of the alloy in the state after solidification was studied by X-ray diffraction. Using a vibrating magnetometer the magnetization in strong magnetic fields has been studied. Analysis of high field magnetization curves allowed to determine the type and quantity of structural defects occurring in the investigated alloys.

P2-23

**THE STUDY OF MAGNETIZATION IN STRONG MAGNETIC FIELDS
FOR $\text{Fe}_{62-x}\text{Co}_{10}\text{Nb}_x\text{Y}_8\text{B}_{20}$ ($x = 0, 1, 2$) ALLOYS**

M. Szota², S. Garus¹, J. Garus¹, K. Gruszka¹ and K. Błoch¹

¹*Institute of Physics, Częstochowa University of Technology,*

Armii Krajowej av. 19, 42-200 Częstochowa, Poland

²*Materials Engineering Institute, Częstochowa University of Technology,*

Armii Krajowej av. 19, 42-200 Częstochowa, Poland

The magnetization process in the area called the approach to ferromagnetic saturation for $\text{Fe}_{62-x}\text{Co}_{10}\text{Nb}_x\text{Y}_8\text{B}_{20}$ ($x = 0, 1, 2$) bulk alloys was analyzed. Using the LakeShore vibrating magnetometer in the fields range of 0 T to 2 T the research were performed. In the studied alloys, in strong magnetic fields, the structural defects affect on magnetization process and the type of defects was designated – the basis of the Kronmüller theory. The article shows that the addition of niobium instead of the iron slightly decreases the saturation magnetization and decreases the value of the coercivity field.

P2-24

COMPARISON OF MAGNETIC PROPERTIES OF AMORPHOUS AND CRYSTALLINE $\text{Fe}_{60}\text{Co}_{10}\text{W}_2\text{Nb}_2\text{Y}_8\text{B}_{18}$ ALLOY

S. Garus¹, M. Nabiałek¹, J. Garus¹ and J. Gondro¹

*¹Institute of Physics, Częstochowa University of Technology,
Armii Krajowej av. 19, 42-200 Częstochowa, Poland*

The article examined the magnetic properties of the alloy $\text{Fe}_{60}\text{Co}_{10}\text{W}_2\text{Nb}_2\text{Y}_8\text{B}_{18}$. The material has been prepared in two ways: by rapid cooling in the copper form - an amorphous state, and slowly cooled on a copper plate - crystalline state. Were analyzed X-ray diffraction and magnetic properties such as saturation magnetization, coercivity field. The amorphous structure of the alloy is usually characterized by better soft magnetic properties than the crystalline structure, however the research showed that in the amorphous $\text{Fe}_{60}\text{Co}_{10}\text{W}_2\text{Nb}_2\text{Y}_8\text{B}_{18}$ alloy was the lower saturation magnetization and higher coercivity field value.

P2-25**MEASUREMENTS OF MAGNETIC PROPERTIES OF POLYMER-METALLIC COMPOSITES**A. Jakubas¹, P. Gębara², A. Gnatowski³ and K. Chwastek¹¹*Faculty of Electrical Engineering, Częstochowa University of Technology, Dąbrowskiego 69, 42-201 Częstochowa, Poland*²*Faculty of Mechanical engineering and Computer Science, Częstochowa University of Technology, Dąbrowskiego 69, 42-201 Częstochowa, Poland*³*Faculty of Production Engineering and Materials Technology, Częstochowa University of Technology, Dąbrowskiego 69, 42-201 Częstochowa, Poland*

In the paper the results of examination of magnetic properties of polymer composites doped with nano-fillers are presented. In this case, soft magnetic composites (SMCs) for electrical engineering applications may be described as structures obtained from the pulverized magnetic material (iron, nano-crystalline, amorphous ferromagnet etc.) glued with polymer. A magnetic nano-particle is surrounded with insulating material, what results in unique magnetic properties dependent on the type of magnetic material, its granulation and percentage contents as well as on the properties of the binder (melting temperature, elasticity, mechanical strength etc.). Such composites reveal a number of advantages in comparison to conventional iron laminates.

SMCs are produced by densification, pressing and thermal processing of mixtures of polymer and ferromagnet. These stages allow one to obtain any shapes and placement of other components in the structure already at the processing stage. Additionally in this way quite different materials may be combined, what is unavailable in other technologies.

The carried out theoretical and experimental studies shall make it possible to carry out an analysis of magnetic properties in novel developed composites in dependence on the type of polymer, magnetic material and their proportion. The aim of the project is to optimize the structure of composites in the context of improvement of their properties.

P2-26**THE INFLUENCE OF TEMPERATURE ON UNIDIRECTIONAL EFFECT IN DOMAIN WALL PROPAGATION**J. Onufer¹, J. Ziman¹, M. Rezníček and S. Kardoš²¹*Department of Physics, Faculty of Electrical Engineering and Informatics, Technical University of Košice, Park Komenského 2, 042 00 Košice, Slovakia*²*Department of Technologies in Electronics, Faculty of Electrical Engineering and Informatics, Technical University of Košice, Park Komenského 2, 042 00 Košice, Slovakia*

It has been reported recently that domain wall mobility in a microwire can be significantly different for cases when magnetization reversal caused by domain wall motion results in different orientation of magnetization [1]. In other words, the process of magnetization reversal runs easier when the sample is magnetized with one orientation of magnetization compared with the opposite one. This behaviour has been called unidirectional effect. It has already been shown that domain wall velocity versus applied magnetic field dependences with higher domain wall mobility are more strongly influenced by applied tensile stress and circular magnetic field created by dc electric current flowing through the microwire compared to those with lower domain wall mobility [2].

In this contribution we present an experimental study of the influence of temperature on unidirectional effect. Glass-coated amorphous $\text{Fe}_{77.5}\text{Si}_{15}\text{B}_{7.5}$ microwire with metallic nucleus radius of about 15 μm and glass coating thickness of about 7.5 μm was used in our experiment.

It was confirmed that domain wall mobility increases with increasing temperature for both types of domain wall velocity versus applied magnetic field dependences. However, the effect of temperature was stronger for dependences with higher domain wall mobility. For the temperature interval 100-300 K the relative change of domain wall mobility in high field (for field interval 370-520 A/m) was about 21 % for the slower wall and about 32 % for the faster wall. Stresses coming from the different thermal expansion coefficients of glass coating and metal core may be responsible for this difference.

- [1] J. Onufer, J. Ziman, M. Kladivová, Unidirectional effect in domain wall propagation observed in bistable glass coated-microwire, *J. Magn. Magn. Mater.* 396 (2015), 313-317.
- [1] J. Onufer, J. Ziman, M. Kladivová, Influence of stress and DC current on unidirectional effect in domain wall propagation, *Journal of Electrical Engineering.* 66, 7 (2015), 108-111.

P2-27**STRUCTURE AND MAGNETIC PROPERTIES OF Fe-B-Si-Zr METALLIC GLASSES**R. Babilas¹, A. Radoń¹ and P. Gębara²¹*Institute of Engineering Materials and Biomaterials, Silesian University of Technology, Konarskiego 18a, 44-100 Gliwice, Poland*²*Institute of Physics, Częstochowa University of Technology, al. Armii Krajowej 19, 42-200 Częstochowa, Poland*

Fe-based glassy alloys have been mainly prepared due to the attractive properties for many magnetic applications. The required magnetic properties are especially large saturation magnetization, low coercive force and high permeability [1-3]. Fe-based metallic glasses with critical cooling rates around 10^6 K/s have been obtained in alloy systems containing metalloids (B, C, Si, P) and early transition elements (Zr, Nb, Hf). It was reported that the Fe-Zr-B alloys show excellent magnetic properties in the nanocrystalline state and good magnetic behaviors in the amorphous state [4].

Fe-based amorphous alloys were characterized by X-ray diffraction (XRD), differential scanning calorimetry (DSC), transmission Mössbauer spectroscopy (MS) and vibrating sample magnetometry (VSM). The studies were performed on $(\text{Fe}_{0.75}\text{B}_{0.15}\text{Si}_{0.1})_{100-x}\text{Zr}_x$ ($x = 0, 1, 3$) metallic glasses in the form of ribbons. The samples were prepared by the “chill-block melt spinning” technique in the argon protective atmosphere [5].

The XRD patterns show the broad diffraction halo that is typical for amorphous metallic alloys. The crystallization behavior associated with onset (T_x) and peak (T_p) crystallization temperatures was examined by DSC method. The Mössbauer spectroscopy allows to study the local environments of the Fe atoms in the glassy state, showing the changes in the amorphous structure due to the changing of Zr addition. From hysteresis loops obtained from VSM measurements, coercive force and magnetic saturation induction were determined versus different Zr content. The obtained magnetic properties allow to classify the studied amorphous alloys in as-cast state as soft magnetic materials.

[1] H.S. Chen, *Rep. Prog. Phys.* 43 (1980) 353-432.

[2] B. Shen, Ch. Chang, A. Inoue, *Intermetallics* 15 (2007) 9-16.

[3] G. Herzer, *Acta Mater.* 61 (2013) 718-734.

[4] B. Yao, Y. Zhang, L. Si, H. Tan, Y. Li, *J. All. Comp.* 370 (2004) 1-7.

[5] R. Babilas, *Mat. Character.* 107 (2015) 7-13.

P2-28**STRUCTURE AND COERCIVITY OF AMORPHOUS RAPIDLY QUENCHED FeCrB ALLOY**J. Kecer¹ and L. Novák¹*¹Department of Physics, Faculty of Electrical Engineering and Informatics, Technical University of Košice, Park Komenského 2, 042 00 Košice, Slovakia*

Rapidly quenched amorphous ferromagnetic materials are becoming increasingly used as magnetically soft materials. For this reason it is very important to study not only the relationship between the changes in their structure and their magnetic properties but also stability of these properties. This study is focused on comparison of the properties of amorphous rapidly quenched FeCrB ribbons of three compositions with those of amorphous FeB ribbon.

The changes in the structure of amorphous rapidly quenched ferromagnetic materials, which are caused by introduction of atomic hydrogen and its consequent spontaneous release from material, are reported in the paper. Hysteresis loops which were measured in equidistant time instants during the processes of hydrogenation and dehydrogenation provided the values of coercivity, magnetic polarization of saturation was measured in the magnetic field strength of 1,6 kA/m, and the total (effective) anisotropy was determined from the curve of initial magnetic polarization.

Introduction of atomic hydrogen in the samples resulted in a conspicuous increase in coercivity (2-3 times higher than the initial value). The total anisotropy was changed only slightly and it cannot explain so large coercivity increase. For this reason the changes in the thickness of the domain wall (due to the introduction of hydrogen) and also the changes in the size of clusters (due to inhomogeneous increase in internal stresses in the process of hydrogenation) have been studied. The obtained results could be explained by the fact that during dehydrogenation relaxation of stress induced by hydrogen takes place continuously, which facilitates the diffusion of boron atoms at short distances and reduces internal stresses transferred into material during the preparation process. Moreover, the size of atomic clusters which act as stress centers also changes.

P2-29**MAGNETIC PROPERTIES OF $\text{Ni}_{0.2}\text{Zn}_{0.8}\text{Fe}_2\text{O}_4$ FERRITE FIBERS PREPARED BY NEEDLE-LESS ELECTROSPINNING TECHNIQUES**M. Streckova¹, E. Mudra¹, M. Sebek¹, T. Sopcak¹, J. Kovac² and J. Duzsa¹¹*Institute of Materials Research, Slovak Academy of Sciences, Watsonova 47, 040 01 Kosice, Slovak Republic*²*Institute of Experimental Physics, Slovak Academy of Sciences, Watsonova 47, 040 01 Košice, Slovak Republic*

One-dimensional nanostructures have received considerable attention due to their tunable physical and electroactive properties, such as mechanical strength, toughness, ferromagnetism, ferroelectricity, etc. The cost-effective and versatile technique for the preparation of fiber nanostructures in the large scale is electrospinning. The preparation of nanostructured materials became available with the expansion of electrospinning from polymers to composites and to ceramics. The typical property of as-prepared fibrous materials is a high surface-to-volume ratio which makes them useful for potential applications such as nanoelectronic devices, sensors, solar cells, photonics, multiferroic materials, molecular sieves, high-temperature insulation, catalysis, biomedical separation, and microwave absorbers. In this work the synthesis and experimental set up of $\text{Ni}_{0.2}\text{Zn}_{0.8}\text{Fe}_2\text{O}_4$ fibers is presented by means of needle-less electrospinning techniques. The pure single phase spinel ferrite was obtained after conventional thermal treatment of PVA/metal nitrate precursor fibers at 800°C for 4 hours adjusted according to the results obtained from TG/DSC analysis. The spinel structure was verified by XRD analysis. The precursor and final fibers morphology was visualized by SEM and TEM. The fibers were arranged and self-assembled to yield dense and continuous fibrous structure. The mass magnetization, coercivity and saturation magnetization of the fibrous samples were measured in the wide range of temperatures on the magnetic properties measurement system (MPMS).

P2-30

STUDY OF THE MAGNETIZATION PROCESSES IN AMORPHOUS AND NANOCRYSTALLINE FINEMET BY THE NUMERICAL DECOMPOSITION OF THE HYSTERESIS LOOPS

J. Kováč¹ and L. Novák²

¹*Inst. of Exp. Physics, Slovak Academy of Sciences, Watsonova 47, 040 01 Košice, Slovakia*

²*Department of Physics, Faculty of Electrical Engineering and Informatics, Technical University of Košice, Letná 9, 042 00 Košice, Slovakia*

The magnetization processes in amorphous and nanocrystalline FINEMET ribbons were studied by the numerical decomposition of the quasi-static hysteresis loop to the contributions of the rotational magnetization (DR) the domain wall movement (DWM) and the domain wall annihilation and nucleation (DWAN) processes following the hyperbolic model of hysteresis. The hysteresis data measured during decreasing of the excitation magnetic field were used for the separation of these processes.

The significant differences in behavior of these two materials were found. The process of the domain wall annihilation is most dominant in the amorphous alloy. The domain wall movement is blocked in this material by internal stresses introduced during the process of preparation. On the contrary, this process - the domain wall movement - is markedly prevailing in nanocrystalline ribbon. In this material, the internal stresses are removed by thermal treatment. In addition, as it is well known, the magnetic anisotropy in nanocrystalline FINEMET reaches very low values. The result is that the DWM is energetically the most advantageous process to change magnetization in this material.

Acknowledgment

This work was realized within the project ITMS 26220120019.

P2-31

**MESOPOROUS SILICA SBA-15 FUNCTIONALIZED BY
NICKEL-PHOSPHONIC UNITS STUDIED BY RAMAN AND SQUID
MAGNETOMETRY**

M. Laskowska¹ and L. Laskowski¹

*¹Czestochowa University of Technology, Institute of Computational Intelligence,
Al. Armii Krajowej 36, 42-201 Czestochowa, Poland*

In the present work we present mesoporous silica SBA-15 containing propyl-nickel phosphonate study towards confirmation of synthesis procedure correctness. The structure of mesoporous sample were tested by TEM microscopy and X-Ray scattering. To probe bounding between nickel atoms and phosphonic units the Raman spectroscopy was carried out. As a support of Raman scattering, the theoretical calculations were made based on density functional theory, with the B3LYP method. By comparison of the calculated vibrational spectra of the molecule with experimental results, distribution of the active units inside silica matrix has been determined. Magnetic measurements were carried out to find nickel ions concentration inside mesoporous matrix, and also to determine nickel ions environment. Both magnetic and Raman research allowed on probing of synthesis efficiency.

P2-32**MAGNETIC AND STRUCTURAL CHARACTERIZATION OF NICKEL AND IRON BASED HEUSLER RIBBON Ni_2FeZ ($\text{Z} = \text{In, Sn, Sb}$)**

L. Bujnakova¹, T. Ryba^{2,3}, Z. Vargova¹, V. Komanicky³, J. Kovac⁴, R. Gyepes⁵ and R. Varga³

¹*Inst. Chem., Fac.Sci., UPJS, Moyseova 11, 041 54 Kosice, Slovakia*

²*RV Magnetics, a.s., Hodkovce 21, 044 21 Hodkovce, Slovakia*

³*Inst. Phys., Fac. Sci., UPJS, Park Angelinum 9, 041 54 Kosice, Slovakia*

⁴*IEP SAS, Watsonova 47, 040 01 Kosice, Slovakia*

⁵*Dept. Chem., Fac. of Education, J. Selye University, Komárno, Slovakia*

Heusler alloys are intermetallic materials with promising technological applications such as spintronics, thermoelectrics, magnetocaloric cooling, sensors etc.[1-2]. One of the few disadvantages of Heusler alloy is their complicated production process that consists of melting pure elements together and further long-term thermal treatment at elevated temperature in order to get correct structure with proper chemical short range order. Recently, rapid quenching has been applied for fast and easy production of large amount of Heusler alloy [3]. Additionally, properly selected chemical composition [1] together with the rapid quenching could lead to single step production of Heusler alloys with desired structure and chemical short-range ordering.

In this article, we study the comparison of structural, chemical and magnetic properties of Ni_2FeZ ($\text{Z}=\text{In, Sn, Sb}$) Heusler ribbons produced by melt-spinning. Microstructural study reveals polycrystalline structure. It is shown that correct L_{21} structure can be obtained by single step production for Ni_2FeSb full Heusler alloys. On the other hand, more phases occurs in case of Ni_2FeSn alloys and further thermal treatment is necessary to get correct chemical short range order. Finally, Ni_2FeIn produces multiphase system that does not contain Heusler structure, most probably because of immiscibility of Fe in In.

Additionally, magnetic characterization has been performed, showing high Curie temperatures (above 500 K for Ni_2FeSb and Ni_2FeSn and 800K for Ni_2FeIn).

This research was supported by the projects APVV-0027-11 and Slovak VEGA grant. No. 1/0164/16.

[1] T. Graf, C. Felser, S.S.P. Parkin, *Prog. Solid State Chem.* 39 (2011), 1.

[2] A. Hirohata, M. Kikuchi, N. Tezuka, K. Inomata, J.S. Claydon, Y.B. Xu, G. van der Laan, *Curr. Opin. Sol. State Mat. Sci.* 10 (2006), 93.

[3] J.L.S.Llamazeres, T.Sanchez, J.D.Santos, et al. *Appl. Phys. Lett.*, 92 (2008) 012513.

P2-33

XAFS SIGNALS MEASURED ON POLYCRYSTALLINE Fe AND $\text{Zr}_{60}\text{Cu}_{20}\text{Fe}_{20}$ ALLOY IN TRANSMISSION AND TOTAL ELECTRON YIELD MODE

K. Saksl^{1, 2}, S. Michalik³, O. Milkovič⁴, J. Gamcová², V. Girman² and D. Balga¹

¹*Institute of Materials Research, Slovak Academy of Sciences, Watsonová 47, 04001 Košice, Slovakia*

²*Institute of Physics, Faculty of Science, P.J. Šafárik University, Park Angelinum 9, 041 54 Košice, Slovak Republic*

³*Diamond Light Source Ltd., Harwell Science and Innovation Campus, Didcot, Oxfordshire OX11 0DE, UK*

⁴*Institute of Materials, Technical university of Košice, Letná 9, 042 00 Košice, Slovakia*

X-ray absorption fine structure spectroscopy (XAFS) has been established as a valuable tool for the determination of atomic scale structure for many types of materials. In this paper we compare difference between the total electron yield (TEY) and absorption coefficients measured at *K* absorption edge of magnetic polycrystalline Fe and $\text{Zr}_{60}\text{Cu}_{20}\text{Fe}_{20}$ alloy. The presented results serve as a demonstration of capabilities and limitations of the TEY and transmission XAFS measurement modes.

P2-34**STRUCTURAL AND THERMOMAGNETIC PROPERTIES OF** **$\text{Fe}_{86-x}\text{Zr}_7\text{M}_x\text{Nb}_2\text{Cu}_1\text{B}_4$ {M=Co, Ni, (CoCr); x=0 or 6} ALLOYS**A. Łukiewska¹*¹Institute of Physics, Czestochowa University of Technology, Armii Krajowej Avenue 19, 42-200 Czestochowa, Poland*

The effect of the substitution of Co, Ni or (CoCr) for the part of Fe atoms on the thermal stability, structure and some magnetic properties, i.e. magnetization and magnetocaloric effect of $\text{Fe}_{86-x}\text{Zr}_7\text{M}_x\text{Nb}_2\text{Cu}_1\text{B}_4$ {M=Co, Ni, (CoCr); x=0 or 6} alloys has been studied. All investigations were carried out for the alloys in the as-quenched state and after the accumulative annealing for 10 min at 600 K, 700 K and 750 K. The annealing temperatures were chosen according to differential scanning calorimetry curves (DSC) recordered by NETSCH STA 449F1 Jupiter set-up at the heating rate of 10 K/min. The results obtained from X-ray diffractometry studies indicate that the replacement of 6 at.% Fe with Co, Ni and (CoCr) in the amorphous $\text{Fe}_{86}\text{Zr}_7\text{Nb}_2\text{Cu}_1\text{B}_4$ alloy reduces the thermal stability of the alloy. The pronounced decrease of the crystallization temperature was observed after Ni addition to $\text{Fe}_{86}\text{Zr}_7\text{Nb}_2\text{Cu}_1\text{B}_4$ alloy. To explain magnetic behavior of the samples the thermomagnetic curves $\sigma(T)$ were measured in magnetizing field induction from 5 mT up to 1 T. From the families of the isothermal magnetic curves $\sigma(B)$ the Arrott's plots were constructed and the positive value of these plots slope near the Curie temperature shows that the ferromagnetic- paramagnetic phase transition in the investigated alloys is of the second order type. The values of the magnetic entropy changes ($-\Delta S_M$) versus temperature (magnetocaloric effect) were also calculated from those families. The maximum of the magnetic entropy changes occurs near the Curie temperature of the alloys. In $-\Delta S_M(T)$ curves obtained for $\text{Fe}_{80}\text{Zr}_7\text{Ni}_6\text{Nb}_2\text{Cu}_1\text{B}_4$ and $\text{Fe}_{80}\text{Zr}_7\text{Co}_3\text{Cr}_3\text{Nb}_2\text{Cu}_1\text{B}_4$ alloys after annealing at 600 K and then 700 K the distinct shift of maxima toward the lower temperatures was observed. It is due to the invar effect.

P2-35

THE CORRELATION OF MAGNETIC AND STRUCTURAL PROPERTIES OF Ni-Ti-Zr BULK METALLIC GLASS AT ELEVATED TEMPERATURES

M. Lisnichuk¹, J. Katuna¹, K. Saksl^{1,2}, V. Girman¹, J. Gamcová¹, D. Balga², M. Ďurišin², J. Kováč³ and P. Sovák¹

¹*Institute of Physics, Faculty of Science, P.J. Šafárik University, Park Angelinum 9, 041 54 Košice, Slovak Republic*

²*Institute of Materials Research, Slovak Academy of Sciences, Watsonová 47, 040 01 Košice, Slovakia*

³*Institute of Experimental Physics of SAS, Watsonová 47, 040 01 Košice, Slovakia*

Ni-Ti-Zr bulk metallic glass (BMG) is due to its known shape memory properties a promising alloy for a wide range of engineering materials in the field of micromechanical systems. In this paper, its structure and surface was investigated via X-ray diffraction and scanning electron microscopy with energy dispersive X-ray spectroscopy (SEM/EDX). The evolution of the saturation magnetization after thermal treatment was measured by vibrating-sample magnetometer at maximum applied field of 1T in the temperature range of 300–1100 K.

Acknowledgment

This work was realized within the project ITMS 26220120019.

P2-36**TEMPERATURE EVOLUTION OF HYPERFINE MAGNETIC FIELDS ON 57-Fe IN A Fe-Co-Si-B-Mo-P METALLIC GLASS**

M. Cesnek¹, M. Miglierini^{1,2}, T. Kmječ³, J. Kohout³, N. Amini^{2,4} and D. Janičkovič⁵

¹*Department of Nuclear Reactors, Czech Technical University in Prague, V Holešovičkách 2, 180 00 Prague, Czech Republic*

²*Institute of Nuclear and Physical Engineering, Slovak University of Technology, Ilkovičova 3, 812 19 Bratislava, Slovak Republic*

³*Charles University in Prague, Faculty of Mathematics and Physics, V Holešovičkách 2, 180 00 Prague, Czech Republic*

⁴*Department of Physics, Bu-Ali Sina University, 65174-4161, Hamedan, Iran*

⁵*Institute of Physics, Slovak Academy of Sciences, Dúbravská cesta 9, 845 11 Bratislava, Slovak Republic*

This contribution shows the results from the studies of magnetic behaviour of the Fe₅₀Co₁₂Si₁₆B₉Mo₅P₈ metallic glass. Amorphous state of the ribbon-shaped sample was proved by X-ray diffraction. Magnetic properties were characterized by temperature dependences of magnetization which were measured in zero field cooled (ZFC) and field cooled (FC) regimes in the range 50 K – 400 K with applied external magnetic fields up to 25 mT. Structural and magnetic features were studied by transmission ⁵⁷Fe Mössbauer spectroscopy (MS). MS spectra of the as-quenched samples were recorded in the temperature range 4.2 K – 415 K. They exhibit broadened spectral lines which are characteristic for an amorphous structure and were refined using distributions of hyperfine magnetic fields. The latter gradually collapsed with increasing temperature of measurement. Average values of hyperfine magnetic fields obtained from MS are compared with the results of magnetization measurements. Curie temperature of the investigated metallic glass was determined from both types of experiments to be T_c ~ 397 K. Additional differential scanning calorimetry experiments have revealed that the onset of crystallization is expected at the temperature of ~835 K. However, MS spectrum, which was recorded at room temperature using a sample annealed for one hour in a protective Ar atmosphere, shows that nanocrystalline grains are formed already at notably lower temperature. Their analysis is also briefly reported.

This work was supported by the grants GACR 14-12449S, VEGA 1/0182/16 and VEGA 2/0189/14.

P2-37

STRUCTURE AND MAGNETIC PROPERTIES OF IRON/IRON-OXIDE NANOPARTICLES PREPARED BY PRECIPITATION FROM SOLID STATE SOLUTION

O. Milkovič¹, M. Sopko¹, J. Gamcová² and I. Škorvánek³

¹*Institute of Materials, Technical university of Košice, Letná 9, 042 00 Košice, Slovakia*

²*Institute of Materials Research, Slovak Academy of Sciences, Watsonová 47, 04001 Košice, Slovakia*

³*Institute of Physics, Faculty of Science, P.J. Šafárik University, Park Angelinum 9, 041 54 Košice, Slovak Republic*

⁴*Institute of Experimental Physics of SAS, Watsonová 47, 040 01 Košice, Slovakia*

The influence of precipitation temperature on structural and magnetic properties of iron/iron-oxide nanoparticles is investigated. Nanoparticles were prepared by precipitation of γ -Fe precipitates in Cu-Fe solid solution and subsequently isolated by matrix dissolution. Precipitation annealing temperatures were 773 K, 873 K and 973 K. Nanoparticles core-shell structure and morphology were characterized by X-ray diffraction, high-resolution transmission electron microscopy and selected area electron diffraction. These measurements showed that average diameter of nanoparticles increases with precipitation temperature from 8,5 nm to 20,5 nm. The measurements of magnetization as a function of temperature and applied field have been performed by SQUID magnetometer in temperature range from 5 K to 200 K.

P2-38

THE STRUCTURAL CHARACTERIZATION OF Ni-Ti-Zr BULK METALLIC GLASS USING TRANSMISSION AND SCANNING ELECTRON MICROSCOPY

J. Katuna¹, M. Lisnichuk¹, K. Saks^{1,2}, V. Girman¹, J. Gamcová¹, D. Balga², M. Ďurišin², J. Kováč³ and P. Sovák¹

¹*Institute of Physics, Faculty of Science, P.J. Šafárik University, Park Angelinum 9, 041 54 Košice, Slovak Republic*

²*Institute of Materials Research, Slovak Academy of Sciences, Watsonová 47, 040 01 Košice, Slovakia*

³*Institute of Experimental Physics of SAS, Watsonová 47, 040 01 Košice, Slovakia*

BMGs in contrast to its crystalline counterparts, exhibit unique mechanical and structural properties, which make them attractive for practical applications. Especially Ni-Ti-Zr BMG is a promising alloy for micromechanical systems because of its known shape memory properties. Shape memory properties are connected with structural phase transformation. In this paper, the room-temperature-structure of Ni-Ti-Zr BMG is investigated using transmission electron microscopy (TEM) and the surface and chemical analysis is documented using scanning electron microscopy (SEM). Moreover, the influence of temperature on magnetic behavior measured by vibrating-sample magnetometer is reported.

Acknowledgment

This work was realized within the project ITMS 26220120019.

P2-39

THE INFLUENCE OF PULSE HEATING ON THE RAYLEIGH REGION IN AMORPHOUS FINEMET ALLOY

L. Novák¹, J. Kováč² and L. Hubáč²

¹*Department of Physics, Technical University of Košice, Park Komenského 2, 042 00 Košice, Slovakia*

²*Inst. of Exp. Physics, Slovak Academy of Sciences, Watsonova 47, 040 01 Košice, Slovakia*

Magnetization processes in ferromagnetic materials can be described in four ways - reversible and irreversible domain wall motion, rotation of the vector of magnetic polarization and paraprocess in high magnetic fields. The process of reversible domain wall motion is characteristic for the range of small exciting magnetic fields - Rayleigh region.

The method of pulse annealing was used for modification of magnetic properties of material. The results of magnetic measurements in this region obtained on the amorphous FINEMET samples are presented. The magnetic properties of the samples were investigated after application of three different types of pulse heating and subsequently compared with results obtained on the sample subjected to classical annealing.

Besides of magnetization processes in Rayleigh region full hysteresis loops for both amorphous and nanocrystalline samples were also measured. Processing of these measurements provides data about the other magnetic parameters as coercivity, magnetoelastic anisotropy as well as thickness of domain walls.

The reason of the observed significant differences in the behavior of the investigated samples we are finding in different influences on the internal stresses what are the cause of the changes in total magnetic anisotropy and subsequently in different thickness of domain walls.

Acknowledgment

This work was realized within the project ITMS 26220120019.

P2-40**EFFECT OF THICKNESS OF ELECTROPLATED NiFe CORES ON THE NOISE OF FLUXGATES**M. Butta¹*¹Department of Measurement, Faculty of Electrical Engineering, Czech Technical University in Prague, Technická 2 – 16627 Praha, Czech Republic*

A typical rule of the thumb of fluxgate sensors design is to avoid large core thickness because this would result in a low sensitivity due to the increased core demagnetizing factor (lower coupling to the external magnetic field). Nevertheless, this simple criterion becomes complicated when other phenomena have to be taken into account, such as the effect of field induced anisotropy.

It has been recently shown that radial anisotropy can be induced in NiFe ring cores by electroplating this film under the influence of a large magnetic field. The radial anisotropy reduces the noise of the fluxgate because it is orthogonal to the direction of magnetization all over the circumference of the ring.

We wanted to understand how the thickness influences the field-induced anisotropy and finally what is its effect on the noise of the fluxgate sensor.

We electroplated the ring-cores in a yoke with about 720 kA/m radial field. Four cores were obtained for each value of thickness to have statistically relevant data. The shape of the ring's B-H loop significantly depends on the thickness. For 2 μm thickness the B-H loop shows very moderate radial anisotropy, whereas at 12 μm thickness there was a clear field-induced anisotropy orthogonal to the direction of magnetization. Cores with intermediate thickness have anisotropy monotonically increasing with thickness up to 12 μm ; for larger thickness the anisotropy does not further increase.

Then, we used the electroplated cores for fluxgate sensors exciting them in all cases with the same excitation current and using the same pick-up coil (2nd harmonic was extracted by a lock-in amplifier). We observed that as the thickness increased from 2 to 12 μm , the higher field-induced anisotropy makes the noise of the sensor drop by one order of magnitude. The sensor's noise decreased despite increasing its demagnetizing factor: this means that the reduction of sensor's noise was mainly due to the larger anisotropy in the thicker cores. This also explains why for thicknesses larger than 12 μm the noise starts to increase: in such cores the anisotropy does not further increase but on the other hand the demagnetizing factor does. Therefore, we explain the minimum of 60 pT/ $\sqrt{\text{Hz}}$ at 1 Hz found for 12 μm thickness as an optimum solution between highest induced anisotropy and lowest demagnetizing factor.

P2-41**INFLUENCE OF CO DOPING ON INDUCED ANISOTROPY AND DOMAIN STRUCTURE IN MAGNETIC FIELD ANNEALED (Fe_{1-x}Co_x)₇₉Mo₈Cu₁B₁₂ ALLOY**B. Kunca¹, J. Marcin¹, P. Švec², J. Kováč¹, P. Švec Sr.² and I. Škorvánek¹¹*Institute of Experimental Physics, Slovak Academy of Sciences, Watsonova 47, 040 01 Košice, Slovakia*²*Institute of Physics, Slovak Academy of Sciences, Dúbravská cesta 9, 842 28 Bratislava, Slovakia*

FeMoCuB-based nanocrystalline alloys show good soft magnetic behavior. However, stability of their magnetic properties towards elevated temperatures is poor, mainly because of low Curie temperature [1]. Improvement of thermal and magnetic properties could be achieved by Co doping. With rising Co content, Curie temperature is shifted to higher temperatures, which makes such compositions interesting candidates for high temperature applications. In this work, nanocrystallization and induced anisotropy were investigated in a system of alloys (Fe_{1-x}Co_x)₇₉Mo₈Cu₁B₁₂ (where x=0, 0.2, 0.5). Ribbons were isothermally annealed at 703K for 1 hour in presence of zero (ZF), longitudinal (LF), and transverse (TF) magnetic field with magnitude up to 640kA/m. The XRD and TEM analysis has revealed formation of nanocrystalline structure of BCC grains in all samples. Temperature dependence of magnetization, measured from 200K to 870K, showed a marked increase of Curie temperature with rising Co content. For Co-free samples, hysteresis loops with high coercivity are nearly identical for all thermally treated samples and hence, the effect of induced anisotropy is not present. In Co doped samples, small increase of coercivity values was observed after ZF annealing. Thermal treatment under LF conditions resulted in a squared hysteresis loops, with accompanied coercivity reduction. Sheared hysteresis loops were achieved by TF annealing, with sufficiently low values of coercivity. Domain structure in these samples was investigated by Kerr microscopy. Complicated domains structures with the presence of maze-shaped patterns were observed after ZF thermal treatment. Samples annealed in applied magnetic field showed uniform domain structure parallel (LF), and perpendicular to the direction of ribbon axis (TF) respectively. Correlations between Co doping, Curie temperature and magnetic properties after annealing will be discussed.

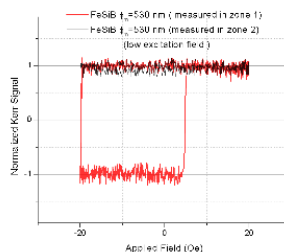
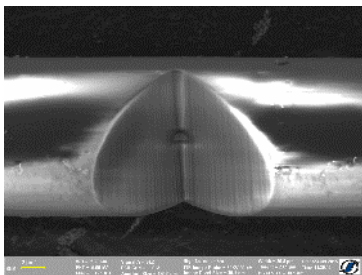
*Acknowledgment**This work was realized within the project ITMS 26220120019.*

[1] E. Illeková et al.: J. Magn. Magn. Mat. 304 (2006) e636-e638.

P2-42**FORMATION AND MOTION OF DOMAIN WALLS IN RAPIDLY SOLIDIFIED AMORPHOUS MAGNETIC NANOWIRES**M. Ţibu¹, M. Lostun¹, D. A. Allwood², H. Chiriac¹, N. Lupu¹ and T.-A. Óvári¹¹National Institute of R&D for Technical Physics, 700050 Iaşi, Romania²Dept. of Materials Science and Engineering, Sheffield University, S1 3JD, UK

Amorphous glass-coated wires with metallic nucleus diameters below 1 μm have been recently prepared by rapid solidification. They exhibit bistable magnetic behavior on the axial direction due to their specific domain structure. Therefore, the propagation of domain walls in these ultrathin magnetic wires is of high interest for applications in domain wall logic devices and in miniature magnetic sensors. However, such applications require an accurate control over the dynamics of the domain walls, as well as over their formation and motion, since the speed of these devices will directly depend on the velocity of the domain walls.

Here we report on the influence of artificial defects on the dynamics of domain walls in rapidly solidified amorphous nanowires. Artificial defects such as the one shown below have been made using a focused ion beam (FIB) system.



Notch in an $\text{Fe}_{77.5}\text{Si}_{17.5}\text{B}_{15}$ amorphous nanowire – left, and its effect on the MOKE hysteresis loops before (zone 1) and after the notch (zone 2) – right.

The influence of artificial defects on the nucleation of new domains and propagation of domain walls along the samples has been investigated using a set-up based on a NANOMOKE-2 equipment for the study of magneto-optical Kerr effect (MOKE). We have found that it is possible to generate and pin a domain wall in well-defined regions of the samples. The simultaneous use of nucleation pulses and artificial defects can yield a good and efficient control over the domain wall movement in magnetic amorphous nanowires.

Acknowledgment – Work supported by the Romanian Executive Agency for Higher Education, Research, Development and Innovation Funding (UEFISCDI) under Contract no. 46/2013 (Project PN-II-ID-PCE-2012-4-0424) and by the European Commission under Grant no. 316194 (NANOSSENS).

P2-43**HOPKINSON EFFECT IN SOFT AND HARD MAGNETIC FERRITES**J. Sláma¹, M. Ušáková¹, M. Šoka¹, R. Dosoudil¹ and V. Jančárik¹¹*Faculty of Electrical Engineering and Information Technology, Slovak University of Technology in Bratislava, Ilkovičova 3, 812 19 Bratislava, Slovakia*

Some of the temperature dependencies of magnetic susceptibility $\chi(T)$ reveal a presence of a peak just below the Curie temperature T_C , i.e. Hopkinson effect. The accepted explanation of the Hopkinson effect is based on domain wall motion. Heating of soft magnetic material leads to the domain wall mobility increase and consequently the magnetic susceptibility increment as well. The Hopkinson effect occurrence based only on idea of domain wall motion is obviously inapplicable to the hard magnetic materials as well as to the case of single-domain particles. However, we observed the Hopkinson effect in many $\chi(T)$ dependencies of the hexagonal (Br, Sr) ferrite samples, or in (not only single domain) particle ferrite samples. We investigated the Hopkinson effect in ferrites with spinel structure as well as with hexagonal structure. The explanation of experimentally observed Hopkinson peak based on superparamagnetic state of particles at a critical temperature just below T_C is proposed. The Hopkinson peak turns out to be associated with the transition from the region of stable magnetization to super-paramagnetism in contrast to other explanations of Hopkinson effect.

In the present work we discuss fluctuations of magnetization above the blocking temperature in particles with arbitrary magnetic energy, and the influence of these fluctuations on magnetic susceptibility. We want present an answer to the question of the existence of the Hopkinson effects, which had been indicated in ferrites with spinel structure and hexagonal structure.

Acknowledgement

This work was supported by the Slovak Research and Development Agency under the contract no. APVV-0062-11 and by the Scientific Grant Agency of the Ministry of Education, Science, Research and Sport of the Slovak Republic, and in part by the Slovak Academy of Sciences, under projects no. 1/0571/15 and 1/0405/16.

P2-44**INFLUENCE OF VITROVAC CONTENT ON MAGNETIC PROPERTIES IN COMPOSITE MATERIALS BASED ON THE MIXTURE OF TWO FERROMAGNETS**L. Hegedűs¹, P. Kollár¹, J. Füzer¹, R. Bureš², M. Fáberová² and P. Kurek²¹*Institute of Physics, Faculty of Science, P. J. Šafárik University, 041 54 Košice, Slovakia*²*Institute of Materials Research, Slovak Academy of Sciences, 040 01 Košice, Slovakia*

Soft magnetic composite materials (SMCs) play an important role in nowadays industry, replacing the traditional materials such as electrical steels and soft ferrites, especially at medium and higher frequency applications. The material can be tailored for a specific application by changing the composition of the material and by adaptation the fabrication process.

The aim of this work was to investigate the morphology, phase composition and magnetic properties of SMCs with various magnetic content and crystallization-temperature to minimize the total magnetic losses. The prepared sample series was based on the mixture of two different ferromagnets Vitrovac 6155 (amorphous Co-based) and Somaloy 700 (polycrystalline Fe-based) without addition of insulating material. Two series of the samples were prepared. The samples were prepared by conventional powder metallurgy with particular fraction (5, 20, 30, 50 wt. % of Vitrovac 6155) in the form of a ring for magnetic measurements in AC fields and electric resistivity measurements. The mixed powders were uniaxially pressed at 800 MPa and heat treated (at 450°C and 530°C, respectively) in an electric furnace in air atmosphere. The samples annealed at 450°C consist of amorphous Co-based powder and polycrystalline Fe-based powder (A series). The samples annealed at 530°C consist of crystalline Co-based powder and polycrystalline Fe-based powder (B series). A series exhibits substantial lower values of total losses compared to that for B series. The Vitrovac 6155 content causes the increase of the specific resistivity of both sample series.

*Acknowledgment**This work was realized within the project ITMS 26220120019.*

P2-45**MAGNETIC PROPERTIES OF Fe-BASED SOFT METALLIC ALLOY AFTER ION IRRADIATION**M. Hasiak¹ and M. Miglierini^{2,3}¹*Department of Mechanics and Materials Science, Wrocław University of Science and Technology, Smoluchowskiego 25, 50 370 Wrocław, Poland*²*Institute of Nuclear and Physical Engineering, Slovak University of Technology, Ilkovičova 3, 812 19 Bratislava, Slovakia*³*Department of Nuclear Reactors, Faculty of Nuclear Sciences and Physical Engineering, Czech Technical University in Prague, V Holešovičkách 2, 180 00 Prague 8, Czech Republic*

Fe-based metallic glasses are interesting from a basic research point of view because they do not exhibit any topological order in the structural arrangement of the constituent atoms. Their magnetic properties can be easily affected by impurities and/or structural modifications that are introduced during or after the production process. In this respect, an influential role is played by ion irradiation.

In this paper we investigate the effects of ion irradiation on microstructure and magnetic properties of the as-quenched $^{57}\text{Fe}_{75}\text{Mo}_8\text{Cu}_1\text{B}_{16}$ metallic glass. Magnetization characteristics were recorded in a wide range of temperatures (50-400 K) under external DC magnetic fields of up to 0.1 T. Zero field cooled and field cooled mode magnetization versus temperature characteristics demonstrate an impact of magnetic field on low temperature magnetic properties. The analysis of the hysteresis loops recorded at different temperatures shows that the coercivity depends on temperature and also ion irradiation. We have also performed magnetocaloric effect studies for ion irradiated samples. They were calculated for magnetic fields of up to 1 T. Microstructure of ribbon-shaped samples was investigated at room temperature by conversion electron Mössbauer spectrometry which is especially suitable for surface modified materials.

From the obtained results we can conclude that ion irradiation affects microstructure and magnetic behaviour of the as-quenched $^{57}\text{Fe}_{75}\text{Mo}_8\text{Cu}_1\text{B}_{16}$ metallic glass.

This work was supported by the grants GACR 14-12499S and VEGA 1/0182/16.

P2-46**FeSiBAlNiMo HIGH ENTROPY ALLOY PREPARED BY MECHANICAL ALLOYING**

R. Bureš¹, H. Hadraba², M. Fáberová¹, P. Kollár³, J. Füzér³, P. Roupčová² and M. Strečková¹

¹*Institute of Materials Research, Slovak Academy of Sciences, Watsonova 47, 040 01 Kosice, Slovak Republic*

²*Institute of Physics of Materials, Academy of Sciences of Czech Republic, Žitkova 22, 616 62 Brno, Czech Republic*

³*Institute of Physics, Faculty of Science, Pavol Jozef Safarik University in Kosice, Park Angelinum 9, 041 54 Kosice, Slovak Republic*

Traditional strategy of physical metallurgy is based on one principal element as matrix. There are iron based alloys, nickel based super alloys etc, as well as metal matrix composites. Novel alloy design concept is based on multiple principal elements in equimolar or near-equimolar ratios [published by Yeh]. Solid solution of many elements will tend to be more stable because of their large mixing entropies. High entropy alloys (HEA) are composed of at least 5 principal elements. Nowadays, unique structure and physical properties of HEA's are often subject of study. FeSiBAlNi HEA system was inspired by FeSiB metallic glasses with good glass formation ability, thermal stability and soft magnetic properties. The amorphous high entropy alloys have been successfully fabricated using the mechanical alloying method. The as-milled FeSiBAlNi(Nb) powders are soft magnetic materials as it was published by Wang. The Nb addition does not improve the soft magnetic properties of FeSiBAlNi HEA. FeSiBAlNiMo equiatomic high entropy alloy was prepared by mechanical milling. Mechanical alloying process was monitored using X-ray diffraction. Prepared powder HEA was consolidated using cold pressing and sintering at 580°C and 1100°C in Ar/10H₂ protective atmosphere. Properties of the consolidated samples were investigated by measurement of coercivity, resistivity, elastic modulus, hardness and transverse rupture strength (TRS). Structure of the samples were analyzed using scanning electron microscopy and X-ray diffraction. Low temperature sintering at 580°C led to low elastic (E-modulus=7.5 GPa) and mechanical (TRS=5 MPa) properties, but lower coercivity (H_c=400 A/m). High temperature sintering at 1100°C produced higher strength (TRS=345 MPa), but nearly four times higher coercivity (H_c=1450 A/m). Nano-crystalline phase based on complex borides was confirmed by XRD in high temperature sintered sample. Main constituents of low temperature sintered HEA were alpha iron and AlNi solid solution.

P2-47**EFFECT OF SAMPLE THICKNESS ON GMI BEHAVIOR OF AMORPHOUS $(\text{Fe}_1\text{Ni}_1)_{73}\text{Nb}_7\text{B}_{20}$ RIBBONS**F. Andrejka¹, J. Marcin¹, D. Janičkovič², P. Švec² and I. Škorvánek¹¹*Institute of Experimental Physics, Slovak Academy of Sciences, Watsonova 47, 040 01 Košice, Slovakia*²*Institute of Physics, Slovak Academy of Sciences, Dúbravská cesta 9, 842 28 Bratislava, Slovakia*

The influence of sample thickness on giant magnetoimpedance (GMI) effect was investigated in amorphous $(\text{Fe}_1\text{Ni}_1)_{73}\text{Nb}_7\text{B}_{20}$ single-layer, bilayer and trilayer ribbons. The ribbons were prepared by planar flow casting technique from a single crucible with one, two and three nozzles, respectively. Our interest was centered mainly on the relationship between the thickness and GMI effect at frequency range 0.1 – 100 MHz. In order to improve GMI effect, the soft magnetic ribbons were annealed at temperature 673 K (below the onset of crystallization) for 1 hour. Such heat treatment resulted in thermal relaxation of the internal stresses, which are induced in the amorphous structure during rapid quenching. The hysteresis loops with coercivity below 1 A/m were observed for all annealed samples. The highest value of the percentage change of magnetoimpedance $\Delta Z/Z \sim 133\%$ is achieved for trilayer ribbon. The frequency where $\Delta Z/Z$ reaches maximum continuously increased with a decrease of the sample thickness from 1 MHz for trilayer to 2,8 MHz for single-layer). The correlations between the GMI and ribbon thickness are discussed in terms of skin effect. The observed values of field sensitivity ($\eta \sim 26\%/Oe$) could be of potential interest for magnetic sensors applications.

*Acknowledgment**This work was realized within the project ITMS 26220120019.*

P2-48**EVIDENCE OF GRIFFITHS LIKE PHASE IN NANOCRYSTALLINE MANGANITE $\text{La}_{0.85}\text{Ca}_{0.15}\text{MnO}_3$** M. Pękała¹, J. Szydłowska¹, K. Pękała² and V. Drozd³¹*Chem. Dept., Warsaw University, Warsaw, Poland*²*Phys. Dept., Warsaw University of Technology, Warsaw, Poland*³*Florida Intl. University, Miami, USA*

Nanocrystalline and polycrystalline mixed valence manganites $\text{La}_{0.85}\text{Ca}_{0.15}\text{MnO}_3$ were prepared by citrate sol-gel method and sintered at 750 °C and 1300 °C, respectively. The mean crystallite sizes of nano- and polycrystalline samples are about 8.3 nm and 100 nm, respectively, as determined from X-ray diffraction patterns. Magnetic characterization was made by means of AC susceptibility and electron spin resonance methods in a broad temperature range. The ferromagnetic Curie temperatures T_C derived from a temperature derivative of AC susceptibility are equal to 106 K and 98 K for the nanocrystalline and polycrystalline manganites, respectively. The characteristic features of the Griffiths like phase, detected by both the methods, unanimously prove that the small magnetic clusters with short range magnetic ordering, exist in paramagnetic matrix of the nanocrystalline manganite above the Curie temperature. An analysis of resonance spectra allows to detect the upper temperature limit for an existence of Griffiths like phase at temperature T_{GI} , which is somewhat higher than the T_G of the magnetic susceptibility. This proves that the high frequency field is able to excite the relatively smaller magnetic clusters / systems responsible for the Griffiths like phase in the nanocrystalline manganite studied. Results are discussed applying the core – shell model, and compared with similar systems.

P2-49**EFFECT OF LASER SCRIBING ON THE MAGNETIC PROPERTIES OF CONVENTIONAL GO SILICON STEEL.**I. Petryshynets¹, V. Puchý¹, F. Kováč¹ and M. Šebek¹¹*Division of Metals Systems, Institute of Materials Research, Watsonova 47, 040 01 Košice, Slovakia*

The grain oriented (GO) steels are iron - 3% silicon alloys developed with a strong also called the Goss – type texture to provide very low core loss and high permeability in the rolling direction. These steels are predominantly employed for the transformers with high efficiency. With an additional surface treatment after the rolling process it is possible to improve the magnetic properties of the core material; especially the core losses. At the same time it is well known that laser radiation influence on domain structure with subsequent decrease of specific power losses.

In the present work the influence of laser treatment technique on the magnetic domains modification with positive impact on the magnetic properties of grain-oriented silicon steel has been investigated. The conventional GO steel with silicon content 3 % wt, taken from industrial line after final heat treatment, was chosen as an experimental material. The laser scribing was applied on the material surface in order to induce thermal stresses, which influence on the modification of the internal structure of magnetic domains. The final domain structures were optimized in relation to the minimization of magnetic losses of the experimental material and to the optimization of thermal stresses application on the surface. The magneto-optical Kerr effect was employed to obtain a visible contrast between antiparallel domains. The domain structures showed that domain-walls positions did not repeat precisely from cycle to cycle, particularly at high inductions, and that the average domain-wall spacing decreased with increasing density of laser scribing lines. The pinning effects are attributed to the presence of non-magnetic inclusions and surface defects. A semi quantitative relationship has been found between the domain patterns and used fiber laser treating method. The obtained samples with modified domain structure leads to a significant decrease of coercivity measured in DC magnetic field from 20 A/m to 12 A/m.

P2-50**MICROWAVE SINTERED Fe/MgO SOFT MAGNETIC COMPOSITE**

M. Fáberová¹, R. Bureš¹, P. Kollár², J. Füzer², S. Dobák², F. Onderko²,
M. Strečková¹ and P. Kurek¹

¹*Institute of Materials Research, Slovak Academy of Sciences, Watsonova 47,
040 01 Košice, Slovak Republic*

²*Institute of Physics, Faculty of Science, Pavol Jozef Šafárik University in Kosice,
Park Angelinum 9, 041 54 Košice, Slovak Republic*

Soft magnetic composites (SMC) are produced by the powder metallurgy method from ferromagnetic particles coated with a thin electrically insulating layer. Widely used shaping method is cold pressing, which introduce an elastic and plastic deformation to the composite. Structural discontinuities, imperfections as well as residual stresses induce changes of magnetic and mechanical properties. Inorganic coatings with high thermal stability are investigated to allow stress relaxation heat treatment at temperature higher than 600°C. Advanced compaction methods are investigated with focusing on optimization of intrinsic structure of SMC's. Microwave sintering is progressive heat treatment technique. Microwave heating is fundamentally different from conventional heating in the way how thermal energy is delivered to the material.

SMC based on Fe and MgO was prepared. Technically pure iron particles were dry coated by MgO nano-particles using the Resonant Acoustic Mixing method. Fe/MgO powders with 1, 2, 3, 5, 10 and 13.85 wt.% of MgO were uniaxially cold pressed at pressure of 600 MPa. Sintering was provided in multimode microwave cavity with controlled power from 100 W to 3 kW at constant temperature of 800°C, for 15 minutes, in dry air atmosphere.

Magnetic and mechanical properties of green compact as well as sintered samples were measured. Coercivity, permeability, resistivity, elastic modulus and transverse rupture strength values in dependence on MgO content were investigated. The influence of MgO content ratio on properties was different in case of as pressed green samples in comparison to sintered bodies. This provided a possibility to consider by mechanisms of microstructure and properties development of Fe/MgO composite. Microstructure of prepared SMC was investigated by scanning electron and optical microscopy. The coercivity of the green compacts with 1-5 wt.% of MgO exhibits approximately 460 A/m and after sintering decreases to approximately 290 A/m. The real part of the complex permeability in the frequency range 100-1000 Hz is higher for sintered compacts, on the other hand is lower at higher frequencies. It was observed that increasing the content of MgO causes decreasing of the permeability.

P2-51**IMPROVEMENT OF MAGNETIC PROPERTIES AND CRYSTALLOGRAPHIC TEXTURE OF Fe-Si STEELS BY THERMAL PROCESSING IN HIGH MAGNETIC FIELD**F. Kováč¹, I. Petryshynets¹, J. Marcin² and I. Škorvánek²¹*Division of Metals Systems, Institute of Materials Research, Watsonova 47, 040 01 Košice, Slovakia*²*Laboratory of Nanomaterials and Applied Magnetism, Institute of Experimental Physics, Watsonova 47, 040 01 Košice, Slovakia*

Non-oriented electrical steels belong to important group of the soft magnetic materials that are typically used as core parts in a variety of electrical rotating equipments. Their good soft magnetic characteristics strongly rely on the ability to control the grain size and crystallographic texture as well as chemistry of the final steel sheets products. The most appropriate texture for NO steels is so-called “rotating cube” with the easy magnetization direction (100), which provides isotropic magnetic properties in all plane directions of sheet steels.

In this work, we report on the effects high static magnetic field on the formation of desirable crystallographic orientation of grains (rotation cube or Goss) during the primary recrystallization of NO steels. Vacuum degassed NO steel with the silicon content about 1% wt. was taken from industrial line after final cold rolling with 80% of deformation and then it was subjected to the laboratory annealing at the temperature of primary recrystallization. Whole annealing process was carried in external magnetic field of 14T. The analysis of crystallographic orientation of experimental material was studied by EBSD technique. The magnetic measurements show that the coercivity values of the samples annealed in the magnetic field of 14 T can be reduced by approx. 3% in comparison with samples annealed under zero field conditions.

I3-01**ENERGY-EFFICIENT REFRIGERATION NEAR ROOM TEMPERATURE WITH TRANSITION METAL BASED MAGNETIC REFRIGERANTS**

E. Brück¹, H. Yibole¹, Van Thang Nguyen¹, Xuefei Miao¹, M. Boeije¹, L. Caron², Lian Zhang^{1,3}, F. Guillou⁴ and N. Van Dijk¹

¹*Fundamental Aspects of Materials and Energy, Department of Radiation Science and Technology, Faculty of Applied Sciences, Delft University of Technology, Delft, The Netherlands*

²*Max-Planck-Institut für Chemische Physik fester Stoffe, Nöthnitzer Straße 40, 01187 Dresden*

³*BASF Nederland. B.V. Strijviertel 61, 3454 PK, De Meern, The Netherlands*

⁴*European Synchrotron Radiation Facility, 71 Avenue des Martiers, 38000 Grenoble Cedex, France*

With the advent of giant magnetocaloric effects (MCE) that occur in conjunction with magneto-elastic or magneto-structural phase transition of first order (FOT), room temperature applications became feasible. In this context the MnFe(P,X) system is of particular interest as it contains earth abundant ingredients that are not toxic. This material family derives from the Fe₂P compound, a prototypical example known since a long time to exhibit a sharp but weak FOT at 210 K (-63°C).

In this hexagonal system, the Fe atoms occupy two inequivalent atomic positions referred as *3f* (in a tetrahedral environment of non-metallic atoms) and *3g* (pyramidal). One intriguing aspect is the disappearance of the magnetic moments of iron atoms on the *3f* sites when crossing T_C, whereas there is only a limited decrease on the *3g* site. This observation has led to a cooperative description of the FOT linking the loss of long range magnetic order at T_C with the loss of local moments on *3f*. This mechanism has recently been shown to be at the origin of the G-MCE observed in MnFe(P,Si) [1].

The disappearance of the magnetic moments has been ascribed to a conversion from non-bonding *3fd* electrons into a distribution with a pronounced hybridization with the surrounding Si/P atoms. Therefore, one can expect to adjust the properties of these compounds by substitutions on the non-metallic site. This solution has been used to optimize the properties of MnFe(P,Si) materials [2].

[1] Nguyen H. Dung., et al. Mixed Magnetism for Refrigeration and Energy Conversion. *Advanced Energy Materials* 1 (6), 2011 pp. 1215-1219.

[2] Guillou F., et al., Taming the First-Order Transition in Giant Magnetocaloric Materials. *Advanced Materials* 26 (17), 2014 pp. 2671-2675.

I3-02**SOFT MAGNETIC, NANOCRYSTALLINE MATERIALS FOR INDUCTORS AND SHIELDING APPLICATIONS - OPTIMIZED FOR HIGHER FREQUENCY**C. Polak¹*¹Vacuumschmelze GmbH & Co. KG, Gruener Weg 37, 63450 Hanau, Germany*

In recent times miniaturization and energy conservation of electronic devices have been demanded more intensively. There is the need for less environmental loads and accordingly for miniaturization a higher frequency and a smaller thickness have been demanded. Among metallic soft magnetic materials, amorphous and nanocrystalline alloys are the most promising candidates for high frequency applications. These relatively new materials developed during the last decades are meanwhile successfully applied in high grade magnetic cores for inductors. We will survey characteristic features of nanocrystalline alloys particularly relevant for inductor and shielding applications at higher frequencies. In particular we will discuss the optimization of the high frequency properties by applying new annealing and processing technologies.

As an example, we will discuss nanocrystalline materials with huge anisotropy. Tape wound cores were produced using this nanocrystalline ribbons with linear hysteresis loops and particularly low DC permeability down to $\mu_{DC} = 100$. In the cores of these inductive components highly non-uniform field distributions can occur, depending on the design. Thus, for conventional cores with homogeneous permeability distribution a noticeable degradation of component properties can be observed. This work will show new tape wound cores in which a designed permeability distribution is used in order to avoid the above mentioned issues.

On the other hand, we will discuss inductances made of planar sheets used in inductive wireless power transmission systems. Nanocrystalline soft-magnetic shielding material is used to avoid lossy eddy currents being induced in electrically conducting components like batteries or ground layers of electronic circuits.

O3-01**MAGNETOCALORIC EFFECT OVER A WIDE TEMPERATURE RANGE DUE TO MULTIPLE MAGNETIC TRANSITIONS IN GdNi_{0.8}Al_{1.2} ALLOY**

T.P. Rashid¹, S. Nallamuthu¹, K.Arun¹, I. Curlik², S. Ilkovic², A. Dzubinska², M. Reiffers² and R.Nagalakshmi¹

¹*Department of Physics, National Institute of Technology,
Tiruchirappalli 620 0015, India*

²*Faculty of Humanities and Natural Sciences, Presov University, Presov, Slovakia*

The magnetic properties, magnetocaloric effect (MCE) and refrigerant capacity (RC) of the novel polycrystalline GdNi_{0.8}Al_{1.2} alloy are investigated. The temperature dependence of magnetization exhibits multiple magnetic transitions at $T_1 = 17.7$ K, $T_2 = 46.7$ K and $T_3 = 256$ K and thereby displaying a complex magnetic behaviour. The magnetocaloric effect is calculated in terms of the magnetic entropy change ($-\Delta S_M$), from isothermal magnetization data using Maxwell relations. The maximum magnetic entropy change at major transitions T_2 is $9.15 \text{ J kg}^{-1} \text{ K}^{-1}$ (for a field change of 0 – 9 T) and $4.20 \text{ J kg}^{-1} \text{ K}^{-1}$ (0 – 5 T) and at T_3 is $1.10 \text{ J kg}^{-1} \text{ K}^{-1}$ (0 – 9 T) and $0.67 \text{ J kg}^{-1} \text{ K}^{-1}$ (0 – 5 T). The overlap of the two $-\Delta S_M$ peaks expeditiously expand the working temperature range of this material with substantial MCE which in turn yields moderate RC value of 120 J/kg for a field change of 0 – 5 T. These results suggest that the GdNi_{0.8}Al_{1.2} alloy may be a meaningful candidate for magnetic refrigeration working in a wide temperature range.

O3-02**THE SCHOTTKY EFFECT IN YbCoGaO₄ SINGLE CRYSTALS**

I. Radelytskyi¹, T. Zajarniuk¹, A. Szewczyk¹, M. Gutowska¹, H.A. Dabkowska², P. Dłużewski¹ and H. Szymczak¹

¹*Institute of Physics PAS, al.Lotnikow 32/46, 02-668 Warsaw, Poland*

²*The Department of Physics and Astronomy, McMaster University, Hamilton, Ontario, Canada*

Specific heat, magnetic measurements and the scanning transmission electron microscopy studies have been performed on YbCoGaO₄ single crystals. The studied system behaves like a three-dimensional Ising-like spin glass. A typical spin-glass-like cusp was seen only in the longitudinal susceptibility, whereas a paramagnetic behavior was observed in the transverse susceptibility [1]. The single crystals were grown using the optical floating zone image furnace technique [2].

Measurement of the low temperature specific heat did not reveal any anomaly near the spin glass transition temperature as expected for a spin glass. Instead, a previously unobserved in Ising spin glasses Schottky anomaly in YbCoGaO₄ single crystal was seen and analysed. This anomaly is associated with splitting of the lowest Kramers doublet of ²F_{7/2} ground state of Yb³⁺ ions. From the Schottky analysis, exchange interactions Co²⁺-Yb³⁺ as well as g-factor for the lowest Kramers doublet were determined. The magnetocaloric effect induced by Schottky effect in studied crystals has been calculated from specific heat measurements and compared with that determined indirectly from magnetization measurements.

This study was partly financed by the National Centre for Research and Development, Research Project PBS2/A5/36/2013.

[1] R.Szymczak et al., Journal of Physics: Conference Series 303 (2011) 012064.

[2] H. A. Dabkowska, B. D. Gaulin in International School on Crystal Growth of Technologically Important Electronic Materials, Ed.K. Byrappa, Allied Publishers, 2003.

O3-03**ANALYSIS OF THE CRYSTALLIZATION PROCESSES AS A BASIS FOR OPTIMIZATION OF MAGNETIC PROPERTIES OF $\text{Hf}_2\text{Co}_{11}\text{B}$ ALLOYS**A. Musiał¹, Z. Śniadecki¹, J. Kováč², I. Škorvánek² and B. Idzikowski¹¹*Institute of Molecular Physics, Polish Academy of Sciences,**M. Smoluchowskiego 17, PL 60-179 Poznań, Poland*²*Institute of Experimental Physics, Slovak Academy of Sciences, Watsonova 47, 040 01 Košice, Slovakia*

The novel magnetic materials without rare-earth elements should be characterized by possibly high coercive field, magnetization and thus energy product $/BH/_{\max}$. One of the widely used methods to improve the magnetic properties is annealing of the amorphous precursors [1]. During heat treatment formation of magnetic phases is observed. Isothermal annealing of Hf-Co based alloy leads to crystallization of phases which deteriorate hard magnetic properties as HfCo_2 , HfCo_3B_2 [2]. Deep insight into the crystallization dynamics can provide necessary information on the formation mechanisms of the optimum crystalline structure.

The melt-spinning technique was used to synthesize amorphous $\text{Hf}_2\text{Co}_{11}\text{B}$ alloy under argon atmosphere on a copper wheel rotating with velocity 30 ms^{-1} . Ribbons were characterized by means of differential scanning calorimetry (DSC), X-ray diffraction (XRD) and thermomagnetic measurement. DSC measurements have been conducted with different heating rates between 10-40 K/min. Crystallization temperatures for the first, second and third step are equal to $T_{p1} = 594^\circ\text{C}$, $T_{p2} = 614^\circ\text{C}$, $T_{p3} = 654^\circ\text{C}$, respectively, for the heating rate 20 K/min. Kissinger, Ozawa, Augis and Bennet, and Matusita models were used for calculations of crystallization dynamics. Different methods allowed to calculate not only the activation energy but additionally different coefficients as frequency factor k_0 , rate constant k and also Avrami exponent, describing dimensionality of the processes. Crystallization is evolving with temperature from 3D to 2D mode.

On the basis of magnetic measurements Curie temperature T_C was determined to be about 540°C . During cooling process, two other inflections connected with Curie temperatures of $\text{Hf}_2\text{Co}_{11}$ rhombohedral and orthorhombic phases were observed.

[1] M. Rajasekhar, D. Akhtar, S. Ram, J. Phys. D. Appl. Phys. 43 (2010) 135004.

[2] M.A. McGuire, O. Rios, J. Appl. Phys. 117 (2015) 053912.

P3-01**INVESTIGATIONS OF THE MAGNETIZATION REVERSAL****PROCESSES IN NANOCRYSTALLINE Nd-Fe-B ALLOYS DOPED BY Nb**

M. Kaźmierczak¹, P. Gębara¹, P. Pawlik¹, K. Pawlik¹, A. Przybył¹, I. Wnuk¹ and J. J. Wysocki¹

¹*Institute of Physics, Częstochowa University of Technology, Armii Krajowej 19 Av., 42-200 Częstochowa, Poland*

In the present work the magnetic properties and phase constitution of $(\text{Nd}_{10}\text{Fe}_{67}\text{B}_{23})_{100-x}\text{Nb}_x$ (where $x = 5, 6, 7, 8, 9$) alloys in the form of ribbons were investigated. The ribbon samples were obtained by controlled atmosphere melt-spinning technique under an Ar atmosphere. In order to generate the nanocrystalline microstructure and hard magnetic properties, samples were annealed at various temperatures (from 923 K to 1063 K) for 5 min. The X-ray diffraction revealed hard magnetic $\text{Nd}_2\text{Fe}_{14}\text{B}$, the paramagnetic $\text{Nd}_{1+\epsilon}\text{Fe}_4\text{B}_4$ and soft magnetic metastable $\text{Nd}_2\text{Fe}_{23}\text{B}_3$ phases. The shapes of $M_{\text{rev}}(M_{\text{irr}})$ indicate that the magnetization reversal proceeds through the nucleation of reversal domain for ribbon doped with 5 - 7 at.% of Nb and the subsequent pinning domain walls for ribbons doped with 8 and 9 at.% of Nb.

P3-02**MAGNETOCALORIC PROPERTIES OF $(\text{Fe}_{46.9}\text{Co}_{20.1}\text{B}_{22.7}\text{Si}_{5.3}\text{Nb}_5)_{90}\text{M}_{10}$ (M=Tb, Pr, Nd) ALLOYS PREPARED BY MECHANICAL ALLOYING**K. Sarlar¹, A. Adam¹, E. Civan¹ and I. Kucuk¹¹*Department of Physics, Uludag University, Gorukle Campus, 16059 Bursa, TURKEY*

In the present work, the $(\text{Fe}_{46.9}\text{Co}_{20.1}\text{B}_{22.7}\text{Si}_{5.3}\text{Nb}_5)_{90}\text{M}_{10}$ (M=Tb, Pr, Nd) alloys were fabricated by mechanical alloying. The magnetocaloric properties of the $(\text{Fe}_{46.9}\text{Co}_{20.1}\text{B}_{22.7}\text{Si}_{5.3}\text{Nb}_5)_{90}\text{M}_{10}$ (M=Tb, Pr, Nd) samples were determined by the isothermal magnetization curves of the $(\text{Fe}_{46.9}\text{Co}_{20.1}\text{B}_{22.7}\text{Si}_{5.3}\text{Nb}_5)_{90}\text{M}_{10}$ (M=Tb, Pr, Nd) alloys. The values of refrigeration capacity (RC) for the alloys are comparable with those of previously studied magnetocaloric materials. With good RC and negligible hysteresis, these alloys can be used as the magnetic refrigerants.

P3-03**DC MAGNETIC PROPERTIES OF Ni-Fe BASED COMPOSITES**

F. Onderko¹, M. Jakubčín¹, S. Dobák¹, D. Olekšáková², P. Kollár¹, J. Füzér¹, M. Fáberová³, R. Bureš³ and P. Kurek³

¹*Institute of Physics, Faculty of Science P. J. Šafarik University,
Park Angelinum 9, 040 01 Košice, Slovak Republic*

²*Faculty of Mechanical Engineering, Technical University, Letná 9, 042 00 Košice,
Slovak Republic*

³*Institute of Materials Research, Slovak Academy of Sciences, Watsonova 47,
040 01 Košice, Slovak Republic*

Soft magnetic materials based on NiFe (also known as permalloy) possess high permeability, low magnetostriction and low coercivity. These properties determine NiFe alloys for creating magnetic circuits in electrotechnology, fabricated usually in the form of thin sheets. Metallic sheets covered by insulator layer are then laminated to create a magnetic circuit, what is limitation factor for creating magnetic circuit in required shape. Powder metallurgy allows creating magnetic circuit in 3D shape with isotropic magnetic properties by compacting of powder material with insulated particles. The compacted soft magnetic materials have high application potential in electrotechnology (magnetic core in rotors and stators of electric motors). We investigated the magnetic properties of NiFe based soft magnetic composites. The ring shaped samples were prepared from basic material - thin permalloy sheet with Ni/Fe content 81/19 wt. %. The sheet was cut in to small pieces and milled in a planetary ball mill to obtain the powder. The powder was mixed with phenol-formaldehyde resin and pressed to the ring-shaped samples. Complex permeability was measured by impedance/gain-phase analyzer and DC magnetic properties (initial magnetization curve, anhysteretic curve and hysteresis loop) were measured by the fluxmeter based hysteresisgraph. The measured data were analyzed to optimize preparation process for preparation of soft magnetic composites with required magnetic properties.

Acknowledgment

This work was realized within the project ITMS 26220120019.

P3-04**SCALLING ANALYSIS OF THE MAGNETOCALORIC EFFECT IN Co@Au NANOPARTICLES**P. Hrubovčák¹, A. Zeleňáková¹, V. Zeleňák² and V. Franco³¹*Department of Condensed Matter Physics, University of P.J. Šafárik, Park Angelinum 9, 040 01 Košice, Slovakia*²*Department of Inorganic Chemistry, University of P.J. Šafárik, Moyzesova 11, 040 01 Košice, Slovakia*³*Department of Condensed Matter Physics, University of Sevilla, P.O. BOX 1065, 41080 Sevilla*

Magnetocaloric effect (MCE) is associated with large magnetization change induced by external magnetic field in magnetic material. The effect is usually enhanced at the vicinity of phase transition. Since MCE can be utilized for magnetic refrigeration, suitable materials which could replace the conventional refrigerants have been investigated intensively. Despite the extensive research on MCE in various bulk materials, only a small attention has been paid to the nanoparticle systems by now. The possibility of tuning nanoparticles' properties easily enables to tailor the crucial parameters of potential refrigerant.

Among several methods for MCE evaluation that have already been proposed the construction of master (universal) curve is considered to be very interpretable. For the materials from the same universality class, magnetic entropy change dependence on temperature data obtained at different magnetic field changes should collapse in one universal curve after proper rescaling. The shape and parameters of the master curve can provide us with information on the character of the phase transition or critical exponents (α , β , δ).

We studied Co@Au core@shell nanoparticle system and evaluated its properties with respect to MCE. Series of $M(T)$ ZFC data obtained at different magnetic fields were processed by Maxwell relation $(\partial M/\partial T)_H = (\partial S/\partial H)_T$ in order to calculate the entropy change according to equation $\Delta S = \int (\partial M/\partial T)_H dH$. Subsequently, $\Delta S(T)$ dependences at corresponding field change were plotted. The peaks of $\Delta S(T)$ dependences were observed at very low temperature $T \sim 8$ K. Rescaled data $\Delta S(T)/\Delta S_{max}(T)$ vs. $(T-T_C)/(T_r-T_C)$, where T_C is transition temperature and T_r reference temperature, collapsed onto single universal curve. This collapse was found to resemble the universal curve reported for magnetocaloric materials with second order phase transition. Additionally, the value $n=1.67$ of the exponent of field dependence of refrigeration capacity was found to be close to the value $n = 1.47$ reported for the similar systems recently.

*Acknowledgment**This work was realized within the project ITMS 26220120019.*

P3-05**INVESTIGATION OF THE MAGNETIC PHASE TRANSITION IN THE $\text{LaFe}_{11.14}\text{Co}_{0.66}\text{Si}_{1.1}\text{M}_{0.1}$ (WHERE M=Al OR Ga) ALLOYS**P. Gębara¹*¹Institute of Physics, Częstochowa University of Technology,
Armii Krajowej 19 Av., 42-200 Częstochowa, Poland*

The aim of the present work was to study the phase transition in the $\text{LaFe}_{11.14}\text{Co}_{0.66}\text{Si}_{1.1}\text{M}_{0.1}$ (where M= Al or Ga) alloys. Samples were obtained by arc-melting of the high purity of constituent elements under low pressure of Ar. Then specimens were sealed-off in quartz tubes under low pressure of Ar and annealed at 1323K for 15 days. Magnetic properties of prepared samples were measured using LakeShore 7400 rev A VSM at wide temperature range and these results were used to investigation of magnetic phase transition. The positive slope of Arrott plots showed that magnetic phase transition in both investigated samples was of second order nature. More detailed studies of the phase transition have been supported by Landau theory. The temperature dependences of Landau coefficients also revealed second order phase transition in both specimens.

P3-06**MAGNETIC PROPERTIES AND MAGNETOCALORIC EFFECT IN SPUTTER DEPOSITED THIN FILMS OF Mn-RICH HEUSLER ALLOYS FROM Ni-Mn-X (X = Ga, Sn) SYSTEMS**

M. Chojnacki¹, K. Fronc¹, I. Radelytskyi¹, T. Wojciechowski¹, R. Minikayev¹ and H. Szymczak¹

¹*Institute of Physics of the Polish Academy of Sciences, Al. Lotników 32/46, 02-668 Warsaw, Poland*

Ferromagnetic Heusler alloys from the Ni-Mn-X systems (X = Ga, Sn, In, Sb) thanks to their unique magnetic properties such as, among many others, giant magnetocaloric effect (GMCE) and large magnetic-field-induced strain (MFIS), are very popular in many areas of science and technology, such as refrigeration techniques or micro-electro-mechanical system (MEMS) applications.

There are many techniques of the preparation of these alloys both as bulk and thin films materials. One of the most effective and widely used methods for producing thin layers of Heusler alloys is magnetron sputtering.

In this work several different samples of thin films of Ni-Mn-Ga and Ni-Mn-Sn magnetocaloric alloys were prepared. These materials were deposited on amorphous SiO₂ substrates in room temperature by the means of DC magnetron sputtering from pure element sources (Ni, Mn, Ga and Sn). The chemical composition of these alloys oscillated in the Mn-rich region of Ni-Mn-X ternary phase diagram (38-47 at.%) with the amount of Ga or Sn in the range of 14-21 and 10-15 atomic percent respectively. Samples were annealed in the temperature of 775K for 5 hours in vacuum and their composition, structure and magnetic properties were studied with the use of SEM/EDX, XRD and SQUID magnetometer technique.

Magnetization investigations showed that the magnetocaloric effect strongly depends on the composition, both in its intensity and in the temperature range it takes place in. For the alloys from the Ni-Mn-Ga system the MC effect's occurrence temperatures varies from about 200K (with maximum $-\Delta S \approx 0.65 \text{ J/kg}\cdot\text{K}$ in magnetic field of 50kOe), for compositions range of Ni₃₉₋₄₅Mn₃₈₋₄₅Ga₁₄₋₁₆, to about 330K (with maximum $-\Delta S \approx 1.4 \text{ J/kg}\cdot\text{K}$) for Ni₄₂Mn₃₉Ga₁₉. Similar differences were observed for Ni-Mn-Sn system with maximal MCE in the temperature of about 330K (with maximum $-\Delta S \approx 2.3 \text{ J/kg}\cdot\text{K}$ in magnetic field of 50kOe) for the Ni₄₆Mn₄₁Sn₁₃ alloy.

This study was partly financed by the National Centre for Research and Development, Research Project no. PBS2/A5/36/2013.

P3-07**MEASUREMENT OF MAGNETOCALORIC EFFECT WITH MICROCALORIMETRY**

A. Chudikova¹, D. Gonzalez¹, T. Ryba¹, Z. Vargova², V. Komanicky¹,
J. Kacmarcik³, R. Gyepes⁴ and R. Varga¹

¹*Inst. Phys., Fac. Sci., UPJS, Park Angelinum 9, 041 54 Kosice, Slovakia*

²*Inst. Chem., Fac. Sci., UPJS, Moyzesova 11, 041 54 Kosice, Slovakia*

³*Inst. Exp. Phys., SAS, Watsonova 47, 04001 Kosice, Slovakia*

⁴*Dept. of Chemistry, Faculty of Education, J. Selye University, Komárno, Slovakia*

Magnetocaloric effect is based on the temperature change of the substance by re-configuration of its magnetic moments, which are influenced by outer magnetic field. Maximum temperature change appears at the Curie temperature of material. The temperature change increases even further, when material undergoes at the same time phase transition from less-ordered to highly-ordered structure. This is typical for Heusler alloys [1].

Heusler alloys are new perspective materials for different applications in spintronics, magnetocaloric cooling, sensors etc. Ni₂MnZ (Z=Ga, Sn, Sb) are good candidates for applications in shape memory alloy- or magnetocaloric- based devices. They are known to undergo structural phase transformation of martensitic type [2]. Usually, they are prepared by arc-melting of selected elements followed by long-term annealing. However, rapid quenching method has been recently successfully introduced for the preparation of Heusler alloys. It allows a fast production of relatively large amount of material [3].

In order to measure the magnetocaloric effect directly, we have designed a microcalorimeter, which allows us to measure very small temperature differences in samples on a microscopic scale [4]. This technique is very well adapted to carry out continuous measurements during either temperature or magnetic field sweeps. We have tested the system on Ni₂MnGa and Ni₂MnSb rapidly quenched ribbons in the temperature range of 30-90°C.

This research was supported by the projects APVV-0027-11 and Slovak VEGA grant. No. 1/0164/16.

[1] V.K.Pecharsky, et al. *Journal of Applied Physics*, Volume 86, Number 1, 1999

[2] V.A. Chernenko, et al. *Scripta Metallurgica et Materialia*, 33(1995), 1239.

[3] J.L.S. Llamazeres, T. Sanchez, et al. *Appl. Phys. Lett.*, 92 (2008) 012513.

[4] J. Kacmarcik, *Acta Physica Polonica A*, Volume 113, 2008.

P3-08**THE EFFECT OF Ni AND Mn ADMIXTURE ON MAGNETIZATION REVERSAL PROCESSES IN (Pr, Dy)-(Fe, Co)-B RIBBONS**A. Przybył¹*¹Institute of Physics, Faculty of Production Engineering and Materials Technology, Czestochowa University of Technology, al. Armii Krajowej 19, 42-200 Czestochowa, Poland*

The aim of the present paper was to study the influence of Mn and Ni admixture on the phase constitution, magnetic properties and magnetization reversal processes in (Pr, Dy)-(Fe, Co)-B ribbons doped with Zr, Ti, Mn and Ni.

The ingot samples of the $\text{Pr}_8\text{Dy}_1\text{Fe}_{60}\text{Co}_7\text{Mn}_{(6-x)}\text{Ni}_x\text{B}_{14}\text{Zr}_1\text{Ti}_3$ (where $x = 0, 3, 6$) alloys were produced by arc-melting of the high purity constituent elements and then the ribbons were prepared by single roll melt-spinning. Both processes were carried out under the Ar atmosphere. The admixture of Zr was used to improve their glass forming abilities and Dy was substituted to enhance the magnetocrystalline anisotropy of hard magnetic phase. The samples in as-cast state were fully amorphous, therefore the ribbons were annealing at 963K temperature. The magnetic parameters were determined from magnetic hysteresis loops measured in the external magnetic field up to 2T at room temperature. The effect of Mn and Ni additions on the magnetization reversal processes was studied. To determine magnetization reversal processes the rates of irreversible magnetization changes upon the change of external magnetic field H were investigated. The series of recoil curves were obtained for the initially saturated samples and for the thermally demagnetized specimens. Moreover, minor hysteresis loops were used to obtain the field dependences of remanence J_r and coercivity J_{Hc} . In order to characterize interactions between grains of crystalline phases the δM plots were also constructed from recoil curves.

P3-09**APPLICATION OF MODIFIED TAKÁCS MODEL FOR ANALYSIS OF MAGNETOCALORIC EFFECT IN $\text{Fe}_{60}\text{Co}_{10}\text{Mo}_5\text{Cr}_4\text{Nb}_6\text{B}_{15}$** J. Rzaccki¹ and M. Dospial¹*¹Czestochowa University of Technology, Faculty of Production Engineering and Materials Technology, Institute of Physics, 19 Armii Krajowej Av., Czestochowa, Poland*

The paper presents studies on application of modified T(x) model to analysis of magnetocaloric effect. The usability of phenomenological model was studied for $\text{Fe}_{60}\text{Co}_{10}\text{Mo}_5\text{Cr}_4\text{Nb}_6\text{B}_{15}$ sample obtained in the form of ribbon by melt-spinning route. The amorphous structure was confirmed by x-ray and Mossbauer spectroscopy measurements. The initial magnetization curves were measured using vibrating sample magnetometer at different temperatures. Basing on obtained results the temperature dependence of parameters describing initial magnetization curve were determined. Further analysis of magnetocaloric effect was performed basing on the concrete, temperature dependence of magnetization, described in the formalism of modified T(x) model. This approach enabled the accurate construction of the curve describing the magnetic entropy change versus temperature. The obtained theoretical dependence was also compared with experimental data.

P3-10**SCALING OF ANHYSTERETIC CURVES FOR LAFECOSI ALLOY NEAR THE TRANSITION POINT**

R. Gozdur¹, K. Chwastek², M. Najgebauer², M. Lebioda³, Ł. Bernacki¹ and A. Wodzyński²

¹*Department of Semiconductors and Optoelectronic Devices, Łódź University of Technology, Wólczajska 211/215, 90-924 Łódź, Poland*

²*Faculty of Electrical Engineering, Częstochowa University of Technology, Armii Krajowej 17, 42-201 Częstochowa, Poland*

³*Institute of Electrical Engineering Systems, Łódź University of Technology, Stefanowskiego 18/22, 90-924 Łódź, Poland*

La(FeCoSi)_x alloys with $x = 13$ have been the subject of considerable interest to the scientific community interested in magnetic refrigeration, since in these materials the magnetocaloric effect occurs near room temperature. Moreover their magnetic properties may be easily tailored by an appropriate adjustment of chemical composition (in particular by intentional modification of cobalt content) [1-3].

The present paper focuses on the description of anhysteretic curves at temperatures close to the Curie point. The anhysteretic curves are reconstructed from measured hysteresis curves following the procedures described by Bozorth [4] and Krah [5]. Next the obtained $M_{an}(H)$ dependencies are fitted to the Langevin function. The shape parameter in the Langevin function is directly proportional to temperature. A representation of anhysteretic curves in the dimensionless form $M_{an}/M_s(T)$ vs. $H/a(T)$ similar to that presented in Refs. [6-7] allows one to obtain a unified description, which is found valid both below the transition point as well as in the paramagnetic regime. The proposed model might be useful for in-depth study of magnetic properties of La(FeCoSi)_x alloys.

- [1] K. A. Gschneider, Jr., V. K. Pecharsky, Thirty years of near room temperature magn. cooling: where are we today and future prospects, *Int. J. Refrig.* 31 (2008) 945.
- [2] P. Gębara, P. Pawlik, I. Škorvánek, J. Marcin, J. J. Wysocki, Structural and magnetocaloric study of LaFe_{11.0}Co_{0.8}(Si_{0.4}Al_{0.6})_{1.2} alloy, *Acta Phys. Pol. A* 118 (2010) 910.
- [3] J. Liu, J. D. Moore, K. P. Skokov, M. Krautz, K. Löwe, A. Barcza, M. Katter, O. Gutfleisch, Exploring La(Fe,Si)₁₃-based magnetic refrigerants towards application. *Scripta Mater.* 67 (2012) 584.
- [4] R. M. Bozorth, *Ferromagnetism*, IEEE Press 1993.
- [5] J. Krah, A. Berqvist, Numerical optimization of a hysteresis model, *Physica B* 343 (2004) 35.
- [6] P. Allia, M. Coisson, P. Tiberto, F. Vinai, Temperature behaviour of anhysteretic magnetization in granular magnetic systems, *J. Magn. Magn. Mater.* 226-230 (2001) 1904.
- [7] P. Allia, M. Coisson, P. Tiberto, F. Vinai, M. Knobel, M. A. Novak, W. C. Nunes, Granular Cu-Co alloys as interacting superparamagnets, *Phys. Rev. B* 64 (2001) 144420.

P3-11**INFLUENCE OF SPARK PLASMA SINTERING ON MICROSTRUCTURE AND PROPERTIES OF La-Ca-Sr-Mn-O MAGNETOCALORIC CERAMIC MATERIALS**

K. Zmorayová¹, V. Antal¹, J. Kováč¹, J. Noudem² and P. Diko¹

¹*Institute of Experimental Physics, Slovak Academy of Science, Watsonova 47, 040 01 Košice, Slovakia*

²*CRISMAT, UMR 6508 ENSICAEN/CNRS, IUT-Caen, Université de Caen Basse-Normandie, 6 Bd Maréchal Juin, 14050 Caen Cedex 04, France*

Polycrystalline $\text{La}_{0.67}\text{Ca}_{0.33-x}\text{Sr}_x\text{MnO}_3$ ($x = 0.33; 0.03; 0$) perovskite samples prepared by Spark Plasma Sintering (SPS) process are investigated. The different sintering temperature on microstructure and properties of studied LCSM materials are discussed.

The microstructure characterizations are performed by polarized light microscopy and scanning electron microscopy. The microstructural observations reveal changes of grain size of studied LCSM materials as a function of sintering temperature of SPS process. The energy dispersive spectrometer (EDS) analysis confirms that higher sintering temperature causes a change in the phase composition of the investigated LCSM perovskite materials.

Magnetic measurements are performed by the Quantum Design XL5 Magnetic Properties Measurement System (MPMS). The influence of changes in the phase composition and grain size of polycrystalline LCSM materials after SPS and/or oxidation on the magnetization behaviour is described.

Acknowledgment

This work was realized within the framework of the projects: Centre of Excellence of Advanced Materials with Nano- and Submicron Structure (ITMS 26220120019), Infrastructure Improving of Centre of Excellence of Advanced Materials with Nano- and Submicron Structure (ITMS 26220120035), New Materials and Technologies for Energetic (ITMS 26220220061), Research and Development of Second Generation YBCO Bulk Superconductors (ITMS 26220220041), APVV No. 0330-12, VEGA No. No. 2/0121/16, Stefanik Project SK-FR-2013-0025, PhysNet Project (ITMS 26110230097) and SAS Centre of Excellence: CFNT MVEP.

P3-12**MAGNETIC PROPERTIES AND STRUCTURE OF FeCo ALLOYS**D. Olekšáková¹, P. Kollár², F. Onderko², J. Füzér², S. Dobák² and J. Viňáš³¹*Department of Applied Mathematics and Informatics, Faculty of Mechanical Engineering, Technical University in Košice, Letná 9, 042 00 Košice, Slovakia*²*Institute of Physics, Faculty of Science, P. J. Šafárik, Park Angelinum 9, Košice 04154, Slovakia*³*Department Engineering Technologies and Materials, Faculty of Mechanical Engineering, Technical University in Košice, Mäsiarska 74, 040 01 Košice, Slovakia*

Fe-Co alloys are known to have many applications in a wide variety of areas due to their magnetic properties (high Curie temperatures, high saturation magnetization and high permeability). These properties, which depend significantly on grain size, internal strain and crystal structure, are shown to be superior in the nanostructured alloys.

In the present work, the crystalline Fe-Co powders with ratio 50:50 are prepared after 30 h of ball milling. The bulk samples were prepared from these powders in the form of cylinders (diameter 10 mm, height 2.5 mm, weight approx. 2 g). The compaction was performed at a pressure of 800MPa for 5 min at temperature range from 400 ° to 600 °C. In order to prevent oxidation and to remove free gases in the compacted samples, the compaction was performed in vacuum of $5 \cdot 10^{-3}$ Pa.

The mechanical milling was proved to be an effective technique for the synthesis of nanostructured powders of various metal-metal systems. This useful technique can produce a variety of equilibrium and non-equilibrium alloy phases leading to size reduction and particle shape modification. The advantage of this process technology is that the powder can be produced in large quantities and the processing parameters can be easily controlled.

Complex permeability was measured by impedance/gain-phase analyser. Dc magnetic properties were measured by the fluxmeter based on the hysteresisgraph.

The structural and magnetic characteristics were analysed as a dependence on Co content and consequently compared with the conventional Fe-Co alloys.

Acknowledgment

This work was supported by the Scientific Grant Agency of the Ministry of Education of the Slovak Republic and the Slovak Academy of Sciences, projects VEGA 1/0377/16 and KEGA 072TUKE-4/2014 and project ITMS 26220120019.

P3-13**INVESTIGATION OF MAGNETIC ANISOTROPY INFLUENCE ON TOTAL LOSS COMPONENTS OF GRAIN-ORIENTED ELECTRICAL STEELS**W.A. Pluta¹*¹Czestochowa University of Technology, Electrical Engineering Faculty,
Al. Armii Krajowej 17, 42-200 Czestochowa, Poland*

In the electrical industry the most widely used soft magnetic material is electrical steel. Magnetic anisotropy resulting from Goss texture has probably the largest influence on magnetic properties the electrical steel sheet. Modeling of frequency dependence of total loss is important. The aim of the paper is to present the influence of anisotropy and frequency on total loss components of grain-oriented electrical steel sheets.

The experiment was carried out on grain-oriented (GO) electrical steel sheets. The measurements of specific total power loss were carried out in a non-standard Single Sheet Tester (SST) on square samples of 100 mm width. The flux density range was varied from 0.1 T to 1.3T - 1.8 T in dependence on magnetization direction. There were chosen 10 to 12 measurement frequencies from the range of 2 Hz to 100 Hz. Number of frequencies allowed to analyze frequency behavior of chosen magnetic properties of electrical steel.

Angular magnetic properties as well as other physical properties can be represented by a periodic function, but most often a trigonometric function is used. Such a function allows to model total loss components related to crystallographic texture. Angular dependences of total loss components of GO electrical steel has to be described with minimum of 5 components as below:

$$F(x) = A_0 - A_1 \cos(2x) - A_2 \cos(4x) - A_3 \cos(6x) + A_4 \cos(8x)$$

There were presented relationships between the coefficients A_i of above formula calculated for hysteresis and additional eddy current total loss components and anisotropy of ES grades under consideration. Those relationships show some similarities between those calculated for hysteresis and additional eddy current components. There is also visible different anisotropy behavior of the hysteresis and additional eddy current specific total loss components in "low" and "upper" flux density regions.

The analysis allows to propose simplified model for specific total loss calculation according to formula $P_s(\alpha) = C(\alpha)(Ph(\alpha) + Pa(\alpha)) + P_{ce}$ where α is the magnetization angle and $Ph(\alpha)$ and $Pa(\alpha)$ are dependent on magnetic anisotropy.

P3-14**MAGNETOCALORIC EFFECT IN NOVEL $\text{Gd}_2\text{O}_3@\text{SiO}_2$ NANOCOMPOSITES**A. Berkutova¹, A. Zelenáková¹, P. Hrubovčák¹, O. Kapusta¹ and V. Zelenák²¹*Department of Condensed Matter Physics, University of P.J. Šafárik, Park Angelinum 9, 040 01 Košice, Slovakia*²*Department of Inorganic Chemistry, University of P.J. Šafárik, Moyzesova 11, 040 01 Košice, Slovakia*

Lanthanide metals and their alloys have attracted much attention as suitable magnetic materials for a wide range of technological and biomedical applications. For example, Gd and its compounds are of current interest as magnetic resonance contrast media, therapeutic agents in tumor treatment and drug delivery. In addition, gadolinium and its compounds exhibit the large magnetocaloric effect and therefore gadolinium compounds are promising magnetic materials for refrigeration technology applications.

Magnetocaloric effect (MCE) can be observed in all magnetic materials. It is evident from the changes in magnetic part of the entropy of a solid as a result of relation between magnetic sublattice and magnetic field. Also it can give information about magnetic phase transitions and spin structures because of its strong relation with magnetism. MCE in ferromagnets is associated with disorder-order states reached by phase transition below Curie temperature (T_c). In case of paramagnets, MCE can be measured only close to absolute zero temperatures, where the $(\partial M/\partial T)_H$, which is enhanced, but still limited, is easily onset by the negligible lattice heat capacity of a solid.

We have studied magnetic properties (with respect to MCE) of $\text{Gd}_2\text{O}_3@\text{SiO}_2$ nanocomposite prepared by nanocasting of Gd_2O_3 nanoparticles in periodic nanoporous silica matrix with hexagonal symmetry. Magnetic properties were measured by commercial MPMS 5XL (Quantum Design) apparatus in temperature range 1.8-300K in external magnetic field up to 5 T. The MCE was characterized by the magnetic entropy change due to the application of a magnetic field H , which was evaluated from the processing of the temperature and field dependent magnetization curves using a Maxwell relation $\Delta S = \int (\partial M/\partial T)_H dH$. Our results show that the peak of entropy change in studied material was observed at very low temperature $T \sim 4$ K and the change in entropy with the change in applied magnetic field (dS/dH) is reasonably large $\Delta S(T) \sim 9.8$ J/K.kg for this type of nanocomposites. On the base of our study, the $\text{Gd}_2\text{O}_3@\text{SiO}_2$ nanocomposites could be promising for refrigeration technology.

*Acknowledgment**This work was realized within the project ITMS 26220120019.*

P3-15**THE INFLUENCE OF $\text{NiZnFe}_2\text{O}_4$ CONTENT ON MAGNETIC PROPERTIES OF SUPERMALLOY TYPE MATERIAL**

L. Ďáková¹, J. Füzér¹, S. Dobák¹, P. Kollár¹, M. Fáberová², M. Strečková², R. Bureš² and H. Hadrabá³

¹*Institute of Physics, Faculty of Science, Pavol Jozef Šafárik University, Park Angelinum 9, 041 54 Košice, Slovakia*

²*Institute of Materials Research, Slovak Academy of Sciences, Watsonova 47, 040 01 Košice, Slovak Republic*

³*CEITEC IPM, Institute of Physics of Materials ASCR, Žitkova 513/22, 616 62 Brno, Czech Republic*

Soft magnetic material is mostly used as magnetic cores of filters, transformers, deflection, antenna, magnetic heads of multiple path communication and core material for power transformers. The magnetic properties are dependent on the materials composition and also on the method of preparation. Ni–Fe–Mo alloys (supermalloy) have high relative permeability and low eddy current losses. Soft magnetic ferrites of $\text{NiZnFe}_2\text{O}_4$ have low coercivity and high saturation magnetization.

The $\text{Ni}_{80}\text{Fe}_{14.7}\text{Mo}_{0.4}\text{Mn}_{0.5}\text{Si}_{0.3}$ (wt.%) powder sample was prepared by mechanical alloying of the chemical elements: iron, nickel, molybdenum, manganese and silicon in a planetary ball mill Pulverisette 6 (Fritsch) for 24 h. $\text{NiZnFe}_2\text{O}_4$ ferrite was commercially distributed by Sigma Aldrich. Both powders were mixed at selected ratio and compacted at 800MPa.

In this paper, we report the experimental observations of the effects of $\text{NiZnFe}_2\text{O}_4$ content and conditions of heat treatment on the electromagnetic properties of soft magnetic composite $\text{NiFeMoMnSi/NiZnFe}_2\text{O}_4$. The samples contained 5, 10, 15 % of $\text{NiZnFe}_2\text{O}_4$ ferrite and were sintered for 30 minutes at 800 °C and 1000 °C, respectively. The rings were used for measurement of complex permeability and total magnetic losses and cylinders were used for measurement of coercivity and electric resistivity. Permeability was studied in the range from 100 Hz to 40 MHz. The total losses of the samples were measured at different frequencies, ranging between 10 Hz- 100 kHz at 0.1 T. The sample $\text{NiFeMoMnSi/NiZnFe}_2\text{O}_4$ (15 % wt. of ferrite) exhibits the lowest total magnetic losses and the highest magnetic permeability. The sample prepared by sintering at 1000 °C exhibits the worst soft magnetic properties in medium frequencies.

Acknowledgment

This work was realized within the project ITMS 26220120019.

P3-16**THE INFLUENCE OF PREPARATION METHODS ON MAGNETIC PROPERTIES OF Fe/SiO₂ SOFT MAGNETIC COMPOSITES**J. Füzerová¹, J. Füzer², P. Kollár², M. Kabátová³ and E. Dudrová³¹*Department of Applied Mathematics and Informatics, Faculty of Mechanical Engineering, Technical University Košice, Letná 1, 042 00 Košice, Slovakia*²*Institute of Physics, Faculty of Science, Pavol Jozef Šafárik University, Park Angelinum 9, 041 54 Košice, Slovakia*³*Institute of Materials Research, Slovak Academy of Sciences, Watsonova 47, 040 01 Košice, Slovak Republic*

Soft magnetic composites (SMCs) offer an interesting alternative to the traditional laminated silicon iron sheets as core material in electrical machines. SMCs are mostly composed of pure iron powder particles insulated from each other by organic or inorganic material, which insulates and binds ferromagnetic particles and produces a high electrical resistivity.

The shape of the iron powder particles, the polymer type and the preparation procedure of composites were studied in view of magnetic and electrical properties of Fe/SiO₂/polymer soft magnetic composites. Fe/(0.4-2wt.%) SiO₂/polymer composite materials are based on iron powder particles irregularly and/or spherically shape, the SiO₂ component was added in two ways: as a nano-powder and as a sol-gel SiO₂ coating. Ring and cylindrical composite samples were prepared by powder metallurgy, conventional mixing the Fe/SiO₂ powder with shellac dissolved in ethanol and by an unconventional vacuum/pressure impregnation procedure of low-temperature sintered Fe/SiO₂ compacts with shellac dissolved in ethanol. Powder mixtures were dried at RT for 60 min in air and subsequently cold compacted at pressures ranging from 100 to 800 MPa into cylindrical and rings compacts, respectively.

The rings were used for measurement of complex permeability and total magnetic losses and cylinders were used for measurement of coercivity and electric resistivity. Permeability was studied in the range from 1 kHz to 40 MHz. The total losses of the samples were measured at different frequencies, ranging between 2 - 30 kHz at 0.1 T.

The results showed that the resulting soft magnetic properties depend not only on the amount of the electrical-insulating phase, but also on the shape of iron particles, the type of polymer and the preparation method applied. In the case of irregularly shaped iron particles, the vacuum-pressure impregnation is associated with a risk of Fe/Fe connection creation in local surface asperities, which leads to the loss of the insulating function of the layer.

*Acknowledgment**This work was realized within the project ITMS 26220120019.*

P3-17

MAGNETIC PROPERTIES AND STRUCTURE OF NON-ORIENTED ELECTRICAL STEEL SHEETS AFTER DIFFERENT SHAPE PROCESSINGS

T. Bulín¹, E. Švábenská², M. Hapla², Č. Ondrůšek¹ and O. Schneeweiss²

¹Brno University of Technology, Faculty of Electrical Engineering and Communication, Technická 3058/10, 616 00 Brno, Czech Republic

²Institute of Physics of Materials ASCR, Žitkova 22, 616 62 Brno, Czech Republic

Non-oriented electrical steel sheets are the most often used materials in electrical rotary machines. Raw sheets must be formatted by various methods, e.g., punching, laser, spark or water stream cutting. Basic parameters of magnetic, electrical, and mechanical properties of the sheets are usually obtained from the producer, but namely magnetic properties are changed in dependence on additional machining processes. The aim of this study is to describe changes in magnetic properties after punching, laser or spark cutting of the original sheets M470-50A. The basic information of structure was obtained by optical microscopy (OM) and scanning electron microscopy (SEM). For the magnetic measurements toroidal samples were prepared by the mentioned technologies. The magnetic parameters were yielded from the measuring of magnetic hysteresis loops in dependence on saturation fields and frequencies. Simultaneously structures of cut edges were analyzed by OM and SEM. The results are discussed from the point of view of applied cutting methods with the aim to obtain the best magnetic parameters and consequently a higher efficiency of the final product. After laser cutting, important decrease in remanence and increase in total losses were observed in comparison with the punched samples (Fig.1). Results can be used as input parameters in simulation of the electrical machine.

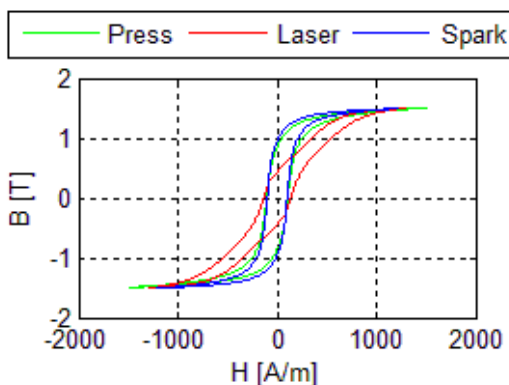


Fig. 1 Hysteresis loops of the samples after different cutting methods.

I4-01**LOW T_c GLASSY MAGNETIC ALLOYS FOR MEDICAL APPLICATIONS**H. Chiriac¹¹*National Institute of R&D for Technical Physics, 700050 Iasi, Romania*

The need for curing various incurable diseases is demanding not only new types of materials, which preferably will mimic the nature functionalities, but also the understanding of their properties in relation with their microstructure. In this context, the use of magnetic hyperthermia for curing cancer appears to be an extremely viable one. In this sense, we have developed a new type of ferromagnetic nanoparticles (the saturation magnetization is higher compared with Fe-oxides and the hysteresis losses are reduced as well), with the nominal compositions $\text{Fe}_{79.7-x}\text{ETM}_x\text{Nb}_{0.3}\text{B}_{20}$ ($\text{ETM} = \text{Cr, Ti, Ta, Mn}$; $x = 12 \div 20$ at.%), with low Curie temperature, which can be tailored easily and precisely in the $0\text{--}70^\circ\text{C}$ by modifying the ETM content, with an accuracy of less than 1°C , more suitable for self-regulating magnetic hyperthermia. The purpose of the present study was to evaluate in vitro the cytotoxicity of $\text{Fe}_{79.7-x}\text{ETM}_x\text{Nb}_{0.3}\text{B}_{20}$ alloy nanoparticles, coated or not by a biocompatible layer. The effect of Fe-ETM-Nb-B magnetic nanoparticles on tumor cells (human osteosarcoma cancer cells) was investigated prior and following particle activation by an a.c. electromagnetic field of 350 mT ($f = 153$ kHz) created by a home-made magnetic-induction hyperthermia unit. In addition, we prepared a ferrofluid based on low Curie $\text{Fe}_{67.2}\text{Cr}_{12.5}\text{Nb}_{0.3}\text{B}_{20}$ particles, to have a suspension of particles with good stability and to avoid their agglomeration, aspects that are important in biomedical applications. The heating power of the ferrofluid was investigated by using the same magnetic induction hyperthermia unit. When the ferrofluid is introduced in the AC magnetic field, its heating curve starts to saturate after 12 min. of continuous heating, when temperature reaches 47°C , and increases afterwards with only 0.6°C during the next 20 min. Cytotoxicity tests performed on osteosarcoma cells showed that the cellular viability was not significantly reduced, the ferrofluid presenting a good biocompatibility. Moreover, a very uniform distribution of the particles in the cell culture was observed in the case of ferrofluid as compared to bare magnetic particles. This represents an advantage for hyperthermia as well as for drug delivery applications, because it will provide a homogenous distribution of the heat and of the bioactive material in the targeted tissue, respectively.

This work was supported by the CNDI–UEFISCDI grant #148/2012 (HYPERTHERMIA).

I4-02**TEMPLATE ASSISTED DEPOSITION OF FERROMAGNETIC NANOSTRUCTURES: FROM ANTIDOT THIN FILMS TO MULTISEGMENTED NANOWIRES AND METALLIC NANOTUBES**

V. M. Prida¹, V. Vega¹, S. González¹, M. Salaheldeen^{1,2}, J. M. Mesquita¹, A. Fernández¹ and B. Hernando¹

¹*Department of Physics, University of Oviedo, Calvo Sotelo s/n, 33007-Oviedo, Asturias, Spain*

²*Department of Physics, Faculty of Science, Sohag University, 82524-Sohag, Egypt*

Ordered arrays of nanostructured ferromagnetic materials have recently attracted the interest of the research community due to their singular magnetic properties and their potential applications in high-density recording media, magnetic sensors or energy conversion and microwave devices. The growth of nanostructured materials by means of different deposition methods employing nanoporous anodic aluminum oxide (AAO) membranes as patterned templates has been widely used during last years due to the outstanding features exhibited by these nanoporous templates. The highly self-ordered hexagonal symmetry of the pores arrangement exhibited by the AAO templates displays narrow pore size distributions with well-defined interpore distances. Furthermore, advanced deposition techniques suitable for conformal coating of 3D structured substrates, such as atomic layer deposition (ALD), allow for additional control of the morphological parameters of AAO membranes, enabling independent control of pores diameter, while keeping constant the interpore distances. The spatial and periodic pores arrangement of the AAO templates, together with the confined growth of the magnetic material at the nanoscale deposited in the nanoporous alumina template, translate into the appearing of cooperative phenomena in the nanostructured materials, which in turn lead to tailor novel functional properties that differ from that of 3D bulk and 2D thin film systems. The synthesis, morphology, structural properties and magnetic behavior of ordered arrays of ferromagnetic nanowires made of Transition Metals (Fe, Ni, Co), and their alloys by means of electrochemical deposition methods, together with magnetic nanotubes grown via ALD deposition technique inside the nanopores of the AAO templates, and ferromagnetic thin films with ordered nanoholes (antidots), designed by replicating the nanoporous arrangement of the AAO substrate on which the metallic layer is deposited by vacuum thermal evaporation technique, will be presented. The main features of the peculiar magnetic properties exhibited by these novel nanostructured materials will be discussed.

O4-01**FOCUSED ION BEAM PATTERNING OF METASTABLE FCC IRON THIN FILMS – A NOVEL TEMPLATE FOR MAGNETIC METAMATERIALS**

M. Urbánek^{1,2}, V. Křižáková², J. Gloss³, M. Horký^{1,2}, L. Flajšman¹, M. Schmid³, T. Šíkola^{1,2} and P. Varga^{1,3}

¹*CEITEC BUT, Brno University of Technology, Purkyňova 656/123, 612 00 Brno, Czech Republic*

²*Institute of Physical Engineering, Faculty of Mechanical Engineering, Technická 2, 616 69 Brno, Czech Republic*

³*Institute of Applied Physics, TU Wien, 1040 Vienna, Austria*

Nanostructured magnetic materials may exhibit phenomena, which are not achievable in their bulk constituents. Due to their unexpected behavior, these materials are often called metamaterials. We have recently shown the possibility to grow metastable fcc Fe thin films which can undergo magnetic and structural (paramagnetic to ferromagnetic, fcc to bcc) phase transformation upon ion-beam irradiation [1]. These films represent an ideal system, where ferromagnetic elements may be selectively written into a paramagnetic matrix by using focused ion beam.

In our experiments we have used epitaxial metastable thin films of fcc Fe₇₈Ni₂₂ evaporated in UHV ($p=3\times 10^{-10}$ mbar) on Cu(100) surface. The films were then selectively irradiated (i.e. transformed) by 30 keV Ga⁺ focused ion beam and magnetic properties of transformed patterns were studied by Magnetic Force Microscopy and Kerr magnetometry. We show that with varying ion dose we are able to selectively write magnetic patterns with spatially modulated magnetic properties (M_s , H_c). Further, we also demonstrate, that with a proper selection of focused ion beam scanning strategy (linear or circular scanning) we are able to control the type of the anisotropy (cubic or uniaxial) of the transformed areas, together with the values of anisotropy constants.

Our results show that the metastable fcc Fe thin films are good template for fabrication of arbitrary magnetic patterns by focused ion beam direct writing. This system presents an ideal candidate for fabrication of magnetic metamaterials [2], due to its unprecedented possibility of spatial variation of magnetic properties by using different irradiation procedures.

[1] Gloss J., et al., Ion-beam-induced magnetic and structural phase transformation of Ni-stabilized face-centered-cubic Fe films on Cu(100). Appl. Phys. Lett. 103, 262405 (2013).

[2] Chumak A. V., et al., Magnon spintronics. Nature Physics. 11, 453-461 (2015).

O4-02**IN-PLANE EDGE MAGNETISM IN GRAPHENE-LIKE NANOSTRUCTURES**S. Krompiewski¹*¹Institute of Molecular Physics, Polish Academy of Sciences,
Mariana Smoluchowskiego 17, 60-179 Poznań, Poland*

This paper is devoted to identification of the most important factors responsible for formation of magnetic moments at edges of graphene-like nanoribbons. The main role is attributed to Hubbard correlations (within unrestricted Hartree-Fock approximation) and intrinsic spin-orbit interactions, but additionally a perpendicular electric field is also taken into account. Of particular interest is the interplay of the in-plane edge magnetism and the energy band gap. It is shown that, with the increasing electric field, typically the following phases develop: magnetic insulator (with in-plane spins), nonmagnetic narrow-band semiconductor, and nonmagnetic band insulator.

Acknowledgments This work was supported by the Polish National Science Centre from funds awarded through the decision No. DEC-2013/10/M/ST3/00488.

O4-03**HIGH-RESOLUTION FULLY VECTORIAL SCANNING KERR
MAGNETOMETRY**L. Flajšman¹, M. Urbánek^{1,2}, V. Křížáková², M. Vaňatka¹ and T. Šíkola^{1,2}¹*CEITEC BUT, Brno University of Technology, Technická 10, 616 00 Brno, Czech Republic*²*Institute of Physical Engineering, Brno University of Technology, Technická 2, 616 69 Brno, Czech Republic*

We report on the development of a high-resolution scanning magnetometer which fully exploits the vectorial nature of the magneto-optical Kerr effect. The three-dimensional nature of magnetization is at the basis of many micromagnetic phenomena and from this data, we can fully characterize magnetization processes of nanostructures in static and dynamic regimes. Our scanning Kerr magnetometer uses a high numerical aperture microscope objective where the incident light beam can be deterministically deviated from the objective symmetry axis, therefore both in-plane (via the longitudinal Kerr effect), and out-of-plane (via the polar Kerr effect) components of the magnetization vector may be detected. These components are then separated by exploiting the symmetries of the polar and longitudinal Kerr effects. From four consecutive measurements we are able to directly obtain the three orthogonal components of the magnetization vector with a resolution of < 600 nm. Performance of the magnetometer is demonstrated by a measurement of 3D magnetization vector maps showing out-of-plane domains and in-plane domain walls in an yttrium-iron-garnet (YIG) film, the angular dependent anisotropy energy function measurements of metastable iron layers and on a study of magnetization reversal in a magnetic disks with diameters ranging from 250 nm to 8 micrometers.

O4-04**TOWARDS MEASURING MAGNETISM WITH ATOMIC RESOLUTION IN A TRANSMISSION ELECTRON MICROSCOPE**J. Ruzs¹, J. C. Idrobo², S. Muto³, J. Spiegelberg¹ and K. Tatsumi³¹*Department of Physics and Astronomu, Uppsala University, Uppsala, Sweden*²*Oak Ridge National Laboratory, TN, USA*³*Institute of Materials & Systems for Sustainability, Nagoya University, Nagoya, Japan*

It was shown about a decade ago that magnetic circular dichroism (MCD) can be measured in transmission electron microscopes (TEMs) [1]. Since then, significant improvements have been achieved in improving both signal to noise ratio (SNR) and spatial resolution, in part also thanks to progress in simulations and theoretical understanding, since electron MCD (EMCD) is – in contrast to the x-ray MCD method – influenced by dynamical diffraction effects.

The original EMCD measurement geometry [1] is however not likely to provide atomic-resolution information. It requires near-parallel beam (limiting spatial resolution) and uses only a small fraction of scattered electrons (reducing SNR). Therefore new experimental geometries have to be developed.

Recently, electron vortex beams (EVBs) have been successfully generated in TEMs [2,3,4]. These electron beams carry a nonzero orbital angular momentum, which can interact with magnetic moments in the sample. It was shown later [5] that it is actually the specific symmetry of the phase distribution in the electron beam wavefunction, which allows to detect EMCD. Alternative beam shapes were proposed, e.g., four-fold astigmatic beams [5].

Important advantage of these new approaches is that it requires a use of convergent electron probes with atomic size and the EMCD should be measured at transmitted beam direction – recovering high resolution and improving SNR.

We will present some of the recent progresses in measuring EMCD at atomic or near-atomic resolution, utilizing the manipulation of the phase of the electron beam wavefunction.

[1] P. Schattschneider *et al.*, Nature 441, 486 (2006).

[2] M. Uchida, and A. Tonomura, Nature 464, 737 (2010).

[3] J. Verbeeck, H. Tian, and P. Schattschneider, Nature 467, 301 (2010).

[4] B. McMorrán *et al.*, Science 331, 192 (2011).

[5] J. Ruzs, J. C. Idrobo, and S. Bhowmick, Phys. Rev. Lett. 113, 145501 (2014).

O4-05**MAGNETIC VORTEX NUCLEATION MODES STUDIED BY ANISOTROPIC MAGNETORESISTANCE AND MAGNETIC TRANSMISSION X-RAY MICROSCOPY**

M. Vaňatka¹, M. Urbánek^{1,2}, R. Jíra², L. Flajšman¹, M. Dhankhar¹, V. Uhlíř¹, M.-Y. Im³ and T. Šíkola^{1,2}

¹*CEITEC BUT, Brno University of Technology, Technická 10, 616 00 Brno, Czech Republic*

²*Institute of Physical Engineering, Brno University of Technology, Technická 2, 616 69 Brno, Czech Republic*

³*Center for X-Ray Optics, Lawrence Berkeley National Laboratory, 1 Cyclotron Road, Berkeley, California 94720, USA*

Behavior of magnetic vortices under applied static or pulsed magnetic fields has been previously studied in many aspects [1,2]. Of particular interest is the vortex nucleation and annihilation, which defines the final state of the vortex. While the vortex annihilation has been studied extensively [3], not much attention has been paid to the vortex nucleation mechanisms and experimental data on vortex nucleation in single disks are missing completely.

In presented work, we show how various vortex nucleation modes in Permalloy nanodisks can be detected by anisotropic magnetoresistance (AMR), i.e. by detection of the electrical resistance changes corresponding to the individual nucleation modes. The AMR data are compared to the calculations of the electrical resistance obtained from micromagnetic simulations. The experimental and simulated AMR spectra are in a very good agreement and we further support our results by direct magnetic imaging (Fig. 1) of vortex nucleation under applied static magnetic fields using Magnetic Transmission X-ray Microscopy (MTXM) performed at the Advanced Light Source at Berkeley, CA, USA.

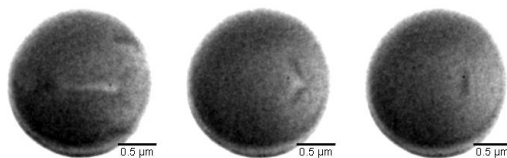


Fig. 1: MTXM images of magnetic vortex nucleation in a single Permalloy disk.

- [1] K.Y. Guslienko, J. Nanosci. Nanotechnol. 8, 2745 (2008).
- [2] V. Uhlíř, M. Urbánek, L. Hladík, J. Spousta, M.-Y. Im, P. Fischer, N. Eibagi, J.J. Kan, E.E. Fullerton, and T. Šíkola, Nat. Nanotechnol. 8, 341 (2013).
- [3] J.F. Pulecio, S.D. Pollard, P. Warnicke, D. a. Arena, and Y. Zhu, Appl. Phys. Lett. 105, 132403 (2014).

O4-06**MAGNETIC PROPERTIES OF HEXAGONAL GRAPHENE NANOMESHES**M. Zwierzycki¹*¹Institute of Molecular Physics, Polish Academy of Sciences, Smoluchowskiego 17, 60-179 Poznań, Poland*

Graphene nanomeshes are the nanostructures consisting of graphene flake with a regular pattern of antidots (holes) punched through it. Thanks to energy gaps opening in electronic spectrum, nanomesh-based FET transistors offer improved I_{on}/I_{off} ratio while supporting up to 100 larger driving currents than nanoribbon-based devices. In this contribution the electronic and magnetic structure of graphene nanomeshes with hexagonally shaped antidots (holes) has been studied. The internal zigzag edges has been found to support magnetic moments with antiferromagnetic ordering being the lowest energy configuration. The energy gap which forms in the necks separating the antidots gap closes upon switching (e.g. by external magnetic field) to ferromagnetic configuration. This change should be observable in transport properties, which makes graphene nanomeshes of this kind promising materials for spintronic applications.

O4-07**MAGNETOTRANSPORT IN Mn-DOPED Bi₂Se₃ TOPOLOGICAL INSULATORS**

V. Tkáč¹, V. Komanický², R. Tarasenko², M. Vališka¹, V. Holý¹, G. Springholz³, V. Sechovský¹ and J. Honolka⁴

¹*Department of Condensed Matter Physics, Faculty of Mathematics and Physics, Charles University, Ke Karlovu 5, CZ-12116 Prague 2, Czech Republic*

²*Institute of Physics, P. J. Šafárik University, Park Angelinum 9, 040 01 Košice, Slovak Republic*

³*Institute of Semiconductor and Solid State Physics, Johannes Kepler University, Altenbergerstrasse 69, A-4040 Linz, Austria*

⁴*Institute of Physics, Academy of Sciences of the Czech Republic, Na Slovance 2, CZ-18221 Prague 8, Czech Republic*

Three-dimensional topological insulators (TIs) are a newly discovered state of matter with insulating bulk and conducting topological surface states (TSSs). In prototype Bi-based chalcogenide TIs like Bi₂Te₃ or Bi₂Se₃, a single spin-helical TSS is generated by strong spin-orbit coupling, which is protected by time-reversal symmetry. Two-dimensional transport through TSSs is predicted to be connected with the presence of weak antilocalization effects. The gapless Dirac cone dispersion of the TSS carries a π Berry phase, which changes the interference of time-reversed scattering loops from constructive to destructive. This effect can be destroyed by applying a magnetic field, which breaks the π Berry phase, leading to a cusp-shaped negative magnetoconductivity.

Magnetic impurities violate time-reversal symmetry and thus may largely affect topological insulator properties and their transport. The mean field produced by magnetic doping may open a uniform gap at the Dirac point, allowing electrons to backscatter.

The present work is devoted to the study of Bi₂Se₃ thin films with Mn dopants, which were grown by molecular beam epitaxy on insulating BaF₂ (111) substrates. We experimentally studied transport properties of the Mn-doped Bi₂Se₃ topological insulators with various thickness and Mn concentrations. Bi₂Se₃-based Hall bars for transport measurements were fabricated using lithography techniques. The measurements of electrical resistivity, magnetoconductance and Hall resistivity have been realized at temperatures down to 0.3 K in magnetic fields up to 14 T in various orientations. The experimental data were successfully described with several theoretical models.

O4-08**Study Of Magnetic Micro-Ellipses By Cantilever Sensor**K. Sečianska¹, J. Šoltýs¹ and V. Cambel¹¹*Institute of Electrical Engineering, SAS, Dúbravská cesta 9, 841 04 Bratislava, Slovakia*

Cantilever sensors have attracted great attention as a highly sensitive and fast sensor platform for numerous applications. In principle every external perturbation can be measured by bending of a cantilever beam or detected by a shift in cantilever's resonance frequency with the greatest accuracy. Measuring micrometer and submicrometer scale magnetic features has proven to be a challenge for conventional magnetometers. Hence, microcantilever magnetometry is a promising experimental technique for measuring magnetism of submicron magnetic particles.

Measurements are performed by a cantilever; however it does not scan over the sample surface as in AFM. In this application, samples are mounted directly on a cantilever. Generally, it can be realized by two methods. Firstly, sample can be placed on cantilever with a micromanipulator and glued. However, this can introduce contamination and negatively change cantilever mechanical properties. The second method is standard MEMS process, where cantilevers and structures are prepared from planar substrate by lithography. Obstacle is that prepared structures are etched by chemicals, which are used to release cantilever in final step. Therefore it would be appropriate to release cantilever first and then prepare structures by lithography. Common method is electron beam lithography (EBL). EBL involves an EB resist, which is usually applied by spin-coating. However, standard spin-coating technique fails to pattern non planar surfaces and cannot apply resist uniformly on pre-structured structures. Therefore alternative methods of resist deposition have to be used, but they are difficult and require special equipment.

We propose a novel method of prototyping of cantilever sensors by means of modification of commercial AFM cantilevers, without the need of difficult and time-consuming cantilever fabrication. We propose an advanced spin-coating of PMMA resist on AFM cantilevers. Using this method we fabricated cantilever sensor for study of magnetic structures. We prepared two arrays of micrometric sized permalloy ellipses on cantilever by EBL. Cantilever was then cut by FIB into halves. By external magnetic field we could set magnetization of arrays and create a magnetic coupling between the cantilever halves. In ideal case coupling could be detected by a shift in resonance peaks. Attractive and repulsive forces between magnetic structures were shown by magnetic force microscopy (MFM).

O4-09**MAGNETIC PHASE TRANSITION ASYMMETRY IN MESOSCALE FERH STRIPES**V. Uhlíř^{1,2}, J. A. Arregi^{2,3} and E. E. Fullerton²¹*Central European Institute of Technology, Brno University of Technology, Purkyňova 123, 612 00 Brno, Czech Republic*²*Center for Memory and Recording Research, University of California, San Diego, La Jolla, California 92093-0401, USA*³*CIC nanoGUNE Consolider, Tolosa Hiribidea 76, E-20018 Donostia–San Sebastián, Spain*

Understanding and ultimately controlling emergent phenomena at the mesoscale requires understanding the interactions and correlations of the individual constituents in complex materials [1] and engineered systems [2]. The nature of first-order phase transitions that exhibit an interplay between multiple degrees of freedom (*i.e.* electronic, structural and/or magnetic) is at the forefront of materials science. We focus on the metamagnetic transition from the antiferromagnetic order (AF) to ferromagnetic order (FM) in FeRh which occurs at approximately 370 K [3]. The transition is accompanied by a volume increase of 1-2%, a reduction in resistivity [4] and a large change in entropy. Unlike bulk single crystals, measurement of the resistance or magnetization [5] of thin films across the phase transition gives a continuous smooth transition that is relatively broad (about 10K).

However, in micron-scale patterned FeRh stripes we observed pronounced supercooling and avalanche-like abrupt transition from the ferromagnetic to the antiferromagnetic phase while the reverse transition remains nearly continuous. We deduce that the asymmetry arises from the differences in the magnetic correlations of FM regions compared to AF regions. Although modest asymmetry signatures are present in full films, the effect is dramatically enhanced at the mesoscale.

- [1] E. Dagotto, Complexity in Strongly Correlated Electronic Systems. *Science* 309, 257 (2005).
- [2] L. J. Heyderman and R. L. Stamps, Artificial ferroic systems: novel functionality from structure, interactions and dynamics. *J. Phys.: Condens. Matter* 25, 363201 (2013).
- [3] M. Fallot and R. Hocart, Sur l'apparition du ferromagnétisme par élévation de température dans des alliages de fer et de rhodium. *Rev. Sci.* 77, 498 (1939).
- [4] J. S. Kouvel and C. C. Hartelius, Anomalous Magnetic Moments and Transformations in the Ordered Alloy FeRh. *J. Appl. Phys.* 33, 1343 (1962).
- [5] S. Maat, J.-U. Thiele, and E. E. Fullerton, Temperature and field hysteresis of the antiferromagnetic-to-ferromagnetic phase transition in epitaxial FeRh films. *Phys. Rev. B* 72, 214432 (2005).

P4-01**MAGNETISM AND STRUCTURE EVOLUTION IN Ni-Zn FERRITES THIN FILMS – CEMS STUDY**

T. Szumiata¹, M. Gzik-Szumiata¹, K. Brzózka¹, B. Górka¹, M. Gawroński¹, A. Javed², K. Farman² and T. Fatima²

¹*Department of Physics, Faculty of Mechanical Engineering, University of Technology and Humanities in Radom, Krasickiego 54, 26-600 Radom, Poland*

²*Department of Physics, University of the Punjab, Quaid-i-Azam Campus, Lahore-54590-Pakistan*

Ni-Zn ferrites are promising ceramic materials for pulsed and microwave applications due to the ability of fast magnetization changes. The structural and magnetic order were effectively studied by means of transmission Mössbauer spectrometry [1,2] in bulk Ni-Zn ferrites. In this work, a conversion electron Mössbauer spectrometry (CEMS) has been utilized for the investigation of structural and magnetic order in 500 nm thick Ni-Zn ferrite films deposited on Si(100) substrate by laser ablation. The most general chemical formula of Ni-Zn ferrites could be denoted by $[\text{Ni}_{x-y}\text{Zn}_{1-x+y-i}\text{Fe}_i]^{\text{A}}[\text{Ni}_y\text{Zn}_{i-y}\text{Fe}_{2-i}]^{\text{B}}\text{O}_4$, where x is a number of all Ni atoms, y – a number of Ni atoms in octahedral positions B and i ($i \leq 1$) is the inversion parameter (which denotes the number of Fe atom in tetrahedral positions A). For $x = 0$ (i.e. ZnFe_2O_4), a doublet of quadrupole splitting $QS = 0.36$ mm/s dominates in CEMS spectra. It represents Fe atoms in tetrahedral B positions and points to the simple spinel structure in paramagnetic state. Moreover, a weak high-field sextet is observed which is attributed to the hematite formed at the partially oxidized surface. For $x = 1$ (i.e. NiFe_2O_4), the CEMS spectrum consists of two high-field sextets of the same intensity which point-out the equal distribution of Fe atoms at A and B positions in the ideal ferromagnetic inverse spinel structure ($i=1$). For $x \neq 0$ and $x \neq 1$, the inversion parameter i can be determined from the intensities of subspectra corresponding to Fe in A and B position. The average hyperfine field in the investigated Ni-Zn ferrites thin films is about 5%-9% smaller than the results reported in Refs. [1,2] which could be a sign of size effects of superparamagnetic character. The average direction of hyperfine magnetic field was found to be close to that characteristic of the random distribution, contrary to expectation of in-plane preference. This is probably due to the existence of the perpendicular anisotropy.

[1] M. Arshed, M. Siddique, M. Anwar-ul-Islam, N.M. Butt, T. Abbas and M. Ahmed, *Solid State Communications* 93 (1995) 599-602.

[2] M. Niyafar, H. Mohammadpour, A. F. R. Rodriguez, *Journal of Magnetism* 20 (2015) 246-251.

P4-02**EXACT DIAGONALIZATION-BASED CALCULATIONS
OF INDIRECT MAGNETIC COUPLING IN GRAPHENE
NANOSTRUCTURES**K. Szałowski¹*¹Department of Solid State Physics, University of Łódź, ulica Pomorska 149/153,
PL 90-236 Łódź, Poland*

In the paper the computational study of indirect, charge carrier-mediated magnetic coupling in a prototypical, ultrasmall graphene nanostructure (nanoflake, quantum dot) is presented. The system of interest consists of charge carriers in the nanostructure interacting with a pair of on-site magnetic impurities and immersed in external electric and magnetic in-plane field. The description is based on Hubbard Hamiltonian with Anderson-Kondo term and terms introducing the external fields. The total energy is calculated by means of exact diagonalization, what allows the fully non-perturbative determination of all the components of indirect coupling between the impurity spins. The exact diagonalization results are supplemented and compared with the outcome of Mean Field Approximation (MFA).

It is demonstrated that MFA provides the accurate quantitative description of coupling energy for the parameters relevant to graphene nanostructures (i.e. for limited Hubbard energy) for the case of interaction which is isotropic in spin space. On the other hand, in the presence of in-plane magnetic field, MFA becomes insufficient since the spin-space anisotropy emerges in the studied interaction. In such a case exact diagonalization constitutes particularly reliable method of describing all the components of anisotropic indirect coupling. It is found that the external magnetic field can induce a strong Ising-like anisotropy, even leading to different signs of particular coupling components. This effect is especially pronounced in charge-doped structures and may lead to complicated magnetic interactions. It has also been confirmed by means of exact diagonalization that the in-plane electric field is able to change the sign and magnitude of indirect coupling. In the presence of combined electric and magnetic field, the electric field can be effectively utilized to control the anisotropy of coupling, for example, to switch on Ising-type anisotropy.

This work has been supported by Polish Ministry of Science and Higher Education by a special purpose grant to fund the research and development activities and tasks associated with them, serving the development of young scientists and doctoral students.

The computational support on Hugo cluster at Laboratory of Theoretical Aspects of Quantum Magnetism and Statistical Physics, P. J. Šafárik University in Košice is gratefully acknowledged.

P4-03

GROWTH OF Pt-Ni NANOPARTICLES OF DIFFERENT COMPOSITION USING ELECTRODEPOSITION AND CHARACTERIZATION OF THEIR MAGNETIC PROPERTIES

M. Kožejová¹, D. Hložná¹, Y. Hua Liu², K. Ráczová¹, E. Čižmár¹, M. Orendáč¹ and V. Komanický¹

¹*Institute of Physics, Faculty of Science, P. J. Šafárik University, Park Angelinum 9, 041 54 Košice, Slovakia*

²*Materials Science Division, Argonne National Laboratory, Argonne, Illinois 60439, USA*

Among the electrodeposition schemes used to form Pt alloys, underpotential codeposition is a simple, reproducible, and scalable approach for producing thin films [1]. The alloy composition is a monotonic function of deposition potential, with chemically homogeneous films being obtained by potentiostatic deposition at room temperature. Given a suitable conductive support, thin alloy catalyst films can be synthesized in a matter of seconds to minutes. We have used this technique to produce Pt-Ni nanoparticles with different composition. We prepared Pt₃Ni and PtNi₃ nanoparticles of various sizes on conductive and atomically smooth highly oriented pyrolytic graphite (HOPG) surfaces. By changing deposition time we can control the size of electrodeposited nanoparticles and their density on the surface. The morphology of nanoparticles was determined by scanning electron microscopy. PtNi₃ particles have spherical shape, while Pt₃Ni particles have more irregular shape. Composition of particles was confirmed by EDAX analysis. We have measured magnetic properties of both systems, superparamagnetic behavior was observed in PtNi₃ nanoparticles with 100 s preparation time and increased change of magnetic entropy ($-\Delta S = 40$ mJ/kg K for 0.7 T change of the magnetic field) was observed in the vicinity of the blocking temperature $T_B = 250$ K.

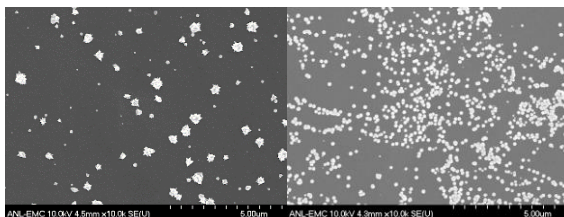


Fig. 1: left Pt₃Ni deposited at -300 mV on HOPG, right PtNi₃ deposited at -600 mV on HOPG

[1] Yihua Liu et al., J. Phys. Chem. C 2012, 116, 7848–7862.

P4-04**LSMO/YBCO HETEROSTRUCTURES AND INVESTIGATION OF “NEGATIVE” RESISTANCE EFFECT IN THE INTERFACE**

M. Sojková¹, T. Nurgaliev², V. Štrbík¹, Š. Chromík¹, B. Blagoev² and M. Španková¹

¹*Institute of Electrical Engineering, Slovak Academy of Sciences, Dúbravská cesta 9, 84104 Bratislava, Slovak Republic*

²*Institute of Electronics, Bulgarian Academy of Sciences, 72 Tsarigradsko Chausse, 1784 Sofia, Bulgaria*

Combinations of ferromagnetic (FM) perovskite manganite and high temperature superconducting (HTS) thin films are of great interest currently both in connection with their attractive physics, originated from the competition of superconductivity and ferromagnetism in the interface, and with their potential application in various spintronics devices. In spite of the conducted intensive research during the last decade, the electrical properties of such thin film structures remain still far from full understanding. Fabrication of HTS/manganite heterostructures and investigation of their electric characteristics in different areas of the sample and in the interface are the aims of this paper.

Heterostructures consisting of high quality ferromagnetic manganite $\text{La}_{0.7}\text{Sr}_{0.3}\text{MnO}_3$ (LSMO) and high temperature superconducting $\text{YBa}_2\text{Cu}_3\text{O}_7$ (YBCO) thin films of thickness about 50 nm were deposited on LaAlO_3 (LAO) single crystal substrates by PLD (A KrF excimer laser operating at 248 nm) method. A standard photolithography process and wet etchings were used to prepare the samples of necessary configurations, suitable for performance of DC, low frequency and microwave measurements.

The samples contained single YBCO, single LSMO areas and a bilayer YBCO/LSMO area. The resistive characteristics of these individual areas were determined using a DC four probe method and analyzed in terms of the interaction of the HTS and FM layers. The measurements in the YBCO/LSMO interface demonstrated “negative” values of the resistance (like the case of “negative” resistance, observed in tunnel barriers [1]). A good interpretation of the obtained results was performed in the framework of a 1 D model which took into account the resistance of the interface R_{if} and the temperature dependence of the resistance of YBCO and LSMO films. It was shown that the effect of “negative” resistance arises because of the redistribution of the measuring electrical current in the interphase area if the resistance of the interface R_{if} is small in comparison with the resistances of the neighboring electrodes.

[1] I. Giaver, Tunneling phenomena in solids, Plenum press New York 1969, pp.19-30.

P4-05**GENERALIZATION OF MAGNETOSTATIC METHOD OF MOMENTS FOR THIN LAYERS WITH REGULAR RECTANGULAR GRIDS**R. Szewczyk¹*¹Industrial Research Institute for Automation and Measurements PIAP,
Al. Jerozolimskie 202;02-486 Warszawa, Poland*

Magnetostatic modelling of field distribution in inductive elements plays the key role in development of different types of sensors. For this purpose the most common method is finite elements method. However, 3D finite elements method have significant limitations for modelling of thin films (which can't be reduced to 2D surfaces) due to very fast increase of the number of tetrahedral elements with the reduction of the thickness of the layer.

For this reason the alternative method is required. Such method is magnetostatic method of moments. Paper presents the generalization of this method for thin layers with rectangular grid. Within the generalization, four key equations describing the influence of rectangular cell's border on the magnetization of cells are stated. On the base of these dependences, the set of $2 \cdot N \cdot M$ linear equations was determined, where N and M are the numbers of rectangular cells in the rows and columns of regular grid. Finally, the set of linear equation is solved and magnetic field distribution is calculated.

Paper presents the most important part of OCTAVE/MATLAB code for modelling the magnetostatic systems, based on thin layer with given thickness. Moreover, the results presenting the influence of thin layer thickness on the magnetic field distribution are presented. To enable validation of the developed software as well as further researches, OCTAVE/MATLAB code is available as open-source software.

P4-06**SPECTROSCOPIC PROPERTIES OF SBA-15 MESOPOROUS SILICA FREE-STANDING THIN FILMS ACTIVATED BY COPPER IONS**L. Laskowski¹ and M. Laskowska¹¹Czestochowa University of Technology, Institute of Intelligent Computational Systems, Al. Armii Krajowej 36, 42-201 Czestochowa, Poland

The present work is devoted to SBA-15 silica thin films containing copper ions anchored inside channels via propyl phosphonate groups. The materials has been prepared in the form of thin films with hexagonally arranged pores, laying rectilinear to substrate surface. The films, that are presented in the present work, has been prepared in the free-standing form. The structural properties of the samples has been investigated by X-ray refractometry, atomic force microscopy (AFM) and transmission electron microscopy (TEM). The molecular structure has been investigated by Raman spectroscopy supported by DFT numerical simulations. Magnetic properties were investigated by QSUID magnetometry and EPR spectroscopy. On the base of varied out researches we was able to determinate of the pores arrangement and verify of activation process related to phosphonate groups in unambiguous way.

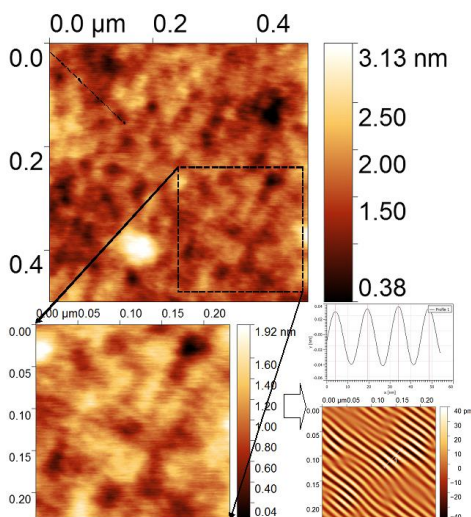


Fig. 1. The AFM microphotographies of the SBA-15 thin film activated by copper ions.

P4-07**TRANSPORT AND MAGNETIC PROPERTIES OF SUPERCONDUCTOR-FERROMAGNET-SUPERCONDUCTOR NANJUNCTIONS**

N. Gál¹, V. Štrbík¹, Š. Beňačka¹, Š. Gaží¹, M. Španková¹, Š. Chromík¹,
M. Sojková¹, M. Pisarčík¹

*¹Institute of Electrical Engineering, Slovak Academy of Sciences,
Dúbravská cesta 9, 84104 Bratislava, Slovak Republic*

Metallic ferromagnet (F) in close proximity with a superconductor (S) can transport supercurrent on long distance (long range proximity effect) through conversion of opposite-spin singlet Cooper pairs (CP) into equal-spin triplet CP, which are not broken by the exchange energy of F. Optimal conditions for the conversion are not clear until now, however, it is accepted that key points to this process include high interface transparency and magnetic inhomogeneity at the SF interface. The aims of our contribution are preparation of lateral SFS nanjunctions (length 40-100 nm and width about 300 nm) based on high critical temperature superconductor $\text{YBa}_2\text{Cu}_3\text{O}_x$ (YBCO) and half-metallic ferromagnet $\text{La}_{0.67}\text{Sr}_{0.33}\text{MnO}_3$ (LSMO) thin films and study of the SFS transport and magnetic properties. The SFS nanjunctions were prepared by Ga^{3+} focused ion beam from in situ deposited bilayer LSMO/YBCO.

P4-08**HIGH RESOLUTION X-RAY CHARACTERIZATION OF MANGANITE FILMS GROWN ON VARIOUS SUBSTRATES**M. Španková¹, V. Štrbík¹, E. Dobročka¹, Š. Chromík¹, N. Gál¹ and M. Sojková¹¹*Institute of Electrical Engineering, Dúbravská cesta 9, 84104 Bratislava, Slovakia*

Colossal magnetoresistance effect discovered in epitaxial manganite thin films led to an increasing interest in the use of the materials for industrial applications.

Epitaxial $\text{La}_{0.67}\text{Sr}_{0.33}\text{MnO}_3$ (LSMO) thin films with increased value of Curie temperature were prepared on single crystal (001) MgO , (001) SrTiO_3 , (001) LaAlO_3 , (001) $\text{La}_{0.26}\text{Sr}_{0.76}\text{Al}_{0.61}\text{Ta}_{0.37}\text{O}_3$ substrates using pulsed laser deposition technique.

We investigate microstructural properties of epitaxial LSMO films using high resolution X-ray diffraction. Linear “h” scans (rocking curves) in reciprocal space and mapping of reciprocal space in the h-k plane perpendicular to $l \equiv [001]$ direction were performed in order to characterize the stress relief mechanism arising from the misfit strain between the LSMO and the underlying substrates. From the series of the rocking curves across the LSMO 004 diffraction (performed around [001] substrate axis) we created 3D views. We registered different kinds of stress relief of the LSMO depending on the substrate used for the LSMO film preparation.

P4-09**LOW-TEMPERATURE PROPERTIES OF ONE-DIMENSIONAL MAGNETO-PHOTONIC CRYSTALS IN MAGNETIC FIELD**

Yu. Kharchenko¹, I. Lukienko¹, O. Miloslavskaya¹, M. F. Kharchenko¹,
A. V. Karavainikov², A. R. Prokopov² and A. N. Shaposhnikov²

¹*B. Verkin Institute LTPE of NASU, Prospekt Nauky 47, Kharkiv, 61103, Ukraine*

²*Taurida National V.I. Vernadsky University, Simferopol, Crimea, Ukraine*

We have studied the temperature properties of optical transmission and Faraday rotation (FR) the microcavity one-dimension magneto-photonic crystals (1D-MPC) and single magneto-optical (MO) layers of the same composition. We investigated the microcavity MPC of the similar compositions:

GGG/(TiO₂/SiO₂)₄/(**M1/M2**)/(SiO₂/TiO₂)₄,

GGG/(TiO₂/SiO₂)₄/(**M1/M3**)/(SiO₂/TiO₂)₄ and

GGG/(TiO₂/SiO₂)₄/(**2M1**)/(SiO₂/TiO₂)₄.

Here GGG is the substrate of (111) gadolinium-gallium garnet Gd₃Ga₅O₁₂, and the main MO layers are $\frac{1}{4}\lambda_R$ – **M1**: Bi_{1.0}Y_{0.5}Gd_{1.5}Fe_{4.2}Al_{0.8}O₁₂, $\frac{3}{4}\lambda_R$ – **M3**: Bi_{2.5}Gd_{0.5}Fe_{3.8}Al_{1.2}O₁₂ та $\frac{3}{4}\lambda_R$ – **M2**: Bi_{2.8}Y_{0.2}Fe₅O₁₂, where λ_R – the wavelength of light the resonance transmission peak in a bandgap of microcavity MPC. The optical thicknesses of TiO₂ and SiO₂ layers of the Bragg's mirrors were chosen as $\frac{1}{4}\lambda_R$. Microcavity MPC which consisted of MO layers (**2M1**) and (**M1/M3**) had a point of magnetic temperature compensation (T_{comp}).

The results showed high stability of the spectral position of the resonance peak of the microcavity MPC in the temperature range from 300K to 20K: changing the position of the resonance peak is not observed within the resolution monochromator (1 nm). The value of Faraday rotation (FR) of the 1D-MPC with the (**M1/M2**) MO layer monotonically depends on temperature. Dependence is non-monotonic character in the microcavity 1D-MPC, which consist of layers **2M1** and (**M1/M3**) — angle of FR changes its sign at ~ 135 K and ~ 30 K, respectively. In films **2M1** and **M3** sign change FR occurs at $T_{\text{comp}} \sim 139$ K and ~ 28 K [1].

Magnetic hysteresis loops of the samples had the form for the type of magnetic anisotropy they had — "easy axis" or "easy plane". Some features of the magnetic hysteresis loop near T_{comp} indicate the formation of a layer between the substrate and the MO layer, particularly for the film GGG/**2M1**. Faraday rotation at the resonant wavelength in microcavity 1D-MPC with layers (**M1/M3**) and (**2M1**) increased ~ 10 times compared to the Faraday rotation in films (**M1/M3**) and (**2M1**).

[1] A.N. Shaposhnikov et al., *Optical Materials* 52 p. 21–25(2016).

P4-10**MAGNETIC PROPERTIES OF NICKEL
HEXACYANOFERRATE/CHROMATE THIN FILMS**M. Fitta¹, T. Korzeniak², P. Czaja³ and M. Bałanda¹¹*Institute of Nuclear Physics Polish Academy of Sciences, Radzikowskiego 152,
31-342 Kraków, Poland*²*Faculty of Chemistry, Jagiellonian University, Ingardena 3, 30-060, Kraków,
Poland*³*Institute of Metallurgy and Materials Science Polish Academy of Sciences,
Reymonta 25, 30-059, Kraków, Poland*

Prussian blue analogues (PBAs) attract the great attention due to their rich palette of properties such as room temperature ferromagnetism or photomagnetism. Additional advantage of PBAs is possibility of their preparation as the low-dimensional assemblies, which can be considered as interesting materials for the fabrication of future molecule- based spintronic devices.

Herein, we present the investigation on the thin films composed of $\text{Ni}^{\text{II}}_{1.5}[\text{Fe}^{\text{III}}_x(\text{CN})_6][\text{Cr}^{\text{III}}_{1-x}(\text{CN})_6]$ ($x = 0, 0.5$ and 1) prepared by sequential adsorption techniques. Magnetic properties of presented films strongly depend on x value. The critical temperature increases with the decrease of x value and is equal to 21 K, 48 K and 68 K for $x = 1, 0.5$ and 0 respectively. Minimum value of coercive field is found for $x = 0$ and H_c increases with increase of Fe content reaching the value of 1.5 kOe for $x = 1$. For all samples the anisotropic magnetic response is observed.

The films were also characterized with infrared spectroscopy, scanning electron microscopy and atomic force microscopy.

This work was supported by the Polish National Science Centre within the frame of Project No. UMO-2011/03/D/ST5/05400.

P4-11**Ni₂FeSi HEUSLER MICROWIRES FOR SPINTRONIC APPLICATIONS**

L. Galdun^{1,2}, T. Ryba¹, V. M. Prida², B. Hernando², V. Zhukova³, A. Zhukov³,
Z. Vargová¹ and R. Varga¹

¹*Inst. Phys., Fac. Sci., UPJS, Park Angelinum 9, Kosice, Slovakia*

²*Dpto. De Física, Universidad de Oviedo, Calvo Sotelo s/n, 33007 Oviedo, Spain*

³*Dpto. Física de Materiales, Fac. Químicas, UPV/EHU, 20009 San Sebastian, Spain*

In recent years, a large class of magnetic X₂YZ compounds well known as Full Heusler alloys, have attracted great interest due to their features suitable for spintronic applications. It should be mentioned, that one of the biggest challenge is the fast and easy preparation of Heusler alloys from cheaper elements belonging to *d*-block (Fe, Co, Ni) and *p*-block (Al, Si), which causes a great benefit in order to replace expensive materials. Therefore, Taylor-Ulitovski technique is one of the rapid quenching methods, which offers fast and easy massive production of glass-covered microwires.

Theoretical calculations have shown that Ni₂Fe-based full-Heusler alloys have been predicted to exhibit spin polarization due to the asymmetry of the density of states (DOS) in the majority and minority spin channel at the Fermi energy level, which can be attributed to the hybridization of Ni and Fe *d* orbitals [1].

On behalf on this, we report on fabrication, structural and magnetic properties of novel Heusler-type glass coated Ni₂FeSi microwires that were prepared by Taylor-Ulitovsky method, having a metallic nucleus diameter about 3.9 μm and total sample diameter of 39 μm. This single step and low cost fabrication technique offers to prepare up to kilometres of glass-coated microwires starting from few grams of cheap elements for diverse applications. The XRD data from the metallic nucleus indicates L2₁ crystalline structure (*a* = 5.56(3) Å), with a possible DO₃ disorder. Magnetic measurements determined the different magnetic and anisotropic behaviour between the inner metallic core and its surface. Curie temperature well above the room temperature (770 K) together with uniform easy magnetization axis of the metallic core predisposes this material as a suitable candidate for spintronic applications.

This work has been financially supported by NanoCEXmat ITMS 26220120035, VEGA 1/0060/13, APVV-0027-11, VVGS-PF-2015-495 and Spanish MINECO research funds under project N° MAT2013-48054-C2-2-R.

[1] Y. Qawasmeh, B. Hamad, J. Appl. Phys., 111, 033905, (2012).

P4-12**SPIN WAVE CHARACTERISTICS OF INHOMOGENEOUS FERROMAGNETIC LAYERED COMPOSITES**A. Urbaniak-Kucharczyk¹¹*Faculty of Physics and Applied Informatics, University of Łódź, Pomorska 149/153, 90 236 Łódź, Poland*

Periodic composite magnetic materials have been increasing interest in the areas of magnetism and spintronic devices, due to their potential application to data-processing devices. Therefore it is important to know the properties of spin waves to minimize their disturbing influence or make use of them in logic devices. Theoretical and experimental approaches dedicated to periodic composite magnetic materials showed that in description of their properties it is necessary to take into account the anisotropic factors. In presented contribution a ferromagnetic layered composite (ABAB....ABA, where A and B are different ferromagnetic materials) is studied by means of Green function approach. In the system considered the spin wave resonance modes are induced entirely by exchange interactions and therefore they strongly depend of inhomogeneity of parameters characterizing magnetic materials.

Spin wave resonance spectra for composite system with spatial distribution of anisotropy across magnetic layers have been calculated. Temperature dependence of anisotropy parameters has been also taken into account. As a result the characteristics of spin wave spectrum have been obtained using the transfer matrix method for several magnetic systems deposited on substrate characterized by parameters corresponding to GaAs for the case of uniform anisotropy parameter and for quadratic distribution of this parameter in magnetic layers, respectively. The effects of damping due spin-spin interaction leading to non-zero line-width of ferromagnetic resonance peaks have been additionally taken into account. The influence of inhomogeneity of anisotropy distribution the spin wave patterns and the shape of resonance lines has been shown. Moreover, the temperature dependence of magnetization of a ferromagnetic layered composite have been calculated and the spin wave parameter B in the Bloch's law $T^{3/2}$ is has been found and presented in dependence of parameters characterizing composite magnetic system.

P4-13**MAGNETIC AND STRUCTURAL CHARACTERIZATION OF NiMnSb HEUSLER RIBBON**

T. Ryba^{1,2}, Z. Vargova³, S. Ilkovic⁴, M. Reiffers⁴, V. Haskova^{2,5}, P. Szabo⁵, J. Kravcak⁶, R. Gyepes⁷ and R. Varga^{1,2}

¹*RV Magnetics, a.s., Hodkovce 21, 044 21 Hodkovce, Slovakia*

²*Institute of Physics, Faculty of Sciences, P. J. Safarik University, Košice 04154, Slovakia*

³*Dept. Inorg. Chem., Fac. Sci., UPJS, Moyzesova 11, 041 54 Kosice, Slovakia*

⁴*Univ. of Presov, Fac. Hum. and Nat. Sci., SK-08078 Presov, Slovakia*

⁵*Institute of Experimental Physics, Slovak Academy of Sciences, Košice 04001, Slovakia*

⁶*Dept. Phys., FEEL, Technical University of Kosice, Kosice, Slovakia*

⁷*Dept. of Chemistry, Faculty of Education, J. Selye University, Komárno, Slovakia*

Heusler alloys, as a perspective material for applications, are characterized by many interesting properties for example: high spin polarization, magnetocaloric effect, shape memory effect and etc. Particularly, the applications in spintronics are significantly influenced by high value of magnetic moment, high spin polarization, high Curie temperature and small Gilbert damping. Heusler alloys, depending on the structure, are divided into two large groups such as full-Heusler alloys with composition X_2YZ and half-Heusler alloys with composition XYZ [1-2]. The typical example of half-Heusler alloys that exhibit high spin polarization is NiMnSb.

In the given contribution, we have studied structural and magnetic properties of NiMnSb half-Heusler ribbons produced by melt spinning. The SEM/EDX and powder X-ray characterizations were used to estimate their composition and structure determination ($C1_0$ – typical for half-Heusler alloy). Magnetic properties have been studied by VSM and spin polarization ($P = 22\%$) has been estimated by Andreev reflection (point contact method).

This research was supported by the projects APVV-0027-11 and Slovak VEGA grant. No. 1/0164/16.

[1] T. Graf, C. Felser, S.S.P. Parkin, *Prog. Solid State Chem.* 39 (2011), 1.

[2] A. Hirohata, M. Kikuchi, N. Tezuka, K. Inomata, J.S. Claydon, Y.B. Xu, G. van der Laan, *Curr. Opin. Sol. State Mat. Sci.* 10 (2006), 93.

P4-14**MAGNETIC PROPERTIES FE AND GD OXIDES EMBEDDED IN MESOPOROUS SILICA**O. Kapusta¹, A. Zelenáková¹, V. Girman¹, P. Hrubovčák¹ and V. Zeleňák²¹*Department of Solid State Physics, P.J. Šafárik University, Park Angelinum 9, 04154 Košice, Slovakia*²*Department of Inorganic Chemistry, P.J. Šafárik University, Moyzesova 11, 04001 Košice, Slovakia*

Currently, there is a need to develop drug delivery systems and monitoring methods. Magnetic resonance imaging (MRI) is a one of widely used diagnostic tool with excellent anatomical detail with or without the application of contrast agents such as iron and gadolinium oxides nanoparticles. Nanostructured materials have been shown to have some advantages over conventional MRI agents. Nanoscale dimensions of these materials have considerable impact on certain parameters like unique magnetic properties, ability to operate on cellular level and surface adaptability for bioagent attachment. One possible way how to prepare nanoparticles is synthesis through impregnation method, where porous matrix serves as a medium for magnetic nanoparticles growth. Nanoparticles size and particle's distribution size are controlled by matrix pores.

In our work, we prepared magnetic nanoparticles of Fe and Gd oxides close to spherical shape with size up to 7 nm inside a periodic porous silica matrix with hexagonal symmetry. Nanoparticles were prepared using wet-impregnation method a by nanocasting, where the mesoporous silica acts as a hard template for the growth of the nanoparticles. Solutions of $\text{Fe}(\text{NO}_3)_3$ and $\text{Gd}(\text{NO}_3)_3$ were used as metal oxides precursors.

The prepared samples structure was characterized by TEM (Transmission Electron microscopy), EDX measurement and magnetic measurements were provided by MPMS apparatus. Magnetic properties were characterized by two basic measurements: i) magnetization dependence on external magnetic field up to 5 T at constant temperature and ii) magnetization dependence on temperature in range of 2 – 300 K in two regimes – ZFC (zero field cooling) and FC (field cooling) at constant external dc magnetic field.

TEM confirmed hexagonal symmetry of porous matrix and nanoparticles size up to 7 nm. Both oxides presence were demonstrated by EDX measurement. Magnetic measurement confirmed superparamagnetic Fe_2O_3 nanoparticles inside porous matrix with blocking temperature about 50 K and coercivity about 2 400 Oe at 2 K and paramagnetic Gd_2O_3 nanoparticles with high magnetization about 90 emu/g at 50 000 Oe. Studied composites are suitable as negative (with Fe) and positive (with Gd) contrast agents for MRI, moreover they can be impregnated with drugs and be used as intelligent drug delivery systems.

*Acknowledgment**This work was realized within the project ITMS 26220120019.*

P4-15**SYSTEMATIC ANALYSIS OF ANISOTROPIC MAGNETORESISTANCE IN (Ga,Mn)As**K. Výborný¹¹*Fyzikální ústav AV ČR, v.v.i., Cukrovarnická 10, Praha 6, CZ-16253*

Contrary to most well-explored ferromagnets, the diluted magnetic semiconductor (Ga,Mn)As allows to tune various material parameters that strongly influence its transport and magnetic properties. Appreciable spin-orbit coupling in this material leads to a relatively large anisotropic magnetoresistance (AMR). I summarise available experimental data that have appeared in literature over last 15 years and compare them to the Boltzmann-equation based model relying on the GaAs host band structure exchange-split through the hybridisation of *p*-states and *d*-states located dominantly on As and Mn atoms, respectively. This model has been previously used as a basis for interpretation of AMR in individual measurements but a systematic survey on state-of-the-art samples has not been performed yet. It is found that the model can account for the measured AMR data but the residual resistivity is too low unless additional scattering is assumed. Components of the AMR (distinguished by symmetries) both on the side of experiments and the model are discussed.

P4-16**PHASE ANALYSIS OF MAGNETIC INCLUSIONS IN NANOMATERIALS BASED ON MULTIWALL CARBON NANOTUBES**

K. Brzózka¹, M. Krajewski², A. Małolepszy³, L. Stobiński^{3,4}, T. Szumiata¹, B. Górka¹, M. Gawroński¹ and D. Wasik²

¹*Department of Physics, Faculty of Mechanical Engineering, University of Technology and Humanities in Radom, Krasickiego 54, 26-600 Radom, Poland*

²*Faculty of Physics, Institute of Experimental Physics, University of Warsaw, Pasteura St.5, 02-093 Warsaw, Poland*

³*Faculty of Chemical and Process Engineering, Warsaw University of Technology, Waryńskiego St. 1, 00-645 Warsaw, Poland*

⁴*Institute of Physical Chemistry, Polish Academy of Sciences, Kasprzaka St. 44/52, 01-224 Warsaw, Poland*

Multiwall carbon nanotubes (MWCNTs), described as multiple rolled layers of graphene, have been intensively studied for last 25 years because of many purposes. The development of an innovative manufacturing process [1] has allowed a supplementary incorporation of magnetic components which makes their possible applications much wider.

Two kinds of nanomaterials based on multiwall carbon nanotubes are the subject of presented study: MWCNTs-COONH₄ as a reference sample and the same material covered by nanoparticles composed of iron oxides. They were produced by chemical vapor deposition using metallic iron as a catalyst and their subsequent chemical processing. Both nanomaterials exhibited weak and somewhat different magnetic properties [1]. Their XRD patterns showed, except for a component attributed to graphite which occurred in both cases, an evidence of presence of hematite in the latter material [1]. In order to identify all magnetic phases, transmission Mössbauer spectroscopy investigations based on ⁵⁷Fe were performed. The experiments were carried out both at room temperature and also at low temperatures. It was stated that in MWCNTs-COONH₄ the impurities were present, originating from catalyst remains, in form of Fe-C nanoparticles. The Mössbauer spectra collected for the nanocomposite composed of MWCNTs-COONH₄ covered with iron oxides showed a complex shape characteristic of temperature relaxation. The following subspectra related to iron-based phases were identified: sextet attributed to hematite, with hyperfine magnetic field reduced due to the temperature relaxations, sextet corresponding to iron carbide as well as two doublets linked to superparamagnetic hematite and ferrihydrites.

- [1] Krajewski M., Małolepszy A., Stobinski L., Lewińska S., Ślawska-Waniewska A., M. Tokarczyk M., Kowalski G., Borysiuk J., Wasik D.: *J. Supercond. Nov. Magn.* 28, 901-904 (2015).

P4-17**INFLUENCE OF Mn DOPING ON MAGNETIC AND STRUCTURAL PROPERTIES OF Co₂FeSi HEUSLER ALLOY**L. Galdun^{1,2}, T. Ryba¹, V. M. Prida², B. Hernando², Z. Vargová¹ and R. Varga¹¹*Inst. Phys., Fac. Sci., UPJS, Park Angelinum 9, Kosice, Slovakia*²*Dpto. De Física, Universidad de Oviedo, Calvo Sotelo s/n, 33007 Oviedo, Spain*

Half-metallic Full-Heusler alloys have been proposed as ideal candidates for spintronic devices due to the theoretical predictions to exhibit 100% spin polarization. This property is a result of a minority band gap in the density of states at Fermi level (E_F) [1]. Co₂-based Full-Heusler alloys have a special interest thanks to their large minority band gap, experimentally observed high spin polarization and high Curie temperature [2].

The electronic calculations have shown that E_F is close to the top of the valence band in the case of Co₂MnSi. On the other hand, E_F is near to the bottom of the conduction band in Co₂FeSi (however under condition of high ordered L2₁ crystalline phase) [3]. In order to find the correct composition (which would stabilize the half-metallic character against the temperature excitation and disorder effects), we have studied the possibilities of preparing the mixed quaternary compound.

Here, we report on results of study of structural and magnetic properties in ternary Co₂FeSi, quaternary Co₂Fe_{0.75}Mn_{0.25}Si and Co₂Mn_{0.5}Fe_{0.5}Si Full-Heusler alloys prepared by melt spinning technique. The rapid quenching method offers the advantage of easy preparation of large amount of Heusler alloys with correct L2₁ crystalline structure, essential for obtaining of the highest degree of spin polarization. Additionally, magnetic measurements reveal well-defined magnetic anisotropy which makes them suitable candidates for spintronic application.

This work has been financially supported by NanoCEXmat ITMS 26220120035, VEGA I/0060/13, APVV-0027-11, VVGS-PF-2015-495 and Spanish MINECO research funds under project N° MAT2013-48054-C2-2-R.

[1] X. Zhu, Y. Wang, et al., J. Phys. Chem. Solids., 75, 391 – 396, (2014).

[2] L. Bainsla, A. I. Mallick, et al, J. Magn. Magn. Mater, 394, 82-86, (2015).

[3] B. Balke, H. C. Kandpal, et al, J. Magn. Magn. Mater., 310, 1823-1825, (2007).

P4-18**EXCHANGE BIAS EFFECT IN NdFeO₃ SYSTEM OF NANO PARTICLES**

M. Vavra^{1,2}, M. Zentková¹, M. Mihalik¹, M. Mihalik jr.¹, J. Lazúrová¹, V. Girman², M. Perovic³, V. Kusigerski³, P. Roupčová⁴ and Z. Jagličić⁵

¹*Institute of Experimental Physics SAS, Watsonova 47, Košice, Slovak Republic*

²*P.J. Šafárik University, Faculty of Science, Košice, Slovak Republic*

³*The Vinca Institute, University of Belgrade, 11001 Belgrade, Serbia*

⁴*Institute of Physics of Materials, ASCR, Žitkova 22, Brno, Czech Republic*

⁵*IMPM & FGG, Jadranska 19, 1000 Ljubljana, Slovenia*

In our paper we study the effect of nano-metric size on the crystal structure, magnetic environment of iron and magnetization in NdFeO₃ system of nano particles (NAP). The physical and structural properties of NdFeO₃ are widely studied and they attract large attention due to interesting magnetic properties such as spin-reorientation phase transition [1]. Magnetic properties of NdFeO₃ are mostly determined by Fe-Fe, Fe-Nd and Nd-Nd exchange interactions. Magnetic ordering of Fe³⁺ ions creates a canted antiferromagnetic ordering of G-type below the Néel temperature at about $T_{N1} = 690$ K and the magnetic moments of Fe³⁺ exhibit spin reorientation from G_x type to combination of G_x and G_z type in the region from 100 K to 200 K. The moments of Nd were found to undergo a collective C-type antiferromagnetic ordering at $T_{N2} = 1.5$ K [2].

The average particle size of NdFeO₃ nanoparticles increases with annealing at 600°C from about 15 nm to 25 nm. The presence of superparamagnetic particles was indicated by Mössbauer measurements in this system of NAP. The reduction of dimensionality induces a decrease of T_{N1} from 691 K to 544 K. The shift of magnetic hysteresis loop in vertical and horizontal direction was observed at low temperatures after cooling in magnetic field. Such behaviour we attribute to exchange bias effect and discuss in the frame of core – shell model.

This work was supported by the project ERDF EU under the contract No. ITMS26220120005.

- [1] T Sławiński W, Przeniosło R, Sosnowska I and Suard E 2005 *Journal of Physics* (Condens. Matter 17) 4605–4614.
- [2] Bartolomé J, Palacios E, Kuźmin M D and Bartolomé F 1997 *Physical Review B* 55 11432.

P4-19**SUPERSPIN GLASS STATE IN MAGNETIC NANOPARTICLES**A. Zelenáková¹, P. Hrubovčák¹ and V. Zelenák²¹*Department of Condensed Matter Physics, University of P.J. Šafárik, Park Angelinum 9, 040 01 Košice, Slovakia*²*Department of Inorganic Chemistry, University of P.J. Šafárik, Moyzesova 11, 040 01 Košice, Slovakia*

Over the past few decades, magnetic nanoparticles (MNPs) have attracted a significant amount of research interest because of their applications in medicine (cancer diagnostics, drug delivery, magnetic hyperthermia) or environmental science posed new trends and challenges in these fields for the incoming 21st century. In addition, fine MNPs are model materials for fundamental investigations of a variety of magnetic phenomena, such as superparamagnetic (SPM) relaxation, spin canting, and superspin glass (SSG) state. The SSG behavior is typically manifested in strongly interacting and dense nanoparticle systems showing spin-glass (SG) properties. The evidence of SSG transition in MNPs is strengthened by standard spin-glass fingerprints, namely the critical slowing down of the relaxation and the divergence of the nonlinear susceptibility at a finite glass transition temperature T_g .

In this contributions, fine nanoparticles based on Fe and Co, coated by diamagnetic shell, were prepared by methods of nanocasting or microemulsions, controlling the particles size. A suite of experimental probes were used to establish the structural and magnetic properties of the prepared nanoparticle systems. We discuss the structural parameters of different nanoparticles in correlations to attributes of superspin glass magnetic state (SSG) reflected on various features (narrow ac susceptibility vs. temperature maximum, saturated FC magnetization at low temperatures, shift of the Cole-Cole arc downwards) and calculated parameters (relaxation time, critical exponent $z\nu \sim 10$ and frequency dependent criterion $p < 0.05$). Our study can opens up the possibility of tailoring the SSG state and its onset temperature by suitable choosing of the particle size, morphology and can bring the new look for the application of MNPs mainly in biomedicine.

Acknowledgment

This work was supported by the Slovak Research and Development Agency under contract No. APVV-0073-14 and project ITMS 26220120019.

P4-20**THE INVESTIGATION OF SPIN-SEEBECK EFFECT IN Ni_xFe_y ALLOYS**Ł. Bernacki¹, R. Gozdur¹ and W. Pawlak²¹*Department of Semiconductor and Optoelectronics Devices,**Lodz University of Technology, Stefanowskiego St. 18/22, 90-924 Lodz, Poland*²*Institute of Materials Science and Engineering, Lodz University of Technology, Stefanowskiego St. 1/15, 90-924 Lodz, Poland*

Thermoelectric effects in magnetic nanostructures and the so-called spin caloritronics have been generating great interests due to potentially higher efficiency of thermoelectric conversion. Spin caloritronics devices allow one to control spin, charge, and heat currents in magnetic/non-magnetic bilayers. It provides new strategies for the thermoelectric power generation that have not been fully explored yet. The spin-Seebeck effect (SSE) generates a non-equilibrium spin currents driven by spin thermoelectric voltage. This effect is strongly measurable in chosen ferromagnetic materials in presence of a temperature gradient and saturation of magnetization.

The paper presents an experimental study of the spin-Seebeck effect (SSE) in a ferromagnetic NiFe/Pt layers based on spin wave excitation in magnetically ordered ferromagnets. This approach was primarily proposed by Uchida K. et al [1,2,3].

The present work focuses on the investigation of the strong SSE in the widely used Ni_xFe_y layers partially covered with Pt layer. The measurements were carried out at room temperature for the $\text{Ni}_x\text{Fe}_y/\text{Pt}$ layers with a different content of nickel. The authors also report the method of SSE excitation and the measurement setup. The results prove that the spin-Seebeck effect leads to the reasonable values of thermoelectric voltage induced in a temperature from 20 to 50 degrees.

- [1] K. Uchida, T. Ota, K. Harii, S. Takahashi, S. Maekawa, Y. Fujikawa, and E. Saitoh, "Spin-Seebeck effects in films NiFe/Pt," *Solid State Commun.*, vol. 150, no. 11–12, pp. 524–528, Mar. 2010.
- [2] Uchida, K. et al. Long-range spin Seebeck effect and acoustic spin pumping. *Nature Mater.* 10, 737–741 (2011).
- [3] Uchida, K., Nonaka, T, Ota, T. & Saitoh, E. Observation of longitudinal spin-Seebeck effect in magnetic insulators. *Appl. Phys. Lett.* 97, 172505 (2010).

P4-21**EFFECT OF THE JAHN TELLER DISTORTION ON DOUBLE EXCHANGE INTERACTION IN $\text{La}_{1-x}\text{K}_x\text{MnO}_3$ NANO PARTICLES**

M. Mihalik¹, M. Zentková¹, M. Vavra^{1,2}, M. Mihalik Jr.¹, J. Lazúrová¹, V. Girman², M Fitta³ and S. Il'kovič⁴

¹*Institute of Experimental Physics SAS, Watsonova 47, Košice, Slovak Republic*

²*P. J. Šafárik University, Faculty of Science, Košice, Slovak Republic*

³*Institute of Nuclear Physics, Polish Academy of Sciences, Radzikowskiego 152, Kraków, Poland*

⁴*Faculty of Humanities and Natural Sciences, University of Prešov, 17 novembra 1, Slovak Republic*

Group of $\text{La}_{1-x}\text{K}_x\text{MnO}_3$ manganites provides a series of new oxides to study magnetocaloric effect [1, 2] and insulator-to-metal transition [3] at room temperature. In this work we study effect of Jahn-Teller (JT) distortion on double exchange interaction in this system. It was shown theoretically that the JT coupling drastically reduces the Anderson–Hasegawa double exchange (DE) [4] and our work probes the extent of this theoretical result on the $\text{La}_{1-x}\text{K}_x\text{MnO}_3$ nano powder system experimentally.

$\text{La}_{0.8}\text{K}_{0.2}\text{MnO}_3$ nanoparticles have been prepared by glycine – nitrate method with very well developed crystal structure even in as prepared sample. Crystal structure and particles size were modified by heat treatment. As prepared nanoparticles and samples annealed at 300°C/2 hours adopt orthorhombic crystal structure (space group $Pnma$) and the average particles size is less than 50 nm. Heat treatment at 600 °C/2 hours and at 900 °C/2 increases the average size of nanoparticles from 60 nm to 135 nm, crystal structure changes to rhombohedral structure (space group $R\bar{3}c$). The annealing reduces JT distortions and increases T_c , θ and μ_s mainly due to the enhancement of ferromagnetic exchange interaction given by the DE interaction. In addition, the increase of DE interactions by reducing of JT distortions we probed by high pressure experiments and by measurements of electrical resistivity.

This work was supported by the project ERDF EU under the contract No. ITMS26220120005.

[1] A.M. Aliev et al., Physica B, 406, 885 (2011).

[2] I.K. Kamilov et al., Bull. Mater. Sci., 32, 443 (2009).

[3] S. B. Bošković et al., Ceram Int 33, 89 (2007).

[4] H. Meskine and S. Satpathy, J. Appl. Phys. 85, 4346 (1999).

P4-22**THE MAGNETIC EQUATION OF STATE AND TRANSPORT PROPERTIES IN REDUCED DIMENSIONS**K. Warda¹ and L. Wojtczak¹*¹Solid State Physics Department, University of Łódź, Pomorska 149/153, 90-236 Łódź, Poland*

In in our earlier paper we developed the equation of state for real gas and applied it to the description of the magnetic systems of the confined geometry such as thin films, nanoparticles and multilayers[1].

Based on the magnetic equation of state we developed the model of calculations of the electrical resistivity for the metallic trilayers and multilayers. The model of calculations is based on the Boltzmann equation for thin films.

It is usually consider that the conductivity in ferromagnetic (FM) materials is governed by s and p electrons. It was shown that in transport of charge in FM material important role play d electrons. The conductivity is determined mainly by the electrons at the Fermi level. In the spin conserving process the s electrons with spin up and spin down can be scattered to s and d band to spin up and down state respectively. The electrons from d band are exchange split and density of states (DOS) of electrons at the Fermi level is different for spin up and spin down.

The new expression for the magnetoresistance (MR) is obtained for trilayers and multilayers. The key parameters in the presented model are: the width of the electron energy band and the shift of the energy level for two spin orientations as well as the Fermi energy and size of the sample (the thickness of magnetic and nonmagnetic layers and the total number of layers). The obtained values of MR exhibit a strong dependence on the magnetization and the size of the considered system. The presented results of the calculations for the temperature dependence of MR are in agreement with the available experimental data.

[1] K. Warda, J. Phys.: Condens. Matter 21 (2009) 345301.

P4-23**THE ELECTRICAL RESISTIVITY OF METALLIC ALLOYS**K. Warda¹ and L. Wojtczak¹*¹Solid State Physics Department, University of Łódź, Pomorska 149/153, 90-236 Łódź, Poland*

We present the model of calculations for the electrical resistivity of the metallic alloys based on the Boltzmann equation for thin films [1,2]. The temperature, magnetic field dependence as well as the concentration dependence of the resistivity for the disordered alloys materials were undertaken lately [3]. We have developed a method for calculation of the electrical resistivity for binary alloys.

An introduced calculations show the important role of surface and the value of the Fermi energy in the considered system. These parameters for the binary system were taken into account in the calculation of electrical resistance.

The results of the calculations are in agreement with the available experimental data.

- [1] K. Warda, L. Wojtczak, D. Baldomir, M. Pereiro, and J. Arias phys. stat. sol. (c) 3, No. 1, (2006) 73–76.
- [2] K. Warda, Transport and magnetic properties in metallic systems of reduced dimensions, Habilitation thesis, Primum Verbum (2014) Łódź.
- [3] M. Ornat, A. Paja, Acta Phys. Pol. A 126 (2014) 1296.

P4-24**STRUCTURE OF MELT-SPUN Co₂MnAl HEUSLER ALLOY**S. Piovarči¹, P. Diko¹, V. Kavečanský¹, T. Ryba², Z. Vargová³ and R. Varga²¹*Institute of Experimental Physics, Slovak Academy of Sciences, Watsonova 47, 040 01 Kosice, Slovakia*²*Institute of Physics, UPJS Kosice, Park Angelinum 9, 040 01 Kosice, Slovakia*²*Institute of Chemistry, UPJS Kosice, Moyzesova 11, 040 01 Kosice, Slovakia*

The growth-related microstructure and texture of the Co₂MnAl type Heusler alloy in the form of a melt-spun ribbon was studied by electron microscopy, electron backscattered diffraction (EBSD) and X-ray diffraction. It is shown that melt spinning produces a single-phase disordered Heusler alloy. The fine grain structure at the wheel side of the ribbon exhibits no texture, while dominant columnar grain structure formed on the free surface side exhibits the <111> fibre texture with a declination by about 10 degrees in the spinning direction. The dendritic growth of columnar crystals cause inhomogeneity of the chemical composition on a micrometre scale with a higher Co and Al concentration in the centre of dendritic arms and a higher concentration of Mn at the dendrite arm boundaries.

Acknowledgment

This work was realized within the framework of the projects: Centre of Excellence of Advanced Materials with Nano- and Submicron Structure (ITMS 26220120019), Infrastructure Improving of Centre of Excellence of Advanced Materials with Nano- and Submicron - Structure (ITMS 26220120035), New Materials and Technologies for Energetics (ITMS 2 6220220061), Research and Development of Second Generation YBCO Bulk Superconductors (ITMS 26220220041), Nanokop (ITMS 26110230061) which are supported by the Operational Programme 'Research and Development' financed through the European Regional Development Fund, APVV No. 0330-I2, VEGA No. 2/0090/13, VVGS-2013-112, SAS Centre of Excellence: CFNT MVEP, VEGA No. 2/0121/16 and Stefanik Project SK-FR-2013-0025.

I5-01**THE ROUTE TO MAGNETIC ORDER IN THE KAGOME ANTIFERROMAGNET**J. Richter¹*¹Institute for Theoretical Physics, University Magdeburg, 39016 Magdeburg, Germany*

The kagome antiferromagnet (KAFM) is a celebrated and challenging model system in frustrated quantum magnetism. In my talk I will review our recent work on the ground state (GS) of the KAFM [1-3]. By using the coupled cluster method at high orders of approximation we calculate the GS energy and the GS magnetic order parameter (sublattice magnetization) of the so called $q=0$ and $q=\sqrt{3}\times\sqrt{3}$ states. In agreement with recent DMRG results we find that the GS of the isotropic Heisenberg AFM is magnetically disordered for spin $s=1/2$ and $s=1$. However, for $s>1$ we get $\sqrt{3}\times\sqrt{3}$ magnetic long order (LRO), where for $s=3/2$ the order parameter is only 7% of the classical value [1].

For the spin- s XXZ KAFM with easy-plane anisotropy magnetic GS LRO can be established also for $s=1$ [2]: Varying the easy-plane anisotropy parameter Δ between $\Delta=1$ (isotropic Heisenberg KAFM) and $\Delta=0$ (XY KAFM) we find that the ground state is disordered for $0.82<\Delta\leq 1$, it exhibits $\sqrt{3}\times\sqrt{3}$ magnetic LRO for $0.28<\Delta<0.82$, and $q=0$ magnetic LRO for $0\leq\Delta<0.28$. We confirm the recent unexpected result of [4] that the selection of the GS LRO by quantum fluctuations is different for small Δ (XY limit) and for Δ close to one (Heisenberg limit).

We also study the role of an interlayer coupling (ILC), unavoidably present in real 3D materials. [3] We consider a stacked $s=1/2$ KHAF with a perpendicular

ILC J_{ILC} . We find that the disordered GS persists until relatively large strengths of the ILC. Only at $J_{\text{ILC}}\sim 0.15$ the disordered phase gives way for $q=0$ magnetic LRO. At larger J_{ILC} the ILC drives a first-order transition to $\sqrt{3}\times\sqrt{3}$ LRO. Evidently, anisotropy, larger spin quantum numbers $s>1/2$, and particularly ILC have relevance for the experimental research on kagome compounds and lead to a rich GS phase diagram.

- [1] O. Götze, D.J.J. Farnell, R.F. Bishop, P.H.Y. Li, and J. Richter, Phys. Rev. B 84, 224428 (2011).
- [2] O. Götze and J. Richter, Phys. Rev. B 91, 104402 (2015).
- [3] O. Götze and J. Richter, arXiv:1510.04898.
- [4] A. L. Chernyshev, M. E. Zhitomirsky, Phys. Rev. Lett. 113, 237202 (2014).

I5-02**LONG-RANGE MAGNETIC ORDER IN A PURELY ORGANIC 2D LAYER ADSORBED ON EPITAXIAL GRAPHENE**A. L. Vázquez de Parga^{1,2}¹*Departamento Física de la Materia Condensada, Universidad Autónoma de Madrid, Cantoblanco 28049, Madrid, Spain*²*IMDEA-Nanociencia, Calle Faraday 9, Cantoblanco 28049, Madrid, Spain*

Graphene grown on Ru(0001) is spontaneously nanostructured forming an hexagonal array of 100 pm high nanodomes with a periodicity of 3 nm and localized electronic states [1]. Cryogenic Scanning Tunnelling Microscopy (STM) and Spectroscopy and Density Functional Theory simulations show that isolated TCNQ molecules deposited on gr/Ru(0001) acquire charge from the substrate and develop a sizeable magnetic moment, which is revealed by a prominent Kondo resonance [2]. The magnetic moment is preserved upon dimer and monolayer formation. The self-assembled molecular monolayer develops spatially extended spin-split electronic bands with only the majority band filled, thus becoming a 2D organic magnet whose predicted spin alignment in the ground state is visualized by spin-polarized STM at 4.6 K [3].

The long range magnetic order is originated by the charge transfer from graphene to TCNQ (which creates the magnetic moments) plus the self-assembly of the molecular adlayer on the periodically corrugated graphene layer (which creates spin-polarized intermolecular bands where the added electrons delocalize). Examples will be shown where the adsorbed molecules accept charge and develop magnetic moments, but do not form bands and, accordingly, no long-range order appear (F4-TCNQ on graphene/Ru(0001))[4], or where molecules do form similar bands, but they are not populated because there is no charge transfer to the molecules (TCNQ on gr/Ir(111)). No long range magnetic order develops in these cases.

[1] A.L. Vázquez de Parga et al. Phys. Rev. Lett. 100, 056807 (2008).

[2] M. Garnica et al. Nano Lett. 14, 4560 (2014).

[3] M. Garnica et al. Nature Physics 9, 368 (2013).

[4] M. Garnica et al. Surf. Sci. 630, 356 (2014).

O5-01**UNUSUAL MAGNETIC-PRESSURE RESPONSE OF AN $S = 1$ QUASI-ONE-DIMENSIONAL ANTIFERROMAGNET NEAR $D/J \sim 1$**

M. K. Peprah¹, P. A. Quintero¹, A. Garcia², J. M. Pérez^{1,3}, J. S. Xia¹,
J. M. Manson⁴, S.E. Brown¹ and M.W. Meisel¹

¹*Dept. of Physics and NHMFL, Univ. of Florida, Gainesville, FL 32611, USA*

²*Dept. of Physics and Astro., Univ. of California, Los Angeles, CA 90095, USA*

³*Dept. of Physics, Univ. of Puerto Rico, Mayagüez, Puerto Rico 00681, USA*

⁴*Dept. of Chemistry and Biochemistry, Eastern Washington Univ., Cheney, WA 99004, USA*

An antiferromagnetic $S = 1$, quasi-one-dimensional chain, $[\text{Ni}(\text{HF}_2)(3\text{-Clpy})_4]\text{BF}_4$ (py = pyridine), has been identified to have nearest-neighbor antiferromagnetic interaction $J/k_B = 4.86$ K and single-ion anisotropy (zero-field splitting) $D/k_B = 4.3$ K, while avoiding long-range order down to 25 mK [1]. With $D/J = 0.88$, this system is close to the $D/J \sim 1$ gapless quantum critical point between the Haldane and Large- D phases [2]. The magnetization was studied over a range of temperatures, $50 \text{ mK} \leq T \leq 1 \text{ K}$, and magnetic fields, $B \leq 10 \text{ T}$ [3]. Strikingly, the magnetic response was relatively independent of temperature for $50 \text{ mK} \leq T \leq 1 \text{ K}$, and this observation is consistent with a significant increase of the specific heat arising from the accumulation of entropy in the vicinity of the quantum critical point.

Using a commercial magnetometer equipped with home-made pressure cells, the low-field (0.1 T), high-temperature ($T \geq 2 \text{ K}$) magnetic susceptibility was studied as function of pressure up to 1.47 GPa. These data suggest the response at ambient pressure [1] changes between 0.24 GPa and 0.35 GPa, and the unusually strong Curie-like response intensifies. Ergo, the pressure may tune the material through the critical point or a structural transition. These studies are being extended by ^1H NMR experiments capable of varying the pressure and of spanning from 300 K to below 100 mK.

Supported by the NSF via DMR-1202033 (MWM), DMR-1410343 (SEB), DMR-1306158 (JLM), DMR-1461019 (UF Physics REU support for JMP), DMR-1157490 (NHMFL), and by the State of Florida.

- [1] J.L. Manson, A.G. Baldwin, B.L. Scott, J. Bendix, R.E. Del Sesto, P.A. Goddard, Y. Kohama, H.E. Tran, S. Ghannadzadeh, J. Singleton, T. Lancaster, J.S. Möller, S.J. Blundell, F.L. Pratt, V.S. Zapf, J. Kang, C. Lee, M.-H. Whangbo, C. Baines, *Inorg. Chem.* **51** (2012) 7520.
- [2] A. F. Albuquerque, C. J. Hamer, J. Oitmaa, *Phys. Rev. B* **79** (2009) 054412.
- [3] J.-S. Xia, A. Ozarowski, P. M. Spurgeon, A. G. Balswin, J. L. Manson, M. W. Meisel, *arxiv.1409.5971* (2014).

O5-02**DOUBLE MAGNETIC RELAXATION AND MAGNETOCALORIC EFFECT IN TWO CLUSTER-BASED MATERIALS $\text{Mn}_9[\text{W}(\text{CN})_6]\text{-L}$**

P. Konieczny¹, R. Pełka¹, W. Nogaś², S. Choraży², M. Kubicki³, R. Podgajny², B. Sieklucka² and T. Wasiutyński¹

¹*Department of Magnetic Research, Institute of Nuclear Physics PAN, Radzikowskiego 152, 31-342 Kraków, Poland*

²*Faculty of Chemistry, Jagiellonian University, Ingardena 3, 30-060 Krakow, Poland*

³*Faculty of Chemistry, Adam Mickiewicz University, Umultowska 89B, 61-614 Poznań, Poland*

Two similar three dimensional molecular based materials were investigated to study the influence of supramolecular anisotropy on their magnetic properties. Both of them are based on pentadecanuclear cyano-bridged high spin $\{\text{M}^{\text{II}}_9\text{W}^{\text{V}}_6(\text{CN})_{48}(\text{solv})_x\}$ clusters which were organized in different manner into compound **1**: $\{\text{Mn}_9[\text{W}(\text{CN})_8]_6(\text{ald-4})_4(\text{MeOH})_{24}\}$ (ald-4= aldrithiol-4) and **2**: $\{\text{Mn}_9[\text{W}(\text{CN})_8]_6(\text{ditbubpy})_8(\text{MeOH})_6(\text{H}_2\text{O})_3(\text{iPr}_2\text{O})_2\}$ (ditbubpy=4,4'-di-tert-butyl-2,2'-bipyridine). The main difference between this compounds are the intercluster distances and overall spatial distribution of building block clusters. No substantial differences between **1** and **2** were observed in typical static magnetic measurements. The exception is the study of magnetocaloric effect where noticeable difference were observed in the low temperature regime. The dissimilarity came out in ac susceptibility measurements, which reveal field induced slow magnetic relaxations. In both compounds there are two relaxation processes, one temperature dependent and the second one which is temperature independent. The temperature dependent relaxations times were used to determine the energy barriers Δ , which $\Delta_1 = 38(4)$ K for **1** and $\Delta_2 = 9(1)$ K for **2**.

O5-03**AC MAGNETIC SUSCEPTIBILITY OF FERROFLUIDS EXPOSED TO AN EXTERNAL ELECTRIC FIELD**M. Rajňák¹, B. Dolník², J. Kováč¹, J. Kurimský², R. Cimbala², K. Paulovičová¹, P. Kopčanský¹ and M. Timko¹¹*Institute of Experimental Physics, Slovak Academy of Sciences, Watsonova 47, 040 01, Košice, Slovakia*²*Faculty of Electrical Engineering and Informatics, Technical University of Košice, Letná 9, 04200 Košice, Slovakia*

Ferrofluids exhibit peculiar dielectric properties when exposed to external magnetic fields. Among the well known magneto-dielectric phenomena, the effect of magneto-dielectric anisotropy has drawn much attention of the ferrofluid research. This effect originates in interactions of magnetic nanoparticles with a magnetic field, forming thus elongated clusters along the field. The total ferrofluid permittivity then can be considerably increased or decreased, depending on the orientation of the magnetic field in regard to a measuring electric field. Here we report on the contrary effect when a magnetic susceptibility is controllable by an electric field. The presented work has connection with our latest structural investigation of a weakly polar ferrofluid in various conditions of electric fields. It has been found that a DC electric field gives rise to forces acting on the magnetite nanoparticles, leading to the formation of aggregates. At this condition we have measured the ferrofluid AC magnetic susceptibility in parallel and perpendicular configuration of magnetic and electric fields at room temperature. The measurements in both configurations yielded a noticeable decrease of the real susceptibility values with increasing electric field strength. The effect is believed to be caused by the confinement of the formed aggregates by the electric polarization forces, reducing so the Brownian relaxation range. Finally, we highlight the necessity of nuclear magnetic resonance and neutron scattering investigations in order to obtain exact information on the magnetic structure induced by the electric forces.

This work was supported by Slovak Academy of Sciences and Ministry of Education: VEGA 2/0045/13, 1/0311/15, 2/0141/16, and Ministry of Education Agency for structural funds of EU, Project No. 26110230061, 26220120046, 26220120003, 26220120055 and 26220220182.

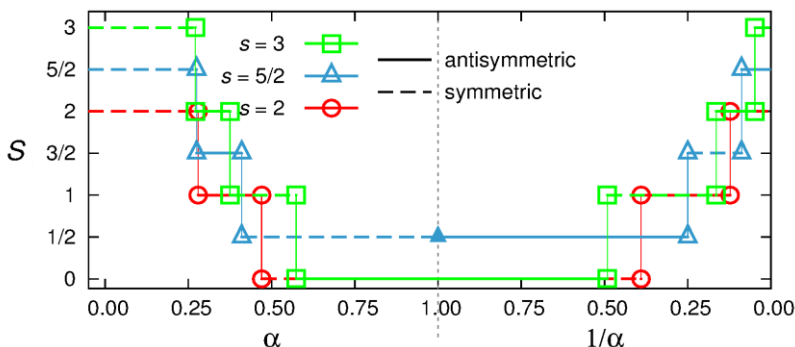
O5-04

UNIVERSAL SEQUENCE OF GROUND STATES IN ANTIFERROMAGNETIC FRUSTRATED RINGS WITH A SINGLE BOND DEFECT

M. Antkowiak¹, G. Kamieniarz¹ and W. Florek¹

Faculty of Physics, A. Mickiewicz University, Umultowska 85, 61-614 Poznań, Poland

We have established the universal sequence of the ground states for antiferromagnetic frustrated rings with the odd number of the local spins s and a single bond defect α described by the isotropic Heisenberg Hamiltonian [1]. The sequence is characterized by the total spin $S \leq s$ and contains all the spin numbers belonging to the interval allowed. It validates the classification of frustration in this type of nanomagnets and is illustrated in the diagram



for $s = 2, 5/2, 3$. The symmetry of the ground states with respect to reflection is also indicated.

For $S' \geq S$, the Lieb-Mattis level ordering [1] $E(S'+1) > E(S')$ is valid, where $E(S')$ is the lowest energy of the states described by the quantum number S' . Our calculations, pointing out the role of bipartiteness [1], have revealed the unexpected features of the model in question: the rings with enlarged nonbipartite structure inherit the Lieb-Mattis theorem consequences of their bipartite archetypes.

[1] G. Kamieniarz, W. Florek, M. Antkowiak, Phys. Rev. B 92 (2015) 140411(R).

P5-01**MAGNETIC-FIELD INDUCED SLOW RELAXATION IN THE ISING-LIKE QUASI-ONE-DIMENSIONAL FERROMAGNET $\text{Ker}(\text{MoO}_4)_2$** V. Tkáč¹, A. Orendáčová¹, L. Dlháň², M. Orendáč¹, R. Boča² and A. Feher¹¹*Centre of Low temperature physics of SAS and P. J. Šafárik University, Park Angelinum 9, 04001 Košice, Slovak Republic*²*Institute of Inorganic Chemistry, Technology and Materials, Faculty of Chemical and Food Technology, Slovak University of Technology, Radlinského 9, 812 37 Bratislava, Slovak Republic*

$\text{Ker}(\text{MoO}_4)_2$ is characterized by a layered crystal structure and a strong magnetic anisotropy. Previous specific heat studies identified a magnetic subsystem of $\text{Ker}(\text{MoO}_4)_2$ as a quasi-two-dimensional array of ferromagnetic Ising chains with an effective spin $\frac{1}{2}$ with an intrachain ferromagnetic interaction, $J_1/k_B \approx 0.9$ K, and interchain antiferromagnetic coupling, $J_2 \approx 0.2 J_1$. A phase transition to the magnetically ordered state has been observed at $T_c = 0.95$ K in zero magnetic field. Using AC susceptibility, spin dynamics of the system has been studied previously in a magnetic field applied along the easy axis a at liquid helium temperatures. Magnetic field dependence of ac susceptibility studied at 2 K indicated intensive slow magnetic relaxation in the field in the range 0.1 -0.5 T, while higher fields suppressed the relaxation [1].

In the current work we present the study of spin dynamics in the field applied along the hard axis c . The temperature dependence of AC susceptibility in zero magnetic field studied at frequencies $f=10, 100$ and 1000 Hz indicated the absence of relaxation at least in the studied temperature range from 2 to 10 K. On the other hand, application of magnetic field revealed the presence of a slow magnetic relaxation, which was studied in detail in the field 0.5 T by measuring a frequency dependence of in phase and out of phase components of AC susceptibility at constant temperatures. The strongest relaxation was observed at 2 K. With increasing temperature, the relaxation process is weaker and vanishes completely above 3.5 K. Corresponding Cole-Cole diagrams were constructed and analysed within a single relaxation process which can be associated with a direct relaxation process with a bottleneck effect, $\tau \approx 1/T^b$, characterized by $b = 1.4$. Unlike temperature, magnetic field has an opposite effect; the slow relaxation at 2 K intensifies with increasing magnetic field at least up to 1 T.

This work was supported by the projects APVV LPP-0202-09, VEGA 1/0143/13, ITMS26220120005 and APVV-14-0073.

[1] V. Tkáč, A. Orendáčová, R. Tarasenko, D.M. Pajerowski, E. Čížmár, M. Orendáč, A.G. Anders, M.W. Meisel and A. Feher, *Acta Physica Polonica* 127 (2015) 353.

P5-02

INFLUENCE OF PRESSURE ON THE MAGNETIC RESPONSE OF THE LOW-DIMENSIONAL QUANTUM MAGNET $\text{Cu}(\text{H}_2\text{O})_2(\text{C}_2\text{H}_8\text{N}_2)\text{SO}_4$

M. K. Peprah¹, D. VanGennep¹, B. D. Blasiola¹, P. A. Quintero¹, R. Tarasenko², J. J. Hamlin¹, M. W. Meisel¹ and A. Orendáčová²

¹*Department of Physics and National High Magnetic Field Laboratory, University of Florida, Gainesville, FL 32611-8440, USA*

²*Institute of Physics, Faculty of Science, P. J. Šafárik University, Košice, Slovak Republic*

One approach to new materials discovery involves enhanced interactive collaborations between experimental and theoretical research teams. For example, experimental studies identified $\text{Cu}(\text{H}_2\text{O})_2(\text{C}_2\text{H}_8\text{N}_2)\text{SO}_4$ as a quasi-two-dimensional $S = 1/2$ spatially-anisotropic triangular-lattice antiferromagnet [1,2]. On the other hand, a theoretical *ab-initio* investigation of the exchange interactions between Cu ions indicate the system is a quasi-one dimensional magnet [3]. These numerical studies were extended to pressures up to 8.2 GPa, thereby allowing the pressure dependence of the calculated exchange interactions to be predicted [4].

The purpose of the present investigation was to study the magnetic response of a single crystal sample of $\text{Cu}(\text{H}_2\text{O})_2(\text{C}_2\text{H}_8\text{N}_2)\text{SO}_4$ to high pressures and to compare the results with the theoretical predictions. Using two different pressure cells, magnetization measurements were performed between 2 K and 10 K with pressures ranging from ambient to 5.0 GPa. The data suggest a possible shift in the magnetization peak of the material at the lowest temperatures and at the highest applied pressures.

This work was supported, in part, by the NSF via DMR-1202033 (MWM), DMR-1461019 (UF Physics REU Program), DMR-1157490 (NHMFL), the State of Florida, and CFNT MVEP—Centre of Excellence of the Slovak Academy of Sciences, SAS and the projects APVV LPP-0202-09 and VEGA 1/0143/13. Instrumentation used with the diamond anvil pressure cell was made possible by the NHMFL User Collaboration Grants Program (JJH).

- [1] M. Kajňáková, M. Orendáč, A. Orendáčová, A. Vlček, J. Černák, O. V. Kravchyna, A. G. Anders, M. Bałanda, J.-H. Park, A. Feher, and M. W. Meisel, Phys. Rev. B 71, 014435 (2005).
- [2] R. Tarasenko, A. Orendáčová, E. Čížmár, S. Matáš, M. Orendáč, I. Potočný, K. Siemensmeyer, S. Zvyagin, J. Wosnitza, and A. Feher, Phys. Rev. B 87, 174401 (2013).
- [3] R. Sýkora, D. Legut, and U.D. Wdowik, Acta Phys. Pol. A 126, 50 (2014).
- [4] R. Sýkora and D. Legut, J. Appl. Phys. 115, 17B305 (2014).

P5-03**EXPERIMENTAL STUDY OF THE MAGNETOCALORIC EFFECT IN $\text{Ni(en)(H}_2\text{O)}_4\text{SO}_4 \cdot 2\text{H}_2\text{O}$ - an $S = 1$ MOLECULAR MAGNET WITH EASY-PLANE ANISOTROPY**

R. Tarasenko¹, A. Orendáčová¹, E. Čížmár¹, M. Orendáč¹, I. Potočník² and A. Feher¹

¹*Centre of Low Temperature Physics of P.J. Šafárik University and SAS, Park Angelinum 9, 041 54 Košice, Slovak Republic*

²*Institute of Chemistry, Department of Inorganic Chemistry, Faculty of Science, P.J. Šafárik University, Moyzesova 11, 041 54 Košice, Slovak Republic*

The title compound $\text{Ni(en)(H}_2\text{O)}_4\text{SO}_4 \cdot 2\text{H}_2\text{O}$ (NEHS) (en = ethylenediamine = $\text{C}_2\text{H}_4\text{N}_2$) crystallizes in the monoclinic structure, $C 2/c$ space group. The crystal structure of the compound is build of $[\text{Ni(en)(H}_2\text{O)}_4]^{2+}$ cations, $[\text{SO}_4]^{2-}$ anions and two water molecules comprising basic structural units. The units are mutually connected by a large number of hydrogen bonds forming a three-dimensional crystal structure. NEHS has been previously identified as a spin 1 single-molecule magnet with a nonmagnetic ground state introduced by easy-plane single-ion anisotropy $D/k_B = 11.6$ K and neglecting in-plane anisotropy $E/D = 0.1$. The good agreement between the experimental value of magnetic entropy and the theoretical entropy for spin 1 indicates the absence of a phase transition to the ordered state below 1.8 K and the crystal field effects play a dominant role for magnetic properties [1]. Consequently, in the first approximation, the magnetocaloric effect in NEHS has been theoretically calculated within a simple model of a spin 1 paramagnet with energy levels split by a crystal field described by D and E parameters. Maximal magnetocaloric effect was found near saturated value of magnetic field as an uniform property for these systems. Magnetocaloric studies have been performed on powder sample NEHS in the temperature range from 1.8 K to 30 K in magnetic fields up to 7 T using isothermal magnetization curves measured in a commercial Quantum Design SQUID magnetometer. Large conventional magnetocaloric effect was found around 6.3 K ($-\Delta S_{\text{max}} = 8.2$ J/kg K for 7 T). Temperature dependence of the isothermal entropy change under different magnetic fields is in good agreement with theoretical predictions from crystal electric field parameters.

This work was supported by the projects APPV-14-0073, APVV LPP-0202-09 and ERDF EU project No. ITMS 26220120005

- [1] R. Tarasenko, A. Orendáčová, K. Tibenská, I. Potočník, M. Kajňáková, A. Vlček, M. Orendáč, A. Feher, *Acta Physica Polonica A* 113, (2008) 481.

P5-04**GENERATION OF Fe_3O_4 NANOPARTICLE AGGREGATES IN A FERROFLUID DRIVEN BY EXTERNAL ELECTRIC FIELD**

J. Kurimský¹, M. Rajňák², R. Cimbala¹, K. Paulovičová², M. Timko²,
P. Kopčanský², M. Kostelec¹, L. Kruželák¹ and M. Kolcun¹

¹*Department Electrical Power Engineering, Technical University of Košice,
Mäsiarska 74, 040 01 Košice, Slovakia*

²*Institute of Experimental Physics SAS, Watsonova 47, 040 01 Košice, Slovakia*

In the paper the experimental study of magnetic nanoparticle aggregation in a transformer oil based ferrofluid driven by external electric field is reported. The studied ferrofluid was composed of the magnetite nanoparticles, oleic acid surfactant and transformer oil carrier fluid.

Generally, it is considered that superparamagnetic nanoparticles do not interact in the absence of external magnetic field. In the paper we present an experimental observation of the particle interactions in a direct current external electric field by optical microscopy. During the observation no external magnetic field was applied. A diluted low-polarity ferrofluid drop on a glass surface was exposed to external static inhomogeneous electric field. This brought up a flow in the fluid after a certain time period. In a further time span, the nanoparticles assembled into apparent thin chains acting as charge traps activated by external electric field.

The space charge accumulation followed by a sudden discharge process is considered to be a consequence of the observable anisotropic particle aggregation caused by electrical field with the intensity over a certain threshold. This is repeated continually and forces accompanying these phenomena contribute to the drop's shape modification.

The study confirms that the interactions of magnetic nanoparticles can be controlled externally by an electric field in the dielectrically featured ferrofluid.

P5-05**ULTRASOUND FREQUENCY ANALYSIS OF A MAGNETIC FLUID IN LOW-INTENSITY EXTERNAL MAGNETIC FIELD**

J. Kurimský¹, M. Rajňák², R. Cimbala¹, B. Dolník¹, J. Tóthová¹, K. Paulovičová², M. Timko², P. Kopčanský², J. Petráš¹, I. Kolcunová¹, J. Džmura¹ and J. Balogh¹

¹*Department Electrical Power Engineering, Technical University of Košice, Mäsiarska 74, 040 01 Košice, Slovakia*

²*Institute of Experimental Physics SAS, Watsonova 47, 040 01 Košice, Slovakia*

This work deals with an interaction of a magnetic fluid (MF) of a dielectric nature with magnetic field by means of ultrasound waves measurements and analysis. Ultrasound is known as a non-destructive inspection tool often used in technical diagnostics, moreover, it has numerous applications in medicine and biology, too. We report the low-frequency ultrasound analysis of a dielectric MF in low-intensity external static magnetic field.

The studied MF was composed of a transformer oil and dispersed magnetite nanoparticles coated with oleic acid. Experiments were conducted using an ultrasonic testing cell. The cell was exposed to a magnetic field of 50 mT in both parallel and perpendicular direction to the waves propagation. A through-transmission mode measurement was used, where two fixed narrow-band transducers with completely shielded crystal for maximum RFI/EMI immunity (Physical Acoustic R15I-AST, the resonant frequency 150 kHz) served as a transmitter and a receiver. In this way we carried out the measurement of the frequency-dependent ultrasonic response to a rectangle calibrating signal of 5 microseconds pulse width. Digitized signals were recorded for further analysis.

We present the frequency domain analysis of the low-frequency ultrasound in MF. The frequency spectrum in MF colloidal system was calculated by Fourier transformation method. Results show that there is a frequency shift in the amplitude-frequency spectrum caused by the step-up magnetic field. The higher the magnetic field, the higher the frequency of the peaks. The effect of particle aggregation in magnetic field on the ultrasound wave propagation is discussed in the paper.

P5-06**STRUCTURAL CHANGES IN LIQUID CRYSTALS WITH ROD-LIKE MAGNETIC PARTICLES STUDIED BY SURFACE ACOUSTIC WAVES**P. Bury¹, J. Kúdelčík¹, M. Veverčík¹, P. Kopčanský², M. Timko² and V. Závášová²¹*Department of Physics, Žilina University, Univerzitná 1, 010 26 Žilina, Slovakia*²*Institute of Experimental Physics, Slovak Academy of Sciences, Watsonova 47, 040 01 Košice, Slovakia*

The effect of rod-like magnetic particles on liquid crystals (6CHBT) structural changes in electric and weak magnetic fields were studied by means of the attenuation of surface acoustic wave (SAW) of frequency 30 MHz propagating along ferronematic liquid crystals. Three low volume concentrations ($\Phi=1\times10^{-5}$, 5×10^{-5} and 1×10^{-4}) of rod-like magnetic particles were added to liquid crystal during its isotropic phase. Several experimental measurements were done including the investigation of the effects of electrical and magnetic fields applied both separately and in conjunction as well as temperature on the SAW attenuation. In contrast to undoped 6CHTB the distinctive SAW attenuation responses induced by both electric and magnetic fields in studied ferronematic liquid crystals have been observed suggesting both structural changes and the orientational coupling between magnetic moments of magnetic particles and the director of the liquid crystal. Observed results confirmed the significant influence of the presence of magnetic particles on the structural properties and following behavior of 6CHTB.

P5-07**THE SPIN-1 J_1 - J_3 HEISENBERG MODEL ON A TRIANGULAR LATTICE: EXACT DIAGONALIZATION STUDY**P. Rubin¹ and A. Sherman¹¹*Institute of Physics, University of Tartu, Ravila 14c, 50411 Tartu, Estonia*

The spin-1 Heisenberg model on a triangular lattice with the ferromagnetic nearest- and antiferromagnetic third-nearest-neighbour exchange interactions, $J_1 = -(1-p)J$ and $J_3 = pJ$, $J > 0$, is studied in the range of the parameter $0 \leq p \leq 1$. This model is of interest as a minimal model for the description of magnetic properties of the compound NiGa_2S_4 . In particular, as we showed earlier with the use of Mori's approach, the model describes key features observed in NiGa_2S_4 - the incommensurate antiferromagnetic short-range order at finite temperature, the quadratic temperature dependence of specific heat, and the shape of the uniform susceptibility.

In the presented work the ground state energies, low-lying state energies, and corresponding spin-spin correlation functions have been found for finite lattices with 16 and 20 sites with periodic boundary conditions. SPINPACK code (Lanczos ED) has been used. We have found qualitative agreement between the dependencies of the ground state energies and spin-spin correlation functions on p with our results obtained earlier by Mori's technique.

P5-08**GROUND STATE SPIN OF HUBBARD LADDER MODELS WITH INFINITE ELECTRON REPULSION**V. O. Cheranovskii¹, E. V. Ezerskaya¹, D. J. Klein² and V. V. Tokarev¹¹*V.N.Karazin Kharkiv National University 61022 Svoboda Sq., 4, Kharkiv, Ukraine*²*Texas A&M University at Galveston, Galveston, TX 77553-1675, USA*

One of the simplest approaches to the study of magnetism of itinerant electrons is the Hubbard model with infinite electron repulsion ($U=\infty$). According to Nagaoka theorem [1], for some types of lattices, the ground state of the one-band $U=\infty$ Hubbard model with one hole in a half-filled band corresponds to a maximal value of total spin. Recently, such a “ferromagnetic” ground state was found numerically for this model on isotropic n -leg ladders with the density of electrons per site ρ in the range $0.8 \leq \rho < 1$ [2].

We consider the ground state and lowest excitations of $U=\infty$ Hubbard model on the n -leg ladders with alternating values of one-site energies α_i for neighboring rungs ($\alpha_i = 0$ & $\alpha_i = \alpha$ for odd & even rungs respectively). Using perturbation theory (PT) in hopping parameter t (for weak interactions between neighbor rungs of the ladder) and a cyclic-spin-permutation technique, we derive effective low-energy Hamiltonians describing this ladder model at different electron densities. We establish the “ferromagnetic” character of ladder ground states at electron density $\rho = 1 - (2n)^{-1}$ and $\alpha \gg |t|$. We also find a stability of this state against the small deviations of the values of α_i . For similar 2-leg ladders with equal one-site energies, a numerical study for finite-ladder fragments demonstrates an instability of the “ferromagnetic” state against these deviations. A numerical study by Davidson’s method for finite fragments of 2-leg ladders shows that with alternating values of α_i the increase of the ratio t/α may decrease the ground state spin of finite fragments due to crossing of lowest energy levels. Using PT in hopping parameter t and extended Nagaoka theorem, we show that the n -leg ladder has “ferromagnetic” ground state at electron density in the interval $1 - (2n)^{-1} \leq \rho < 1$. In other words, donor doping leaves the ladder ground state spin unchanged for $\alpha \gg |t|$. PT considerations for the case of weak acceptor doping, demonstrates a possible instability of the “ferromagnetic” ground state as compared to a similar n -leg ladder with equal one-site energies.

[1] Nagaoka Y. *Phys.Rev.*147, 392 (1966).

[2] Liu.L. et al. *Phys.Rev.Lett.* 108, 126406(4) (2012).

P5-09**STUDY OF STRUCTURAL CHANGES OF WATER-BASED MAGNETIC-FLUID BY ACOUSTIC SPECTROSCOPY**J. Kúdelčík¹, Š. Hardoň¹, P. Bury¹, M. Timko² and P. Kopčanský²¹*Department of Physics, University of Žilina, Univerzitná 1, 010 26 Žilina, Slovakia*²*Institute of Experimental Physics, SAS, Watsonova 47, 040 01 Košice, Slovakia*

The effect of an external magnetic field on the changes in structural arrangement of magnetic nanoparticles in water based magnetic fluid were studied by acoustic spectroscopy. When a magnetic field is increased, the interaction between the magnetic field and the magnetic moments of nanoparticles leads to the aggregation of magnetic nanoparticles to long chains and following increase of acoustic attenuation. The attenuation of acoustic waves measured for a jump changes of the magnetic field to 100, 200 and 300 mT at temperature 20 °C showed that the change of acoustic attenuation is increased slowly to a steady value, but after switching off the magnetic field it decreased immediately to initial value. The dependence of attenuation of acoustic waves in constant magnetic fluid on angle between the wave vector and direction of the applied magnetic field has been measured, too. The measured anisotropy of acoustic attenuation validates structural changes of magnetic fluid in the magnetic field. The observed influences of the various development of magnetic field on the investigated liquid structure are discussed.

P5-10**ENHANCED MAGNETOCALORIC EFFECT IN $\text{NiCl}_2(\text{bipy})$ AT LOW TEMPERATURES**K. Ráczová¹, E. Čížmár¹ and A. Feher¹¹*Institute of Physics, Faculty of Science, P.J. Šafárik University, Park Angelinum 9, 04154 Košice, Slovakia*

We studied magnetothermal properties of the compound $\text{NiCl}_2(\text{bipy})$, $\text{bipy} = 4,4'$ -bipyridine. The crystal structure consists of a two-dimensional framework built by NiCl_2 chains, connected by bipy molecules, which occupy the axial positions of the *trans*- D_{4h} octahedrally coordinated metal atoms. Previously, metamagnetic behavior was observed in $\text{NiCl}_2(\text{bipy})$ below 7 K, the ground-state magnetic structure changes upon the change in the applied magnetic field [1]. Below a critical field the magnetic structure is antiferromagnetic. The intrachain exchange coupling through the Cl_2 bridges is ferromagnetic, and the antiferromagnetic coupling is present between chains [2].

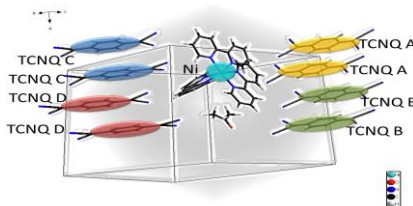
We estimated the value of single-ion anisotropy of Ni ions from magnetic susceptibility and present a study of the magnetocaloric effect (MCE) in $\text{NiCl}_2(\text{bipy})$ from magnetization and specific heat measurements of powdered sample. Above the metamagnetic transition a maximum in the isothermal change of the magnetic entropy is reached near 10 K at field change from 0 T to 9 T with peak value $-\Delta S_M = 8.3 \text{ J.kg}^{-1}.\text{K}^{-1}$. The temperature dependence of ΔS_M above 7 K agrees with the assumption of a positive sign of single-ion anisotropy. Although, inverse MCE is usually observed in ordered antiferromagnets, we observed normal MCE also below transition temperature down to 0.5 K. While maximum temperature change $\Delta T_{\text{ad}} = -4.6 \text{ K}$ during adiabatic demagnetization from 9 T to 0 T is observed at 15 K, the change is still $\Delta T_{\text{ad}} = -2.5 \text{ K}$ at 4 K.

This work was supported by the research project VEGA 1/0145/13 and by ERDF EU project under the contract No. ITMS26220120005.

- [1] M.A. Lawandy, X.Y. Huang, R.J. Wang, J. Li, J.Y. Lu, T. Yuen, C.L. Lin, Inorg. Chem. 38 (1999) 5410.
- [2] R. Feyerherm, A. Loose, M.A. Lawandy, J. Li, Appl. Phys. A 74 [Suppl.] (2002) S778–S780.

P5-11**MAGNETIC HEAT CAPACITY OF ANION-RADICAL SALT
Ni(bipy)₃(TCNQ)₄·(CH₃)₂CO AT VERY LOW TEMPERATURES**D. Šoltésová¹, E. Čížmár¹, G. Vasylets², V. Starodub³ and A. Feher¹¹*Institute of Physics, Faculty of Science, P.J. Šafárik University, Park Angelinum 9, 041 54 Košice, Slovakia*²*Applied Chemistry Department, V.N. Karazin Kharkiv National University, Svobody Sq. 4, 61022 Kharkiv, Ukraine*³*Institute of Chemistry, Jan Kochanowski University of Humanities and Sciences, Świętokrzyska 15G, 25-406 Kielce, Poland*

We report thermodynamic studies of anion-radical salt (ARS) Ni(bipy)₃(TCNQ)₄·(CH₃)₂CO, where TCNQ is 7,7',8,8'-tetracyanoquinodimethane. The ARS based on TCNQ belong to material class, in which the arrangement of ASR has considerable impact on charge transfer and magnetic properties. The studied compound consists of [Ni(bipy)₃]²⁺ cation containing transition metal ion Ni²⁺ and four types of anion-radicals TNCQ^{·-} (A, B, C and D). TNCQ^{·-} radicals form two different types of TCNQ^{·-} stacks (AABB and CCDD), where a strong exchange interaction is expected.



We studied temperature dependence of specific heat on single crystal Ni(bipy)₃(TCNQ)₄·(CH₃)₂CO in magnetic fields up to 5 T in the temperature range 0.4 K to 30 K. In zero magnetic field, upturn at the lowest temperatures was observed in the temperature dependence of specific heat. After the application of the magnetic field parallel to *c*-axes the specific heat displays a broad Schottky-like maximum above 0.4 K. We suggest that observed maximum originates from the single-ion anisotropy of Ni²⁺ ions and the exchange interaction between transition metal ions and TCNQ is negligible. The analysis of the temperature dependence of specific heat below 10 K using single-ion approximation yields the parameters of single-ion anisotropy $D/k_B = -1.95$ K and $E/k_B = 0.3$ K.

This work was supported by the research project VEGA 1/0145/13 and by ERDF EU project under the contract No. ITMS26220120005.

P5-12**THE ENERGY SPECTRUM AND THERMODYNAMICS OF THE SPIN-1/2 XX CHAIN WITH ISING IMPURITIES**E.V. Ezerskaya¹*¹Department of Physics, V.N.Karazin Kharkiv National University, Svoboda sq. 4, 61 022 Kharkiv, Ukraine*

The energy spectrum and thermodynamics of two exactly solvable spin models: finite isotropic XY-chain, or so called XX-chain, with periodic boundaries (“ring”) and impurity Ising spin S_1 and open ends finite XX chain (“line”) with two different edge impurity Ising spins S_1, S_2 are investigated. These Hamiltonians describe some kind of well-known broken-chain effect in real quasi-one dimensional magnets. The Hamiltonians split into the sum of the finite XX-chain Hamiltonians with the effective “impurity” spins ($s = 1/2$) at the ends, owing to z -projections of the impurity spins are good quantum numbers: both Hamiltonians commute with the z -projection of the impurity spin operators ($\sigma_i = -S_i, \dots, +S_i, i = 1, 2$) and z -component of the XX-chain total spin.

The conditions for the appearance of the energy states, localized in the vicinity of impurity spins, have been derived.

The partition functions for above “ring” and “line” models are the sum of partition functions of finite XX chains with impurities. We performed the simulation of the field and the temperature dependencies of the magnetization and heat capacity. One may expect the big effect of impurities in presence of localized levels. For antiferromagnetic (AF) Ising interaction, the field dependence of the magnetization at very low temperatures demonstrates jump associated with the spin-flip of impurity spin in sufficiently strong magnetic field for “ring” and two jumps for “line”. At very low temperatures, the field dependence of the specific heat for both chains has a complex form with the multiple maxima. Additional peaks of specific heat for AF Ising interaction of impurities with XX chain we associate with the local impurity levels and the spin-flip of the impurity spin in strong fields.

The behavior of the average z -projection of impurity spins and longitudinal impurities spin-spin correlation functions at zero and non-zero temperature are studied numerically. It is shown that under certain conditions, the average z -spin projection for impurity sites at $T = 0$ may have the finite jumps and non-monotonic dependence on the magnetic field at low temperatures. The behavior of the impurity spin in the closed chain and open chain can differ substantially, due to the fact that in the closed chain the impurity spin interacts directly with the two neighboring spins.

P5-13**MEASUREMENT OF COMPLEX PERMITTIVITY OF OIL-BASED FERROFLUID**J. Kúdelčík¹, Š. Hardoň¹ and L. Varačka¹¹*Department of Physics, University of Žilina, Univerzitná 1, 010 26 Žilina, Slovakia*

The investigation on dielectric properties of oil-based ferrofluid with magnetite nanoparticles are presented. The changes in complex dielectric permittivity have been measured in an external magnetic field. Two different instruments: IDAX and LCR Meter that enabled the measurement in wide frequency ranges were used. The frequency dependence of permittivity was measured within the frequency range from 1 mHz to 2MHz. In whole measured frequency range the complex permittivity has been studied in the magnetic field applied to the sample in either parallel or perpendicular configurations in regard to the electric field. When a magnetic field is applied, the interaction between the magnetic field and magnetic moments of nanoparticles leads to the aggregation of magnetic nanoparticles to new structures which had influence on the value of dielectric permittivity. The application of electric field is also connected with reduction in the electric dipole moment of particles and their orientation to the electric field direction connected also with formation of chains. The Cole-Cole and Havriliak-Negami relaxation model have been used to analyzing measured data. The various influences of magnetic field development on the investigated liquid are discussed.

P5-14**LOW MAGNETIC FIELD RESPONSE IN FERRONEMATICS**

V. Gdovinova¹, N. Tomasovicova¹, V. Zavisova¹, N. Eber², T. Toth-Katona²,
F. Royer³, D. Jamon³, J. Jadzyn⁴ and P. Kopcansky¹

¹*Institute of Experimental Physics SAS, Kosice, Slovakia*

²*Research Institute for Solid State Physics and Optics,*

Hungarian Academy of Sciences, Budapest, Hungary

³*Université de Saint Etienne, Saint Etienne, France*

⁴*Institute of Molecular Physics, Polish Academy of Sciences, 60179 Poznan, Poland*

The orientational order of liquid crystals (LCs) can be controlled by magnetic or electric fields due to the anisotropy of dielectric permittivity or diamagnetic susceptibility. Very small anisotropy of the diamagnetic susceptibility of liquid crystals causes that liquid crystals are rather control by electric field in practise than by magnetic field. In order to increase the magnetic susceptibility of liquid crystals Brochard and de Gennes' introduce the great idea of doping them with fine magnetic particles so called ferronematics [1]. A linear magnetodielectric response has been detected in planarly oriented ferronematics samples far below the threshold of the magnetic Freedericksz transition in the presence of a weak orienting bias magnetic field (2mT) [2]. In our study, magneto-optical and dielectric properties of magnetic nanoparticle doped nematic LCs has been investigated by means of applying different orienting bias magnetic fields B_{bias} as well as electric fields E_{bias} . The liquid crystals 4-n-hexyl-4'-cyanobiphenyl (6CB) was doped with rod-like and spherical magnetic nanoparticles of 10 nm in diameter. The obtained results ie linear magnetic field dependence of magneto-optical and magnetodielectric effects in low magnetic field region showed that bias fields allow controlling these effects of ferronematic samples. This can be used as liquid sensors for the mapping of magnetic field similar to mapping spacial distribution of temperature by liquid crystals for example.

This work was supported by Ministry of Education Agency for Structural Funds of EU in frame of project PhysNet 26110230097.

[1] F. Brochard and P. G. De Gennes, J. Phys., vol. 31, no. 7, pp. 691-708 (1970).

[2] N. Tomašovičová, M. Timko, Z. Mitróová, M. Koneracká, M. Rajňák, N. Éber, T. Tóth-Katona, X. Chaud, J. Jadzyn and P. Kopčanský, Phys. Rev. E 87, 014501 (2013).

P5-15

ANALYSIS OF THERMAL FIELD IN MINERAL TRANSFORMER OIL BASED MAGNETIC FLUIDS

M. Kostelec¹, J. Kurimský¹, R. Cimbala¹, L. Kruželák¹, M. Rajňák², M. Timko² and P. Kopčanský²

¹*Department of Electrical Power Engineering, Technical University of Košice, Faculty of Electrical Engineering and Informatics, Mäsiarska 74, 041 20 Košice, Slovakia*

²*Institute of Experimental Physics SAS, Watsonova 47, 040 01 Košice, Slovakia*

Growing interest in the use of magnetic fluids in power systems especially in transformers as insulation and a coolant is nowadays registered. Magnetisable nano fluids, which are used in cooling systems as an alternative to mineral transformer oil, are characterised by lower concentration of magnetic nanoparticles. The magnetic fluid has better heat transfer and dielectric properties such as breakdown as mineral transformer oil and it can be used to improve heat flow, thereby increasing the ability of the active parts to resist failures such as electromagnetic pulses. External magnetic field may be used for forced circulation of magnetic fluid. Magnetic force inside the magnetic fluid can be adequately controlled by adjusting the incident magnetic field. This paper presents thermal distribution, fluid flow and cooling ability of mineral transformer oil and magnetic fluid based on mineral transformer oil. The concentration of Fe_3O_4 magnetic nanoparticles is 0.15% volume of mineral transformer oil. The thermal field is generated by steel conductor. Thermal distributions in mineral transformer oil and magnetic fluid are investigated and differences for both cases are discussed in the paper.

P5-16**FRUSTRATED ZIG-ZAG SPIN CHAINS FORMED BY HYDROGEN BONDS IN COMPOUND $[\text{Cu}(\text{H}_2\text{O})(\text{OH})(\text{tmen})]_2[\text{Pd}(\text{CN})_4] \cdot 2\text{H}_2\text{O}$**

E. Čižmár¹, A. Orendáčová¹, M. Orendáč¹, J. Kuchár², A. Feher¹, J.-H. Park³ and M. W. Meisel⁴

¹*Institute of Physics, Faculty of Science, P.J. Šafárik University, Park Angelinum 9, 04154 Košice, Slovakia*

²*Institute of Chemistry, Faculty of Science, P.J. Šafárik University, Moyzesova 11, 04154 Košice, Slovakia*

³*National High Magnetic Field Laboratory, Florida State University, Tallahassee, FL 32310-3706, USA*

⁴*Department of Physics and National High Magnetic Field Laboratory, University of Florida, Gainesville, FL 32611-8440, USA*

The magnetic properties of the novel dimeric compound $[\text{Cu}(\text{tmen})(\text{H}_2\text{O})(\text{OH})]_2[\text{Pd}(\text{CN})_4] \cdot 2\text{H}_2\text{O}$ (*tmen* = N,N,N',N'-tetramethylethylenediamine) were studied over a wide range of temperature and magnetic field. The crystal structure of the compound is modulated, where the co-ordination number of the Cu(II) ion varies between 5 (square-pyramidal) and 6 (deformed octahedral) in every 7th dimeric unit due to the occupancy of the water molecules coordinated to Cu(II). The dimeric units interact with the water molecules of crystallization and $[\text{Pd}(\text{CN})_4]^{2-}$ anions *via* hydrogen bonds (HBs). The *g*-factor of the Cu(II) ions was determined from ESR measurements to be anisotropic with $g_{\parallel}=2.19$ and $g_{\perp}=2.08$, while magnetic measurements revealed a presence of weak antiferromagnetic (AFM) exchange coupling in the compound. Specific heat measurements were realized in the temperature range from 100 mK to 3 K and in zero magnetic field. The temperature dependence of specific heat is characterized by the presence of a Schottky-like maximum at 0.47 K and a λ -anomaly at 0.28 K, indicating the formation of long-range order in the system. The magnetic entropy removed above the long-range ordering temperature represents 75 % of the total magnetic entropy, suggesting the low-dimensional character of the studied system. The comparison of the experimental data with theoretical predictions revealed the presence of AFM intradimer exchange coupling $J/k_B = -1.2$ K and interdimer coupling of similar strength mediated *via* hydrogen bonds between dimeric units forming a frustrated magnetic zig-zag chain structure. These results reveal a significant influence of HBs on the magnetic structure and dimensionality of title compound.

This work was supported by ERDF EU project under the contract No. ITMS26220120005, and the NSF via DMR-1202033 (MWM), DMR- 1157490 (NHMFL), and the State of Florida.

P5-17**TEMPERATURE DEPENDENCE OF A DIELECTRIC RELAXATION IN WEAKLY POLAR FERROFLUIDS**

M. Rajňák¹, J. Kurimský², B. Dolník², R. Cimbala², K. Paulovičová¹,
P. Kopčanský¹ and M. Timko¹

¹*Institute of Experimental Physics, Slovak Academy of Sciences, Watsonova 47,
040 01, Košice, Slovakia*

²*Faculty of Electrical Engineering and Informatics, Technical University of
Košice, Letná 9, 04200 Košice, Slovakia*

In this study we focus on the temperature dependent broadband dielectric response of a ferrofluid based on transformer oil and magnetite nanoparticles covered with oleic acid molecules. For that purpose the method of dielectric spectroscopy has been chosen in the frequency range from 20 Hz up to 2 MHz. The experiments were carried out on thin film ferrofluid samples filling a glass plate capacitor coated with ITO conductive layers. The obtained complex permittivity spectrum shows a pronounced dielectric dispersion in the low frequency range. Following the Cole-Cole fitting parameters we found a nearly Debye-like nature of the detected relaxation process. Taking into account the ferrofluid composition we associate this relaxation with ion impurity polarization on the nanoparticle – oil interface. A strong temperature dependence of the relaxation process has been found when conducting the experiments in the temperature range from 298 K to 358 K. The relaxation maximum shifts considerably to higher frequencies with increasing temperature. The relaxation time of the process exhibits a typical Arrhenius behavior. As the maximal dielectric losses due to the relaxation process appear around the line frequency, we point out a possible drawback when applying the studied ferrofluid in power transformers as a cooling and insulating medium. On the other hand, we propose other reasonable practical applications in the field of electrical engineering.

This work was supported by Slovak Academy of Sciences and Ministry of Education: VEGA 2/0045/13, 1/0311/15, 2/0141/16, and Ministry of Education Agency for structural funds of EU, Project No. 26110230061, 26220120046, 26220120003, 26220120055 and 26220220182.

P5-18**THE RESPONSE OF A MAGNETIC FLUID TO RADIO FREQUENCY ELECTROMAGNETIC FIELD**

B. Dolník¹, M. Rajňák², R. Cimbala¹, I. Kolcunová¹, J. Kurimský¹, J. Balogh¹, J. Džmura¹, J. Petráš¹, P. Kopčanský², M. Timko², J. Briančin³, and M. Fabián³

¹*Department of Electric Power Engineering, FEI, Technical University of Košice, Mäsiarska 74, 041 20 Košice, Slovakia*

²*Institute of Experimental Physics, Slovak Academy of Sciences, Watsonova 47, 040 01, Košice, Slovakia*

³*Institute Geotechnic, Slovak Academy of Science, Watsonova 45, 043 53 Košice, Slovakia*

Electromagnetic pollution generated by the electrical devices has been regarded as a new form of pollution, harmful to the society as air and water pollution. The operation of electronic devices in polluted electromagnetic environment has caused electromagnetic interference (EMI) to become important concerns. Devices that are vulnerable to interference must often be shielded to protect them from the effects of EMI. In this work we describe an interaction of a magnetic fluid (MF) based on transformer oil with alternating magnetic field. The MF was composed of a transformer oil and dispersed magnetite nanoparticles coated with oleic acid. Among the wide range of topics covered, we pay attention to an important field related to the absorption of electromagnetic field by MF as a suitable candidate for applications where it is necessary to electrically isolate, remove excess of heat and to shield electromagnetic fields. We present a method for the determination of shielding effectiveness (SE) of the MF under high-frequency excitation conditions from 750 MHz to 3 GHz by means of magnetic near field measurements and analysis. Herein, we report the effect of magnetic volume fraction in the MF and the effect of the sample thickness on the SE. We have found that the magnetic fluid has a frequency dependent "windows", characterized that either absorb the magnetic field, or facilitate penetration of the magnetic field through the barrier.

P5-19**KINETICS OF NEMATIC TO ISOTROPIC PHASE TRANSITION IN LIQUID CRYSTAL DOPED WITH MAGNETIC NANOPARTICLES**

K. Csach¹, A. Juriková¹, J. Miškuf¹, N. Tomašovičová¹, V. Gdovinová¹, V. Závistová¹, P. Kopčanský¹, N. Éber², K. Fodor-Csorba² and A. Vajda²

¹ *Institute of Experimental Physics, Slovak Academy of Sciences, Watsonova 47, 040 01 Košice, Slovakia*

² *Institute for Solid State Physics and Optics, Wigner Research Centre for Physics, Hungarian Academy of Sciences, H-1525 Budapest, P.O.B. 49, Hungary*

For practical purpose of liquid crystals, the mixtures of substances are used. The transition from crystalline to liquid phase is more complex and proceeds through several intermediate phases. The controlled nematic to isotropic phase transition is usually exploited in liquid crystal based displays.

The binary mixture of bent-core (10DCIPBBC) and rod-shaped (6OO8) liquid crystals (with the weight ratio of 1:1) was chosen as a model substance combining the properties of both types of the liquid crystals. The mixture was doped with the spherical and the rodlike magnetic nanoparticles with the concentrations of $7,5 \times 10^{-4}$ and $8,5 \times 10^{-4}$, respectively. DSC experiments were performed for the pure as well as the doped mixture at different heating rates ranging from 1 to 16 °C/min. The kinetics of nematic to isotropic phase transition was evaluated in the framework of the differential isoconversional method. The addition of the magnetic nanoparticles lowered the phase transition temperature. This effect is more intensive in the case of the rodlike magnetic nanoparticles. Measured enthalpy change decreased from the value of 2 J/g for the pure mixture to the value of about 1,5 J/g for the liquid crystal mixture modified by the magnetic nanoparticles. The calculated apparent activation energy showed non-monotonous behaviour and the sensitivity on the shape of added magnetic nanoparticles.

This work was supported by the project VEGA 2/0045/14 by Slovak Academy of Sciences and No. 26110230097 provided in the frame of Structural funds of the European Union.

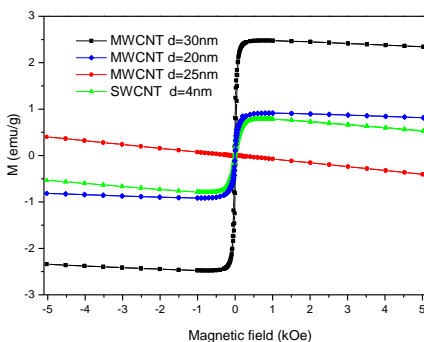
P5-20**CHARACTERIZATION OF CARBON NANOTUBES**

M. Jeníková¹, K. Zakuťanská², J. Kováč¹, V. Girman², P. Kopčanský¹ and N. Tomašovičová¹

¹*Institute of Experimental Physics, Slovak Academy of Science, Watsonova 47, 040 01 Košice, Slovakia*

²*Institute of Physics, Faculty of Sciences, P.J.Šafárik University, Park Angelinum 9, 040 01 Košice, Slovakia*

Interest in study of binary mixtures of nematic liquid crystals and carbon nanotubes (CNTs) is motivated by their common high anisotropic physical properties [1]. CNTs are exceptionally anisometric particles with diameters on the order of nanometers, but lengths ranging from microns to centimeters. They can have either a paramagnetic, ferromagnetic or diamagnetic response to an applied magnetic field depending on their diameter, chirality and Fermi energy level. Control of CNTs orientation becomes a very important for their application in new materials. Among the methods that have been proposed are magnetic and electric field alignment. One from the promising methods is their dispersion in liquid crystal. To prepare stable colloids a fundamental requirement is that they can be well dispersed and preferably also aligned in the composite, and the strong interaction with the surrounding matrix [2]. The magnetic properties of CNTs is one of the crucial parameters to determine the effectiveness of the applied magnetic field. Figure shows the magnetic field dependent magnetization curves of SWCNT and MWCNTs of different size.



- [1] R. Saito, G.Dresselhaus, M.S. Dresselhaus, Physical properties of carbon nanotubes. London: Imperial College Press, 1998.
- [2] J. P. F. Lagerwall and G. Scalia, J. Mater. Chem., 2008,18, 2890–2898.

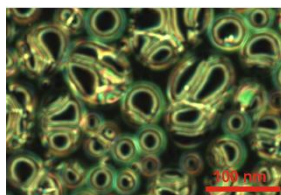
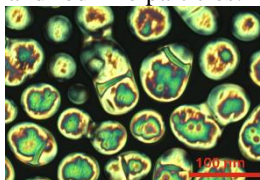
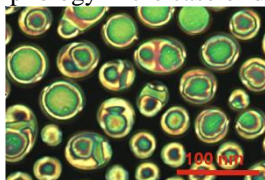
P5-21**THE INFLUENCE OF MAGNETIC PARTICLES AND MAGNETIC FIELD ON THE SHAPE OF DROPLETS OF LIQUID CRYSTAL.**

J. Majorošová¹, V. Gdovinová¹, N. Tomašovičová¹, A. Juríková¹, V. Závišová,
J. Jadzyn² and P. Kopčanský¹

¹*Institute of Experimental Physics, Slovak Academy of Sciences, Watsonova 47,
04353 Košice, Slovakia*

²*Institute of Molecular Physics, Polish Academy of Sciences, Smoluchowskiego
17, 60179 Poznań, Poland*

Ferronematics are suspensions of magnetic particles in nematic liquid crystals (LCs). In this work the thermotropic nematic liquid crystal 4-trans-4'-n-hexyl-cyclohexyl-isothiocyanato-benzene (6CHBT) was dissolved in phenyl-isocyanate and doped with spherical as well as rod-like magnetic particles with volume concentration 10^{-4} . The influence of the shape and volume concentration on the phase transitions from isotropic to nematic phase was studied by three experimental methods: optical microscopy, differential scanning calorimetry and dielectric measurements. The obtained results confirmed the coexistence of isotropic and nematic phase, i.e. nematic or ferronematic droplets in isotropic phase in the wide temperature region (comparing with pure LC) between nematic and isotropic phase. Optical microscopy shows, that there is the difference in the shape of LC droplets morphology in the case of doping with spherical and rod-like particles.



This work was supported by Ministry of Education Agency for Structural Funds of EU No. 26110230097

P5-22**THERMAL CONDUCTIVITY OF LOW-DIMENSIONAL MAGNETIC SYSTEMS**D. Legut¹, D. U Wdowik² and A. Orendáčová³¹*IT4Innovations Center, VSB-Technical University of Ostrava, 17. listopadu 15, 708 33 Ostrava, Czech Republic*²*Institute of Technology, Pedagogical University, ulica Podchorazych 2, 30-084 Cracow, Poland*³*Centre of Low Temperature Physics, Faculty of Science, P.J. Šafárik University Park Angelinum 9, 041 54 Kosice, Slovakia*

The thermal conductivity of low-dimensional magnetic system is investigated. Recently, the lattice vibrations (phonons) and hence thermodynamic quantities were estimated in phases of the KCuF_3 [1]. The strength of exchange interactions and the thermal transport were considered in similar system of CsNiF_3 [2-3]. Both systems are quasi-one dimensional quantum magnets with the the major exchange interaction along the c -axis [1, 2], anti-ferromagnetic and ferromagnetic one, respectively.

A large anisotropy in the thermal conductivity close to the Neel temperature in both systems was measured [4]. Here, we would like to approach the thermal conductivity employing first-principal calculations. The results are compared to the recorded data [4, 5] as well as to the models of Heisenberg and Ising, as the mediators of the heat transport close to the Neel temperature are thought to be magnetic interactions [5].

[1] D. Legut and U. D Wdowik J. Phys.: Condens. Matter 25, 115404 (2013).

[2] D. Legut and J. Rusz, Acta Phys. Pol. A 113, 503 (2008).

[3] V. Tkac , A. Orendacova , M. Orendac , D. Legut , K. Tibenska , A. Feher , M. Poirier and M.W. Meisel, Acta Phys. Pol. A 121, 503 (2012).

[4] H. Miike and K. Hirakawa, J. Phys. Soc Jap. 38, 1279 (1975).

[5] K. Hirakawa, H. Miike, and H. Hayashi, J. Phys. Soc Jap. 33, 266 (1972).

[6] D. Legut and U. D. Wdowik, J. Phys. Condens. Matter. 25, 115404 (2013).

[7] H. Miike and K. Hirakawa, J. Phys. Soc Jap. 38, 1279 (1975).

[8] K. Hirakawa, H. Miike, and H. Hayashi, J. Phys. Soc Jap. 33, 266 (1972).

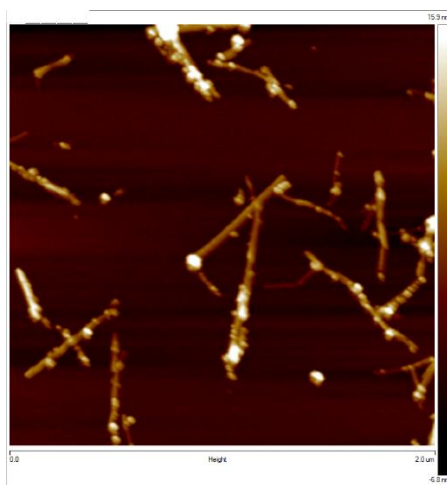
P5-23**AFM STUDIES OF INTERACTION OF MAGNETIC NANOPARTICLES WITH LYOTROPIC LIQUID CRYSTAL**

N. Tomašovičová¹, L. Balejíčková¹, V. Gdovinová¹, M. Kubovčíková¹,
C.-W. Yang², I.-S. Hwang², S. Hayryan², C.-K. Hu² and P. Kopčanský¹

¹*Institute of Experimental Physics SAS, Kosice, Slovakia*

²*Institute of Physics, Academia Sinica in Taipei, Taiwan*

The focus of current worldwide research is to design nanomaterials that are able to assemble into functional superstructures in multiple directions. A powerful tool is using magnetic nanoparticles and magnetic field as an organizing medium to induce the assembly of liquid crystals. Magnetic particles dispersed in thermotropic or lyotropic liquid crystals modify the properties of the hosts. Due to the adsorption of magnetic nanoparticles on fibril surface we suggest the possible ordering of the fibrils by applying an external magnetic field that can be helpful in production of biological liquid crystals. In this work the interaction of lysozyme fibrils and magnetic particles after their mixing was studied. The experiments were carried out for a better understanding of the binding process. Fig. shows AFM image of lysozyme fibrils with adsorbed magnetic particles. Scanned area is 2nm × 2nm.



This work was supported by Ministry of Education Agency for Structural Funds of EU No. 26110230097.

P5-24**THE LOW AND HIGH SPIN GROUND STATES IN NEW TETRANUCLEAR MANGANESE MOLECULES WITH $[\text{Mn}^{\text{II}}_3\text{Mn}^{\text{III}}]$ AND $[\text{Mn}^{\text{II}}_2\text{Mn}^{\text{III}}_2]$ METALLIC CORES**

M. Antkowiak¹, M. Sobocińska², M. Wojciechowski³, G. Kamieniarz¹, J. Utko² and T. Lis²

¹*Faculty of Physics, A. Mickiewicz University, Umultowska 85, 61-614 Poznań, Poland*

²*Faculty of Chemistry, University of Wrocław, Joliot-Curie 14, 50-383 Wrocław, Poland*

³*Institute of Physics, University of Zielona Góra, Szafrana 4a, 65-516 Zielona Góra, Poland*

Molecular-based nanomagnets are important in fundamental physics and are good candidates for applications in the domain of magnetic storage and quantum information processing. A particular subgroup is the family of manganese-based clusters.

In this communication we present the experimental and theoretical results obtained for two recently synthesized [1] tetranuclear magnetic clusters $[\text{Mn}^{\text{II}}_3\text{Mn}^{\text{III}}\text{Cl}(\text{Ph}_3\text{CCOO})_4(\text{CH}_3\text{OCH}_2\text{CH}_2\text{O})_4(\text{CH}_3\text{CN})] \cdot 0.4\text{C}_6\text{H}_5\text{CH}_3 \cdot 0.6\text{CH}_3\text{CN}$ and $[\text{Mn}^{\text{II}}_2\text{Mn}^{\text{III}}_2\text{Cl}_4(\text{CH}_3\text{OCH}_2\text{CH}_2\text{O})_6]$ denoted $\text{Mn}^{\text{II}}_3\text{Mn}^{\text{III}}$ and $\text{Mn}^{\text{II}}_2\text{Mn}^{\text{III}}_2$ respectively.

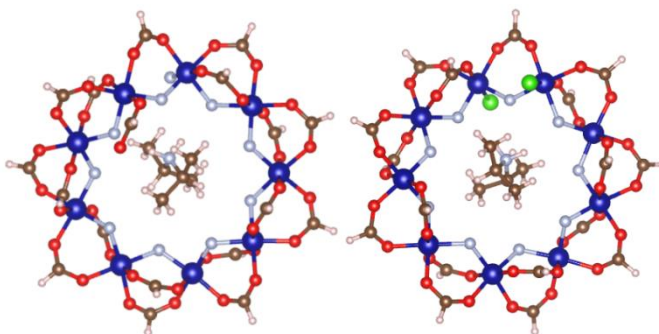
We analysed the magnetic susceptibility and magnetization of both compounds in terms of the Heisenberg spin model using exact diagonalization technique. We achieved quantitative agreement between theory and experiment for $\text{Mn}^{\text{II}}_2\text{Mn}^{\text{III}}_2$ and semi-quantitative for $\text{Mn}^{\text{II}}_3\text{Mn}^{\text{III}}$ and the model predictions for $\text{Mn}^{\text{II}}_3\text{Mn}^{\text{III}}$ are supported by DFT.

We also studied the energy structure of both compounds. The lowest value of the total spin $S=1/2$ found in the ground state of $\text{Mn}^{\text{II}}_3\text{Mn}^{\text{III}}$ is desirable prerequisite for the molecular qubits whereas the highest one $S=9$ for $\text{Mn}^{\text{II}}_2\text{Mn}^{\text{III}}_2$ is expected for the single-molecule magnets. Both compounds provide examples of the bipartite spin systems so that Lieb-Mattis theorem implies the ground state degeneracy and architecture of their low-energy level structure. We emphasize that the topology of interactions in $\text{Mn}^{\text{II}}_3\text{Mn}^{\text{III}}$ is particularly suitable for synthesis of molecules with the ground state $S=1/2$ and the interactions between Mn^{II} ions are crucial to get the lowest energy gap higher than that observed in the chromium-based molecules.

[1] M. Sobocińska et al., Dalton Trans. (2016), in press, DOI: 10.1039/C5DT04869A.

P5-25**THE STUDY OF MAGNETIC MOLECULES CONTAINING CHROMIUM-BASED RINGS WITHIN DENSITY FUNCTIONAL THEORY**B. Brzostowski¹, M. Wojciechowski¹ and G. Kamieniarz²¹*Institute of Physics, University of Zielona Góra, ul. Prof. Szafrana 4a, 65-516 Zielona Góra, Poland*²*Faculty of Physics, A. Mickiewicz University, ul. Umultowska 85, 61-614 Poznań, Poland*

We present a comprehensive study of electronic and magnetic properties of nonmetallic hetero-nuclear chromium-based molecular rings using the DFT package SIESTA. We widely examine three different molecules which realize the rare examples of spin-frustrated nanomagnets and exhibit a particular type of a bond defect.



The molecules provide real systems revealing the correspondence between the strength of the defect and the total spin in the ground state [1]. Five non-equivalent spin configurations with $S=\pm 3/2$ for Cr are considered, the corresponding differences between the total energies of these configurations are calculated and the exchange interaction parameter J are extracted from the spin model, using the broken symmetry approach and different scenarios.

The total, local and orbital projected density of states are presented, as well as the spin densities and magnetic moments are calculated for the metallic centers. Differences in charge and magnetic moments distribution along the rings are compared. The HOMO and LUMO orbitals are plotted and discussed.

[1] G. Kamieniarz et al., Phys. Rev. B92, 140411(R) (2015).

P5-26**CORRELATION BETWEEN THE STRUCTURE AND MAGNETIC SUSCEPTIBILITY OF BiOX ($X=\text{Cl, Br, I}$) SINGLE CRYSTALS**V. Bunda¹, S. Bunda¹, J. Kovac², D. Lotnyk³ and A. Feher³¹Department of Computer Sciences and Web-Design,

Transcarpathian Institute of Arts, Voloshin Str. 37, 880 00 Uzhgorod, Ukraine

²Centre of Low Temperature Physics, Institute of Experimental Physics SAS, Watsonova 47, 040 01 Kosice, Slovak Republic³Centre of Low Temperature Physics, P.J. Šafárik University, Park Angelinum 9, 041 54 Kosice, Slovak Republic

The high-resolution X-ray powder diffraction patterns on the poly- and singlecrystalline BiOX ($X=\text{Cl, Br, I}$) were measured. The BiOX materials possess the Matlockite (PbFCl) type tetragonal crystal structure with $P4/nmm$ (No. 129) as the space group. There are two BiOX molecules per unit cell. The Bi^{3+} and halogen ions reside in the $2c$ ($1/4, 1/4, z$) position while the oxides lie in the $2a$ ($1/4, 3/4, 0$) position. The Bi^{3+} ion is coordinated to four oxides and four + one halogens in a distorted monocapped tetragonal antiprism arrangement yielding C_{4v} as the point symmetry of the Bi^{3+} site.

Magnetic susceptibility measurements were carried out between 2 and 300 K singlecrystalline samples weighing between 2 and 8 mg with a Quantum Design MPMS SQUID magnetometer using an applied magnetic field of 10-100 Oe.

The high temperature inverse susceptibility data were fitted to Curie-Weiss law $\chi = C/(T - \theta)$, where $C = N_A (\mu_{\text{eff}})^2 / 3k$ is the Curie constant, θ the Weiss constant, N_A Avogadro's number, μ_{eff} the effective magnetic moment, and k Boltzmann's constant. The high absolute values of θ for the Bi^{3+} ion suggest significant deviation from the the free ion Curie-type behaviour (see table)

BiOX	C_{\parallel} (emuKmol ⁻¹)	C_{\perp} (emuKmol ⁻¹)	θ_{\parallel} (K)	θ_{\perp} (K)	μ_{\parallel} (μ_B)	μ_{\perp} (μ_B)
BiOCl	29.29	17.84	-3049	-2996	4.84	3.78
BiOBr	208.77	72.73	-5086	-3904	12.92	7.63
BiOI	25.18	46.53	-3224	-8147	4.49	6.10

P5-27**MAGNETIC PROPERTIES OF $\text{BiOCl}:\text{Ti}$ AND $\text{BiOCl}:\text{Sm}$ SINGLE CRYSTALS**S. Bunda¹, V. Bunda¹, J. Kovac², D. Lotnyk³ and A. Feher³¹*Department of Computer Sciences and Web-Design,**Transcarpathian Institute of Arts, Voloshin Str. 37, 880 00 Uzhgorod, Ukraine*²*Centre of Low Temperature Physics, Institute of Experimental Physics SAS, Watsonova 47, 040 01 Kosice, Slovak Republic*³*Centre of Low Temperature Physics, P.J. Šafárik University, Park Angelinum 9, 041 54 Kosice, Slovak Republic*

The activated $\text{BiOCl}:\text{Ti}^{4+}$ and $\text{BiOCl}:\text{Sm}^{2+}$ single crystals were grown by the method of chemical gas transport reaction in closed volume. The TiCl_4 and SmCl_2 was used as activators. Water vapor was used as the transport agent.

The BiOX materials possess the Matlockite (PbFCl) type tetragonal crystal structure with $P4/nmm$ (No. 129) as the space group. The Ti^{4+} and Sm^{2+} ions in BiOCl matrix are coordinated to four oxides and four + one chlorides in a distorted monocapped tetragonal antiprism arrangement yielding C_{4v} as the point symmetry of the Bi^{3+} , Ti^{4+} and Sm^{2+} site.

Magnetic susceptibility measurements were carried out between 2 and 300 K singlecrystalline samples weighing between 2 and 8 mg with a Quantum Design MPMS SQUID magnetometer using an applied magnetic field of 100 Oe.

The temperature dependence of the inverse magnetic susceptibility of $\text{BiOCl}:\text{Ti}^{4+}$ is complex: characteristic to a Cuire-Weiss paramagnet at high temperatures, constant for the lower temperature range between 125 and 15 K and then sharply decreasing below 10 K.

The complex behaviour for $\text{BiOCl}:\text{Sm}^{2+}$ is probably due to the strong mixing of the crystal field components of the first excited free ion ${}^6H_{7/2}$ level with those of the ${}^6H_{5/2}$ ground one.

The fitting C and θ parameters of Cuire-Weiss law and effective magnetic moments μ_{eff} of $\text{BiOCl}:\text{Ti}^{4+}$ and $\text{BiOCl}:\text{Sm}^{2+}$ are present in table.

$\text{BiOCl}:\text{Y}^{n+}$	C (emuKmol ⁻¹)	θ (K)	μ_{eff} (μ_B)
$\text{BiOCl}:\text{Ti}^{4+}$	45.56	-4054	6.04
$\text{BiOCl}:\text{Sm}^{2+}$	22.21	-1853	4.2

I6-01**FERROMAGNETIC CRITICALITY OF URANIUM COMPOUNDS**J. Prokleška¹, P. Opletal¹, M. Vališka¹, M. Míšek² and V. Sechovský¹¹*Charles University in Prague, Faculty of Mathematics and Physics, DCMF, Ke Karlovu 5, 121 16 Prague 2, Czech Republic*²*Institute of Physics, Czech Academy of Sciences, Na Slovance 2, 182 21 Prague 8, Czech Republic*

The critical behavior of itinerant ferromagnets close to the onset of the long range order is a subject of intensive experimental and theoretical studies. In particular the evolution of this phase transition at low temperatures is being discussed including the possible scenarios in the zero temperature limit where quantum phase transition may take place. At low temperatures and in clean systems two scenarios avoiding single quantum critical point are possible – the ferromagnetic fluctuations become critical and the ferromagnet-to-paramagnet transition is of first order, or inhomogeneous magnetic phases may appear between the uniform ferromagnetic phase and the paramagnetic phase. Global detailed investigation of both options is rather rare in literature and still open problem, high quality samples and very rigorous experiment realization are necessary in order to obtain unambiguous results.

The talk will be devoted to the discussion of experimental observations of the critical ferromagnetic behavior in uranium based intermetallic compounds. In particular, the novel findings in UCoGa, U(Co_{1-x}Ru_x)Al and U₄Ru₆Ge₇ compounds will be presented and put into the context of earlier published data on the UCoAl relatives, URhAl, URhGe, UCoGe and U₃P₄ compounds.

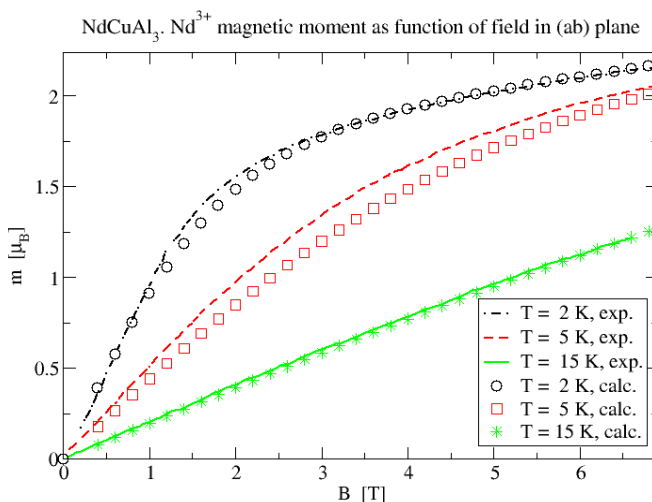
The observed phenomena will be discussed in detail, particular attention will be paid to the comparison across the hexagonal UTX group of compounds, the origin of majority of case-related uranium compounds.

- [1] M. Brando, D. Belitz, F. M. Grosche, and T. R. Kirkpatrick, *Rev. Mod. Phys.* (2016).
- [2] D. Aoki, J. Flouquet, *J. Phys. Soc. Jpn.* 81, 011003 (2012).
- [3] Y. Shimizu et al., *Phys. Rev. B* 91, 125115 (2015).
- [4] D. Aoki et al., *J. Phys. Soc. Jpn.* 80, 094711 (2011).
- [5] A.D. Huxley et al., *J. Phys. Soc. Japan* 76, 1 (2007).

O6-01

MAGNETISM AND CRYSTAL FIELD IN PrCuAl_3 AND NdCuAl_3 P. Novák¹ and M. Diviš²¹Department of Magnetism and Superconductivity, Institute of Physics ASCR, Cukrovarnická 10, 162 53 Praha 6, Czech Republic²Department of Condensed Matter Physics, Faculty of Mathematics and Physics, Charles University, Ke Karlovu 5, 121 16 Praha 2, Czech Republic

During the last five years we developed method to calculate crystal field and magnetism of rare-earth ions in solids. The method is fully *ab-initio* with the exception of a single parameter which adjusts the position of *f*-states relative to other valence states and it was successfully applied to more than 60 rare-earth containing oxides and fluorides ([1] and references therein). In this contribution we use it to explain crystal field and magnetism in PrCuAl_3 and NdCuAl_3 intermetallic compounds. For NdCuAl_3 it works very well as documented in the Figure (experimental points were taken from [2]). It also works for the Pr compound though, due to the more delocalized *f*-electrons, the agreement with experiment is less good. This work was supported by project 15-03777S.



[1] P. Novák, J. Kuneš, and K. Knížek, Opt. Mat. 37, 414, 2014.

[2] D. T. Adroja and V. K. Anand, Phys. Rev. B 86, 104404 (2012).

O6-02**MAGNETIC PROPERTIES OF SOLID SOLUTIONS $\text{HoCo}_{1-x}\text{Ni}_x\text{C}_2$**

H. Michor¹, V. Levytskyi², V. Babizhetskyy², M. Hembara², A. Schümer¹,
S. Özcan¹ and B. Ya. Kotur²

¹*Institute of Solid State Physics, TU Wien, Wiedner Hauptstrasse 8-10, A-1040 Wien, Austria*

²*Department of Inorganic Chemistry, Ivan Franko National University of Lviv, Kyryla and Mefodiya Str., 6, UA-79005 Lviv, Ukraine*

Ternary carbides $R\text{NiC}_2$ ($R = \text{La}, \dots \text{Lu}$) and $R\text{CoC}_2$ ($R = \text{Nd}, \dots \text{Lu}$) crystallize in the non-centrosymmetric orthorhombic CeNiC_2 -type structure, space group $Amm2$ [1,2]. These compounds attracted attention because of various interesting properties such as exotic superconductivity in LaNiC_2 (e.g. [3]), observation of charge density wave (CDW) formation related to Fermi surface nesting features in $R\text{NiC}_2$ with $R = \text{Pr}, \dots \text{Tb}$, and its interplay with rare earth magnetism [4].

In the present study, we report on crystallographic characteristics, magnetic properties, heat capacity and electrical resistivity of a series of polycrystalline solid solutions $\text{HoCo}_{1-x}\text{Ni}_x\text{C}_2$ ($0 \leq x \leq 1$) as well as studies on a HoCoC_2 single crystal grown by the Czochralski technique. Corresponding single crystal data of HoNiC_2 are available in literature [5]. While the latter shows complex antiferromagnetic order at $T_N \sim 2.8$ K, HoCoC_2 displays a ferromagnetic ground state with $T_C = 10.6$ K. The evolution of magnetic ordering in the solid solution $\text{HoCo}_{1-x}\text{Ni}_x\text{C}_2$ indicates a competing nature of these two order parameters and an important influence of crystal field effects. The latter causes a strongly reduced magnitude of the magnetic specific heat anomalies. We are using an approach based on modelling of crystal field and exchange coupling parameters in order to analyse the available magnetic susceptibility and magnetisation data as well as magnetic entropy data evaluated from specific heat measurements.

Our electrical resistivity data of HoNiC_2 further reveal an anomaly at about room temperature which indicates the formation of a CDW state. The transition temperature appears in line with the trend of CDW anomalies reported in Refs. [4] for related compounds $R\text{NiC}_2$ with $R = \text{Pr}, \dots \text{Tb}$.

[1] O. I. Bodak, E. P. Marusin, V. A. Bruskov, *Sov. Phys. Crystallogr.* 25 (1980) 355.

[2] W. Jeitschko, M. H. Gerss, *J. Less-Common Met.* 116 (1986) 147.

[3] T. Yanagisawa and I. Hase, *J. Phys. Soc. Jpn. (JPSJ)* 81 (2012) SB039.

[4] M. Murase *et al.*, *JPSJ* 73 (2004) 2790; N. Yamamoto *et al.*, *JPSJ* 82 (2013) 123701.

[5] Y. Koshikawa, H. Onodera *et al.*, *JMMM* 173 (1997) 72.

O6-03**WEAKLY ANISOTROPIC MAGNETISM IN URANIUM****INTERMETALLIC $\text{U}_4\text{Ru}_7\text{Ge}_6$**

M. Vališka¹, J. Valenta¹, P. Doležal¹, V. Tkáč¹, J. Prokleška¹, M. Diviš¹ and V. Sechovský¹

¹*Faculty of Mathematics and Physics, Charles University, DCMP, Ke Karlovu 5, CZ-12116 Praha 2, Czech Republic*

Uranium intermetallic compounds usually exhibit large magnetocrystalline anisotropy that is born in strong S-O coupling in U ions and together with participation of 5f orbitals in anisotropic covalent bonding. We have grown a high quality single crystal of $\text{U}_4\text{Ru}_7\text{Ge}_6$ by Czochralski method and measured on it XRD, magnetization, AC susceptibility, specific heat and electrical resistivity in various conditions. Magnetization data revealed that this cubic compound represents by its very weak anisotropy a rare exception among U intermetallics. It is ferromagnet below 7.5 K with the easy magnetization axis along the [111] direction. The magnetocrystalline anisotropy appears to be exceptionally weak. The anisotropy fields for the [110] and [100] directions are close to ~0.2 T for both directions. The paramagnetic susceptibility is entirely isotropic. Modified Curie-Weiss law fit of the magnetic susceptibility shows effective moment of 1.37 $\mu\text{B}/\text{U}$, that is significantly lower than the free ion values. First-principle calculations reveal the total magnetic moment of 1.00 $\mu\text{B}/\text{f.u.}$ which is in very good agreement with experimental data (1.0 $\mu\text{B}/\text{f.u.}$ at 7 T). The relativistic spin-orbit coupling splits the crystallographically equivalent U positions in two types. The U ions at the first site bear almost negligible magnetic moment due to the cancelation of the spin and orbital components. The second site has uncompensated spin and orbital moment dominating the total moment. Thermal expansion measurements show a positive length change below T_{C} for [100] direction and almost no response for magnetic easy axis [111]. At the same time we observed a negative longitudinal magnetostriction for [100] direction and only small positive length change for [111]. It shows on possible rhombohedral distortion with an increased lattice angle ($>90^\circ$). This scenario is in agreement with our results of low-temperature X-ray powder diffraction experiments down to 2.8 K. Proposed rhombohedral structure has two different U sites as was obtained by relativistic first-principle calculations. Inspection of Ehrenfest relations indicates strong pressure dependence of T_{C} . Measurements of resistivity and AC susceptibility under hydrostatic pressure reveal suppression of T_{C} to 0 K at a critical pressure around 2 GPa.

O6-04

**MAGNETIC PROPERTIES AND MAGNETOCALORIC EFFECT
IN STRUCTURALLY DISORDERED RECo_2 ($\text{RE} = \text{Y, Gd, Tb}$)
COMPOUNDS**

Z. Śniadecki¹, N. Pierunek¹ and B. Idzikowski¹

¹*Institute of Molecular Physics, Polish Academy of Sciences,
M. Smoluchowskiego 17, 60-179 Poznań, Poland*

The main aim of our research is focused on the investigation of the magnetic properties and magnetocaloric effect in structurally disordered $\text{Y}_{1-x}\text{Tb}_x\text{Co}_2$ and $\text{Y}_{1-x}\text{Gd}_x\text{Co}_2$ ($0 \leq x \leq 1$) alloys. Magnetocaloric effect (MCE) is a property of all magnetic materials, which in an isothermal (*adiabatic*) process leads to magnetic entropy change ΔS_M (*adiabatic temperature change* ΔT_{ad}) due to variation of applied magnetic field $\mu_0 H$ [1]. MCE is utilized in magnetic refrigeration, which is becoming a new alternative for conventional cooling methods.

Samples were prepared by melt-spinning under Ar atmosphere. X-ray diffraction (XRD) was used to determine crystalline structure. Magnetic measurements were performed by vibrating sample magnetometry (VSM) and AC susceptibility measurements. Temperature and magnetic field dependence of specific heat C_P was measured to determine adiabatic temperature change. Curie temperature changes from 35 K for $\text{Y}_{0.8}\text{Tb}_{0.2}\text{Co}_2$ to 236 K for TbCo_2 . $\text{Y}_{1-x}\text{Gd}_x\text{Co}_2$ ($0 \leq x \leq 1$) alloys exhibit similar behavior and T_C increases with Gd content. High values of full width at half maximum of entropy change peak δT_{FWHM} are observed comparing to homogenized compounds. It may be associated with relatively high topological and chemical disorder, as observed for Gd-based compounds and parent YCo_2 [2]. Such broadening is even more pronounced for substitutional alloys. For instance, maximum value of magnetic entropy changes $\Delta S_{Mpk} = 4.55 \text{ J/kgK}$, $\delta T_{FWHM} = 68 \text{ K}$ and refrigerant capacity $\text{RC} = 222 \text{ J/kg}$ for TbCo_2 compound in as-quenched state (measured for $\Delta \mu_0 H = 5 \text{ T}$). Additional features, suggesting cluster glass behavior, are observed at low temperatures and may be the origin of low- T inverse MCE below *ca.* 50 K. Moreover, at temperatures above T_C , additional contribution appearing as a separate peak is visible on $C_P(T, \mu_0 H)$ and $\chi_{AC}(T)$. In TbCo_2 it was detected at around 280 K and can be connected with paramagnetic behavior, which has been observed in other Laves phase compounds already [3].

[1] N. Pierunek *et al.*, IEEE Trans. Magn. 50 (2014) 2506603.

[2] Z. Śniadecki *et al.*, J. Appl. Phys. 115 (2014) 17E129.

[3] J. Herrero-Albillos *et al.*, Phys. Rev. B 76 (2007) 094409.

O6-05**MAGNETIC PHASE DIAGRAMS AND STRUCTURES IN R_2TiIn_8 ($T = Rh, Ir, Co$) AND RELATED TETRAGONAL COMPOUNDS**

P. Javorský¹, P. Čermák², M. Kratochvílová³, J. Zubáč¹, K. Pajskr¹, K. Prokeš⁴ and B. Ouladdiaf⁵

¹Charles University, Faculty of Mathematics and Physics,

Department of Condensed Matter Physics, 12116 Prague 2, The Czech Republic

²Jülich Center for Neutron Science JCNS, FZ Jülich, Outstation at MLZ, Lichtenbergstr. 1, 85747 Garching, Germany

³Center for Correlated Electron Systems, Institute for Basic Science (IBS), Seoul 151-747, Korea

⁴Helmholtz-Centre Berlin for Materials and Energy, SF-2, Glienicker Strasse 100, Berlin 14109, Germany

⁵Institut Laue Langevin, 6 rue Jules Horowitz, BP156, 38042 Grenoble Cedex 9, France

The $R_nT_mX_{3n+2m}$ (R = rare earth or actinide, T = transition metal, X = In or Ga) form a broad family of structurally related tetragonal compounds which is particularly interesting as it involves several archetypal heavy-fermion superconductors based on Ce and also Pu. Most of these compounds order antiferromagnetically. Compounds with magnetic moments oriented along the tetragonal c axis exhibit additional field-induced spin-flip magnetic phase when the magnetic field is applied along the moment direction. There are basically two types of magnetic phase diagram, both contain two phases but differ by the shape of their border. In the case of Nd_2RhIn_8 , we show how the magnetic phase diagram evolves when external pressure is applied.

The magnetic structures exhibit some common features as well. The magnetic structure of the field-induced phase determined in the case of Ho_2RhIn_8 seems to have a general validity in this broad family of materials. We present an overview of magnetic structures determined up to now showing similarities and exceptions, including our recent neutron diffraction studies on Tm_2RhIn_8 .

The RPd_5Al_2 compounds crystallize in the structure which is closely related to that of RTX_5 , member of the above mentioned broad family. Also the magnetic phase diagram of $NdPd_5Al_2$ fits well into the general scheme of this group of compounds.

P6-01**THE MACROSCOPIC AND MICROSCOPIC PROPERTIES STUDY ON CeTIn COMPOUNDS, WHERE $T = \text{Ni, Pd, Pt}$** M.Klicpera^{1,2}, M. Boehm² and P. Javorský¹¹*Charles University in Prague, Faculty of Mathematics and Physics, Department of Condensed Matter Physics, Ke Karlovu 3, 121 16 Prague 2, Czech Republic*²*Institut Laue-Langevin, 71 avenue des Martyrs - CS 20156, 38042 Grenoble Cedex 9, France*

Intermetallic ternary RTX compounds, where R is rare-earth element, T transition element d-metal and X p-metal, crystallizing in hexagonal ZrNiAl -type structure, form a large family of compounds with a variety of interesting and often exotic ground state properties. Most of these compounds order magnetically at low temperatures, often with complex magnetic structures, but there are also some compounds without magnetic transition down to very low temperatures. In the presented study, we present on the electronic properties of CeTIn compounds with $T = \text{Ni, Pd}$ and Pt investigated by both macroscopic (magnetization, specific heat, electrical resistivity) and microscopic (neutron scattering) techniques.

CeNiIn is a valence fluctuator without magnetic order at least down to 50 mK and with Kondo like behavior. Heavy-fermion CePdIn orders antiferromagnetically below 1.8 K and exhibits second magnetic transition at around 0.9 K. CePtIn do not reveal any sign of magnetic order down to 60 mK and behaves in a complex way at low temperatures, i.e. the specific heat strongly increases with decreasing temperature, ranking CePtIn among heavy-fermion compounds. Moreover, a non-Fermi-liquid behavior has been proposed in CePtIn . A dramatic change of the electronic properties in CeTIn compounds with isostructural and isoelectronic Ni-Pd-Pt substitution can be explained by different radii of d-elements rather than by their different character. A tuning of Ni-Pd content in CeTIn allows approaching the physical properties of CePtIn which is documented clearly e.g. on specific heat data: C/T increases logarithmically with decreasing temperature similarly for both CePtIn and $\text{CeNi}_{0.4}\text{Pd}_{0.6}\text{In}$. The crystal field excitations in CePtIn were investigated within our very recent inelastic neutron scattering experiment revealing only one CF excitation at around 10 meV and no other magnetic excitation up to 50 meV. Such a result is somewhat surprising as we expect two CF excitations for this compound; nevertheless, the magnetic specific heat data are fully consistent with this one CF excited doublet scenario.

P6-02**CRYSTAL FIELD IN NdPd_5Al_2 AND ITS INFLUENCE ON MAGNETIC PROPERTIES**J. Zubáč¹, M. Diviš¹, B. Fåk² and P. Javorský¹¹*Charles University, Faculty of Mathematics and Physics,**Department of Condensed Matter Physics, 12116 Prague 2, The Czech Republic*²*Institut Laue-Langevin, 71 avenue des Martyrs, 38000 Grenoble, France*

RPd_5Al_2 compounds (R is rare earth element or actinide) have aroused an interest of scientific community after the discovery of a paramagnetic unconventional heavy-fermion superconductor NpPd_5Al_2 (first Np SC) by Aoki et al. in 2007 [1] followed by reporting of a pressure-induced superconductivity in a Kondo lattice antiferromagnet CePd_5Al_2 [2]. These findings motivated further investigations of isostructural homologues. Nd-based materials, which are generally considered as the nearest magnetic analogues of cerium compounds, are predominantly governed by crystal-field effects and RKKY interactions and can provide useful information about the effect of these phenomena on properties of RPd_5Al_2 and related tetragonal compounds.

We report on crystal field (CF) in NdPd_5Al_2 studied by various methods. The tetragonal CF splits the $^4\text{I}_{9/2}$ ground state of Nd^{3+} ions into 5 Kramers doublets and influences fundamentally the magnetocrystalline anisotropy. We have investigated CF directly by inelastic neutron scattering and observed peaks corresponding to the transitions between CF states in INS spectra. The analysis of the spectra measured at different temperatures leads to the energy-level scheme consisting of five doublets at 0, 3.0, 7.4, 8.6 and 17.1 meV. We confront information about CF obtained by neutron scattering with magnetic and specific heat measurements and with the first principles calculations. Our findings will be also discussed with respect to related tetragonal RPd_5Al_2 , $R_2\text{TX}_8$ and RTX_5 compounds.

[1] D. Aoki et al., J. Phys. Soc. Jpn. 76, 063701 (2007).

[2] F. Honda et al., J. Phys. Soc. Jpn. 77, 043701 (2008).

P6-03**ANOMALOUS HALL EFFECT IN $\text{Ho}_{0.5}\text{Lu}_{0.5}\text{B}_{12}$ ANTIFERROMAGNET WITH CAGE-GLASS CRYSTAL STRUCTURE**

N. E. Sluchanko¹, V. N. Krasnorussky¹, A. V. Bogach¹, V. V. Glushkov^{1,2}, S. V. Demishev^{1,2}, A. L. Khoroshilov², A. V. Dukhnenko³, N. Yu. Shitsevalova³, V. B. Filipov³, S. Gabani⁴, K. Flachbart⁴ and G. E. Grechnev⁵

¹*Prokhorov General Physics Institute of RAS, 38 Vavilov str., Moscow, 119991 Russia*

²*Moscow Institute of Physics and Technology, 9 Institutskii per., 141700, Dolgoprudnyi, Russia*

³*Frantsevich Institute for Problems of Materials Science of NASU, 3 Krzhizhanovskii str., Kiev, 03680 Ukraine*

⁴*Institute of Experimental Physics of SAS, 47 Watsonova str., 040 01 Košice, Slovak Republic*

⁵*Verkin Institute for Low Temperature Physics and Engineering of NASU, 47 Nauky Av., Kharkiv, 61103 Ukraine*

To shed more light on the origin of the anomalous Hall effect (AHE) in antiferromagnetic (AF) metals with frustration-induced, non-collinear magnetic order, it is useful to investigate model compounds with *fcc* crystal structure and different type of disorder in the location of magnetic moments. For our AHE study we have chosen the *fcc* metallic AF solid solution $\text{Ho}_{0.5}\text{Lu}_{0.5}\text{B}_{12}$ with Ho magnetic ions embedded in a rigid covalent boron cage of the dodecaboride lattice. Within this research detailed investigation of resistivity (ρ) and Hall effect (ρ_H) were undertaken on high quality single crystals of $\text{Ho}_{0.5}\text{Lu}_{0.5}\text{B}_{12}$ ($T_N \approx 3.4$ K) both in paramagnetic and AF phases in magnetic field up to 8 T. The acquired anomalous resistivity components $\Delta\rho$ and $\Delta\rho_H^{\text{AHE}}$ demonstrate the scaling behavior $\Delta\rho_H^{\text{AHE}} \sim \Delta\rho^2$ which is typical for the topological Berry-phase induced anomalous Hall effect in strongly disordered *fcc* antiferromagnets [1]. Further analysis allowed us to conclude that the intrinsic, spin-chirality mechanism of AHE may be considered as dominating in the AF state of $\text{Ho}_{0.5}\text{Lu}_{0.5}\text{B}_{12}$, independently of the details of comprehensive non-coplanar spin configurations created by holmium magnetic moments and spin density waves in various AF phases with a multiple-*q* magnetic structure [2-3].

This work was supported by the ERDF EU grant under contract No. ITMS26220120005.

[1] N. Nagaosa, J. Sinova, S. Onoda, et.al., Rev. Mod. Phys. 82, 1539 (2010).

[2] K. Siemensmeyer, K. Babicht, Th. Lonkai, et.al., J. Low Temp. Phys. 146, 581 (2007).

[3] N. E. Sluchanko, A. L. Khoroshilov, M. A. Anisimov, et.al., Phys. Rev. B, 91, 235104 (2015).

P6-04**MAGNETIC ANISOTROPY IN ANTIFERROMAGNET GdB_6**

M. Anisimov¹, V. Glushkov^{1,2}, S. Demishev^{1,2}, N. Samarin¹, A. Bogach¹,
A. Samarin², N. Shitsevalova³, A. Levchenko³, V. Filipov³, S. Gabani⁴,
K. Flachbart⁴ and N. Sluchanko^{1,2}

¹*A.M. Prokhorov General Physics Institute of RAS, Vavilov str. 38,
119991 Moscow, Russia*

²*Moscow Institute of Physics and Technology (State University), Institutskii lane 9,
141700 Dolgoprudny, Moscow region, Russia*

³*I.M. Frantsevich Institute for Problems of Materials Science NASU,
Krzhizhanovskiy str. 3, 03680 Kiev, Ukraine*

⁴*Institute of Experimental Physics of Slovak Academy of Science, Watsonova 47,
040 01 Košice, Slovak Republic*

The antiferromagnet (AF) GdB_6 is characterized by two successive first-order AF transitions into magnetic structures AF(I) and AF(II) (AF(I) ordering appears below $T_{N1} \approx 15$ K, and the AF(II) phase exists at temperatures $T < T_{N2} \approx 5-10$ K) which are still a subject of discussion [1, 2]. To shed more light on the mechanisms responsible for the formation of the unusual AF(II) phase we performed a comprehensive study of magnetoresistance (MR) below T_{N2} in magnetic fields ($\mu_0 H < 8$ T) oriented along the main crystallographic directions $\mathbf{H} \parallel \langle 100 \rangle$, $\langle 110 \rangle$, $\langle 111 \rangle$. The data obtained allow to detect the appearance of a considerable anisotropy of MR in the AF(II) state. In particular, the angular distribution of charge carriers scattering obtained from MR data at $T < T_{N2}$ shows the form of a cross with maxima along the direction $\mathbf{H} \parallel \langle 110 \rangle$ and along the four cavern-satellites (along $\mathbf{H} \parallel \langle 111 \rangle$), the last ones disappear above 5 T. The magnetic H - T phase diagram reconstructed from our data for $\mathbf{H} \parallel \langle 100 \rangle$, $\langle 110 \rangle$ and $\langle 111 \rangle$ contains several additional transitions (1) in the range 0.7–1.7 T only for the direction $\mathbf{H} \parallel \langle 111 \rangle$, and (2) a new phase transition in the range 1.7–5 T for $\mathbf{H} \parallel \langle 111 \rangle$, $\langle 100 \rangle$. The results are discussed in terms of a complex scenario which includes spin-polarons formation in the paramagnetic and in the AF(I) phase of GdB_6 . On the other hand, taking into account the effects observed in the AF(II) phase, we propose the development of a structural instability which leads to possible structural transitions and to anisotropy in the transport characteristics of GdB_6 at $T < T_{N2}$.

This work was supported by the ERDF EU grant under contract No. ITMS26220120005.

[1] M. Amara et al., *Phys. Rev. B* 72, 064447 (2005).

[2] M. Anisimov et al., *Acta Phys. Pol. A* 126, 348 (2014).

P6-05**TRANSPORT PROPERTIES OF DILUTED MAGNETIC HEXABORIDES** **$R_{0.01}La_{0.99}B_6$ ($R = Ce, Pr, Nd, Gd, Eu, Ho$)**

M. Anisimov¹, V. Glushkov^{1,2}, S. Demishev^{1,2}, N. Samarin¹, N. Shitsevalova³,
A. Levchenko³, V. Filipov³, A. Bogach¹, V. Voronov¹, S. Gabani⁴, K. Flachbart⁴
and N. Sluchanko^{1,2}

¹*A.M. Prokhorov General Physics Institute of RAS, Vavilov str. 38,
119991 Moscow, Russia*

²*Moscow Institute of Physics and Technology (State University), Institutskii lane 9,
141700 Dolgoprudny, Moscow region, Russia*

³*I.M. Frantsevich Institute for Problems of Materials Science NASU,
Krzhizhanovskiy str. 3, 03680 Kiev, Ukraine*

⁴*Institute of Experimental Physics of Slovak Academy of Science, Watsonova 47,
040 01 Košice, Slovak Republic*

In this study we present the results of low temperature investigations of the charge transport (resistivity, magnetoresistance) which were carried out on $R_xLa_{1-x}B_6$ ($R = Ce, Pr, Nd, Gd, Eu, Ho$) solid solutions in the regime of isolated magnetic impurity ($x \sim 1\%$).

The data obtained demonstrate a strong increase of resistivity of the $R_{0.01}La_{0.99}B_6$ compounds with the temperature lowering in the range $T < 20$ K. It was found that instead of the logarithmic behavior, predicted by Kondo model, the low temperature magnetic contribution to resistivity obeys the power law $\Delta\rho_m(T) \sim T^{-\alpha}$, which corresponds to the regime of weak localization of charge carriers [1] with critical exponent values $\alpha \approx 0.2$ (Pr, Nd), 0.39 (Ho) and 0.5 (Ce), see [2]. The problem with Kondo-type fitting $\Delta\rho_m(T) \sim -\ln T$ may be recognized also in the data published previously in [3, 4] for $Ce_xLa_{1-x}B_6$ and $Nd_xLa_{1-x}B_6$. The analysis of current data allows to conclude in favor of the formation of many-body spin-polaron states in the vicinity of magnetic rare-earth ions in the LaB_6 matrix.

This work was supported by the ERDF EU grant under contract No. ITMS26220120005.

[1] W.L. McMillan, *Phys. Rev. B* 24, 2739 (1981).

[2] N.E. Sluchanko, M.A. Anisimov et al., *JETP Lett.* 101, 36 (2015).

[3] K. Samwer, *Z. Physik B* 25, 269 (1976).

[4] J. Stankiewicz et al., *Phys. Rev. Lett.* 108, 257201 (2012).

P6-06**ELECTRON SPIN RESONANCE IN PARAMAGNETIC AND ANTI-FERROMAGNETIC STATES OF $\text{Ho}_{0.5}\text{Lu}_{0.5}\text{B}_{12}$**

M. I. Gilmanov^{1,2}, A. V. Semeno², S. V. Demishev^{1,2}, V. V. Glushkov^{1,2},
A. L. Khoroshilov^{1,2}, V. N. Krasnorussky², N. Y. Shitzevalova³, V. B. Filipov³,
K. Flachbart⁴ and N. E. Sluchanko²

¹*Moscow Institute of Physics and Technology, 141700, Institutsky lane., 9, Dolgoprudniy, Russia*

²*General Physics Institute RAS, 119991, Vavilov str., 38, Moscow, Russia*

³*Institute for Problems of Materials Science of National Academy of Sciences of Ukraine, 3 Krzhizhanovskogo Street, 03680 Kiev, Ukraine*

⁴*Institute of Experimental Physics of SAS, 47 Watsonova Street, SK-04001 Kosice, Slovak Republic*

It was shown [1] that the low-temperature negative magnetoresistance in $\text{Ho}_x\text{Lu}_{1-x}\text{B}_{12}$ compounds is attributed to charge-carrier scattering on nanosize magnetic clusters of Ho^{3+} ions with anti-ferromagnetic (AF) exchange inside. Moreover, additional spin polarization in the vicinity of Ho^{3+} ions was found to modify the charge carrier's characteristics. To probe these manybody polarization states it is promising to investigate the effect of electron spin resonance (ESR) in these unusual compounds.

In this contribution we report the first observation of the electron spin resonance in cage-glass compound $\text{Ho}_{0.5}\text{Lu}_{0.5}\text{B}_{12}$ at the frequency $f=60\text{GHz}$. It is shown that the complicated microwave magnetoabsorption signal $(\mu\rho)^{1/2}$ is formed from combination of magnetoresistance $\rho(H)$ and permeability $\mu(H)$, which allows to perform the procedure of its calibration [2].

A broad resonance line with a width of $\Delta w \approx 1\text{T}$ is observed in both paramagnetic and AF phases. The transition from paramagnetic to AF state is characterised by considerable broadening as well as by decreasing of resonance line intensity. It is also remarkable that the g-factor of the observed ESR line is isotropic and equal to $g \approx 4.4$ in both phases, which cannot be described in terms of isolated Ho^{3+} ion response and should be interpreted as an effect of strong electron correlations.

[1] N. E. Sluchanko et. al. Physical review B 91, 235104 (2015).

[2] A. V. Semeno et. al. Physical review B 79, 014423 2009.

P6-07**MAGNETORESISTANCE ANISOTROPY IN HoB₁₂**

A. Khoroshilov^{1,2}, V. Krasnorussky¹, A. Bogach¹, V. Glushkov^{1,2}, S. Demishev^{1,2},
A. Levchenko³, N. Shitsevalova³, V. Filipov³, S. Gabani⁴, K. Flachbart⁴,
K. Siemensmeyer⁵ and N. Sluchanko^{1,2}

¹*A.M.Prokhorov General Physics Institute of RAS, 119991 Moscow, Russia*

²*Moscow Institute of Physics and Technology, Moscow Region 141700 Russia*

³*Institute for Problems of Materials Science, NASU, 03680 Kiev, Ukraine*

⁴*Institute of Experimental Physics of SAS, 040 01 Košice, Slovak Republic*

⁵*Hahn Meitner Institut Berlin, D 14109 Berlin, Germany*

We report results of transverse magnetoresistance (MR) $\Delta\rho/\rho(T, H, \varphi)$ measurements carried out on high quality single crystals of Ho¹¹B₁₂ at temperatures 1.9-300 K, in magnetic field up to 80 kOe, and for angles $\varphi = 0 - 360^\circ$ between the magnetic field direction and sample surface $\mathbf{n} \parallel \langle 110 \rangle$.

The obtained results demonstrate a strong anisotropy of MR in the antiferromagnetic (AF) state. It was shown that the anisotropic picture of MR $\Delta\rho/\rho(H, \varphi)$ presented in polar coordinates (H, φ) has a fourfold symmetry.

A comprehensive analysis of MR derivations $d[\Delta\rho/\rho(H, \varphi)]/dH$ allowed us to reconstruct the complex AF phase diagram and to characterize the angle-field areas which correspond to different regimes of charge carriers scattering. In particular, it was shown that in low fields $H \leq 20$ kOe and for all \mathbf{H} directions the positive linear magnetic contribution to MR $\Delta\rho/\rho = A \cdot H$ dominates, which is connected with charge carriers scattering on spin density waves (SDW). However, at fields $H > 20$ kOe the MR behavior becomes strongly anisotropic. At angles $\langle 100 \rangle \pm 36^\circ$ and in the range of $H \sim 20-40$ kOe the SDW contribution still dominates, but it exhibits smaller values of the A coefficient. For $\mathbf{H} \sim 40-50$ kOe and for directions in the interval $\langle 111 \rangle - 18^\circ \div \langle 111 \rangle + 36^\circ$ negative magneto-resistance prevails in the SDW contribution, but in the range $\langle 110 \rangle \pm 10^\circ$ SDW scattering still dominates. At even higher fields up to the AF-paramagnetic phase boundary and for directions $\langle 100 \rangle \pm 36^\circ$ a coexistence of two components - a positive linear and a negative quadratic ($-\Delta\rho/\rho = B \cdot H^2$) is observed.

The data obtained are analyzed and compared both with results of magnetic neutron scattering experiments and angular dependences of magnetization of Ho¹¹B₁₂.

This work was supported by the ERDF EU grant under contract No. ITMS26220120005.

P6-08**GLASS FORMING ABILITIES AND CRYSTALLIZATION PROCESS IN AMORPHOUS Pr-Fe-Co-Zr-Nb-B ALLOYS OF VARIOUS B CONTENTS**K. Pawlik¹, P. Pawlik¹ and J. J. Wysocki¹¹*Institute of Physics, Czestochowa University of Technology, Al. Armii Krajowej 19, 42-200 Czestochowa, Poland*

The influence of boron contents on the glass forming abilities and magnetic properties of melt-spun ribbon samples produced for $\text{Pr}_9\text{Fe}_{50+x}\text{Co}_{13}\text{Zr}_1\text{Nb}_4\text{B}_{23-x}$ ($x=0, 2, 5, 8$) alloys, were investigated. For all compositions, the rapidly solidified samples were fully amorphous, which was confirmed by XRD and Mössbauer spectroscopy. DSC and DTA studies revealed good glass forming abilities for all investigated specimens and allowed to determine thermal stability parameters of the amorphous phase. For all alloy ribbons, very large supercooled liquid region before crystallization ΔT_x reaching 100K was measured. Kissinger plots were constructed to determine the activation energies for crystallization. Annealing of specimens at temperatures from 923K to 1033K for 5 min, resulted in significant change of the phase constitution. The XRD studies have shown presence of hard magnetic $\text{Pr}_2\text{FeCo}_{14}\text{B}$ and paramagnetic $\text{Pr}_{1+x}\text{Fe}_4\text{B}_4$ phases. For $x=0, 5$ and 8 alloy ribbons annealed at temperatures higher than 1000K, the secondary crystallization of α -(Fe,Co) phase occurs. This is in a good agreement with DSC results. Anomaly of both thermal and magnetic properties was observed for the $\text{Pr}_9\text{Fe}_{52}\text{Co}_{13}\text{Zr}_1\text{Nb}_4\text{B}_{21}$ alloy ribbons.

P6-09**INFLUENCE OF PRESSURE ON THE ELECTRIC TRANSPORT PROPERTIES OF CARBON-DOPED EuB_6** G. Pristáš¹, S. Gabáni¹, I. Baťko¹, M. Baťková¹, V. Filipov² and E. Konovalova²¹*Institute of Experimental Physics, Slovak Academy of Sciences, Watsonova 47, 040 01 Košice, Slovakia*²*Institute for Problems of Material Science, National Academy of Sciences of Ukraine, Kiev, Ukraine*

EuB_6 reveals ferromagnetic order and metal-insulator transition at $T_c=12.6$ K. Due to very low number of intrinsic charge carriers, even a small doping with carbon can drastically modify the electric and magnetic properties of this compound. In this work we have studied influence of hydrostatic pressure on the electrical resistivity of $\text{EuB}_{5.99}\text{C}_{0.01}$ with $T_c=3.9$ K, which is intrinsically inhomogeneous due to fluctuations of carbon content. We observed shift of low-temperature resistivity maximum from 4.6 K (at 1 bar) to 5.2 K (at 30.3 kbar) with increasing value of the applied pressure. The maximum in $dp/dT(T)$ (which reveals temperature of bulk ferromagnetic ordering) does not change the position within experimental resolution. This behavior is different from stoichiometric EuB_6 , where the pressure increases the FM ordering temperature. The origin of this discrepancy is in increasing of volume fraction of the phase that is not compatible with ferromagnetic ordering with increasing pressure. Our results support the picture that carbon-rich regions play a role of "spacers", which prevent a percolation of the ferromagnetic phase [1]. The magnetoresistance has been measured between 1.5 K and 30 K. With increasing value of applied magnetic field the resistivity is monotonically decreasing. Above 1 T we have observed transition to "metallic" behavior.

This work was supported by project No. EU ERDF-ITMS 26220120005.

- [1] M. Baťková, I. Baťko, K. Flachbart, Z. Janu, K. Jurek, J. Kováč, M. Reiffers, V. Sechovský, N. Shitsevalova, E. Šantavá, J. Šebek, Phys. Rev. B 78, 224414-1 (2008).

P6-10**PREPARATION AND BASIC PHYSICAL PROPERTIES OF YbT_2X_2 ($\text{T} - \text{Pd, Au}$; $\text{X} - \text{Si, Ge}$) COMPOUNDS**J. Kaštil¹, K. Vlášková², J. Prchal², M. Mišek¹, J. Kamarád¹ and Z. Arnold¹¹*Institute of Physics ASCR, v.v.i., Na Slovance 2, Prague, Czech Republic*²*Charles University in Prague, Faculty of Mathematics and Physics, Prague, Czech Republic*

The research of strongly correlated electron systems is very lively topic in present-day condensed matter physics. The interest is driven by number of discoveries of new exotic phenomena. CeAu_2Si_2 and YbRh_2Si_2 are two examples of recently studied compounds with the same structure as YbT_2X_2 showing extraordinary properties. CeAu_2Si_2 orders magnetically below 10 K and simultaneously the external hydrostatic pressure above 12 GPa leads to appearance of superconductivity [1]. The region of coexistence of magnetic order and superconductivity is several GPa wide. YbRh_2Si_2 is heavy fermions compound very near to a QCP which can be reached by magnetic field of 0.06 T [2]. The intermediate valence state of Yb can lead to complex behavior of magnetic properties under extreme hydrostatic pressure and magnetic field. In present work we focused on three isostructural candidates YbPd_2Si_2 , YbPd_2Ge_2 and YbAu_2Si_2 where we expect formation of magnetic ordering and complex behavior of physical properties under extreme hydrostatic pressure. The selected intermetallic compounds form naturally layered tetragonal structure of ThCr_2Si_2 type. We prepared samples of the compounds and performed the basic characterization of their properties. The flux growth method was used to successfully prepare the singlecrystals of YbPd_2Si_2 and YbPd_2Ge_2 . The samples of YbPd_2Si_2 were of sufficient size and quality to perform first measurements. The heat capacity was measured in temperature range from 0.35 K to 300 K in several magnetic fields. Below 2 K the $C/T(T)$ dependence showed an increase with decreasing temperature. The $\gamma = 140 \text{ mJ} \cdot \text{mol}^{-1} \cdot \text{K}^{-2}$ was determined by extrapolation of $C/T(T)$ to zero temperature. Magnetization was measured in temperature range from 1.9 K to 200 K in different magnetic field and hydrostatic pressures up to 0.8 GPa. The dc-susceptibility was decreasing with increasing temperature until it reached minimum at 10 K and then we observed a maximum at 69 K. Analysis of the magnetic properties showed decreasing valence of Yb from 2.8 to 2.6 with respect to temperature.

[1] Z. Ren et al., Physical Review X 4 (2014) 031055.

[2] H. Pfau et al., Nature 484 (2012) 493-497.

P6-11**CHARGE TRANSPORT AND MAGNETISM IN $\text{Tm}_{0.03}\text{Yb}_{0.97}\text{B}_{12}$**

V. Glushkov¹, A. Azarevich¹, M. Anisimov¹, A. Bogach¹, S. Demishev¹,
A. Dukhnenko², V. Filipov², K. Flachbart³, S. Gabáni³, S. Gavrilkin⁴,
N. Shitsevalova² and N. Sluchanko¹

¹*Prokhorov General Physics Institute of RAS, Vavilov str. 38, Moscow 119991 Russia*

²*Frantsevich Institute for Problems of Materials Science NAS, Krzhizhanovsky str. 3, Kiev 03680 Ukraine*

³*Institute of Experimental Physics, Slovak Academy of Sciences, Watsonova 47, 040 01 Košice, Slovak Republic*

⁴*Lebedev Physical Institute of RAS, Leninskii pr. 53, Moscow 119991 Russia*

Substitution of Tm with Yb in $\text{Tm}_{1-x}\text{Yb}_x\text{B}_{12}$ initiates a metal-insulator transition from the antiferromagnetic metal TmB_{12} to the narrow gap semiconductor YbB_{12} ($\varepsilon_g \approx 18$ meV) [1]. The suppression of long range magnetic order at $x_c \approx 0.7$ is followed by a strong renormalization of the $\text{Tm}_{1-x}\text{Yb}_x\text{B}_{12}$ band spectrum. The corresponding many-body resonance ($\Delta \approx 6$ meV), which appears at the Fermi level, is characterized by a large effective mass of charge carriers ($m_{\text{eff}} \approx 24m_0$, m_0 - free electron mass) [1-2]. This transformation induces also a rise of the Seebeck coefficient, which changes from $S = -2 \mu\text{V/K}$ (for TmB_{12}) up to $S = -230 \mu\text{V/K}$ (for $\text{Tm}_{0.2}\text{Yb}_{0.8}\text{B}_{12}$) [1]. However, the range of ytterbium rich solid solutions $\text{Tm}_{1-x}\text{Yb}_x\text{B}_{12}$ ($0.8 < x < 1$) stays to be unexplored up to now.

Here we report the transport and magnetic properties of polycrystalline $\text{Tm}_{0.03}\text{Yb}_{0.97}\text{B}_{12}$ samples measured at temperatures 1.8 - 300 K in magnetic fields up to 9 T. The maximum of magnetic susceptibility found at 50 K is shown to be induced by the spin gap $\Delta = 9.2$ meV, which equals approximately to the activation energy of Hall constant ($E_H \approx \varepsilon_g/2$) in the intrinsic conductivity range ($T > 100$ K). The large diffusive thermopower $S = AT$, $A = -29 \mu\text{V/K}^2$ found below 10 K and the magnetic susceptibility divergence $\chi \sim T^{-\alpha}$ ($\alpha \approx 0.63$) seem to be associated with the narrow many-body resonance. The estimated relaxation time of charge carriers ($\tau \sim 0.6$ ps) was found to agree with the inverse valence fluctuation rate in YbB_{12} ($\tau \sim 0.4$ ps) [3] that requires a correct consideration of the 4f-5d hybridization effects in the ground state of the Yb-rich compounds.

The financial support from RFBR project 15-02-03166 is acknowledged.

[1] N. E. Sluchanko et al., JETP Lett., 89, 256 (2009).

[2] A. V. Bogach et al., JETP, 116, 838 (2013).

[3] P. A. Alekseev et al., Phys. Rev. B, 89, 115121 (2014).

P6-12**X-RAY DIFFRACTION STUDY OF $\text{CeT}_2\text{Al}_{10}$ ($T = \text{Ru, Os}$) AT LOW TEMPERATURE AND UNDER PRESSURE**

Y. Kawamura¹, J. Hayashi¹, K. Takeda¹, C. Sekine¹, T. Tanida², M. Sera², S. Nakano³, T. Tomita⁴, H. Takahashi⁵ and T. Nishioka⁶

¹*Muroran Institute of Technology, Muroran, Hokkaido 050-8585, Japan*

²*Hiroshima University, Higashi-Hiroshima, Hiroshima 739-8530, Japan*

³*National Institute for Materials Science, Tsukuba, Ibaraki 305-0044, Japan*

⁴*ISSP, University of Tokyo, Kashiwa, Chiba 277-8581, Japan*

⁵*Nihon University, Sakurajosui, Setagaya, Tokyo 156-8550, Japan*

⁶*Kochi University, Kochi 780-8520, Japan*

The orthorhombic $\text{YbFe}_2\text{Al}_{10}$ -type $\text{CeRu}_2\text{Al}_{10}$ and $\text{CeOs}_2\text{Al}_{10}$ show a unique antiferromagnetic transition at $T_N \sim 27$ K and $T_N \sim 29$ K, respectively [1, 2]. When the de Gennes law is applied to $\text{RT}_2\text{Al}_{10}$ ($R = \text{rare earth}, T = \text{Ru, Os}$) system, the T_N of $\text{CeRu}_2\text{Al}_{10}$ and $\text{CeOs}_2\text{Al}_{10}$ are over 100 times higher than that would be expected. Although the driving force of this high T_N is proposed from standpoints of both experiment and theory, it has not clarified yet. One proposed idea is CDW transition induce this high T_N . In general, CDW transition is induced by structural transition or modification. In addition, T_N of $\text{CeRu}_2\text{Al}_{10}$ and $\text{CeOs}_2\text{Al}_{10}$ abruptly disappears at a critical pressure $P_C \sim 4$ GPa and 2.5 GPa, respectively [2,3]. Thus, there is a possibility of structural transition or modification at P_C or T_N . The purpose of this study is to investigate around P_C or T_N from structural point of view. The experiment under pressure is performed by diamond anvil pressure cell. A mixture of methanol and ethanol in a ratio of 4:1 was used as a pressure-transmitting medium. Synchrotron X-ray diffraction study at low temperature and under pressure was performed by GM refrigerator installed at BL-18C of Photon Factory at KEK in Tsukuba.

Both $\text{CeRu}_2\text{Al}_{10}$ and $\text{CeOs}_2\text{Al}_{10}$ do not have peak appearance or annihilation between P_C or T_N . That means there is no structural change. In addition, the lattice parameters monotonically decrease with pressure; There is no structural deformation in this experimental accuracy. We have evaluated the bulk modulus of $\text{CeT}_2\text{Al}_{10}$ ($T = \text{Fe, Ru, Os}$). The bulk modulus of $\text{CeFe}_2\text{Al}_{10}$ is smallest in spite of the lattice constant is smallest among $\text{CeT}_2\text{Al}_{10}$. This is because transition metal is the essential factor to decide the hardness in $\text{CeT}_2\text{Al}_{10}$.

[1] A. M. Strydom, *Physica B* 404, 2981 (2009).

[2] T. Nishioka, et al., *J. Phys. Soc. Jpn.* 78, 123705 (2009).

[3] K. Umeo, et al, *J. Phys. Soc. Jpn.* 80, 064709 (2011).

P6-13**SPECIFIC HEAT STUDY ON $\text{CeCu}_x\text{Al}_{4-x}$ AND $\text{Ce}_x\text{La}_{1-x}\text{CuAl}_3$ COMPOUNDS**K. Vlášková¹, M. Klicpera² and P. Javorský¹¹*Department of Condensed Matter Physics, Charles University in Prague, Ke Karlovu 5, 121 16 Prague 2, Czech republic*²*Institut Laue-Langevin, 71 Avenue des Martyrs – CS 20156, 38042 Grenoble Cedex 9, France*

CeCuAl_3 crystallizes in the tetragonal BaNiSn_3 -type structure and orders antiferromagnetically below $T_N = 2.7$. The magnetic behavior of CeCuAl_3 is generally discussed as a result of the interplay between the RKKY and Kondo interaction. The magnetic properties are also influenced by the low-lying first excited crystal field (CF) level. Highly interesting phenomenon was revealed by inelastic neutron scattering experiments: the spectra of CeCuAl_3 showed an additional peak beside two peaks which are ascribed to CF energy transitions. This peak could have his origin in a strong magneto-elastic coupling, so called vibron state.

In this work, we investigate the influence of two different substitutions on the magnetic and structural properties of CeCuAl_3 . In the $\text{CeCu}_x\text{Al}_{4-x}$ compounds we can tune the properties of lattice and influence the phonon excitations, as well as modify the local surroundings of Ce^{3+} ions and hence affect CF. We have prepared polycrystalline samples with $x = 0.95$ and $x = 1.05$. The analysis of the heat capacity data allows us to extract the magnetic contribution and to determine CF energy levels. We have also prepared $(\text{Ce}_x\text{La}_{1-x})\text{CuAl}_3$ series in the whole concentration range and performed the heat capacity measurements. The magnetic order is gradually suppressed by La substitution as expected. We followed the development of magnetic contribution to specific heat and the first excited CF level. In the low-cerium concentrations where no transition is observed we obtained the pure Schottky contribution.

P6-14**VARIATIONS OF ANTIFERROMAGNETISM IN UIrGe IN MAGNETIC FIELDS AND EXTERNAL PRESSURES**M. Vališka¹, J. Prchal¹ and V. Sechovský¹¹*Department of Condensed Matter Physics, Faculty of Mathematics and Physics, Charles University, Ke Karlovu 5, CZ-12116 Prague 2, Czech Republic*

UIrGe is one of the UTX (T = transition metal, X = p-electron element) compounds crystallizing in the orthorhombic TiNiSi-type structure. It has been found antiferromagnetic (AF) below the Néel temperature $T_N \sim 16$ K [1]. The strongly reduced U magnetic moments ($0.36 \mu_B$ at 1.8 K) form a non-collinear AF structure with a non-zero hard-axis AF component [2]. Application of a magnetic field H along the c -axis leads to a metamagnetic transition (MT) with a critical field $\mu_0 H_c \sim 14$ T at 2 K [3]. The AF structure is consequently destroyed and all the U moments ($0.38 \mu_B$ at 2 K) point along the field direction [4]. A similar MT is induced in $\mu_0 H_c \sim 21$ T applied along the b -axis [3].

We have grown a new UIrGe single crystal and measured on it the magnetization (M), specific heat (C_p), electrical resistivity/magnetoresistance (ρ) (both for current i along the main crystallographic axes a , b and c , respectively), thermal expansion/magnetostriction, linear - $\Delta L/L$, volume - $\Delta V/V$ (both along a , b and c , respectively) with respect to temperature T and H applied along a , b and c , respectively, in longitudinal and transversal geometry, respectively.

Character of anomalies in temperature and magnetic-field dependences of the electrical resistivity accompanying the magnetic phase transitions at T_N and $\mu_0 H_c$, respectively, will be discussed considering the symmetry of the AF structure and its impact on the topology of Fermi surface reconstruction (gap formation near T_N reflecting the propagation vector of the emerging AF structure and gap modification/removal due to the AF structure destruction near $\mu_0 H_c$).

The relevant experimental data near the magnetic phase transitions will be analyzed by means of Ehrenfest relations and predictions concerning pressure dependence of T_N will be drawn. Validity of these predictions will be discussed in the light of results of direct measurements of the crystal subjected to external hydrostatic pressure.

[1] V. Sechovský, L. Havela, in: K.H.J. Buschow (Ed.), Handbook of Magnetic Materials, vol. 11, North Holland, Amsterdam, 1998, p. 1 and references therein.

[2] K Prokeš et al., Physica B 350 (2004) e199.

[3] S. Yoshii, J. Phys. Conf. Ser. 51 (2006) 151.

[4] K Prokeš et al., J. Phys.: Condens. Matter 20 (2008) 104221.

P6-15**EFFECT OF SOLVENTS ON MAGNETIC PROPERTIES OF METAL-ORGANIC FRAMEWORK MOF-76(Gd)**M. Almáši¹, V. Zeleňák¹ and A. Zeleňáková²¹*Department of Inorganic Chemistry, P.J. Šafárik University, Moyzesova 11, SK-04154 Košice, Slovak Republic*²*Department of Solid State Physics, P.J. Šafárik University, Park Angelinum 9, SK-04154 Košice, Slovak Republic*

The assembly of organic molecules and metal ions may yield novel types of three-dimensional networks that contain channels with various sizes and shapes and which are denoted as metal-organic frameworks (MOFs). MOFs represent an interesting class of crystalline hybrid inorganic-organic porous materials, which have attracted a great deal of research interest due to their promising applications in the fields like gas storage and separation, catalysis, magnetism and others.

MOF-76 represents a large family of compounds, which consists of predominantly lanthanide ions and benzene-1,3,5-tricarboxylate linker (BTC). These 3D transformable frameworks exhibit permanent porosity and extremely high thermal stability. In our previous work, we have investigated stability and applications of MOF-76 containing Ce(III), Ho(III), Tm(III) and Lu(III) ions. Here we continue in our research with gadolinium form namely, $\{[\text{Gd}(\text{BTC})(\text{H}_2\text{O})]\cdot\text{DMF}\}_n$. The framework contain approximately $6.7 \times 6.7 \text{ \AA}^2$ sinusoidally shaped channels propagating along the *c* crystallographic axis. The channels are filled with DMF molecules, which could be removed by the thermal treatment. The shortest distance between two Gd(III) atoms in the helical strands is 4.723 Å (1), while shortest distance between Gd(III) atoms within the frameworks is 8.005 Å.

It is well known, that magnetic exchange interactions are traditionally established through direct and super-exchange mechanisms between metal centers or metal centers and various ligands. The exchange interactions can also occur through intermolecular hydrogen bonds. We have investigated magnetic properties of three samples: as synthesized (containing DMF in the cavity system), activated (without solvent) and water exchanged MOF-76(Gd). We have studied the effect of solvent on their magnetic properties using a SQUID based magnetometer in external *dc* field up to 5 T in the temperature range of 2 - 300 K. Obtained results will be presented and explained.

This work was supported by the Slovak Research and Development Agency under contract No. APVV-0073-14.

P6-16**CHARACTERIZATION OF NEW UNiX₂ SPLATS AND STUDY OF THEIR PHYSICAL PROPERTIES**Z. Molcanova¹, M. Mihalik¹, M. Mihalik jr.¹, M. Paukov² and L. Havela²¹*Institute of Experimental Physics, SAS, Watsonova 47, 040 01 Košice, Slovakia*²*Department of Condensed Matter Physics, Charles University, Ke Karlovu 5, 121 16 Prague 2, Czech Republic*

We explored crystal structure, magnetic and transport properties of UNiX₂ (X = Ge, Si) materials prepared by a conventional metallurgical technique and by rapid solidification – splat cooling. The samples were prepared by arc melting in argon atmosphere and subsequently processed in a high-vacuum splat cooler. The splat cooling technique can facilitate stabilization of the polymorphous modifications. Our quenched UNiGe₂ sample contained also significant amount of amorphous phase.

Although RNiX₂ (R = U and Ce, X = Si and Ge) compounds do not melt congruently, CeNiGe₂ and UNiSi₂ single crystals can be grown by the Czochralsky method from Ge- or Si- rich precursor [1]. Any UNiGe₂ sample has been not prepared till now. RNiX₂ crystallizes in orthorhombic CeNiSi₂-type layered structure, which is constructed from deformed fragments of the CeGa₂Al₂ and α -ThSi₂ structures. UNiSi₂, which orders ferromagnetically at $T_C = 95$ K, displays the anisotropic behaviour of the magnetization. The easy magnetization direction is in the *ac* plane. From the result of the magnetic susceptibility along the *ac* plane, the effective magnetic moment is obtained to be $\mu_{\text{eff}} \sim 2.47\mu_B$, which is larger than that of polycrystalline sample, $\mu_{\text{eff}} \sim 1.9\mu_B$ [2]. We did not find any report on UNiGe₂ in the literature but UNiGe (TiNiSi type of crystal structure) has been studied [3]. This compound is antiferromagnetic below $T_N \approx 50$ K and we expect that UNiGe₂ if exists, is magnetic, too.

In summary, we prepared new intermetallic compound UNiGe₂ and as well as already known UNiSi₂ by splat cooling and we studied their physical properties with particular emphasis on transport and magnetic properties. In the case of UNiSi₂ we compare our results with results obtained on polycrystalline and single crystalline samples and in the case of UNiGe₂ our study represents new original contribution to the subject.

This work was supported by the project ERDF EU, No. ITMS26220120005.

[1] Ohashi, M. et al.: J. Phys. Soc. Jpn. Vol. 75, Suppl. (2006) 124–126.

[2] Kaczorowski, D. et al.: Solid State Communications, Vol. 99, No. 12, (1996) 949-953.

[3] Adamska, M. et al.: JMMM, 323 (2011) 3217–3222.

P6-17**MAGNETIC PROPERTIES OF A DyCo₂ CRYSTAL**J. Prchal¹, V. Latoňová¹, M. Kratochvílová¹ and V. Sechovský¹*Charles University in Prague, Faculty of Mathematics and Physics, Department of Condensed Matter Physics, Ke Karlovu 5, 121 16 Praha 2, Czech Republic*

DyCo₂ is a member of a group of compounds crystallizing in the cubic MgCu₂-type Laves phase. It is interesting for the presence of two magnetic sublattices of different character of magnetic moment – localized and itinerant – coming from the Dy and Co sublattice, respectively. Most of the RECo₂ compounds (RE = rare-earth element) were studied in the past in the form of polycrystalline samples, including DyCo₂. We succeeded to grow a high-quality crystal of DyCo₂ and performed a systematic study of its bulk properties – electric resistivity, magnetization, magnetic susceptibility and specific heat – with respect to orientation of magnetic field along different crystallographic directions. These measurements confirmed a first-order magnetic transition at the Curie temperature $T_C = 142\text{K}$, what is a bit higher than for the polycrystalline sample ($T_C^{\text{poly}} = 136\text{K}$). From magnetization curves the easy [100] and the hard axis [111] were determined. Measurements of the AC-magnetic susceptibility in the paramagnetic area performed in order to check the presence of the so called paramagnetism did not show any anomaly that had been observed on polycrystalline samples – similar to other single crystals [1].

[1] F. Bartolomé, C.M. Bonilla, J. Herrero-Albillos et al., *Eur. Phys. J. B* 86 (2013) 489.

P6-18**EXPERIMENTAL STUDY OF PHYSICAL PROPERTIES OF NEW $\text{Gd}_{1-x}\text{Ce}_x\text{Ni}_5$ SYSTEM**A. Džubinská¹, M. Reiffers¹, J. I. Espeso² and J. Rodríguez Fernández²¹*Faculty of Humanities and Natural Sciences, Prešov University, 081 16 Prešov, Slovakia*²*Departamento CITIMAC, Universidad de Cantabria, 39005 Santander, Spain*

GdNi_5 is known as ferromagnetic compound $T_C = 31.8$ K. CeNi_5 is the well-known spin fluctuation compound without magnetic ordering up to lowest temperatures. In order to study the influence of different rare-earths on ground state connected with spin fluctuation we have been prepared new system of $\text{Gd}_{1-x}\text{Ce}_x\text{Ni}_5$ polycrystalline samples with concentration $x = 0; 0.2; 0.5$ and 0.8 . We performed RXD study, which confirm the hexagonal crystal structure and single phase samples. The measurement of magnetic properties ($M(T)$, $M(B)$) showed that increasing content of Ce depresses the transition temperature T_C to 2 K for $x = 0.8$. Heat capacity measurements confirmed these results. The Sommerfeld coefficient γ determined for all samples order of $\sim 100 \text{ mJ} \cdot \text{mol}^{-1} \cdot \text{K}^{-2}$. However, the application of magnetic field depresses in all cases the γ value to the order of $\sim 30 \text{ mJ} \cdot \text{mol}^{-1} \cdot \text{K}^{-2}$, which is the value typical for normal metals. This is confirmation of rather important magnetic contribution to the heat capacity, which still presented 2 K. Therefore, it is necessary to measure heat capacity at lower temperatures.

P6-19**MAGNETORESISTANCE OF THE $\text{CeCo}_{1-x}\text{Fe}_x\text{Ge}_3$ ALLOYS**P. Skokowski¹, K. Synoradzki¹ and T. Toliński¹*Institute of Molecular Physics, Polish Academy of Sciences,
ul. Smoluchowskiego 17, 60-179 Poznań, Poland*

A transition from CeCoGe_3 to the CeFeGe_3 compound, i.e. the $\text{CeCo}_{1-x}\text{Fe}_x\text{Ge}_3$ series has been studied by magnetoresistance measurements. CeCoGe_3 shows a complicated magnetic structure with three antiferromagnetic phase transitions at $T_{N1} = 21$ K, $T_{N2} = 12$ K, and $T_{N3} = 8$ K [1]. CeFeGe_3 is a non-magnetic heavy fermion with high Kondo temperature (over 100 K) [2]. Our X-ray diffraction studies have shown that all the studied compounds are isostructural, single phase, and crystallize in the tetragonal BaNiSn_3 -type structure without inversion symmetry. The 3d elements are nonmagnetic in these alloys and the magnetic moment is mainly due to the Ce ions. Previously, it was reported that at the concentration $x \approx 0.6$ the system is in the vicinity of the quantum critical point (QCP) [3,4]. In the present research we have performed the isothermal magnetoresistivity investigations (down to 2 K) on polycrystalline samples with $x = 0.3, 0.4$, and 0.6 to gain further insight into the possible existence of QCP in the $\text{CeCo}_{1-x}\text{Fe}_x\text{Ge}_3$ series. The temperature and magnetic field dependences of the magnetoresistance are analyzed and discussed in frames of the appropriate models.

[1] K. Kaneko et al., Journal of Physics: Conference Series 150, 042082 (2009).

[2] H. Yamamoto et al., Phys. Lett. A 196, 83 (1994).

[3] S.N. de Medeiros et al., J. Magn. Magn. Mater. 226-230, 152 (2001).

[4] S.L. Bud'ko et al., Physica B 259-261, 118 (1999).

P6-20**CRYSTAL STRUCTURE AND PHYSICAL PROPERTIES OF THE NOVEL Eu COMPOUNDS**I. Čurlík¹, F. Gastaldo², M. Giovannini², A. M. Strydom³ and M. Reiffers¹¹*Faculty of Humanities and Natural Sciences, University of Prešov,**17. novembra 1, SK-081 16 Prešov, Slovakia*²*Department of Chemistry, University of Genova, Via Dodecaneso 31,**I-16146 Genova, Italy*³*Highly Correlated Matter Research Group, Department of Physics,**University of Johannesburg, South Africa*

New intermetallic compounds based on the rare-earth element Eu have been synthesized – $\text{Eu}_3\text{Pd}_2\text{Sn}_2$, EuPd_2Sn_4 , and EuPdSn_2 . The pure elements have been weighed in the stoichiometric ratio inside a glove box, in order to avoid Eu oxidation, and closed in a Ta crucible. Afterwards, all the compounds have been synthesized by induction melting and their crystal structure was established by X-ray powder diffraction. All the three compounds were found to crystallize in orthorhombic lattices.

In this work we present the first results of the magnetic properties, electrical resistivity and heat capacity measurements for these compounds.

The temperature dependent susceptibility $\chi(T)$ is found to follow the Curie-Weiss law above 50 K, 25 K and 20 K; with a paramagnetic temperature value $\theta_P = -5.1$ K, 5.5 K, 13 K; for $\text{Eu}_3\text{Pd}_2\text{Sn}_2$, EuPd_2Sn_4 , EuPdSn_2 , respectively. The values of the effective magnetic moment for all three compounds are very close to the theoretical free-ion value for Eu^{2+} .

Concerning the magnetic properties, for these Eu based compounds an antiferromagnetic transition was observed in all three cases. In addition, in EuPd_2Sn_4 and EuPdSn_2 compounds also the ferromagnetic type of interaction is present (indicated also from the sign of the paramagnetic temperatures θ_P), which is manifested more intensively with applied external magnetic field. The measurements of specific heat $C_p(T)$ and electrical resistivity $\rho(T)$ fully confirm this scenario.

P6-21**CROSSOVER BETWEEN FERMI-LIQUID AND NON-FERMI-LIQUID IN $\text{Th}_{1-x}\text{U}_x\text{Be}_{13}$ ($0 \leq x \leq 1$)**

N. Miura¹, K. Uhlířová², Jiří Prchal², C. Tabata¹, V. Sechovský², H. Hidaka¹,
T. Yanagisawa¹ and H. Amitsuka¹

¹*Graduate School of Science, Hokkaido University, Sapporo, Japan*

²*Faculty of Mathematics and Physics, Charles University, Prague, Czech Republic*

Physics of the first discovered U-based heavy-fermion superconductor [1], UBe_{13} ($T_c \sim 0.8$ K, $\gamma \sim 1000$ mJmol⁻¹K⁻²), remains among the main topics of condensed matter research. This compound exhibits anomalous “Non-Fermi-liquid” (NFL) state above T_c , whose origin could be crucial to understand the unconventional superconductivity of this system. Our previous studies on the diluted magnetic system $\text{Th}_{1-x}\text{U}_x\text{Be}_{13}$ ($x \leq 0.11$) revealed that the low-temperature properties in the dilute U limit is described as Fermi liquid (FL), and imply that the anomalous NFL state in the pure UBe_{13} could be attributed to a quantum criticality due to the competition between the crystalline-electric-field singlet state versus the Kondo-Yosida singlet state [2,3]. In order to see how the low-temperature state changes from FL to NFL with x , we have performed magnetic susceptibility (χ), specific heat (C), and electric resistivity (ρ) measurements on the $\text{Th}_{1-x}\text{U}_x\text{Be}_{13}$ single crystals in the entire range of U concentration $0 \leq x \leq 1$. The obtained Weiss temperature derived from fitting the high-temperature susceptibility data by Curie-Weiss law is negative for the whole range of x and its absolute value increases with increasing x . The electronic specific-heat coefficient at low temperature also increases monotonically with increasing x . Interestingly, the characteristic temperature of the Fermi-liquid state estimated from $\chi(T)$ and $\rho(T)$ data decreases continuously and monotonically with increasing x , and vanishes above $x^* \sim 0.8$, where the NFL behavior becomes obvious in $C/T(T)$ and $\rho(T)$ dependences. These results strongly suggest that a crossover of the low- T state between FL and NFL occurs around x^* . The origin of the anomalous metallic state in UBe_{13} from the aspect of the x variations of single U-site effects, U-U inter-site correlations, lattice parameters, etc. will be discussed.

[1] H. R. Ott, H. Rudigier, Z. Fisk, and J. L. Smith, PRL 50, 1595 (1983).

[2] S. Yotsushashi, K. Miyake, and H. Kusunose, JPSJ 71, 389 (2002).

[3] N. Miura, C. Tabata, S. Mombetsu, S. Yamazaki, Y. Shimizu, H. Hidaka, T. Yanagisawa, and H. Amitsuka, to be published in JPSJ.

P6-22**HALL COEFFICIENT IN TOROIDAL MAGNETIC ORDERED STATE OF UNi₄B**H. Saito¹, N. Miura¹, C. Tabata¹, H. Hidaka¹, T. Yanagisawa¹ and H. Amitsuka¹¹*Graduate School of Science, Hokkaido University, N10W8, Sapporo, Japan*

Toroidal moment is one of the parameters which describe the strength of the magnetoelectric coupling. In the last several years, the toroidal order, which is the ordered periodic array of toroidal moments, has attracted much interest in connection with insulators called multiferroics. Recently, S. Hayami *et al.* showed theoretically that such an exotic order can occur also in metallic systems, and exotic phenomena such as magnetization induced by electric current can occur in the ferrotoroidal ordered metal [1].

UNi₄B, one of such the candidates, crystalizes in the orthorhombic structure (symmetry: *Cmcm*, D_{2h}^{17} , No. 63) [2]. Below T_N ($= 20.4$ K), it orders antiferromagnetically in a magnetic structure where the magnetic moments carried by the 2/3 of U ions make the vortices in each triangular planes [3]. This magnetic structure is equivalent to that assumed in the above theory. Our recent magnetization measurements under electric current showed that electric current actually induces magnetization in the toroidal magnetic ordered state of UNi₄B [4]. Thus the validity of the theory is confirmed in part by the experiments.

In order to make a further test for the theory, Hall-coefficient measurements have been performed for the first time. The theory predicts Hall voltage which is proportional to the square of the electric current, I_2 is induced by in-plane current even in zero magnetic field. However, such behavior of the Hall voltage is not observed within the accuracy of our measurements.

[1] S. Hayami *et al.*, Phys. Rev. B 90, 024432 (2014).

[2] Y. Haga *et al.*, Physica B 403 900 (2008).

[3] S. A. M. Mentink *et al.*, Phys. Rev. Lett. 73, 1031 (1994).

[4] H. Saito *et al.*, JPS autumn meeting, 9aBK-13 (2014).

I7-01**SAMARIUM HEXABORIDE: THE FIRST STRONGLY CORRELATED TOPOLOGICAL INSULATOR?**

O. Rader¹, P. Hlawenka¹, K. Siemensmeyer¹, E. Weschke¹, A. Varykhalov¹, J. Sánchez-Barriga¹, N. Y. Shitsevalova², A. V. Dukhnenko², V. B. Filipov², S. Gabáni³, K. Flachbart³ and E. D. L. Rienks¹

¹*Helmholtz-Zentrum Berlin für Materialien und Energie, Berlin, Germany*

²*Institute for Problems of Materials Science, National Academy of Sciences of Ukraine, Kiev, Ukraine*

³*Institute of Experimental Physics, Slovak Academy of Sciences, Košice, Slovakia*

Topological insulators represent a new phase of matter with an insulating bulk and a metallic surface caused by an odd number of spin-polarized, Dirac-cone surface states in the surface Brillouin zone which are topologically protected by time-reversal symmetry. This protection by time-reversal symmetry constitutes an important connection to magnetism and potential way of functionalization. It is important to note that topological insulators are defined by their band structure and do not require electron correlation.

For fundamental but also for practical reasons, there has been a quest for topological insulators based on strong electron correlation. In this context, SmB₆ has been a prime candidate. SmB₆ is historically the first mixed-valent compound and first Kondo insulator. Additionally, it features a low-temperature resistivity which has remained unexplained for over three decades. Recent predictions as the first topological insulator caused by electron correlation have been supported by a large number of angle-resolved photoemission studies in the literature.

By proper distinction of Sm and boron terminated samples we demonstrate that the existence of surface states (at Γ -bar and X-bar) is independent of the termination. Secondly, we show that both types of surface states appear massive, most clearly the one at the zone center Γ -bar which develops a Rashba spin splitting for boron termination excluding an odd number of Dirac cones. This demonstrates in an elegant way that the features in photoelectron spectroscopy reported in the literature support a trivial rather than a topological nature of SmB₆. To explain the metallic surface at low temperature, we demonstrate a surface shift of the 4f and a reduced f-d hybridization at the surface which together cause the metallic surface state around the X-bar point.

I7-02**SCANNING TUNNELING MICROSCOPY STUDY
OF SUPERCONDUCTING VORTEX MOTION**

T. Samuely¹, M. Timmermans², D. Lotnyk¹, B. Raes², J. Van de Vondel² and V. V. Moshchalkov²

¹*Centre of Low Temperature Physics, Faculty of Science,
P. J. Šafárik University in Košice, Slovakia*

²*Institute for Nanoscale Physics and Chemistry (INPAC), KU Leuven, Belgium*

Our innovative scanning tunneling microscopy mode is capable of visualizing periodic dynamics at the nanoscale with unprecedented temporal resolution. [1] Hence, it allowed us to investigate in detail the behavior of superconducting vortices oscillating in ac magnetic field. We observed the hitherto well-known vortex motion along the so called “tin roof” potential. In this case, the vortex trajectory coincides with one of the primitive vectors of the Abrikosov lattice and the crystal lattice. On top of that, we observed a transverse trajectory. We analyze the differences of the observed trajectories and their time evolution.

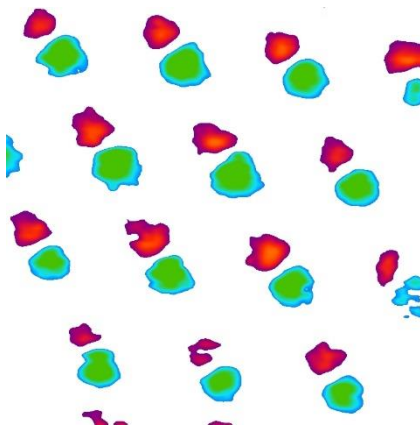


Figure: First harmonic of the differential conductance reveals vortices oscillating in ac magnetic field along the so called “tin roof” potential.

This work was supported by the ERDF EU grant No. ITMS 26220120005, APVV 0605-14, VEGA 1-0409-15.

[1] M. Timmermans, T. Samuely, B. Raes, J. Van de Vondel, and V. V. Moshchalkov, ACS NANO, 8, 2782-2787 (2014).

O7-01**TRANSITION FROM MOTT INSULATOR TO SUPERCONDUCTOR IN GaNb_4S_8 AT HIGH PRESSURE**

X. Wang¹, K. Syassen¹, J. Litterst³, J. Prchal⁴, V. Sechovsky⁴, D. Johrendt⁵ and M. M. Abd-Elmeguid^{2,4}

¹*MPI for Solid State Research, Stuttgart, Germany*

²*Institute of Physics II, University of Cologne, Cologne, Germany*

³*Institute of Condensed Matter Physics, TU Braunschweig, Braunschweig, Germany*

⁴*Department of Condensed Matter Physics, Charles University, Prague, Czech Republic*

⁵*Department of Chemistry and Biochemistry, LMU Munich, Munich, Germany*

In strongly correlated insulating systems, the metal insulator (MI) transition is driven by strong correlation effects associated with electron-electron interactions and the interplay between the charge, spin and orbital degrees of freedom. These are strongly coupled to the lattice and consequently can be tuned by external pressure.

We have investigated the effect of pressure on the transport, magnetic, and structural properties of GaNb_4S_8 (cubic fcc GaMo_4S_8 type structure) which belongs to a new class of Mott insulators. The interesting aspect to study this compound is that the electronic conduction originates from hopping of localized electrons ($S = 1/2$) among widely separated tetrahedral Nb_4 metal clusters. We find that the Mott insulating state at ambient pressure, transforms to a metallic and superconducting state at pressure of 10.5 GPa with critical temperature of $T_c = 2.1$ K at 10 GPa which increases with pressure up to 4 K at 23 GPa. We further show from our recent μSR experiments at ambient pressure and high pressure ac- susceptibility measurements on GaNb_4S_8 that short range magnetic order exists below 30 K that is strongly suppressed with pressure as the system approaches the superconducting state. We discuss the possibility of a nonconventional pressure-induced superconducting state in GaNb_4S_8 .

O7-02**TESTING THE THIRD LAW OF THERMODYNAMICS AT $T \rightarrow 0$ IN MAGNETIC SYSTEMS**J. G. Sereni¹*¹Low Temperature Division (CAB - CNEA) and Conicet, 8400 San Carlos de Bariloche, Argentina*

The fruitful research carried on low temperature ($T \leq 1\text{ K}$) thermal properties in magnetic systems was recently powered by the search of Quantum Critical Points (QCP) at $T \rightarrow 0$. Despite of the unattainability of the $T = 0$ limit, the characteristic energies of these systems were driven to low enough values that they provide a fertile field to test the validity of third law of thermodynamics in real systems. As a consequence of the available information different subtle properties and constraints on the thermal dependence of the entropy (S_m) can be revised.

In the light of the third law of thermodynamics, resumed as $S_m \geq 0$, in this review we analyze: i) the thermodynamic conditions to be fulfilled by any magnetic system to reach a QCP and their alternative specific heat (C_m) behaviors observed at $T \rightarrow 0$. ii) the allowed thermal dependencies of $S_m(T \rightarrow 0)$ as $\partial^2 S_m / \partial T^2$ derivatives, iii) with the consequent upper limit of the density of magnetic excitations in very heavy fermions (i.e. $C_m(T \rightarrow 0) / T \geq 4 \text{ J/mol K}^2$). iv) The appearance of 'entropy bottlenecks' in magnetically frustrated systems, related to v) the access to exotic ground states.

Each topic is backed by low temperature specific heat results, mainly performed on Ce and Yb intermetallic compounds.

O7-03**PROTON DISORDER IN D₂O – ICE – A NEUTRON DIFFRACTION STUDY**

K. Siemensmeyer¹, J.-U. Hofmann¹, S. V. Isakov², B. Klemke¹, R. Moessner³, J. P. Morris⁴ and D.A. Tennant⁵

¹*Helmholtz-Zentrum Berlin, Hahn Meitner Platz 1, D-14109 Berlin, Germany,*

²*Google, Brandschenkestrasse 110, 8002 Zürich, Switzerland*

³*Max Planck Institut für Physik komplexer Systeme, D-01187 Dresden, Germany*

⁴*Xavier University, Cincinnati, OH 45207, USA*

⁵*Neutron Sciences Directorate, ORNL, Oak Ridge TN 37831, USA*

Water ice (H₂O) at low pressure can be understood as a hexagonal structure where each Oxygen atom is bound to two Hydrogen atoms. Further, each bond between Oxygen atoms is occupied by only one Hydrogen atom. These are the famous ice - rules that give rise to a highly disordered ground state with a residual entropy of $R \ln(3/2)$. We have measured the diffuse scattering from a large D₂O – ice crystal using neutron diffraction. Different to previous descriptions of the ice - structure by Monte Carlo methods we are able to explain the data using an analytical method: The structure is mapped to a divergence-free dipolar model which is solved within a large-N approach. We obtain remarkable agreement between model and neutron results. The correlation length obtained at $T = 30\text{ K}$ seems to be limited by the instrumental resolution.

[1] Analytical theory for proton correlations in common water ice *Ih*, S. V. Isakov, R. Moessner, S. L. Sondhi, D. A. Tennant, Phys. Rev. B91, 245152 (2015).

[2] Electromagnetism on ice: classical and quantum theories of proton disorder in hexagonal water ice, O. Benton, O. Sikora, N. Shannon, arXiv 1504.04158.

O7-04**STRUCTURAL AND PHYSICAL PROPERTIES OF NEW COMPOUNDS IN THE Yb–Pd–Sn TERNARY SYSTEM**

F. Gastaldo¹, M. Giovannini^{1,2}, A. Strydom³, I. Čurlík⁴, M. Reiffers⁴, P. Solokha¹ and A. Saccone¹

¹*Department of Chemistry and Industrial Chemistry, University of Genova, Via Dodecaneso 31, 15046, Genova, Italy*

²*CNR-SPIN, Corso Ferdinando Maria Perrone 24, 16152, Genova, Italy*

³*Highly Correlated Matter Research Group, Department of Physics, University of Johannesburg, South Africa*

⁴*Faculty of Humanities and Natural Sciences, University of Prešov, Prešov, Slovakia*

Phase equilibria in the Yb–Pd–Sn ternary system at 600 °C were investigated in the whole concentration range (except the Pd-rich corner). Besides the known intermetallic compounds, new ternary intermetallics were revealed in the system and physical measurements have been performed on these compounds. In particular, among the new discovered compounds, Yb₃Pd₄Sn₁₃ emerges as a new member of the R₃T₄Sn₁₃ family (R = rare earth element, T = transition metal) and its crystal structure was determined by XRPD analysis. Measurements of magnetic susceptibility on Yb₃Pd₄Sn₁₃ indicate that Yb is in the magnetic Yb³⁺ state, but with a strongly reduced effective moment. Similarly to the analogous Yb₃Rh₄Sn₁₃ [1,2], the novel compound Yb₃Pd₄Sn₁₃ seems to exhibit superconductivity (T_c = 2.4 K), with clear superconducting phase transition anomalies consistently found in the magnetic susceptibility, electrical resistivity and specific heat. As for the other new compounds, structural characterization on single-crystal and powder data and physical properties of some of them will be presented.

[1] J.L. Hodeau et al. *Solid State Commun.* 36 (1980) 839.

[2] J.P. Remeika et al. *Solid State Commun.* 34 (1980) 923-926.

07-05

SYNTHESIS AND PHYSICAL PROPERTIES CePdIn_5 , A NEW COMPOUND OF $\text{Ce}_n\text{Pd}_m\text{In}_{3n+2m}$ HOMOLOGOUS SERIES

K. Uhlířová¹, J. Prokleška¹, B. Vondráčková¹, M. Kratochvilová¹, M. Dušek², J. Custers¹ and V. Sechovský¹

¹Charles University in Prague, Faculty of Mathematics and Physics, Ke Karlovu 3, 121 16 Praha 2, Czech Republic

²Institute of Physics of the CAS, Na Slovance 2, 182 21 Prague, Czech Republic

The family of $\text{Ce}_n\text{T}_m\text{In}_{3n+2m}$ ($n = 1, 2; m = 1$; T = transition metal) heavy fermion compounds have been intensively studied group of materials due to presence of magnetic order and superconductivity in a broad range of the temperature-pressure phase diagram. Besides the well know CeTIn_5 and $\text{Ce}_2\text{TIn}_{11}$ ($T = \text{Co, Rh, Ir}$) compounds, new materials CePtIn_7 , Ce_2PtIn_8 , $\text{Ce}_3\text{PtIn}_{11}$, Ce_2PdIn_8 , $\text{Ce}_5\text{Pd}_2\text{In}_{19}$ and $\text{Ce}_3\text{PdIn}_{11}$ have been discovered recently [1-5].

We report on synthesis and characterization of $\text{Ce}_n\text{Pd}_m\text{In}_{3n+2m}$, compounds with focus on a new compound CePdIn_5 . Similar to other compounds [3], single crystals of CePdIn_5 we prepared by indium flux growth method. The compounds were characterized by microprobe analysis and single crystal x-ray diffraction. The CePdIn_5 phase tends to grow as a thin layer on Ce_2PdIn_8 single crystals hampering the studies of the physical properties. As a solution samples have been isolated by focused ion beam method.

CePdIn_5 crystallizes in the HoCoGa_5 -type tetragonal structure with room temperature lattice parameters $a = 0.4693$ nm and $c = 0.7538$ nm. The compound remains paramagnetic down to 0.4 K where a superconducting transition is observed. Comparing the results of CePdIn_5 with other $\text{Ce}_n\text{Pd}_m\text{In}_{3n+2m}$ compounds develop from pure superconducting state in CePdIn_5 ($T_c = 0.4$ K) and Ce_2PdIn_8 ($T_c = 0.7$ K) via coexistence of superconductivity and antiferromagnetism in $\text{Ce}_3\text{PdIn}_{11}$ ($T_c = 0.4$ K, $T_N = 1.7$ K) to pure antiferromagnetic CeIn_3 ($T_N = 10$ K) resembling the proposed generic phase diagram [6].

[1] Z. M. Kurenbaeva et al., Intermetallics 16 (2008) 979.

[2] A. Tursina et al., J. Sol. State Chem. 200 (2013) 7.

[3] M. Kratochvilová et al., J. Cryst. Growth 397 (2014) 47.

[4] M. Kratochvilová et al., Scientific Reports 5 (2015) 15904.

[5] J. Prokleška et al., Phys. Rev. B 92 (2015) 161114(R).

[6] Q. Si et. al., Physica B 378 (2006) 23.

O7-06**SUPERCONDUCTOR – INSULATOR TRANSITION**

P. Szabó¹, T. Samuely¹, V. Hašková¹, J. Kačmarčík¹, M. Žemlička², M. Grajcar², R. Hlubina², R. Martoňák² and P. Samuely¹

¹*Centre of Low Temperature Physics, Inst. Exp. Phys., Slovak Academy of Science and Institute of Physics, P. J. Šafárik University, 040 01 Košice, Slovakia*

²*Comenius University, Dpt. Solid State Physics, 84248 Bratislava, Slovakia*

Superconductivity is characterized by the order parameter $\Psi = \Delta e^{i\phi}$, with the amplitude Δ and phase ϕ . Two fundamental approaches describe SIT as a consequence of closing Δ (fermionic scenario) or the phase fluctuations (bosonic mechanism). In the first case disorder-enhanced Coulomb interaction breaks Cooper pairs into fermionic states leading to superconductor-(bad) metal transition (SMT) with $\Delta \rightarrow 0$ at $T_c \rightarrow 0$. At even higher disorder metal-insulator transition (MIT) follows due to Anderson localization. The bosonic scenario assumes a single quantum phase transition. There, on the superconducting side even in a homogeneously disordered system superconducting “puddles” with variant Δ emerge. In the insulating state Cooper pairs with a finite amplitude are still present, but their global phase coherence is lost. Many characteristics in both scenarios are very similar [1] and probably only a probe directly sensitive to the local variations of the superconducting energy gap/order parameter can discern the realized mechanism. The scanning tunneling microscope (STM) is a unique probe with such a capability. The most of available STM experiments on thin films close to SIT support the bosonic mechanism and raise the question about its universality. We will discuss our recent transport, microwave [2] and subkelvin STM [3] measurements supplemented by the band-structure calculations on the ultrathin MoC superconducting films close to SIT in the framework of an alternative, fermionic scenario.

This work was supported by the ERDF EU grant under contract No. ITMS26220120005.

- [1] V F Gantmakher, V T Dolgoplov, Physics - Uspekhi 53, 1 (2010).
- [2] M. Žemlička, P. Neilinger, M. Trgala, M. Rehák, D. Manca, M. Grajcar, P. Szabó, P. Samuely, Š. Gaži, U. Hübner, V. M. Vinokur, E. Il'ichev, Phys. Rev. B 92, 224506.
- [3] P. Szabó, T. Samuely, V. Hašková, J. Kačmarčík, M. Žemlička, M. Grajcar, J. G. Rodrigo, and P. Samuely, Phys. Rev. B 93, 014505 (2016).

O7-07**SUPERCONDUCTING STATE IN $\text{LaPd}_2\text{Al}_{(2-x)}\text{Ga}_x$** P. Doležal¹, M. Klicpera², J. Pásztorová³, J. Prchal¹ and P. Javorský¹¹*Department of Condensed Matter Physics, Charles University in Prague, Ke Karlovu 5, 121 16 Praha 2, Czech Republic*²*Institut Laue-Langevin, 71 avenue des Martyrs – CS 20156, 38042 Grenoble Cedex 9, France*³*Institut for Condensed Matter and Complex Systems, University of Edinburgh, Edinburgh EH9 3FD, United Kingdom*

The RT_2X_2 compounds (R: f-element, T: d-element and X: p-element) crystallize generally in the tetragonal centrosymmetric ThCr_2Si_2 -type or CaBe_2Ge_2 -type crystal structure. Superconductivity in these compounds is almost exclusively connected to ThCr_2Si_2 -type structure, where the inversion centre takes place at the atomic position of R. The Compounds crystallizing in CaBe_2Ge_2 -type structure have the centre of inversion out of any atomic position, but still are centrosymmetric.

$\text{LaPd}_2\text{Al}_{(2-x)}\text{Ga}_x$ compounds crystallize in the centrosymmetric tetragonal CaBe_2Ge_2 -type structure ($P4/nmm$) and undergo structural phase transition at low temperatures to structure with a lower orthorhombic symmetry ($Cmma$). This transition is analogous to a distortion in the basal plane.

Whole $\text{LaPd}_2\text{Al}_{(2-x)}\text{Ga}_x$ series exhibits a superconducting state with the critical temperatures between 1.6 K and 2.7 K. Our recent study on polycrystalline samples [1] revealed substantial deviations from the BCS theory: the unusual curvature of field dependence of the critical temperature $T_c(H)$, non-exponential temperature dependence of the electronic specific heat in the superconducting state and significantly lower value of the weak-coupling BCS limit. The present study is focused on investigation of the structural phase transition in the whole series and on the physical properties of a new LaPd_2Al_2 single crystal, grown by a recrystallization of the polycrystalline sample. The transport properties investigated at ambient and hydrostatic pressure in various magnetic fields will be presented.

[1] M. Klicpera, J. Pásztorová, P. Javorský, *Superconductor Science and Technology* 085001, 27, (2014)

O7-08**THE EFFECT OF Sm ADDITION ON SUPERCONDUCTING PROPERTIES OF YBCO BULK SUPERCONDUCTORS**D. Volochová¹, P. Diko¹, S. Piovarči¹, V. Antal¹ and J. Kováč¹¹*Institute of Experimental Physics, Slovak Academy of Sciences, Watsonova 47, 040 01 Košice, Slovakia*

The effect of Sm addition on the microstructure and superconducting properties of Y-Ba-Cu-O (YBCO) bulk superconductors has been studied. Precursor powders $\text{YBa}_2\text{Cu}_3\text{O}_{7-\delta}$ (Y-123), Y_2O_3 and CeO_2 were enriched with different amounts of $\text{SmBa}_2\text{Cu}_3\text{O}_y$ (Sm-123) or Sm_2O_3 powders with the aim to increase critical current density, J_c , in self field as well as in higher magnetic fields, by introducing additional pinning centers. YBCO bulk superconductors with $\text{SmBa}_2\text{Cu}_3\text{O}_y$ (Y123-Sm) or Sm_2O_3 (Y123-SmO) addition were prepared by the optimized Top Seeded Melt Growth (TSMG) process in the form of single grains. Microstructure of prepared samples was studied by polarized light microscope, scanning electron microscope (SEM) equipped with Energy Dispersive Spectrometer (EDS). The superconducting properties were measured using a commercial MPMS magnetometer in magnetic fields up to 6 T at 77 K. Microstructure analysis revealed that Sm_2O_3 addition leads to a higher amount of smaller Y_2BaCuO_5 (Y-211) particles, what is related to high critical current densities ($J_c \sim 7 \times 10^4 \text{ A/cm}^2$) of the YBCO samples with Sm_2O_3 addition in low magnetic fields. The influence of Sm addition on Y_2BaCuO_5 particle size, critical temperature, T_c , critical current density, J_c , and maximum trapped magnetic field, B_{Zmax} , is reported.

Acknowledgment

This work was realized within the framework of the projects: Centre of Excellence of Advanced Materials with Nano- and Submicron Structure (ITMS 26220120019), Infrastructure Improving of Centre of Excellence of Advanced Materials with Nano- and Submicron Structure (ITMS 26220120035), New Materials and Technologies for Energetic (ITMS 26220220061), Research and Development of Second Generation YBCO Bulk Superconductors (ITMS 26220220041), APVV No. 0330-12, VEGA No. 2/0121/16, PhysNet Project (ITMS 26110230097), NANOKOP Project (ITMS 26110230061).

O7-09**HALL EFFECT AND HIDDEN QUANTUM CRITICALITY IN $\text{Mn}_{1-x}\text{Fe}_x\text{Si}$**

V. V. Glushkov¹, I. I. Lobanova², V. Yu. Ivanov¹, V. V. Voronov¹,
V. A. Dyadkin³, N. M. Chubova⁴, S. V. Grigoriev⁴ and S. V. Demishev^{1,2}

¹*Prokhorov General Physics Institute of RAS, Vavilov street 38,
119991 Moscow, Russia*

²*Moscow Institute of Physics and Technology, Institutskiy lane 9,
141700 Dolgoprudny, Moscow region, Russia*

³*Swiss-Norwegian Beamlines at the European Synchrotron Radiation Facility,
38000 Grenoble, France*

⁴*Petersburg Nuclear Physics Institute, Gatchina, 188300 Saint-Petersburg, Russia*

The study of the ordinary Hall effect in the quantum critical (QC) regime allows choosing between different scenarios of non-Fermi liquid behavior in strongly correlated electron systems [1-3]. In the case of localized magnetic moments a collapse of the Fermi surface is expected exactly at the QC point resulting in an abrupt change of the Hall constant at zero temperature [2]. In contrast, no direct evidence of the Lifshitz transition at QC point is provided for itinerant magnets in the spin density wave model of quantum criticality [3].

Here we report the study of Hall effect in the single crystals of $\text{Mn}_{1-x}\text{Fe}_x\text{Si}$ ($x < 0.3$) carried out in magnetic fields below 8 T at temperatures 2-60 K. Separating between the ordinary and anomalous Hall effect in the paramagnetic phase of $\text{Mn}_{1-x}\text{Fe}_x\text{Si}$ ($x < 0.3$) allows to identify a sign inversion of normal Hall constant, which is definitely associated with the hidden QC point $x^* \sim 0.11$. The effective hole doping produced by the increase of Fe content allows to make some verifiable predictions in the field of fermiology, magnetic interactions, and QC phenomena in $\text{Mn}_{1-x}\text{Fe}_x\text{Si}$. The established change of electron and hole concentrations is considered as a main “driving force”, which tunes the QC regime in $\text{Mn}_{1-x}\text{Fe}_x\text{Si}$ by modulating the Ruderman-Kittel-Kasuya-Yosida exchange interaction between the localized magnetic moments of Mn ions.

This work was supported by the RAS Programmes “Electron spin resonance, spin-dependent electronic effects and spin technologies”, “Electron correlations in strongly interacting systems” and by RFBR project 13-02-00160.

[1] A. Yeh *et al.*, Nature 419, 459 (2002).

[2] S. Paschen *et al.*, Nature 432, 881 (2004).

[3] T. Combier *et al.*, J. Phys. Soc. Jpn. 82, 104705 (2013).

[4] V. V. Glushkov *et al.*, Phys. Rev. Lett. 115, 256601 (2015).

O7-10**ELECTRIC CURRENTS AND VORTEX PINNING IN REBaCuO SUPERCONDUCTING TAPES**M. Jirsa^{1,2}, M. Rameš¹, I. Ďuran², T. Melíšek³ and P. Kováč³¹*Institute of Physics, Czech Academy of Sciences, Na Slovance 2, CZ-18221 Praha 8, Czech Republic*²*Institute of Plasma Physics, Czech Academy of Sciences, Za Slovankou 3, CZ-182 00 Praha 8, Czech Republic*³*Institute of Electrical Engineering, Slovak Academy of Sciences, Dúbravská cesta 9, SK-841 04 Bratislava, Slovak Republic*

We studied electromagnetic properties of several superconducting RE-BaCuO tapes of main wire suppliers. The tapes were tested by magnetic induction technique (vibrating sample magnetometer) and by current transport. The aim was to find the best candidates for wiring a new generation of superconducting magnets for fusion reactors. In the induction tests the critical current density and the pinning force density were studied as a function of magnetic field at several temperatures. From these data and the sample dimensions the engineering currents were deduced and compared with the results of transport experiments. These were done at 77 K, magnetic fields up to 1 T, and different angles between magnetic field and the sample plane. The induction and transport tests provided complementary results giving us a deeper insight into the tape behavior. The induction tests enabled study of vortex pinning up to very low temperatures and very high magnetic fields, where transport measurements, at least in our case, were not possible. The transport tests were possible only at around liquid nitrogen boiling point, 78 K, and at magnetic fields up to 1 T. They gave us information on the tape connectivity and quality on a much longer length and enabled reliable tests of the angular dependence of the transport current. Some tapes were prepared on ferromagnetic substrates, where the evaluation of induced superconducting magnetic moments was quite tricky. The transport experiment was even in this case quite straightforward and easy.

P7-01**THERMODYNAMIC PROPERTIES OF A CUBIC HUBBARD CLUSTER AT QUARTER FILLING**K. Szałowski¹, T. Balcerzak¹, M. Jaščur², A. Bobák² and M. Žukovič²¹*Department of Solid State Physics, University of Łódź, ulica Pomorska 149/153, PL 90-236 Łódź, Poland*²*Department of Theoretical Physics and Astrophysics, Faculty of Science, P. J. Šafárik University, Park Angelinum 9, 041 54 Košice, Slovak Republic*

In the paper the thermodynamic description of a zero-dimensional, cubic cluster consisting of 8 atoms, in the framework of an extended Hubbard model is presented. The electron hopping between nearest neighbours t_1 and second nearest neighbours t_2 , as well as on-site coulombic energy U and nearest-neighbour coulombic energy V is taken into account. The study is focused on the case of quarter-filling (presence of 4 electrons), which yields the paramagnetic ground state. By means of exact numerical diagonalization, a full set of eigenstates and eigenenergies of the Hamiltonian is obtained. The further thermodynamic analysis is based on the canonical ensemble formalism, leading to the exact results for the system in question [1].

The temperature dependence of such quantities as entropy, specific heat and magnetic susceptibility, as well as the spin-spin correlations and double occupancy per site is calculated. In particular, the presence of a double-peak structure in the specific heat and a single peak in the magnetic susceptibility is found. The behaviour of these maxima as a function of parameters U/t_1 and V/t_1 , as well as hopping ratio t_2/t_1 is discussed. For instance, the low-temperature maximum of the specific heat and corresponding maximum of susceptibility is quite sensitive to U/t_1 . In order to explain such behaviour, the Schottky model involving two degenerate states: the ground state and the first excited state, is employed. It can be concluded that such a model describes well the position of the mentioned peaks. On the other hand, the high-temperature maximum of the specific heat origins from electron hopping and is rather weakly sensitive to U/t_1 . However, the influence of t_2/t_1 parameter on this peak is quite pronounced.

This work has been supported by Polish Ministry of Science and Higher Education by a special purpose grant to fund the research and development activities and tasks associated with them, serving the development of young scientists and doctoral students.

- [1] K. Szałowski, T. Balcerzak, M. Jaščur, A. Bobák, M. Žukovič, Bull. Soc. Sci. Lettres Łódź 66 Sér. Rech. Déform. (2016) – in press; preprint arXiv:1511.08490v1 (2015).

P7-02**PARAMAGNETISM OF TASAKI-HUBBARD MODEL**V. Baliha¹, O. Derzhko¹ and J. Richter²¹*Institute for Condensed Matter Physics, National Academy of Sciences of Ukraine, Svientsitskii Street 1, 79011 L'viv, Ukraine*²*Institut für theoretische Physik, Otto-von-Guericke-Universität Magdeburg, P.O. Box 4120, 39016 Magdeburg, Germany*

We consider the standard Hubbard model on the N -site one-dimensional Tasaki lattice (i.e., the sawtooth chain with the hopping parameter along the zigzag path $t_2 > 0$ which is $\sqrt{2}$ times larger than the hopping parameter along the basal straight line $t_1 > 0$) [1,2] and assume that the number of electrons n is less than $N/2$. The model under consideration has completely dispersionless (flat) lowest-energy one-electron band and belongs to the class of Mielke-Tasaki ferromagnets [2]. That is, the ground state of the model is ferromagnetic if the electron density $n/N = 1/2$. However, the ground state in the thermodynamic limit is paramagnetic if the electron density $n/N < 1/2$.

The aim of our study is to examine the paramagnetic properties of the described strongly correlated electron system and to compare them to the properties of the conventional Curie paramagnet. To this end, we extend the consideration of Refs. 3 and 4 by introducing into the model an infinitesimally small external magnetic field. We also focus on the case when $n/N \rightarrow 1/2$ to follow how the observable paramagnetic properties indicate approaching the point of Mielke-Tasaki ferromagnetism.

[1] H. Tasaki, Phys. Rev. Lett. 69, 1608 (1992).

[2] O. Derzhko, J. Richter, and M. Maksymenko, Int. J. Mod. Phys. B 29, 1530007 (2015).

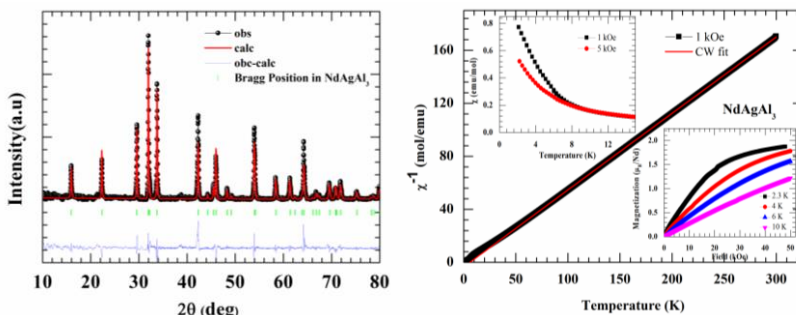
[3] O. Derzhko, A. Honecker, and J. Richter, Phys. Rev. B 76, 220402 (R) (2007).

[4] O. Derzhko, J. Richter, A. Honecker, M. Maksymenko, and R. Moessner, Phys. Rev. B 81, 014421 (2010).

P7-03

MAGNETIC, THERMODYNAMIC AND TRANSPORT PROPERTIES OF POLYCRYSTALLINE NdAgAl₃ COMPOUNDS. Nallamuthu¹, A. Džubinská², M. Reiffers² and R. Nagalakshmi¹¹*Department of Physics, National Institute of Technology,
Tiruchirappalli 620 015, India*²*Faculty of Humanities and Natural Sciences, Presov University, Presov, Slovakia*

We present the detailed study of magnetic, thermodynamic and transport properties of polycrystalline NdAgAl₃ compounds. The compound has crystallized in BaNiSn₃-type tetragonal structure with the space group of I4mm, which is distorted from BaAl₄ tetragonal structure. Recently several RTX₃ compounds have been reported last few decades, which exhibited much interesting ground state properties. Because of the interesting physical properties, this found the motivation for this study. We are concentrating on RTX₃ compounds. Our recent report of RCuGa₃ series (R = La, Pr, Nd and Gd) shows magnetocrystalline anisotropy behavior [1]. Also recently was reported that single crystal of CeAgAl₃ [2] shows ferromagnetic transition at $T_C = 3$ K. Therefore, we performed the comprehensive study of polycrystalline NdAgAl₃ crystal structure and physical properties. Heat capacity and magnetic measurements indicate the ferromagnetic nature of ordering of the compounds at $T_C \sim 2$ K. The compound shows Schottky anomaly in heat capacity data. The resistivity measurement presents a low temperature drop around magnetic ordering temperature. Compound shows negative magnetoresistance (MR) due to the ferromagnetic ordering.



[1] R. Nagalakshmi, et.al., Journal of Magnetism and Magnetic Materials 386 (2015) 37–43.

[2] Takahiro Muranaka and Jun Akimitsu. Physica C 460–462 (2007) 688–690.

P7-04**MAGNETIC PHASE DIAGRAM OF $\text{UCo}_{1-x}\text{Ru}_x\text{Al}$ WITH LOW Ru CONCENTRATION**P. Opletal¹, J. Prokleška¹, J. Valenta¹ and V. Sechovský¹¹*Charles University in Prague, Faculty of Mathematics and Physics, Department of Condensed Matter Physics, Ke Karlovu 5, 121 16 Prague 2, the Czech Republic*

In recent years it was shown that second order ferromagnetic (FM) transition is not always suppressed by external parameters into a quantum critical point (QCP) as one would expect. In some materials second order FM transition is suppressed until tricritical point (TCP) is reached [1]. At TCP the character of FM transition changes into the first order one and it is quickly suppressed. Simultaneously metamagnetic transition of the first order appears at TCP. This metamagnetic behavior is characterized by critical endpoint (CEP), where metamagnetic transition becomes first order transition. CEP can be further suppressed by external parameters down until QCP is reached. Some materials which exhibit this kind of behavior are ZrZn_2 , UGe_2 , URhAl or UCoAl .

UCoAl is paramagnet down to low temperatures and exhibits metamagnetic transition with critical field of ~ 0.7 T [2]. By applying hydrostatic pressure CEP of UCoAl is suppressed until QCP is reached at 13 T and 2.9 GPa [3]. TCP and FM ordering can be reached by applying uniaxial pressure along the c-axis or by doping. Doping already by 1% of Ru on Co position induces ferromagnetic ordering with $T_C = 16$ K.

We prepared single crystals of $\text{UCo}_{1-x}\text{Ru}_x\text{Al}$ of composition 1%, 0.5% and 0.25% of Ru. All single crystals were investigated in ambient and hydrostatic pressure. We focused on evolution of magnetism with changing composition and hydrostatic pressure. Phase diagram (p,H,T) for each single crystal was determined using el. resistivity, thermal expansion and magnetization in ambient and hydrostatic pressure.

- [1] M. Brando, D.B., F. M. Grosche, T. R. Kirkpatrick, *Metallic Quantum Ferromagnets*. <http://arxiv.org/abs/1502.02898>, 2015.
- [2] Sechovsky, V., et al., Systematics across the UTX series (T = Ru, Co, Ni; X = Al, Ga, Sn) of high-field and low-temperature properties of non-ferromagnetic compounds. *Physica B+C*, 1986. 142(3): p. 283-293.
- [3] Kimura, N., et al., Quantum critical point and unusual phase diagram in the itinerant-electron metamagnet UCoAl . *Physical Review B*, 2015. 92(3): p. 035106.

P7-05**MAGNETORESISTANCE STUDY OF C-AXIS ORIENTED YBCO THIN FILM**

M. Chrobak¹, W.M. Woch¹, M. Kowalik¹, R. Zalecki¹, M. Giebułtowski¹, J. Przewoźnik¹, Cz. Kapusta¹ and G. Szwachta^{2,3}

¹*Solid State Physics Department, Faculty of Physics and Applied Computer Science, AGH University of Science and Technology, al. A. Mickiewicza 30, 30-059 Kraków, Poland*

²*Department of Surface Engineering and Materials Characterization, Faculty of Metals Engineering and Industrial Computer Science, AGH University of Science and Technology, al. A. Mickiewicza 30, 30-059 Krakow, Poland*

³*Academic Centre for Materials and Nanotechnology, AGH University of Science and Technology, al. A. Mickiewicza 30, 30-059 Krakow, Poland*

The c-axis orientation YBa₂Cu₃O₈ thin film was prepared directly on MgO substrate by the pulse laser deposition. The thickness of the film was 170 nm. The superconducting critical temperature was $T_{c50\%} = 89$ K and the width of superconducting transition was $\Delta T = 1.6$ K. The temperature dependencies of magnetoresistance were measured up to 90 kOe. The widths of the transition to the superconducting state versus applied magnetic field were derived and they were fitted using the formula: $\Delta T = CH^m + \Delta T_0$. The irreversibility fields as a function of temperature were obtained and fitted by the de Almeida and Thouless like equation:

$$H_{irr} = H_{irr0} \left(1 - \frac{T}{T_{c0}} \right)^n.$$

P7-06**PHASE DIAGRAMS AND REENTRANT TRANSITIONS OF A SPIN ELECTRON MODEL ON A DOUBLY DECORATED HONEYCOMB LATTICE**H. Čenčariková¹ and J. Strečka²¹*Institute of Experimental Physics, Slovak Academy of Sciences, Watsonova 47, 04001 Košice, Slovak Republic*²*Department of Theoretical Physics and Astrophysics, Faculty of Science, P. J. Šafárik University, Park Angelinum 9, 040 01 Košice, Slovak Republic*

The generalized decoration-iteration transformation is used to examine the finite-temperature phase diagrams, critical properties and thermodynamics of a coupled spin-electron model on a doubly decorated honeycomb lattice. The hybrid spin-electron model takes into account the hopping term for the mobile electrons placed on decorating lattice sites, the nearest-neighbor Ising coupling between the mobile electrons and the localized spins placed on nodal lattice sites, as well as, the further-neighbor Ising coupling between the localized spins. The finite-temperature phase diagram and spontaneous magnetization are examined in detail for both ferromagnetic as well as antiferromagnetic further-neighbor Ising interaction between the localized spins. It is shown that the fractional electron concentration along with the further-neighbor Ising interaction are responsible for a rich variety of phase diagrams including the spontaneously ordered ferromagnetic phase, the spontaneously ordered antiferromagnetic phase and the disordered paramagnetic phase. Under certain conditions, reentrant phase transitions may be detected at the phase boundaries between the paramagnetic phase and the spontaneously ordered ferromagnetic or antiferromagnetic phase. In addition, the complete picture of thermal dependences of the uniform and staggered magnetizations of the localized Ising spins and mobile electrons are presented. It is evidenced that thermal variations of the uniform and staggered spontaneous magnetizations are basically influenced by the annealed bond disorder and the quantum reduction of the spontaneous magnetization, respectively. The loop character in thermal dependences of the spontaneous magnetizations verifies a presence of interesting reentrant phase transitions connected with two consecutive critical points.

This work was financially supported by ERDF EU (European Union European regional development fond) grant provided under the contract No. ITMS26220120005.

P7-07**SPIN-GLASS BEHAVIOR IN LaCu_4Mn COMPOUND**K. Synoradzki¹¹*Institute of Molecular Physics Polish Academy of Sciences, Smoluchowskiego 17, 60-179 Poznań, Poland*

The experimental results of the X-ray powder diffraction, magnetic susceptibility, electrical resistivity, and specific-heat measurements of the LaCu_4Mn compound are presented. LaCu_4Mn is an intermetallic compound that crystallizes in the hexagonal CaCu_5 -type structure (P6/mmm space group, No. 191), where the atoms on the 3g (1/2, 0, 1/2) site create a kagome lattice, which can cause the spin frustration and leads to a variety of interesting states of matter, such as spin-ice, spin-liquid, and spin-glass states. The Rietveld refinement reveals a random distribution of Mn and Cu atoms on the 3g and 2c site, where about 80% of Mn atoms occupy the 3g site. The lattice parameters are $a = 5.252(1) \text{ \AA}$ and $c = 4.176(1) \text{ \AA}$. The low-field zero-field-cooled and field-cooled DC magnetic susceptibilities show splitting below the spin freezing temperature $T_f = 35 \text{ K}$. At 2 K the magnetization $M(H)$ exhibits hysteresis with coercivity field of $\sim 0.5 \text{ T}$. The AC susceptibility measurements exhibit a frequency-dependent cusp, associated with a frequency-dependent freezing temperature. Moreover, there is no clear sign of long range magnetic order in specific heat and resistivity measurements. Additionally, the value of the frustration parameter f , i.e. the ratio of the Curie-Weiss temperature and the freezing temperature, indicates moderate frustration strength in LaCu_4Mn . The frustration mechanism is attributed to the site disorder and to competing interactions between the Mn ions.

P7-08**CLEAN BULK YBaCuO SUPERCODUCTORS DOPED BY
PARAMAGNETIC IONS OF Sm AND Yb**M. Jirsa^{1,2}, D. Volochová², J. Kováč² and P. Diko²¹*Institute of Physics, Czech Academy of Sciences, Na Slovance 2,
CZ-18221 Praha 8, Czech Republic*²*Institute of Experimental Physics, Slovak Academy of Sciences, Watsonova 47,
SK- 04001 Kosice, Slovakia*

The recently acquired experience of the material contamination by paramagnetic ions diffusing from supporting rods and/or the melt-texture seed were employed in the new step of developing clean cuprate technology with the aim to create well defined superconducting structures. This technology was employed to study the possibility to create new vortex pinning sites in bulk YBaCuO by doping it by tiny amounts of paramagnetic ions. Small samples of about $1,5 \times 1,5 \times 0,6 \text{ mm}^3$ were cut from the pellet and measured by vibrating sample magnetometer (VSM) in the field range $\pm 9 \text{ T}$. Temperatures ranged from 300 K to 10 K for the samples in the non-superconducting tetragonal state and from 300 K to 70 K for those in the orthorhombic, superconducting state, reached by samples' annealing in oxygen. In the latter case, we observed the reversible paramagnetic moment above the critical temperature of the sample and compared it with that from the tetragonal state. Below T_c an irreversible magnetic moment enabled us to evaluate critical current density (by means of the extended Bean model) and to compare the effect of doping in individual materials. A correlation of pinning enhancement with increasing paramagnetic moment was observed. The normalized pinning force density as a function of the reduced magnetic field was analyzed in terms of the classical model and discussed with respect to the material anisotropy, giving us at least a rough idea on the type of effective pinning centers.

P7-09**STM STUDIES OF THE SUPERCONDUCTOR-INSULATOR TRANSITION IN MoC ULTRATHIN FILMS**

P. Szabó¹, V. Hašková¹, T. Samuely¹, J. Kačmarčík¹, M. Žemlička², M. Grajcar² and P. Samuely¹

¹*Centre of Low Temperature Physics @ Institute of Experimental Physics, Slovak Academy of Sciences & Šafárik university, SK-04001 Košice, Slovakia*

²*DEP, Comenius University, SK-84248 Bratislava, Slovakia*

Low temperature STM and transport studies on ultrathin MoC films provide evidence that, in contrast to TiN, InO_x and NbN, where the bosonic scenario of SIT is found upon increased disorder, the superconducting energy gap or order parameter decreases, as superconductivity is suppressed from bulk $T_c = 8.5$ K to 1.3 K at the unchanged strength of the superconducting coupling $2\Delta/k_B T_c = 3.85$. The global superconducting coherence is manifested by the presence of superconducting vortices and most importantly, the superconducting state is very homogeneous for all the thicknesses down to 3 nm where the strong disorder is characterized by $k_F l$ close to unity. All this points to the fermionic route of the SIT in MoC thin films, with a split quantum transition: first happens the superconductor-(bad)metal transition (SMT), later, at even higher disorder it is followed by the metal-insulator transition (MIT) [1].

Also the SMT transition caused by magnetic field is studied on the 3-nm thick MoC film at subKelvin temperatures via STM tunneling and transport measurements. We will discuss importance of superconducting fluctuations and Coulomb repulsion in the normal state close to the upper critical field B_{c2} .

This work was supported by the ERDF EU grant under contract No. ITMS26220120005.

[1] P. Szabo et al., Phys. Rev. B 93, 014505 (2016).

P7-10

SUPERCONDUCTIVITY OF NIOBIUM THIN FILM IN THE BiOCl/Nb HETEROSTRUCTURE

D. Lotnyk¹, V. Komanicky¹, V. Bunda² and A. Feher¹¹*Institute of Physics, Faculty of Science, P.J. Safarik University,
Park Angelinum 9, 04154 Kosice, Slovakia*²*Transcarpathian Institute of Arts, Voloshiv st. 37, 88000 Uzhgorod, Ukraine*

In the past decades much attention is paid to the nanoscale heterostructures such as metal/semiconductor, semiconductor/superconductor, and also to their superlattices. Nanosized materials reveal new, extraordinary properties compared to the bulk (or even mesoscale) ones which could be applied as a replacement to current semiconductor technology due to smaller sizes hence lower energy costs.

In the current paper electrical transport properties of 25 nm thick Nb film sputtered on the photosensitive semiconductor (BiOCl) were investigated. Resistive superconducting transitions were measured under influence of green (532 nm) and red (640 nm) laser excitations (Fig. 1). As a reference resistive curves of Nb film sputtered on glass (circles) were measured.

The superconducting transition temperature (T_c) shifts towards to the lower temperatures with increasing excitation energy. Also the second peak on dp/dT curves is revealed (see insert).

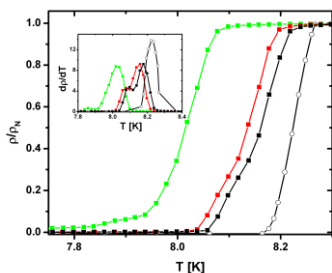


Fig. 1. Temperature dependences normalized resistivity of Nb thin films on glass (circles); on BiOCl without laser excitation (black squares), under green (green squares) and red (red squares) laser excitation

The decrease of T_c could correspond to the more effective influence of the interface between two materials to superconducting wave functions. Applying the laser excitation on the photosensitive semiconductor sufficiently changes density of states of semiconductor on the interface which manifests in more effective proximity effect. That could explain the second, low temperature peak on dp/dT curves. Such effect could be used for laser induced superconductor – insulator transition at thinner Nb films.

This work was supported by the ERDF EU (European Union European regional development fond) grant, under the contract No. ITMS 26220120005, APVV 0605-14, VEGA 1-0409-15.

P7-11

NON BCS SUPERCONDUCTING DENSITY OF STATES IN B-DOPED DIAMOND

O. Onufrienko¹, T. Samuely¹, G. Zhang², P. Szabó¹, V. V. Moshchalkov² and P. Samuely¹

¹Centre of Low Temperature Physics, Institute of Experimental Physics, Slovak Academy of Sciences & Faculty of Science, P. J. Safarik University, 04001 Kosice, Slovakia

²INPAC-Institute for Nanoscale Physics and Chemistry, KU Leuven, Celestijnenlaan 200D, B-3001 Heverlee, Belgium

In the presented work, we investigated the superconducting boron doped diamond polycrystal prepared by chemical vapor deposition by means of scanning tunneling spectroscopy. The local density of states obtained from the differential conductance spectra measured at 0.5 K exhibits features inconsistent with the standard theoretical model of Bardeen, Cooper and Schrieffer. We present and discuss various theoretical models in an attempt to explain this unorthodox behavior.

This work was supported by the ERDF EU (European Union European regional development fond) grant, under the contract No. ITMS 26220120005, APVV 0605-14 and VEGA 1-0409-15.

P7-12**INFLUENCE OF THERMO – CHEMICAL TREATMENTS ON SUPERCONDUCTING PROPERTIES OF LITHIUM DOPED $\text{YBa}_2\text{Cu}_3\text{O}_{7-\delta}$ BULK SUPERCONDUCTORS**V. Antal¹, D. Volochová¹, V. Kavečanský¹, J. Kováč¹ and P. Diko¹¹*Institute of Experimental Physics, Slovak Academy of Sciences, Watsonova 47, Košice, 040 01, Slovakia*

$\text{YBa}_2\text{Cu}_3\text{O}_{7-\delta}$ bulks single – grain superconductors doped by lithium were fabricated by the Top – Seeded Melt – Growth process. Lithium could create nanosized non-superconducting regions in $\text{YBa}_2\text{Cu}_3\text{O}_{7-\delta}$ by substitution of the Cu atoms in both the CuO chains and the CuO_2 planes. Formed nanosized non-superconducting regions could be effective pinning centres and enhance the superconducting properties of $\text{YBa}_2\text{Cu}_3\text{O}_{7-\delta}$ bulk superconductors at high and intermediate magnetic fields.

In our work we investigated lithium doped $\text{YBa}_2\text{Cu}_3\text{O}_{7-\delta}$ bulks after additional thermo - chemical treatments in atmospheres with different oxygen partial pressure. These investigations pointed out that annealing atmosphere has an essential influence on a distribution of lithium atoms between the CuO chains and the CuO_2 planes and it could have direct reflection on the superconducting properties of $\text{YBa}_2\text{Cu}_3\text{O}_{7-\delta}$ such as the transition temperatures. Also, X-ray analysis and light optical microscopy confirmed that lithium has influence on the size and concentration of non-superconducting Y_2BaCuO_5 particles and in such way the pinning properties of $\text{YBa}_2\text{Cu}_3\text{O}_{7-\delta}$ at low magnetic fields could be influenced.

Acknowledgements:

This work was realized within the framework of the projects: Centre of Excellence of Advanced Materials with Nano- and Submicron Structure (ITMS 26220120019), Infrastructure Improving of Centre of Excellence of Advanced Materials with Nano- and Submicron Structure (ITMS 26220120035), New Materials and Technologies for Energetic (ITMS 26220220061), Research and Development of Second Generation YBCO Bulk Superconductors (ITMS 26220220041), APVV No. 0330-12, VEGA No. 2/0121/16, SAS Centre of Excellence: CFNT MVEP, PhysNet (ITMS 26110230097), NANOKOP (ITMS 26110230061).

P7-13**SUPERCONDUCTIVITY IN $\text{Lu}_x\text{Zr}_{1-x}\text{B}_{12}$ DODECABORIDES WITH CAGE-GLASS CRYSTAL STRUCTURE**

N. E. Sluchanko^{1,2}, A. N. Azarevich¹, A. V. Bogach¹, S. Yu. Gavrilkin³,
M. I. Gilmanov², V. V. Glushkov^{1,2}, S. V. Demishev^{1,2}, K. V. Mitsen³,
A. V. Levchenko⁴, N. Yu. Shitsevalova⁴, V. B. Filipov⁴, S. Gabani⁵ and
K. Flachbart⁵

¹*Prokhorov General Physics Institute of RAS, 38 Vavilov str., Moscow, 119991 Russia*

²*Moscow Institute of Physics and Technology, 9 Institutskii per., 141700, Dolgoprudnyi, Russia*

³*Lebedev Physical Institute of RAS, Moscow, 119991 Russia*

⁴*Frantsevich Institute for Problems of Materials Science of NASU, 3 Krzhizhanovskii str., Kiev, 03680 Ukraine*

⁵*Institute of Experimental Physics of SAS, 47 Watsonova str., 040 01 Košice, Slovak Republic*

We probed the evolution of superconducting transition temperature T_c and the normal state parameters for substitutional solid solutions $\text{Lu}_x\text{Zr}_{1-x}\text{B}_{12}$ using resistivity, heat capacity and both dynamic (electron spin resonance) and static magnetization measurements. In studies of high-quality single crystals it was found [1] that the unusually strong suppression of superconductivity in $\text{Lu}_x\text{Zr}_{1-x}\text{B}_{12}$ ($x < 0.08$) BSC-type superconductors is caused by the emergence of static spin polarization in the vicinity of non-magnetic lutetium impurities. The analysis of received results points to a formation of static magnetic moments with $\mu_{\text{eff}} \approx 6\mu_B$ per Lu-ion ($^1\text{S}_0$ ground state, $4f^{14}$ configuration) incorporated in the superconducting ZrB_{12} matrix. The size of these spin polarized nanodomains was estimated to be about 5 Å.

[1] Sluchanko N.E., Azarevich A.N., Anisimov M.A., et al., Phys. Rev. B 93, 085130 (2016).

P7-14**INFLUENCE OF PRESSURE ON THE ELECTRON-PHONON INTERACTION IN SUPERCONDUCTORS**

Mat. Orendáč¹, S. Gabáni¹, G. Pristáš¹, E. Gažo¹, K. Flachbart¹ and N. Shitsevalova²

¹*Institute of Experimental Physics, SAS, Watsonova 47, 04001 Košice, Slovakia*
²*Institute for Problems of Materials Science, NASU, Krzhizhanovsky 3, 03680 Kiev, Ukraine*

The electron-phonon interaction (EPI) is a very important and ubiquitous process in solids, affecting almost all their physical properties. In metals, where the relaxation processes depend on both electrons and phonons, all thermodynamic and transport properties are dictated by EPI. The most dramatic manifestation of EPI is the superconducting state in metals.

Here we report the effect of high pressure on EPI in superconducting systems like YB₆ ($T_c \approx 6$ K), Pb ($T_c \approx 7.2$ K) and Nb ($T_c \approx 9.2$ K), and in LaB₆ in which superconductivity was not yet observed. The expected pressure effect should correspond to the predicted and observed negative pressure effect on T_c in all of these studied materials (except for LaB₆). To determine the influence of pressure on EPI we utilized the Bloch-Grüneisen fit (as ‘thermal spectroscopy’) of precise temperature dependence of resistivity measurements in the normal state up to 2.8 GPa. Based on this fit the observed negative pressure effect on EPI values, $d\lambda/dp$, were as follows: $d\lambda/dp \approx -0.049$ GPa⁻¹ for YB₆, $d\lambda/dp \approx -0.13$ GPa⁻¹ for Pb, $d\lambda/dp \approx -0.018$ GPa⁻¹ for Nb, and $d\lambda/dp \approx -0.0074$ GPa⁻¹ for LaB₆. These values are in good agreement with theoretical predictions.

This work was supported by project No. EU ERDF-ITMS 26220120005.

P7-15**SIMPLIFIED PARQUET EQUATION SOLVER FOR THE ANDERSON IMPURITY MODEL**V. Pokorný¹, V. Janiš¹ and A. Kauch¹*¹Institute of Physics, Czech Academy of Sciences, Na Slovance 2,
182 21 Praha 8, Czech Republic*

We present an analytic solver for the single-impurity Anderson model based on simplified parquet equations. This scheme uses the two-particle self-consistency to control the Kondo asymptotics and the critical behavior of this model. The equations can be written in the real-frequency representation which gives us direct access to spectral functions without the need for any numerical analytic continuation technique. We obtain the correct Kondo scale as well as magnetic susceptibility behavior in the critical regime. We also compare our results to the ones obtained by the (numerically exact) continuous-time quantum Monte Carlo to assess the reliability of this approximation.

P7-16**ANOMALOUS HALL EFFECT IN MnSi**V. V. Glushkov¹, I. I. Lobanova², V. Yu. Ivanov¹ and S. V. Demishev^{1,2}¹*Prokhorov General Physics Institute of RAS, Vavilov street 38,
119991 Moscow, Russia*²*Moscow Institute of Physics and Technology, Institutskiy lane 9,
141700 Dolgoprudny, Moscow region, Russia*

Anomalous (ρ_H^a) and normal (R_{HB}) contributions to Hall effect in chiral magnet MnSi ($T_c \approx 29.1$ K) were extracted from the analysis of the temperature dependencies of low field Hall resistivity. The suppression of long range magnetic order is found to induce the change in the ρ_H^a behavior governed by Berry phase effects below Curie temperature ($\rho_H^a = \mu_0 S_2 \rho^2 M$) to the regime dominated by skew scattering of charge carriers in the paramagnetic phase ($\rho_H^a = \mu_0 S_1 \rho M$). The crossover between the intrinsic ($\rho_H^a \sim \rho^2$) and extrinsic ($\rho_H^a \sim \rho$) anomalous Hall effect is shown to be accompanied by the rapid decrease of the charge carriers concentration from $n/n_{Mn}(T < T_c) \approx 1.5$ to $n/n_{Mn}(T > T_c) \approx 0.94$ ($n_{Mn} \approx 4.2 \cdot 10^{22} \text{ cm}^{-3}$ is the concentration of Mn ions). We argue that the observed crossover in anomalous Hall effect may be initiated by the change of the spin fluctuations rate in the vicinity of T_c . The possible realization of the electronic phase transition in MnSi resulted in the observed transformation of the electronic structure under the onset of long-range magnetic order should be independently checked by high precision electron photoemission studies.

This work was supported by the Programme of Russian Academy of Sciences “Electron correlations in strongly interacting systems”.

[1] V. V. Glushkov *et al.*, JETP Lett. 101, 459 (2015).

P7-17**ELECTROMAGNON CONTRIBUTION TO THE COOPER PAIR FORMATION AND SUPERCONDUCTIVITY**Z. Bak¹*¹Institute of Physics, Jan Dlugosz University, 42-200 Częstochowa, al. Armii Krajowej 13/15, 42-200 Częstochowa, Poland*

Since the discovery of superconductivity /SC/, there has been a drive to understand the mechanisms by which it occurs. Thirty years after discovery of SC there is no consensus on what kind of thermal excitations contributes to the pair formation. Despite of some inconsistencies is the classical concept of phonons serving as the pairing medium is the main candidate. Lately, vivid theoretical interest focuses on the paramagnons as the pairing glue for some organic superconductors, heavy-fermion systems and possibly high temperature superconductors. Till now both pairing agents studied separately, but there is a need for the theory, which accounts for the interplay of magnetic and elastic mechanisms effects when simultaneously present. In such situation there arises fundamental interaction between the electric and magnetic states of the SC material, called magnetoelectricity with novel type of elementary excitations called electromagnons. Strong magnetoelectric coupling can be achieved in materials with frustrated spin structures e.g. due to the Dzyaloshinsky-Moriya interaction. In this case magnetoelectric coupling creates a new quasiparticle excitation—the electromagnon—at terahertz frequencies. In our contribution we address the concept of the electromagnon based mechanism of SC.

The aim of the paper is to assess, whether formation of electromagnons can facilitate the SC transition. We show that the electromagnon condensation in any magnetic superconductor reduces the destructive effect of magnetic fluctuations on Cooper pairs, on the other hand the destructive effect of induced ferroelectric moments can enhance destruction.

The mass effect is usually used as the verification cross-test of the phonon based S.C., we show that electromagnon formation modifies the mass effect making this method useless. Finally, we will present a model of multicomponent condensate superconductivity with electromagnon contribution taken into account.

P7-18**SUPERCONDUCTING AND MAGNETIC PROPERTIES OF Sn-DOPED $\text{EuBa}_2\text{Cu}_3\text{O}_{7-\delta}$ Compound**

A. Dvurečenskij¹, A. Cigán¹, I. Van Driessche², M. Škrátek¹, M. Majerová¹, J. Maňka¹ and E. Bruneel²

¹*Institute of Measurement Science, Slovak Academy of Sciences, Dúbravská cesta 9, 841 04 Bratislava, Slovakia,*

²*Department of Inorganic and Physical Chemistry, Gent University, Krijgslaan 281 (53), 9000 Gent, Belgium*

During the study of Sn doping of RE-123 HT superconductors, most results were reported for Sn doping of the Y-123 superconductor. In this case, some inconsistent results were also reported, e.g. the question of Sn entering the Y-123 phase or the question of an effect of increasing the Sn content on the critical transition temperature. Only several results were reported for the Eu-123 system, disregarding the Sn addition in the melt textured Eu-Ba-Cu-O compounds to increase the critical current density and to supply, in the crystal growth process, more oxygen using oxide precursors. In the paper, we studied superconducting and magnetic properties of sintered samples of the nominal composition of $\text{EuBa}_2\text{Cu}_{3-x}\text{Sn}_x\text{O}_{7-\delta}$, with x ranging from 0 to 1.5. The samples prepared by the solid state reaction technique from Eu_2O_3 , BaCO_3 , CuO and SnO_2 precursors were sintered at about 1 323 K for 72 h in flowing oxygen of 20 ml/min.

All the samples show superconducting ordering, except for the one with $x=1.5$. The increasing Sn-content deteriorates the superconducting properties of the Sn doped samples. T_c^{on} , determined from ZFC $M(T)$ at 0.8 kAm^{-1} , decreases from $\sim 95 \text{ K}$ to 62 K likewise the magnetization hysteresis. At 20 K , the magnetization loops with the Sn content $x \leq 0.03$ indicate the so-called second peak effect, while the ones with a higher Sn content of $x \geq 0.10$ show an evident (para) magnetic “tail”.

ZFC, FC $M(T)$ and $M(H)$ magnetic dependences measured by the Quantum Design SQUID magnetometer MPMS XL-7 were analysed at low and high values of the temperature (2K - 300 K) and magnetic applied field (0.8 kAm^{-1} - 5.8 MAmm^{-1}) and analysed with respect to non-superconducting phases, e.g. BaCuO_2 and BaSnO_3 that were identified by the XRD. At 300 K , the samples with $x=0$ and 1.5 show paramagnetic magnetization curves up to magnetic field of 5.8 MAmm^{-1} . ZFC and FC $M(T)$ dependences of the sample with the highest Sn doping show bifurcation and AFM ordering starting at $\sim 100 \text{ K}$ and characteristics of AFM transition at 60 K (ZFC) and 46 K (FC) at 0.8 kAm^{-1} , respectively.

P7-19**TRAPPED FIELD OF YBCO BULK SUPERCONDUCTORS PREPARED BY INFILTRATION GROWTH PROCESS**L. Vojtkova¹, P. Diko¹ and S. Piovarči¹¹*Institute of Experimental Physics, Slovak Academy of Sciences,
Watsonova 47, 04001 Košice*

Single grain YBCO bulk superconductors were prepared from different starting precursors. In the first case, Y211 powder was used as the solid phase and the composition of liquid phase was a mixture of Y123+BaCuO₂+CuO powders. In the second case the solid phase was prepared as a mixture of Y₂O₃+BaCuO₂ instead of the conventionally used Y211 solid phase and as the liquid phase a mixture of Y₂O₃+BaCuO₂+CuO powders was used. The trapped field measurements at 77 K were performed and microstructure of samples was studied by polarized light microscopy and scanning electron microscopy. The influence of different starting compositions and the final size of Y211 particles on measured trapped field is shown.

Acknowledgment

This work was realized within the framework of the projects: ITMS 26220120019, ITMS 26220120035, ITMS 26220220061, ITMS 26220220041, APVV No. 0330-12, VEGA No. 2/0121/16 and Stefanik Project SK-FR-2013-0025, SAS Centre of Excellence: CFNT MVEP, PhysNet ITMS 26110230097, NANOKOP ITMS 26110230061.

P7-20

ON THE MAGNETIC PENETRATION DEPTH IN SUPERCONDUCTING ULTRATHIN LEAD FILMS

A. P. Durajski¹ and R. Szczesniak¹

*¹Institute of Physics, Czestochowa University of Technology,
Ave. Armii Krajowej 19, 42-200 Czestochowa, Poland*

In the present paper, we report a theoretical study of the magnetic London penetration depth in ultrathin Pb films consisting of five to ten monolayers.

Our calculations were performed within the framework of the strong-coupling Eliashberg approach. We observed that for thin films, the thermodynamic parameter exhibits an oscillatory behaviour connected with a quantum size effect. Moreover, we proved that the London penetration depth of Pb films cannot be correctly described using the Bardeen-Cooper-Schrieffer (BCS) theory of superconductivity due to the strong-coupling and retardation effects. The Eliashberg theory, used in this paper, goes beyond the BCS theory to include these effects which allows to describe the superconducting state on the quantitative level.

P7-21**DC NANOSQUID FROM Nb THIN FILMS**V. Štrbík¹, M. Pisarčík¹, Š. Gaží¹ and M. Španková¹*¹Institute of Electrical Engineering, Slovak Academy of Sciences,
Dúbravská cesta 9, 84104 Bratislava, Slovak Republic*

A dc nanoSQUID is superconducting quantum interference device sensitive to a magnetic field at the single spin level or a few Bohr magnetons. The nanoSQUID requires either nano-sized Josephson junctions or a part of superconducting ring with nano-sized dimensions. A focused ion beam (FIB) milling is a suitable technique to prepare the nanoSQUIDs. In this contribution we will present the fabrication of Nb-based thin film nanoSQUID using both Ar ion beam and FIB etchings. The Josephson weak links of width about 100 nm were obtained. The nanoSQUID resistance vs. temperature dependences, current-voltage characteristics and voltage vs. magnetic field dependences will be presented. The nanoSQUID sensitivity in units of Bohr magneton will be evaluated.

P7-22**MAGNETIC AND STRUCTURAL CHARACTERIZATION OF SUPERCONDUCTIVE Ni₂NbSn HEUSLER ALLOY**P. Kanuch¹, T. Ryba¹, J. Gamcová¹, M. Kanuchova², M. Durisin³, K. Saks³, Z. Vargova⁴ and R. Varga¹¹*Institute of Physics, Faculty of Sciences, P.J. Safarik University, Kosice 04154 Slovakia*²*FBERG, Technical University of Kosice, Kosice 04001, Slovakia*³*Institute of Materials Research, Slovak Academy of Sciences, Kosice 04001 Slovakia*⁴*Dept. Inorg. Chem., Fac. Sci., UPJS, Moyzesova 11, Kosice 04154, Slovakia*

Superconductive materials have many great features e.g. levitation or conducting electricity with no resistance. Magnetic superconductors are a special type of superconductors, in which the ferromagnetism and superconducting can coexist at the same time what leads us to a totally new phenomenon of electromagnetic invisibility [1].

Thanks to the wide range of physical properties e.g. high spin polarization, magnetic ordering, shape memory effect and many more, Heusler alloys are one of the most interesting groups for technical use, especially the superconducting Heusler alloys that can be cheaply and easily produced [2].

In the given contribution we have studied the structural and magnetic properties of rapidly quenched Ni₂NbSn alloy. The SEM, XPS and powder X-ray characterizations were used to estimate their composition and structure. Magnetic properties were studied by SQUID and the conducting properties at PPMS. It was shown that Ni₂NbSn has a critical temperature 2,2 K. Moreover, it shows transition to ferromagnetic phase at 2,5K. The coexistence of the ferromagnetism and superconductivity in rapidly quenched Ni₂NbSn alloy is confirmed by hysteresis loop measurement.

This research was supported by the projects APVV-0027-11 and Slovak VEGA grant. No. 1/0164/16.

- [1] F. Gömöry, R. Tebano, A. Sanchez, E. Pardo, C. Navau, I. Husek, F. Strycek, P. Kovac, *Superconductor Science and Technology*, Volume 15, Number 9 (2002).
- [2] T. Graf, C. Felser, S.S.P. Parkin, *Prog. Solid State Chem.* 39 (2011).

P7-23**EVOLUTION OF LOCK-IN EFFECT IN Cu_xTiSe_2 SINGLE CRYSTALS**Z. Medvecká^{1,2}, T. Klein¹, V. Cambel³, J. Šoltýs³, G. Karapetrov⁴,F. Levy-Bertrand¹, B. Michon¹, C. Marcenat⁵, Z. Pribulová² and P. Samuely²¹*Institute NEEL, CNRS & Université Grenoble Alpes, F-38042 Grenoble, France*²*Center of Low Temperature Physics, Institute of Experimental Physics SAS & P.J. Šafárik University, 040 01 Košice, Slovakia*³*Institute of Electrical Engineering SAS, 84104 Bratislava, Slovakia*⁴*Department of Physics, Drexel University, Philadelphia, PA 19104, USA*⁵*CEA & Université Grenoble Alpes, INAC-SPSMS, F-38000, France*

Lock-in effect in superconductors develops when vortices penetrating into the sample remain locked along the planes even though magnetic field is not parallel with the planes. This effect is usually observed in high temperature superconductors (HTS) with layered structure, large mass anisotropy ($\Gamma > 7$), large Ginzburg-Landau parameter ($\kappa > 10$) or coherence length smaller than the interlayer distance ($\xi^c \ll d$). Cu_xTiSe_2 belongs to the group of layered transition metal dichalcogenides that display similarities with the HTS. As the phase diagram of Cu_xTiSe_2 shows [1], charge density waves present in pure TiSe_2 are suppressed by intercalation of copper and at certain Cu concentration dome of superconducting state appears. Despite similarities with HTS, with the small anisotropy $\Gamma = 1.7$ and $\kappa \sim 10$ values no intrinsic lock-in effect is expected to be present in this material.

However, we have already observed the signatures of the lock-in effect in Cu_xTiSe_2 and reasoned that it could have an extrinsic origin [2]. In such a scenario vortices lock on an additional layered structure where superconductivity is at least partially suppressed. Here we compare our results of lock-in observation on three single crystals of Cu_xTiSe_2 . Samples with different copper doping and geometry were investigated by local Hall probe magnetometry in magnetic fields applied at various angles relative to the sample layers.

[1] E. Morosan, H.W. Zandbergen, B.S. Dennis, J.W.G. Bos, Y. Onose, T.Klimczuk, A.P. Ramirez, N.P. Ong and R.J. Cava, *Nature Phys.* 2, 544 (2006).

[2] Z. Medvecká, T. Klein, V. Cambel, J. Šoltýs, G. Karapetrov, F. Levy-Bertrand, B. Michon, C. Marcenat, Z. Pribulová and P. Samuely, *PRB* 93, 100501 (R) (2016)

P7-24**VORTEX LATTICE IN HEAVY-FERMION CeCoIn₅ PROBED BY AC-CALORIMETRY**

J. Kačmarčík¹, P. Pedrizzini², C. Marcenat³, Y. Fasano², V. Correa², Z. Pribulová¹ and P. Samuely¹

¹*Centre of Low Temperature Physics @ Institute of Experimental Physics, Slovak Academy of Sciences and P. J. Šafárik University, 040 01 Košice, Slovakia*

²*Lab. Bajas Temperaturas and Instituto Balseiro, Centro Atómico Bariloche (CNEA), Bariloche, Argentina*

³*Univ. Grenoble Alpes, CEA, INAC SPSMS, F-38000 Grenoble, France*

The heavy-fermion CeCoIn₅ presents a superconducting phase that can coexist with magnetic order when properly tuning different external parameters. This material is an interesting candidate to study the microscopic coupling giving rise to unconventional phenomena. One of its remarkable properties is the occurrence of vortex lattice structural changes as revealed by reciprocal-space imaging by small-angle neutron scattering at low temperatures [1]. The vortex lattice changes between hexagonal, rhombic and even square symmetries for certain ranges of temperatures and magnetic fields.

We have performed a detailed thermodynamic study of CeCoIn₅ by means of very sensitive ac-calorimetry. Continuous measurements while sweeping the temperature or magnetic field allowed us to inspect possible vortex-lattice structural phase transitions down to the sub-Kelvin temperature range. We will discuss our findings and compare them with the vortex phase diagram proposed from neutron data.

This work was supported by the ERDF EU grant under contract No. ITMS26220120005 and the Argentina-Slovakia bilateral collaboration program Conicet-SAS.

[1] A. Bianchi et al., Science 319 (2008) 177.

P7-25

SUPPRESSION OF SUPERCONDUCTIVITY IN HOMOGENEOUSLY DISORDERED ULTRATHIN MoC FILMS INTRODUCED BY INTERFACE BETWEEN THE SAMPLE AND THE SUBSTRATE

V. Hašková¹, M. Kopčík¹, P. Szabó¹, T. Samuely¹, J. Kačmarčík¹, M. Žemlička², M. Grajcar² and P. Samuely¹

¹*Centre of Ultra Low Temperature Physics, Institute of Experimental Physics, Slovak Academy of Sciences, and P. J. Šafárik University, SK-04001 Košice, Slovakia*

²*Department of Experimental Physics, Comenius University, SK-84248 Bratislava, Slovakia*

We investigated homogeneously disordered ultrathin MoC films by means of tunneling microscopy and spectroscopy at very low temperatures. In this contribution we intend to demonstrate the influence of the interface between a thin film sample and the substrate on the superconducting properties of the system. Our films were prepared by reactive magnetron sputtering of Mo target in a mixture of argon and acetylene on 2 types of substrates: single-crystalline *c*-cut sapphire and amorphous SiO₂. The difference between the two samples in terms of the value of superconducting energy gap and superconducting transition temperature will be discussed.

This work was supported by the ERDF EU grant under contract No. ITMS26220120005.

P7-26**HALL PROBE MAGNETOMETRY OF SUPERCONDUCTING YB₆**

M. Marcin¹, Z. Pribulová¹, J. Kačmarčík¹, S. Gabáni¹, T. Mori², V. Cambel³, J. Šoltýs³ and P. Samuely¹

¹*Centre of Low Temperature Physics @ Institute of Experimental Physics, Slovak Academy of Sciences and P. J. Šafárik University, 040 01 Košice, Slovakia*

²*Advanced Materials Laboratory, National Institute for Materials Science, Namiki 1-1, 305 0044 Tsukuba, Japan*

³*Institute of Electrical Engineering SAS, Dubravská cesta 9, 84104 Bratislava, Slovakia*

Discovery of superconductivity in MgB₂ at about 40 K [1] revived the interest in binary compounds, specifically borides. Anyway, the expectations of finding another high-temperature superconductor in this group, has not been met. YB₆ is a superconductor with the second highest critical temperature among borides, yet it is limited to 8.4 K [2]. It was shown that superconductivity here is mediated mainly by the very soft phonon mode originating from the rattling motion of the Y ion in the spacious cage of the B₆ octahedron. It leads to strong superconducting coupling, with the superconducting energy gap Δ and critical temperature T_c ratio being $2\Delta/kT_c > 4$ [3].

Here we present local magnetometry of two YB₆ samples with slightly different stoichiometry, with $T_c \sim 6.2$ and 7.4 K. We inspected mechanism of magnetic field penetration into and vortex distribution inside the sample using an array of miniature Hall probes. From measurements at different temperatures, the temperature dependence of the lower critical magnetic field H_{c1} was determined for both samples. The coupling ratios $2\Delta/kT_c$ were determined and compared with those from specific heat measurements performed on the same samples.

This work was supported by the ERDF EU grant under contract No. ITMS26220120005.

- [1] J. Nagamatsu, N. Nakagawa, T. Muranaka, Y. Zenitani and J. Akimitsu, *Nature* 410, 63 (2001).
- [2] C. Buzea and T. Yamashita, *Supercond. Sci. Technol.*, 14 (2001) R115.
- [3] P. Szabó, J. Girovský, Z. Pribulová, J. Kačmarčík, T. Mori and P. Samuely, *Supercond. Sci. Technol.* 26 (2013) 045019.

P7-27**ANGULAR DEPENDENCIES OF ESR PARAMETERS****IN ANTIFERROQUADRUPOLEAR PHASE OF CeB₆**

A. V. Semeno¹, M. I. Gilmanov^{1,2}, N. E. Sluchanko¹, V. N. Krasnorussky¹,
N. Y. Shitzevalova³, V. B. Filipov³, K. Flachbart⁴ and S.V. Demishev¹

¹*General Physics Institute RAS, 119991, Vavilov str., 38, Moscow, Russia*

²*Moscow Institute of Physics and Technology, 141700,*

Institutsky lane., 9, Dolgoprudniy, Russia

³*Institute for Problems of Materials Science of National Academy of Sciences of Ukraine, 3 Krzhyzhanovskogo Street, 03680 Kiev, Ukraine*

⁴*Institute of Experimental Physics of SAS, 47 Watsonova Street, SK-04001 Kosice, Slovak Republic*

Angular dependencies of ESR line parameters (g -factor and the linewidth ΔH) were experimentally explored in the antiferroquadrupolar (AFQ) phase of CeB₆ at $T=1.8\text{K}$. The data was obtained in two experimental geometries with different directions of the wavevector \mathbf{k} relatively to the external magnetic field \mathbf{H} with the use in each case of identical cylindrical cavities operating at frequency $f=60\text{GHz}$. Previous ESR study was done in the case of $\mathbf{k} \parallel \mathbf{H}$ for the direction of external magnetic field along [110] crystallographic axis [1]. In the present study this method was applied for $\mathbf{H} \parallel [100]$ and $\mathbf{H} \parallel [111]$. We found that while g -factors for [110] and [111] are close to each other $g \approx 1.6$ it's considerably different for [100] $g \approx 1.75$. The geometry with $\mathbf{k} \perp \mathbf{H}$ allowed rotating the sample thus resulting in detailed angular dependencies of $g(\varphi)$ and $\Delta H(\varphi)$ including major crystallographic directions. In the agreement with $\mathbf{k} \parallel \mathbf{H}$ experiment g -factor shows gradual increase approaching to [100] direction. The increase of g -factor is correlated with the increase of the linewidth from the average value $\Delta H \approx 1.7\text{kOe}$ to $\Delta H \approx 3.5\text{kOe}$ at [100]. The obtained $g(\varphi)$ dependence was compared with the predicted g -factor behavior for Γ_8 state of Ce³⁺ ion in AFQ phase [2]. It turned that experimental g -factor values were at all angles considerably lower then theoretically calculated limits ($2 < g < 2.2$) and in addition had different symmetry. From the other hand it's different from Γ_7 state of Ce³⁺ ion which implies isotropic $g(\varphi)$ behavior with $g \approx 1.4$. Thus the found ESR line characteristics raise new question concerning the magnetic state of Ce³⁺ ion in CeB₆ requiring further investigations.

[1] S.V. Demishev et. al., Phys.Rev.B, 80, 245106 (2009).

[2] P.Schlottmann, Phys. Rev. B, 86, 075135 (2012).

P7-28

THERMODYNAMIC CRITICAL FIELD IN HEXAGONAL BaSn₅ SUPERCONDUCTOR

M.W. Jarosik¹ and A.D. Woźniak¹

*¹Institute of Physics, Częstochowa University of Technology,
Ave. Armii Krajowej 19, 42-200 Częstochowa, Poland*

In presented work the dependence of the thermodynamic critical field on the temperature and the free energy difference between the superconducting and the normal state for hexagonal BaSn₅ superconductor has been investigated. The complicated numerical analysis has been conducted in the framework of strong coupling Eliashberg formalism. It has been stated that maximal value of the thermodynamic critical field is equal to 3.5 meV.

P7-29**UNIFORMLY DISORDERED ULTRATHIN SUPERCONDUCTING MoC FILMS CLOSE TO INSULATING STATE. TRANSPORT STUDIES.**

J. Kačmarčík¹, P. Szabó¹, M. Rajňák¹, M. Žemlička², M. Grajcar², P. Markoš² and P. Samuely¹

¹*Centre of Low Temperature Physics, Institute of Experimental Physics, Slovak Academy of Science and Institute of Physics, P. J. Šafárik University, 040 01 Košice, Slovakia*

²*Comenius University, Dpt. Solid State Physics, 84248 Bratislava, Slovakia*

Electronic transport properties of the homogeneously disordered MoC superconducting films down to 3-nm thickness are studied from room temperatures down to 300 mK and in magnetic fields up to 18 T. We have found that the superconducting transition temperature T_c of the films is well correlated with the sheet resistance following the Finkelstein formula of T_c (R_{\square}) based on weakening of the Coulomb screening in two-dimensional systems but the two-dimensional character of the electron movement is questioned, here. The transition temperature of our films is even better correlated with the product of Fermi momentum and the electronic mean free path, $k_F l$ being close to unity for the thinnest and most disordered films.

The temperature dependence of the sheet resistance at magnetic fields slightly above the upper critical magnetic field shows a reentrant behavior, first displaying decrease in resistance with decreasing temperature, later changed by its rapid growth of at lower T . The data are analysed in the framework of the theory of quantum corrections to the conductivity of disordered metals developed by Altshuler and Aronov and Galitski and Larkin. The quantum phase transition from the superconducting ground state to a bad metal or insulator induced by magnetic field is also addressed and scaling hypothesis is tested on the magnetotransport data at low temperatures and in fields close to critical.

This work was supported by the ERDF EU grant under contract No. ITMS26220120005.

P7-30**DETECTING OF LIGHT BY MEANS OF “HTSC / PHOTOSEMICONDUCTOR” HYBRID CONTACT STRUCTURES**V. Bunda¹, S. Bunda¹, D. Lotnyk², V. Komanicky² and A. Feher²¹*Department of Computer Sciences and Web-Design,**Transcarpathian Institute of Arts, Voloshin Str. 37, 880 00 Uzhgorod, Ukraine*²*Centre of Low Temperature Physics, P.J. Šafárik University,**Park Angelinum 9, 041 54 Kosice, Slovak Republic*

The important factor, causing perspective of use HTSC V. photonics, are in comparison large value of superconducting gap $2\Delta_0$. So, for the $\text{Y}_1\text{Ba}_2\text{Cu}_3\text{O}_{7.8}$ compound ($T_c=92$ K) the relation of cooper's pairs binding energy at zero temperature $2\Delta_0$ to value of the superconducting transition critical temperature T_c lies V. a interval $2\Delta_0 / k_B T_c = 4 \div 8$. It meets to photon energy of infra-red range of a spectrum. On the other hand, the occurrence HTSC materials with the T_c values $> 77\text{K}$ enables to use as semiconductor making HJ and HCS and such technological conventional (Ge, Si, GaAs, InAlAs) and unconventional (BiOHal; LnOHal; Ln-lanthanide; Hal= Cl,Br, I, F) semi- and photosemiconductors, the application of which before was impossible owing to a strong temperature degradation of conductivity (effect of a charge carrier "freezing").

In this abstract we report the formation process of " $\text{YBa}_2\text{Cu}_3\text{O}_{7.8}$ (ceramics) / BiOHal (singlecrystal)" HCS's and the results of investigation our physical properties. The features of the physical properties "HTSC-SC" HCS's become much more significant within the temperature range $T < T_c$, due to the changes in the spectra of elementary excitations of HTSC. The " $\text{YBa}_2\text{Cu}_3\text{O}_{7.8}$ - BiOCl:Ti" and " $\text{YBa}_2\text{Cu}_3\text{O}_{7.8}$ -BiOI "HCS's are heterophotoreistors with large spectral sensitivity ($0.31 - 0.80 \mu\text{m}$) and which are suitable for photoelectric analysis of polarisation plane of linearly polarised irradiation.

P7-31**EFFECT OF PRESSURE ON CRITICAL PARAMETERS AND MICROSTRUCTURE OF DOPED MgB_2 MATERIAL**

G. Gajda¹, A. Morawski², A. Presz², R. Diduszko³, T. Cetner², K. Gruszk⁴, S. Hossain⁵ and D. Gajda¹

¹*International Laboratory of HMF and LT, Gajowicka 95, 53-421 Wrocław, Poland*

²*Institute of High Pressure Physics PAS, Sokolowska 29/37, 01-142 Warszawa, Poland*

³*Tele and Radio Research Institute, Ratuszowa 11, 03-450 Warszawa, Poland*

⁴*Częstochowa University of Technology, Faculty of Production engineering and materials technology, Institute of Physics, Armii Krajowej 19, 42-200 Częstochowa*

⁵*University of Wollongong and Institute for Superconducting and Electronic Materials, Wollongong, New South Wales 2522, Australia*

The results of the irreversibility magnetic field and critical temperature were showed for cylindrical sample. These samples were doped with samarium, erbium and europium oxide in range from 1-3%. Furthermore, the MgB_2 material was made the carbon encapsulated boron. The cylindrical samples were paced in the Nb foil and steel container with dimensions of 6x6 [mm]. The next step were annealed in 1 GPa pressure at 800 °C by 1 h (at argon gas). We show results for samples after HIP process and without HIP process. All the samples were prepared and annealed at the Institute of High Pressure Physics in Warsaw. The measurements of the critical temperature and the hysteresis loop were done at International Laboratory of High Magnetic Fields and Low Temperatures Wrocław by using a vibrating magnetometer (VSM) up to 14T. The critical current density (J_c) was determined from the Bean model. The calculations allows to determine the pinning force and changes of J_c and F_p in depending on the processing methods. The XRD analysis were made by the Tele @ Radio Research Institute and the Częstochowa University of Technology, Faculty of Production engineering and materials technology, Institute of Physics, Armii Krajowej 19, 42-200 Częstochowa.

P7-32**LOCAL MAGNETOMETRY USING SCANNING HALL PROBE MICROSCOPE**Z. Pribulová¹, Z. Medvecká¹, J. Kačmarčík¹, E. Gažo¹ and P. Samuely¹*¹Centre of Low Temperature Physics @ Institute of Experimental Physics, Slovak Academy of Sciences and P. J. Šafárik University, 040 01 Košice, Slovakia*

Recently, a new Scanning Hall Probe Microscope (SHPM), designed and fabricated by attocube, was implemented in our low-temperature laboratory. In SHPM, a high resolution Hall sensor is scanned in close proximity to the sample surface mapping the Hall voltage as a function of location. This directly yields the spatial distribution of the local magnetic field. The coarse and fine movement of the sample is realized using piezo-drivers, with the step size that could be as fine as 10 nm at low temperatures. Anyway, the lateral resolution of the mapping is limited by the sensor dimensions, being 400 nm x 400 nm in our case. While other local probes may have better spatial resolution, SHPM with its ability to non-invasively bring quantitative information of the local magnetic field stands up to be a unique tool for the study of superconductors and magnetic materials. Here we present our first measurements of the vortex matter in a 100 nm thick film of Niobium. Measurements were performed at temperatures between 1.8 K and 9 K in low magnetic fields of a fraction of militesla.

P7-33**PHOTON-ASSISTED CHARGE TRANSPORT IN A HYBRID JUNCTION WITH TWO NON-COLLINEAR FERROMAGNETS AND A SUPERCONDUCTOR**K. Bocian¹ and W. Rudziński¹*¹Faculty of Physics, Adam Mickiewicz University,
ul. Umultowska 85, 61-614 Poznań, Poland*

Photon-assisted transmission (PAT) through a three-terminal hybrid system based on a quantum dot coupled to two ferromagnetic (F) and one superconducting (S) electrodes is studied in the sub-gap regime. Linear conductance is calculated within the nonequilibrium Green function technique. The effect of PAT on the local and non-local conductances for arbitrary angles between the magnetic moments of the F electrodes is studied. A generalized formula for the Andreev reflection magnetoresistance (ARMR) is proposed and it is found that the linear conductance may be significantly modified by the photon-assisted tunneling, while ARMR remains practically unaffected by PAT. Also, the conditions for the ARMR inversion have been determined for an interplay between the transport processes occurring in the system, magnetic polarization of the F leads and the angular configuration of the magnetic moments in the F leads. The influence of the non-vanishing intradot Coulomb correlations on PAT in the considered three-terminal hybrid system is also discussed.

P7-34**MAGNETIC-FIELD INDUCED TRANSITION IN A SPIN-GLASS STATE OF CATION DEFICIENT LaMnO_3** V. Eremenko¹, V. Sirenko¹, E. Čížmár², A. Baran³, and A. Feher²¹*B. Verkin Institute for Low Temperature Physics and Engineering NASU, Kharkov 61103, Ukraine*²*Institute of Physics, Faculty of Science, P. J. Šafárik University in Košice, Park Angelinum 9, 04154 Košice, Slovakia*³*Department of Physics, Faculty of Electrical Engineering and Informatics, Technical University of Košice, Park Komenského 2, 042 00 Košice, Slovakia*

Novel pattern of spin-glass transition in a magnetic field is discovered by means of complex susceptibility measurements in a bias magnetic field. A field induced transition is inferred from a shift of cusp temperature and from dynamic scaling in perfect single crystals of LaMnO_3 , randomized by cation vacancies. Measurements span the time interval over five decades, when transition temperature T^* is approached from above, and below T^* in a bias field up to 7 kOe. We observed Ising behavior in a close vicinity to T^* and Heisenberg behavior apart from it in bias field of the strength H up to about 1 kOe. Related change in symmetry properties of Hamiltonian is not accompanied by modification of dynamic scaling. Occurrence of polymorphic transition in spin glass indicates the novel type of polyamorphism. This is important feature in common with ordinary glasses.

This work has been supported by the research project VEGA 1/0145/13.

I8-01**RECENT RESEARCH IN MAGNETIC SHAPE MEMORY ALLOYS**J.M. Barandiaran^{1,2} and V.A. Chernenko^{1,2,3}¹*University of the Basque Country (UPV/EHU), Leioa 48940, Spain*²*BCMaterials, Technology Park of Biscay, 500, Derio 48160, Spain*³*Ikerbasque, Basque Foundation for Science, Bilbao 48013, Spain*

FerroMagnetic shape memory alloys (FMSMAs), such as the Ni₂MnGa Heusler compound and off-stoichiometric alloys, represent a new type of active materials which couple the martensitic transformation (MT) with ferromagnetism, enabling outstanding effects like magnetically induced strains, up to 12%, in bulk single crystals under a moderate magnetic field. High strains, high frequency response and large power density has driven the research and development of FSMAs as magnetic actuators or sensing devices.

Metamagnetic Shape Memory Alloys (MMSMAs) are a special kind of Magnetic Shape Memory Alloys in which the martensitic transformation is accompanied with a large drop in magnetization on cooling, resulting in a weakly magnetic or non magnetic martensite, in stark contrast and contrary to the conventional behaviour of magnetic materials. Such feature enables the reverse transformation into austenite to be driven by a moderate magnetic field, which also produces large inverse magnetocaloric, magnetoresistance and magnetostrain effects. This has a large interest for possible applications in magnetic refrigeration. Typical MMSMAs are Ni-Mn-X (X=In, Sn, Sb) Heusler alloys.

In this work we review our last years work on these alloys, either in bulk and single crystal form. Very recently, we have also found shape memory and superelastic effect in nanopillars shaped into Ni-Mn-Ga and Ni-Fe-(Co)-Ga FSMA single-crystals. Those effects provide a promising evidence for thermal and magnetic actuation at the nanoscale.

O8-01**MAGNETIC DOMAIN STRUCTURE TRANSFORMATION DURING FERROELASTIC TWIN BOUNDARY PASSAGE IN Ni-Mn-Ga SINGLE CRYSTAL**V. Kopecký¹, O. Perevertov¹, L. Fekete¹ and O. Heczko¹¹*Department of Functional Materials, Institute of Physics, ASCR, Na Slovance 2, CZ-182 02 Prague, Czech Republic*

Some off-stoichiometric martensitic Ni-Mn-Ga Heusler alloys exhibit up to 12% magnetic field induced strain [1] by magnetically induced reorientation (MIR), which is one of the magnetic shape memory effects. The reorientation is caused by magnetic-field induced motion of twin boundaries that are coherent interfaces between differently oriented ferroelastic domains called twin variants. This interface between twin variants (ferroelastic domains) is also magnetic domain wall as it separates the variants with different magnetic domain structure due to different crystallographic orientation. This multiferroic boundary, in contrast with pure magnetic domain wall, can be moved by small mechanical stress.

We investigated the changes of magnetic domain structure in-situ during the passage of single twin boundary of Type I and II [2] induced by mechanical stress. For in-situ observation we could not employ the usual Kerr microscopy due to vanishing Kerr effect [3] and optical microscopy with magneto-optical indicator film (MOIF) was used instead. This allowed in-situ observation of domain evolution during mechanical loading, however, with lower resolution determined by the properties of indicator film (garnet) and the strength of stray field. After the in-situ experiment the details of the domain structure were investigated by magnetic force microscopy (MFM). We found that radical changes of the magnetic domain structure occurred by moving twin boundary by mechanical stress (compression/tension). The well-defined pattern disappeared and peculiar granular or rake pattern formed, e.g., the usual labyrinth domain structure typical for crystal with uniaxial magnetic anisotropy changed to the rake [4], stripe-like domains after the passage although the structure orientation of the variants was the same. This demonstrates the possibility to manipulate the magnetic pattern by mechanical stress. The origin of these patterns and its effect on magnetic shape memory effect will be discussed.

We acknowledge the support of Czech Science Foundation No. 15-00262S.

[1] A. Sozinov et al., Appl. Phys. Lett., 102, 021902 (2013).

[2] L. Straka et al., Acta Mater. 59, 7450 (2011).

[3] M. Veis et al., J. Appl. Phys. 115, 17A936 (2014).

[4] A. Neudert et al., Advanced Eng. Mat. 2012, 14, No. 8 (2012).

O8-02**INVESTIGATION OF MAGNETOELASTIC PROPERTIES
OF $\text{Ni}_{0.36}\text{Zn}_{0.64}\text{Fe}_2\text{O}_4$ FERRITE MATERIAL IN LOW MAGNETIZING
FIELDS CORRESPONDING TO RAYLEIGH REGION**M. Kachniarz¹, A. Bieńkowski² and R. Szewczyk²¹*Industrial Research Institute for Automation and Measurements PIAP,
al. Jerozolimskie 202, 02-486 Warsaw, Poland*²*Institute of Metrology and Biomedical Engineering,
Warsaw University of Technology, sw. Andrzeja Boboli 8, 02-525 Warsaw, Poland*

Magnetic properties of ferromagnetic materials are very interesting subject of investigation developed for many years. One of the lesser-known area of magnetism is behaviour of ferromagnetic materials in region of low magnetizing fields, significantly lower than saturation coercive field, and their magnetomechanical properties in this region.

This paper presents result of study on magnetoelastic properties of $\text{Ni}_{0.36}\text{Zn}_{0.64}\text{Fe}_2\text{O}_4$ ferrite material in so called Rayleigh region, which cover region of low magnetizing fields. Investigated material was formed into frame-shaped magnetic core and subjected to the influence of external compressive stress. Special measurement system was developed to perform described experiment. Magnetoelastic characteristics of the material were investigated and modelling was performed utilizing Rayleigh model, which utilizes second order polynomials to approximate hysteresis loop in low magnetizing fields. Rayleigh model was extended with the influence of stress on the magnetic properties of the material in Rayleigh region. Comparison of experimental and modelling results indicates, that developed model is correct.

O8-03**MAGNETIC PHASE DIAGRAM OF $\text{TbMn}_{1-x}\text{Fe}_x\text{O}_3$ ($0 \leq x \leq 1$)
SUBSTITUTIONAL SYSTEM**

M. Mihalik jr.¹, M. Mihalik¹, Z. Jagličić², R. Vilarinho³, J. Agostinho Moreira³,
A. Almeida³ and M. Zentková¹

¹*Institute of Experimental Physics Slovak Academy of Sciences, Watsonova 47,
Košice, Slovak Republic*

²*Institute of Mathematics, Physics and Mechanics and Faculty of Civil and
Geodetic Engineering, University of Ljubljana, Slovenia*

³*IFIMUP and IN-Institute of Nanoscience and Nanotechnology,
Departamento de Física e Astronomia da Faculdade de Ciências,
Universidade do Porto, Porto, Portugal*

We present the magnetic phase diagram of $\text{TbMn}_{1-x}\text{Fe}_x\text{O}_3$ ($0 \leq x \leq 1$) substitutional system as obtained by specific heat and magnetization measurements. We have found that magnetism for $x \leq 0.1$ is driven by the Mn sublattice wherein Fe ions only affect this sublattice, but do not order magnetically. The onset of magnetism of Fe sublattice takes place around $x = 0.3$ and is magnetically coupled with ordered Mn sublattice at this concentration. At higher x -concentrations, the dominant magnetic ion in the system is iron and the magnetic ordering temperature increases with x . The magnetic ordering temperature can be tuned near the room temperature for concentrations around $x = 0.5$. Such a tuning may have the application potential in magnetic hyperthermia, or magnetic switching. The highest ordering temperature was observed to be 661 K for concentration $x = 1$, i.e. TbFeO_3 . We have also observed the spin-reorientation transition of the Fe sublattice and we have traced it in concentration range $0.5 \leq x \leq 1$. We will compare our data with the data for $x = 0.5$ published before [1] and we will address the question, whether there is one spin reorientation transition in the whole concentration range, or two independent: one around $x = 0.5$ and another for $x \geq 0.7$.

We observed the ordering of Tb sublattice for $x = 0$, and for x approaching 1 and it was not observed for any other concentration and for temperatures higher than 2 K.

This work was supported by ERDF EU under the contract No. ITMS 26220120005, by Fundação para a Ciência e Tecnologia, through the Project PTDC/FIS-NAN/0533/2012, and by QREN, through the Project Norte-070124-FEDER-000070 Nanomateriais Multifuncionais.

[1] Hariharan Nhalil et al., J. Appl. Phys. 117 (2015), 173904.

O8-04**MAGNETIC PROPERTIES OF THE $\text{Bi}_{0.65}\text{La}_{0.35}\text{Fe}_{0.5}\text{Sc}_{0.5}\text{O}_3$ PEROVSKITE**

A. V. Fedorchenko^{1,2}, E. L. Fertman², V. A. Desnenko², O. V. Kotlyar²,
E. Čizmár¹, V. V. Shvartsman³, D. C. Lupascu³, S. Salamon⁴, H. Wende⁴,
A. N. Salak⁵, D. D. Khalyavin⁶, N. M. Olekhnovich⁷, A. V. Pushkarev⁷,
Yu. V. Radyush⁷ and A. Feher¹

¹*Institute of Physics, Faculty of Science, P.J. Safarik University in Kosice, Kosice 04154, Slovakia*

²*B.Verkin Institute for Low Temperature Physics and Engineering of NASU, Kharkov 61103, Ukraine*

³*Institute for Materials Science and CENIDE, University of Duisburg-Essen, Essen 45141, Germany*

⁴*Faculty of Physics and CENIDE, University of Duisburg-Essen, Duisburg 47048, Germany*

⁵*University of Aveiro, (CICECO), Aveiro 3810-193, Portugal*

⁶*STFC, Rutherford Appleton Laboratory, Chilton, Didcot, Oxfordshire, OX11 0QX, United Kingdom*

⁷*Scientific-Practical Materials Research Centre of NASB, Minsk 220072, Belarus*

Magnetic properties of polycrystalline multiferroic $\text{Bi}_{0.65}\text{La}_{0.35}\text{Fe}_{0.5}\text{Sc}_{0.5}\text{O}_3$ synthesized under high-pressure (6 GPa) and high-temperature (1500 K) conditions were studied using a SQUID magnetometer technique. Temperature dependent static magnetic properties were measured in both zero-field-cooled (ZFC) and field-cooled (FC) modes in magnetic field H up to 6 kOe over the temperature range of 5–300 K. The field dependent magnetization $M(H)$ was measured in magnetic fields up to 50 kOe at different temperatures up to $T=230$ K. Neutron powder diffraction measurements revealed that the compound crystallizes into a distorted perovskite structure with the orthorhombic $Pnma$ symmetry [1]. A long-range magnetic ordering of the antiferromagnetic type with a weak ferromagnetic contribution takes place below $T_N \sim 220$ K. We report on an unusual magnetic field dependence of the magnetization. Detailed analysis of the initial magnetization curves is evident of a magnetic phase separation of the compound: at least two different magnetic phases coexist. Magnetic hysteresis loops taken below T_N possess a huge coercive field up to $H_c \sim 10$ kOe. Magnetic moment does not saturate up to 50 kOe. Besides, it was found that ZFC magnetization dependences measured in low (up to $H=100$ Oe) and enough high ($H=6$ kOe) magnetic fields are strongly different, which suggest a strong magnetic field effect on the properties of the compound.

This work was supported by the TUMOCs project. This project has received funding from the European Union's Horizon 2020 research and innovation programme under the Marie Skłodowska-Curie grant agreement No 645660. Also this work was supported by the Slovak Grant Agency VEGA 1/0145/13. S. Salamon thanks Stiftung Mercator (MERCUR) for the financial support.

[1] D. Khalyavin et al. *Zeitschrift für Kristallographie - Crystalline Materials*, 2015, Vol. 230 (12), pp. 767–774.

P8-01**SPIN DISORDER RESISTIVITY OF THE HEUSLER Ni_2MnGa -BASED ALLOYS**J. Kamarád¹, J. Kaštil¹, F. Albertini², S. Fabbri^{2,3} and Z. Arnold¹¹*Institute of Physics ASCR, v.v.i., Na Slovance 2, 182 21 Praha 8, Czech Republic*²*IMEM CNR, Parco Area delle Scienze 37/A, I-43124 Parma, Italy*³*MIST E-R Laboratory, via Piero Gobetti 101, I-40129 Bologna, Italy*

The multifunctional (magneto-elastic, magneto-caloric, magneto-electric...) properties of the Heusler alloys are a consequence of a strong sensitivity of both, the crystal and the electronic structure to external conditions. The shape memory effect of the Ni_2MnGa -based alloys is caused by a reversible martensitic trans-mation from the high-temperature cubic austenite (A) into the low-temperature martensite (M) with a lower crystal symmetry. We have studied electrical resistivity of the off-stoichiometric $(\text{NiCo})_2\text{Mn}(\text{GaIn})$ alloys in a wide range of temperature (3K – 550K) and magnetic field (0T – 4.5T). The resistivity of ferro-magnetic materials is usually written as $\rho(T) = \rho_0 + \rho_{\text{ph}}(T) + \rho_{\text{sd}}(T)$, where, the residual resistivity ρ_0 and the temperature linearly dependent resistivity $\rho_{\text{ph}} \sim AT$ are caused by a scattering of conduction electrons on impurities and on phonons, resp. An additional spin-disorder part of resistivity in magnetic materials, $\rho_{\text{sd}}(T) \sim BT^2$, describes a scattering mechanism on magnetic fluctuations. It reaches the maximum at the Curie temperature T_C and remains constant above T_C [1].

We have observed a small step decrease of resistivity ($\Delta\rho \sim 10\mu\Omega\text{cm}$) at the M-A transition temperature $T_{\text{M-A}}$ in the Co- and In-free $\text{Ni}_{1.85}\text{Mn}_{1.21}\text{Ga}_{0.94}$ alloy due to a difference in scattering of electrons on different structural defects in M and A phases of the alloy, similarly as it was observed in the stoichiometric Ni_2MnGa alloy [2]. In the case of the $(\text{NiCo})_2\text{Mn}(\text{GaIn})$ alloys, we have revealed an enormous increase of the step change of $\Delta\rho(T_{\text{M-A}})$, up to $\sim 200\mu\Omega\text{cm}$, that is caused by an increase of $\rho(T)$ of martensite phase of the alloys. Simultaneously, resistivity $\rho_{\text{sd}}(T)$ of austenite phase of the $(\text{NiCo})_2\text{Mn}(\text{GaIn})$ alloys is just slightly dependent on composition of the alloys and the maximum values of $\rho_{\text{sd}}(T_C^{\text{A}})$ vary from $\sim 40\mu\Omega\text{cm}$ up to $\sim 70\mu\Omega\text{cm}$, in good agreement with theoretical calculations [3]. Due to high sensitivity of $T_{\text{M-A}}$ temperature of the alloys to magnetic field, the very pronounced magneto-resistance effects have been observed at temperatures in vicinity of $T_{\text{M-A}}$ of the studied alloys.

- [1] B.R. Coles, Adv. Phys. 7 (1958) 40; [2] V.V. Khovailo et al., J. Phys.: Condens. Matter 16 (2004) 1951; [3] J. Kudrnovsky et al., Phys. Rev. B 86 (2012) 144423.

P8-02**MAGNETIC CHARACTERIZATION OF MELT-SPUN CoNiGa FERROMAGNETIC SUPERELASTIC ALLOY**

J. Mino^{1,2}, M. Ipatov², J. Gamcova¹, V. Zhukova², Z. Vargova¹, A. Zhukov^{2,3,4} and R. Varga¹

¹*Department of condensed matter physics, Faculty of science, University of Pavol Jozef Safarik, Srobarova 2, 040 01 Kosice*

²*Material Physics department, Faculty of Chemistry, University of the Basque Country, UPV/EHU, Plaza Elhuyar, 2., 20018, San Sebastian, Spain*

³*IKERBASQUE, Basque Foundation for Science, 48011 Bilbao, Spain*

⁴*Dpto. de Física Aplicada, EUPDS, UPV/EHU, 200018, San Sebastian, Spain*

Ferromagnetic nature of some superelastic alloys allows us to use them as sensors, not only as actuators contrary to traditional NiTi shape memory alloys. Superelasticity in alloys is caused by martensitic transformation between two phases with different lattice structures and their parameters. Ferromagnetic alloy of CoNiGa composition shows a considerable recoverable superelastic strain up to 8.6% [1]. Usually, shape memory alloys are prepared by growing of single crystals [2] or by arc-melting [3] followed with annealing in the high temperatures for a long time. Preparing sample with rapid quenching can help to reduce or avoid thermal treatment.

In the given contribution a melt-spun ribbons with Co₄₉Ni₂₁Ga₃₀ composition have been prepared. Structural characterization was executed on the Co₄₉Ni₂₁Ga₃₀ ribbon by X-Ray Diffraction. Microstructure of the ribbon was examined by SEM and revealed polycrystalline structure with grains size varies from 10µm to 30µm. Temperature range of martensitic transformation was identified from dependence of resistance and magnetization on temperature made by PPMS and SQUID, respectively. Start of martensitic transformation has been observed at 150K and end of it above 325K.

This work was supported by Spanish MINECO under MAT2013-47231-C2-1-P and Slovak project APVV-0027-011 and VEGA grant No. 1/0164/16. Technical and human support provided by SGIker (UPV/EHU, MICINN, GV/EJ, ERDF and ESF) is gratefully acknowledged.

[1] J. Dadda, H.J. Maier, D. Niklasch, et al. , Metall. Mater. Trans. A, 39 (9), (2008) 2026.

[2] I.V. Kireeva, C. Picornell, J. Pons, et al., Acta Mater., 68 (2014) 127.

[3] M. Vollmer, P. Krooß, Ch. Segel, et al. J. Alloy Compd., 633 (2015) 288.

P8-03**MAGNETO-CRYSTALLINE ANISOTROPY OF $\text{NdFe}_{x-1}\text{Mn}_x\text{O}_3$ SINGLE CRYSTALS**

M. Mihalik¹, M. Mihalik jr.¹, M. Zentková¹, J. Lazúrová¹, K. Uhlířová² and M. Kratochvílová²

¹*Institute of Experimental Physics SAS, Watsonova 47, Košice, Slovak Republic*

²*Department of Condensed Matter Physics, Faculty of Mathematics and Physics, Charles University in Prague, Ke Karlovu 5, Prague, Czech Republic*

In our paper we study magneto-crystalline anisotropy of $\text{NdFe}_{0.9}\text{Mn}_{0.1}\text{O}_3$ single crystal and the obtained results we discuss and compare with NdFeO_3 . Magnetic properties of NdFeO_3 are mostly determined by three magnetic interactions (Fe-Fe, Fe-Nd and Nd-Nd), which are present in this material. Magnetic ordering of Fe^{3+} ions creates a canted antiferromagnet below the Néel temperature at about 690 K [1]. Upon cooling, the magnetic moments of Fe^{3+} exhibit reorientation from the a -axis to the c -axis in the spin reorientation region (103-165 K) [2]. The Schottky anomaly in heat capacity at about 2 K is connected with the Nd-Fe interaction and small sharp peak associated with Nd ordering appears below 1 K [3]. Low concentration substitution of Mn for Fe ($x=0.1$) can be regarded as an external parameter affecting magnetic ordering of Fe^{3+} ions. Recently, we have shown that the Néel temperature decreases from $T_N = 691$ K to $T_N = 621$ K, and the anomaly in AC susceptibility, related to spin reorientation, vanishes with substitution [4]. Low temperature heat capacity measurement revealed that this substitution shifts a Schottky-type anomaly to higher temperatures. Another anomaly is generated by doping at $T_{\text{max}} = 11$ K. The anomaly is smeared out by magnetic field confirming its magnetic origin.

Our present study on oriented single crystals revealed huge magneto-crystalline anisotropy with respect to principal crystallographic axes, even magnetic transition takes place at different temperatures, as it is evidenced from magnetization measurements and magnetic isotherms. These measurements enable us to trace the development of ferromagnetic component from magnetic transition to $T = 2$ K. The Mn-substitution makes the spin reorientation transition very sharp and shifts the magnetic transition to the lower temperatures.

This work was supported by the project ERDF EU under the contract No. ITMS26220120005.

- [1] K.P. Belov, et al. Phys. Solid State, 13 (1971) 518, D. Treves, J. Appl. Phys., 3a (1965) 1033.
- [2] I. Sosnowska, et al., Physica, 136B (1986) 394-396.
- [3] F. Bartolomé, et al., Solid State Communications, 91 (1994) 177-182.
- [4] M. Zentkova et al., Acta Physica Polonica A, 126 (2014) 306-307.

P8-04**TUNING OF MAGNETISM IN $\text{DyFe}_{x-1}\text{Mn}_x\text{O}_3$ SINGLE CRYSTALS BY IRON SUBSTITUTION**

M. Zentková¹, M. Mihalik¹, M. Mihalik Jr.¹, J. Lazúrová¹, K. Uhlířová²,
M. Kratochvílová², M. K. Peprah³ and M. W. Meisel³

¹*Institute of Experimental Physics SAS, Watsonova 47, Košice, Slovak Republic*

²*Department of Condensed Matter Physics, Faculty of Mathematics and Physics, Charles University in Prague, Ke Karlovu 5, Prague, Czech Republic*

³*Department of Physics and NHMFL, University of Florida, Gainesville, USA*

This work reports the effects of Fe doping on the thermal and magnetic properties of single crystals $\text{DyFe}_{x-1}\text{Mn}_x\text{O}_3$. Parent compound DyMnO_3 exhibits magnetic ordering below $T_N(\text{Mn}) = 41$ K, where the Mn-spins order in a longitudinal spin density wave propagating along the *c*-direction. This structure changes to a cycloidal phase below $T_s(\text{Mn}) = 18$ K, while a ferroelectric phase exists below this temperature and another ordering appears at $T_N(\text{Dy}) \sim 6.5$ K [1, 2]. The cycloidal Mn-spin structure, with the inverse Dzyaloshinskii-Moriya interaction, is the driving force for the ferroelectric order and the frustration is the origin of the multiferroicity [3]. The magnetic frustration can be tuned by modifications of exchange interactions induced by substitution and our work probes the extent of this conjecture. Single crystals of $\text{DyMn}_{1-x}\text{Fe}_x\text{O}_3$, where $x = 0.00, 0.01, 0.02, 0.05, 0.1$, were grown by the optical floating zone method, and all resulting crystals adopted the *Pnma* orthorhombic crystal structure. With the doping, the crystal parameters change linearly and volume of the elementary cell decreases, while the temperatures of all the characteristic transitions decrease with doping. No sign of the transition to the cycloidal phase was observed for $x > 0.02$. Magnetic fields up to 9 T do not significantly affect transitions near 41 K and 18 K, but the transition at 6.5 K shifts to higher temperatures and washes it out for concentrations $x < 0.02$. Our study on oriented single crystals revealed a huge magneto-crystalline anisotropy with respect to principal crystallographic axes. Signatures of magnetic field induced transition can be observed in magnetic isotherms taken along all axes at 2 K, and only the field induced transition appears at a different magnetic field.

This work was supported by the project ERDF EU under the contract No. ITMS26220120005, and by the NSF via DMR-1202033 (MWM) and DMR-1157490 (NHMFL).

[1] T. Kimura et al.: *Phys. Rev. B* 71 (2005) 224425.

[2] T. Kimura et al.: *J. Phys.: Condens. Matter* 20 (2008) 434204.

[3] S-W. Cheong et al.: *Nat. Mater.* 6 (2007) 13.

P8-05**IDENTIFICATION OF MAGNETIC PHASES IN HIGHLY CORROSION-RESISTANT STEEL BY MÖSSBAUER SPECTROMETRY**L. Pašteka^{1,2}, M. Miglierini^{2,3} and M. Bujdoš¹¹*Institute of Laboratory Research on Geomaterials, Faculty of Natural Sciences, Comenius University in Bratislava, Ilkovičova 6, 842 15 Bratislava, Slovakia*²*Institute of Nuclear and Physical Engineering, Faculty of Electrical Engineering and Information Technology, Slovak University of Technology in Bratislava, Ilkovičova 3, 812 19 Bratislava, Slovakia*³*Department of Nuclear Reactors, Czech Technical University in Prague, V Holešovičkách 2, 180 00 Prague, Czech Republic*

Mössbauer spectrometry (MS) is widely used method for characterization of structural and/or magnetic properties of steels via hyperfine interactions at ⁵⁷Fe nuclei. This method can determine iron oxidation states and iron lattices (e.g., bcc – body-centered cubic, fcc – face-centered cubic). In this work we report on three types of samples of LC 200N corrosion-resistant steel that were treated using different procedures: (i) hardening, (ii) hardening with consequent rapid quenching in liquid nitrogen, and (iii) no particular treatment, i.e. non-hardened steel. The investigated samples of the LC 200 N steel were cut from original rods with the diameter of 25 mm using brass wire electric discharge machining (EDM). One side of the disks was polished in order to remove contamination imposed by EDM.

We have employed unconventional backscattering MS method which enables scanning of rather thick samples. Both sides of all disks were inspected. These types of steel exhibit different magnetic features, that are reflected in distinct Mössbauer parameters like ratios of non-magnetic singlets to magnetic sextets. The original non-hardened steel shows notable contribution of magnetically soft ferritic phases. Their content is decreased on account of austenite after both hardening procedures.

This work was supported by the grants GACR 14-12449S, VEGA 1/0182/16, VEGA 1/0203/14, UK/271/2016 and UK/272/2016.

P8-06**SUPERPARAMAGNETIC BEHAVIOUR OF IRON IN BIOLOGICAL TISSUES STUDIED BY MÖSSBAUER SPECTROMETRY**I. Bonková¹, M. Miglierini², M. Bujdoš¹ and M. Kopáni³¹*Institute of Laboratory Research on Geomaterials, Faculty of Natural Sciences, Comenius University in Bratislava, Ilkovičova 6, 842 15 Bratislava, Slovakia*²*Institute of Nuclear and Physical Engineering, Faculty of Electrical Engineering and Information Technology, Slovak University of Technology in Bratislava, Ilkovičova 3, 812 19 Bratislava, Slovakia*³*Department of Medical Physics, Biophysics, Informatics and Telemedicine, Faculty of Medicine, Comenius University in Bratislava, Sasinkova 4, 811 08 Bratislava, Slovakia*

In the current work, we focus on characterization of iron in biological tissues from the point of view of demonstration its magnetic properties. We have studied three types of biological tissues. Original samples that were extracted according to the Helsinki Declaration were lyophilized (dried in a vacuum) thus providing powder forms. We have investigated biological samples prepared from human brain, human and horse spleen. As a principal method of study, ⁵⁷Fe Mössbauer spectrometry (MS) in transmission mode was used. This technique enables simultaneous examination of both structural arrangement and magnetic states of iron atoms located in the samples. MS experiments were performed at room (~300 K) and liquid helium (4.2 K) temperature. A conventional constant acceleration spectrometer with ⁵⁷Co source in a rhodium matrix was used. At room temperature Mössbauer spectra show doublet-like features. Such behaviour is typical for fluctuating magnetic moments that acquire at room temperature arbitrary positions. On the other hand, low temperature MS measurements show significant contributions of sextets that confirmed the expected superparamagnetic behaviour. Different contents of magnetic spectral components suggest differences in the blocking temperatures observed for the three inspected biological tissues.

This work was supported by the grant VEGA 1/0836/15, UK/241/2016 and UK/242/2016.

P8-07**ASSESSMENT OF THE MAGNETOSTRICTIVE PROPERTIES OF THE SELECTED CONSTRUCTION STEELS**A. Juś¹, P. Nowak² and R. Szewczyk¹¹*Institute of Metrology and Biomedical Engineering, Faculty of Mechatronics, Warsaw University of Technology, Andrzej Boboli 8, 02-525 Warsaw, Poland*²*Industrial Research Institute for Automation and Measurements, Al. Jerozolimskie 202, 02-486 Warsaw, Poland*

The paper presents results of research on the effects of mechanical stresses on the magnetostrictive hysteresis loops of 13CrMo4-5 and X30Cr13 steels. Stress dependence of the magnetic hysteresis loops of these steels was presented previously [1, 2]. Measurements of stress dependence of magnetostriction fill the gap in the state of the art enabling description of relationships between stresses applied to the samples and its magnetoelastic and magnetostrictive properties.

Presented studies are the starting point for work to develop a unified model of both Villari (magnetoelastic) and Joule (magnetostrictive) effects under stresses in steels. The formulated model will be the basis for the development of generalized methods of interpreting the results of non-destructive testing of the state of the internal stresses in steels based on these phenomena.

Research were conducted using the unique measuring system developed by authors [3], partially based on [4]. The system allows to conduct strain gauges testing of magnetostriction under compressive and tensile stresses in frame-shaped samples made of different materials, with simultaneous magnetoelastic properties testing.

- [1] D. Jackiewicz, R. Szewczyk, J. Salach, A. Bieńkowski, and M. Kachniarz, "Influence of Stresses on Magnetic B-H Characteristics of X30Cr13 Corrosion Resisting Martensitic Steel," in *Recent Advances in Automation, Robotics and Measuring Techniques*, 2014, vol. 267, pp. 607–614.
- [2] M. Kachniarz, D. Jackiewicz, M. Nowicki, A. Bieńkowski, R. Szewczyk, and W. Winiarski, "Magnetoelastic Characteristics of Constructional Steel Materials," in *Mechatronics - Ideas for Industrial Application*, 2015, vol. 317, pp. 307–315.
- [3] O. Gińko, A. Juś, and R. Szewczyk, "Test Stand for Measuring Magnetostriction Phenomena Under External Mechanical Stress with Foil Strain Gauges," in *Challenges in Automation, Robotics and Measurement Techniques. Proceedings of AUTOMATION-2016, March 2-4, 2016, Warsaw, Poland*, 2016, vol. 440, pp. 843–853.
- [4] M. Urbański, T. Charubin, P. Rozum, M. Nowicki, and R. Szewczyk, "Automated System for Testing Ferromagnetic Materials," in *Challenges in Automation, Robotics and Measurement Techniques. Proceedings of AUTOMATION-2016, March 2-4, 2016, Warsaw, Poland*, 2016, vol. 440, pp. 817–825.

P8-08**MAGNETIC SUSCEPTIBILITY OF MULTIFERROIC PEROVSKITES**M. Maryško¹, V. V. Laguta¹, P. Novák¹ and I. P. Raevski²¹*Institute of Physics of ASCR, Na Slovance 2, 18221 Prague 8, Czech Republic*²*Institute of Physics, Southern Federal University, Rostov on Don 344090, Russia*

The perovskite compounds $A(\text{Fe}_{0.5}\text{M}_{0.5})\text{O}_3$ with nonmagnetic ions A^{2+} (Ba, Cd, Sr, Pb) and M^{5+} (Nb, Sb) were studied using the SQUID measurements of the dc and ac susceptibilities. The magnetic properties of these oxides depend crucially on the degree of the ordering of the Fe^{3+} ions in the octahedral sublattice [1][2], and also on the presence or absence of the Pb^{2+} ion [3]. Our experiments suggest that this ordering may lead to a perfect linear dependence of the inverse susceptibility vs T plot in the high temperature region (up to $T=380$ K) as was found for $\text{Sr}(\text{Fe}_{0.5}\text{Sb}_{0.5})\text{O}_3$. In this case we can reliably determine the effective moment of the Fe^{3+} . For all other compounds the observed curvature of the $1/\chi$ vs T plot reflects a more complicated arrangement or a disorder of the Fe^{3+} ions in the octahedral sublattice, which is discussed in the context with the recent theoretical calculations of the exchange interactions between the Fe^{3+} ions [2]. In the low temperature region information on the spin-glass like state coexisting with the antiferromagnetic phase is obtained from the temperature dependence of the ac susceptibility at different frequencies.

[1] I.P. Raevski et.al., *Ferroelectric*, 444, 47 (2013).

[2] R.O. Kuzian et al., *Phys.Rev. B*89, 024402-1 (2014).

[3] I.P. Raevski et al., *Phys.Rev. B*80, 024108-1. (2009).

I9-01**STRESS MONITORING & ANNIHILATION IN STEELS BASED ON MAGNETIC TECHNIQUES**E. Hristoforou¹, P. Vourna¹, A. Ktena¹ and P. Svec²¹*Sensor Lab, National TU of Athens, Athens 15780, Greece*²*Slovak Academy of Sciences, Bratislava, Slovakia*

In this presentation, we demonstrate our technology permitting stress tensor distribution monitoring in the bulk and the surface of ferromagnetic steels, concerning the determination of their residual stresses and plastic deformation, by using magneto-elastic non-contact and non-destructive methods with an uncertainty better than 1%. The speed of stress monitoring can reach 30 m/s under certain circumstances. Therefore, the steel producer, manufacturer or user can quantitatively measure the precise amplitude of the stress tensor distribution and its gradient on and in the produced or used steel.

This technology apart from allowing for the knowledge of the stress tensor distribution can also be used for obtaining stress annihilation or control, by means of being used as the feedback control of the automated system to precisely control stresses at any local point of the under test and treatment steel, using the existing or new technologies like thermos-mechanical treatment.

This technology, changing the map of non-destructive testing of steels, will allow for advanced steel production methods and procedures: those manufacturers who are to adopt this method will offer steel products with properly measured and obtained characteristics along the whole area and volume of the steel, governed by the corresponding stress distribution.

The sensing system and methodology can be used in the steel manufacturing products such as pipeline manufacturers, steel tool manufacturers, as well as the users of these products, like energy (classic thermoelectric or hydroelectric stations, as well as nuclear stations), oil & gas applications, shipping, automotive industry, railway & train industry and construction.

The method is under standardization process in National, European, American and International Standardization Bodies; in parallel, the method is currently being adopted from certification bodies, ship classes, specific institutions etc. in the form of directives and procedures to be followed by steel manufacturers and users.

O9-01**MAGNETIC PROPERTIES OF THE IONIC LIQUIDS****Edimim(FeX₄) (X = Cl and Br) IN ITS SOLID STATE**

I. de Pedro¹, A. García-Sáiz¹, J.L. Espeso¹, L.F. Barquín¹ and J. Rodríguez-Fernández¹

¹*CITIMAC, Facultad de Ciencias, Universidad de Cantabria, Santander 39005, Spain*

In recent years, there has been a tremendous expansion in the design and synthesis of ionic liquids (ILs). Among them, the magnetic ionic liquids (MILs)^{1,2} have highlighted, fueled by the possibility of combining the ILs properties with additional ones. These can be intrinsic thermochromic, magnetoelectrochromic or luminescent properties, depending on the used paramagnetic ion.

Here, we present two novel MILs, comprised of 1-ethyl-2,3-dimethylimidazolium (Edimim) cation and tetrahaloferrate(III) (FeX₄) (X = Cl and Br) anion³. They have been characterized by thermal, structural, magnetic and neutron studies. Their crystal structure is characterized by layers of cations (in non-planar configuration) and anions stacked upon one another in a 3D configuration, with several non-bonding interactions: hydrogen bond, anion- π , and halide-halide. The magnetic susceptibility and heat capacity measurements indicate the existence of a long-range antiferromagnetic ordering at approximately 3 K and 9 K for Edimim[FeCl₄] and Edimim[FeBr₄], respectively. The magnetic structure of the chloride-based compound shows that the 3D magnetic ordering takes place via Fe-Cl---Cl-Fe magnetic pathways, displaying a stronger superexchange magnetic interaction between the planes.

[1] García-Saiz A.; et al.; *Chem. Eur. J.*, 2014, 20, 72.

[2] García-Saiz A.; et al.; *Inorg. Chem.*, 2014, 53, 8384.

[3] García-Saiz A.; et al.; *RSC Adv.*, 2015 ,5, 60835.

09-02

MAGNETIC ANISOTROPY OF HARD MILLED SURFACE

A. Mičietová¹, J. Uriček¹, M. Čilliková¹, M. Neslušan¹ and P. Kejzlar²

*¹Faculty of Mechanical Engineering, University of Žilina,
Univerzitná 1, 010 26 Žilina, Slovak Republic*

*²Institute for Nanomaterials, Technical University in Liberec,
Studentská 1402/2, 46117 Liberec, Czech Republic*

This paper deals with investigation of hard milled surface as a surface undergoing severe plastic deformation at elevated temperatures. Such surface exhibits quite remarkable magnetic anisotropy (expressed in term of Barkhausen noise) and differs from ground surfaces. The main reason can be viewed in cutting temperature exceeding the Curie temperature needed to disturb magnetic domains configuration. The new domain alignment is configured during rapid cooling. Domains are not randomly but preferentially oriented in the direction of the cutting speed at the expense of feed direction. Barkhausen noise signals (measured in two perpendicular directions as cutting speed and feed direction) indicate that the mechanism of Bloch Wall motion during cyclic magnetization in hard milled surfaces differ from surfaces produced by grinding cycles.

O9-03**CHARACTERISATION OF ODS STEELS AFTER GAMMA IRRADIATION FOR APPLICATION IN ALLEGRO REACTOR**V. Slugeň¹, I. Bartošová¹ and J. Dekan¹*¹Institute of Nuclear and Physical Engineering, Slovak University of Technology in Bratislava, Ilkovičova 3, 812 19 Bratislava, Slovak Republic*

Oxide-dispersion-strengthened (ODS) characterization using various spectroscopic techniques is presented. Microstructure of 15% chromium ODS steels was studied in term of vacancy defects presence and their accumulation after defined irradiation treatment, respectively. Studied materials originated from Kyoto University and studied via IAEA collaborative project focused on generation IV reactors (Allegro). Samples were characterized “as received” by positron annihilation lifetime spectroscopy, Mössbauer spectroscopy and their microstructure was examined by transmission electron microscopy as well. Samples were afterwards irradiated in Washington State University Nuclear Radiation Center via a strong gamma source (6TBq). Damage induced by gamma irradiation was evaluated by positron lifetime measurements in emphasis on defect accumulation in the materials. We have demonstrated strong defect production induced by gamma irradiation which results from positron measurement data.

O9-04**MRI GRADIENT ECHO PULSE SEQUENCE AS A PHYSICAL TOOL IN DIFFERENTIATION OF NATIVE AND RECONSTRUCTED FERRITIN**

L. Balejcikova^{1,2}, O. Strbak¹, L. Baciak³, J. Kovac², M. Masarova¹, A. Krafcik¹, M. Peteri⁴, P. Kopcansky² and I. Frollo¹

¹*Institute of Measurement Science SAS, Dubravská cesta 9, 841 04 Bratislava 4, Slovakia*

²*Institute of Experimental Physics SAS, Watsonova 47, 040 01 Kosice, Slovakia*

³*Faculty of Chemical and Food Technology STU, Radlinského 9, 812 37 Bratislava, Slovakia*

⁴*Faculty of Electrical Engineering University of Zilina, Univerzitná 1, 010 26 Zilina, Slovakia*

Ferritin is a biological iron storage macromolecule, which consist of protein shell (apoferritin) and mineral core. Due to its biocompatible properties attracts interest in biomedical applications. It also plays a crucial role in pathological processes of disrupted iron homeostasis and iron accumulation, linked with various disorders (e.g. neuroinflammation, neurodegeneration, cirrhosis, etc). Iron overloaded ferritin, with the help of MRI techniques, has such potential to become a non-invasive biomarker of these processes. However, there is still lacking the method, which enables distinguish between physiological and pathological ferritin. With the help of MRI Gradient Echo (GE) pulse sequence, we managed to clearly distinguish between native and reconstructed ferritin (Fig. 1). It can serve as starting point in developing of method for differentiation of physiological and pathological ferritin. Such method is necessary in early diagnostics of iron-based disorders. Native ferritin represents the physiological ferritin model system, while reconstructed ferritin served as the pathological (iron overloaded) ferritin model system.

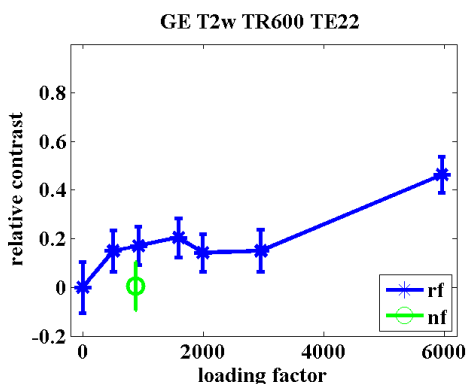


Figure 1: MRI relative contrast of native (nf) and reconstructed ferritin (rf) in comparison with loading factor, acquired with GE pulse sequence at 0.2 T.

P9-01**MAGNETIC AND MÖSSBAUER STUDY OF A CERIUM-BASED REACTIVE SORBENT**Y. Jiraskova^{1,2}, J. Bursik², O. Zivotsky³, J. Lunacek³ and P. Janos⁴¹*Ceitec IPM*, ²*Institute of Physics of Materials, AS CR, Žitkova 22, 616 62 Brno, Czech Republic*³*Institute of Physics, VŠB-Technical University of Ostrava, 17.listopadu 15, 708 33 Ostrava-Poruba, Czech Republic*⁴*Faculty of the Environment, University of Jan Evangelista Purkyně, Králova Výšina 7, 400 96 Ústí nad Labem, Czech Republic*

A new type of magnetically modified composites, namely a cerium-based reactive sorbent, can be applied to a decomposition of some dangerous organophosphate materials. Its composition based on the Fe-oxide grains covered by the active Ce-oxide nano-grains calls for macro- and microscopic magnetic investigations.

The powder samples in the as-prepared state and exposed to treatment at several calcination temperatures were followed by X-ray diffraction and transmission electron microscopy to see the phase composition and morphology, by the hysteresis curve measurements to determine magnetic characteristics and Henkel plots, and by the Mössbauer measurements to look at the microscopic magnetic properties. Selected samples were measured also at high and/or low temperatures to obtain information in more details.

Based on the calcination temperature the samples were divided into two groups yielding various magnetic behaviours. The first group consists of the samples annealed below 873 K. These samples exhibit low values of the coercivity and the remnant magnetization and the high saturation magnetization. The negative interparticle interactions start practically at zero magnetic field and reach their minima in weak fields about 2.4 - 3.2 kA/m. Above this temperature the changes in the magnetic behaviour are influenced by the iron oxide transformations and by the growth of the crystallite size contributing to the magnetic hardening.

The as-prepared sample and samples after treatments at 773 K–873 K–973 K were measured also between room temperature and 2 K and the field cooled and zero field cooled curves are compared and discussed from the viewpoint of the low-temperature Mössbauer spectra analysis.

P9-02

ANALYSIS OF STRUCTURE TRANSFORMATIONS IN RAIL SURFACE INDUCED BY PLASTIC DEFORMATION VIA BARKHAUSEN NOISE EMISSION

M. Neslušan¹, K. Zgutová², K. Kolařík³ and J. Šramka²

¹*Faculty of Mechanical Engineering, University of Žilina, Univerzitná 1, 010 26 Žilina, Slovak Republic*

²*Faculty of Civil Engineering, University of Žilina, Univerzitná 1, 010 26 Žilina, Slovak Republic*

³*Faculty of Nuclear Science and Physical Engineering, Czech Technical University in Prague, Trojanova 13, 120 00 Praha 2, Czech Republic*

This paper reports about magnetic Barkhausen noise emission of the rail surface exposed to long time cyclic plastic deformation. Severe plastic deformation of the rail surface induces remarkable structure transformation and alteration of stress state which contribute to valuable decrease of Barkhausen noise emission compared to untouched surface of the rail. The paper analyses correlation between Barkhausen noise signals (as well as extracted Barkhausen noise envelopes) and surface state (expressed in terms of micrographs, microhardness readings and residual stresses). This study would contribute to a possible concept for preventing unexpected rails deformation (or cracking) due to their thermal dilatation via Barkhausen noise technique.

P9-03**MÖSSBAUER STUDY OF CHANGES IN OLIVINE AFTER TREATMENTS IN AIR**M. Kądziołka-Gaweł¹ and Z. Adamczyk²*¹Institute of Physics, Silesian University, Uniwersytecka 4, 40-700 Katowice, Poland**²Institute of Applied Geology, Silesian University of Technology, Akademicka 2, 44-100 Gliwice, Poland*

The transformation mechanism of Fe cations in natural olivine $(\text{Fe, Mg})_2\text{SiO}_4$ after heating in air has been studied using ^{57}Fe Mössbauer spectroscopy and X-ray diffraction measurement. As the object of the study we selected the olivine rock from Krzeniów (Poland). Three transitions are seen. Fe^{2+} ions in olivine transform at temperatures 500°C-700°C to the nanoparticles of $\gamma\text{-Fe}_2\text{O}_3$. In temperatures range 800°C-900°C the transformation mechanism changes and appear two new phases $\alpha\text{-Fe}_2\text{O}_3$ and MgFe_2O_4 . Heating of investigated sample in temperature 1180°C occurs to formation of magnetic $\gamma\text{-Fe}_2\text{O}_3$ from $\alpha\text{-Fe}_2\text{O}_3$.

P9-04

HIGH SENSITIVITY CURRENT TRANSDUCER BASED ON FLUXGATE SENSOR WITH ULTRALOW COERCIVITY CORE

P. Frydrych¹, M. Nowicki² and R. Szewczyk¹

¹Institute of Metrology and Biomedical Engineering,

Warsaw University of Technology, Warsaw, Poland

²Research Institute for Automation and Measurements, Warsaw, Poland

Presented current transducer is using fluxgate sensor in Förster configuration as zero detection sensor. Transducer operates as compensation sensor. Typical difficulties caused by hysteresis bias were overcome by using ultralow coercivity core. Transducer consists of two ring shaped cores, and three kind of coils: magnetization, measurement and compensation coils.

Transducer exhibits high sensitivity and wide operation range. Sensor is resistant to external magnetic field disturbances and insensitive for angle between core axis and measured wire. It can operate in wide temperature ranges.

P9-05**BSA EFFECT ON CONTRAST PROPERTIES OF MAGNETITE NANOPARTICLES DURING MRI**

O. Strbak¹, M. Kubovcikova², L. Baciak³, I. Khmara⁴, D. Gogola¹, M. Koneracka², V. Zavisova², I. Antal², M. Masarova¹, P. Kopcansky² and I. Frollo¹

¹*Institute of Measurement Science SAS, Dubravska cesta 9,*

841 05 Bratislava, Slovakia

²*Institute of Experimental Physics SAS, Watsonova 47, 040 01 Kosice, Slovakia*

³*Faculty of Chemical and Food Technology STU, Radlinskeho 9,*

812 37 Bratislava, Slovakia

⁴*Safarik University, Faculty of Science, Pk Angelinum 9, 041 54 Kosice, Slovakia*

Proteins are biomarkers of many serious diseases (e.g. inflammation, cancer), and their changes in concentration levels are associated with various pathological processes. We tried to find out whether the presence of protein has influence on the contrast properties of MRI contrast agents. If so, it could provide additional information to the anatomical picture, without additional invasive diagnostics.

Our model system consisted of BSA as a specific protein, and magnetite nanoparticles stabilized with PEG as a carrier. MRI measurements were performed on 4.7 T (VARIAN) and 0.2 T (ESAOTE) systems. Images were acquired with standard T2 weighted protocols, and relative contrast, T2 relaxation time, and relaxivity r_2 were evaluated and compared.

The best concentration interval for contrast imaging of our model system is in range of 4-60 $\mu\text{g/ml}$ of magnetite. Difference in relative contrast of nanoparticles with and without BSA reaches nearly 20 %, which is in range visible to the naked eye. Differences in T2 are as follows (magnetite concentration [$\mu\text{g/ml}$] - relative T2 [%]): 0.5-19; 1-36; 2-7; 4-0.6; 7-10; 15-5; 30-1.5; 60-3; 120-2. The relaxivity values of nanoparticles are $358.73 \pm 1.4 \text{ mM}^{-1}\text{s}^{-1}$ without BSA, and $375.16 \pm 3.2 \text{ mM}^{-1}\text{s}^{-1}$ with BSA.

We have found that BSA protein affects the MRI contrast properties of magnetite nanoparticles up to 20 % in relative contrast, and almost 10 % in T2. In clinical practice it could have potential in providing additional information about the presence of protein as biomarker, without supplementary diagnostics.

This work was supported by the Slovak Research and Development Agency under Contract nos. APVV-14-0120, APVV-14-0932, and APVV-0431-12.

P9-06

THE EFFECT OF CRYO-ROLLING AND ANNEALING ON MAGNETIC PROPERTIES IN NON-ORIENTED ELECTRICAL STEEL

T. Kvačkaj¹, P. Bella², R. Bidulský¹, R. Kočíško¹, P. Petroušek¹, A. Fedoriková¹, J. Bidulská¹, P. Jandačka³, M. Lupták¹ and M. Černík⁴

¹*Faculty of Metallurgy, Technical University of Košice, Letná 9,
042 00 Košice, Slovakia*

²*ŽP VVC s.r.o., Kolkáreň 35, 976 81, Podbrezová, Slovakia*

³*Institute of Physics, VSB-Technical University of Ostrava, 17.listopadu 15/2172,
70833 Ostrava, Czech Republic*

⁴*U.S. Steel Košice, s.r.o., Research and Technology center, Vstupný areál
U.S.Steel, 044 54, Košice, Slovakia*

The goal of the present work is to compare progressive technology - rolling at cryogenic temperature and classical rolling at ambient temperature followed by investigation of their impact on the final microstructure and the magnetic properties of non-oriented electrical steel. Non-oriented electrical steel is characterized by high magnetic induction, low magnetic losses and low coercive force. The best magnetic properties are achieved by means of preferable texture and optimal grain size. In this paper is analyzed percentage of different textural components after cryo-rolling and after rolling at ambient temperature. To obtain maps of inverse pole figures (IPF) the electron backscatter diffraction (EBSD) method was used. The main contribution of this study was that the samples rolled at cryo conditions and after final annealing reached better magnetic properties than at ambient temperature, which was reflected by low magnetic losses and coercive force.

P9-07**COMPARISON OF IRON OXIDES-RELATED MRI ARTIFACTS IN HEALTHY AND NEUROPATHOLOGICAL HUMAN BRAIN TISSUE**

M. Masarova¹, A.Krafčík¹, M.Teplan¹, O. Strbak¹, D.Gogola¹, P. Boruta² and I. Frollo¹

¹*Institute of Measurement Science SAS, Dubravská cesta 9,
841 05 Bratislava, Slovakia*

²*Slovak Medical University, Limbova 12, 833 03 Bratislava, Slovakia*

Accumulated biogenic iron influences the MRI contrast of the T2 weighted images and causes hypo-intense artefacts. Iron accumulation in the form of iron oxide nanocrystals is associated with presence of neurodegenerative processes. The aim of this study is to investigate whether it is possible, with standard MRI sequences, to distinguish between healthy tissue and neuropathological tissue with accumulated iron.

Eighteen healthy volunteers were included in the study, as well as 13 patients with Multiple sclerosis (MS) or Parkinson disease (PD) patients. All subjects underwent MR examination at Siemens Magnetom Verio 3T system (Siemens HealthCare, Erlangen, Germany) by standard T2 weighted gradient-echo (GE) sequence. Mean value of absolute intensity of investigated region of interest (ROI) in basal ganglia or related structures (BGRS) was compared with the reference ROI in gray matter for each subject, each slice, for both, patients and group of healthy volunteers. Final relative contrast values were such acquired.

Our results indicate that we are able to statistically distinguish between healthy and diseased groups. Shapiro-Wilk test has shown that neither group was distributed normally. Subsequent non-parametric Kruskal-Wallis test confirmed that both investigated groups were significantly different ($p < 10^{-10}$). Leave-one-out cross-validation was implemented in order to simulate new patient approaching for diagnostics. “New” patient relative contrast distribution was classified according to comparison with pathological and control distributions via Kruskal-Wallis test. 84.6 % sensitivity and 94.4 % specificity was achieved.

These preliminary results suggest that MRI is feasible diagnostic tool for MS and PD, with the possibility to be further used in the research of iron quantification and non-invasive diagnostics of neuropathological diseases associated with the accumulation of biogenic iron oxide nanocrystals in brain tissue.

P9-08**ThALES - THREE-AXIS LOW ENERGY NEUTRON SPECTROSCOPY AT THE INSTITUT LAUE-LANGEVIN**

M.Klicpera^{1,2}, M. Boehm², S. Roux², J. Kulda¹, V. Sechovský¹, P. Svoboda¹, J. Saroun³ and P. Steffens²

¹Charles University in Prague, Faculty of Mathematics and Physics, Department of Condensed Matter Physics, Ke Karlovu 3, 121 16 Prague 2, Czech Republic

²Institut Laue-Langevin, 71 avenue des Martyrs - CS 20156, 38042 Grenoble Cedex 9, France.

³Nuclear Physics Institute AS CR, 25068 Rez, Czech Republic

Neutron inelastic scattering studies using three-axis spectrometers are indispensable for measuring elementary excitations of magnetic correlated systems. It yields the most complete information on the role of space and time correlations and their interplay in the behavior of condensed matter systems. Moreover, neutrons couple with comparable strength to both the structural and magnetic degrees of freedom, while the two scattering components can be separated using polarized neutron techniques.

The new cold neutron spectrometer *ThALES* at the Institut Laue-Langevin has been optimized for exploring correlated magnetic systems beyond the experimental possibilities of its predecessor IN14 spectrometer [1-3] in terms of data collection rate, kinematical range and neutron polarization analysis. *ThALES* covers momentum transfers up to 2 \AA^{-1} and energy transfers up to 18 meV with enhanced energy resolution ($\sim 0.05 \text{ meV}$ at incident wavenumber $k_i = 1.5 \text{ \AA}^{-1}$). New Heusler monochromator will provide a polarized neutron flux comparable to the old IN14 in its unpolarized mode. The challenge of measuring magnetic excitations in mm^3 -sized samples has been addressed by combining the virtual source concept with a focusing guide and a Si 111 focusing monochromator.

We present first results demonstrating the capabilities of this spectrometer for measuring magnetic correlated systems. The commissioning phase of *ThALES* has been finished in 2015. The instrument is now available to the user community.

The ThALES project is a collaboration between ILL and Charles University, financed by the Czech Ministry of Science and Education (Project no. LM2010001).

[1] Boehm M., Roux S. et al., JMMM 310 (2007) e965-e967.

[2] Boehm M., Roux S. et al., Meas. Sci. Technol 19 (2008) 034024.

[3] Boehm M., Čermák P. et al., J. Phys. Soc. Jap. 82, (2013) SA026.

P9-09**THERMAL EXPANSION MEASUREMENT METHODS**

P. Proschek¹, P. Opletal², A. Bartha², J. Valenta², J. Prokleška^{1,2} and V. Sechovský^{1,2}

¹*Department of Condensed Matter Physics, Charles University, Ke Karlovu 5, 121 16 Praha 2, Czech Republic*

²*Department of Condensed Matter Physics, Charles University, Ke Karlovu 5, 121 16 Praha 2, Czech Republic*

Measurement of elastic properties (thermal expansion and magnetostriction) under (multi)extreme conditions is a difficult task. In the vicinity of the room temperature or above it an abundance of methods is available, with decreasing temperature and adding magnetic field and/or hydrostatic pressure their number is limited. Dilatometric cells (either planparallel or tilted plate design) provide superior sensitivity in low temperatures and applied magnetic fields, however, cannot be used in hydrostatic cell. Common choice for the measurement of thermal expansion under hydrostatic pressure are methods based on strain-gauges, with mediocre sensitivity and more importantly a difficult or even impossible usage at very low temperatures ($T \sim 3\text{K}$).

Our aim was to construct a simple yet sensitive measurement method, which could be used for the measurement of thermal expansion and magnetostriction at very low temperatures ($T < 2\text{K}$) and applied hydrostatic pressures. Our design is based on the measurement of the electrical capacitance of the (specifically chosen) capacitor consisting of a base plate (25 μm polished copper foil), insulation (7.6 μm kapton foil) and polished sample. This allows the measurement of in plane expansion/contraction of rather small sample depending on the field and/or temperature with or without presence of hydrostatic pressure with sensitivity comparable to the use of strain-gauges.

The presentation will discuss the technicalities in detail, as well as test measurements with different samples (HoCo₂, UCoAl, Ce₂RhIn₈) under different conditions and their comparison with reference measurements.

P9-10**EFFECT OF STOCHASTIC DYNAMICS ON THE NUCLEAR MAGNETIC RESONANCE IN A FIELD GRADIENT**J. Tóthová¹ and V. Lisý^{1,2}*¹Department of Physics, Faculty of Electrical Engineering and Informatics, Technical University of Košice, Park Komenského 2, 042 00 Košice, Slovakia**²Laboratory of Radiation Biology, Joint Institute for Nuclear Research, 141980 Dubna, Russian Federation*

Nuclear magnetic resonance (NMR) has proven to be an effective means of studying molecular self-diffusion and diffusion in various materials and has a wide range of applications. The influence of diffusion on the signal of the NMR experiment, such as the spin echo, is described by the diffusion suppression function $S(t)$. In the literature, $S(t)$ is usually calculated using the Bloch-Torrey equation for the spin magnetization. Another way is to evaluate $S(t)$ through the time-dependent resonance frequency offset in the rotating frame, which is expressed through the position $x(t)$ of the nuclear spin at time t . It is assumed that $x(t)$ is a Gaussian random process. The known results in both the approaches are, however, valid only within the Einstein-Fick diffusion approximation. The current theories of the diffusion-based NMR thus ignore possible memory effects in the dynamics of the spin-bearing particles. Recent attempts to overcome this limitation operate with the positional autocorrelation function (PAF), which is not defined for unbounded particle motion, described by the standard or generalized Langevin equation. In the present contribution, the attenuation function $S(t)$ for an ensemble of spins in a magnetic-field gradient is expressed through an accumulation of the phase shifts in the rotating frame due to the changes of the particle displacements. Instead of the PAF we deal with the mean square displacement $X(t)$, the well defined and experimentally measured function. The obtained new formulas for $S(t)$ and the NMR line broadening due to the particle motion in a simple experiment, when the nuclear induction signal is read-out in the presence of a field gradient, significantly differ from the known ones and are applicable for any kind of the stochastic motion of spins, including their non-markovian Brownian motion and anomalous diffusion. The classical expression valid for normal diffusion is just a special (long-time) case within our consideration. Our method is also applicable to the NMR pulse sequences based on the refocusing principle. This is demonstrated by describing the spin echo experiment developed by Hahn.

P9-11**THE INFLUENCE OF ANNEALING TEMPERATURE ON THE MAGNETIC PROPERTIES OF CRYO-ROLLED NON-ORIENTED ELECTRICAL STEEL**

T. Kvačkaj¹, P. Bella², R. Bidulský¹, R. Kočíško¹, A. Fedoriková¹, P. Petroušek¹, J. Bidulská¹, P. Jandačka³, M. Lupták¹, L. Gembalová⁴ and M. Černík⁵

¹ *Faculty of Metallurgy, Technical University of Košice, Letná 9, 042 00 Košice, Slovakia*

² *ŽP VVC s.r.o., Kolkáreň 35, 976 81, Podbrezová, Slovakia*

³ *Institute of Physics and IT4 Innovations centre, HGF, VSB-Technical University of Ostrava, 17.listopadu 15/2172, 70833 Ostrava, Czech Republic*

⁴ *Institute of Clean Technologies for Mining and Utilization of Raw Materials for Energy Use, HGF, VSB-Technical University of Ostrava, 17.listopadu 15/2172, 70833 Ostrava, Czech Republic*

⁵ *U.S. Steel Košice, s.r.o., Research and Technology center, Vstupný areál U.S.Steel, 044 54, Košice, Slovakia*

The paper is focused on a comparison of the magnetic properties of the non-oriented electrical steel containing 3.5% Si. Two methods were used - conventional rolling at ambient temperature and a progressive rolling in cryogenic conditions. The total deformation of the samples was $\varepsilon = 15\%$. Subsequently, the samples were heat treated at temperatures $T = \langle 900; 1000; 1100 \rangle$ °C. Measuring of the magnetic properties was carried out in an alternating magnetic field at frequencies $f = \langle 50; 100; 150 \rangle$ Hz. At a frequency of 50 Hz were achieved smallest magnetic losses and therefore further measurements were made at a given frequency. Followed measurements of the magnetic induction were conducted at different intensities of magnetic field. EBSD analyses were performed to obtain the IPF maps on which the resulting structure was evaluated after processing of the material. The specific magnetic losses were compared for different processing methods. The suitable condition is cryo-rolling followed by annealing at 900 °C, for which the smallest magnetic losses was measured.

P9-12**THE EFFECT OF RESIDUAL STRESSES ON THE COERCIVE FIELD STRENGTH OF DRAWN WIRES**M. Suliga¹, R. Kruzel¹, K. Chwastek², A. Jakubas² and P. Pawlik¹¹*Faculty of Materials Processing and Production Technology, Częstochowa University of Technology, Al. AK 19, 42-201 Częstochowa, Poland*²*Faculty of Electrical Engineering, Częstochowa University of Technology, Al. AK 17, 42-201 Częstochowa, Poland*

Residual stresses occurring in ferromagnetic materials after processing affect their magnetic properties. This effect may be useful for nondestructive testing purposes, as the monitoring of residual stress level is crucial in failure analysis for safety reasons. Wire drawing is an example of industrial process, where such monitoring is extremely important.

Coercive field strength in soft magnetic materials is affected by a number of factors i.e. microstructure (in particular the presence of inclusions acting as pinning sites for domain walls), intrinsic and stress-induced anisotropy and eddy currents. This quantity may be used as an indicator of residual stress level in drawn wires.

The present paper considers the effect of drawing speed velocity on coercive field strength in high (0.85 wt %) carbon steel wires. Magnetic M - H dependencies have been determined using a vibrating sample magnetometer VSM 7301 from Lakeshore.

P9-13**MAGNETIC AURA MEASUREMENT IN DIAGNOSTICS AND CONTROL OF A SMALL TURBOJET ENGINE**R. Andoga¹ and L.Főző²*¹Department of Avionics, Technical University of Košice, Rampová 7, 040 21 Košice, Slovakia**²Department of Aviation Engineering, Technical University of Košice, Rampová 7, 040 21 Košice, Slovakia*

Different information sources can be used in diagnostics and control of a turbojet engine. These sources are usually represented by measured values from sensors evaluating the thermo-dynamic process of the engine and its state parameters, like temperatures, pressures, speeds, vibrations, etc. We present a novel idea of expanding this broad range of parameters by measurement of magnetic aura of a small turbojet engine. Manifestation of the inner processes in magnetic aura can hold valuable information, which can be used to obtain diagnostic information of the engine as well as be used to enhance its control. The presented article shows pilot experimental results and basic concepts of possible application of magnetic aura measurements in diagnostics and control on the laboratory object of a small turbojet engine MPM-20.

We deal with the main hypothesis that an object like a small turbojet engine manifests its thermodynamic parameters and energy also by its magnetic aura. Magnetic aura is defined as a density of magnetic volume expressed by intensity of magnetic field shape of which is set by the geometry of magnetically conductive object. Several measurements have been done in order to confirm and evaluate the existence of magnetic aura in the Laboratory of intelligent control systems of aircraft engines. A series of measurements in the free space of the laboratory to set the baseline magnetic field, measurements of the object of small turbojet engine in its unpowered state and at last the measurements of magnetic aura surrounding the engine during its operational states.

The article further deals with information obtained from magnetic aura measurements in enhancing solution of two cybernetic tasks with the engine MPM-20, which is diagnostic of its state as well as possibilities of improvements of its control. We design a special class of algorithms and models in order to enhance the currently designed diagnostic system of the engine with a new set of parameters resulting from magnetic aura measurement and select the ones, which are usable in diagnostics. The same approach is taken, where the situational control system of the engine is enhanced by application of feedback information from the magnetic aura measurement. These concepts are to be experimentally proven in future research.

P9-14**MECHANOCHEMICAL PREPARATION AND MAGNETIC PROPERTIES OF $\text{Fe}_3\text{O}_4/\text{ZnS}$ NANOCOMPOSITE**Z. Bujňáková¹, A. Zorkovská¹ and J. Kováč²¹*Institute of Geotechnics, Slovak Academy of Sciences, Watsonova 45, 040 01, Košice, Slovakia*²*Institute of Experimental Physics, Slovak Academy of Sciences, Watsonova 47, 040 01, Košice, Slovakia*

Powder nanocomposite of $\text{Fe}_3\text{O}_4/\text{ZnS}$ was prepared by mechanochemical synthesis in a planetary ball mill. In this reaction natural magnetite mineral Fe_3O_4 was used, together with zinc acetate $(\text{CH}_3\text{COO})_2\text{Zn} \cdot 2\text{H}_2\text{O}$ and sodium sulfide $\text{Na}_2\text{S} \cdot 9\text{H}_2\text{O}$, as precursors for the zinc sulfide ZnS . Pure natural magnetite was milled under the same conditions, for comparison. Particle size analysis and X-ray diffraction revealed that the sample is composed of small nanocrystalline particles, containing Fe_3O_4 and ZnS . When comparing the non-milled and milled Fe_3O_4 samples, the reduction of saturation magnetization (from $90 \text{ Am}^2/\text{kg}$ to $69 \text{ Am}^2/\text{kg}$, respectively) can be observed, as a consequence of the milling process (strong size reduction, increase of specific surface area and surface disorder). The non-milled magnetite showed distinctive Verwey-transition at around 120 K, this becomes suppressed after milling, what is a sign of strong structural disorder and presence of defects. The magnetization of the $\text{Fe}_3\text{O}_4/\text{ZnS}$ nanocomposite was the lowest ($34 \text{ Am}^2/\text{kg}$), what is reasonable, since the weight fraction of the ferromagnetic component is decreased. Nevertheless, the $\text{Fe}_3\text{O}_4/\text{ZnS}$ sample demonstrates ferromagnetic behavior as well, and the structure is less perturbed by milling, the Verwey-transition, although less impressive, but is preserved.

The unique combination of magnetic and fluorescent properties in such a bifunctional material like $\text{Fe}_3\text{O}_4/\text{ZnS}$ seems to be very promising in wide range of applications, especially in the field of nanomedicine.

P9-15**ESTIMATION OF MULTICHANNEL MAGNETOMETER NOISE FLOOR IN ORDINARY LABORATORY CONDITIONS**D. Praslička¹, P. Lipovský¹, J. Hudák¹ and M. Šmelko¹*¹Department of Aviation Technical Studies, Faculty of Aeronautics, Technical University of Košice, Rampová 7, 041 21 Košice, Slovakia*

The article deals with the method for estimation of noise floor in each channel of a multichannel magnetometer in ordinary laboratory conditions. Attention to the environment is important to obtain accurate noise measurements of any given sensor. Magnetic noise sources operating nearby or far away from the measurement place such as powerlines, switched supplies, mechanical vibrations either stochastic or deterministic, or local magnetic field variations can cause inaccurate sensor noise readings. Often there is not the possibility to test the magnetic sensor in a magnetically shielded chamber and even with the use of the chamber it is not possible to suppress the DC and extremely low frequencies fields to the exactly zero value.

In the article we deal with the statistical method of big data set processing to separate ambient noise from inherent noises of the multichannel magnetometer, thus providing characterization of their noise performances in an ordinary laboratory with changing ambient conditions. In the experiments we used the four-channel magnetometer of VEMA series developed at our Department. This magnetometer has simultaneously sampled channels at 1 kHz. For each channel variances and correlations of recorded signals were analyzed and also the power spectral densities for 250 Hz bandwidth were specified. Based on the experimental results we obtained the noise floor estimation for each channel. The proposed method is also suitable for other and not only magnetic multichannel sensor systems.

P9-16**NON-STATIONARY NOISE ANALYSIS OF MAGNETIC SENSORS USING ALLAN VARIANCE**K. Draganová¹, V. Moucha¹, T. Volčko¹ and K. Semrád¹¹*Department of Aviation Technical Studies, Faculty of Aeronautics, Technical University of Košice, Rampová 7, 041 21 Košice, Slovakia*

The Allan variance is a method of analyzing a sequence of data in the time domain and can also be used to determine the noise types in a system as a function of the averaging time even in cases, which cannot be adequately handled with a classical statistical approach. It is one of the methods for identifying and quantifying the different noise types that exist in inertial sensor data and the theory is very good applicable also for magnetic sensors [1], which become nowadays together with accelerometers and gyroscopes a common part of inertial measurement units. After computation of Allan variance as a function of different averaging times without the need of any transformations we obtain the characteristic regions with different slopes that specify the noise types existing in inertial sensors, including white and quantization noise, random walk and flicker noise.

However the Allan variance is the most common time domain measure of frequency stability and several versions of it that provide for example better statistical confidence or can better distinguish noise types have been developed, there is still a problem with determination of those output data series, which exhibit non-stationary behavior over time, for example due to the interference, disturbances or temperature changes. Therefore during the noise analysis it is necessary to consider dynamic characteristics and time-varying nature of the noise stability.

The presented paper describes methodology for non-stationary noise analysis of the magnetic sensors' data verified by the simulations and experiments and results of obtained data analysis are graphically presented and statistically evaluated and underline the correctness of the initial hypothesis and confirm suitability of the dynamic Allan variance approach also for magnetic sensors with the non-stationary behavior of noise.

- [1] DRAGANOVÁ, K., KMEC, F., BLAŽEK, J., PRASLIČKA, D., HUDÁK, J., LAŠŠÁK, M. Noise Analysis of Magnetic Sensors Using Allan Variance. In *Acta Physica Polonica A*, Vol. 126, No. 1 (2014), p. 394-395. ISSN 1898-794X.

P9-17**CALIBRATION OF MAGNETOMETER FOR SMALL SATELLITES USING NEURAL NETWORK**

T. Kliment¹, D. Praslička¹, P. Lipovský¹, K. Draganová¹ and O. Závodský^{2,3}

¹*Department of Aviation Technical Studies, Technical University of Košice, Rampová 7, 041 21 Košice, Slovakia*

²*Slovak Organization for Space Activities (SOSA), Zámocká 18, 811 01 Bratislava, Slovakia*

³*Department of Telecommunications and Multimedia, University of Žilina, Univerzitná 1, 010 26 Žilina, Slovakia*

Methodology shown in the article was designed for a pre-flight calibration of the magnetometer used in the first Slovak satellite skCUBE, where the magnetometer performs stabilisation and navigation tasks. The article presents the scalar calibration method that uses a neural network for the determination of parameters of the inverse model of the vector magnetometer. Vogel's method was used for the generation of the data sets. Using this methodology, the knowledge of the true orthogonal decomposition of the measured magnetic field vector is not necessary. In comparison with the conventional thin-shell test, this calibration solves non-linearities using Taylor's activation functions and can work with the dataset of any size. Utilisation of the one-layered, feed-forward neural network with the back propagation algorithm has suppressed the systematic errors of vector magnetometers, namely the multiplicative, additive, orthogonality and linearity errors.

The experiment was performed in a 3D Helmholtz coil system, when the Earth's magnetic field was suppressed and at the same time the stimulation field was created. Complete suppression of the Earth's magnetic field was achieved by special positioning of the satellite. Honeywell HMC5883L was used for the verification of the methodology. The standard deviation of the scalar error of the uncalibrated sensor was substantially reduced. In the end we present a global map of scalar errors before and after the calibration. Random distribution of the error in the map of scalar errors after the calibration confirms efficiency of the methodology and adequacy of the inverse model.

P9-18**BARKHAUSEN NOISE INVESTIGATIONS OF 5.5 MM WIRE RODS WITH VARIOUS CARBON CONTENT**M. Suliga¹ and T. Garstka¹*¹Faculty of Production Engineering and Materials Technology, Częstochowa University of Technology, Al. Armii Krajowej 19, 42-200 Częstochowa, Poland*

In this paper, the results of testing of wire rods by the magnetic method based on Barkhausen noise (BN) analysis were presented. Continuing the preliminary works [1], eight samples of Ø5.5 mm wire rod with wide range of carbon content, from 0.05% to 0.85%, were examined to better recognize contribution of the microstructure and stress level on Barkhausen effect, and the same, to find quick and reliable non-destructive tool to control of wire rods and wires.

The Barkhausen noise examinations were carried out using the measurement equipment developed at Faculty of Production Engineering and Materials Technology of Częstochowa University of Technology. To meet demands of wire rod testing, special design of the measuring head was elaborated too.

The measurements of BN were done in few points on the length of each sample, to average the local fluctuations. The typical parameters like amplitude, root mean square value of BN as well as shape and the time dependences of the BN envelope peak shift were analyzed.

As an effect of these investigation, first of all, strong dependence between carbon content in steel and Barkhausen noise peak shift was found as was expected. Also other parameters of BN e.g. root mean square value were studied and discussed in confrontation to the results of mechanical properties testing of wire rods. Obtained results are point of entry for further investigations of wire rods and final wires with different carbon content and after various variants of drawing.

- [1] Garstka T., Dyja H., An attempt of characterization of stress state in high carbon C68d steel wire rod by Barkhausen noise method, *Przegląd Elektrotechniczny*, R. 91 No 4/2015, pp 20-23.

P9-19**SUPERCONDUCTIVITY AND QUANTUM CRITICALITY IN $\text{Cr}_{100-z}\text{Os}_z$** P.R. Fernando¹, C.J. Sheppard¹ and A.R.E. Prinsloo¹¹*Department of Physics, University of Johannesburg,**Corner of University and Kingsway, 2006 Auckland Park, South Africa*

Previous studies on the magnetic phase diagram (MPD) of $\text{Cr}_{100-z}\text{Os}_z$ focused on diluent concentrations up to $z \approx 2$ [1]. This is surprising as the MPDs of many Cr alloys with group-8 metals, such as Cr with Re and Ru, show interesting properties, including quantum critical behavior (QCB) [2,3], as well as superconducting (SC) behavior existing with antiferromagnetism (AFM) [1]. It is noted that SC properties in $\text{Cr}_{100-z}\text{Os}_z$ alloys with $z > 25$ were previously reported [4]. However, studies of these Cr alloys with high diluent concentrations of group-8 metals showed that these alloys include binary phases such as Cr_3X , that contains a cubic A15 phase, shown to be SC [5,6] that need to be probed further.

In order to extend investigations into the physical properties and the magnetic phase diagram of the $\text{Cr}_{100-z}\text{Os}_z$ system, the present study focuses on the characteristics of alloys with $2 \leq z \leq 30.6$. XRD analysis, as well as the measurement of several transport and magnetic properties were utilized.

Structural analysis show that samples with $z < 20$ has a bcc structure, while those with $z > 22$ include a cubic A15-type structure. Physical properties measurements indicate that the AFM disappears at $z \approx 14$ and that samples with concentrations $z \geq 13$, lower than the mentioned $z > 25$ [4], show SC behavior.

The magnetic phase diagram of $\text{Cr}_{100-z}\text{Os}_z$ is constructed from the Néel transition temperatures obtained from various measurements. The commensurate spin-density-wave (CSDW) to paramagnetic (PM) phase line reaches a maximum at $z \approx 4$, where after it decreases sharply. Fitting parameters of a power law fit to this CSDW-PM phase line indicate possible QCB. The present results suggest that this phase line terminates in a narrow SC dome near a magnetic quantum critical point, similar to that previously observed in certain heavy fermion systems [7], but not previously reported for other Cr alloys.

[1] Fawcett E. *et al.*, Rev. Mod. Phys 66(1) (1994) 25.[2] Reddy L. *et al.*, J. appl. Phys 103(7) (2008) 07C903.[3] Jacobs B.S. *et al.*, J. Appl. Phys. 113 (2013) 17E126.[4] Blaugher R.D. *et al.*, J. Low. Temp. Phys. 1(6) (1969) 539.[5] Van Reuth E.C. *et al.*, Acta Cryst. B24 (1968) 186.[6] Flukiger R. *et al.*, Solid State Commun. 14 (1974) 443.[7] Löhneysen H. *et al.*, Rev. Mod. Phys. 79 (2007) 1015.

P9-20**MAGNETIC PROPERTIES OF $\text{Sc}_{1-x}\text{Ti}_x\text{Fe}_2$ UNDER HIGH PRESSURE**Z. Arnold¹, M. Mišek¹, O. Isnard², J. Kaštil¹ and J. Kamarád¹¹*Institute of Physics AS CR, v.v.i., Na Slovance 2, Prague 8, Czech Republic*²*Institut Néel, CNRS / Université Joseph Fourier, 38042 Grenoble, France*

The pseudo-binary $\text{Sc}_{1-x}\text{Ti}_x\text{Fe}_2$ system crystallizes in the hexagonal MgZn_2 type structure ($\text{P6}_3/\text{mmc}$) and exhibits, as function of x , different forms of $3d$ magnetism. ScFe_2 is ferromagnet with $T_C = 540$ K and average magnetic moment $1.37 \mu_B/\text{Fe}$. TiFe_2 is antiferromagnet with $T_N = 280$ K and different magnetic moments on 6h sites ($1.4 \mu_B/\text{Fe}$) and 2a sites ($\sim 0 \mu_B/\text{Fe}$). Within the $\text{Sc}_{1-x}\text{Ti}_x\text{Fe}_2$ series this different behavior leads to complex magnetic diagram with magnetic ground state varying from ferromagnetic for Sc- rich compounds through canted states where ferromagnetism and antiferromagnetism coexists to an antiferromagnetic ground state for Ti-rich compositions. Since the substitution of Ti by Sc is accompanied with an increase of the volume of elementary cell, the application of the high pressure can have similar effect as substitution of Sc by Ti.

To get more detailed information about the effect of volume change on the character of magnetism and exchange interactions we have studied effects of hydrostatic pressure up to 1 GPa on magnetic properties of polycrystalline $\text{Sc}_{1-x}\text{Ti}_x\text{Fe}_2$ ($x = 0.65; 0.9$ and 1) compounds in temperature range $5 - 380$ K using a SQUID magnetometer with magnetic field up to 7T and miniature Cu-Be pressure cell.

Both the TiFe_2 and $\text{Sc}_{0.1}\text{Ti}_{0.9}\text{Fe}_2$ exhibit antiferromagnetic structure at high temperatures with $T_N = 283$ K and $T_N = 260$ K, respectively. Their antiferromagnetic states are very stable under high pressure, $dT_N/dp = -1$ K/GPa and $dT_N/dp \sim 0$ K/GPa for TiFe_2 and $\text{Sc}_{0.1}\text{Ti}_{0.9}\text{Fe}_2$ respectively. Contrary to TiFe_2 that exhibit antiferromagnetic ground state at low temperatures, the magnetization of $\text{Sc}_{0.1}\text{Ti}_{0.9}\text{Fe}_2$ exhibits remarkable increase below 50 K indicating the coexistence of ferromagnetism and antiferromagnetism. The magnetic isotherms at different temperatures showed moderate decrease of magnetization with pressure. The temperature of appearance of ferromagnetic contribution decreases with increasing pressure, $dT_0/dp = -17$ K/GPa.

$\text{Sc}_{0.35}\text{Ti}_{0.65}\text{Fe}_2$ compound exhibits complex ferromagnetic structure with $T_C = 348$ K and another ferro-ferro transition at 108 K. Application of pressure leads not only to decrease of T_C with a slope $dT_C/dp = -27$ K/GPa but also to significant decrease of both temperature and magnetization of ferro-ferro transition. The role of volume at these transitions will be discussed.

P9-21**INFLUENCE OF MAGNETIC SHIELD ON THE HIGH FREQUENCY ELECTROMAGNETIC FIELD PENETRATION THROUGH THE BUILDING MATERIAL**

I. Kolcunová¹, M. Pavlík¹, J. Zbojovský¹, S. Ilenin¹, Z. Čonka¹, M. Kanálik¹, D. Medveď¹, A. Mészáros¹, L. Beňa¹ and M. Kolcun¹

¹Technical University of Košice, Faculty of Electrical Engineering and Informatics, Department of Electric Power Engineering, Mäsiarska 74, 042 01 Košice, Slovak Republic

This paper concerns with the task how to protect the inhabitants against the electromagnetic radiation inside the building. Widespread usage of the mobile communication led to building of more and more new GSM base-station antennas. These antennas are often placed in the areas with high population density. People living near these base-station antennas are daily exposed to GSM electromagnetic fields. These antennas emit electromagnetic radiation in standard mobile operator's frequencies, i.e. 900 MHz, 1.8 GHz and 2.1 GHz. Many studies have shown potential biological and thermal effects of GSM electromagnetic fields, therefore people are concerned about their health. Electromagnetic wave does not penetrate the wall of the building as a whole. Small part of the wave is reflected and small part is absorbed by the building material. This paper deals with the measurements of the penetration of electromagnetic waves through the commercially available building materials and it compares the measured results for frequencies 900 MHz, 1.8 GHz and 2.1 GHz. After that the surface of the chosen building material was coated with a magnetic conductive paint in order to improve the shielding effect of the building material. The results of experiment should show how the magnetic shield will reduce the penetration of electromagnetic waves through the building wall.

P9-22

**ADDITIONAL MODIFICATION OF THERMOMAGNETIC PROPERTIES
OF OBJECTS OF LOW RELATIVE PERMEABILITY IN
ELECTROMAGNETIC FIELD**

D. Medved¹, M. Pavlík¹, J. Zbojovský¹, S. Ilenin¹, Z. Čonka¹, M. Kanálik¹,
I. Kolcunová¹, A. Mészáros¹, L. Beňa¹ and M. Kolcun¹

*¹Technical University of Košice, Faculty of Electrical Engineering and
Informatics, Department of Electric Power Engineering, Mäsiarska 74, 042 01
Košice, Slovak Republic*

The paper presents a characteristics of the foodstuff heating phenomenon using induction heating process by an induction cooker. The simulation setup is prepared according to the proposed magnetic material and configuration of the pot and induction cooker. The material properties of pot were varied among the several alternatives. The helical coil is designed based on the limitation of the induction cooker size and given number of coil turns and coil tube diameter with specific supplied electric current density. The data from the simulation analysis have to determine the enhancing of the highest heat transfer from induction cooker into pot. These data led to the modification of the material and geometrical properties of the pot in accordance to a minimum heating time and enhanced safety operation achieving, especially to the close unshielded magnetic objects.

P9-23**ELECTRO-RHEOLOGICAL PROPERTIES OF TRANSFORMER OIL-BASED MAGNETIC FLUIDS**

K. Paulovičová¹, J. Tóthová², M. Rajňák¹, M. Timko¹, P. Kopčanský¹ and V. Lisý^{2,3}

¹*Institute of Experimental Physics, SAS, Watsonova 47, 040 01 Košice, Slovakia*

²*Department of Physics, Technical University of Košice, Park Komenského 2, 042 00 Košice, Slovakia*

³*Laboratory of Radiation Biology, Joint Institute for Nuclear Research, 141980 Dubna, Moscow Region, Russia*

The control of the viscosity of a suspension by an electric field has been intensively studied during the last decade because of both the fundamental interest and numerous possible applications (active damping, viscous coupling, etc.). Most of these studies have shown that the viscosity increases when an electric field is applied to a suspension of dielectric particles. This effect is due to a chain formation of the particles of the suspension, induced by their polarization under the electric field.

The aim of this work was to study rheological behavior of nanofluids affected by electric field and temperature. We used transformer oil-based magnetic fluids (TOMFs), the suspensions of permanently magnetized colloidal particles (Fe_3O_4) coated by a stabilizing surfactant and immersed in transformer oil. For their exquisite and thermal properties they have a potential to become an alternative to conventional transformer oils used in the transformer, the most significant and essential part in the modern power grid system for transmission and distribution of electric power. The rheological characterization of TOMF was performed using the rotational rheometer MCR 502. The temperature dependence of the viscosity was measured at 25, 50 and 75°C in shear rate and electric field range 10-1000 s^{-1} and 0-6 kVcm^{-1} , respectively. It is assumed that the electric field induced viscosity change can play a key role in the streamer initiation and affect in this way the breakdown field strength of TOMF. Our recent study on TOMF showed that the interfacial relaxation processes contribute to the total dielectric response of TOMF. Moreover, by means of dielectric spectroscopy on thin TOMF layers with applied DC bias voltage, we found strong indications that the external electric field induces aggregation of the magnetic nanoparticles. We have clearly demonstrated visually observable pattern formation in TOMF exposed to a DC electric field. Unusual viscosity dependencies on the shear rate at different temperatures and electric fields have been observed. This is the subject of our current investigations.

P9-24**SOLID STATE ^{13}C NUCLEAR MAGNETIC RESONANCE STUDY OF MORPHOLOGY AND MOLECULAR MOBILITY OF POLYHYDROXYBUTYRATE**A. Baran¹, P. Vrábek¹ and D. Olčák¹*¹Department of Physics, Faculty of Electrical Engineering and Informatics, Technical University of Košice, Park Komenského 2, 04200 Košice, Slovakia*

Biodegradable polymers with properties comparable to conventional polymers used in industry are environmentally friendly materials which have been extensively studied in recent years [1]. Polyhydroxybutyrate, or PHB is a semicrystalline [2] biodegradable and biocompatible polymer [3] with mechanical properties very similar to isotactic polypropylene [4].

The physical properties of polymers are strongly dependent on their structure and morphology, which can be influenced by changing the crystallization conditions and by quenching or annealing at different temperatures. The aim of the present work is to study the influence of quenching on morphology and molecular dynamics of PHB using ^{13}C NMR spectroscopy. The analysis of single pulse MAS ^{13}C NMR spectra of virgin and quenched PHB indicates semicrystalline character of both samples, however, in the case of quenched PHB an increase of amorphous phase ratio was observed. The carbon spin-lattice relaxation times $T_1(^{13}\text{C})$ measured at ambient temperature indicate an increase in local mobility in quenched PHB in comparison to the virgin one. The changes in morphology and molecular mobility can be associated with the increase of free volume in quenched PHB sample.

- [1] Armentano I., Fortunati E., Burgos N., Dominici F., Luzi F., Fiori S., Jimenez A., Yoon K., Ahn J., Kang S., and Kenny J.M., *eXPRESS Polymer Letters* 9, (2015) 583.
- [2] Nozirov F., Fojud Z., Klinowski J., and Jugra S., *Solid State Nuclear Magnetic Resonance* 21, (2002), 197.
- [3] Zhang M., Thomas N. L., *Advances in Polymer Technology* 30, (2011), 67.
- [4] Doi Y., Kanesawa Y., Kawaguchi Y. and Kunioka M., *Macromolecular Chemical Rapid Communication* 10, (1989), 227.

P9-25**OPTIMIZED FREQUENCY SELECTIVE SURFACE FOR THE DESIGN OF MAGNETIC TYPE THIN BROADBAND RADIO ABSORBERS**V. Babayan¹, N. E. Kazantseva¹, Yu. N. Kazantsev², J. Vilčáková¹ and R. Moučka¹¹*Centre of Polymer Systems, Tomas Bata University in Zlin, Tr. T. Bati 5678, Zlin, 760 01, Czech Republic*²*Fryazino Branch of Kotel'nikov Institute of Radio Engineering and Electronics, Russian Academy of Sciences, pl. Vvedenskogo 1, Fryazino 141190, Russia*

Nowadays, the solution of problems associated with electromagnetic interference and the negative impact of electromagnetic radiation on human beings are of particular importance due to the rapid penetration of electronics to virtually all fields of a modern life. One of the means to address these concerns is the use of radio absorbers (RAs). For the optimal design of RAs the reduction of weight and thickness as well as broadening of operating frequency range of absorber must be considered simultaneously. In the current work, the aforementioned conditions are satisfied owing to the incorporation of an optimized frequency selective surface (FSS) into the structure of magnetic type RA representing the polymer composite filled with carbonyl iron. Carbonyl iron type and its concentration in a composite have been varied in such a way to achieve the frequency dispersion of complex permeability in 1–20 GHz region.

Generally, the width of operating frequency range of RA depends on resonance frequency and quality factor (Q-factor) of FSS as well as on its position in absorber. As a rule, the lower the value of Q-factor the wider will be an operating frequency range of RA. However, the realization of FSS with a Q-factor lower than 1.3 with the aid of productive and low-cost technology is rather challenging. Having this fact in mind, we came up with a novel FSS the unique structure of which allows one to achieve the value of a Q-factor as low as 0.5.

The optimized FSS represents an array of flat electrically conductive elements deposited on the both sides of nonconductive polymer foil so that on the one of the sides the elements are having a closed-loop structure and on the opposite side are representing solid fragments connecting projections of the neighboring closed loops. The effectiveness of FSS application in RAs operating in microwave region was successfully verified both numerically as well as experimentally. The thickness of designed RAs varied from 1.5 mm to 3 mm depending on the composition of RA.

Acknowledgments: This work was supported by the Ministry of Education, Youth and Sports of the Czech Republic – Program NPU I (LO1504).

P9-26**APPLICATIONS OF BISTABLE MAGNETIC MICROWIRES**

R. Sabol¹, P. Klein¹, T. Ryba¹, R. Varga^{1,2}, M. Rovnak³, I. Sulla⁴, D. Mudronova⁵, J. Gálik⁶, I. Poláček⁷ and R. Hudák⁷

¹*RVmagnetics s.r.o., Hodkovce 21, 04421 Košice, Slovakia*

²*Inst. Phys., Fac. Sci., UPJS, Park Angelinum 9, 041 54 Košice, Slovakia*

³*Faculty of Civil Engineering, TU Košice, Košice 042 00, Slovakia*

⁴*Dept. Anat. Hist. Phys., UVMP, Komenskeho 74, 041 81 Kosice, Slovakia*

⁵*Dept. Microbiol. Immun., UVMP, Komenskeho 74, 041 81 Kosice, Slovakia*

⁶*Institute of Neurobiology, SAS, Soltesovej 4, 04001 Kosice, Slovakia*

⁷*Dept. Biomed. Eng. Meas., Fac. Mech. Eng., TU Košice, Košice 042 00, Slovakia*

Amorphous glass-coated microwires belong to a family of materials with outstanding properties [1]. They are composite materials that consist of metallic core covered by insulating glass cover. Very cheap preparation technique called Taylor-Ulitovsky method allows to produce up to few kilometres in a quite short time.

As a result of magnetoelastic anisotropy, magnetic domain structure consists of large monodomain with axial magnetization in the centre of the wire which is surrounded by radial domain structure. Magnetization can have only two states +Ms or -Ms and such property is also called magnetic bistability. The switching between these two states of magnetization runs through domain wall propagation in a single large Barkhausen jump at the field so called switching field.

The switching field is very sensitive to many external parameters like temperature, magnetic field, frequency or mechanical stresses, which can be successfully employed in construction of miniaturized sensors [2].

In the given contribution, we shows few examples of applications of bistable magnetic microwires in civil engineering, electronics and biomedical solutions for sensing the stress, temperature and position.

This research was supported by the projects APVV-0027-11 and Slovak VEGA grant. No. 1/0164/16.

[1] M. Vazquez Handbook of Magnetism and Advanced Magnetic Materials (Wiley, Chichester, U. K., 2007), p. 2193.

[2] R. Varga, Acta Physica Slovaca 65 (2012), 411.

P9-27**KINETICS OF SOLID STATE SYNTHESIS OF QUATERNARY $\text{Cu}_2\text{FeSnS}_4$ (STANNITE) NANOCRYSTALS FOR SOLAR ENERGY APPLICATIONS**

P. Baláž¹, A. Zorkovská¹, I. Škorvánek², M. Baláž¹, E. Dutková¹, Z. Bujňáková¹, J. Trajić³ and J. Briančin¹

¹*Institute of Geotechnics of Slovak Academy of Sciences, Watsonova 45, 04001 Košice, Slovakia*

²*Institute of Experimental Physics of Slovak Academy of Sciences, Watsonova 47, 04001 Košice, Slovakia*

³*Institute of Physics Belgrade, Pregrevica 118, 11080 Belgrade, Serbia*

There is a general paradox in present research and application of chalcogenide solar materials. On one side, CIGS($\text{CuIn}_{1-x}\text{Ga}_x\text{Se}_2$) thin film solar cells attracted a big attention owing to its high power conversion efficiency and good stability. On the other side, these materials represent the potential environmental problem with Se toxicity and In and Ga limited availability and high price. Quaternary semiconductor nanocrystals provide promising alternatives to conventional photovoltaic materials because of their environmental acceptance (application of S instead of toxic Se), cheapness and availability (application of earth-abundant Fe, Zn and Sn instead of scarce In and Ga). For example kesterite (CZTS) and stannite (CITS) combine many advantageous characteristics for photovoltaic applications, such as composition from the abundant and non-toxic constituents, suitable band gap, high absorption coefficient and high radiation stability.

Stannite $\text{Cu}_2\text{FeSnS}_4$ has been recently prepared by several techniques such as solution-based synthesis, hot injection and microwave irradiation. However, these techniques are complex, time consuming, need high temperature and toxic organic solvents. In this study we demonstrate the use of elemental precursors (Cu, Fe, Sn, S) to obtain CITS by a solid state one-pot mechanochemical synthesis. In the processing route, the unique nanostructures and properties are developed. We report the kinetics of the mechanochemical synthesis. Methods of XRD, SEM, EDS, Raman and UV-Vis spectroscopy and magnetic and surface area measurements were applied. CITS polymorphs with tetragonally body-centered structure with crystallite sizes 17-19 nm were obtained. The magnetic measurements performed by SQUID magnetometry allowed us to study the kinetics of magnetic phase transformation during solid state synthesis in more details. The weak ferromagnetic properties of the final nanocrystalline product after maximum milling time were also documented. The obtained results confirm the excellent structural properties of synthesized $\text{Cu}_2\text{FeSnS}_4$ nanocrystals.

[1] Baláž Peter: Mechanochemistry in Nanoscience and Minerals Engineering, Springer, Berlin Heidelberg 2008.

P9-28**MECHANOCHEMICAL SYNTHESIS AND CHARACTERIZATION OF TERNARY CuFeS₂ and CuFeSe₂ NANOPARTICLES**

E. Dutková¹, I. Škorvánek², M.J. Sayagués³, A. Zorkovská¹, J. Kováč⁴ and J. Kováč, Jr.⁴

¹*Institute of Geotechnics, Slovak Academy of Sciences, 040 01 Košice, Slovakia*

²*Institute of Experimental Physics, Slovak Academy of Sciences, 040 01 Košice, Slovakia*

³*Institute of Material Science of Seville (CSIC-US), 410 92 Seville, Spain*

⁴*Institute of Electronics and Photonics, Slovak University of Technology and International Laser Centre, 81219 Bratislava, Slovakia*

Semiconducting nanomaterials with the novel physical and chemical properties different from bulk materials become more important due to their potential applications in solar power engineering, spintronics, thermoelectric devices etc.

The mechanochemical synthesis of ternary CuFeS₂ and CuFeSe₂ nanoparticles with the chalcopyrite structure by high-energy milling in a planetary mill in an argon atmosphere from copper, iron and sulphur or selenium for 60 minutes was reported. CuFeS₂ and CuFeSe₂ nanoparticles crystallize in the tetragonal structure with the crystallite size of about 38±1 nm and 32±1, respectively. The Raman spectra also proved the formation of pure CuFeS₂ and CuFeSe₂ nanoparticles. Low temperature magnetic data for CuFeS₂ support the coexistence of antiferromagnetic spin structure with paramagnetic contribution. On the other hand, CuFeSe₂ nanoparticles exhibit at low temperatures a weak ferromagnetic or ferrimagnetic behavior. Furthermore, the magnetic measurements revealed a presence of very small amount of elemental Fe impurity in both types of as-prepared nanoparticles. TEM measurements also revealed the presence of nanocrystals with the size of 10-30 nm with the tendency to form agglomerates. The optical band gap of CuFeS₂ and CuFeSe₂ nanoparticles has been detected larger than band gap of bulk material. The quantum size effect of the particles was confirmed also by PL measurement. It is demonstrated that mechanochemical synthesis can be successfully employed in the one step preparation of CuFeS₂ and CuFeSe₂ nanoparticles.

Acknowledgements

This work was promoted by the Slovak Research and Development Agency under the contract No. APVV-14-0103 and the Slovak Grant Agency VEGA (project 2/0027/14).

P9-29**ELIMINATION OF MAGNETIC NANOPARTICLES WITH VARIOUS SURFACE MODIFICATIONS FROM THE BLOODSTREAM *IN VIVO***

I. Khmara¹, V. Zavisova², M. Koneracka², N. Tomasovicova², M. Kubovcikova², J. Kovac², M. Muckova³ and P. Kopcansky²

¹*Pavol Jozef Safarik University, Faculty of Science, Park Angelinum 9, 041 54 Kosice, Slovakia*

²*Institute of Experimental Physics SAS, Watsonova 47, 040 01 Kosice, Slovakia*

³*Hameln, rds a.s., Horna 36, 900 01 Modra, Slovakia*

The magnetic nanoparticles (MNPs) with the core diameter 10 nm stabilized by sodium oleate and bovine serum albumin in phosphate buffer have been modified by different biocompatible substances such as poly(ethylene glycol) (PEG), dextrane (DEX), and polyvinylpyrrolidone (PVP). Prepared biocompatible magnetic fluids were characterized by scanning electron microscopy (SEM), dynamic light scattering (DLS) and Laser Doppler Electrophoretic (LDE) methods to obtain information about particle size distribution and their stability. To study the elimination of different modified magnetic nanoparticles from the bloodstream, the biocompatible samples were diluted in water for injection (1:1) and applied intravenously to the mice's bloodstream with further blood specimens' collecting in given time intervals. Magnetic moment of the lyophilized blood samples was measured by SQUID magnetometer.

Time dependence of magnetic moment of MNPs and MNPs modified by DEX, PEG and PVP normalized to the Fe₃O₄ showed that the circulation time of MNPs in the bloodstream depends on the substance used for modification. The magnetic nanoparticles stabilized only with sodium oleate were trapped by reticuloendothelial system within 1 hour while MNPs modified by DEX, PEG and PVP circulated in blood up to 3 hours.

This work was supported by the Slovak Research and Development Agency under Contract nos. APVV-14-0120 and APVV-14-0932.

P9-30**DYNAMICS OF ^1H - ^{13}C CROSS POLARIZATION IN NUCLEAR MAGNETIC RESONANCE OF POLYHYDROXYBUTYRATE**M. Kovaľáková¹, O. Fričová¹, M. Hutníková¹, V. Hronský¹ and D. Olčák¹¹*Department of Physics, Faculty of Electrical Engineering and Informatics, Technical University of Košice, Park Komenského 2, 04200 Košice, Slovakia*

Polyhydroxybutyrate (PHB) is a biodegradable thermoplastic polymer belonging to polyhydroxyalkanoates [1]. Its structure contains methyl (CH_3), methylene (CH_2), methine (CH) and carbonyl (CO) carbons which are present in amorphous and crystalline regions of the polymer. The aim of this study was to obtain information on the dynamics of ^1H - ^{13}C NMR cross polarization (CP) [2] of functional groups with directly bonded hydrogens. The integral line intensities obtained from ^1H - ^{13}C NMR cross polarization (CP) spectra measured at increasing contact times plotted versus contact times create CP build-up curves and their analysis provides desired information.

The ^1H - ^{13}C CP NMR measurements were performed on as-supplied PHB sample at magic angle spinning (MAS) rate of 10 kHz. The measurements required setting Hartmann-Hahn (HH) condition which was inferred from the HH matching profiles [3] measured for each studied functional group. The measured CP build-up curves displayed oscillatory course which indicates the presence of ^1H - ^{13}C spin pairs isolated from lattice [4]. The frequency of the observed oscillations is directly proportional to ^1H - ^{13}C dipolar coupling constant which is related to the C-H distance and its value also reflects mobility of particular functional group [5]. The Fourier transforms of the CP build-up curves made it possible to calculate the values of dipolar coupling constants from the line splitting in Pake-like powder patterns [6]. The mobility of particular group was assessed comparing the obtained values with the value calculated for rigid lattice.

- [1] Chodák, I., Monomers, Polymers and Composites from Renewable Resources, Chapter 22 – Polyhydroxyalkanoates: Origin, Properties and Applications, 2008, Pages 451–477.
- [2] Kolodziejewski, W.; Klinowski J., Chemical Reviews 2002, 102, 613–628.
- [3] Stejskal, E.O.; Schaefer, J.; Waugh, J. S., Journal of Magnetic Resonance 1977, 28 (1), 105–112.
- [4] Müller, L.; Kumar, A.; Baumann, T.; Ernst, R. R., Physical Review Letters 1974, 32, 1402–1406.
- [5] E. R. Andrew and R. G. Eades, Proc. R. Soc. London, Ser. A 216, 1953, 398.
- [6] Bertani, P., Raya, J., Hirschinger, J., C.R. Chimie 7, 2004, 363–369.

P9-31**MECHANOCHEMICAL REDUCTION OF CHALCOPYRITE CuFeS_2 : CHANGES IN COMPOSITION AND MAGNETIC PROPERTIES**

P. Baláž¹, A. Zorkovská¹, J. Kováč², M. Tešínský¹, M. Baláž¹, T. Osserov³, G. Guseynova³ and T. Ketegenov⁴

¹*Institute of Geotechnics, Slovak Academy of Sciences, Watsonova 45, 04001 Košice, Slovakia*

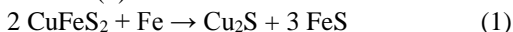
²*Institute of Experimental Physics, Slovak Academy of Sciences, Watsonova 47, 04353 Košice, Slovakia*

³*K.I.Satpayev Kazakh National Research Technical University, Satpayev Street 22a, 050013 Almaty, Kazakhstan*

⁴*Al-Farabi Kazakh National University, Al-Farabi avenue 71, 050040 Almaty, Kazakhstan*

The mechanochemical reactions have attracted considerable scientific and technical interest in recent years. As a consequence, the unique nanostructures and properties are developed by these processes. High-energy milling of sulphides with a reactive metal in so – called mechanochemical reduction mode will lead to products in nano-range and composition which simplify the following metallurgical processing. Chalcopyrite CuFeS_2 , a ternary semiconductor with its antiferromagnetic properties represents promising candidate as an advanced material for use in inexpensive nano-electronic (solar cells, magnetic area) as well as copper ore source in metallurgical operations [1-2].

In this work the process of mechanochemical reduction of chalcopyrite with element iron according to reaction (1) is studied



The reduction was performed in planetary mills Pulverisette 6 and Premium 7 (Fritsch, Germany) in an argon atmosphere for 30 minutes. The composition and properties of nano-powders prepared by high-energy milling were analyzed by XRD and magnetic measurements. For comparison, the high-energy milling of chalcopyrite itself was also performed. Most of the reaction takes place during 30 minutes with chalcocite Cu_2S and troilite FeS as the only reaction products.

The magnetic measurements performed by MPMS XL5 magnetometer reveal significant increase of saturation magnetization after milling. The temperature dependence of magnetic moment in the temperature range 2-300 K for sample milled 30 minutes shows striking kink around temperature 130 K connected with the presence of phase transition.

The obtained results illustrate the possibility of mechanochemistry to manipulate the properties of solids to obtain materials with unique properties.

[1] B.Li, Z.Huang, M.Zhong, Z.Wei, J.Li, RSC Advances 5 (2015) 91103-91107.

[2] P.Baláž, Mechanochemistry in Nanoscience and Minerals Engineering, Springer, Berlin Heidelberg 2008.

P9-32

UTILIZATION OF EDDY CURRENT TOMOGRAPHY IN AUTOMOTIVE INDUSTRY

P.Nowak¹, M. Nowicki¹, A.Juś² and R.Szewczyk¹

¹Warsaw University of Technology, Faculty of Mechatronics,

sw. A. Boboli 8, 02-525 Warsaw, Poland

²Industrial Research Institute for Automation and Measurements,

Al. Jerozolimskie 202, 02-486 Warsaw, Poland

Paper presents utilized innovative setup for eddy current tomography and possibility of its utilization in automotive industry. Described tomography setup is designed for testing axisymmetric objects thus motor valve was selected for exemplary testing. Tests were conducted on motor valve in original state. Afterwards reference defect was created on element and measurements were repeated. Significant difference between tests results were observed, thus potential for utilization in automotive industry was confirmed.

Finite Element Method simulations were applied in order to confirm the measurement results. Calculations were conducted in open-source FEM software, which solves Maxwell equations in the A-V form. High consistency of the modeling results and measurements results presents possibility for inverse tomographic transformation and thus objects shape reconstruction.

P9-33**MÖSSBAUER SPECTROSCOPY STUDY OF LABORATORY PRODUCED ODS STEELS**J. Degmová¹, J. Dekan¹, J. Simeg Veterníková¹ and V. Slugeň¹*¹Institute of Nuclear and Physical Engineering, Slovak University of Technology, Ilkovičova 3, 812 19 Bratislava, Slovakia*

The investigated ODS (Oxide Dispersion Strengthened) steels were received from laboratories involved in the Coordinated Research Project F11014 "Benchmarking of Structural Materials Pre-selected for Advanced Nuclear Reactors". Namely from India (IGCAR), Russia (Bochvar Institute) and Japan (Kyoto University). The application of Mössbauer spectroscopy on these materials is aimed to reveal the complex information about studied materials via unique characteristics as micro-magnetic properties and homogeneity of admixtures distribution in steels. All studied steels are ferritic and they mainly differ in content of elements as Cr or Al. Chosen fitting model consists of bcc Fe, bcc Fe with Cr substitution and paramagnetic bcc Cr rich component. All of these features can be detected in all studied samples, however, in some cases in very low amount (about 1%). These ODS steels as aimed in further study for He implantations.

P9-34**DUAL-CONTROLLED PHOTSENSITIVE MESOPOROUS SILICA-COATED MAGNETITE NANOPARTICLES**E. Beňová¹, O. Kapusta², A. Zeleňáková² and V. Zeleňák¹¹*Department of Inorganic Chemistry, P.J. Šafárik University, Moyzesova 11, 04001 Košice, Slovakia*²*Department of Solid State Physics, P.J. Šafárik University, Park Angelinum 9, 04154 Košice, Slovakia*

Magnetic nanocomposites consisting of magnetic cores and mesoporous silica shells have been extensively studied in the past two decades, both in terms of precise control over the synthesis and appropriate applications. These magnetic nanocomposites have wide range of applications since they combine different advantageous properties in one multifunctional nanocomposite. They attracted an attention as bioimaging devices, contrast agents for MRI diagnostics, as well as for hyperthermia and cancer treatment. We combined the advantages of mesoporous silica and magnetic particles to fabricate a nanocomposite with high surface area, magnetic separability and targeted drug delivery systems, which carries the drug directly to a specific organ or location in the body under an external magnetic field. Various synthesis strategies including thermal decomposition, co-precipitation and hydrothermal approaches can be used for obtaining magnetic mesoporous silica nanoparticles.

In this work, we present mesoporous silica modified by magnetite nanoparticles and photosensitive organic ligands for controlled drug delivery. Two types of the superparamagnetic magnetite mesoporous silica nanoparticles were prepared by hydrothermal method using triethanolamine (TEA) which play an important role in the formation of Fe_3O_4 nanoparticles. The mesoporous silica was modified by the photo-switchable derivative of p-coumaric acid (CA), which under the influence of UV irradiation subjects reversible photo-dimerization and creates “gates” on the surface of the pores. The prepared mesoporous materials were characterized by transmission electron microscopy (TEM), nitrogen adsorption, thermal analysis (TG-DTA) and UV-Vis spectroscopy which confirmed the photo-dimerization processes of CA anchored on mesoporous silica nanoparticles. Magnetic properties were investigated using a SQUID based magnetometer in external dc field up to 5 T and in the temperature range of 2 – 300 K. Magnetic characteristics as blocking temperature and relaxation time were analyzed in accordance to the particle size. Prepared composites have potential to be used as active drug delivery system controlled by magnetic field and UV light.

*Acknowledgment**This work was realized within the project ITMS 26220120019.*

P9-35

ISOLATED DC AND AC CURRENT AMPLIFIER WITH MAGNETIC FIELD SENSOR IN LOOP AND AMORPHOUS RING CORE

O. Petruk¹, M. Kachniarz¹ and R. Szewczyk²

¹*Industrial Research Institute for Automation and Measurements PIAP, al. Jerozolimskie 202, 02-486 Warsaw, Poland*

²*Institute of Metrology and Biomedical Engineering, Warsaw University of Technology, sw. Andrzeja Boboli 8, 02-525 Warsaw, Poland*

Measurement of the leakage current in power lines overvoltage protection is a very important issue from the point of view of the energy industry. This kind of measurement requires isolated measurement system for current measurement. Practical implementation of such measurement system is difficult, because it is necessary to ensure galvanic isolation for several kilovolts.

This paper presents innovative isolated DC and AC current amplifier, which can be utilized in this type of measurement. Developed amplifier contains magnetic field sensor in the feedback loop. Amorphous ring core with air gap is utilized as a part of galvanic isolation separating input and output current. In the paper outline of the amplifier is presented. Then PCB project was developed and electronic circuit of the amplifier was manufactured. Developed device was investigated with DC and AC current and the results are presented in the paper. Obtained results were compared with other solutions used so far. Results indicate that developed device is very useful in described application.

P9-36

NOVEL METHOD OF OFFSET VOLTAGE MINIMIZATION IN HALL-EFFECT SENSOR

O. Petruk¹, M. Kachniarz¹ and R. Szewczyk²

¹*Industrial Research Institute for Automation and Measurements PIAP, al. Jerozolimskie 202, 02-486 Warsaw, Poland*

²*Institute of Metrology and Biomedical Engineering, Warsaw University of Technology, sw. Andrzeja Boboli 8, 02-525 Warsaw, Poland*

Hall-effect sensors are widely utilized in measurements of magnetic field in both industrial and scientific applications. Important problem in application of Hall-effect sensors is offset voltage, which has negative influence on the metrological properties of the sensor. Offset voltage is unavoidable and undesired problem in practical applications of Hall-effect sensor.

The paper presents numerical model and validation of new methodology of offset voltage minimization in Hall-effect sensor. Model of Hall-effect sensor with multiple electric pins was developed. Mathematical description of influence of magnetic field on current flow in the Hall-effect structure was formulated. Simulations were carried out using Finite Elements Method (FEM) in ELMER FEM software. Performed investigation of actual parameters of newly designed Hall-effect sensor confirms effectiveness of the described method.

P9-37

AIR-GAP TOROIDAL MAGNETIC MICRO-FORCE SENSOR

M. Nowicki¹, M. Kachniarz¹, A. Juś², T. Charubin² and R. Szewczyk²

¹*Industrial Research Institute for Automation and Measurements PIAP,
al. Jerozolimskie 202, 02-486 Warsaw, Poland*

²*Institute of Metrology and Biomedical Engineering,*

Warsaw University of Technology, sw. Andrzeja Boboli 8, 02-525 Warsaw, Poland

Micro-force measurements are very important in modern nanoscale technology. It is very complicated issue requiring utilization of specialized measurement techniques. Among many force sensors, magnetoelastic sensors are intensively developed. They utilize toroidal cores made of amorphous alloys, where axial stress is acting on the core. They are however suitable for relatively high values of force such as encountered in civil engineering constructions monitoring, heavy industry etc.

In this paper new innovative method of micro-force measurement based on air gap influence on magnetic circuits properties is presented. Magnetic toroidal core with air gap is put under transverse compressive stress perpendicular to the magnetic field direction generated by low-mass calibration weight. Change of the air gap induced by the force acting on the core causes change of its magnetic parameters. In the paper possibility of utilization of various magnetic parameters dependence on the force applied is investigated. Obtained results indicate a possibility of application of the developed sensor in micro-force measurements.

P9-38**NANOCRYSTALLINE MAGNETIC GLASS-COATED MICROWIRES
USABLE AS TEMPERATURE SENSORS IN BIOMEDICAL
APPLICATIONS**R. Hudak¹, I. Polacek¹, P. Klein³, R. Varga^{2,3}, R. Sabol³ and J. Zivcak¹¹*Department of Biomedical Engineering and Measurement, Faculty of Mechanical Engineering, Technical University of Kosice, Letna 9, 042 00 Kosice, Slovakia*²*Department of Condensed Matters Physics, Institute of Physics, Faculty of Science, P. J. Safarik University, Park Angelinum 9, 041 54 Kosice, Slovakia*³*RVmagnetics s.r.o., Hodkovce 21, 04421 Kosice, Slovakia*

For a control and study of post-implantation biomechanical processes of a Ti64 implants, an ability of wireless in-vivo measurement of various parameters (i.e. temperature in this case) at the tissue-implant interface is required. Compared to other types of sensors, which consist of sensing and transmitting element, nanocrystalline magnetic glass-coated microwires combine the both itself. Thanks to pyrex coating, the microwires are biocompatible and due to their size they do not intervene into the surface structure of implants.

Studied as-cast microwire has low Curie temperature due to high amount of molybdenum and is not magnetically bistable at room temperature. Therefore the microwire was specially annealed under axial stress above crystallization temperature in order to create its bistability at room temperature [1] and enhance its temperature sensitivity in the range from 37 °C up to 42 °C.

Extreme temperature sensitivity in the range of body temperature was achieved using effect of superparamagnetism, moreover, due to this effect, switching field increased almost linear way. Temperature dependence of the switching field has been studied in two TiAl₆V₄ samples, representing implants, with different types of fixation.

This research was supported by the projects Slovak VEGA grant. No. 036TUKE-4/2013 and VEGA grant. No. 1/0164/1.

- [1] R. Hudak, R. Varga, I. Polacek, P. Klein, I. Skorvanek, V. Komanicky, R. del Real, M. Vazquez, Addition of molybdenum into amorphous glass-coated microwires usable as temperature sensors in biomedical applications, *Physica Status Solidi A* 213, No. 2, 377–383 (2016), DOI 10.1002/pssa.201532574.

P9-39**INFLUENCE OF TEMPERATURE ON MAGNETOSTRICTIVE DELAY LINE PROPERTIES**J. Salach¹ and Y. D. Jackiewicz²*¹Institute of Metrology and Biomedical Engineering,**Warsaw University of Technology, A. Baboli 8, 02-525 Warszawa, Poland**²Industrial Research Institute for Automation and Measurements PIAP,**Jerozolimskie 202, 02-486 Warsaw, Poland*

Magnetostrictive delay line is a very interesting method for small values of force and stresses measurement. In this method, impulse transition time between exciting and detecting coil is measured. The transit time is changed under the stresses influence on the delay line. This change can be converted into force signal. Properties of the delay line mainly depend on the material's Young's modulus. Due to the fact that this parameter is temperature dependent, the temperature will influence the properties of the delay line. This paper presents a study on the influence of temperature on the delay line force measurement. During the test delay line was placed in the laboratory furnace for a temperature setting. The results confirmed the effect of temperature on the properties of the delay line. Such information will enable the correction of the indications of the magnetostrictive delay line. Moreover, knowing the dynamics between the measurement and the temperature variation increases the measurement resolution of the sensor utilizing delay line principle.

P9-40

**IMPLEMENTATION OF CONDUCTANCE TOMOGRAPHY
IN DETECTION OF THE HALL SENSORS INHOMOGENEITY**

O. Petruk¹, P. Nowak² and R. Szewczyk²

¹*Industrial Research Institute for Automation and Measurements PIAP,
al. Jerozolimskie 202, 02-486 Warsaw, Poland*

²*Institute of Metrology and Biomedical Engineering,
Warsaw University of Technology, sw. Andrzeja Boboli 8, 02-525 Warsaw, Poland*

Tomography is a useful tool for objects reconstruction in non-destructive testing. Many kinds of tomography, depending on the penetrating wave character, are available and adapted for specific application. This paper presents new kind of tomography - conductance tomography extended with a Hall effect. Its development was motivated by the need on inhomogeneity detection in thin film Hall effect sensor, particularly graphene Hall effect sensors.

Paper presents complete description of the tomographic method and tomography software developed in the GNU Octave. Inverse transformation is based on gradient optimization method. Each shape reconstruction was done with the Finite Element Method using the open source software: Elmer FEM and Salome. Results confirmed the suitability of the work.

P9-41

MODELLING THE INFLUENCE OF STRESSES ON MAGNETIC CHARACTERISTICS OF THE ELEMENTS OF THE TRUSS USING EXTENDED JILES-ATHERTON MODEL

D. Jackiewicz² and R. Szewczyk¹

¹*Industrial Research Institute for Automation and Measurements PIAP, Jerozolimskie 202, 02-486 Warsaw, Poland*

²*Institute of Metrology and Biomedical Engineering, Warsaw University of Technology, A. Boboli 8, 02-525 Warszawa, Poland*

Steel truss structures are commonly used in civil engineering. Their mechanical parameters, especially the durability, are critical, and often human life depends on it. Therefore it is very important to monitor the critical elements of the truss. For this purpose magnetoelastic method of measurement may be used. It is a method having several advantages over other methods, particularly because of use of elements which are already parts of the structure. The study of structural elements have already been conducted.

However, to take advantage of the magnetoelastic characteristics measurement to assess the state of stress, one should have a model of the influence of stress on magnetic properties. The influence of stresses on hysteresis loops was modelled with the extended Jiles-Atherton model. The obtained results of the modelling are consistent with the experimental measurements results. The results of modelling create new possibilities of explanation of the physical phenomena connected with magnetization of the magnetic materials under stresses, which is especially important for the assessment of the state of the constructional steel during its exploitation in industrial conditions.

I N D E X O F A B S T R A C T S

PLENARY

PL-01 MAGNETO-OPTICAL DOMAIN IMAGING

R. Schäfer

PL-02 SPIN CONFIGURATION AND MAGNETIZATION REVERSAL OF INDIVIDUAL CoFe BASED CYLINDRICAL NANOWIRES

M. Vazquez, C. Bran, A. Asenjo, R. Perez, O. Chubykalo-Fesenko, E. Palmero, E. Berganza and J.A. Fernandez Roldan

PL-03 INVESTIGATION OF Ce AND Yb INTERMETALLICS: THE IMPORTANCE OF PHASE DIAGRAMS AND CRYSTAL CHEMISTRY

M. Giovannini

1. THEORETICAL PROBLEMS OF MAGNETICALLY ORDERED MATERIALS, MAGNETIZATION PROCESSES

II-01 EFFECT OF ELECTRON CONFINEMENT ON MAGNETISM OF NANOSTRUCTURES

M. Przybylski

O1-01 MICROSCOPIC ORIGIN OF HEISENBERG AND NON-HEISENBERG EXCHANGE INTERACTIONS IN FERROMAGNETIC BCC Fe

Y. O. Kvashnin, R. Cardias, A. Szilva, I. Di Marco, M. I. Katsnelson, A. I. Lichtenstein, L. Nordström, A. B. Klautau and O. Eriksson

O1-02 MAGNETISM AND TRANSPORT PROPERTIES OF Mn-DOPED TOPOLOGICAL INSULATOR Bi_2Te_3 AND Bi_2Se_3 : AB INITIO CALCULATIONS

K. Carva, P. Baláž, V. Tkáč, R. Tarasenko, V. Sechovský, J. Kudrnovský, F. Máca and J. Honolka

O1-03 NON- PLATEAU BEHAVIOR OF THE ZERO-TEMPERATURE MAGNETIZATION IN SPIN-CLUSTERS AND CHAINS

V. Ohanyan, O. Rojas, J. Strecka and S. Bellucci

O1-04 AB INITIO THEORY OF GILBERT DAMPING IN RANDOM ALLOYS

I. Turek, J. Kudrnovsky and V. Drchal

O1-05 PHOTO-MECHANICAL COUPLING IN MAGNETIC SHUTTLE DEVICE

A. Parafilo, S. Kulinich, L. Gorelik, M. Kiselev, R. Shekhter and M. Jonson

O1-06 BROKEN SYMMETRY IN THE MAGNETISATION DYNAMICS

J. Tóbiš and V. Cambel

P1-01 EXACT STUDIES OF THE HUBBARD PAIR-CLUSTER IN EXTERNAL FIELDS

T. Balcerzak and K. Szałowski

P1-02 THERMODYNAMICS OF FRUSTRATED MAGNETS: HIGH-TEMPERATURE EXPANSION REVISITED

J. Richter, A. Lohmann and H.-J. Schmidt

P1-03 SPONTANEOUS MAGNETIZATION AND PHASE DIAGRAMS OF THE MIXED SPIN-1/2 AND SPIN-S ISING MODEL ON THE BETHE LATTICE

C. Ekiz and J. Strečka

P1-04 MAGNETIC HYSTERESIS AS A CHAOTIC SEQUENCE

P. Frydrych, M. Nowicki and R. Szewczyk

- P1-05 APPLICATION OF ANISOTROPIC VECTOR PREISACH MODEL FOR BULK MATERIALS**
P. Frydrych, R. Szewczyk and M. Nowicki
- P1-06 LOCALIZED-MAGNON CHAINS AND INTERCHAIN COUPLINGS**
O. Krupnitska, O. Derzhko and J. Richter
- P1-07 SPIN-CHAIN OF ALTERNATING ISING SPINS-CANTED AND HEISENBERG SPINS WITH TWO DIFFERENT LOCAL ANISOTROPY AXES: ZERO TEMPERATURA PHASE DIAGRAM AND MAGNETIZATION, AND THERMODYNAMICS MAGNETIZATION AND SUSCEPTIBILITY**
J. Torrico, M. L. Lyra, O. Rojas, S. M. de Souza, M. Rojas, M. Hagiwara, Y. Han and J. Strečka
- P1-08 BREAKDOWN OF A MAGNETIZATION PLATEAU IN FERRIMAGNETIC MIXED-SPIN HEISENBERG CHAINS DUE TO A QUANTUM PHASE TRANSITION TOWARDS A SPIN-LIQUID PHASE**
J. Strečka
- P1-09 INVERSE MAGNETOCALORIC EFFECT IN THE SPIN-1/2 FISHER'S SUPER-EXCHANGE ANTIFERROMAGNET**
L. Gálisová and J. Strečka
- P1-10 ISOTHERMAL ENTROPY CHANGE AND ADIABATIC CHANGE OF TEMPERATURE DURING THE MAGNETIZATION PROCESS OF THE ISING OCTAHEDRON AND DODECAHEDRON**
K. Karl'ová, J. Strečka and T. Madaras
- P1-11 SELF-CONSISTENT MODEL OF A SOLID FOR THE LATTICE AND MAGNETIC PROPERTIES DESCRIPTION**
T. Balcerzak, K. Szałowski and M. Jaščur
- P1-12 FRACTIONAL SCALING OF MAGNETIC COERCIVITY IN ELECTRICAL STEELS**
M. Najgebauer
- P1-13 THEORETICAL STUDY OF THE FRUSTRATED ISING ANTIFERROMAGNET ON THE HONEYCOMB LATTICE**
A. Bobák, T. Lučivjanský, M. Žukovič, M. Borovský and T. Balcerzak
- P1-14 DEPENDENCE OF "LIFETIME" OF THE SPIRAL MAGNETIC DOMAIN ON THE MATERIAL PARAMETERS**
V. N. Mal'tsev and A. A. Nesterenko
- P1-15 ULTRAFast SPIN TRANSFER TORQUE GENERATED BY A FEMTOSECOND LASER PULSE**
P. Baláž, K. Carva, P. Maldonado and P. Oppeneer

- P1-16 THERMAL ENTANGLEMENT AND QUANTUM NON-LOCALITY ALONG THE MAGNETIZATION CURVE OF THE SPIN-1/2 ISING-HEISENBERG TRIMERIZED CHAIN**
J. Pavličko and J. Strečka
- P1-17 STRONG-COUPLING APPROACH TO THE SPIN-1/2 ORTHOGONAL-DIMER CHAIN**
T. Verkholyak and J. Strečka
- P1-18 STUDY OF AXIAL DIMENSION OF STATIC HEAD-TO-HEAD DOMAIN BOUNDARY IN AMORPHOUS GLASS-COATED MICROWIRE**
M. Kladivová, J. Ziman, J. Kecer and P. Duranka
- P1-19 THEORETICAL INVESTIGATIONS ON THE STRUCTURAL, MAGNETIC AND ELECTRONIC PROPERTIES OF $\text{Fe}_{2-x}\text{MnGe}:\text{Cu}_x$ ALLOY**
K. Gruszka and M. Nabiałek
- P1-20 MAGNETIZATION CURVES OF GEOMETRICALLY FRUSTRATED EXCHANGE-BIASED FM-AFM BILAYERS**
M. Pankratova and M. Žukovič
- P1-21 ENHANCED MAGNETOCALORIC EFFECT DUE TO SELECTIVE DILUTION IN A TRIANGULAR ISING ANTIFERROMAGNET**
M. Borovský and M. Žukovič
- P1-22 MOKE STUDY OF THE DOMAIN WALL DYNAMICS IN MAGNETIC MICROWIRES**
O. Váhovský and R. Varga
- P1-23 MIXED SPIN-1/2 AND SPIN 3/2 ISING MODEL WITH THREE-SITE FOUR-SPIN INTERACTIONS ON A DECORATED TRIANGULAR LATTICE**
V. Štubňa and M. Jaščur
- P1-24 CRITICAL DYNAMICS OF PLANAR MAGNETS: RENORMALIZATION GROUP ANALYSIS**
M. Dančo, M. Hnatič and T. Lučivjanský

2. AMORPHOUS, NANOCRYSTALLINE AND OTHER SOFT MAGNETIC MATERIALS

- I2-01 STRUCTURAL ORIGIN OF CREEP INDUCED MAGNETIC ANISOTROPY OF AMORPHOUS ALLOYS**
M. Ohnuma, P. Kozikowski, G. Herzer and C. Polak
- I2-02 DEVELOPMENT OF SELECTED AMORPHOUS AND NANOCRYSTALLINE SOFT MAGNETIC SYSTEMS WITH ENHANCED FUNCTIONAL PROPERTIES**
P. Svec, I. Janotova, J. Zigo, I. Matko, D. Janickovic, J. Marcin, I. Skorvanek and P. Svec Sr.
- O2-01 INFLUENCE OF ANNEALING CONDITIONS ON THE MAGNETIC PROPERTIES OF $\text{Fe}_{73.5}\text{Cu}_1\text{Nb}_3\text{Si}_{13.5}\text{B}_9$ GLASS-COATED NANOWIRES**
S. Corodeanu, T. A. Óvári, G. Stoian, L. C. Whitmore, H. Chiriac and N. Lupu
- O2-03 Co_2FeX (X = Al, Si) HEUSLER COMPOUNDS PREPARED BY PLANAR FLOW CASTING AND ARC MELTING METHODS: MICROSTRUCTURE AND MAGNETISM**
A. Titov, O. Zivotsky, Y. Jiraskova, J. Bursik, A. Hendrych and D. Janickovic
- O2-04 EFFECTS OF SWIFT HEAVY-IONS ON Fe-BASED METALLIC GLASSES STUDIED BY SYNCHROTRON DIFFRACTION**
S. Michalik, M. Pavlovic, J. Gamcova, P. Sovak and M. Miglierini
- O2-05 OPTIMISATION OF FRAME-SHAPED FLUXGATE SENSOR'S CORE MADE OF AMORPHOUS ALLOY USING GENERALIZED MAGNETOSTATIC METHOD OF MOMENTS**
R. Szewczyk and P. Frydrych
- O2-06 SIZE DEPENDENT HEATING EFFICIENCY OF MULTICORE IRON OXIDE PARTICLES IN LOW-POWER ALTERNATING MAGNETIC FIELDS**
I. S. Smolkova, N. E. Kazantseva, L. Vitkova, V. Babayan, J. Vilcakova and P. Smolka
- O2-07 LOSS PREDICTION IN 6.5% ELECTRICAL STEELS**
J. Szczyglowski
- O2-08 EFFECT OF DISK VELOCITY IN MELT SPINNING METHOD ON MAGNETIC PROPERTIES OF AMORPHOUS RIBBONS**
N. Amini, M. Miglierini and M. Hasiak

- P2-01 BOSON PEAK AND RELAXATION PHENOMENA IN $\text{Zn}(\text{PO}_3)_2\text{Er}(\text{PO}_3)_3$ PHOSPHATE GLASS**
M. Orendáč, K. Tibenská, E. Čížmár, V. Tkáč, A. Orendáčová,
E. Černošková, J. Holubová and Z. Černošek
- P2-02 THE COMPARISON HARDNESS AND COERCIVITY EVOLUTION IN VARIOUS $\text{Fe}(\text{TM})$ BASED GLASSES (INCLUDING FINEMET PRECURSOR) DURING RELAXATION AND CRYSTALLIZATION**
Z. Weltsch, K. Kitti and A. Lovas
- P2-03 THE CHANGES IN MAGNETIC AND MECHANICAL PROPERTIES OF FINEMET - TYPE ALLOYS DURING ISOTHERMAL, AND PULSE HEAT TREATMENTS**
L. Hubač, L. Novák and A. Lovas
- P2-04 DC MAGNETIC PROPERTIES OF AMORPHOUS VITROVAC RIBBON**
P. Kollár, Z. Birčáková, J. Füzer and M. Kuźmiński
- P2-05 ANALYSIS OF THE THERMAL AND MAGNETIC PROPERTIES OF AMORPHOUS $\text{Fe}_{61}\text{Co}_{10}\text{B}_{20}\text{Y}_8\text{Me}_1$ (WHERE $\text{Me} = \text{W}, \text{Zr}, \text{Nb}, \text{Mo}$) RIBBONS**
P. Pietrusiewicz and M. Nabialek
- P2-06 EFFECT OF CURRENT ANNEALING ON DOMAIN STRUCTURE IN AMORPHOUS AND NANOCRYSTALLINE FeCoMoB MICROWIRES**
P. Klein, R. Varga, G. A. Badini-Confalonieri and M. Vazquez
- P2-07 INVESTIGATION OF MAGNETIZATION PROCESSES FROM THE ENERGY LOSSES IN SOFT MAGNETIC COMPOSITE MATERIALS**
Z. Birčáková, P. Kollár, B. Weidenfeller, J. Füzer, R. Bureš and M. Fáberová
- P2-08 HIGH-FREQUENCY ABSORBING PERFORMANCES OF CARBONYL IRON/ MnZn FERRITE/PVC POLYMER COMPOSITES**
R. Dosoudil and M. Ušáková
- P2-09 MICROSTRUCTURAL AND MAGNETIC CHARACTERISTICS OF DIVALENT Zn, Cu AND Co DOPED Ni FERRITES**
M. Šoka, R. Dosoudil and M. Ušáková
- P2-10 NICKEL/ZINC RATIO AND LANTHANUM SUBSTITUTION EFFECT ON STRUCTURAL AND MAGNETIC PROPERTIES OF NICKEL ZINC FERRITES**
V. Jančárik, M. Šoka, M. Ušáková and R. Hartánský

- P2-11 THE ROLE OF TEMPERATURE ON THE MAGNETIZATION PROCESS IN CoFeZrB/FeCuNbMoSiB HYBRID FERROMAGNETS**
S. Dobák, J. Füzer and P. Kollár
- P2-12 MAGNETIC PROPERTIES OF AMORPHOUS GEHLENITE GLASS MICROSPHERES**
M. Majerová, A. Dvurečenskij, A. Cigáň, M. Škrátek, A. Prnová, J. Kraxner, D. Galusek and J. Maňka
- P2-13 THERMOPOWER CHARACTERIZATION OF STRUCTURAL RELAXATION AND CRYSTALLIZATION IN FINEMET TYPE AMORPHOUS PRECURSOR ALLOY**
K. Bán, A. Szabó, R. Ipach and B. Szabó
- P2-14 COMPLEX MAGNETOIMPEDANCE IN JOULE HEATED Co_{71.1}Fe_{3.9}Si₁₀B₁₅ MICROWIRES**
E. Komova, P. Klein, R. Varga and J. Kozár
- P2-15 MAGNETIC PROPERTIES OF NANOCRYSTALLINE ALLOYS AFTER ELECTRONS IRRADIATION**
J. Sitek, D. Holková, J. Dekan and P. Novák
- P2-16 ACCENTS IN MODERN HIGH SATURATION NANOCRYSTALLINE Fe-RICH ALLOYS**
B. Butvinová, P. Butvin, I. Maťko, D. Janičkovič, M. Kuzminski, A. Slawska-Waniewska, P. Švec Sr. and M. Chromčíková
- P2-17 IMAGING OF MAGNETIC DOMAIN STRUCTURE IN FeSi/Mn_{0.8}Zn_{0.2}Fe₂O₄ COMPOSITE USING MAGNETIC FORCE MICROSCOPY**
M. Streckova, I. Batko, M. Batkova, R. Bures, M. Faberova, H. Hadraba and I. Kubena
- P2-18 EFFECTS OF COBALT ADDITION ON MAGNETIC PROPERTIES IN Fe-Co-Si-B-P-Cu ALLOYS**
M. Kuhnt, M. Marsilius, T. Strache, K. Durst, C. Polak and G. Herzer
- P2-19 MAGNETIC PROPERTIES OF Ni_{0.3}Zn_{0.7}Fe₂O₄ FERRITES WITH Fe IONS PARTLY SUBSTITUTED BY Eu**
E. Ušák, M. Ušáková, M. Šoka and D. Vašut
- P2-20 STRUCTURAL RELAXATIONS IN THE AMORPHOUS FeMeMoCrNbB (Me = NI OR CO) ALLOYS**
J. Rzącki and K. Bloch
- P2-21 THE STRUCTURE AND POROSITY OF Fe_{62-x}Co₁₀W_yMe_xY₈B_{20-y} (WHERE Me = Mo, Nb; x = 0, 1, 2; y = 0, 1, 2) ALLOYS IN THE AMORPHOUS AND CRYSTALLINE STATE**
J. Gondro, S. Garus, M. Nabiałek, J. Garus and P. Pietrusiewicz

- P2-22 STRUCTURAL RELAXATIONS IN THE MASSIVE ALLOYS**
Fe₆₀Co₁₀W_xMo₂Y₈B_{20-x} (X = 0, 1, 2)
 K. Bloch, S. Garus, M. Nabiałek and J. Garus
- P2-23 THE STUDY OF MAGNETIZATION IN STRONG MAGNETIC**
FIELDS FOR Fe_{62-x}Co₁₀Nb_xY₈B₂₀ (X = 0, 1, 2) ALLOYS
 M. Szota, S. Garus, J. Garus, K. Gruszką and K. Bloch
- P2-24 COMPARISON OF MAGNETIC PROPERTIES OF AMORPHOUS**
AND CRYSTALLINE Fe₆₀Co₁₀W₂Nb₂Y₈B₁₈ ALLOY
 S. Garus, M. Nabiałek, J. Garus and J. Gondro
- P2-25 MEASUREMENTS OF MAGNETIC PROPERTIES OF**
POLYMER-METALLIC COMPOSITES
 A. Jakubas, P. Gębara, A. Gnatowski and K. Chwastek
- P2-26 THE INFLUENCE OF TEMPERATURE ON UNIDIRECTIONAL**
EFFECT IN DOMAIN WALL PROPAGATION
 J. Onufer, J. Ziman, M. Rezníček and S. Kardoš
- P2-27 STRUCTURE AND MAGNETIC PROPERTIES OF Fe-B-Si-Zr**
METALLIC GLASSES
 R. Babilas, A. Radoń and P. Gębara
- P2-28 STRUCTURE AND COERCIVITY OF AMORPHOUS RAPIDLY**
QUENCHED FeCrB ALLOY
 J. Kecer and L. Novák
- P2-29 MAGNETIC PROPERTIES OF Ni_{0.2}Zn_{0.8}Fe₂O₄ FERRITE FIBERS**
PREPARED BY NEEDLE-LESS ELECTROSPINNING
TECHNIQUES
 M. Streckova, E. Mudra, M. Sebek, T. Sopcak, J. Kovac and J. Duzsa
- P2-30 STUDY OF THE MAGNETIZATION PROCESSES IN**
AMORPHOUS AND NANOCRYSTALLINE FINEMET BY THE
NUMERICAL DECOMPOSITION OF THE HYSTERESIS LOOPS
 J. Kováč and L. Novák
- P2-31 MESOPOROUS SILICA SBA-15 FUNCTIONALIZED BY**
NICKEL-PHOSPHONIC UNITS STUDIED BY RAMAN AND
SQUID MAGNETOMETRY
 M. Laskowska and L. Laskowski
- P2-32 MAGNETIC AND STRUCTURAL CHARACTERIZATION OF**
NICKEL AND IRON BASED HEUSLER RIBBON Ni₂FeZ
(Z = In, Sn, Sb)
 L. Bujnakova, T. Ryba, Z. Vargova, V. Komanicky, J. Kovac, R. Gyepes
 and R. Varga
- P2-33 XAFS SIGNALS MEASURED ON POLYCRYSTALLINE Fe AND**
Zr₆₀Cu₂₀Fe₂₀ ALLOY IN TRANSMISSION AND TOTAL
ELECTRON YIELD MODE
 K. Saksl, S. Michalik, O. Milkovič, J. Gamcová, V. Girman and D. Balga

- P2-34 STRUCTURAL AND THERMOMAGNETIC PROPERTIES OF $\text{Fe}_{86-x}\text{Zr}_7\text{M}_x\text{Nb}_2\text{Cu}_1\text{B}_4$ {M=Co, Ni, (CoCr); x=0 OR 6} ALLOYS**
A. Łukiewska
- P2-35 THE CORRELATION OF MAGNETIC AND STRUCTURAL PROPERTIES OF Ni-Ti-Zr BULK METALLIC GLASS AT ELEVATED TEMPERATURES**
M. Lisnichuk, J. Katuna, K. Saksli, V. Girman, J. Gamcová, D. Balga, M. Ďurišin, J. Kováč and P. Sovák
- P2-36 TEMPERATURE EVOLUTION OF HYPERFINE MAGNETIC FIELDS ON 57-Fe IN A Fe-Co-Si-B-Mo-P METALLIC GLASS**
M. Cesnek, M. Miglierini, T. Kmječ, J. Kohout, N. Amini and D. Janičkovič
- P2-37 STRUCTURE AND MAGNETIC PROPERTIES OF IRON/IRON-OXIDE NANOPARTICLES PREPARED BY PRECIPITATION FROM SOLID STATE SOLUTION**
O. Milkovič, M. Sopko, J. Gamcová and I. Škorvánek
- P2-38 THE STRUCTURAL CHARACTERIZATION OF Ni-Ti-Zr BULK METALLIC GLASS USING TRANSMISSION AND SCANNING ELECTRON MICROSCOPY**
J. Katuna, M. Lisnichuk, K. Saksli, V. Girman, J. Gamcová, D. Balga, M. Ďurišin, J. Kováč and P. Sovák
- P2-39 THE INFLUENCE OF PULSE HEATING ON THE RAYLEIGH REGION IN AMORPHOUS FINEMET ALLOY**
L. Novák, J. Kováč and L. Hubáč
- P2-40 EFFECT OF THICKNESS OF ELECTROPLATED NiFe CORES ON THE NOISE OF FLUXGATES**
M. Butta
- P2-41 INFLUENCE OF Co DOPING ON INDUCED ANISOTROPY AND DOMAIN STRUCTURE IN MAGNETIC FIELD ANNEALED $(\text{Fe}_{1-x}\text{Co}_x)_{79}\text{Mo}_8\text{Cu}_1\text{B}_{12}$ ALLOY**
B. Kunca, J. Marcin, P. Švec, J. Kováč, P. Švec Sr. and I. Škorvánek
- P2-42 FORMATION AND MOTION OF DOMAIN WALLS IN RAPIDLY SOLIDIFIED AMORPHOUS MAGNETIC NANOWIRES**
M. Tibu, M. Lostun, D. A. Allwood, H. Chiriac, N. Lupu and T.-A. Óvári
- P2-43 HOPKINSON EFFECT IN SOFT AND HARD MAGNETIC FERRITES**
J. Sláma, M. Ušáková, M. Šoka, R. Dosoudil and V. Jančárik
- P2-44 INFLUENCE OF VITROVAC CONTENT ON MAGNETIC PROPERTIES IN COMPOSITE MATERIALS BASED ON THE MIXTURE OF TWO FERROMAGNETS**
L. Hegedús, P. Kollár, J. Füzer, R. Bureš, M. Fáberová and P. Kurek

- P2-45 MAGNETIC PROPERTIES OF Fe-BASED SOFT METALLIC ALLOY AFTER ION IRRADIATION**
M. Hasiak and M. Miglierini
- P2-46 FeSiBAINiMo HIGH ENTROPY ALLOY PREPARED BY MECHANICAL ALLOYING**
R. Bureš, H. Hadraba, M. Fáberová, P. Kollár, J. Füzer, P. Roupcová and M. Strečková
- P2-47 EFFECT OF SAMPLE THICKNESS ON GMI BEHAVIOR OF AMORPHOUS $(\text{Fe}_{10}\text{Ni}_{90})_{73}\text{Nb}_7\text{B}_{20}$ RIBBONS**
F. Andrejka, J. Marcin, D. Janičkovič, P. Švec and I. Škorvánek
- P2-48 EVIDENCE OF GRIFFITHS LIKE PHASE IN NANOCRYSTALLINE MANGANITE $\text{La}_{0.85}\text{Ca}_{0.15}\text{MnO}_3$**
M. Pękała, J. Szydłowska, K. Pękała and V. Drozd
- P2-49 EFFECT OF LASER SCRIBING ON THE MAGNETIC PROPERTIES OF CONVENTIONAL 60 SILICON STEEL**
I. Petryshynets, V. Puchý, F. Kováč and M. Šebek
- P2-50 MICROWAVE SINTERED Fe/MgO SOFT MAGNETIC COMPOSITE**
M. Fáberová, R. Bureš, P. Kollár, J. Füzer, S. Dobák, F. Onderko, M. Strečková and P. Kurek
- P2-51 IMPROVEMENT OF MAGNETIC PROPERTIES AND CRYSTALLOGRAPHIC TEXTURE OF Fe-Si STEELS BY THERMAL PROCESSING IN HIGH MAGNETIC FIELD**
F. Kováč, I. Petryshynets, J. Marcin and I. Škorvánek

3. MAGNETIC MATERIALS FOR ENERGY APPLICATIONS (PERMANENT MAGNETS, MAGNETOCALORIC MATERIALS, MOTORS, TRANSFORMERS, ...)

- I3-01 ENERGY-EFFICIENT REFRIGERATION NEAR ROOM TEMPERATURE WITH TRANSITION METAL BASED MAGNETIC REFRIGERANTS**
E. Brück, H. Yibole, Van Thang Nguyen, Xuefei Miao, M. Boeije, L. Caron, Lian Zhang, F. Guillou and N. Van Dijk
- I3-02 SOFT MAGNETIC, NANOCRYSTALLINE MATERIALS FOR INDUCTORS AND SHIELDING APPLICATIONS - OPTIMIZED FOR HIGHER FREQUENCY**
C. Polak
- O3-01 MAGNETOCALORIC EFFECT OVER A WIDE TEMPERATURE RANGE DUE TO MULTIPLE MAGNETIC TRANSITIONS IN $\text{GdNi}_{0.8}\text{Al}_{1.2}$ ALLOY**
T. P. Rashid, S. Nallamuthu, K. Arun, I. Curlik, S. Ilkovic, A. Dzubinska, M. Reiffers and R. Nagalakshmi
- O3-02 THE SCHOTTKY EFFECT IN YbCoGaO_4 SINGLE CRYSTALS**
I. Radelytskyi, T. Zajarniuk, A. Szewczyk, M. Gutowska, H. A. Dabkowska, P. Dłużewski and H. Szymczak
- O3-03 ANALYSIS OF THE CRYSTALLIZATION PROCESSES AS A BASIS FOR OPTIMIZATION OF MAGNETIC PROPERTIES OF $\text{Hf}_2\text{Co}_{11}\text{B}$ ALLOYS**
A. Musiał, Z. Śniadecki, J. Kováč, I. Škorvánek and B. Idzikowski
- P3-01 INVESTIGATIONS OF THE MAGNETIZATION REVERSAL PROCESSES IN NANOCRYSTALLINE Nd-Fe-B ALLOYS DOPED BY Nb**
M. Kaźmierczak, P. Gębara, P. Pawlik, K. Pawlik, A. Przybył, I. Wnuk and J. J. Wysłocki
- P3-02 MAGNETOCALORIC PROPERTIES OF $(\text{Fe}_{46.9}\text{Co}_{20.1}\text{B}_{22.7}\text{Si}_{5.3}\text{Nb}_5)_{90}\text{M}_{10}$ ($\text{M}=\text{Tb}, \text{Pr}, \text{Nd}$) ALLOYS PREPARED BY MECHANICAL ALLOYING**
K. Sarlar, A. Adam, E. Civan and I. Kucuk
- P3-03 DC MAGNETIC PROPERTIES OF Ni-Fe BASED COMPOSITES**
F. Onderko, M. Jakubčín, S. Dobák, D. Olekšáková, P. Kollár, J. Füzer, M. Fáberová, R. Bureš and P. Kurek
- P3-04 SCALLING ANALYSIS OF THE MAGNETOCALORIC EFFECT IN Co@Au NANOPARTICLES**
P. Hrubovčák, A. Zeleňáková, V. Zeleňák and V. Franco

- P3-05 INVESTIGATION OF THE MAGNETIC PHASE TRANSITION IN THE $\text{LaFe}_{11.14}\text{Co}_{0.66}\text{Si}_{1.1}\text{M}_{0.1}$ (WHERE M=Al OR Ga) ALLOYS**
P. Gębara
- P3-06 MAGNETIC PROPERTIES AND MAGNETOCALORIC EFFECT IN SPUTTER DEPOSITED THIN FILMS OF Mn-RICH HEUSLER ALLOYS FROM Ni-Mn-X (X = Ga, Sn) SYSTEMS**
M. Chojnacki, K. Fronc, I. Radelytskyi, T. Wojciechowski, R. Minikayev and H. Szymczak
- P3-07 MEASUREMENT OF MAGNETOCALORIC EFFECT WITH MICROCALORIMETRY**
A. Chudikova, D. Gonzalez, T. Ryba, Z. Vargova, V. Komanicky, J. Kacmarcik, R. Gyepes and R. Varga
- P3-08 THE EFFECT OF Mn AND Ni ADMIXTURE ON MAGNETIZATION REVERSAL PROCESSES IN (Pr, Dy)-(Fe, Co)-B RIBBONS**
A. Przybył
- P3-09 APPLICATION OF MODIFIED TAKACS MODEL FOR ANALYSIS OF MAGNETOCALORIC EFFECT IN $\text{Fe}_{60}\text{Co}_{10}\text{Mo}_5\text{Cr}_4\text{Nb}_6\text{B}_{15}$**
J. Rzakci and M. Dospial
- P3-10 SCALING OF ANHYSTERETIC CURVES FOR LAFECOSI ALLOY NEAR THE TRANSITION POINT**
R. Gozdur, K. Chwastek, M. Najgebauer, M. Lebioda, Ł. Bernacki and A. Wodzyński
- P3-11 INFLUENCE OF SPARK PLASMA SINTERING ON MICROSTRUCTURE AND PROPERTIES OF La-Ca-Sr-Mn-O MAGNETOCALORIC CERAMIC MATERIALS**
K. Zmorayová, V. Antal, J. Kováč, J. Noudem and P. Diko
- P3-12 MAGNETIC PROPERTIES AND STRUCTURE OF FeCo ALLOYS**
D. Olekšáková, P. Kollár, F. Onderko, J. Füzér, S. Dobák and J. Viňáš
- P3-13 INVESTIGATION OF MAGNETIC ANISOTROPY INFLUENCE ON TOTAL LOSS COMPONENTS OF GRAIN-ORIENTED ELECTRICAL STEELS**
W. A. Pluta
- P3-14 MAGNETOCALORIC EFFECT IN NOVEL $\text{Gd}_2\text{O}_3@\text{SiO}_2$ NANOCOMPOSITES**
A. Berkutova, A. Zelenáková, P. Hrubovčák, O. Kapusta and V. Zeleňák
- P3-15 THE INFLUENCE OF $\text{NiZnFe}_2\text{O}_4$ CONTENT ON MAGNETIC PROPERTIES OF SUPERMALLOY TYPE MATERIAL**
L. Ďáková, J. Füzér, S. Dobák, P. Kollár, M. Fáberová, M. Strečková, R. Bureš and H. Hadraba

**P3-16 THE INFLUENCE OF PREPARATION METHODS ON
MAGNETIC PROPERTIES OF Fe/SiO₂ SOFT MAGNETIC
COMPOSITES**

J. Füzervová, J. Füzer, P. Kollár, M. Kabátová and E. Dudrová

**P3-17 MAGNETIC PROPERTIES AND STRUCTURE OF NON-
ORIENTED ELECTRICAL STEEL SHEETS AFTER DIFFERENT
SHAPE PROCESSINGS**

T. Bulín, E. Švábenská, M. Hapla, Č. Ondrůšek and O. Schneeweiss

4. MAGNETIC THIN FILMS AND SURFACES, SPINTRONICS, PARTICLES AND NANOSTRUCTURES

I4-01 LOW T_c GLASSY MAGNETIC ALLOYS FOR MEDICAL APPLICATIONS

H. Chiriac

I4-02 TEMPLATE ASSISTED DEPOSITION OF FERROMAGNETIC NANOSTRUCTURES: FROM ANTIDOT THIN FILMS TO MULTISEGMENTED NANOWIRES AND METALLIC NANOTUBES

V. M. Prida, V. Vega, S. González, M. Salaheldeen, J. M. Mesquita, A. Fernández and B. Hernando

O4-01 FOCUSED ION BEAM PATTERNING OF METASTABLE FCC IRON THIN FILMS – A NOVEL TEMPLATE FOR MAGNETIC METAMATERIALS

M. Urbánek, V. Křížáková, J. Gloss, M. Horký, L. Flajšman, M. Schmid, T. Šíkola and P. Varga

O4-02 IN-PLANE EDGE MAGNETISM IN GRAPHENE-LIKE NANOSTRUCTURES

S. Krompiewski

O4-03 HIGH-RESOLUTION FULLY VECTORIAL SCANNING KERR MAGNETOMETRY

L. Flajšman, M. Urbánek, V. Křížáková, M. Vaňatka and T. Šíkola

O4-04 TOWARDS MEASURING MAGNETISM WITH ATOMIC RESOLUTION IN A TRANSMISSION ELECTRON MICROSCOPE

J. Rusz, J. C. Idrobo, S. Muto, J. Spiegelberg and K. Tatsumi

O4-05 MAGNETIC VORTEX NUCLEATION MODES STUDIED BY ANISOTROPIC MAGNETORESISTANCE AND MAGNETIC TRANSMISSION X-RAY MICROSCOPY

M. Vaňatka, M. Urbánek, R. Jíra, L. Flajšman, M. Dhankhar, V. Uhlíř, M.-Y. Im and T. Šíkola

O4-06 MAGNETIC PROPERTIES OF HEXAGONAL GRAPHENE NANOMESHES

M. Zwierzycki

O4-07 MAGNETOTRANSPORT IN Mn-DOPED Bi_2Se_3 TOPOLOGICAL INSULATORS

V. Tkáč, V. Komanicky, R. Tarasenko, M. Vališka, V. Holý, G. Springholz, V. Sechovský and J. Honolka

O4-08 STUDY OF MAGNETIC MICRO-ELLIPSES BY CANTILEVER SENSOR

K. Sečianska, J. Šoltýs and V. Cambel

- O4-09 MAGNETIC PHASE TRANSITION ASYMMETRY IN MESOSCALE FeRh STRIPES**
V. Uhlíř, J. A. Arregi and E. E. Fullerton
- P4-01 MAGNETISM AND STRUCTURE EVOLUTION IN Ni-Zn FERRITES THIN FILMS – CEMS STUDY**
T. Szumiata, M. Gzik-Szumiata, K. Brzózka, B. Górka, M. Gawroński, A. Javed, K. Farman and T. Fatima
- P4-02 EXACT DIAGONALIZATION-BASED CALCULATIONS OF INDIRECT MAGNETIC COUPLING IN GRAPHENE NANOSTRUCTURES**
K. Szałowski
- P4-03 GROWTH OF Pt-Ni NANOPARTICLES OF DIFFERENT COMPOSITION USING ELECTRODEPOSITION AND CHARACTERIZATION OF THEIR MAGNETIC PROPERTIES**
M. Kozejová, D. Hložná, Y. Hua Liu, K. Ráciová, E. Čížmar, M. Orendáč and V. Komanický
- P4-04 LSMO/YBCO HETEROSTRUCTURES AND INVESTIGATION OF “NEGATIVE” RESISTANCE EFFECT IN THE INTERFACE**
M. Sojková, T. Nurgaliev, V. Štrbík, Š. Chromik, B. Blagoev and M. Španková
- P4-05 GENERALIZATION OF MAGNETOSTATIC METHOD OF MOMENTS FOR THIN LAYERS WITH REGULAR RECTANGULAR GRIDS**
R. Szewczyk
- P4-06 SPECTROSCOPIC PROPERTIES OF SBA-15 MESOPOROUS SILICA FREE-STANDING THIN FILMS ACTIVATED BY COPPER IONS**
L. Laskowski and M. Laskowska
- P4-07 TRANSPORT AND MAGNETIC PROPERTIES OF SUPERCONDUCTOR-FERROMAGNET-SUPERCONDUCTOR NANOFUNCTIONS**
N. Gál, V. Štrbík, Š. Beňačka, Š. Gaži, M. Španková, Š. Chromik, M. Sojková and M. Pisarčík
- P4-08 HIGH RESOLUTION X-RAY CHARACTERIZATION OF MANGANITE FILMS GROWN ON VARIOUS SUBSTRATES**
M. Španková, V. Štrbík, E. Dobročka, Š. Chromik, N. Gál and M. Sojková
- P4-09 LOW-TEMPERATURE PROPERTIES OF ONE-DIMENSIONAL MAGNETO-PHOTONIC CRYSTALS IN MAGNETIC FIELD**
Yu. Kharchenko, I. Lukienko, O. Miloslavskaya, M. F. Kharchenko, A. V. Karavainikov, A. R. Prokopov and A. N. Shaposhnikov

- P4-10 MAGNETIC PROPERTIES OF NICKEL HEXACYANOFERRATE/CHROMATE THIN FILMS**
M. Fitta, T. Korzeniak, P. Czaja and M. Bałanda
- P4-11 Ni_2FeSi HEUSLER MICROWIRES FOR SPINTRONIC APPLICATIONS**
L. Galdun, T. Ryba, V. M. Prida, B. Hernando, V. Zhukova, A. Zhukov, Z. Vargová and R. Varga
- P4-12 SPIN WAVE CHARACTERISTICS OF INHOMOGENEOUS FERROMAGNETIC LAYERED COMPOSITES**
A. Urbaniak-Kucharczyk
- P4-13 MAGNETIC AND STRUCTURAL CHARACTERIZATION OF NiMnSb HEUSLER RIBBON**
T. Ryba, Z. Vargova, S. Ilkovic, M. Reiffers, V. Haskova, P. Szabo, J. Kravcak, R. Gyepes and R. Varga
- P4-14 MAGNETIC PROPERTIES FE AND GD OXIDES EMBEDDED IN MESOPOROUS SILICA**
O. Kapusta, A. Zeleňáková, V. Girman, P. Hrubovčák and V. Zeleňák
- P4-15 SYSTEMATIC ANALYSIS OF ANISOTROPIC MAGNETORESISTANCE IN $(\text{Ga},\text{Mn})\text{As}$**
K. Vyborný
- P4-16 PHASE ANALYSIS OF MAGNETIC INCLUSIONS IN NANOMATERIALS BASED ON MULTIWALL CARBON NANOTUBES**
K. Brzózka, M. Krajewski, A. Małolepszy, L. Stobiński, T. Szumiata, B. Górka, M. Gawroński and D. Wasik
- P4-17 INFLUENCE OF Mn DOPING ON MAGNETIC AND STRUCTURAL PROPERTIES OF Co_2FeSi HEUSLER ALLOY**
L. Galdun, T. Ryba, V. M. Prida, B. Hernando, Z. Vargová and R. Varga
- P4-18 EXCHANGE BIAS EFFECT IN NdFeO_3 SYSTEM OF NANO PARTICLES**
M. Vavra, M. Zentková, M. Mihalik, M. Mihalik jr., J. Lazúrová, V. Girman, M. Perovic, V. Kusigerski, P. Roupčova and Z. Jaglicic
- P4-19 SUPERSPIN GLASS STATE IN MAGNETIC NANOPARTICLES**
A. Zeleňáková, P. Hrubovčák and V. Zeleňák
- P4-20 THE INVESTIGATION OF SPIN-SEEBECK EFFECT IN Ni_xFe_y ALLOYS**
Ł. Bernacki, R. Gozdur and W. Pawlak
- P4-21 EFFECT OF THE JAHN TELLER DISTORTION ON DOUBLE EXCHANGE INTERACTION IN $\text{La}_{1-x}\text{K}_x\text{MnO}_3$ NANO PARTICLES**
M. Mihalik, M. Zentková, M. Vavra, M. Mihalik Jr., J. Lazúrová, V. Girman, M. Fitta and S. Il'kovič

P4-22 THE MAGNETIC EQUATION OF STATE AND TRANSPORT PROPERTIES IN REDUCED DIMENSIONS

K. Warda and L. Wojtczak

P4-23 THE ELECTRICAL RESISTIVITY OF METALLIC ALLOYS

K. Warda and L. Wojtczak

P4-24 STRUCTURE OF MELT-SPUN Co_2MnAl HEUSLER ALLOY

S. Piovarči, P. Diko, V. Kavečanský, T. Ryba, Z. Vargová and R. Varga

5. LOW-DIMENSIONAL MAGNETIC MATERIALS, MOLECULAR MAGNETS AND FERROFLUIDS

- I5-01 THE ROUTE TO MAGNETIC ORDER IN THE KAGOME ANTIFERROMAGNET**
J. Richter
- I5-02 LONG-RANGE MAGNETIC ORDER IN A PURELY ORGANIC 2D LAYER ADSORBED ON EPITAXIAL GRAPHENE**
A. L. Vázquez de Parga
- O5-01 UNUSUAL MAGNETIC-PRESSURE RESPONSE OF AN $S = 1$ QUASI-ONE-DIMENSIONAL ANTIFERROMAGNET NEAR $D/J \sim 1$**
M. K. Peprah, P. A. Quintero, A. Garcia, J. M. Pérez, J. S. Xia, J. M. Manson, S.E. Brown and M. W. Meisel
- O5-02 DOUBLE MAGNETIC RELAXATION AND MAGNETOCALORIC EFFECT IN TWO CLUSTER-BASED MATERIALS $Mn_9[W(CN)_6]_L$**
P. Konieczny, R. Pelka, W. Nogaś, S. Choraży, M. Kubicki, R. Podgajny, B. Sieklucka and T. Wasiutyński
- O5-03 AC MAGNETIC SUSCEPTIBILITY OF FERROFLUIDS EXPOSED TO AN EXTERNAL ELECTRIC FIELD**
M. Rajňák, B. Dolník, J. Kováč, J. Kurimský, R. Cimbala, K. Paulovičová, P. Kopčanský and M. Timko
- O5-04 UNIVERSAL SEQUENCE OF GROUND STATES IN ANTIFERROMAGNETIC FRUSTRATED RINGS WITH A SINGLE BOND DEFECT**
M. Antkowiak, G. Kamieniarz and W. Florek
- P5-01 MAGNETIC-FIELD INDUCED SLOW RELAXATION IN THE ISING-LIKE QUASI-ONE-DIMENSIONAL FERROMAGNET $KEr(MoO_4)_2$**
V. Tkáč, A. Orendáčová, Ľ. Dlháň, M. Orendáč, R. Boča and A. Feher
- P5-02 INFLUENCE OF PRESSURE ON THE MAGNETIC RESPONSE OF THE LOW-DIMENSIONAL QUANTUM MAGNET $Cu(H_2O)_2(C_2H_8N_2)SO_4$**
M. K. Peprah, D. VanGennep, B. D. Blasiola, P. A. Quintero, R. Tarasenko, J. J. Hamlin, M. W. Meisel and A. Orendáčová
- P5-03 EXPERIMENTAL STUDY OF THE MAGNETOCALORIC EFFECT IN $Ni(en)(H_2O)_4SO_4 \cdot 2H_2O$ - an $S = 1$ MOLECULAR MAGNET WITH EASY-PLANE ANISOTROPY**
R. Tarasenko, A. Orendáčová, E. Čížmár, M. Orendáč, I. Potočník and A. Feher

- P5-04 GENERATION OF Fe_3O_4 NANOPARTICLE AGGREGATES IN A FERROFLUID DRIVEN BY EXTERNAL ELECTRIC FIELD**
J. Kurimský, M. Rajňák, R. Cimbala, K. Paulovičová, M. Timko, P. Kopčanský, M. Kosterec, L. Kruželák and M. Kolcun
- P5-05 ULTRASOUND FREQUENCY ANALYSIS OF A MAGNETIC FLUID IN LOW-INTENSITY EXTERNAL MAGNETIC FIELD**
J. Kurimský, M. Rajňák, R. Cimbala, B. Dolník, J. Tóthová, K. Paulovičová, M. Timko, P. Kopčanský, J. Petráš, I. Kolcunová, J. Džmura and J. Balogh
- P5-06 STRUCTURAL CHANGES IN LIQUID CRYSTALS WITH ROD-LIKE MAGNETIC PARTICLES STUDIED BY SURFACE ACOUSTIC WAVES**
P. Bury, J. Kúdelčík, M. Veveričík, P. Kopčanský, M. Timko and V. Závishová
- P5-07 THE SPIN-1 J1-J3 HEISENBERG MODEL ON A TRIANGULAR LATTICE: EXACT DIAGONALIZATION STUDY**
P. Rubin and A. Sherman
- P5-08 GROUND STATE SPIN OF HUBBARD LADDER MODELS WITH INFINITE ELECTRON REPULSION**
V. O. Cheranovskii, E. V. Ezerskaya, D. J. Klein and V. V. Tokarev
- P5-09 STUDY OF STRUCTURAL CHANGES OF WATER-BASED MAGNETIC-FLUID BY ACOUSTIC SPECTROSCOPY**
J. Kúdelčík, Š. Hardoň, P. Bury, M. Timko and P. Kopčanský
- P5-10 ENHANCED MAGNETOCALORIC EFFECT IN $\text{NiCl}_2(\text{bipy})$ AT LOW TEMPERATURES**
K. Ráczová, E. Čížmár and A. Feher
- P5-11 MAGNETIC HEAT CAPACITY OF ANION-RADICAL SALT $\text{Ni}(\text{bipy})_3(\text{TCNQ})_4 \cdot (\text{CH}_3)_2\text{CO}$ AT VERY LOW TEMPERATURES**
D. Šoltéssová, E. Čížmár, G. Vasylets, V. Starodub and A. Feher
- P5-12 THE ENERGY SPECTRUM AND THERMODYNAMICS OF THE SPIN-1/2 XX CHAIN WITH ISING IMPURITIES**
E. V. Ezerskaya
- P5-13 MEASUREMENT OF COMPLEX PERMITTIVITY OF OIL-BASED FERROFLUID**
J. Kúdelčík, Š. Hardoň and L. Varačka
- P5-14 LOW MAGNETIC FIELD RESPONSE IN FERRONEMATICS**
V. Gdovinova, N. Tomasovicova, V. Zavisova, N. Eber, T. Toth-Katona, F. Royer, D. Jamon, J. Jadzyn and P. Kopcansky
- P5-15 ANALYSIS OF THERMAL FIELD IN MINERAL TRANSFORMER OIL BASED MAGNETIC FLUIDS**
M. Kosterec, J. Kurimský, R. Cimbala, L. Kruželák, M. Rajňák, M. Timko and P. Kopčanský

- P5-16 FRUSTRATED ZIG-ZAG SPIN CHAINS FORMED BY HYDROGEN BONDS IN COMPOUND**
 $[\text{Cu}(\text{H}_2\text{O})(\text{OH})(\text{tmen})]_2[\text{Pd}(\text{CN})_4] \cdot 2\text{H}_2\text{O}$
E. Čížmár, A. Orendáčová, M. Orendáč, J. Kuchár, A. Feher, J.-H. Park and M. W. Meisel
- P5-17 TEMPERATURE DEPENDENCE OF A DIELECTRIC RELAXATION IN WEAKLY POLAR FERROFLUIDS**
M. Rajňák, J. Kurimský, B. Dolník, R. Cimbala, K. Paulovičová, P. Kopčanský and M. Timko
- P5-18 THE RESPONSE OF A MAGNETIC FLUID TO RADIO FREQUENCY ELECTROMAGNETIC FIELD**
B. Dolník, M. Rajňák, R. Cimbala, I. Kolcunová, J. Kurimský, J. Balogh, J. Džmura, J. Petráš, P. Kopčanský, M. Timko, J. Briančin and M. Fabián
- P5-19 KINETICS OF NEMATIC TO ISOTROPIC PHASE TRANSITION IN LIQUID CRYSTAL DOPED WITH MAGNETIC NANOPARTICLES**
K. Csach, A. Juríková, J. Miškuf, N. Tomašovičová, V. Gdovinová, V. Závišová, P. Kopčanský, N. Éber, K. Fodor-Csorba and A. Vajda
- P5-20 CHARACTERIZATION OF CARBON NANOTUBES**
M. Jeníková, K. Zakuťanská, J. Kováč, V. Girman, P. Kopčanský and N. Tomašovičová
- P5-21 THE INFLUENCE OF MAGNETIC PARTICLES AND MAGNETIC FIELD ON THE SHAPE OF DROPLETS OF LIQUID CRYSTAL**
J. Majorošová, V. Gdovinová, N. Tomašovičová, A. Juríková, V. Závišová, J. Jadzyn and P. Kopčanský
- P5-22 THERMAL CONDUCTIVITY OF LOW-DIMENSIONAL MAGNETIC SYSTEMS**
D. Legut, D. U. Wdowik and A. Orendáčová
- P5-23 AFM STUDIES OF INTERACTION OF MAGNETIC NANOPARTICLES WITH LYOTROPIC LIQUID CRYSTAL**
N. Tomašovičová, L. Balejíčková, V. Gdovinová, M. Kubovčíková, C.-W. Yang, I.-S. Hwang, S. Hayryan, C.-K. Hu and P. Kopčanský
- P5-24 THE LOW AND HIGH SPIN GROUND STATES IN NEW TETRANUCLEAR MANGANESE MOLECULES WITH $[\text{Mn}^{\text{II}}_3\text{Mn}^{\text{III}}]$ AND $[\text{Mn}^{\text{II}}_2\text{Mn}^{\text{III}}_2]$ METALLIC CORES**
M. Antkowiak, M. Sobocińska, M. Wojciechowski, G. Kamieniarz, J. Utko and T. Lis
- P5-25 THE STUDY OF MAGNETIC MOLECULES CONTAINING CROMIUM-BASED RINGS WITHIN DENSITY FUNCTIONAL THEORY**
B. Brzostowski, M. Wojciechowski and G. Kamieniarz

**P5-26 CORRELATION BETWEEN THE STRUCTURE AND
MAGNETIC SUSCEPTIBILITY OF BiOX (X=Cl, Br, I) SINGLE
CRYSTALS**

V. Bunda, S. Bunda, J. Kovac, D. Lotnyk and A. Feher

**P5-27 MAGNETIC PROPERTIES OF BiOCl:Ti AND BiOCl:Sm SINGLE
CRYSTALS**

S. Bunda, V. Bunda, J. Kovac, D. Lotnyk and A. Feher

6. RARE-EARTH AND 5f-SYSTEMS

I6-01 FERROMAGNETIC CRITICALITY OF URANIUM COMPOUNDS

J. Prokleška, P. Opletal, M. Vališka, M. Míšek and V. Sechovský

O6-01 MAGNETISM AND CRYSTAL FIELD IN PrCuAl_3 AND NdCuAl_3

P. Novák and M. Diviš

O6-02 MAGNETIC PROPERTIES OF SOLID SOLUTIONS $\text{HoCo}_{1-x}\text{Ni}_x\text{C}_2$

H. Michor, V. Levytskyy, V. Babizhetskyy, M. Hembara, A. Schumer, S. Özcan and B. Ya. Kotur

O6-03 WEAKLY ANISOTROPIC MAGNETISM IN URANIUM INTERMETALLIC $\text{U}_4\text{Ru}_7\text{Ge}_6$

M. Vališka, J. Valenta, P. Doležal, V. Tkáč, J. Prokleška, M. Diviš and V. Sechovský

O6-04 MAGNETIC PROPERTIES AND MAGNETOCALORIC EFFECT IN STRUCTURALLY DISORDERED RECo_2 ($\text{RE} = \text{Y, Gd, Tb}$) COMPOUNDS

Z. Śniadecki, N. Pierunek and B. Idzikowski

O6-05 MAGNETIC PHASE DIAGRAMS AND STRUCTURES IN R_2TIn_8 ($\text{T} = \text{Rh, Ir, Co}$) AND RELATED TETRAGONAL COMPOUNDS

P. Javorský, P. Čermák, M. Kratochvílová, J. Zubáč, K. Pajskr, K. Prokeš and B. Ouladdiaf

P6-01 THE MACROSCOPIC AND MICROSCOPIC PROPERTIES STUDY ON CeTIn COMPOUNDS, WHERE $\text{T} = \text{Ni, Pd, Pt}$

M. Klicpera, M. Boehm and P. Javorský

P6-02 CRYSTAL FIELD IN NdPd_5Al_2 AND ITS INFLUENCE ON MAGNETIC PROPERTIES

J. Zubáč, M. Diviš, B. Fåk and P. Javorský

P6-03 ANOMALOUS HALL EFFECT IN $\text{Ho}_{0.5}\text{Lu}_{0.5}\text{B}_{12}$ ANTIFERROMAGNET WITH CAGE-GLASS CRYSTAL STRUCTURE

N. E. Sluchanko, V. N. Krasnorussky, A. V. Bogach, V. V. Glushkov, S. V. Demishev, A. L. Khoroshilov, A. V. Dukhnenko,

N. Yu. Shitsevalova, V. B. Filipov, S. Gabani, K. Flachbart and G. E. Grechnev

P6-04 MAGNETIC ANISOTROPY IN ANTIFERROMAGNET GdB_6

M. Anisimov, V. Glushkov, S. Demishev, N. Samarin, A. Bogach, A. Samarin, N. Shitsevalova, A. Levchenko, V. Filipov, S. Gabani, K. Flachbart and N. Sluchanko

- P6-05 TRANSPORT PROPERTIES OF DILUTED MAGNETIC HEXABORIDES $R_{0.01}La_{0.99}B_6$ ($R = Ce, Pr, Nd, Gd, Eu, Ho$)**
M. Anisimov, V. Glushkov, S. Demishev, N. Samarin, N. Shitsevalova, A. Levchenko, V. Filipov, A. Bogach, V. Voronov, S. Gabani, K. Flachbart and N. Sluchanko
- P6-06 ELECTRON SPIN RESONANCE IN PARAMAGNETIC AND ANTI-FERROMAGNETIC STATES OF $Ho_{0.5}Lu_{0.5}B_{12}$**
M. I. Gilmanov, A. V. Semeno, S. V. Demishev, V. V. Glushkov, A. L. Khoroshilov, V. N. Krasnorussky, N. Y. Shitsevalova, V. B. Filipov, K. Flachbart and N. E. Sluchanko
- P6-07 MAGNETORESISTANCE ANISOTROPY IN HoB_{12}**
A. Khoroshilov, V. Krasnorussky, A. Bogach, V. Glushkov, S. Demishev, A. Levchenko, N. Shitsevalova, V. Filipov, S. Gabani, K. Flachbart, K. Siemensmeyer and N. Sluchanko
- P6-08 GLASS FORMING ABILITIES AND CRYSTALLIZATION PROCESS IN AMORPHOUS $Pr-Fe-Co-Zr-Nb-B$ ALLOYS OF VARIOUS B CONTENTS**
K. Pawlik, P. Pawlik and J. J. Wysocki
- P6-09 INFLUENCE OF PRESSURE ON THE ELECTRIC TRANSPORT PROPERTIES OF CARBON-DOPED EuB_6**
G. Pristáš, S. Gabáni, I. Baťko, M. Baťková, V. Filipov and E. Konovalova
- P6-10 PREPARATION AND BASIC PHYSICAL PROPERTIES OF YbT_2X_2 ($T = Pd, Au$; $X = Si, Ge$) COMPOUNDS**
J. Kaštil, K. Vlášková, J. Prchal, M. Míšek, J. Kamarád and Z. Arnold
- P6-11 CHARGE TRANSPORT AND MAGNETISM IN $Tm_{0.03}Yb_{0.97}B_{12}$**
V. Glushkov, A. Azarevich, M. Anisimov, A. Bogach, S. Demishev, A. Dukhnenko, V. Filipov, K. Flachbart, S. Gabáni, S. Gavrilkin, N. Shitsevalova and N. Sluchanko
- P6-12 X-RAY DIFFRACTION STUDY OF CeT_2Al_{10} ($T = Ru, Os$) AT LOW TEMPERATURE AND UNDER PRESSURE**
Y. Kawamura, J. Hayashi, K. Takeda, C. Sekine, T. Tanida, M. Sera, S. Nakano, T. Tomita, H. Takahashi and T. Nishioka
- P6-13 SPECIFIC HEAT STUDY ON $CeCu_xAl_{4-x}$ AND $Ce_xLa_{1-x}CuAl_3$ COMPOUNDS**
K. Vlášková, P. Javorský and M. Klicpera
- P6-14 VARIATIONS OF ANTIFERROMAGNETISM IN $U_{1-x}Ir_xGe$ IN MAGNETIC FIELDS AND EXTERNAL PRESSURES**
M. Vališka, J. Prchal and V. Sechovský
- P6-15 EFFECT OF SOLVENTS ON MAGNETIC PROPERTIES OF METAL-ORGANIC FRAMEWORK MOF-76(Gd)**
M. Almáši, V. Zelenák and A. Zelenáková

- P6-16 CHARACTERIZATION OF NEW UNiX₂ SPLATS AND STUDY OF THEIR PHYSICAL PROPERTIES**
Z. Molcanova, M. Mihalik, M. Mihalik jr., M. Paukov and L. Havela
- P6-17 MAGNETIC PROPERTIES OF A DyCo₂ CRYSTAL**
J. Prchal, V. Latoňová, M. Kratochvílová and V. Sechovský
- P6-18 EXPERIMENTAL STUDY OF PHYSICAL PROPERTIES OF NEW Gd_{1-x}Ce_xNi₅ SYSTEM**
A. Džubinská, M. Reiffers, J. I. Espeso and J. Rodríguez Fernández
- P6-19 MAGNETORESISTANCE OF THE CeCo_{1-x}Fe_xGe₃ ALLOYS**
P. Skokowski, K. Synoradzki and T. Toliński
- P6-20 CRYSTAL STRUCTURE AND PHYSICAL PROPERTIES OF THE NOVEL Eu COMPOUNDS**
I. Čurlík, F. Gastaldo, M. Giovannini, A. M. Strydom and M. Reiffers
- P6-21 CROSSOVER BETWEEN FERMI-LIQUID AND NON-FERMI-LIQUID IN Th_{1-x}U_xBe₁₃ (0≤x≤1)**
N. Miura, K. Uhlířová, J. Prchal, C. Tabata, V. Sechovský, H. Hidaka, T. Yanagisawa and H. Amitsuka
- P6-22 HALL COEFFICIENT IN TOROIDAL MAGNETIC ORDERED STATE OF UNi₄B**
H. Saito, N. Miura, C. Tabata, H. Hidaka, T. Yanagisawa and H. Amitsuka

7. STRONGLY CORRELATED ELECTRON SYSTEMS, SUPERCONDUCTING MATERIALS

I7-01 SAMARIUM HEXABORIDE: THE FIRST STRONGLY CORRELATED TOPOLOGICAL INSULATOR?

O. Rader, P. Hlawenka, K. Siemensmeyer, E. Weschke, A. Varykhalov,
J. Sánchez-Barriga, N. Y. Shitsevalova, A. V. Dukhnenko, V. B. Filipov,
S. Gabáni, K. Flachbart and E. D. L. Rienks

I7-02 SCANNING TUNNELING MICROSCOPY STUDY OF SUPERCONDUCTING VORTEX MOTION

T. Samuely, M. Timmermans, D. Lotnyk, B. Raes, J. Van de Vondel and
V. V. Moshchalkov

O7-01 TRANSITION FROM MOTT INSULATOR TO SUPERCONDUCTOR IN GaNb_4S_8 AT HIGH PRESSURE

X. Wang, K. Syassen, F. J. Litterst, J. Prchal, V. Sechovsky, D. Johrendt
and M. M. Abd-Elmeguid

O7-02 TESTING THE THIRD LAW OF THERMODYNAMICS AT $T \rightarrow 0$ IN MAGNETIC SYSTEMS

J. G. Sereni

O7-03 PROTON DISORDER IN D_2O - ICE, A NEUTRON DIFFRACTION STUDY

K. Siemensmeyer, J.-U. Hofmann, S. V. Isakov, B. Klemke,
R. Moessner, J. P. Morris and D. A. Tennant

O7-04 STRUCTURAL AND PHYSICAL PROPERTIES OF NEW COMPOUNDS IN THE Yb-Pd-Sn TERNARY SYSTEM

F. Gastaldo, M. Giovannini, A. Strydom, I. Čurlík, M. Reiffers,
P. Solokha and A. Saccone

O7-05 SYNTHESIS AND PHYSICAL PROPERTIES CePdIn_5 , A NEW COMPOUND OF $\text{Ce}_n\text{Pd}_m\text{In}_{3n+2m}$ HOMOLOGOUS SERIES

K. Uhlířová, J. Prokleška, B. Vondráčková, M. Kratochvilová, M. Dušek,
J. Custers and V. Sechovský

O7-06 SUPERCONDUCTOR – INSULATOR TRANSITION

P. Szabó, T. Samuely, V. Hašková, J. Kačmarčík, M. Žemlička,
M. Grajcar, R. Hlubina, R. Martoňák and P. Samuely

O7-07 SUPERCONDUCTING STATE IN $\text{LaPd}_2\text{Al}_{(2-x)}\text{Ga}_x$

P. Doležal, M. Klicpera, J. Pásztorová, J. Prchal and P. Javorský

O7-08 THE EFFECT OF Sm ADDITION ON SUPERCONDUCTING PROPERTIES OF YBCO BULK SUPERCONDUCTORS

D. Volochová, P. Diko, S. Piovarčí, V. Antal and J. Kováč

- 07-09 HALL EFFECT AND HIDDEN QUANTUM CRITICALITY IN $\text{Mn}_{1-x}\text{Fe}_x\text{Si}$**
V. V. Glushkov, I. I. Lobanova, V. Yu. Ivanov, V. V. Voronov,
V. A. Dyadkin, N. M. Chubova, S. V. Grigoriev and S. V. Demishev
- 07-10 ELECTRIC CURRENTS AND VORTEX PINNING IN REBaCuO SUPERCONDUCTING TAPES**
M. Jirsa, M. Rameš, I. Ďuran, T. Melíšek and P. Kováč
- P7-01 THERMODYNAMIC PROPERTIES OF A CUBIC HUBBARD CLUSTER AT QUARTER FILLING**
K. Szałowski, T. Balcerzak, M. Jaščur, A. Bobák and M. Žukovič
- P7-02 PARAMAGNETISM OF TASAKI-HUBBARD MODEL**
V. Baliha, O. Derzhko and J. Richter
- P7-03 MAGNETIC, THERMODYNAMIC AND TRANSPORT PROPERTIES OF POLYCRYSTALLINE NdAgAl_3 COMPOUND**
S. Nallamuthu, A. Džubinská, M. Reiffers and R. Nagalakshmi
- P7-04 MAGNETIC PHASE DIAGRAM OF $\text{UCo}_{1-x}\text{Ru}_x\text{Al}$ WITH LOW Ru CONCENTRATION**
P. Opletal, J. Prokleška, J. Valenta and V. Sechovský
- P7-05 MAGNETORESISTANCE STUDY OF C-AXIS ORIENTED YBCO THIN FILM**
M. Chrobak, W. M. Woch, M. Kowalik, R. Zalecki, M. Giebułtowski,
J. Przewoźnik, Cz. Kapusta and G. Szwachta
- P7-06 PHASE DIAGRAMS AND REENTRANT TRANSITIONS OF A SPIN-ELECTRON MODEL ON A DOUBLY DECORATED HONEYCOMB LATTICE**
H. Čenčariková and J. Strečka
- P7-07 SPIN-GLASS BEHAVIOR IN LaCu_4Mn COMPOUND**
K. Synoradzki
- P7-08 CLEAN BULK YBaCuO SUPERCONDUCTORS DOPED BY PARAMAGNETIC IONS OF Sm AND Yb**
M. Jirsa, D. Volochová, J. Kováč and P. Diko
- P7-09 STM STUDIES OF THE SUPERCONDUCTOR-INSULATOR TRANSITION IN MoC ULTRATHIN FILMS**
P. Szabó, V. Hašková, T. Samuely, J. Kačmarčík, M. Žemlička,
M. Grajcar and P. Samuely
- P7-10 SUPERCONDUCTIVITY OF NIOBIUM THIN FILM IN THE BiOCl/Nb HETEROSTRUCTURE**
D. Lotnyk, V. Komanicky, V. Bunda and A. Feher

- P7-11 NON BCS SUPERCONDUCTING DENSITY OF STATES IN B-DOPED DIAMOND**
O. Onufriienko, T. Samuely, G. Zhang, P. Szabó, V. V. Moshchalkov and P. Samuely
- P7-12 INFLUENCE OF THERMO – CHEMICAL TREATMENTS ON SUPERCONDUCTING PROPERTIES OF LITHIUM DOPED $\text{YBa}_2\text{Cu}_3\text{O}_{7-\delta}$ BULK SUPERCONDUCTORS**
V. Antal, D. Volochová, V. Kavečanský, J. Kováč and P. Diko
- P7-13 SUPERCONDUCTIVITY IN $\text{Lu}_x\text{Zr}_{1-x}\text{B}_{12}$ DODECABORIDES WITH CAGE-GLASS CRYSTAL STRUCTURE**
N. E. Sluchanko, A. N. Azarevich, A. V. Bogach, S. Yu. Gavrilkin, M. I. Gilmanov, V. V. Glushkov, S. V. Demishev, K. V. Mitsen, A. V. Levchenko, N. Yu. Shitsevalova, V. B. Filipov, S. Gabani and K. Flachbart
- P7-14 INFLUENCE OF PRESSURE ON THE ELECTRON-PHONON INTERACTION IN SUPERCONDUCTORS**
Mat. Orendáč, S. Gabáni, G. Pristáš, E. Gažo, K. Flachbart and N. Shitsevalova
- P7-15 SIMPLIFIED PARQUET EQUATION SOLVER FOR THE ANDERSON IMPURITY MODEL**
V. Pokorný, V. Janiš and A. Kauch
- P7-16 ANOMALOUS HALL EFFECT IN MnSi**
V. V. Glushkov, I. I. Lobanova, V. Yu. Ivanov and S. V. Demishev
- P7-17 ELECTROMAGNON CONTRIBUTION TO THE COOPER PAIR FORMATION AND SUPERCONDUCTIVITY**
Z. Bak
- P7-18 SUPERCONDUCTING AND MAGNETIC PROPERTIES OF Sn-DOPED $\text{EuBa}_2\text{Cu}_3\text{O}_{7-\delta}$ COMPOUND**
A. Dvurečenskij, A. Cigáň, I. Van Driessche, M. Škrátek, M. Majerová, J. Maňka and E. Bruneel
- P7-19 TRAPPED FIELD OF YBCO BULK SUPERCONDUCTORS PREPARED BY INFILTRATION GROWTH PROCESS**
L. Vojtkova, P. Diko and S. Piovarči
- P7-20 ON THE MAGNETIC PENETRATION DEPTH IN SUPERCONDUCTING ULTRATHIN LEAD FILMS**
A. P. Durajski and R. Szczesniak
- P7-21 DC NANOSQUID FROM Nb THIN FILMS**
V. Štrbík, M. Pisarčík, Š. Gaži and M. Španková

- P7-22 MAGNETIC AND STRUCTURAL CHARACTERIZATION OF SUPERCONDUCTIVE Ni_2NbSn HEUSLER ALLOY**
P. Kanuch, T. Ryba, J. Gamcová, M. Kanuchova, M. Durisin, K. Saksli, Z. Vargova and R. Varga
- P7-23 EVOLUTION OF LOCK-IN EFFECT IN Cu_xTiSe_2 SINGLE CRYSTALS**
Z. Medvecká, T. Klein, V. Cambel, J. Šoltýs, G. Karapetrov, F. Levy-Bertrand, B. Michon, C. Marcenat, Z. Pribulová and P. Samuely
- P7-24 VORTEX LATTICE IN HEAVY-FERMION CeCoIn_5 PROBED BY AC-CALORIMETRY**
J. Kačmarčík, P. Pedrizzini, C. Marcenat, Y. Fasano, V. Correa, Z. Pribulová and P. Samuely
- P7-25 SUPPRESSION OF SUPERCONDUCTIVITY IN HOMOGENEOUSLY DISORDERED ULTRATHIN MoC FILMS INTRODUCED BY INTERFACE BETWEEN THE SAMPLE AND THE SUBSTRATE**
V. Hašková, M. Kopčík, P. Szabó, T. Samuely, J. Kačmarčík, M. Žemlička, M. Grajcar and P. Samuely
- P7-26 HALL PROBE MAGNETOMETRY OF SUPERCONDUCTING YB_6**
M. Marcin, Z. Pribulová, J. Kačmarčík, S. Gabáni, T. Mori, V. Cambel, J. Šoltýs and P. Samuely
- P7-27 ANGULAR DEPENDENCIES OF ESR PARAMETERS IN ANTIFERROQUADRUPOLEAR PHASE OF CeB_6**
A. V. Semeno, M. I. Gilmanov, N. E. Sluchanko, V. N. Krasnorussky, N. Y. Shitzevalova, V. B. Filipov, K. Flachbart and S. V. Demishev
- P7-28 THERMODYNAMIC CRITICAL FIELD IN HEXAGONAL BaSn_5 SUPERCONDUCTOR**
M. W. Jarosik and A. D. Woźniak
- P7-29 UNIFORMLY DISORDERED ULTRATHIN SUPERCONDUCTING MoC FILMS CLOSE TO INSULATING STATE. TRANSPORT STUDIES.**
J. Kačmarčík, P. Szabó, M. Rajňák, M. Žemlička, M. Grajcar, P. Markoš and P. Samuely
- P7-30 DETECTING OF LIGHT BY MEANS OF “HTSC / PHOTOSEMICONDUCTOR “ HYBRID CONTACT STRUCTURES**
V. Bunda, S. Bunda, D. Lotnyk, V. Komanicky and A. Feher

- P7-31 EFFECT OF PRESSURE ON CRITICAL PARAMETERS AND MICROSTRUCTURE OF DOPED MgB_2 MATERIAL**
G. Gajda, A. Morawski, A. Presz, R. Diduszko, T. Cetner, K. Gruszka, S. Hossain and D. Gajda
- P7-32 LOCAL MAGNETOMETRY USING SCANNING HALL PROBE MICROSCOPE**
Z. Pribulová, Z. Medvecká, J. Kačmarčík, E. Gažo and P. Samuely
- P7-33 PHOTON-ASSISTED CHARGE TRANSPORT IN A HYBRID JUNCTION WITH TWO NON-COLLINEAR FERROMAGNETS AND A SUPERCONDUCTOR**
K. Bocian and W. Rudziński
- P7-34 MAGNETIC-FIELD INDUCED TRANSITION IN A SPIN-GLASS STATE OF CATION DEFICIENT LaMnO_3**
V. Eremenko, V. Sirenko, E. Čížmár, A. Baran and A. Feher

8. MULTIFUNCTIONAL MAGNETIC MATERIALS (MULTIFERROIC, MAGNETOELASTIC, SHAPE MEMORY, ...)

I8-01 RECENT RESEARCH IN MAGNETIC SHAPE MEMORY ALLOYS

J. M. Barandiaran and V. A. Chernenko

O8-01 MAGNETIC DOMAIN STRUCTURE TRANSFORMATION DURING FERROELASTIC TWIN BOUNDARY PASSAGE IN Ni-Mn-Ga SINGLE CRYSTAL

V. Kopecky, O. Perevertov, L. Fekete and O. Heczko

O8-02 INVESTIGATION OF MAGNETOELASTIC PROPERTIES OF $\text{Ni}_{0.36}\text{Zn}_{0.64}\text{Fe}_2\text{O}_4$ FERRITE MATERIAL IN LOW MAGNETIZING FIELDS CORRESPONDING TO RAYLEIGH REGION

M. Kachniarz, A. Bieńkowski and R. Szewczyk

O8-03 MAGNETIC PHASE DIAGRAM OF $\text{TbMn}_{1-x}\text{Fe}_x\text{O}_3$ ($0 \leq x \leq 1$) SUBSTITUTIONAL SYSTEM

M. Mihalik jr., M. Mihalik, Z. Jagličić, R. Vilarinho, J. Agostinho Moreira, A. Almeida and M. Zentková

O8-04 MAGNETIC PROPERTIES OF THE $\text{Bi}_{0.65}\text{La}_{0.35}\text{Fe}_{0.5}\text{Sc}_{0.5}\text{O}_3$ PEROVSKITE

A. V. Fedorchenko, E. L. Fertman, V. A. Desnenko, O. V. Kotlyar, E. Čížmár, V. V. Shvartsman, D. C. Lupascu, S. Salamon, H. Wende, A. N. Salak, D. D. Khalyavin, N. M. Olekhovich, A. V. Pushkarev, Yu. V. Radyush and A. Feher

P8-01 SPIN DISORDER RESISTIVITY OF THE HEUSLER Ni_2MnGa -BASED ALLOYS

J. Kamarád, J. Kaštil, F. Albertini, S. Fabbri and Z. Arnold

P8-02 MAGNETIC CHARACTERIZATION OF MELT-SPUN CoNiGa FERROMAGNETIC SUPERELASTIC ALLOY

J. Mino, M. Ipatov, J. Gamcova, V. Zhukova, Z. Vargova, A. Zhukov and R. Varga

P8-03 MAGNETO-CRYSTALLINE ANISOTROPY OF $\text{NdFe}_{x-1}\text{Mn}_x\text{O}_3$ SINGLE CRYSTALS

M. Mihalik, M. Mihalik jr., M. Zentková, J. Lazúrová, K. Uhlířová and M. Kratochvílová

P8-04 TUNING OF MAGNETISM IN $\text{DyFe}_{x-1}\text{Mn}_x\text{O}_3$ SINGLE CRYSTALS BY IRON SUBSTITUTION

M. Zentková, M. Mihalik, M. Mihalik Jr., J. Lazúrová, K. Uhlířová, M. Kratochvílová, M. K. Peprah and M. W. Meisel

P8-05 IDENTIFICATION OF MAGNETIC PHASES IN HIGHLY CORROSION-RESISTANT STEEL BY MÖSSBAUER SPECTROMETRY

L. Pašteka, M. Miglierini and M. Bujdoš

P8-06 SUPERPARAMAGNETIC BEHAVIOUR OF IRON IN BIOLOGICAL TISSUES STUDIED BY MÖSSBAUER SPECTROMETRY

I. Bonková, M. Miglierini, M. Bujdoš and M. Kopáni

P8-07 ASSESMENT OF THE MAGNETOSTRICTIVE PROPERTIES OF THE SELECTED CONSTRUCTION STEELS

A. Juš, P. Nowak and R. Szewczyk

P8-08 MAGNETIC SUSCEPTIBILITY OF MULTIFERROIC PEROVSKITES

M. Maryško, V. V. Laguta, P. Novák and I. P. Raevski

9. APPLICATIONS AND OTHER MAGNETIC MATERIALS NOT INCLUDED IN 1-8

- I9-01 STRESS MONITORING & ANNIHILATION IN STEELS BASED ON MAGNETIC TECHNIQUES**
E. Hristoforou, P. Vourna, A. Ktena and P. Svec
- O9-01 MAGNETIC PROPERTIES OF THE IONIC LIQUIDS Edimim(FeX₄) (X =Cl and Br) IN ITS SOLID STATE**
I. de Pedro, A. García-Sáiz, J. L. Espeso, L. F. Barquín and J. Rodríguez-Fernández
- O9-02 MAGNETIC ANISOTROPY OF HARD MILLED SURFACE**
A. Mičietová, J. Uriček, M. Čilliková, M. Neslušan and P. Kejzlar
- O9-03 CHARACTERISATION OF ODS STEELS AFTER GAMMA IRRADIATION FOR APPLICATION IN ALLEGRO REACTOR**
V. Slugeň, I. Bartošová and J. Dekan
- O9-04 MRI GRADIENT ECHO PULSE SEQUENCE AS A PHYSICAL TOOL IN DIFFERENTIATION OF NATIVE AND RECONSTRUCTED FERRITIN**
L. Balejčikova, O. Strbak, L. Baciak, J. Kovac, M. Masarova, A. Krafčík, M. Peteri, P. Kopcansky and I. Frollo
- P9-01 MAGNETIC AND MÖSSBAUER STUDY OF A CERIUM-BASED REACTIVE SORBENT**
Y. Jiraskova, J. Bursík, O. Zivotsky, J. Lunacek and P. Janos
- P9-02 ANALYSIS OF STRUCTURE TRANSFORMATIONS IN RAIL SURFACE INDUCED BY PLASTIC DEFORMATION VIA BARKHAUSEN NOISE EMISSION**
M. Neslušan, K. Zgutová, K. Kolařík and J. Šramka
- P9-03 MÖSSBAUER STUDY OF CHANGES IN OLIVINE AFTER TREATMENTS IN AIR**
M. Kądziołka-Gaweł and Z. Adamczyk
- P9-04 HIGH SENSITIVITY CURRENT TRANSDUCER BASED ON FLUXGATE SENSOR WITH ULTRALOW COERCIVITY CORE**
P. Frydrych, M. Nowicki and R. Szewczyk
- P9-05 BSA EFFECT ON CONTRAST PROPERTIES OF MAGNETITE NANOPARTICLES DURING MRI**
O. Strbak, M. Kubovcikova, L. Baciak, I. Khmara, D. Gogola, M. Koneracka, V. Zavisova, I. Antal, M. Masarova, P. Kopcansky and I. Frollo

- P9-06 THE EFFECT OF CRYO-ROLLING AND ANNEALING ON MAGNETIC PROPERTIES IN NON-ORIENTED ELECTRICAL STEEL**
T. Kvačák, P. Bella, R. Bidulský, R. Kočiško, P. Petroušek, A. Fedoriková, J. Bidulská, P. Jandačka, M. Lupták and M. Černík
- P9-07 COMPARISON OF IRON OXIDES-RELATED MRI ARTIFACTS IN HEALTHY AND NEUROPATHOLOGICAL HUMAN BRAIN TISSUE**
M. Masarova, A. Krafčík, M. Teplan, O. Strbak, D. Gogola, P. Boruta and I. Frollo
- P9-08 ThALES - THREE-AXIS LOW ENERGY NEUTRON SPECTROSCOPY AT THE INSTITUT LAUE-LANGEVIN**
M. Klicpera, M. Boehm, S. Roux, J. Kulda, V. Sechovský, P. Svoboda, J. Saroun and P. Steffens
- P9-09 THERMAL EXPANSION MEASUREMENT METHODS**
P. Proschek, P. Opletal, A. Barthá, J. Valenta, J. Prokleška and V. Sechovský
- P9-10 EFFECT OF STOCHASTIC DYNAMICS ON THE NUCLEAR MAGNETIC RESONANCE IN A FIELD GRADIENT**
J. Tóthová and V. Lisý
- P9-11 THE INFLUENCE OF ANNEALING TEMPERATURE ON THE MAGNETIC PROPERTIES OF CRYO-ROLLED NON-ORIENTED ELECTRICAL STEEL**
T. Kvačák, P. Bella, R. Bidulský, R. Kočiško, A. Fedoriková, P. Petroušek, J. Bidulská, P. Jandačka, M. Lupták, L. Gembalová and M. Černík
- P9-12 THE EFFECT OF RESIDUAL STRESSES ON THE COERCIVE FIELD STRENGTH OF DRAWN WIRES**
M. Suliga, R. Kruzel, K. Chwastek, A. Jakubas and P. Pawlik
- P9-13 MAGNETIC AURA MEASUREMENT IN DIAGNOSTICS AND CONTROL OF A SMALL TURBOJET ENGINE**
R. Andoga and L. Fózó
- P9-14 MECHANOCHEMICAL PREPARATION AND MAGNETIC PROPERTIES OF $\text{Fe}_3\text{O}_4/\text{ZnS}$ NANOCOMPOSITE**
Z. Bujňáková, A. Zorkovská and J. Kováč
- P9-15 ESTIMATION OF MULTICHANNEL MAGNETOMETER NOISE FLOOR IN ORDINARY LABORATORY CONDITIONS**
D. Praslička, P. Lipovský, J. Hudák and M. Šmelko
- P9-16 NON-STATIONARY NOISE ANALYSIS OF MAGNETIC SENSORS USING ALLAN VARIANCE**
K. Draganová, V. Moucha, T. Volčko and K. Semrád

- P9-17 CALIBRATION OF MAGNETOMETER FOR SMALL SATELLITES USING NEURAL NETWORK**
T. Kliment, D. Praslička, P. Lipovský, K. Draganová and O. Závodský
- P9-18 BARKHAUSEN NOISE INVESTIGATIONS OF 5.5 MM WIRE RODS WITH VARIOUS CARBON CONTENT**
M. Suliga and T. Garstka
- P9-19 SUPERCONDUCTIVITY AND QUANTUM CRITICALITY IN $\text{Cr}_{100-z}\text{Os}_z$**
P. R. Fernando, C. J. Sheppard and A. R. E. Prinsloo
- P9-20 MAGNETIC PROPERTIES OF $\text{Sc}_{1-x}\text{Ti}_x\text{Fe}_2$ UNDER HIGH PRESSURE**
Z. Arnold, M. Mišek, O. Isnard, J. Kaštil and J. Kamarád
- P9-21 INFLUENCE OF MAGNETIC SHIELD ON THE HIGH FREQUENCY ELECTROMAGNETIC FIELD PENETRATION THROUGH THE BUILDING MATERIAL**
I. Kolcunová, M. Pavlík, J. Zbojovský, S. Ilenin, Z. Čonka, M. Kanálik, D. Medveď, A. Mészáros, Ľ. Beňa and M. Kolcun
- P9-22 ADDITIONAL MODIFICATION OF THERMOMAGNETIC PROPERTIES OF OBJECTS OF LOW RELATIVE PERMEABILITY IN ELECTROMAGNETIC FIELD**
D. Medveď, M. Pavlík, J. Zbojovský, S. Ilenin, Z. Čonka, M. Kanálik, I. Kolcunová, A. Mészáros, Ľ. Beňa and M. Kolcun
- P9-23 ELECTRO-RHEOLOGICAL PROPERTIES OF TRANSFORMER OIL-BASED MAGNETIC FLUIDS**
K. Paulovičová, J. Tóthová, M. Rajňák, M. Timko, P. Kopčanský and V. Lisý
- P9-24 SOLID STATE ^{13}C NUCLEAR MAGNETIC RESONANCE STUDY OF MORPHOLOGY AND MOLECULAR MOBILITY OF POLYHYDROXYBUTYRATE**
A. Baran, P. Vrábel and D. Olčák
- P9-25 OPTIMIZED FREQUENCY SELECTIVE SURFACE FOR THE DESIGN OF MAGNETIC TYPE THIN BROADBAND RADIO ABSORBERS**
V. Babayan, N. E. Kazantseva, Yu. N. Kazantsev, J. Vilčáková and R. Moučka
- P9-26 APPLICATIONS OF BISTABLE MAGNETIC MICROWIRES**
R. Sabol, P. Klein, T. Ryba, R. Varga, M. Rovnak, I. Sulla, D. Mudronova, J. Gálik, I. Poláček and R. Hudak

- P9-27 KINETICS OF SOLID STATE SYNTHESIS OF QUATERNARY $\text{Cu}_2\text{FeSnS}_4$ (STANNITE) NANOCRYSTALS FOR SOLAR ENERGY APPLICATIONS**
P. Baláž, A. Zorkovská, I. Škorvánek, M. Baláž, E. Dutková, Z. Bujňáková, J. Trajić and J. Briančin
- P9-28 MECHANOCHEMICAL SYNTHESIS AND CHARACTERIZATION OF TERNARY CuFeS_2 and CuFeSe_2 NANOPARTICLES**
E. Dutková, I. Škorvánek, M. J. Sayagués, A. Zorkovská, J. Kováč and J. Kováč Jr.
- P9-29 ELIMINATION OF MAGNETIC NANOPARTICLES WITH VARIOUS SURFACE MODIFICATIONS FROM THE BLOODSTREAM IN VIVO**
I. Khmara, V. Zavisova, M. Koneracka, N. Tomasovicova, M. Kubovcikova, J. Kovac, M. Muckova and P. Kopcansky
- P9-30 DYNAMICS OF ^1H - ^{13}C CROSS POLARIZATION IN NUCLEAR MAGNETIC RESONANCE OF POLYHYDROXYBUTYRATE**
M. Kovaľaková, O. Fričová, M. Hutníková, V. Hronský and D. Olčák
- P9-31 MECHANOCHEMICAL REDUCTION OF CHALCOPYRITE CuFeS_2 : CHANGES IN COMPOSITION AND MAGNETIC PROPERTIES**
P. Baláž, A. Zorkovská, J. Kováč, M. Tešínský, M. Baláž, T. Osserov, G. Guseynova and T. Ketegenov
- P9-32 UTILIZATION OF EDDY CURRENT TOMOGRAPHY IN AUTOMOTIVE INDUSTRY**
P. Nowak, M. Nowicki, A. Juś and R. Szewczyk
- P9-33 MÖSSBAUER SPECTROSCOPY STUDY OF LABORATORY PRODUCED ODS STEELS**
J. Degmová, J. Dekan, J. Simeg Veterníková and V. Slugeň
- P9-34 DUAL-CONTROLLED PHOTSENSITIVE MESOPOROUS SILICA-COATED MAGNETITE NANOPARTICLES**
E. Beňová, O. Kapusta, A. Zeleňáková and V. Zeleňák
- P9-35 ISOLATED DC AND AC CURRENT AMPLIFIER WITH MAGNETIC FIELD SENSOR IN LOOP AND AMORPHOUS RING CORE**
O. Petruk, M. Kachniarz and R. Szewczyk
- P9-36 NOVEL METHOD OF OFFSET VOLTAGE MINIMIZATION IN HALL-EFFECT SENSOR**
O. Petruk, M. Kachniarz and R. Szewczyk

- P9-37 AIR-GAP TOROIDAL MAGNETIC MICRO-FORCE SENSOR**
M. Nowicki, M. Kachniarz, A. Juś, T. Charubin and R. Szewczyk
- P9-38 NANOCRYSTALLINE MAGNETIC GLASS-COATED MICROWIRES USABLE AS TEMPERATURE SENSORS IN BIOMEDICAL APPLICATIONS**
R. Hudak, I. Polacek, P. Klein, R. Varga, R. Sabol and J. Zivcak
- P9-39 INFLUENCE OF TEMPERATURE ON MAGNETOSTRICTIVE DELAY LINE PROPERTIES**
J. Salach and D. Jackiewicz
- P9-40 IMPLEMENTATION OF CONDUCTANCE TOMOGRAPHY IN DETECTION OF THE HALL SENSORS INHOMOGENEITY**
O. Petruk, P. Nowak and R. Szewczyk
- P9-41 MODELLING THE INFLUENCE OF STRESSES ON MAGNETIC CHARACTERISTICS OF THE ELEMENTS OF THE TRUSS USING EXTENDED JILES-ATHERTON MODEL**
D. Jackiewicz and R. Szewczyk

INDEX OF AUTHORS

Abd-Elmeguid M. M.	O7-01	264
Adam A.	P3-02	150
Adamczyk Z.	P9-03	328
Agostinho Moreira J.	O8-03	311
Albertini F.	P8-01	313
Allwood D. A.	P2-42	134
Almáši M.	P6-15	254
Almeida A.	O8-03	311
Amini N.	O2-08, P2-36	92, 128
Amitsuka H.	P6-21, P6-22	260, 261
Andoga R.	P9-13	338
Andrejka F.	P2-47	139
Anisimov M.	P6-04, P6-05, P6-11	243, 244, 250
Antal I.	P9-05	330
Antal V.	P3-11, O7-08, P7-12	159, 271, 285
Antkowiak M.	O5-04, P5-24	206, 230
Arnold Z.	P6-10, P8-01, P9-20	249, 313, 345
Arregi J. A.	O4-09	176
Arun K.	O3-01	146
Asenjo A.	PL-02	51
Azarevich A.	P6-11	250
Azarevich A. N.	P7-13	286
Babayan V.	O2-06, P9-25	90, 350
Babilas R.	P2-27	119
Babizhetskyy V.	O6-02	236
Baciak L.	O9-04, P9-05	325, 330
Badini-Confalonieri G. A.	P2-06	98
Bak Z.	P7-17	290
Bałanda M.	P4-10	186
Baláž M.	P9-27, P9-31	352, 356
Baláž P.	O1-02, P1-15, P9-27, P9-31	55, 74, 352, 356
Balcerzak T.	P1-01, P1-11, P1-13, P7-01	60, 70, 72, 274
Balejčíková L.	P5-23, O9-04	229, 325
Balga D.	P2-33, P2-35, P2-38	125, 127, 130
Baliha V.	P7-02	275
Balogh J.	P5-05, P5-18	211, 224

Bán K.	P2-13	105
Baran A.	P7-34, P9-24	307, 349
Barandiaran J. M.	I8-01	308
Barquín L. F.	O9-01	322
Bartha A.	P9-09	334
Bartošová I.	O9-03	324
Baťko I.	P2-17, P6-09	109, 248
Baťková M.	P2-17, P6-09	109, 248
Bella P.	P9-06, P9-11	331, 336
Bellucci S.	O1-03	56
Beňa Ľ.	P9-21, P9-22	346, 347
Beňačka Š.	P4-07	183
Beňová E.	P9-34	359
Berganza E.	PL-02	51
Berkutova A.	P3-14	162
Bernacki Ł.	P3-10, P4-20	158, 196
Bidulská J.	P9-06, P9-11	331, 336
Bidulský R.	P9-06, P9-11	331, 336
Bieńkowski A.	O8-02	310
Birčáková Z.	P2-04, P2-07	96, 99
Blagoev B.	P4-04	180
Blasiola B. D.	P5-02	208
Bloch K.	P2-20, P2-22, P2-23	112, 114, 115
Bobák A.	P1-13, P7-01	72, 274
Bocian K.	P7-33	306
Boča R.	P5-01	207
Boehm M.	P6-01, P9-08	240, 333
Boeije M.	I3-01	144
Bogach A.	P6-04, P6-05, P6-07, P6-11	243, 244, 246, 250
Bogach A. V.	P6-03, P7-13	242, 286
Bonková I.	P8-06	318
Borovský M.	P1-13, P1-21	72, 80
Boruta P.	P9-07	332
Bran C.	PL-02	51
Briančin J.	P5-18, P9-27	224, 352
Brown S. E.	O5-01	203

Brück E.	I3-01	144
Bruneel E.	P7-18	291
Brzostowski B.	P5-25	231
Brzózka K.	P4-01, P4-16	177, 192
Bujdoš M.	P8-05, P8-06	317, 318
Bujnakova L.	P2-32	124
Bujňáková Z.	P9-14, P9-27	339, 352
Bulín T.	P3-17	165
Bunda S.	P5-26, P5-27, P7-30	232, 233, 303
Bunda V.	P5-26, P5-27, P7-10, P7-30	232, 233, 283, 303
Bureš R.	P2-07, P2-17, P2-44, P2-46, P2-50, P3-03, P3-15	99, 109, 136, 138, 142, 151, 163
Bursík J.	O2-03, P9-01	87, 326
Bury P.	P5-06, P5-09	212, 215
Butta M.	P2-40	132
Butvin P.	P2-16	108
Butvinová B.	P2-16	108
Cambel V.	O1-06, O4-08, P7-23, P7-26	59, 175, 296, 299
Cardias R.	O1-01	54
Caron L.	I3-01	144
Carva K.	O1-02, P1-15	55, 74
Cesnek M.	P2-36	128
Cetner T.	P7-31	304
Cigán A.	P2-12, P7-18	104, 291
Cimbala R.	O5-03, P5-04, P5-05, P5-15, P5-17, P5-18	205, 210, 211, 221, 223, 224
Civan E.	P3-02	150
Corodeanu S.	O2-01	86
Correa V.	P7-24	297
Csach K.	P5-19	225
Curlik I.	O3-01	146
Custers J.	O7-05	268
Czaja P.	P4-10	186
Čenčariková H.	P7-06	279
Čermák P.	O6-05	239
Černík M.	P9-06, P9-11	331, 336

Černošek Z.	P2-01	93
Černošková E.	P2-01	93
Čilliková M.	O9-02	323
Čížmár E.	P2-01, P4-03, P5-03, P5-10, P5-11, P5-16, P7-34, O8-04	93, 179, 209, 216, 217, 222, 307, 312
Čonka Z.	P9-21, P9-22	346, 347
Čurlík I.	P6-20, O7-04	259, 267
Dabkowska H. A.	O3-02	147
Ďáková Ľ.	P3-15	163
Dančo M.	P1-24	83
de Pedro I.	O9-01	322
de Souza S. M.	P1-07	66
Degmová J.	P9-33	358
Dekan J.	P2-15, O9-03, P9-33	107, 324, 358
Demishev S.	P6-04, P6-05, P6-07, P6-11	243, 244, 246, 250
Demishev S. V.	P6-03, P6-06, O7-09, P7-13, P7-16, P7-27	242, 245, 272, 286, 289, 300
Derzhko O.	P1-06, P7-02	65, 275
Desnenko V. A.	O8-04	312
Dhankhar M.	O4-05	172
Di Marco I.	O1-01	54
Diduszko R.	P7-31	304
Diko P.	P3-11, P4-24, O7-08, P7-08, P7-12, P7-19	159, 200, 271, 281, 285, 292
Diviš M.	O6-01, O6-03, P6-02	235, 237, 241
Dlháň Ľ.	P5-01	207
Dłużewski P.	O3-02	147
Dobák S.	P2-11, P2-50, P3-03, P3-12, P3-15	103, 142, 151, 160, 163
Dobročka E.	P4-08	184
Doležal P.	O6-03, O7-07	237, 270
Dolník B.	O5-03, P5-05, P5-17, P5-18	205, 211, 223, 224
Dosoudil R.	P2-08, P2-09, P2-43	100, 101, 135
Dospial M.	P3-09	157
Draganová K.	P9-16, P9-17	341, 342
Drchal V.	O1-04	57
Drozd V.	P2-48	140

Dudrová E.	P3-16	164
Dukhnenko A.	P6-11	250
Dukhnenko A. V.	P6-03, I7-01	242, 262
Durajski A. P.	P7-20	293
Đuran I.	O7-10	273
Duranka P.	P1-18	77
Đurišin M.	P2-35, P2-38, P7-22	127, 130, 295
Durst K.	P2-18	110
Dušek M.	O7-05	268
Dutková E.	P9-27, P9-28	352, 353
Duzsa J.	P2-29	121
Dvurečenskij A.	P2-12, P7-18	104, 291
Dyadkin V. A.	O7-09	272
Dzubinska A.	O3-01	146
Džmura J.	P5-05, P5-18	211, 224
Džubinská A.	P6-18, P7-03	257, 276
Eber N.	P5-14	220
Éber N.	P5-19	225
Ekiz C.	P1-03	62
Eremenko V.	P7-34	307
Eriksson O.	O1-01	54
Espeso J. I.	P6-18	257
Espeso J. L.	O9-01	322
Ezerskaya E. V.	P5-08, P5-12	214, 218
Fåk B.	P6-02	241
Fabbrici S.	P8-01	313
Fáberová M.	P2-07, P2-17, P2-44, P2-46, P2-50, P3-03, P3-15	99, 109, 136, 138, 142, 151, 163
Fabián M.	P5-18	224
Farman K.	P4-01	177
Fasano Y.	P7-24	297
Fatima T.	P4-01	177
Fedorchenko A. V.	O8-04	312
Fedoriková A.	P9-06, P9-11	331, 336

Feher A.	P5-01, P5-03, P5-10, P5-11, P5-16, P5-26, P5-27, P7-10, P7-30, P7-34, O8-04	207, 209, 216, 217, 222, 232, 233, 283, 303, 307, 312
Fekete L.	O8-01	309
Fernández A.	I4-02	167
Fernandez Roldan J. A.	PL-02	51
Fernando P. R.	P9-19	344
Fertman E. L.	O8-04	312
Filipov V.	P6-04, P6-05, P6-07, P6-09, P6-11	243, 244, 246, 248, 250
Filipov V. B.	P6-03, P6-06, I7-01, P7-13, P7-27	242, 245, 262, 286, 300
Fitta M.	P4-10, P4-21	186, 197
Flachbart K.	P6-03, P6-04, P6-05, P6-06, P6-07, P6-11, I7-01, P7-13, P7-14, P7-27	242, 243, 244, 245, 246, 250, 262, 286, 287, 300
Flajšman L.	O4-01, O4-03, O4-05	168, 170, 172
Florek W.	O5-04	206
Fodor-Csorba K.	P5-19	225
Főző L.	P9-13	338
Franco V.	P3-04	152
Fričová O.	P9-30	355
Frollo I.	O9-04, P9-05, P9-07	325, 330, 332
Fronc K.	P3-06	154
Frydrych P.	P1-04, P1-05, O2-05, P9-04	63, 64, 89, 329
Fullerton E. E.	O4-09	176
Füzer J.	P2-04, P2-07, P2-11, P2-44, P2-46, P2-50, P3-03, P3-12, P3-15, P3-16	96, 99, 103, 136, 138, 142, 151, 160, 163, 164
Füzerová J.	P3-16	164
Gabáni S.	P6-03, P6-04, P6-05, P6-07, P6-09, P6-11, I7-01, P7-13, P7-14, P7-26	242, 243, 244, 246, 248, 250, 262, 286, 287, 299
Gajda D.	P7-31	304
Gajda G.	P7-31	304
Gál N.	P4-07, P4-08	183, 184
Galdun L.	P4-11, P4-17	187, 193
Gálik J.	P9-26	351

Gálisová L.	P1-09	68
Galusek D.	P2-12	104
Gamcová J.	O2-04, P2-33, P2-35, P2-37, P2-38, P7-22, P8-02	88, 125, 127, 129, 130, 295, 314
Garcia A.	O5-01	203
García-Sáiz A.	O9-01	322
Garstka T.	P9-18	343
Garus J.	P2-21, P2-22, P2-23, P2-24	113, 114, 115, 116
Garus S.	P2-21, P2-22, P2-23, P2-24	113, 114, 115, 116
Gastaldo F.	P6-20, O7-04	259, 267
Gavrilkin S.	P6-11	250
Gavrilkin S. Yu.	P7-13	286
Gawroński M.	P4-01, P4-16	177, 192
Gaži Š.	P4-07, P7-21	183, 294
Gažo E.	P7-14, P7-32	287, 305
Gdovinová V.	P5-14, P5-19, P5-21, P5-23	220, 225, 227, 229
Gębara P.	P2-25, P2-27, P3-01, P3-05	117, 119, 149, 153
Gembalová L.	P9-11	336
Gilmanov M. I.	P6-06, P7-13, P7-27	245, 286, 300
Giovannini M.	PL-03, P6-20, O7-04	52, 259, 267
Girman V.	P2-33, P2-35, P2-38, P4-14, P4-18, P4-21, P5-20	125, 127, 130, 190, 194, 197, 226
Gloss J.	O4-01	168
Glushkov V.	P6-04, P6-05, P6-07, P6-11	243, 244, 246, 250
Glushkov V. V.	P6-03, P6-06, O7-09, P7-13, P7-16	242, 245, 272, 286, 289
Gnatowski A.	P2-25	117
Gogola D.	P9-05, P9-07	330, 332
Gondro J.	P2-21, P2-24	113, 116
Gonzalez D.	P3-07	155
González S.	I4-02	167
Gorelik L.	O1-05	58
Górka B.	P4-01, P4-16	177, 192
Gozdur R.	P3-10, P4-20	158, 196
Grajcar M.	O7-06, P7-09, P7-25, P7-29	269, 282, 298, 302
Grechnev G. E.	P6-03	242

Grigoriev S. V.	O7-09	272
Gruszká K.	P1-19, P2-23, P7-31	78, 115, 304
Guillou F.	I3-01	144
Guseynova G.	P9-31	356
Gutowska M.	O3-02	147
Gyepes R.	P2-32, P3-07, P4-13	124, 155, 189
Gzik-Szumiatá M.	P4-01	177
Hadraba H.	P2-17, P2-46, P3-15	109, 138, 163
Hagiwara M.	P1-07	66
Hamlin J. J.	P5-02	208
Han Y.	P1-07	66
Hapla M.	P3-17	165
Hardoň Š.	P5-09, P5-13	215, 219
Hartánský R.	P2-10	102
Hasiak M.	O2-08, P2-45	92, 137
Hašková V.	P4-13, O7-06, P7-09, P7-25	189, 269, 282, 298
Havela L.	P6-16	255
Hayashi J.	P6-12	251
Hayryan S.	P5-23	229
Heczko O.	O8-01	309
Hegedűs L.	P2-44	136
Hembara M.	O6-02	236
Hendrych A.	O2-03	87
Hernando B.	I4-02, P4-11, P4-17	167, 187, 193
Herzer G.	I2-01, P2-18	84, 110
Hidaka H.	P6-21, P6-22	260, 261
Hlawenka P.	I7-01	262
Hložná D.	P4-03	179
Hlubina R.	O7-06	269
Hnatič M.	P1-24	83
Hofmann J.-U.	O7-03	266
Holková D.	P2-15	107
Holubová J.	P2-01	93
Holý V.	O4-07	174
Honolka J.	O1-02, O4-07	55, 174
Horký M.	O4-01	168

Hossain S.	P7-31	304
Hristoforou E.	I9-01	321
Hronský V.	P9-30	355
Hrubovčák P.	P3-04, P3-14, P4-14, P4-19	152, 162, 190, 195
Hu C.-K.	P5-23	229
Hua Liu Y.	P4-03	179
Hubač L.	P2-03, P2-39	95, 131
Hudák J.	P9-15	340
Hudak R.	P9-26, P9-38	351, 363
Hutníková M.	P9-30	355
Hwang I.-S.	P5-23	229
Charubin T.	P9-37	362
Cheranovskii V. O.	P5-08	214
Chernenko V. A.	I8-01	308
Chiriac H.	O2-01, P2-42, I4-01	86, 134, 166
Chojnacki M.	P3-06	154
Chorąży S.	O5-02	204
Chrobak M.	P7-05	278
Chromčíková M.	P2-16	108
Chromik Š.	P4-04, P4-07, P4-08	180, 183, 184
Chubova N. M.	O7-09	272
Chubykalo-Fesenko O.	PL-02	51
Chudíkova A.	P3-07	155
Chwastek K.	P2-25, P3-10, P9-12	117, 158, 337
Idrobo J. C.	O4-04	171
Idzikowski B.	O3-03, O6-04	148, 238
Ilenin S.	P9-21, P9-22	346, 347
Ilkovic S.	O3-01, P4-13	146, 189
Il'kovič S.	P4-21	197
Im M.-Y.	O4-05	172
Ipach R.	P2-13	105
Ipatov M.	P8-02	314
Isakov S. V.	O7-03	266
Isnard O.	P9-20	345
Ivanov V. Yu.	O7-09, P7-16	272, 289
Jackiewicz D.	P9-39, P9-41	364, 366

Jadzyn J.	P5-14, P5-21	220, 227
Jaglicic Z.	P4-18	194
Jagličić Z.	O8-03	311
Jakubas A.	P2-25, P9-12	117, 337
Jakubčín M.	P3-03	151
Jamon D.	P5-14	220
Jančárik V.	P2-43	135
Jančárik V.	P2-10	102
Jandačka P.	P9-06, P9-11	331, 336
Janičkovič D.	I2-02, O2-03, P2-16, P2-36, P2-47	85, 87, 108, 128, 139
Janiš V.	P7-15	288
Janos P.	P9-01	326
Janotova I.	I2-02	85
Jarosik M. W.	P7-28	301
Jaščur M.	P1-11, P1-23, P7-01	70, 82, 274
Javed A.	P4-01	177
Javorský P.	O6-05, P6-01, P6-02, P6-13, O7-07	239, 240, 241, 252, 270
Jeníková M.	P5-20	226
Jíra R.	O4-05	172
Jiraskova Y.	O2-03, P9-01	87, 326
Jírša M.	O7-10, P7-08	273, 281
Johrendt D.	O7-01	264
Jonson M.	O1-05	58
Juríková A.	P5-19, P5-21	225, 227
Juś A.	P8-07, P9-32, P9-37	319, 357, 362
Kabátová M.	P3-16	164
Kačmarčík J.	P3-07, O7-06, P7-09, P7-24, P7-25, P7-26, P7-29, P7-32	155, 269, 282, 297, 298, 299, 302, 305
Kądziołka-Gaweł M.	P9-03	328
Kachniarz M.	O8-02, P9-35, P9-36, P9-37	310, 360, 361, 362
Kamarád J.	P6-10, P8-01, P9-20	249, 313, 345
Kamieniarz G.	O5-04, P5-24, P5-25	206, 230, 231
Kanálík M.	P9-21, P9-22	346, 347
Kanuch P.	P7-22	295

Kanuchova M.	P7-22	295
Kapusta Cz.	P7-05	278
Kapusta O.	P3-14, P4-14, P9-34	162, 190, 359
Karapetrov G.	P7-23	296
Karavainikov A. V.	P4-09	185
Kardoš S.	P2-26	118
Karl'ová K.	P1-10	69
Kaštil J.	P6-10, P8-01, P9-20	249, 313, 345
Katsnelson M. I.	O1-01	54
Katuna J.	P2-35, P2-38	127, 130
Kauch A.	P7-15	288
Kavečanský V.	P4-24, P7-12	200, 285
Kawamura Y.	P6-12	251
Kazantsev Yu. N.	P9-25	350
Kazantseva N. E.	O2-06, P9-25	90, 350
Kaźmierczak M.	P3-01	149
Kecer J.	P1-18, P2-28	77, 120
Kejzlar P.	O9-02	323
Ketegenov T.	P9-31	356
Khalyavin D. D.	O8-04	312
Kharchenko M. F.	P4-09	185
Kharchenko Yu.	P4-09	185
Khmara I.	P9-05, P9-29	330, 354
Khoroshilov A.	P6-07	246
Khoroshilov A. L.	P6-03, P6-06	242, 245
Kiselev M.	O1-05	58
Kitti K.	P2-02	94
Kladivová M.	P1-18	77
Klautau A. B.	O1-01	54
Klein D. J.	P5-08	214
Klein P.	P2-06, P2-14, P9-26, P9-38	98, 106, 351, 363
Klein T.	P7-23	296
Klemke B.	O7-03	266
Klicpera M.	P6-01, P6-13, O7-07, P9-08	240, 252, 270, 333
Kliment T.	P9-17	342
Kmječ T.	P2-36	128

Kočiško R.	P9-06, P9-11	331, 336
Kohout J.	P2-36	128
Kolařík K.	P9-02	327
Kolcun M.	P5-04, P9-21, P9-22	210, 346, 347
Kolcunová I.	P5-05, P5-18, P9-21, P9-22	211, 224, 346, 347
Kollár P.	P2-04, P2-07, P2-11, P2-44, P2-46, P2-50, P3-03, P3-12, P3-15, P3-16	96, 99, 103, 136, 138, 142, 151, 160, 163, 164
Komanický V.	P2-32, P3-07, O4-07, P4-03, P7-10, P7-30	124, 155, 174, 179, 283, 303
Komova E.	P2-14	106
Koneracka M.	P9-05, P9-29	330, 354
Konieczny P.	O5-02	204
Konovalova E.	P6-09	248
Kopáni M.	P8-06	318
Kopčanský P.	O5-03, P5-04, P5-05, P5-06, P5-09, P5-14, P5-15, P5-17, P5-18, P5-19, P5-20, P5-21, P5-23, P9-23, O9-04, P9-05, P9-29	205, 210, 211, 212, 215, 220, 221, 223, 224, 225, 226, 227, 229, 325, 330, 348, 354
Kopčík M.	P7-25	298
Kopecky V.	O8-01	309
Korzeniak T.	P4-10	186
Kosterec M.	P5-04, P5-15	210, 221
Kotlyar O. V.	O8-04	312
Kotur B. Ya.	O6-02	236
Kováč F.	P2-49, P2-51	141, 143
Kováč J.	P2-29, P2-30, P2-32, P2-35, P2-38, P2-39, P2-41, O3-03, P3-11, O5-03, P5-20, P5-26, P5-27, O7-08, P7-08, P7-12, O9-04, P9-14, P9-29, P9-31	121, 122, 124, 127, 130, 131, 133, 148, 159, 205, 226, 232, 233, 271, 281, 285, 325, 339, 354, 356
Kováč J.	P9-28	353
Kováč Jr. J.	P9-28	353
Kováč P.	O7-10	273
Kováľaková M.	P9-30	355
Kowalik M.	P7-05	278
Kozár J.	P2-14	106

Kozikowski P.	I2-01	84
Kožejevová M.	P4-03	179
Krafcik A.	O9-04, P9-07	325, 332
Krajewski M.	P4-16	192
Krasnorussky V.	P6-07	246
Krasnorussky V. N.	P6-03, P6-06, P7-27	242, 245, 300
Kratochvilová M.	O7-05	268
Kratochvilová M.	O6-05, P6-17, P8-03, P8-04	239, 256, 315, 316
Kravec J.	P4-13	189
Kraxner J.	P2-12	104
Krompiewski S.	O4-02	169
Krupnitska O.	P1-06	65
Kruzel R.	P9-12	337
Kruželák L.	P5-04, P5-15	210, 221
Křižáková V.	O4-01, O4-03	168, 170
Ktena A.	I9-01	321
Kubena I.	P2-17	109
Kubicki M.	O5-02	204
Kubovčíková M.	P5-23, P9-05, P9-29	229, 330, 354
Kucuk I.	P3-02	150
Kúdelčík J.	P5-06, P5-09, P5-13	212, 215, 219
Kudrnovský J.	O1-02, O1-04	55, 57
Kuhnt M.	P2-18	110
Kuchár J.	P5-16	222
Kulda J.	P9-08	333
Kulinich S.	O1-05	58
Kunca B.	P2-41	133
Kurek P.	P2-44, P2-50, P3-03	136, 142, 151
Kurimský J.	O5-03, P5-04, P5-05, P5-15, P5-17, P5-18	205, 210, 211, 221, 223, 224
Kusigerski V.	P4-18	194
Kuzminski M.	P2-16	108
Kuźmiński M.	P2-04	96
Kvačkaj T.	P9-06, P9-11	331, 336
Kvashnin Y. O.	O1-01	54
Laguta V. V.	P8-08	320

Laskowska M.	P2-31, P4-06	123, 182
Laskowski L.	P2-31, P4-06	123, 182
Latoňová V.	P6-17	256
Lazúrová J.	P4-18, P4-21, P8-03, P8-04	194, 197, 315, 316
Lebioda M.	P3-10	158
Legut D.	P5-22	228
Levchenko A.	P6-04, P6-05, P6-07	243, 244, 246
Levchenko A. V.	P7-13	286
Levy-Bertrand F.	P7-23	296
Levytskyy V.	O6-02	236
Lian Zhang	I3-01	144
Lichtenstein A. I.	O1-01	54
Lipovský P.	P9-15, P9-17	340, 342
Lis T.	P5-24	230
Lisnichuk M.	P2-35, P2-38	127, 130
Lisý V.	P9-10, P9-23	335, 348
Litterst F. J.	O7-01	264
Lobanova I. I.	O7-09, P7-16	272, 289
Lohmann A.	P1-02	61
Lostun M.	P2-42	134
Lotnyk D.	P5-26, P5-27, I7-02, P7-10, P7-30	232, 233, 263, 283, 303
Lovas A.	P2-02, P2-03	94, 95
Lučivjanský T.	P1-13, P1-24	72, 83
Lukienko I.	P4-09	185
Łukiewska A.	P2-34	126
Lunacek J.	P9-01	326
Lupascu D. C.	O8-04	312
Lupták M.	P9-06, P9-11	331, 336
Lupu N.	O2-01, P2-42	86, 134
Lyra M. L.	P1-07	66
M Giebułtowski	P7-05	278
Máca F.	O1-02	55
Madaras T.	P1-10	69
Majerová M.	P2-12, P7-18	104, 291
Majorošová J.	P5-21	227

Mal'tsev V. N.	P1-14	73
Maldonado P.	P1-15	74
Małolepszy A.	P4-16	192
Maňka J.	P2-12, P7-18	104, 291
Manson J. M.	O5-01	203
Marcenat C.	P7-23, P7-24	296, 297
Marcin J.	I2-02, P2-41, P2-47, P2-51	85, 133, 139, 143
Marcin M.	P7-26	299
Markoš P.	P7-29	302
Marsilius M.	P2-18	110
Martoňák R.	O7-06	269
Maryško M.	P8-08	320
Masarova M.	O9-04, P9-05, P9-07	325, 330, 332
Matko I.	I2-02	85
Mat'ko I.	P2-16	108
Medvecká Z.	P7-23, P7-32	296, 305
Medved' D.	P9-21, P9-22	346, 347
Meisel M. W.	O5-01, P5-02, P5-16, P8-04	203, 208, 222, 316
Melišek T.	O7-10	273
Mesquita J. M.	I4-02	167
Mészáros A.	P9-21, P9-22	346, 347
Mičietová A.	O9-02	323
Miglierini M.	O2-04, O2-08, P2-36, P2-45, P8-05, P8-06	88, 92, 128, 137, 317, 318
Mihalik jr. M.	P4-18, P4-21, P6-16, O8-03, P8-03, P8-04	194, 197, 255, 311, 315, 316
Mihalik M.	P4-18, P4-21, P6-16, O8-03, P8-03, P8-04	194, 197, 255, 311, 315, 316
Michalik S.	O2-04, P2-33	88, 125
Michon B.	P7-23	296
Michor H.	O6-02	236
Milkovič O.	P2-33, P2-37	125, 129
Miloslavskaya O.	P4-09	185
Minikayev R.	P3-06	154
Mino J.	P8-02	314
Míšek M.	I6-01, P6-10, P9-20	234, 249, 345

Miškuf J.	P5-19	225
Mitsen K. V.	P7-13	286
Miura N.	P6-21, P6-22	260, 261
Moessner R.	O7-03	266
Molcanova Z.	P6-16	255
Morawski A.	P7-31	304
Mori T.	P7-26	299
Morris J. P.	O7-03	266
Moshchalkov V. V.	I7-02, P7-11	263, 284
Moučka R.	P9-25	350
Moucha V.	P9-16	341
Muckova M.	P9-29	354
Mudra E.	P2-29	121
Mudronova D.	P9-26	351
Musiał A.	O3-03	148
Muto S.	O4-04	171
Nabiałek M.	P1-19, P2-05, P2-21, P2-22, P2-24	78, 97, 113, 114, 116
Nagalakshmi R.	O3-01, P7-03	146, 276
Najgebauer M.	P1-12, P3-10	71, 158
Nakano S.	P6-12	251
Nallamuthu S.	O3-01, P7-03	146, 276
Neslušan M.	O9-02, P9-02	323, 327
Nesterenko A. A.	P1-14	73
Nishioka T.	P6-12	251
Nogaš W.	O5-02	204
Nordström L.	O1-01	54
Noudem J.	P3-11	159
Novák L.	P2-03, P2-28, P2-30, P2-39	95, 120, 122, 131
Novák P.	P2-15, O6-01, P8-08	107, 235, 320
Nowak P.	P8-07, P9-32, P9-40	319, 357, 365
Nowicki M.	P1-04, P1-05, P9-04, P9-32, P9-37	63, 64, 329, 357, 362
Nurgaliev T.	P4-04	180
Ohanyan V.	O1-03	56
Ohnuma M.	I2-01	84

Olčák D.	P9-24, P9-30	349, 355
Olekhnovich N. M.	O8-04	312
Olekšáková D.	P3-03, P3-12	151, 160
Onderko F.	P2-50, P3-03, P3-12	142, 151, 160
Ondrůšek Č.	P3-17	165
Onufer J.	P2-26	118
Onufriienko O.	P7-11	284
Opletal P.	I6-01, P7-04, P9-09	234, 277, 334
Oppeneer P.	P1-15	74
Orendáč M.	P2-01, P4-03, P5-01, P5-03, P5-16	93, 179, 207, 209, 222
Orendáč Mat.	P7-14	287
Orendáčová A.	P2-01, P5-01, P5-02, P5-03, P5-16, P5-22	93, 207, 208, 209, 222, 228
Osserov T.	P9-31	356
Ouladdiaf B.	O6-05	239
Óvári T.-A.	O2-01, P2-42	
Özcan S.	O6-02	134, 236
Pajskr K.	O6-05	239
Palmero E.	PL-02	51
Pankratova M.	P1-20	79
Parafilo A.	O1-05	58
Park J.-H.	P5-16	222
Pásztorová J.	O7-07	270
Pašteka L.	P8-05	317
Paukov M.	P6-16	255
Paulovičová K.	O5-03, P5-04, P5-05, P5-17, P9-23	205, 210, 211, 223, 348
Pavličko J.	P1-16	75
Pavlík M.	P9-21, P9-22	346, 347
Pavlovic M.	O2-04	88
Pawlak W.	P4-20	196
Pawlik K.	P3-01, P6-08	149, 247
Pawlik P.	P3-01, P6-08, P9-12	149, 247, 337
Pedrazzini P.	P7-24	297
Pękała K.	P2-48	140

Pękała M.	P2-48	140
Peška R.	O5-02	204
Peprah M. K.	O5-01, P5-02, P8-04	203, 208, 316
Perevertov O.	O8-01	309
Pérez J. M.	O5-01	203
Perez R.	PL-02	51
Perovic M.	P4-18	194
Peteri M.	O9-04	325
Petráš J.	P5-05, P5-18	211, 224
Petroušek P.	P9-06, P9-11	331, 336
Petruk O.	P9-35, P9-36, P9-40	360, 361, 365
Petryshynets I.	P2-49, P2-51	141, 143
Pierunek N.	O6-04	238
Pietrusiewicz P.	P2-05, P2-21	97, 113
Piovarči S.	P4-24, O7-08, P7-19	200, 271, 292
Pisarčík M.	P4-07, P7-21	183, 294
Pluta W. A.	P3-13	161
Podgajny R.	O5-02	204
Pokorný V.	P7-15	288
Poláček I.	P9-26, P9-38	351, 363
Polak C.	I2-01, P2-18, I3-02	84, 110, 145
Potočník I.	P5-03	209
Praslička D.	P9-15, P9-17	340, 342
Presz A.	P7-31	304
Prchal J.	P6-10, P6-14, P6-17, P6-21, O7-01, O7-07	249, 253, 256, 260, 264, 270
Pribulová Z.	P7-23, P7-24, P7-26, P7-32	296, 297, 299, 305
Prida V. M.	I4-02, P4-11, P4-17	167, 187, 193
Prinsloo A. R. E.	P9-19	344
Pristáš G.	P6-09, P7-14	248, 287
Prnová A.	P2-12	104
Prokeš K.	O6-05	239
Prokleška J.	I6-01, O6-03, O7-05, P7-04, P9-09	234, 237, 268, 277, 334
Prokopov A. R.	P4-09	185
Proschek P.	P9-09	334

Przewoźnik J.	P7-05	278
Przybył A.	P3-01, P3-08	149, 156
Przybylski M.	I1-01	53
Puchý V.	P2-49	141
Pushkarev A. V.	O8-04	312
Quintero P. A.	O5-01, P5-02	203, 208
Ráčzová K.	P4-03, P5-10	179, 216
Radelytskyi I.	O3-02, P3-06	147, 154
Rader O.	I7-01	262
Radoń A.	P2-27	119
Radyush Yu. V.	O8-04	312
Raes B.	I7-02	263
Raevski I. P.	P8-08	320
Rajňák M.	O5-03, P5-04, P5-05, P5-15, P5-17, P5-18, P7-29, P9-23	205, 210, 211, 221, 223, 224, 302, 348
Rameš M.	O7-10	273
Rashid T. P.	O3-01	146
Reiffers M.	O3-01, P4-13, P6-18, P6-20, O7-04, P7-03	146, 189, 257, 259, 267, 276
Rezničák M.	P2-26	118
Rienks E. D. L.	I7-01	262
Richter J.	P1-02, P1-06, I5-01, P7-02	61, 65, 201, 275
Rodríguez Fernández J.	P6-18	257
Rodríguez-Fernández J.	O9-01	322
Rojas M.	P1-07	66
Rojas O.	O1-03, P1-07	56, 66
Roupcová P.	P2-46, P4-18	138, 194
Roux S.	P9-08	333
Rovnak M.	P9-26	351
Royer F.	P5-14	220
Rubin P.	P5-07	213
Rudziński W.	P7-33	306
Rusz J.	O4-04	171
Ryba T.	P2-32, P3-07, P4-11, P4-13, P4-17, P4-24, P7-22, P9-26	124, 155, 187, 189, 193, 200, 295, 351
Rzacki J.	P3-09	157

Rzącki J.	P2-20	112
Sabol R.	P9-26, P9-38	351, 363
Saccone A.	O7-04	267
Saito H.	P6-22	261
Saksl K.	P2-33, P2-35, P2-38, P7-22	125, 127, 130, 295
Salaheldeen M.	I4-02	167
Salach J.	P9-39	364
Salak A. N.	O8-04	312
Salamon S.	O8-04	312
Samarin A.	P6-04	243
Samarin N.	P6-04, P6-05	243, 244
Samuely P.	O7-06, P7-09, P7-11, P7-23, P7-24, P7-25, P7-26, P7-29, P7-32	269, 282, 284, 296, 297, 298, 299, 302, 305
Samuely T.	I7-02, O7-06, P7-09, P7-11, P7-25	263, 269, 282, 284, 298
Sánchez-Barriga J.	I7-01	262
Sarlar K.	P3-02	150
Saroun J.	P9-08	333
Sayagués M. J.	P9-28	353
Sebek M.	P2-29	121
Sečianska K.	O4-08	175
Sechovský V.	O1-02, O4-07, I6-01, O6-03, P6-14, P6-17, P6-21, O7-01, O7-05, P7-04, P9-08, P9-09	55, 174, 234, 237, 253, 256, 260, 264, 268, 277, 333, 334
Sekine C.	P6-12	251
Semeno A. V.	P6-06, P7-27	245, 300
Semrád K.	P9-16	341
Sera M.	P6-12	251
Sereni J. G.	O7-02	265
Shaposhnikov A. N.	P4-09	185
Shekhter R.	O1-05	58
Sheppard C. J.	P9-19	344
Sherman A.	P5-07	213
Shitsevalova N.	P6-04, P6-05, P6-07, P6-11, P7-14	243, 244, 246, 250, 287
Shitsevalova N. Y.	P6-06, I7-01, P7-27	245, 262, 300

Shitsevalova N. Yu.	P6-03, P7-13	242, 286
Shvartsman V. V.	O8-04	312
Schäfer R.	PL-01	50
Schmid M.	O4-01	168
Schmidt H.-J.	P1-02	61
Schneeweiss O.	P3-17	165
Schumer A.	O6-02	236
Sieklucka B.	O5-02	204
Siemensmeyer K.	P6-07, I7-01, O7-03	246, 262, 266
Simeg Veterníková J.	P9-33	358
Sirenko V.	P7-34	307
Sitek J.	P2-15	107
Skokowski P.	P6-19	258
Sláma J.	P2-43	135
Slawska-Waniewska A.	P2-16	108
Slugeň V.	O9-03, P9-33	324, 358
Sluchanko N.	P6-11	250
Sluchanko N.	P6-04, P6-05, P6-07	243, 244, 246
Sluchanko N. E.	P6-03, P6-06, P7-13, P7-27	242, 245, 286, 300
Smolka P.	O2-06	90
Smolkova I. S.	O2-06	90
Śniadecki Z.	O3-03, O6-04	148, 238
Sobocińska M.	P5-24	230
Sojková M.	P4-04, P4-07, P4-08	180, 183, 184
Solokha P.	O7-04	267
Sopcak T.	P2-29	121
Sopko M.	P2-37	129
Sovák P.	O2-04, P2-35, P2-38	88, 127, 130
Spiegelberg J.	O4-04	171
Springholz G.	O4-07	174
Starodub V.	P5-11	217
Steffens P.	P9-08	333
Stobiński L.	P4-16	192
Stoian G.	O2-01	86
Strache T.	P2-18	110
Strbak O.	O9-04, P9-05, P9-07	325, 330, 332

Strečka J.	O1-03, P1-03, P1-07, P1-08, P1-09, P1-10, P1-16, P1-17, P7-06	56, 62, 66, 67, 68, 69, 75, 76, 279
Strečková M.	P2-17, P2-29, P2-46, P2-50, P3-15	109, 121, 138, 142, 163
Strydom A.	O7-04	267
Strydom A. M.	P6-20	259
Suliga M.	P9-12, P9-18	337, 343
Sulla I.	P9-26	351
Svoboda P.	P9-08	333
Syassen K.	O7-01	264
Synoradzki K.	P6-19, P7-07	258, 280
Szabó A.	P2-13	105
Szabó B.	P2-13	105
Szabó P.	P4-13, O7-06, P7-09, P7-11, P7-25, P7-29	189, 269, 282, 284, 298, 302
Szałowski K.	P1-01, P1-11, P4-02, P7-01	60, 70, 178, 274
Szczesniak R.	P7-20	293
Szczygłowski J.	O2-07	91
Szewczyk A.	O3-02	147
Szewczyk R.	P1-04, P1-05, O2-05, P4-05, O8-02, P8-07, P9-04, P9-32, P9-35, P9-36, P9-37, P9-40, P9-41	63, 64, 89, 181, 310, 319, 329, 357, 360, 361, 362, 365, 366
Szilva A.	O1-01	54
Szota M.	P2-23	115
Szumiata T.	P4-01, P4-16	177, 192
Szwachta G.	P7-05	278
Szydłowska J.	P2-48	140
Szymczak H.	O3-02, P3-06	147, 154
Šebek M.	P2-49	141
Šíkola T.	O4-01, O4-03, O4-05	168, 170, 172
Škorvánek I.	I2-02, P2-37, P2-41, P2-47, P2-51, O3-03, P9-27, P9-28	85, 129, 133, 139, 143, 148, 352, 353
Škrátek M.	P2-12, P7-18	104, 291
Šmelko M.	P9-15	340
Šoka M.	P2-09, P2-10, P2-19, P2-43	101, 102, 111, 135

Šoltésová D.	P5-11	217
Šoltýs J.	O4-08, P7-23, P7-26	175, 296, 299
Španková M.	P4-04, P4-07, P4-08, P7-21	180, 183, 184, 294
Šramka J.	P9-02	327
Štrbík V.	P4-04, P4-07, P4-08, P7-21	180, 183, 184, 294
Štubňa V.	P1-23	82
Švábenská E.	P3-17	165
Švec P.	I2-02, P2-41, P2-47	85, 133
Švec Sr. P.	I2-02, P2-16, P2-41, I9-01	85, 108, 133, 139, 321
Tabata C.	P6-21, P6-22	260, 261
Takahashi H.	P6-12	251
Takeda K.	P6-12	251
Tanida T.	P6-12	251
Tarasenko R.	O1-02, O4-07, P5-02, P5-03	55, 174, 208, 209
Tatsumi K.	O4-04	171
Tennant D. A.	O7-03	266
Teplan M.	P9-07	332
Tešínský M.	P9-31	356
Tibenská K.	P2-01	93
Tibu M.	P2-42	134
Timko M.	O5-03, P5-04, P5-05, P5-06, P5-09, P5-15, P5-17, P5-18, P9-23	205, 210, 211, 212, 215, 221, 223, 224, 348
Timmermans M.	I7-02	263
Titov A.	O2-03	87
Tkáč V.	O1-02, P2-01, O4-07, P5-01, O6-03	55, 93, 174, 207, 237
Tóbbik J.	O1-06	59
Tokarev V. V.	P5-08	214
Toliňský T.	P6-19	258
Tomašovičová N.	P5-14, P5-19, P5-20, P5-21, P5-23, P9-29	220, 225, 226, 227, 229, 354
Tomita T.	P6-12	251
Torrico J.	P1-07	66
Toth-Katona T.	P5-14	220
Tóthová J.	P5-05, P9-10, P9-23	211, 335, 348

Trajić J.	P9-27	352
Turek I.	O1-04	57
Uhlíř V.	O4-05, O4-09	172, 176
Uhlířová K.	P6-21, O7-05, P8-03, P8-04	260, 268, 315, 316
Urbánek M.	O4-01, O4-03, O4-05	168, 170, 172
Urbaniak-Kucharczyk A.	P4-12	188
Uriček J.	O9-02	323
Ušák E.	P2-19	111
Ušáková M.	P2-08, P2-09, P2-10, P2-19, P2-43	100, 101, 102, 111, 135
Utko J.	P5-24	230
Váhovský O.	P1-22	81
Vajda A.	P5-19	225
Valenta J.	O6-03, P7-04, P9-09	237, 277, 334
Vališka M.	O4-07, I6-01, O6-03, P6-14	174, 234, 237, 253
Van de Vondel J.	I7-02	263
Van Dijk N.	I3-01	144
Van Driessche I.	P7-18	291
Van Thang Nguyen	I3-01	144
Vaňatka M.	O4-03, O4-05	170, 172
VanGennep D.	P5-02	208
Varačka L.	P5-13	219
Varga P.	O4-01	168
Varga R.	P1-22, P2-06, P2-14, P2-32, P3-07, P4-11, P4-13, P4-17, P4-24, P7-22, P8-02, P9-26, P9-38	81, 98, 106, 124, 155, 187, 189, 193, 200, 295, 314, 351, 363
Vargová Z.	P2-32, P3-07, P4-11, P4-13, P4-17, P4-24, P7-22, P8-02	124, 155, 187, 189, 193, 200, 295, 314
Varykhalov A.	I7-01	262
Vasylets G.	P5-11	217
Vašut D.	P2-19	111
Vavra M.	P4-18, P4-21	194, 197
Vázquez de Parga A. L.	I5-02	202
Vazquez M.	PL-02, P2-06	51, 98
Vega V.	I4-02	167
Verkholyak T.	P1-17	76

Veveričík M.	P5-06	212
Vilarinho R.	O8-03	311
Vilčáková J.	O2-06, P9-25	90, 350
Viňáš J.	P3-12	160
Vitkova L.	O2-06	90
Vlášková K.	P6-10, P6-13	249, 252
Vojtkova L.	P7-19	292
Volčko T.	P9-16	341
Volochová D.	O7-08, P7-08, P7-12	271, 281, 285
Vondráčková B.	O7-05	268
Voronov V.	P6-05	244
Voronov V. V.	O7-09	272
Vourna P.	I9-01	321
Vrábel P.	P9-24	349
Vyborny K.	P4-15	191
Wang X.	O7-01	264
Warda K.	P4-22, P4-23	198, 199
Wasik D.	P4-16	192
Wasiutyński T.	O5-02	204
Wdowik D. U.	P5-22	228
Weidenfeller B.	P2-07	99
Weltsch Z.	P2-02	94
Wende H.	O8-04	312
Weschke E.	I7-01	262
Whitmore L. C.	O2-01	86
Wnuk I.	P3-01	149
Wodzyński A.	P3-10	158
Woch W. M.	P7-05	278
Wojciechowski M.	P5-24, P5-25	230, 231
Wojciechowski T.	P3-06	154
Wojtczak L.	P4-22	198
Wojtczak L.	P4-23	199
Woźniak A. D.	P7-28	301
Wysłocki J. J.	P3-01, P6-08	149, 247
Xia J. S.	O5-01	203
Xuefei Miao	I3-01	144

Yanagisawa T.	P6-21, P6-22	260, 261
Yang C.-W.	P5-23	229
Yibole H.	I3-01	144
Zajarniuk T.	O3-02	147
Zakuťanská K.	P5-20	226
Zalecki R.	P7-05	278
Závišová V.	P5-06, P5-14, P5-19, P5-21, P9-05, P9-29	212, 220, 225, 227, 330, 354
Závodský O.	P9-17	342
Zbojovský J.	P9-21, P9-22	346, 347
Zelevák V.	P3-04, P3-14, P4-14, P4-19, P6-15, P9-34	152, 162, 190, 195, 254, 359
Zeleváková A.	P3-04, P3-14, P4-14, P4-19, P6-15, P9-34	152, 162, 190, 195, 254, 359
Zentková M.	P4-18, P4-21, O8-03, P8-03, P8-04	194, 197, 311, 315, 316
Zgutová K.	P9-02	327
Zhang G.	P7-11	284
Zhukov A.	P4-11, P8-02	187, 314
Zhukova V.	P4-11, P8-02	187, 314
Zigo J.	I2-02	85
Ziman J.	P1-18, P2-26	77, 118
Zivcak J.	P9-38	363
Zivotsky O.	O2-03, P9-01	87, 326
Zmorayová K.	P3-11	159
Zorkovská A.	P9-14, P9-27, P9-28, P9-31	339, 352, 353, 356
Zubáč J.	O6-05, P6-02	239, 241
Zwierzyci M.	O4-06	173
Žemlička M.	O7-06, P7-09, P7-25, P7-29	269, 282, 298, 302
Žukovič M.	P1-13, P1-20, P1-21, P7-01	72, 79, 80, 274



LABORATORY EQUIPMENTS AND SUPPLIES

Import/Export /services

Equipments for CryoBank

Nitrogen and Helium Dewars

Compresors, Chillers, Cryogyn, Cryoskin

Apparatus for Production and Treatment of Materials

Supplies Technical and Special Gases, Liquid Helium and Nitrogen

Thermometers - Ge sensors with very low magnetoresistance,
Pt sensors, thermocouples

Microscopes Nikon, IT and Computers, MRI, CT, Sonographs

Engineering and cryogenic consultations

**CONTACT: Cryosoft Ltd.,
B. Němcovej 14,
P. O. Box G-14, SK 040 01 Košice
Slovakia**

Tel./Fax: ++421 55 729 5948

E- mail: cryosoft@mail.t-com.sk

www: <http://www.cryosoft.euweb.cz>

16th Czech and Slovak Conference on Magnetism

Book of Abstracts

Publisher: Slovak Physical Society

Year of publication: 2016

Impression: 320 copies

Number of pages: 436

First edition

ISBN 978-80-971450-9-5

ISBN 978-80-971450-9-5

